UNIVERSITAT POLITÈCNICA DE CATALUNYA
BARCELONATECH

SEMI-AUTOMATIC LAND COVER CLASSIFICATION AND URBAN MODELLING BASED ON MORPHOLOGICAL FEATURES

Remote Sensing, Geographical Information Systems, and Urban Morphology: Defining Models of Land Occupation along the Mediterranean Side of Spain

NICOLA COLANINNO

PhD

URBAN AND ARCHITECTURE MANAGEMENT AND VALUATION

2016

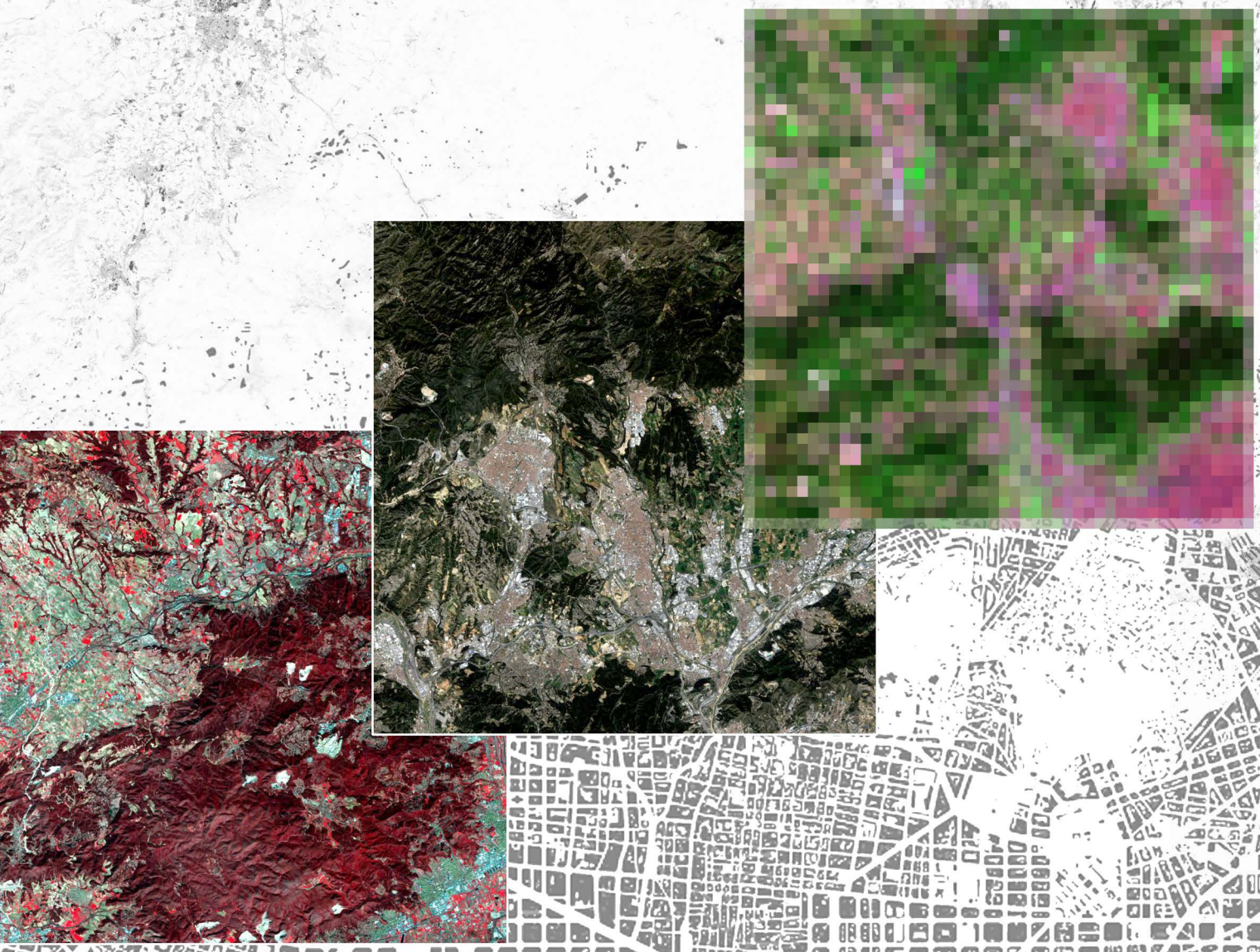

PhD in Urban and Architecture Management and Valuation

PhD THESIS

SEMI-AUTOMATIC LAND COVER CLASSIFICATION AND URBAN MODELLING BASED ON MORPHOLOGICAL FEATURES

Remote Sensing, Geographical Information Systems, and Urban Morphology: Defining Models of Land Occupation along the Mediterranean Side of Spain

PhD Candidate
Nicola Colaninno

PhD Director
Josep Roca Cladera

Universidad Politécnica de Cataluña (UPC) - Barcelona TECH
Departamento de Tecnología de la Arquitectura (TA)
CPSV Centro de Políticas de Suelo y Valoraciones
ETSAB Escuela Técnica Superior de Arquitectura de Barcelona

At the end of this long journey, what remains is not just an increased knowledge, but mostly an increased curiosity, and further questions...and the desire to find proper answers!

Dedicated to Tommaso and Eleonora, both departure and arrival

…to Giuseppe, a variable…and Carmela, a constant

…to Valentina, my traveling partner

FOREWORD

Primarily, this work is the result of an important learning process, in which, paradoxically, the first end-user is the same author. Indeed, this essay relies on an effort to report step-by-step my own training and achievements, either in the fields of geomatics and the spatial analysis.

An important impetus which has motivated this investigation is the global interest shown by several international authorities on the spatial analysis and the interaction among human settlements and natural environment, the consequences of such interaction, and the sustainability of the urban growth. Because currently there exists an increasing attention about the possibility of generating a heavy negative impact upon the environment, urban planners now need to reconsider the development policies in order to face the future urban expansion. For example in the USA, towards the end of the twentieth century, issues about the urban sprawl have generated an important national debate on the land use policies that includes smart growth managing and the capability of measuring and managing urban growth (Brueckner, 2000; Cheng, 2003). Such a debate is currently an international issue!

In fact, the research work underpinning this essay, framed within the field of the spatial analysis and with special emphasis on urban morphology, was first inserted in the national project financed by the Spanish Ministry of Education and Science (MEC) in 2006. The project was aimed at analysing the processes of urbanization occurred along the Spanish Mediterranean side, from Gerona to Cadiz, in the period between 1956, the year in which the first Planning Act came into force, also including the period 1980/81, when the first democratic councils were formed, and until 2006, date which probably marks a peak of the urbanizing processes in Spain before the crisis.

In this sense, the spatial analysis provides a key instrument to the study and measuring of the urban sprawl. In particular, the spatial analysis arises from the quantitative geography, which implies the use of statistics applied to the geographical space, which is thus intended as the main environment for whatever analysis. Actually, the use of spatial statistics has experimented a significant increase, during the last decades, together with an equally rapid development of statistical applications integrated into geographic information systems. Hence, the combined use of statistics and Geographic Information Systems (GIS), has provided an essential set of tools for spatial planning (Martori, et al., 2008).

Indeed, during the last decades, geospatial technologies have completely changed the way we deal with environment analysis, as well as the manner of approaching questions of land management and spatial planning. The appearance of GIS in the mid-1960s mostly revealed a progress in computer technology and the emergence of a quantitative approach in geography.

GIS have developed dramatically since the late 1970's, in terms of both technical and processing capabilities (Huisman, et al., 2009). It has evolved from a tool for mapping and data management, during the first phase, into an efficient spatial data-handling and analysis technology and, more recently, into geographic information science (GISc). Currently, the commercial success of GIS that occurred around the early 1980s has greatly increased the fields of application, potentialities (Weng, 2010), and end-users. Hence, since in the 1990's there has been an increasing trend in applications that use GIS technologies for spatial analysis. On the other hand, the impressive development that has experimented during the last decades the use of the remotely sensed information (either from satellite and/or aerial imagery) in the field of the spatial analysis, has strengthened even more the capabilities for monitoring and managing the environment.

In particular, the Remote Sensing (RS) is becoming more effective and accessible for almost all of the world. In fact, currently, plenty of satellites are operating around the Earth recollecting information at different spatial, spectral, and temporal resolution. The combination of RS technologies, and derived data, with GIS provides powerful and effective tools for understanding spatial dynamics along the Earth's surface.

According to Ehlers (2010), independently of the degree of integration between RS and GIS it is clear that there exists a trend of convergence in the development of applications and processes aimed to the land management and planning either at local, regional, and even at coarser scales. The joint use of both technologies in the field of spatial planning, beside the use of statistical models, provides a recognized solution for critical questions such as urban development, resources management, and natural hazard assessments between others (Ehlers, 2010).

So, if on one hand, this work is part of that research line which aims to strengthen the idea that these two technologies are complementary and necessary to each other; on the other hand, the work aims to demonstrate

the utility of this synergy in the field of spatial analysis and land management. In particular, beyond the results, the main value of the work relies on suggesting a suitable approach to the overall analysis about key environmental aspects (such vegetation, water, agriculture, and, in particular the built-up environment), including the generation of primary data about the land cover, up to the spatial analysis of different urban models. Moreover, the work shows that from scratch, it is possible obtain robust data and analysis, at global level, in many cases using freely available information and open-source software.

From the standpoint of the RS approach, both image enhancement and classification techniques are covered for information extraction, while GIS are used for data management, spatial analysis, and mapping. Still, spatial analysis assumptions rely on some of the most recognized theories of the modern urbanism. In this sense, and due to the didactical value, it is the intention of this essay to provide basic knowledge and further standpoints mainly to urban planners, decision-makers, non-specialist digital image analyst, and students.

ACKNOWLEDGEMENTS

My interest in the field of the urban studies arises during the last stage of the university studies at the school of architecture in Rome "La Sapienza". In particular, some of the most representative works in this field were developed under the supervision of Professor Susanna Menichini, Professor Marcello Vittorini, and Dr. Mario Cerasoli.

After that, a further impetus to the study of urban dynamics based on the use of new technologies is due to Professor Josep Roca who, during the post-graduate studies at the Universitat Politècnica de Catalunya, strongly encouraged me to develop interesting approaches and methodologies for spatial analysis and urban modelling. Actually, with the support of Professor Roca, in 2008 I get a scholarship, first funded by UPC, then by the Regional Government of Catalunya, and finally by the Ministry of Education and Science of the Spanish Government, in order to develop my research and my training as a Doctor.

Besides, acknowledgments are also due to the research funding, granted to develop more extensive research projects, provided by the same Spanish Ministry of Education and Science, the Ministry of Science and Innovation, the Ministry of Development, the Ministry of Housing, and the European Union through the INTERREG IIIB Program (South Western Europe).

During the period in which I have developed this research work I have been particularly fascinated by the use of the new technologies for the spatial analysis, and in particular the Remote Sensing (RS) and the Geographical Information Systems (GIS).

From the technical standpoint the first teachings in the field of both RS and GIS come from the support of Bahaaeddin Alhaddad, at that time my supervisor and colleague. While, in the most advanced stage of my PhD studies, a fundamental support in these fields comes from Alejandro Marambio, both colleague and friend. Indeed, I had (and I still have) the good fortune to work with Alejandro who, with his extraordinary insight and ability, has contributed to the development of the work also through many discussions on the theoretical foundations of digital image processing and analysis.

Particularly, in the field of remote sensing I also have to thank Professor José António Tenedório who, for its excellent teaching capacities, has had quite an impact on the author's abilities about digital data analysis in the field of remote sensing.

Furthermore, I wish to extend my most sincere gratitude to several professionals, part of the Center of Land Policy and Valuations (CPSV), which have contributed to this work, and in particular Malcolm Burns for improving my skills in the field of the spatial planning; Carlos Marmolejo and Jorge Cerda for their encouragement and technical support in both spatial planning and statistical issues; Montserrat Moix for GIS and computational endorsement; Rolando Biere for his help in terms of organization of the work and administrative questions.

Besides, important improvements to the work are due to collaboration with Karin Pfeffer, assistant Professor at the Department of Human Geography of the University of Amsterdam, who, during the academic year 2009/2010, received me as visiting researcher, and has supervised my work during that period.

I also wish to extend my appreciation to others colleagues and friends that likewise played their part, both through direct and indirect discussion and encouragements, and in particular I would like to mention (in alphabetical order) Andrea, Edison, Francesco, Juan, Marco, Massimo, and Sergio.

Finally, but not at the end, I am grateful to my family and to Valentina, to whom this book is dedicated, for their immeasurable love and support and encouragement during this difficult journey.

Again I would like to strongly acknowledge both the Regional Government of Catalunya and the Ministry of Education of the Spanish Government for the financial support, as well as the U.S. Geological Survey for data provision, and Polytechnic University of Catalonia (UPC) for the software and infrastructure availability; and it is my hope that this work could provide inspiration and support to students, researchers, and planners who intend to develop more in-depth investigation on the use of remote sensing and GIS in the field of spatial planning.

CURRICULUM VITAE

Nicola Colaninno is graduated in architecture, since the year 2005, at the school of architecture Ludovico Quaroni of the University "*La Sapienza*" in Rome. In the 2006 he has undertaken a stage at the European Parliament in Brussels, focused on the analysis of some relevant European programs about the urban development and environment.

During the academic year 2006/2007 he has held a master in Urban Management and Valuation at the *Universidad Politécnica de Cataluña* (UPC)-Barcelona TECH, obtaining in 2008 a scholarship for training professors, granted by the Ministry of Education of the Spanish Government, and for developing a PhD within the program of Urban and Architectural Management Valuations at the UPC. In the same framework of the PhD program, and during the academic year 2009/2010 he has got a grant for an internship abroad, developed at the Department of Geography, Planning and International Development Studies of the *Universiteit van Amsterdam* (UvA).

Nicola is currently researcher at the CPSV (Centre for Land Policy and Valuations), and works as specialist in Remote Sensing and GIS at the Virtual City Modelling Laboratory (LMVC) of the UPC. Besides, he collaborates as external referee for the journal "Architecture, City and Environment" (ACE) of the UPC and supports the teaching team of the research Master in Urban Management and Valuation of the UPC, and the Master in Urbanism and Sustainability of the School of Professional & Executive Development at the UPC.

In 2013 is part of the technical staff of the "UNESCO Chair/Intermediate Cities: Urbanization and Development", for the development of a "base plan", for the city of Jacmel in Haiti, based on the methodological model of planning as developed within the program UIA-CIMES and the UNESCO Chair, and coordinated by UN-Habitat.

The main researches are focused on urban and regional planning and analysis, supported by the use of new technologies such as Remote Sensing and GIS. Many achievements of the analysis processes have been included in research projects funded by local, national, and international organizations, and some key results and experiments have been presented at scientific conferences and meetings, or published in journals or acts.

MAIN PUBLICATIONS AND WORKS

Colaninno, N., & Roca, J. (2012). Cataluña: Un desarrollo metropolitano policéntrico. Dispersión y compactación en los procesos de crecimiento urbano, a escala territorial. In F. Gaja i Díaz, *De-construction. La desconfiguración del litoral mediterráneo español* (pp. 19-74). Valencia: Universidad Politécnica de Valencia.

Colaninno, N., Roca, J., Burns, M., & Alhaddad, B. (2012). Defining densities for urban residential texture, through land use classification, from Landsat TM imagery: case study of Spanish Mediterranean coast. In M. Shortis, W. Wagner, & J. Hyyppä (Ed.), *International Archives of the Photogrammetry, Remote Sensing and Spatial Information Sciences. Proceedings of ISPRS Vol. XXXIX-B7.* Melbourne: International Society for Photogrammetry and Remote Sensing (ISPRS).

Colaninno, N., Cerda, J., & Roca, J. (2011). Spatial patterns of land use: morphology and demography in a dynamic evaluation of urban sprawl phenomena along the Spanish Mediterranean coast. *51st European Congress of Regional Science Association International. Special Session: Processes of Urbanisation along the European Coastal Areas.* Barcelona: ERSA.

Colaninno, N., Roca, J., & Pfeffer, K. (2011). An automatic classification of urban texture: form and compactness of morphological homogeneous structures in Barcelona. *51st European Congress of Regional Science Association International. O Session: Barcelona as a case study.* Barcelona: ERSA.

Colaninno, N., Alhaddad, B., & Roca, J. (2009). The effectiveness of morphology and street networks in determining models of urban growth at different spatial scales analysis. In M. Ulrich, & D. Civco (Ed.), *Remote Sensing for Environmental Monitoring, GIS Applications, and Geology IX. Proceedings of SPIE Vol. 7478.* Berlin: SPIE the International Society for Optics and Photonics.

Colaninno, N., & Roca, J. (2008). Modelli di urbanizzazione costiera: morfologia e complessità strutturale, a scala urbana e territoriale, nella Regione Metropolitana di Barcellona. (CPSV/UPC, Ed.) *Architecture, City and Environment/Arquitectura, Ciudad y Entorno (ACE), Año 3*(7).

2014: Creación de información territorial, antecedentes y la situación actual, para las provincias de Santo Domingo y San Pedro de Macorís, en República Dominicana
Técnico - Investigador
Universidad Politécnica de Cataluña (UPC), BarcelonaTECH
Departamento de Construcciones Arquitectónicas I, Centro de Política de Suelo y Valoraciones (CPSV)

2013/2014: Máster en Urbanismo y Sostenibilidad-Sistemas de Información Geográfica Aplicados al Territorio
Profesor Invitado
School of Professional & Executive Development
Universitat Politècnica de Catalunya (UPC)-BarcelonaTech

2013: Projet d'amélioration urbaine de la ville de Jacmel: quartier du Mayard": desarrollo de un "plan base" para la ciudad de Jacmel en Haití
Técnico - investigador
Ayuntamiento de Barcelona; Obra social "la Caixa"; Asociación Catalana de Universidades Públicas (ACUP); Catedra UNESCO CIMES, Universidad de Lleida (UdL); Universidad Politécnica de Cataluña (UPC); Universidad Autónoma de Barcelona (UAB)

2012/2013: Máster en Urbanismo y Sostenibilidad-Sistemas de Información Geográfica Aplicados al Territorio
Profesor Invitado
School of Professional & Executive Development
Universitat Politècnica de Catalunya (UPC)-BarcelonaTech

2012: Delimitación y diagnosis de los barrios marginales de la periferia de Santo Domingo, República Dominicana
Técnico - Investigador
Centro de Cooperación para el Desarrollo (CCD-UPC); Instituto Dominicano de Desarrollo Integral (IDDI); Departamento de Construcciones Arquitectónicas I; Centro de Política de Suelo y Valoraciones (CPSV)-UPC

2009/2012: Desarrollo de una plataforma para el modelado prospectivo de los procesos de urbanización en las zonas costeras
Técnico - investigador
Universidad Politécnica de Cataluña (UPC), Departamento de Construcciones Arquitectónicas I, Centro de Política de Suelo y Valoraciones (CPSV)
Ministerio de Ciencia e Innovación, Dirección General de Investigación y gestión del Plan Nacional I+D+i;

2007/2009: 20 paisajes urbanos por 50 años: estudio sobre la evolución de veinte paisajes urbanos en los últimos cincuenta años con objeto de la exposición "50 años de urbanismo en españa"
Técnico - investigador
Universidad Politécnica de Cataluña (UPC), BarcelonaTECH, Centro de Política de Suelo y Valoraciones (CPSV)
Ministerio de Vivienda

2006/2009: El proceso de urbanización en la Costa Mediterránea: ¿Hacia un modelo insostenible de ocupación del suelo? Un análisis retrospectivo (1956-2006) y prospectivo (2006-2026)
Técnico - investigador
Universidad Politécnica de Cataluña (UPC), BarcelonaTECH, Centro de Política de Suelo y Valoraciones (CPSV)
Ministerio de Educación y Ciencia

CONTENTS

ABSTRACT

From a global point of view, as argued by Levy (1999), *the modern city has undergone radical changes in its physical form*, both in terms of territorial expansion as well as in terms of internal physical transformations. A morphological approach to the spatial analysis of the urban environment has provided evidence that the syntax of the "traditional urban fabric" has changed dramatically. *Cities that were dense, compact and continuous have become diffuse, loose and discontinuous*, and this has produced a radical shift in the urban model. Indeed, cities have passed f*rom a closed fabric, to a peri-urban fabric which is open and fragmented*; from a territorial system, formed from the different urban elements (such as plot, street, constructed space and open space), to an increasing presence of *autonomous and atomized elements which do not relate to each other*. Consequently, *this shift has been accompanied by a significant change in scale, with the appearance of imposing megastructures and relationships between buildings that are now only functional* (Levy, 1999).

Today, *approximately 75% of the European population lives in urban areas*, which makes the urban future of the continent a major cause of concern. *More than a quarter of the European Union's territory has by now been directly affected by urban land use. By 2020, approximately 80 % of Europeans will be living in urban areas, and in seven countries the proportion will be 90 % or more* (Brazil, Cavalcanti, & Longo, 2014). As a result, the demand for urban land, both within and around cities, is becoming increasingly acute. On a daily basis, we are all witnesses to the rapid, visible and conflicting changes in land use, which is shaping the urban and suburban landscape like never before (European Environment Agency, 2006).

In the recent epoch, there has been considerable debate regarding the role of spatial planning in order to improve sustainable trends of land use concerning the European Mediterranean area in general, undertaken either at regional, national, and European level. It is practically impossible not to speak about European cities without taking into account the phenomena of uncontrolled expansion, and dispersion of artificial soil in rural areas, in a discontinuous but abundant way. If we look at how urbanization has spread over the territory during the last twenty or thirty years, and we concentrate on its forms of occupying the soil, we have the clear suspicion that urbanization, above all in the Mediterranean area and even more so towards the immediate coastline, has undergone a process of "uncontrolled" and "uncoordinated" planning, almost without care for environmental problems.

During the last decades, Spain has also been undergoing an important process of urban growth, which has implied the consumption of a large amount of land, although the overall population growth rate, mostly within specific geographic areas, has remained at least unchanged or even, in some cases, decreased. Such a phenomenon has been quite remarkable on the Mediterranean side of Spain, where the current dynamics of urban development have required more and more space without the need for satisfying a real demand for housing. Actually, most of the development has been justified by the increasing economic interests generated by the industry of mass tourism.

Actually, as argued by Gaja (2008), urban development in Spain has been strongly linked to this model of economic development, which relies, since its launch in the 50's, on three main factors, i.e.: emigration, building and mass tourism. On the other hand, it is also plausible (to us) to think that building and tourism in particular have most incisively conditioned political decisions in matters of urban growth during the last decades, and mostly within certain geographical contexts.

Nowadays in Spain, and mostly on the Mediterranean side, several urban areas are facing the important phenomena of urban sprawl, also feared by the European Union. Excessive alternating between urban and non-urban areas make it more and more difficult to identify the natural space currently configured around cities, such as residual areas between built structures. New "urban forms" are drawing new Mediterranean cities, which were previously dominated by the compactness of the urban fabric, and are now the result of the sum of peri-urban areas, dispersed and have a low density.

In particular, the administrative regions along the Mediterranean side, although characterized by their own peculiarities and speeds, in terms of land management and planning, are affected by critical territorial transformations. Indeed, if Catalonia, for instance, is probably moving toward a consolidation of the metropolitan structure, looking for a polycentric system, higher densities, and a sort of re-equilibration of territorial system (Nel·lo, 2001; Marmolejo & Stallbohm, 2008); on the other hand, Valencia is depicted as "a tsunami of

urbanization". There, between 1987 and 2000 the increase in artificial areas (which includes transport infrastructure, mines and landfills) was estimated at 39948.40 hm^2, of which 16557.24 was designated to residential uses, 12376.36 for infrastructure and productive uses (industrial, commercial, etc.), 8487.26 were designated to mining, landfills, and construction, and 2527.51 were used for green nonfarm areas (Gaja, 2012).

In the case of Murcia, Sánchez Morales (2012) speaks about "a regular inopia". Here, the blind trust in obtuse real estate development, especially directed at the tourism sector, is the inexcusable motivation for the current profound crisis, with its devastating effects on the development of the Region; a deep economic identity crisis, which comes to boost a differentiated regional tourist model, and in which the cities are still immersed. It is a model which tried to incorporate "Resorts" in its development (Sánchez Morales, 2012).

The region of Andalucía is defined, by Marcos Rodríguez, et al. (2012), as a case of "destruction at all coast" caused by the "urban overproduction" that, over four decades, has spread to the farthest and best preserved corners of the Andalusian coastline. Indeed, in 2005 the first kilometre of coastline of the Mediterranean side of Spain was already 34% urbanized, the Andalusian coastline had reached values over 59%.

With regard to the Balearic Islands, Cabellos Barreiro (2012) speaks about the dualism between "Destruction and Protection" of the coastal environment. Indeed, despite its relatively small dimensions, the Archipelago has experienced, and exported, one of the most important phenomenon of landscape transformation as a result of mass tourism.

Urban growth has two contradictory aspects. If, on one hand, urban development provides socio-economic improvements; on the other hand, the land use change due to urban growth causes certain deterioration of the environment, such as the loss of natural and agricultural land, an increase in water and energy consumption, among others. Hence, the need to quantify the effects of changes of the land use structure, upon environmental, economic, and social sustainability, is more and more significant, on a global scale (Vitousek, 1994; Cheng, 2003).

Accurate information about the patterns of land use, over time, is a fundamental requirement for a better understanding of urban models. Indeed, during the last few decades, the knowledge of land use and land cover composition and configuration has become increasingly crucial as effective tools for assessing urban growth and environmental development.

However, it is critical here to emphasise that, although the notions of land cover and land use are strictly related and, in many cases, they are used alternately, the term "land cover" commonly identifies the overall natural and semi-natural categories; such as croplands, forest and water bodies, for instance. In particular, the concept of Land Cover *corresponds to a physical description of the space, i.e. the observed (bio) physical cover of the earth's surface* (Di Gregorio & Jansen 1997; Eurostat, 2001). Or in other words, it could be defined as an inventory of the layers which are currently covering the ground. On the other hand, the concept of land use mostly refers to the use to which land is designated, such as the different types of crops or different urban uses (residential, industrial, commercial, etc.).

Currently, even though plenty of approaches to image classification through the use of Remote Sensing (RS) techniques have been proposed, Land Cover/Land Use classification is still an exciting challenge. This is because of the complexity of the landscape, or limitations in remote sensing data (Weng, 2010), but it is also probably due to a lack of standardization and an effective clarity to the questions to which RS products can provide answers. At any rate, the increasing development of RS and GIS technologies, during the last few decades, has provided further capabilities for measuring, analysing, understanding and modelling the "physical expressions" of the urban growth phenomena. This is either in terms of pattern and process (Bhatta, 2012), and is based on land use/land cover mapping and change detection over time. As argued by Bhatta (2012), *determining the rate of urban growth and urban spatial configuration, from remote sensing data, is a prevalent approach in contemporary urban geographic studies*.

In particular, a GIS is a computer-based system designed for enabling the collection, management, analysis, and spatial visualization of a large quantity of geographically referenced data, in a raster or vector format to which specific alphanumeric attributes are associated. Remote Sensing (RS), is generally used for detecting, collecting, storing, and interpreting primary information from several environmental features, including the land cover composition. This is done from a distance, i.e. without coming directly (physically) into contact with an object, but by sensing and measuring the amount of energy emitted by the earth's surface.

The use of new technologies, which arose from the field of computational science during the last few decades and in particular since the 1960's, have been broadly implemented and recognized as powerful tools for

analysis and modelling of the environment. Indeed, the increasing availability of satellite information has increased the ability to acquire a huge amount of data from large geographical areas, globally, and in digital format including different scales of analysis and different time periods. In addition to this, the standardization of sensors and image processing techniques provides important improvements for spatial analysis, land management and planning.

Based on such a technological approach, here we first aim to set up a suitable methodology for detecting generalized land cover classes using an assisted automatic (or semi-automatic) pixel-based approach, calibrated on Landsat Thematic Mapper (TM) multispectral imagery, at 30 meters of spatial resolution. Additionally, through the use of Geographical Information System (GIS), we provide spatial analysis and modelling of different urban models, from a morphological standpoint, in order to define the main patterns of land occupation at a municipal scale along the Mediterranean side of Spain for the year 2011.

Actually, the form of urban settlements should be wholly understood and measured, as it provides basic information for supporting decision-making concerning land management and spatial planning at all levels of government. The availability of reliable and updated spatial information provides the main tool for facing the challenge of handling modern territorial changes. Spatial analysis, as a scientific field related to quantitative geography, represents an effective approach for the synthesis of the modern patterns of urban development.

In this sense, our objectives focus on two main issues. Firstly, RS techniques have been used to set up a proper semi-automatic classification methodology, based on the use of Landsat imagery, capable of handling huge geographical areas quickly and efficiently. This process is basically aimed at detecting the urban areas along the Mediterranean side of Spain, for the year 2011, dependent on the administrative division of Autonomous Communities. Secondly, the spatial patterns of urban settlements have been analysed by using a GIS platform for quantifying a set of spatial metrics from the urban form. Hence, the quantification of different morphological features is obtained including the analysis of the urban profile, the urban texture, and the street network pattern. Then, an automatic classification of different urban morphological models has been proposed, based on a statistical approach (namely factor and cluster analysis).

The urban profile (here intended as two-dimensional geometry in a Cartesian plane) is the result of different features, both internal and external, related to the spatial composition and configuration of its component parts. We aim to measure the morphology of the urban profile as a whole and the spatial relationship between urban patches in terms of distance, i.e. the external features. However, we need to measure those internal features that affect the urban outline, such as the morphology of the street network and the spatial configuration of the built-up pixels, i.e. an analysis at cell level. In particular, the spatial metrics have been selected dependent on four concepts, i.e. the land occupation extent, measured by surface area and density metrics; the urban form, which relies on shape metrics; the structure of the urban profile, defined through the degree of fragmentation; and the urban dispersion, defined by measuring the spatial distribution of the urban patches in terms of distance between them.

Actually, spatial analysis commonly relies on several dimensions; such as *growth rate (of a population or built-up area), density (population density, residential density, employment density), spatial configuration (fragmentation, accessibility, proximity), beside other variables like per-capita consumption of land, land-use efficiency etc.* (Bhatta, 2012). Our approach is "purely" morphological, thus we aim to set up spatial models able to synthesize some of the most critical aspects of urban form.

Through the use of factor analysis, a set of primary spatial metrics of the urban profile and the urban texture has been synthesized into four main morphological indices. Three of them refer to the urban profile, i.e. fragmentation, convolution, and dispersion; and one synthetic index of compactness for urban texture. Additionally, an index of the degree of street network complexity and the urban area of the settlements (in terms of urban land surface) have been taken into account. Based on such a set of measurements, an automatic process for classifying similar patterns of urban structures was designed by using a cluster analysis technique.

Once the different morphological models for all of the municipalities along the Mediterranean side of Spain were classified, a synchronic analysis was undertaken to compare the different patterns of land occupation. Since we can consider the morphological dimension as a key component of the most debated urban phenomenon, i.e. urban sprawl, we believe that the quantitative approach provided here suggests a suitable estimation of an important aspect of urban expansion. In addition, the research also emphasizes that the study of urban phenomena relies, intrinsically, on a multidisciplinary approach, thus in turn contributing to and taking advantage of other

disciplines. Indeed, understanding and modelling urban phenomena currently needs innovative concepts, reliable and diverse data, and feasible methods of analysis and modelling (Cheng, 2003).

Following on from this, more than as a point of arrival, this study can be interpreted as a starting point, i.e. the investigation. Beyond the results, it aims to emphasize the need for a global effort to define the most suitable parameters for providing effective analysis of the urban environment. Moreover, the work also emphasises the value of using a technological approach, namely GIS and RS, in land management and spatial planning.

Universidad Politécnica de Cataluña, Barcelona TECH
Departamento de Tecnología de la Arquitectura
Centro de Políticas de Suelo y Valoraciones
Nicola Colaninno, Josep Roca Cladera

KEYWORDS

- Urbanism
- Urban Geography
- Land Management
- Spatial Analysis
- Modelling
- Urban Morphology
- Land Cover
- Land Use
- Geomatics
- Geographical Information Systems (GIS)
- Remote Sensing (RS)
- Image Processing

LIST OF FIGURES

Chapter 1
INTRODUCTION

Chapter 2
URBAN GROWTH AND LAND CONSUMPTION ALONG THE MEDITERRANEAN SIDE OF SPAIN

Chapter 3
URBAN MODELLING AND TECHNOLOGICAL APPROACH TO THE SPATIAL ANALYSIS: A STATE OF THE ART

LIST OF TABLES

Chapter 2
URBAN GROWTH AND LAND CONSUMPTION ALONG THE MEDITERRANEAN SIDE OF SPAIN

Chapter 3
URBAN MODELLING AND TECHNOLOGICAL APPROACH TO THE SPATIAL ANALYSIS: A STATE OF THE ART

Chapter 4
LAND COVER CLASSIFICATION THROUGH REMOTE SENSING TECHNIQUES

Chapter 1

INTRODUCTION

It is an acknowledged fact that the "form" of a city has profoundly changed during the last century. We refer to a world scenario in which the rapid development experienced by Western countries during the early 20th century, is currently being followed by an equally rapid development of fast-growing countries, such as China, Brazil or India, for example. The second half of the 20th century has been undoubtedly the era that has experienced the highest development of urbanization on a global scale. Actually, there is a large consensus about the growing rate of the urban population, which has grown from about 750 million people in 1950 to around 2˙500 in 2000 and, by 2030 this is expected to swell to almost 5 billion, when three out of five people will live in cities (UNFPA, 2007). According to a 2014 United Nations report, the urban population currently represents more than 50% of the world's population, and by 2050, it is predicted to reach 66% (United Nations, 2014). Figure 1.1 shows a suggested representation of this impressive development[1].

Fig. 1.1: Earth at Night[2] (Source: Elvidge & Simmon, 2012. Image Credit: NASA, NOAA NGDC, Suomi-NPP, Earth Observatory)

A lot of "classical" urban paradigms are going to change, or in most of the cases they have already changed. The interaction between the city and the surrounding landscape is going to become more and more difficult to define, due to the complexity and diversity that new models of urban growth are generating over the territory. At present, although the growth process of cities is normally linked to the increasing rate of population

[1] *Today, the most urbanized regions include North America (82 per cent living in urban areas in 2014), Latin America and the Caribbean (80 per cent), and Europe (73 per cent). In contrast, Africa and Asia remain mostly rural, with 40 and 48 per cent of their respective populations living in urban areas. All regions are expected to urbanize further over the coming decades. Africa and Asia are urbanizing faster than the other regions and are projected to become 56 and 64 percent urban, respectively, by 2050* (United Nations, 2014).

[2] *This remarkably complete view of Earth at night is a composite of cloud-free, nighttime images. The images were collected during April and October 2012 by the Suomi-NPP satellite from polar orbit about 824 kilometers (512 miles) above the surface using its Visible Infrared Imaging Radiometer Suite (VIIRS). VIIRS offers greatly improved resolution and sensitivity compared to previous global nightlight detecting instrumentation on DMSP satellites. It also has advantages compared to cameras on the International Space Station. While the space station passes over the same point on Earth every two or three days, Suomi-NPP passes over the same point twice a day at about 1:30 am and 1:30 pm local time. Easy to recognize here, city lights identify major population centers, tracking the effects of human activity and influence across the globe. That makes nighttime images of our fair planet among the most interesting and important views from space* (Elvidge & Simmon, 2012).

within certain geographical contexts, further socio-economic factors are driving an impressive urban expansion even when little or no population pressure is present. Such factors are mostly linked to forces which include both micro- and macro- socio-economic trends. Indeed, mainly in the case of highly urbanized areas, we observe a "centrifugal" movement of human pressure from the city centre towards the peripheral areas, due to the desire of seeking new lifestyles, or maybe adapting existing urban paradigms to a suburban environment, far from the inner city and following the adjacent crowns of the consolidated city. This generates the phenomena of urban pressure and dispersion, which often affects the productive agricultural space.

The complexity produced by the modern socio-economic dynamics always results in an equivalent complexity of the urban shapes, so that a good understanding of the urban outline can allow a more extensive knowledge concerning the growth dynamics. Similarly, if we focus on the European scenario, it is quite obvious that, also here, the modern dynamics of urban development have remarkably modified the landscape over the last century, and most of all over the last few decades. We, daresay, over the last thirty or forty years, depending on the geographical areas.

Today, *approximately 75% of the European population lives in urban areas*, which makes the urban future of the continent a major cause for concern. *More than a quarter of the European Union's territory has by now been directly affected by urban land use; by 2020, approximately 80 % of Europeans will be living in urban areas, and in seven countries the proportion will be 90 % or more* (Brazil, Cavalcanti, & Longo, 2014). As a result, the demand for urban land is becoming increasingly acute, both within and around cities. On a daily basis, we are all being witnesses to the rapid, visible and conflicting changes in land use, which is shaping the urban and suburban landscape like never before (European Environment Agency, 2006).

In particular, in the most recent of times (roughly the last two decades), there has been considerable debate about urban development in the European Mediterranean area. A debate in which even European Authorities have become involved, and that debate mostly regards the role of spatial planning in promoting sustainable trends for land use. Great transformations along the Spanish Mediterranean coast, for instance, have generated considerable changes in the traditional structure of the urban landscape, and the rapidity of these modern dynamics has had a significant impact upon the spatial patterns of the interaction. This is in morphological terms, as well as in terms of functional patterns, both between the city and the territory and between cities. Indeed, far from the typical Mediterranean model of a city, it is currently impossible to speak about European cities without taking into account the phenomena of uncontrolled expansion, and dispersion of the artificial soil within the surrounding environment, according to a spatially discontinuous, but abundant, process.

Actually, as argued by Gaja (2008), the urban development in Spain has been strongly linked to the model of economic development, which relies, since its launch in the 1950's, on three main factors, i.e.: emigration, building, and mass tourism. On the other hand, it is also plausible (to us) to think that building and tourism in particular, have most incisively conditioned political decisions in matters of urban growth during the last few decades, and mainly in certain geographical contexts.

1.1. OUTLINE OF THE MAIN ISSUES

The urban environment is a very complex and dynamic context, since it is affected by a large number of factors which evolve continuously. However, most of the processes that develop in the framework of urban areas are connected to the physical space. Therefore, precise measurement, analysis and understanding of urban growth dynamics need accurate spatial and temporal information about these physical spaces.

The modern increase in large peri-urban areas sprawled out over the territory (as mentioned during the previous section), often caused by uncontrolled, uncoordinated and unplanned growth, has inevitably brought with it a blurring of clearly identifiable boundaries between the city and rural areas, and/or between adjacent cities.

Actually, since urbanization is a process of concentration of the population within urban areas, when one aims to understand the urban growth phenomena, two main models (forms) of urbanization should be taken into account, which are basically concerned with the direction and movement of the population. On one hand, a centripetal flow of persons, i.e. a movement from the outside to the inner city, gave rise to the model of nineteenth century urbanization, based on the attraction of rural people to the manufacturing centres of industrialized cities.

Universidad Politécnica de Cataluña, Barcelona TECH
Departamento de Tecnología de la Arquitectura
Centro de Políticas de Suelo y Valoraciones
Nicola Colaninno, Josep Roca Cladera

In this way, urban centres were growing and progressively centralizing large volumes of population, decision-making power and resources. On the other hand, the centrifugal movements caused cities to change the relationship with the surrounding space, hence changing the scale of influence and gradually "absorbing" territories, and incorporating adjacent urban settlements into a metropolitan space, which now provides a unique territorial and economic entity spread over a wider space (Cerda, 2012).

Spatial analysis and modelling, as a scientific field related to quantitative geography and the emerging field of regional science, represents an effective approach to the synthesis of the modern urban and regional dynamics, consistent with the "capture" and simulation of the main forms and functions. In particular, although most urban modelling techniques deal with the city in terms of location of its economic and demographic activities, there is an increasing tendency to link approaches to the study of urban morphology (Batty, 2008), in terms of spatial configuration and composition. Indeed, the form of urban settlements should be wholly understood and measured, since it provides basic information for spatial planning that, in turn, provides the main tool for facing the current challenge of modern territorial changes.

The urban space, understood to be an area with certain well-defined dimensioned forms and relationships, is a commonly shared idea used to define the city. Moreover, the interaction between the urban space and the surrounding environment often generates globally recognizable dynamics, which can be quantified based on widely recognized parameters. Actually, although certain rules of urban growth are strongly dependent on the geographical contexts, it is relevant to evaluate those areas affected by high levels of land consumption, both at the city level as well as at a territorial scale. This consumption is due to urbanization processes, and the composition and configuration of the urban texture, which then means defining whether an urban sprawl phenomenon is leading the territorial policies of development, for instance. Indeed, even if the rate of land consumption represents a basic indicator in most of the studies, it is important to highlight the need to further quantify the forms of urban growth in terms of urban fabric, street patterns, fragmentation of the urban profile, and so on. In other words, we require an integrated approach for better quantification of urban models in terms of compactness versus sprawl.

The discipline of urban morphology provides a relevant tool for supporting the analysis of the urban forms, including the understanding and measurement of the main types of territorial patterns, as well as the model of land occupation in terms of urban texture at different scales of analysis, either at local, urban, as well as at territorial level. Computational science and new technologies allow the standardization of certain parameters and make it possible to manage large geographical areas and data while using a globally shared language.

Actually, if we consider that a huge amount of data concerning the Earth's surface is currently freely available on a large scale, thanks to satellite platforms for instance, we may well understand the need for establishing generalized methodologies for analysing such data, from several standpoints, quickly and in an objective way.

1.2. MOTIVATIONS OF THE INVESTIGATION

An important impetus which has motivated this investigation is the global interest shown by many international authorities in the analysis of the spatial interaction between human settlements and the natural environment, the consequences of such interaction and the sustainability of urban growth on the natural environment. Indeed, due to the possibility of generating a heavy negative impact upon the natural environment, urban planners are currently requested to reconsider the development policies in order to face future urban expansion. For example in the USA, towards the end of the twentieth century, issues concerning urban sprawl generated important national debate on the land use policies, that included smart growth managing and the ability to measure growth rates (Brueckner, 2000; Cheng, 2003).

Models of urban development have also been studied from the social and economic point of view in emerging countries such as India (Thangavel, 2000) and China (Yeh & Li, 2001b), and these are dependent on topics such as compactness and dispersion (Cheng, 2003).

In Europe, the main political institutions have clearly shown similar interests since 1985, when the Council, on a proposal from the European Commission, adopted a policy to develop the CORINE program (coordination of information on the environment). This was an experimental project for gathering, coordinating and ensuring the

consistency of information about the state of the environment and natural resources in Europe, and for assessing the impact of spatial planning and policy upon regional development. Hence, an information system about the European environment was created (the CORINE Land Cover system), together with nomenclatures and methodologies developed and agreed at EU level. In addition, a European Environment Agency (EEA) was set up, and the European environment information and observation network (EIONET) was established. *CORINE land cover is now recognized by decision-makers as a key reference data set for spatial and territorial analysis at different territorial levels. Within the European Commission, services such as Regional Policy DG, Environment DG and Agriculture DG as well as in the EEA and its European Topic Centres (ETCs), there is a growing need to use spatial analysis for integrated environmental assessment* (Büttner, Feranec, & Jaffrain, 2002).

At the same time, many initiatives have been undertaken during the last few decades by Spanish national institutions, aimed at the analysis and management of the environment. This is easily justified due to the impressive development that Spain has experienced since the early 1980's, and thus with it, the necessity to quantify the consequences of this kind of growth.

The research work underpinning this essay, situated within the field of spatial analysis, and with special emphasis on urban morphology, was first introduced into the national project financed by the Spanish Ministry of Education and Science (MEC) in 2006[3]. The project was aimed at analysing the processes of urbanization that occurred along the Mediterranean side of Spain, from Gerona to Cadiz, in the period from 1956 (the year in which the first Planning Act came into force), also including the period 1980/81 (when the first democratic councils were formed) and until 2006, (a date which probably marks a peak in the urbanizing processes in Spain before the crisis). The project was also aimed at investigating the most plausible prospective results of urbanization over the next 20 years (2006-2026).

In particular, the investigation sought to carry out a balanced assessment, drawing upon new technologies (GIS, Remote Sensing, Virtual Reality, Cellular Automata and Neural Networks), of the first 50 years of the Planning Act along the Mediterranean Arc[4] from a varied number of perspectives, be they morphological, environmental or socio-economic. More specifically, the project involved quantifying the progressive occupation of the territory, which occurred with an ever increasingly dispersed urban form, representing a growing consumption of natural resources and placing the subsistence of natural ecosystems at risk. Furthermore, the research sought to project the continuation of sprawl over the following 20 years, in order to identify different scenarios resulting from current urban development.

In a second phase, the investigation was included within another project, financed by the Spanish Ministry of Science and Innovation (MICINN) in 2009[5], while still in the grip of uncontrolled dispersed urbanization along the Spanish coastline, and the concomitant negative environmental consequences. It had the overall objective of developing a platform to enable the evaluation for the processes of urbanization already carried out, as well as anticipating the expansion of the same processes in the foreseeable future (2010-2025). Based on the assumption that this would help counter the process of urban sprawl, the study had been generalized for the geographical region of the whole Iberian Coast, thus including Portugal. Here, the analysis of the main characteristics of different models of land occupation was remarked to be an essential instrument to assist administrators and urban planners for spatial planning, as well as the decision-making process. Similarly to the previous project, this work also drew upon new technologies, such as GIS and Remote Sensing, and methods for modelling and defining future scenarios such as Cellular Automata and Neural Networks.

Finally, a contribution of this investigation was also included in a research project carried out by the Spanish Ministry of Housing, during the period 2007-2008, entitled "20x50, twenty urban landscapes over fifty years", which aimed to investigate how some urban areas of Spain had developed during the second half of the

[3] THE PROCESS OF URBANISATION ON THE MEDITERRANEAN COAST. TOWARDS AN UNSUSTAINABLE MODEL OF LAND OCCUPATION? A RETROSPECTIVE (1956-2006) AND PROSPECTIVE (2006-2026) ANALYSIS [2006-2009]. Spanish Ministry of Education and Science (MEC), (SEJ2006-09630), 2006.

[4] The delimitation and quantification of the urban expansion (1956-2006), was focused on different sections of the Spanish Mediterranean coastline and, in particular, along the coastline of Barcelona, Valencia, Alicante, Murcia, Málaga, Cadiz and part of Mallorca.

[5] THE DEVELOPMENT OF A PLATFORM FOR THE PROSPECTIVE MODELLING OF PROCESSES OF URBANISATION ON COASTAL AREAS (MODELCOSTA) [2010-2013]. Spanish Ministry of Science and Innovation (MICINN), (CSO2009-09057), 2009

20th century. Twenty urban landscapes were selected[6] and the observation period was set for the 50 years from 1956 to 2006 for several reasons: First, the year 1956 marked the approval of the first piece of planning legislation in Spain, which established the model of urban planning and land management in which Spain is still firmly rooted. Interestingly, the year 2006 also marked the 50th anniversary of the aerial photography flight carried out by the United States Air Force over the Iberian Peninsula and Balearic Islands (known as "American flight"), and which over time had been ceded to the Spanish Ministry of Defense from its United States counterpart. Moreover, in 2006, the work on the drafting of new planning legislation was also undertaken, which resulted in the approval of a new Act in 2007. This incorporated new criteria to ensure that urban growth corresponded to the requirements of sustainable development, by minimizing its negative impact upon the territory and supporting the regeneration of the existing built-up city[7].

1.3. STATEMENTS AND KEY QUESTIONS

Urban growth means population growth, economic growth and physical development; hence the increase in urban areas is the response to the demand for land for housing location and all related activities. Such a process, as previously highlighted, is commonly termed urbanization, and a range of approaches and concepts have been developed to understand and define it. Imagine concepts like suburbs, edge cities, counter-urbanization, urban sprawl, etc. (Cerda, 2012). Actually, *population growth has often been pointed out as a primary cause of urban sprawl in Europe, in recent decades*[8] (ESPON FOCI 2009, Glaeser et al. 2001, Glaeser 2005; Christiansen & Loftsgarden, 2011).

Historically, a city was formed from just a compact set of buildings in which little open spaces were mainly intended for human movements and markets at a small scale. The advent of the railway and tramway were the first examples which, in the second half of the nineteenth and early twentieth century, "broke" the traditional forms of a city. The first nuclei of urbanization began to rise around stations and stops. From the 1950's, the use of the automobile has induced people to locate several urban activities around the peripheral areas, thus facilitating the spread of urbanization over a larger portion of territory and thus increasing the distances between the urban centres. This kind of process was also facilitated by the construction of motorway networks around major conurbations, belts and radial axes (Pozuea, 2000; Cerda, 2012). However, discontinuous and dispersed growth is often the result of an unplanned process that does not take into account the provision for infrastructure, or issues such as the "best" location for urban functions. In fact, it is basically a spontaneous model of growth, frequently referred to as urban sprawl, which mostly depends on existing infrastructure, and where real estate management and individual interests play a decisive role.

During the last century, the continued "struggle" and the alternation between phenomena of urbanization and suburbanization, centralization and decentralization, linked to population flows, has generated different forms of the urban landscape, finally establishing the current urban settlements as we know them today.

Currently, the phenomenon of decentralization of the population and expansion of the urban space towards suburban areas generates new dynamics among the different urban uses that often result in different urban forms. According to Cerda and Marmolejo (2007), this phenomenon can be schematically delineated based on four different phases of development.

---

[6] Of the twenty areas initially selected, two urban landscapes located in the Canary Islands had to be omitted due to a lack of information derived from the covering provided by the original flights. Hence, only eighteen urban landscapes were finally analysed.

[7] In April 2008, the former Ministry of Housing inaugurated an exhibition in Madrid, carried out in collaboration with the Centre of Land Policy and Valuations (CPSV) of the Technical University of Catalonia (UPC), under the title of "5X50, five urban landscapes over fifty years". The exhibition was focused on five urban areas: Spain's two largest metropolitan areas, Madrid and Barcelona, as clear examples today of how the urban phenomenon spreads beyond the limits of the municipal map; two urban environments of the Mediterranean coast, around Murcia and Alicante, reflecting how tourism development has influenced Spain in certain locations; and, finally, Cordoba, a medium sized provincial capital city, oblivious to the previously mentioned phenomenon, but not exempt from the process of urban expansion. The following link indicates the changes experienced by the 18 urban landscapes in the final study:
http://www.fomento.gob.es/MFOM/LANG_CASTELLANO/_ESPECIALES/SIU/OTROS_PROYECTOS/PAISAJES_20x50/

[8] *Increasing populations in cities provided pressure on the housing market and more expensive homes. In addition, an increasing population could lead to urban problems, such as traffic, congestion, air pollution, noise and crime. These factors will cause the population to either be forced (due to high housing costs), or choose to move out of cities* (Christiansen & Loftsgarden, 2011).

The first phase is characterized by the "coexistence" of residential uses, industrial districts and services around the Central Business District (CBD). This stage is defined as the initial phase of modern urban development, because now the market (which is the place of exchange of goods and services) is explicitly embodied in the city centre.

The second phase is the one known as “metropolization”, which shows several kinds of phenomena occurring in the urban space. Indeed, if on one hand we are witnessing a significant attraction of the rural population moving towards the city but primarily locating in the peripheral areas due to lower land values; on the other hand, there is a relative residential mobility of the population from the central to the adjoining peripheral areas, either due to the effect of externalizing central areas, or the increasing availability of land rentals in peripheral areas. The distribution of work, commerce and services still does not react significantly to the residential displacements at this stage. This daily mobility (journeys) towards central areas is the reason why we see increasing levels of congestion and externalization.

The third phase, i.e. the suburbanization, is characterized by the “reaction” of commercial uses and services to the dynamics of the decentralization of residential uses, in the sense that commerce, as well as services now move towards the periphery (decentralization) in order to get closer to homes and their needs (territorial profitability). In this phase, the spatial distribution of jobs still does not undergo a significant reaction to the new urban forms, thus increasing the transportation congestion towards the city centre.

In the final phase, the labour market is also migrating to the periphery, thus improving its accessibility. The decentralization of major urban functions creates the conditions that, based on an almost fractal (or alveolar) geometry, replicate the urban functionality. This gives value to discontinuous urban settlements far from the consolidated urban area, and generates the important phenomena of landscape fragmentation (Cerda & Marmolejo, 2007).

The excessive alternation of urban and non-urban areas, often following a discontinuous pattern of growth, makes it more and more difficult to identify and quantify the actual urban space. The natural areas currently appear to be configured as residual space among built-up structures, and “new” urban forms are shaping a “new” European model of city. If this was once dominated by the compactness of the urban fabric, it is now resulting from the sum of several fragmented peri-urban areas dispersed within the territory, and has a low density.

Actually, in Spain, during the last twenty or thirty years mainly, we have witnessed a significant urban explosion and change of “classical” paradigms, in terms of urban forms, which were already being experienced in other countries during the first half of the twentieth century. Indeed, the general concept of “Mediterranean city”, as a synonym of compactness, relatively high density and diversity, no longer finds a clear correspondence in the current urban models. Especially within large cities, only the central nucleus (or nuclei) preserves the aforementioned attributes. Here, the diffusion of low density urban fabric outside the compact urban zone has caused, in many cases, a loss of meaning of the classical division of the territory into urban and rural areas. Indeed, large portions of rural areas have been “invaded” by low density built-up areas[9], primarily aimed at residential uses, with the consequence that the Mediterranean urban model, in certain geographical areas, is gradually losing its character of compactness[10].

Along the Mediterranean side of Spain in particular, we have witnessed a radical transformation of the urban model at a territorial level, and a progressive (often unplanned) increase in the amount of seasonal housing and second homes, including many urbanizations linked to the massive tourism phenomenon (in recent decades), such as airports, resorts, hotels and golf courses. Here, the production system generally associated with agriculture is currently mixed with the “urban production system”, and this is occupying larger and larger sections of the available terrain in coastal areas (Vespere 2008). These dynamics are generating a sort of “identity crisis” in terms of urban development, in several Mediterranean countries in Europe. The “traditional” urban forms are giving rise to something different; allowing us to speculate as to what is currently the Mediterranean model of a city, and its

[9] *High utilization of housing (high density) can reduce development pressure, while an opposite development can promote urban sprawl. This aspect has also emerged as political objectives and requirements for utilization of housing. The rationality behind this aspect is simple. High utilization can accommodate more people within a given area. Lower utilization consequently leads to a larger use of areas in order to house the same population. In this way, the development policy can be a driving force behind urban sprawl* (Christiansen & Loftsgarden, 2011).

[10] According to Stefano Benni et al. (2007), excessive soil consumption for residential use, if it is not based on a very efficient design, ends up degrading the whole territorial context of peri-urban zones, causing the most common effects of urban dispersion, fragmentation of agricultural structures, inconsistency of physical space and economic activities.

Universidad Politécnica de Cataluña, Barcelona TECH
Departamento de Tecnología de la Arquitectura
Centro de Políticas de Suelo y Valoraciones
Nicola Colaninno, Josep Roca Cladera

future. Actually, a significant contradiction, in terms of urban forms, is currently occurring in certain areas along the Mediterranean side of Spain. In fact, if on one hand we find the traditional model of a city (figure 1.2), we now find new urban developments just a few kilometers away, that keep nothing of the original essence of the old town (figure 1.3).

Fig. 1.2: Altea, on the Costa Blanca, in the Autonomous Community of Valencia, Spain (Source: Capper, 2011)

Fig. 1.3: A view of the beach of Benidorm on the Costa Blanca, in the Autonomous Community of Valencia, Spain (Source: Tarrach, 2015)

The recent models of urban development, mostly affected by economic dynamics, have generated significant urban dispersion phenomena, linked to a generalized hyper-production in the real estate sector, and which are now difficult to measure. The possible "dissolution" of the traditional model of a compact city is a recurring theme in the analysis and reflection concerning the field of urbanism, which is now addressing the difficult challenge of quantifying the features of the present phenomena of development. Hence, in this light, a series of general questions arise, including:

- What is the actual urban space, for instance, or what is currently the most effective model for a Mediterranean city?
- To what extent do geographical features affect the modelling of urban forms and how can we measure the most common models of urban growth?
- How do we generate precise and updated information about urban expansion and how can urban sprawl be classified?

Although there is a big debate going on within the scientific community about the most sustainable model of a city (Williams, 2000); generally, planners and researchers widely agree that a compact model should be pursued, because it is relatively more sustainable from the point of view of urban development (Newton 2000; Kasanko et al. 2007). As urban development strongly affects the territory at a local, regional, as well as national level, there is an increasing need to measure urban phenomena at different scales.

Indeed, in Europe, according to the European Environment Agency, it has been highlighted that u*rban growth raises questions at different levels of governance*, and in particular:

- *Where does urban growth occur? Which urban areas have expanded most rapidly in recent times? Was the development compact or sprawled? What trends are expected in coming years?*
- *What are the drivers behind urban sprawl? Which can be controlled and at what level?*
- *How sustainable is urbanization? What are the consequences beyond city boundaries?*
- *To what extent do European, national and local policies trigger urban sprawl?*

Therefore, *answering these questions* (first) *requires an appropriate delineation of urban areas* (European Environment Agency, 2011), but most of all, it is necessary to classify and quantify the different forms of urban models based on standard and generalized methodologies.

1.3.1. Land Use and Land Cover Change: An Introduction

Urban growth has two contradictory aspects. If, on one hand, urban development also provides socio-economic improvements; on the other hand, the land use change, due to the urban growth, causes certain deterioration of the environment, such as the loss of natural and agricultural land and the increased consumption of water and energy, among others. Hence, the need to quantify the effects of changes of the land use structure, upon environmental, economic and social sustainability, is more and more significant at a global scale (Vitousek, 1994; Cheng, 2003).

Accurate information about the patterns of land use, over time, is a fundamental requirement for a better understanding of urban models. Indeed, the knowledge of the land use and land cover composition and configuration, has become increasingly vital, during the last decades, as an effective tool for assessing urban growth and environmental development. Actually, in the framework of sustainable development, at an international level, land use/cover change (LUCC) has attracted a great deal of attention[11]. In particular, an efficient understanding of land use/cover change is based on different geographical levels, as it affects global to local issues, and a range of disciplines.

With regard to the urban environment, the growth process is the result of the human interaction with the natural environment, and then the transformation, both physically and functionally, of non-urban land uses into urban uses. Hence, the ability to quantify and model such land use/cover transformations (changes) allows understanding and explanation of those mechanisms behind urban growth, thus providing effective tools for supporting decision making in land management and urban planning (Cheng, 2003). However, it is crucial to highlight that, although the notions of land cover and land use are strictly related and, in many cases, they are used alternatively, the term “land cover” commonly identifies overall natural, and semi-natural, categories such as croplands, forest and water bodies, for instance. The concept of Land Cover *corresponds to a physical description of*

[11] For instance, the International Geosphere-Biosphere Programme (IGBP), the International Human Dimensions Programme on Global Environmental Change (IHDP), NASA's Land Cover and Land Use Change Program (Cheng, 2003), or the CORINE Land Cover Project in Europe could be mentioned.

the space, i.e. the observed (bio) physical cover of the earth's surface (Di Gregorio & Jansen 1997; Eurostat, 2001). Or, in other words, it could be defined as an inventory of the layers which are currently covering the ground[12].

On the other hand, the concept of land use mostly refers to the use to which land is designated, such as the different types of crops, or different urban uses (residential, industrial, commercial, etc.). In particular, *for land use, various approaches are proposed into the literature. Two main "schools" may be distinguished. Land use in terms of "functional dimension" corresponds to the description of areas in terms of their socio-economic purpose: areas used for residential, industrial or commercial purposes, for farming or forestry, for recreational or conservation purposes, etc. Links with land cover are possible; it may be possible to infer land use from land cover and conversely. But situations are often complicated and the link is not so evident. Another approach, termed "sequential", has been particularly developed for agricultural purposes. The definition is a series of operations on land, carried out by humans, with the intention of obtaining products and/or benefits through using land resources. For example, a sequence of operations such as ploughing, seeding, weeding, fertilizing and harvesting*[13] (Mücher et al. 1993; Eurostat, 2001).

Currently, while land use and land cover are two quite different matters, and the difference between those concepts is necessary, it is often ignored, such that a generalization of the concept frequently generates practical problems. This occurs particularly when data from the classifications at different scales of analysis need to be compared or combined.

1.3.2. Urban Growth Modelling: Quantifying Urban Complexity

The purpose of urban modelling is to abstract, simplify and characterize the urban environment, in order to understand its complexity. According to Cheng (2003), *in the domain of urban planning, modelling can be utilized for analysing, evaluating, forecasting and simulating urban systems to support decision-making.* Besides, *from the perspective of spatial science, modelling must take both the spatial and temporal dimensions of urban systems into account*. Finally, *modelling can be conceptual, symbolic or mathematical, depending on the purposes of the specific application.*

According to Cerda (2012), the mathematical modelling of cities is a newly developed branch of science, which arises from the computational advances occurring in recent years. While theoretical mathematical models have existed for several decades, their implementation and resolution have only been possible in a practical way in recent decades. Actually, the development of city modelling is based on urban economy modelling and we can identify three major groups of urban modelling: the spatial interaction models, the discrete choice models (transport and land use) and the simulation models[14]:

- The spatial interaction models emerge in the same analogy with Newton's law, which postulated that the interaction between two populations is directly proportional to their size and inversely proportional to the square of the distance between them. In the field of social sciences, in 1941, Stewart coined the concept of demographic gravitation. From the morphological point of view, the combination of two main aspects, such as the structure and the spatial distribution of the settlements, provides important tools for classifying the different forms of land occupation (Cerda & Marmolejo, 2007).

[12] *This description enables various biophysical categories to be distinguished - basically, areas of vegetation (trees, bushes, fields, lawns), bare soil (even if this is a lack of cover), hard surfaces (rocks, buildings) and wet areas and bodies of water (sheets of water and watercourses, wetlands). This definition has an impact on the development of classification systems, data collection and information systems in general. It is said that Land Cover is "observed". This means that observation can be made from various "sources of observation" at varying distances between the source and the earth's surface: the human eye, aerial photographs and satellite sensors* (Eurostat, 2001).

[13] *Contrary to land cover, land use is difficult to "observe". For example, it is often difficult to decide if grasslands are used or not for agricultural purposes. The information coming from the source of observation may not be sufficient and may require additional information. In the case of agricultural use, farmers may provide information, for example, if cattle are present or not, and if they are grazing. It is also possible to use characteristics on the spot indicating the presence or absence of cattle. For the FUNCTIONAL approach, inference from land cover may be helpful. For the SEQUENTIAL approach, a more exhaustive recording of various attributes will be needed, for example, a multi-temporal approach. In the latter, land use will be understood as FUNCTIONAL.* (Eurostat, 2001).

[14] Although further techniques are used in urban modelling, such as optimization or econometrics (traditional and spatial), their application is not massive, nor does it have representative and identifiable icons (Cerda, 2012).

- The discrete choice models (transport and land use), in turn, are either based on models designed under the assumption that activities are located in order to minimize transportation costs (this approach can be classified as "maximum accessibility"), and where the transportation system has a predominant role[15]; in models where more market elements are introduced, such as land prices (rentals) and property prices (this approach is classified as a "linear market model"); as well as models that use zonal attributes to evaluate location options (Cerda & Marmolejo, 2007).
- Urban simulation models (cellular automata and agent-based models) are part of the logic of simulation, in which models of urban growth are no longer deterministic, but stochastic (Cerda & Marmolejo, 2007).

The use of mathematical models allow a better understanding of a complex space like the urban environment, based on recognized scientific analysis and management of information and data in planning practices. Indeed, *this is the major objective of modelling spatial and temporal urban growth*. On the other hand, *urban growth modelling should be considered as an interdisciplinary field as it involves numerous scientific and technical areas, e.g. geographical information science (GIS), remote sensing (RS), urban geography, complexity theory, land use/cover modelling etc. Understanding urban growth and applying this knowledge to planning are both closely linked with these areas. Hence, a systematic and "holistic" perspective should be adopted in the process of modelling* (Cheng, 2003).

1.4. OBJECTIVES OF THE RESEARCH

The management of several issues concerning urban growth is currently dependent upon the ability to measure the increasingly rapid transformations that occur nowadays at a global scale. The complexity of managing environmental and natural resources, social issues and also functional questions, need to be answered properly. Updated spatial information, depending on its accuracy, can allow better management and planning practices for supporting decision-making at all levels of government, in order to achieve a sustainable use of the space. On the other hand, spatial planning surely provides effective tools and methods capable of handling such information with the aim of designing a balanced coexistence between urban growth and the natural environment.

In this context, our work mainly aims to provide a generalized approach, based on the use of new technologies, capable of automatically detecting information from the urban land cover (within a well-defined geographical context, this being the Mediterranean side of Spain), and then measuring different forms of land occupation. Subsequently, the ability to obtain suitable information and quantify specific urban features is a fundamental prerequisite for setting up improved practices for land management and planning.

1.4.1. General Objectives

Our work relies on three main points: Firstly, we aim to provide an overall description of the modern process of urban growth, often defined as uncontrolled, which has occurred along the Spanish Mediterranean coastline during the last twenty or thirty years. The comparison with urban growth that occurred in other geographical areas of Spain highlights the real and critical phenomenon of urban expansion, and seems to have moved in the opposite direction with respect to the sustainable development promoted by European institutions since the nineties. Here, our work relies on a comparative analysis, over time, of widely recognized data provided by different administrative entities at European and National level.

The second objective is essentially focused on the use of two technologies, i.e. Remote Sensing (RS) and the Geographical Information Systems (GIS), as essential tools for achieving a semi-automatic, generalized and normalized inventory of land cover composition. Here, special emphasis is placed on extracting information about urban land cover and providing previous theoretical descriptions about some main topics, including RS as well as GIS. Our work offers a proper methodological process, based on widely recognized approaches and techniques, capable of quickly obtaining information about urban areas from wider geographical areas.

[15] Various models arise from the basic models proposed by Alonso (1964) or Wilson (1964)

Finally, based on the use of GIS, spatial metrics and a statistical approach, we aim to set up a proper quantification and analysis of certain key features associated with urban form. The automatic classification of a number of similar models of land occupation, from a morphological standpoint, will be proposed for all municipalities within the autonomous communities along the Mediterranean side of Spain, for the year 2011.

1.4.2. Specific Objectives and Structure of the Work

The structure of this study has six main chapters and the specific objectives of the research will be developed through the defining of several tasks, of which firstly, in Chapter 1, we aim to justify the reasons that led to this research, the framing of the scientific field, and the scheduling of some key questions.

Following on in Chapter 2, we attempt to offer a quite extensive overview of the scenario of the urban growth that has occurred since the second half of the past century in Europe, and in particular in Spain, placing special emphasis upon the current state of urban development along the Mediterranean side of Spain. Here, indeed, an exceptional acceleration of urban expansion has been seen during the last few decades.

An initial excursus of the European situation relies on analysing several studies undertaken by the best recognized European institutions. Then, apart from an overall analysis of the European scenario, some specific cases are highlighted and an extensive examination is provided for Spain. In this, many national institutions have provided a quite extensive and interesting collection of reports and analysis during recent years. In particular, the analysis about the exceptional urban growth phenomenon that happened along the Mediterranean side of Spain during the last few decades was based on the data provided by the European Environment Agency through the project “CORINE Land Cover” and covered three temporal stages, i.e. 1990, 2000 and 2006. Additionally, several works of investigation conducted by eminent exponents of the Spanish academic scenario have been analysed. Here, the analysis follows the administrative division of the five Autonomous Communities bordering the Mediterranean.

In Chapter 3, in order to frame the scientific field and lend support to the technical significance of the investigation, we provide a description of some of the key themes and projects in spatial analysis and planning. The study is basically made up of two parts, where the first focuses on the analysis of the most important urban models and the dynamics behind their development which have been theorized since the last century by the scientific community in the field of urban studies. The analysis ranges from the most typical approaches, such as those of Lewis Mumford or Camillo Sitte, up to the most recent ones from Francesco Indovina, Giuseppe Dematteis and Walter Christaller. The second part of the chapter mainly focuses on the examination of objectives, methodologies, and results of some of the most relevant projects. These were done at different geographical and administrative levels, based on the use of new technologies applied to spatial analysis and planning, ranging from the international scenario (Europe and America) down to the national (Spain) and regional levels (Catalonia).

Chapters 4 and 5 stress the significance of a technological approach to spatial analysis. In particular, Chapter 4 discusses the use of Remote Sensing (RS), either for collecting digital data (imagery) from the environment as well as for image processing aimed at extracting suitable information from the land cover composition. After a brief overview of some of the main topics in the field of Remote Sensing and placing particular emphasis on those techniques employed, the study, at this point, aims to provide a proper standardized methodology for automatic (or semi-automatic) classification of land cover classes, based on satellite imagery delivered by the Landsat missions. In particular, the focus is on the detection of impervious areas, by applying a quick and reliable methodology able to manage relatively large geographical areas. Chapter 5 is centred on the analysis and modelling of different patterns of land occupation, from a morphological standpoint, through the use of Geographical Information Systems (GIS). The objectives, at this point in particular, are based on the previously detected urban land cover, on one hand, to provide an effective approach for defining the main morphological features of urban settlements, in terms of urban outline, urban texture and street pattern; whilst on the other hand, the study aims to implement a methodology for automatic classification of different urban models, at a municipal level, based on synthetic morphological features. Both objectives are achieved by using statistical techniques, such as factorial and cluster analysis.

The intersecting objective of the research, at this point, is to strengthen the idea that new technologies can really support all of the processes of planning and decision-making, both at the detection phase as well as for

analysis and modelling. Indeed, today, increasing amounts of satellite information, algorithms and GIS platforms are freely available, such that major potentialities arise from the integrated use of such technologies in the field of land management and spatial planning, and the ability to provide standardized processes and information on a global scale.

The image below (figure 1.4) shows a schematic example of the integrated use of RS and GIS, applied to a theoretical process of spatial analysis and planning, starting with the collection of data (based on satellite information), until the analysis and modelling operations handled through the use of GIS.

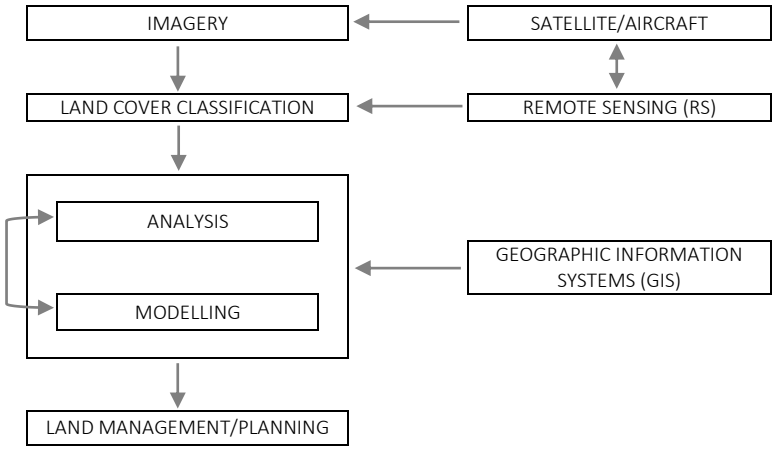

Fig. 1.4: Schematic example of the integrated use of RS and GIS, applied to spatial analysis and planning (Source: By authors).

Finally, Chapter 6 initially provides reflection about the relevance of the results obtained through the use of RS and GIS applied to urban modelling based on a morphological approach. The analysis is provided for all municipalities found within the Autonomous Communities bordering the Mediterranean side of Spain. Following on from that, the study highlights the value of such an approach by speculating about the interaction between urban morphological models in terms of compactness vs. sprawl, and other spatial features such as, in particular, topography, geography, and processes of metropolization. In conclusion, the main limitations and gaps within the investigation are remarked upon, and possible perspectives and future developments are suggested.

1.5. A TECHNOLOGICAL APPROACH TO THE SPATIAL ANALYSIS

Urban growth often generates strong demographic and environmental pressure, so the availability of suitable tools and methods for modelling this process, and the impact upon the natural resources, is vital to properly assess land management and planning practices. Indeed, *land use planning and necessary supporting data are crucial for developing countries* (Bocco, Mendoza, & Velázquez, 2001).

In order to understand and define the dynamics of development of a territory and the processes of evolution and the interactions within a heterogeneous landscape (such as urban areas), it is of fundamental importance to accurately quantify spatial patterns of growth over time (Wu, Jelinski, Luck, & Tueller, 2000). Because of this, new technologies for spatial analysis, which arose from the field of computational science, have been broadly implemented and recognized as powerful tools for analysis and modelling of the environment, especially during the last few decades and particularly since the 1960's.

As argued by Weng (2010), *the appearance of Geographic Information Systems (GIS) in the mid-1960s reflects the progress in computer technology and the influence of quantitative revolution in geography. GIS has evolved dramatically from a tool of automated mapping and data management in the early days into a capable spatial data-handling and analysis technology and, more recently, into geographic information science (GISc)*.

GIS is a computer-based system designed to enable the collection, management, analysis, and spatial visualization of large quantities of geographically referenced data in a raster or vector format, to which specific alphanumeric attributes can be associated[16]. The development of GIS technologies has provided a variety of analytical tools for the analysis and management of the environment, both for urban or natural space. Indeed, the integration of traditional statistical methods, set up for urban analysis, and the technological approach based on GIS, allows the enhancement of the ability to manage large databases and improve the spatial efficiency of the results (García Almirall, 1998).

Remote Sensing (RS), which was born with basically military purposes in mind, is now (also) generally used for detecting, collecting, storing and interpreting information about the environment, and the land cover composition. This is done remotely from a distance, i.e. without coming directly (physically) into contact with an object, but by sensing and measuring the amount of energy emitted by the earth's surface. The increasing availability of satellite information has increased the ability to acquire a huge amount of data globally, and in digital format, over large geographical areas, allowing for different scales of analysis and differing time periods[17]. Similarly to GIS, the standardization of sensor image processing procedures also provides important improvements in spatial analysis.

According to Weng (2012), the demand for remotely sensed data is growing increasingly in relation to cartography and the analysis of the spatial distribution of environmental or socio-economic data. This is due to the ability to manage information concerning huge geographic areas in a raster format ready for analysis in a GIS, and also convertible into a data format suitable for subsequent analysis and modelling.

We could argue that, RS technologies are primarily employed for data-collection and image processing, while GIS are predominantly employed as tools for data-handling, analysis and visualization. The integrated use of both technologies provides plenty of potential in terms of Earth Observation (EO): monitoring, measuring and mapping different environmental features, including urban phenomena at varying scales of analysis. In the latter case, the use of census data, as ancillary information, gives us the ability to set up further demographic and socio-economic analysis in relation to the spatial distribution of the phenomenon under investigation. Indeed, GIS technology provides a flexible (virtual) space for “spatializing” digital data and modelling (Weng, 2010).

[16] GIS is generally formed by a user interface system, which provides a powerful set of tools for spatial data manipulation and analysis, together with functions for displaying and generating geo-referenced products.

[17] Actually, besides information about biophysical parameters, such as temperature, biomass or elevation, the remote sensing systems, which commonly depend upon satellite platforms or aircraft, have the ability to collect data about the land cover composition at different time periods, thus making it possible to monitor changes over time, and analyse growth dynamics in place on the earth's surface. This ability also allows the measurement of natural phenomena such as hurricanes, for instance, or monitoring the activity of volcanoes.

Universidad Politécnica de Cataluña, Barcelona TECH
Departamento de Tecnología de la Arquitectura
Centro de Políticas de Suelo y Valoraciones
Nicola Colaninno, Josep Roca Cladera

Chapter 2

URBAN GROWTH AND LAND CONSUMPTION ALONG THE MEDITERRANEAN SIDE OF SPAIN

This section provides an overall reflection about the different urban growth dynamics occurring in Spain during the last decades, and also in relation to the European scenario. However, above all, we focus our analysis on measuring the urban phenomena along the Mediterranean side of Spain, which is perhaps one the geographical contexts most affected by consistent human pressure.

The significant trend of concentration of population, production and land consumption has occurred since the second half of the last century, towards the Spanish coastline, which is an ecologically fragile, flat and relatively limited space, and seems to have accelerated over the last few decades. An example of this process is the rapid growth rate of housing production, both for permanent and seasonal residential uses. Wherever this growth has been more intense, the territorial and environmental balance has been upset by consumption of non-renewable resources, such as water and soil. Many studies, in different disciplines, have highlighted the environmental and territorial effects of the "coastal development" of the Spanish territory, in relation to urban expansion and to the resulting building typologies, produced by this model of development (González Reverté, 2008).

Therefore, in order to give our contribution for understanding and explaining which kind of urban models we are facing, it is vital to define the main relationships established between the natural environment and human involvement, and their specific weight on each other. This has often resulted in conflicts in the balance between the urban/non-urban combination, and especially in recent years.

Certainly, the urbanization process is affected by natural and/or administrative factors, however, it is clear that there is a tendency to occupy the most "productive" and profitable portions of the landscape. Indeed, if we look at how urbanization has spread throughout the territory over the last twenty or thirty years, and we concentrate on its forms of occupying the soil, we have the clear suspicion that urbanization, especially in the Mediterranean area, and even more so along the immediate coastline, has undergone a process of uncontrolled, uncoordinated planning, almost without care for environmental problems or administrative rules.

An important piece of evidence is that, in 2006, the first kilometre of coastline along the Spanish Mediterranean side was 30% urbanized. This percentage, which was as low as 22% in 1990, flatly decreases in the second kilometre (16% in 2006) to reach very low values at a distance of 20 or 40 kilometres. In fact, as early as the sixties, the Spanish Mediterranean coastline became a privileged stage for the implementation of two of the main drivers of economic development: tourism and construction. The Law about Centres and Tourist Zones of 1963 marked a strategy that strongly favours urban growth, and which has never been rectified (Gaja, 2012).

The consequences of the present-day dynamics of growth processes require new methods of analysing and quantifying urban development phenomena. In fact, there has been considerable debate, undertaken by the European Authorities in recent years, about the European Mediterranean space in general, regarding the role of spatial planning in order to promote sustainable trends of land use. The current configuration, or perhaps misconfiguration, along the Mediterranean side of Spain, together with the traditional landscape profile associated with it, has been profoundly altered by a phenomenon, described by Gaja (2008) as a "real estate tsunami", which has decisively subdued the coastline to actions and interventions of a very different nature. Such interventions help to highlight how certain geographical areas often respond not only to physical and bio-geographical realities, but also to economic and socio-political approaches (Peiró, 2012).

In particular, the urban models of several cities along the Spanish side of the Mediterranean are currently conditioned by real estate interests. Here, the expansion of residential tourism and real estate specialization has indeed resulted in rapid economic growth as well as a deep territorial impact that inevitably makes the model less desirable from a sustainable development perspective, and regarding more traditional tourism models.

In this context, the most touristic cities have to face two obstacles. The first one is the struggle for competitiveness in a market that requires an increasing (critical) and fast restructuring of the facilities supply in order to satisfy the current requirements of the demand (Anton, 2004 b). Secondly, there is the less visible but critical struggle with the real estate sector that competes to get most of the available resources (González Reverté, 2008).

2.1. URBAN GROWTH DYNAMICS: SPAIN WITHIN THE EUROPEAN SCENARIO

In the most recent decades, urban growth in Europe has taken place at a rate much higher than population growth (figure 2.1). This progression has resulted in a huge urban footprint, which has generally affected the whole European territory, thus producing, as a consequence, an important fragmentation of the rural and natural space, in addition to the increase in demand for transport infrastructure and energy.

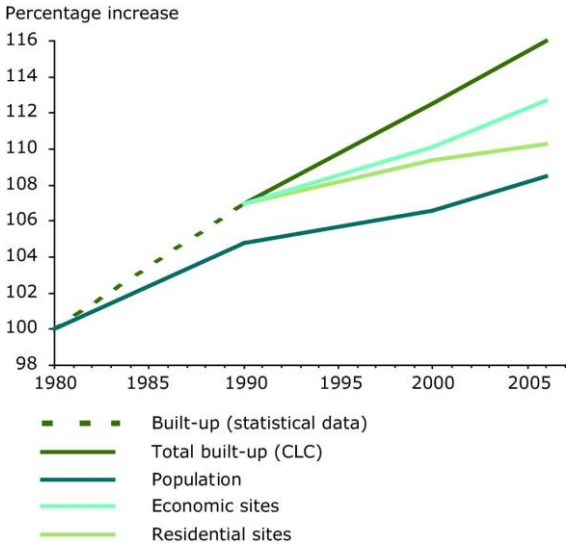

Fig. 2.1: Overall Built-up area and population increase trends, in selected European countries (Source: European Environment Agency, 2011)

Particularly during the last twenty or thirty years, urbanisation has arguably been the most significant change in land use in Europe since the Second World War. Indeed, over 70% of Europe's population now lives in urban areas, which, in turn, have grown in terms of urban area by almost 80% over the last fifty years (EEA 2006).

The most obvious signs of this shift towards urbanisation are the urban sprawl phenomena and the emergence of peri-urban areas, often characterised by scattered built-up residential uses, industrial or commercial areas and dense transport networks. Moreover, we have witnessed an increase of green belts, recreational facilities, urban woodlands and golf courses, as well as the conversion of farmhouses into housing, and the transformation of agricultural land uses and rural areas within easy reach of the city, into hobby farms (PLUREL project[18], 2011).

An overview of the spatial distribution of urban morphological zones in Europe (figure 2.2) provides an interesting perspective about the higher levels of urban concentration. Hence, it is possible to highlight that the major concentration of urban areas forms a kind of axis, known as the European megalopolis or dorsal, extending from the UK (London, Birmingham) to northern Italy (Milan, Turin), passing through northern France (Paris, Lille) Belgium, the Netherlands and western Germany (the Ruhr area, Düsseldorf, Cologne and Bonn).

There are also many cities with more than 50˙000 inhabitants in central and Eastern Europe (namely in capitals such as Berlin, Bucharest, Budapest, Prague, Sofia and Warsaw). Fewer large cities are found in southern

[18] PLUREL is an Integrated Project funded within the 6th Research Framework Programme of the European Union. During its lifetime, 36 partners from 14 European countries and China have participated in the project. It has been coordinated by Dr. Kjell Nilsson, Danish Centre for Forest, Landscape and Planning; University of Copenhagen. The project started in 2007 and finished in March 2011. The PLUREL project aimed to achieve a deeper understanding of the changing relationships between urban and rural land use with an emphasis on the most dynamic portion, that of peri-urban areas. It developed methods and tools to assess the environmental, social and economic impacts of land use changes. Potential strategies and good practice examples were identified in order to promote the sustainable development of land use systems in Rural-Urban Regions, especially the peri-urban areas (PLUREL project, 2011). More details, about the PLUREL project, can be found in chapter 2 of the present study.

Europe, with the biggest ones being Barcelona, Lisbon, Madrid, Porto and Rome (European Environment Agency, 2011).

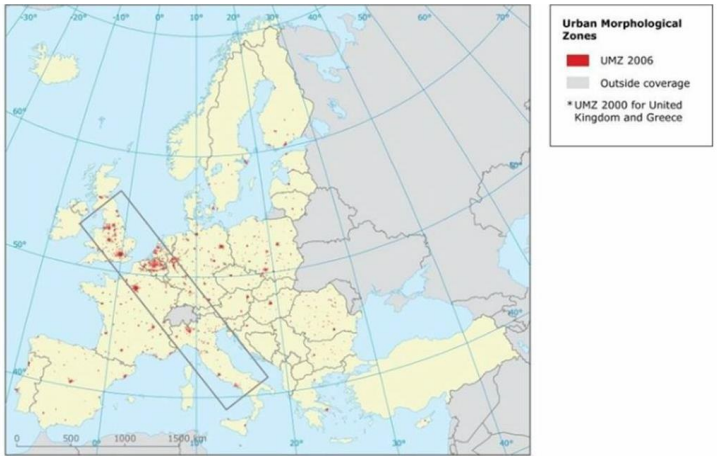

Fig 2.2: Urban morphological zones in Europe. Source: EEA/ETC LUSI (Source: European Environment Agency, 2011)

Really, the most worrying problem is not the city growth itself, but rather the uncontrolled spread of artificial uses over the territories, with the consequent loss of natural and rural areas, together with all the problems connected to the sustainable management of the environment.

Between 2000 and 2006, the artificial land cover increased by 2.4% in Europe, which was the largest (proportional) increase among all land uses. Although the total amount of artificial areas represents only 4% of the whole European context, the way urban uses spread over the territory, actually results in more than a quarter of the EU territory being directly affected by urban uses. Following the results of the PLUREL project (2010), peri-urban (discontinuous) areas grew 4 times faster than continuous urban areas. Indeed, despite the distribution of the main urban agglomerations, growth of artificial areas, as shown in figure 2.3, does not only happen around the major urban centres but also spreads across Europe around smaller cities and towns and along many rural regions. On the other hand, the average population density (at European level), i.e. population per built-up area, decreases dramatically, and this trend shows that the main ongoing tendencies, in terms of urban growth, tend to be sprawl phenomena (European Environment Agency, 2011).

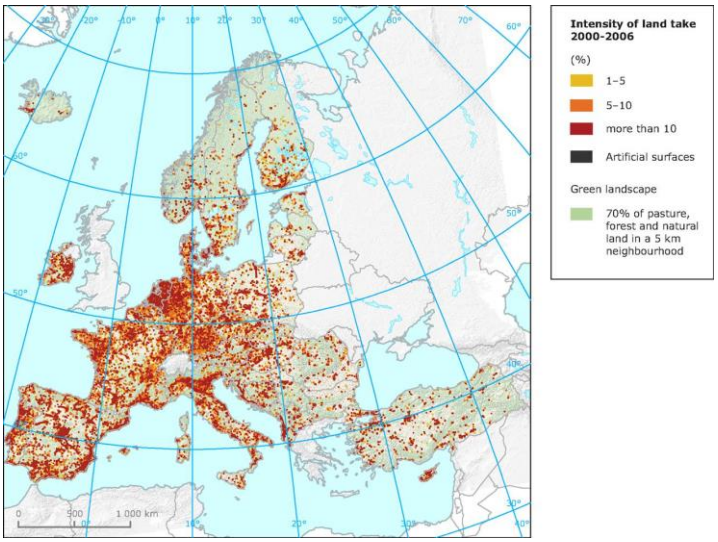

Fig 2.3: Spatial distribution and intensity of artificial land take 2000-2006 (Source: European Environment Agency, 2011)

The European territorial system, in this logic of development, has experienced major changes especially in the areas extending outside the compact urban structure. These areas, generally defined as peri-urban have given the landscape certain features that are quite different from the typical urban structure of the traditional compact nuclei (Benni et al., 2007). The excessive alternation between urban and non-urban areas, which is becoming more and more difficult to identify in several European regions, configures the natural space around cities only as residual areas among buildings. New urban forms are generating new models of cities.

Lots of European cities, which were formerly characterized by the compactness of the urban fabric, are now a result of the sum of peri-urban, dispersed, low-density residential areas. In fact, recent models of urban development, affected by various economic dynamics, have represented a strong conceptual change in the way of urbanizing, generating phenomena of urban dispersion or diffusion which are now difficult to measure. This possible dissolution of the compact city is a recurring theme of analysis and reflection in the field of urbanism, addressing a quantification of the present phenomena.

According to the Observatory of Sustainability in Spain (OSE), within Europe, and in the period between 2000 and 2006, there has been an increase in artificial areas of 686˙414 ha in the 36 countries. Despite not being a very high percentage, in relative terms, there are significant spatial differences, with respect to the urbanization processes, among the various regions included in the analysis.

Considering the contribution of each country to the total increase in urban land and infrastructure in Europe, Spain is the country that has contributed the most (21.4%) to the increase in artificial soil in Europe between 2000 and 2006. Spain is followed by France (12.9%), Germany (10.1%) and Italy (7.4%). Malta on the other hand has been the country with the smaller annual average increase of artificial areas in this period, with 0.001% (figure 2.4).

Although the differences between countries are strongly related to the extent and density of population. In the case of Spain, data about artificialization at the national level, as shown by the image below, clearly highlights a process of "dangerous" urban expansion[19].

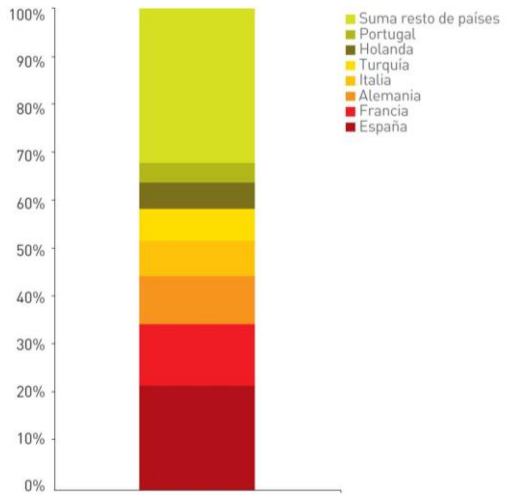

Fig 2.4: Average annual increase of artificial surfaces with respect to the total artificial surface area in Europe, between 2000 and 2006 (%)[20] (Source: OSE, 2011)

There is no doubt that, during the last decades, Spain in particular has been undergoing an important process of urban growth. This has implied the consumption of a large amount of land[21], although the total

[19] OSE, Observatory of Sustainability in Spain. Chapter 8: natural environment and territory, paragraph 8.5: land cover changes

[20] LEAC Database (based on CORINE Land Cover 2000-2006 changes, version 13, 02/2010), ETC/LUSI. AEMA based on data from the Project CLC. [[http://www.eea.europa.eu/data-andmaps/figures/mean-annual-urban-land-take-as-a-percentage-oftotal-europe-23-urban-land-take-1990]).

[21] The Spanish model of economic growth in the late nineties is characterized by the dominance of a major movement in real estate speculation. The price growth and housing activity shows an explosive path that has contributed to expand income and employment well above the rest of the Eurozone economies. Actually, in Spain, approximately 30% of the demand for housing is linked to speculation (Bellod Redondo, 2007).

population has hardly increased. In parallel, the Spanish economy has experienced significant economic growth from the late nineties to the present. In addition to this economic development, we have seen intense speculation in the property sector. Between 1999 and 2004, the average price per square meter rose by 142%. Additionally, the Spanish economy grew in the same period well above the European average. Thus, the strong interests in housing activity are most likely an explanatory cause of this new process of growth (Bellod Redondo, 2007).

There are two alternative explanations to account for the strong expansion in construction activity in recent years in Spain. On the one hand, it could be argued that the rapid growth of house prices is the "normal" product of the expansionary phase of the business cycle that Spain has experienced since 1994. It would be, therefore, an increase based on the evolution of macroeconomic variables (GDP, inflation, demography...). On the other hand, it might be suspected that the market has undergone a speculative process that has led housing prices well beyond what is reasonable. This means that we would be facing a "speculative bubble" which goes beyond basic macroeconomic dynamics (Bellod Redondo, 2007).

2.1.1. The Sprawl Phenomenon in Europe

Although the European government has promoted a process of socio-economic convergence during the last decades, the European Union is still the result of several countries with very different backgrounds and historical paths, as well as different socio-economic structures. This involves a wide range of developments, either in terms of land management and planning, thus making it really difficult to provide useful measurements for controlling the urban growth process at a European level as a whole.

Historical trends, since the mid-1950's, show that European cities have expanded on average by 78%, whereas the population has grown by only 33%. A major consequence of this trend is that European cities have become much less compact. Indeed, evidence demonstrates without a doubt that this phenomenon has characterized the growth of several European cities over the past 50 years (European Environment Agency, 2006).

Phenomena of alarming urban expansion have mostly occurred when the speed of urban growth has exceeded the rate of the population growth. In particular, it has been quite remarkable for medium-sized cities surrounding a big metropolis. Actually, in this case, the highest levels of discrepancy have occurred between urban development and population growth rates. This kind of expansion, commonly referred to as urban sprawl or uncontrolled urban expansion, is occurring unevenly across Europe, indeed in some areas it is more evident than others.

This phenomenon, in reality, is the outcome of a set of forces including both micro and macro-economic trends, and social issues. The quality of the transport system, the price of land, individual housing preferences, demographic trends, traditions and cultural constraints, among others, are factors that determine the type of development of an urban area (European Environment Agency, 2006). Dematteis (1986) highlighted that the modern processes of peri-urbanization and reticular diffusion of the cities give rise to urban peripheries that result in very different forms than those traditionally found in Europe since the industrial revolution in the sixties. This change of paradigms is the result of profound modifications in urban structures (de-urbanization, counter-urbanization), mostly due to modern developments, in terms of information and communication technology (post-Fordism).

An urban development characterized by lower densities, either in terms of persons per urban area as well as urban area upon non-urban area, has led to the increased rate of land consumption in several European cities. Indeed, the overall area consumed per person in European cities has more than doubled in the last 50 years. Over the past 20 years, the extension of the built-up environment in many countries of Western Europe and Eastern Europe increased by 20%, while the population grew by only 6%. Moreover, in terms of mobility, the number of miles traveled in urban areas by road was expected to increase by 40% between 1995 and 2030[22] but was already reached in 2006 (European Environment Agency, 2006).

[22] *During the ten year period 1990–2000, the growth of urban areas and associated infrastructure throughout Europe consumed more than 8,000 km² (a 5.4 % increase during the period), equivalent to complete coverage of the entire territory of the state of Luxembourg. This is equivalent to the consumption of 0.25 % of the combined area of agriculture, forest and natural land. These changes may seem small. However, urban sprawl is concentrated in particular areas which tend to be where the rate of urban growth was already high during the 1970s and 1980s (*European Environment Agency, 2006).

Such a model of development may be detected around small towns or in the countryside, along transportation corridors, and along many parts of the coastline, mostly if connected to the river valleys, as a typical model of urbanization exemplified by the so called “inverse T" model of urban sprawl. This can be observed along the Rhone valley, in southern France and along the Mediterranean coastline of Spain[23] (European Environment Agency, 2006).

In general, it would be possible to delineate several scenarios in Europe, based on values of urban sprawl, as calculated in the the framework of research work provided by Arribas-Bel, et al. (2011), in which they define a “Baltic City” where people usually live in the core (i.e. low decentralization) but have relatively long commutes, and where density and scattering reach middle values, while the amount of urban open space and the mixed use are high. The Northern European City model, which would be similar to the Baltic, shows slightly better connections, more density and decentralization. The Atlantic model implies shorter commutes, higher density and decentralization, medium-low scattering and availability of open space, and less mixed uses than the other regions. Finally, the Mediterranean City shows low average values of commuting times, density and decentralization, with small amounts of open space, a high degree of mixed uses, and a mixed pattern of scattering[24].

In particular, the areas with the most visible effects of urban sprawl are located in highly populated countries or regions and with extremely dynamic economic activity (Belgium, Netherlands, Germany, southern and western, northern Italy, the Paris region), or where economic growth has experienced a rapid increase (Ireland, Portugal, eastern Germany, the Region of Madrid). On the other hand, the dispersion is particularly evident in countries or regions that have benefited from regional policies.

Along the coastal regions of Europe, the highest rate of population growth is often accompanied by an urban growth which is strongly linked to the phenomena of uncontrolled expansion of the urban fabric on the territory (as shown in figure 2.5). During the period 1990-2000, the urbanization of the coastal area grew by about 30% faster than in inland areas, with the highest growth rates (20-35%) in the coastal areas of Portugal, Ireland and Spain[25].

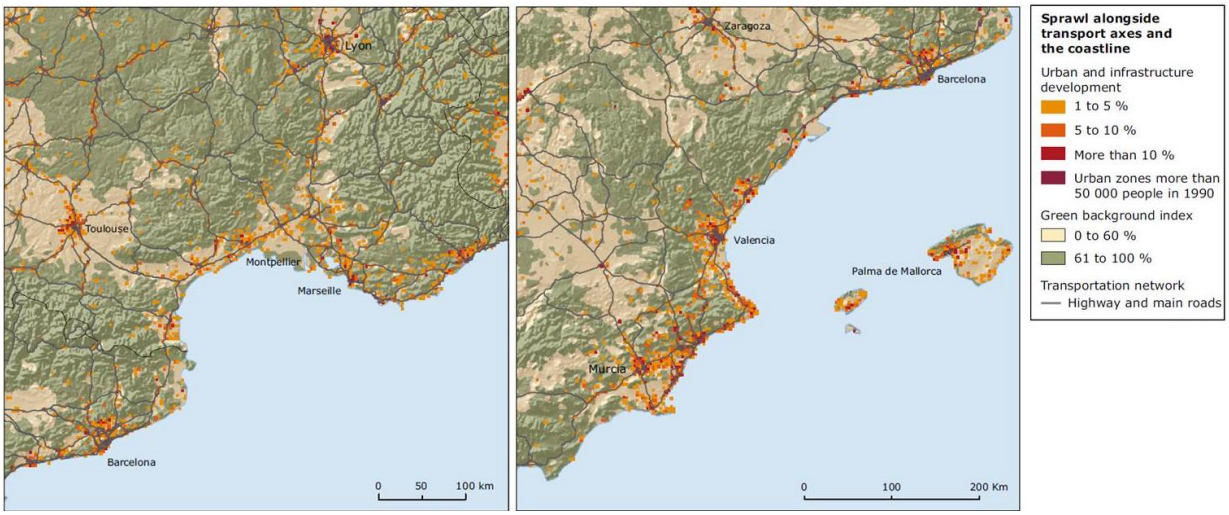

Fig 2.5: Sprawl phenomenon alongside transport axes and the coastline. The case of Rhone valley in France (left side), and the Mediterranean coastline of Spain, along the Regions of Catalonia, Valencia, and Murcia (right side) (Source: EEA, 2006)

[23] In the case of Spain, the artificial areas sometimes cover up to 50% of the total available area.

[24] More details can be found in: Arribas-Bel, Daniel, Nijkamp, Peter and Scholten, Henk. 2011. Multidimensional urban sprawl in Europe: A self-organizing map approach. *Computers, Environment and Urban Systems.* 2011, 35, pp. 263-275.

[25] *Urban sprawl has also produced increased demands for raw materials typically produced in remote locations and requiring transportation. The consumption of concrete in Spain, for example, has increased by 120 % since 1996, reaching a level of 51.5 million tons in 2005* (European Environment Agency, 2006).

The determining factors for the proliferation of urban sprawl, and the resulting dynamics, are completely interconnected and essential to explain the concept of sustainable development, and the concept of "ecosystem" in the functioning of the city and its surroundings. The interconnectedness of environmental impacts, at all levels, provides some of the greatest future challenges in Europe, for the design of effective policy solutions to combat the problems of urban sprawl (European Environment Agency, 2006).

2.1.2. In Europe: A Change of Urban Paradigms

The European Continent provides, without a doubt, one of the most urbanized areas on the planet. Today, *about 75% of the European population lives in urban areas*. However, the future of European cities is a matter of great concern. More than a quarter of the European Union territory is directly affected by land consumption for urban uses. It is estimated that *in 2020, approximately 80% of Europeans will live in urban areas, while in some areas the percentage could rise to 90% or more*. As a result, the demand for natural areas, especially around major metropolitan areas, is expected to increase rapidly (European Environment Agency, 2006).

According to Christiansen, et al. (2011), although Couch, et al. (2007) considers the urban sprawl phenomenon, in Europe, as beginning with the Industrial Revolution, with London as an example[26]; indeed European cities, as a whole, have developed more rapidly during the last 50 years, but at different rates and with remarkable regional differences (table 1.1).

Time-lag	North West Europe (+Denmark)	Western Europe	Mediterranean	New Member States
1950-1960	Urban population: 75%. Start process of suburbanization	High variability between cities and countries. No common pattern	Urban population: 45%. Compact and densely populated cities	Urban population: 40%. Compact cities by centralized planning and reliance on public transport
1960-1970		Start process of suburbanization in many cities		
1970-1980	Revitalization. Recovering the city centre in terms of both population and urbanization	Revitalization. Recovering the city centre in terms of both population and urbanization		
1980-1990		Revitalization. Recovering the city centre in terms of both population and urbanization	Increasing the process of sprawl	Towards the end of 1980's start of political changes
1990-2000	High rates of sprawl in Ireland. Denmark showed the lowest rates of sprawl	Average rates of sprawl. Steady growth of German cities	Rapid increase in urban sprawl	Post socialist period. Most cities are declining and sprawling. Romania and Poland show the highest shares of declining cities
2000-2005	Continuous long-term decline in UK (Merseyside, Tyne and Greater Glasgow)	Growth of German cities at lower rates. Few German cities show continuous decline (Leipzig being a prototype of decline and sprawl)	Most of the Spanish and French cities show continuous growth. Sprawl is still important in Spain	Decline in most Polish cities

Table 2.1: Urban trends in regions of Europe for period 1950-2005 (Source: ESPON, 2010; Christiansen, et al., 2011)

[26] *In the 1800's, London was the largest city in Europe. People flocked to cities to work as cities became economically important. London's urban structure was at the time very dense. Distance between residence and work was usually short, often within the same quarter. This structure led to a number of problems which also exist today, for instance noise pollution. The industrial revolution also created an emerging middle class and elite merchants, who could afford housing in suburbs. Here they could establish homes with gardens and move away from problems associated with the city* (Couch, et al.; Christiansen, et al., 2011).

In general, it seems like since the 1950's and 1960's European cities are becoming less and less compact, even with certain differences in the patterns of growth speed. In particular, the cities of southern Europe, which traditionally accounted for a compact city model, as opposed to cities in northern Europe, are experiencing important changes in the urban growth model. In fact, while in northern Europe urban sprawl is starting to decline, in southern Europe, in particular as low density urbanization, it is now increasing. It seems that, especially since 1990, the countries of the Mediterranean area have experienced a rapid increase in urban growth and sprawl (Christiansen, et al., 2011).

The land consumption pattern has completely changed, mostly during the last twenty years: transportation, housing, communications, tourism and leisure, have become major drivers of land consumption (European Environment Agency, 2006).

While, historically, the growth dynamics of European cities was primarily dependent upon the increase in population; since the post-war period, after different development phases (such as urbanization, suburbanization, and de-urbanization), a new urbanization phase, mainly characterized by urban spreading, is now driving the urban development of the European cities, which often appear more scattered, discontinuous, and less compact, although according to different velocities and intensity depending on the geographical area (European Environment Agency, 2006).

From an overall standpoint, and according to Nilsson and Nielsen (2011), in Europe the urban expansion "*(...) will continue at a rate of 0,4-0,7% per year (...) Discontinuous development containing settlements of less than 20.000 inhabitants and with an average density of at least 40 people per km^2, are growing four times faster than urban areas* "(Christiansen, et al., 2011). This sprawling tendency is extremely significant because of the subsequent increase in soil consumption rate.

Indeed, if we take into account that, as reported by the European Environment Agency in 2010, most of the land "consumed" to generate urban expansion is taken in particular for agricultural, farmland, and pasture uses, as shown in figure 2.6, and since land cannot, in general terms, be created, the meaning of the problems which the European institutions have to face during the next few years seem clear.

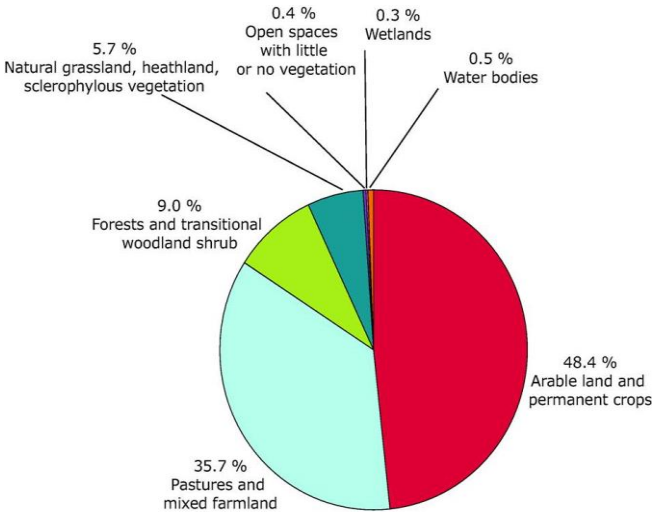

Fig 2.6: Relative contribution of land-cover categories to uptake by urban and other artificial land development (Source: European Environment Agency, 2010)

2.1.3. In Spain: The Loss of The Mediterranean Pattern?

Far from a typical Mediterranean model, today it is practically impossible not to discuss Spanish cities on the Mediterranean side without taking into account phenomena of urban sprawl (also feared by the European Union), which bring dynamics of dispersion of artificial soil in rural, and natural areas, discontinuous but plentiful.

There is excessive alternating between urban and non-urban, which is more and more difficult to identify, currently configured natural space around cities such as residual areas between built-up structures. New "urban forms" are drawing new Mediterranean cities, which were dominated by the compactness of the urban fabric, while now are the result of the sum of peri-urban areas, dispersed and with low density (figure 2.7).

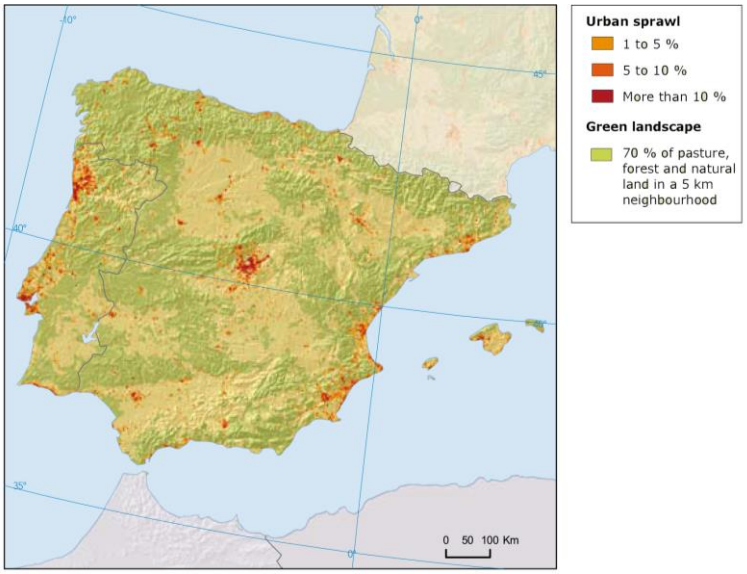

Fig 2.7: Polarized urban sprawl around major cities and the coast of Portugal and Spain (1990–2000) (Source: European Environment Agency, 2006)

The entry of Spain into the European Union (1986), the Treaty of Maastricht (1992) and the completion of the European project for the introduction of the Euro (2002) allowed the Spanish economy to access an unprecedented mass of capitals. The “insatiable” attempt to attract international investment produced the most profitable business of property speculation in Spain, particularly remarkable since 2000 (López, et al., 2010; Ginard Bosch & Murray Mas, 2012).

The high prices of homes in traditional touristic areas and in the big cities served as bait to capture much of the money in circulation (OMM, 2011; Ginard Bosch & Murray Mas, 2012). In this sense, urban development in Spain has been the main engine of the economy, in addition to the support for industry and services, and has enabled mass tourism and property speculation to take place. In particular between 1987 and 2006, there has been an intense process of land consumption mostly caused by the increase in artificial areas. In particular, both continuous and discontinuous urban fabric[27], together with infrastructure and construction sites, with a net growth of 307˙065 ha, have represented around 52 % of the total amount of artificial surface in this period (OSE, 2011). However, in terms of increasing consumption of land for artificial uses; during the most expansive urbanization period in Spain, i.e. between 2000 and 2006 , roads and rail networks and associated land, apart from construction sites, have provided the highest rate of change (positive), measured in percentage values (figure 2.7), far beyond 100%.

At present, it is an acknowledged fact that the transportation infrastructure in particular (road and rail networks) is one the main drivers that leads to the dispersion of urbanization (either housing, economics, or productive uses) and the fragmentation of the landscape. Indeed, the degree of landscape fragmentation provides a key indicator of the unsustainability of urban development. Hence, it is quite alarming that, according to European Environment Agency (2011), and consistent with the values in the figure 2.8, the landscape

[27] In 2006, urban fabric accounted for the largest proportion of the total artificial surface, and the amount of discontinuous urban fabric around the 0.67% and the continuous urban fabric around 0.58%, followed by industrial or commercial areas (0,29%) and mineral extraction sites (0,15%) (European Environment Agency , 2011)

fragmentation in the Iberian Peninsula is the highest with respect to the Mediterranean side of Europe. Besides this, the phenomenon is most marked in Portugal and north-eastern Spain.

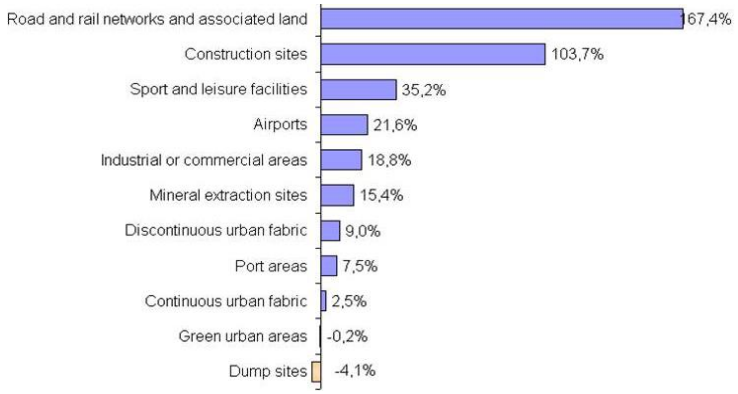

Fig 2.8: Change in artificial surfaces in Spain. 2000-2006 (%) (Source: IGN.MF; European Environment Agency , 2011)

As previously stated, the period between 2000 and 2006 has been the most expansive growth period in Spain, in terms of urban expansion, with an average annual growth of 2.6% versus 1.9% in the previous period (1987-2000). However, in terms of housing, despite the remission of the upward cycle of the housing boom, which occurred in 2007, and the decline in the number of built housing, which approximately has taken place since 2008 to the present (2011), the average annual increase of urban plots, according to the Land Registry, has been on average of 3.34% until 2010, far above the annual growth that occurred between 2000 and 2006. This shows the inertia of the development model based on the property sector, especially in 2008-2009 (with a maximum of 5.64% annual growth), which began to fall but still reached values around 2%, similarly for the period 2006-2008 (OSE, 2011).

Indeed, from the residential perspective, despite the great tensions that have occurred resulting from important migration flows that have occurred during the past few decades, the massive urban development of land has placed Spain in the ranking of housing production per capita in Europe, well above the real needs arising from new household formation (Romano, et al., 2010). Figure 2.9 shows how, since 1998 and for nearly a decade, in Spain it has exceeded the number of 400˙000 homes per year, which had been held as the absolute maximum of production for the sector. While the 960˙000 homes per year was reached in 2006, corresponding to about 20 dwellings per 1˙000 inhabitants (Gaja, 2012). On the other hand, the “obvious”, and maybe even expected, effect that the current crisis has had upon production trends in the housing sector after 2006 is quite noticeable.

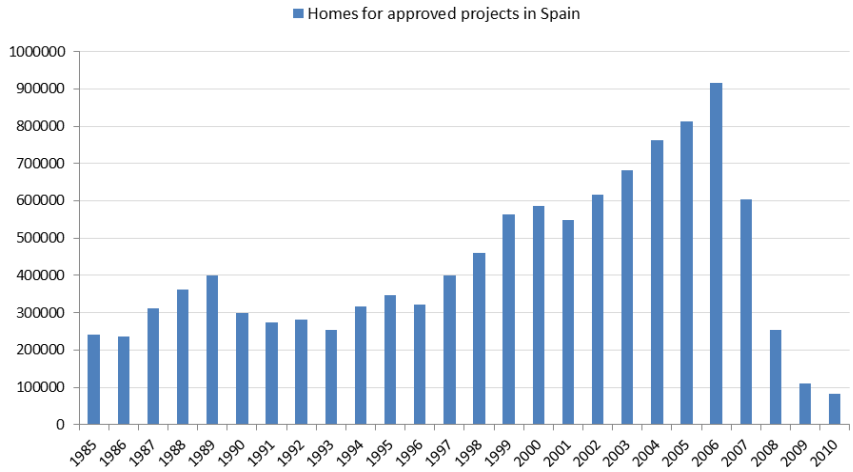

Fig 2.9: Homes for approved projects in Spain, from 1985 to 2010. (Source: Superior Council of Colleges of Architects of Spain)

In the Mediterranean European Countries, undoubtedly, the exceptional patterns of urbanization have been influenced by an attractive climate and favourable landscape topography. In this particular geographical context, then including Spain, the process of urbanization tends to take place in the proximity of coastal areas and near the main urban agglomerations. Over the years, most of the housing expansions and main road infrastructures have been placed close to the coastline. Since the transport infrastructures, as we have pointed out, represent a key point of urban expansion and fragmentation, it seems clear that the coastal areas are currently one of the most sensitive scenarios subjected to human pressure.

As argued by Gaja (2012), urban development in Spain, and the change in growth model, is basically understandable through four widely recognized main stages. The first is between 1939 and 1957 (marked by the end of the war, the creation of the Ministry of Housing and the approval of the Stabilization Plan in 1959) in which, despite the relatively low construction activity, provides the basis for what will happen in the following years. The second phase, properly defined as "development", between 1957 and 1973 (ended with the first oil crisis), in which we saw a true expansion, consolidation and maturation of the growth model. The third, from 1973 to 1996, in a particular context of social, political, and economic crisis, which is possible to identify as a transition stage and in which with its ups and downs, swings, progress and regression, the model continues to strengthen. The last one is that of the urban overproduction, the "tsunami", which mainly occurred between 1996 and 2007 and is the culmination and climax of the model. The Federation of Promoters and Builders estimated that in 2008 Spain needed more than 300˙000 homes a year, but during the 2003-2007 period, triple that figure had been reached (Gaja, 2012).

Urbanization has always been one of the main problems for the coastline. Many municipalities have made every effort to convert the highest possible percentage of their territory (including protected natural areas) to developable land without worrying about building comfortable cities. Between 1990 and 2000, the Spanish population increased by 5%, while urbanization increased by 25.4% (Marcos, Jiménez, & Del Río, 2012). Today, in Spain, there is an amount of soil already classified as developable sufficient to build about 20 million houses. This amount of soil is waiting for new economic good times to continue consuming the territory (Gaja, 2012).

This growth model is mostly based on residential uses, which consequently implies a major incentive to build road, rail networks, and other related infrastructure, and has placed Spain among the first countries, in a ranking on a European level, in terms of land consumption, as shown in the following figure 2.10.

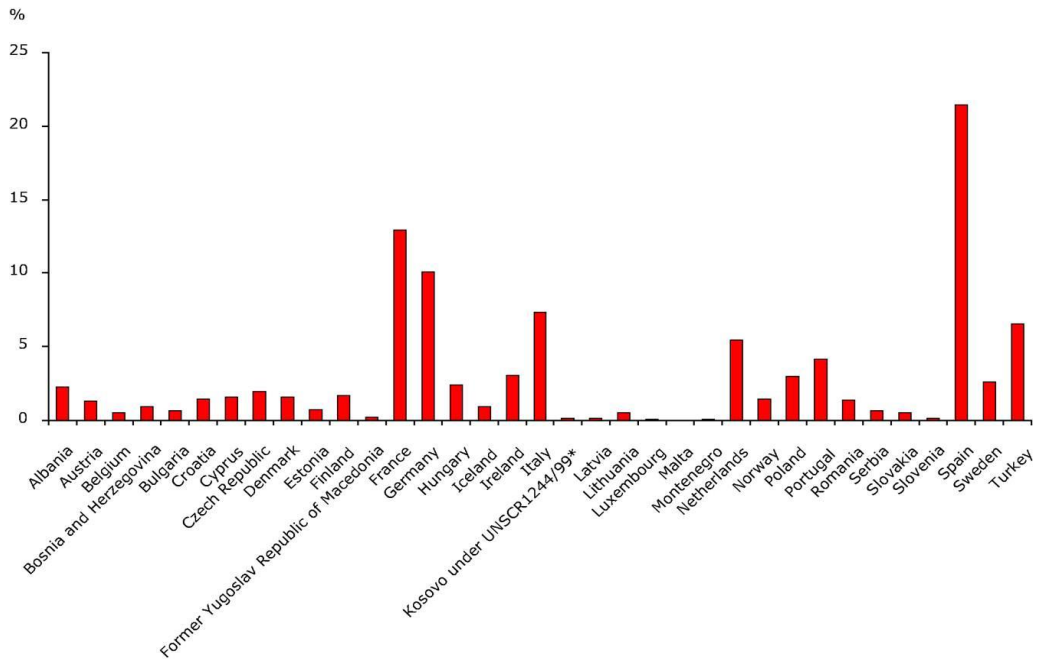

Fig 2.10: Mean annual urban land take as a percentage of total urban land take during the 2000-2006 period (Source: European Environment Agency, 2012)

In Spain, economic growth and tourism has led to an increase in urbanization rates, especially along the Mediterranean side. Clear examples of this phenomenon are the Costa del Sol and the Costa Brava, which have developed considerably over the course of the 1950's and 1960's. In particular, the expansion of the residential sector, both for primary and secondary housing, is on average responsible for over 45% of the transformation of the coastal territory into artificial surfaces. There is a growing demand for residential investments along the coasts of the Iberian Peninsula, generally encompassing Spain and Portugal, due to the mass tourism from other parts of Europe, mostly Northern Europe. In addition, there is also a domestic demand for coastal locations from inland populations (European Environment Agency, 2006). This has led to the development of the combined production of housing, infrastructure, and leisure facilities, such as golf courses and marinas.

The results of the analysis of the "production" of primary and secondary housing within the Mediterranean side of Spain, which González Reverté (2008) exposes in research work about models of touristic cities[28], confirm that the Spanish coastal land, in addition to providing some of the major metropolitan areas, is the growth engine of real estate in Spain. Indeed, this is corroborated by some of the indicators analysed, i.e.: 0.53 houses per inhabitant, which is an annual growth rate of 1.99% of primary residences between 1991 and 2001, and 13.39% of the whole housing park built between 1991-2001. There is also a tendency to the "littoralisation", or a "coast-lization", of the housing production, although it is accompanied by the emergence of such real estate dynamics in other areas beyond the first part of the coastline. The lift-off of housing production, in the second line and interior, is very strongly pursued by the metropolitan relocation of urban uses over the territory (decrease in the average size of families, new migrations, housing price differential), emergence of new geographic locations for residential developments (urban extensions, new developments, urbanization of well-connected spaces, etc..), or "consumption" of leisure (buying and selling of apartments and second homes for tourism).

Despite the "developmentalism", which has led Spain to make significant changes in its urban model of growth, the decline in the numbers on the benefits of the tourism industry, which was one of the engines of this model, has been constant over the last decade. In 2006, Spain was still the second destination for world tourism, but for the third consecutive year experienced a drop during the summer months. In 2004, the budget to keep the set of tourism infrastructure (airports, ports, hotels, beaches, etc.) exceeded by 25% the revenue from tourism. The excessive consumption of resources (land, water, electricity) and environmental degradation caused by this activity was, and still is, greater than the benefits to the society. Actually, it is an unsustainable model. In 2007, the tourism industry accumulated its sixth consecutive year of declining revenues. Despite the drop in profitability, in the same year it was planned to build 202˙500 new hotel rooms, mostly spread between Andalusia (126˙750), Canary Islands (52˙500) and the Region of Murcia (23˙000) (Marcos Rodríguez, et al., 2012).

If we analyse the urban parcel data, provided by the Land Registry during the 2006-2010 period, we see that in the last few years of the past decade, Spain has continued to develop urban land, despite the crisis and population loss[29], increasing the artificial surface to 13.38% in just four years, and in more detail in a 15.15% in undeveloped urban plots and 11.99% in built urban plots. This represents an annual growth rate of the area of urban parcels of 3.34%, this being for the built urban plots somewhat less than 3.00% (OSE, 2011).

2.2. 1990-2006: OVERALL FEATURES ABOUT URBANIZATION AND DEMOGRAPHY ALONG THE MEDITERRANEAN SIDE OF SPAIN

Based on theoretical concepts about urban sprawl, as well as key indices (such as land consumption, population densities, urban fragmentation and dispersion), this study, at this point, aims to provide an overall representation of the urban models and the main changes of growth patterns that occurred in Spain during the last few decades. In particular, the analysis relies on a temporal comparison through the period between 1990 and 2006, placing special emphasis on the urban development along the Spanish side of the Mediterranean.

First of all, from the geographical standpoint, *Spain consists of 17 Autonomous Communities and 2 Autonomous Cities, Ceuta and Melilla, situated in the North of Africa. From an administrative standpoint there are*

[28] González Reverté, F. (2008). El papel de los destinos turísticos en la transformación sociodemográfica del litoral mediterráneo español. *Boletín de la A.G.E.*(47), pp. 79-107.

[29] Worth mentioning that the period of analysis 2006-2010, is temporarily located further beyond of the housing boom

Universidad Politécnica de Cataluña, Barcelona TECH
Departamento de Tecnología de la Arquitectura
Centro de Políticas de Suelo y Valoraciones
Nicola Colaninno, Josep Roca Cladera

three levels: the Central Government, whose responsibilities reach the whole of the national territory; the Autonomic Government, the scope of whose responsibilities is limited to the territory of the individual Autonomous Community, and, finally, the Local Government, made up of the Town Councils in the municipalities; the Provincial Councils in the provinces, and the Inter-Island and Island Councils in the Canary and the Balearic Islands, respectively (European Environment Agency , 2011).

The Mediterranean side of Spain is represented by five Autonomous Communities. The continental part of the peninsula makes up the regions of Catalonia, Valencia, Murcia, and Andalucía (which also occupies an important part of its territory on the Atlantic side), while the fifth region is formed by the archipelago of Balearic Islands, as shown in figure 2.11.

Fig 2.11: Spain, from satellite, and the administrative division of the Autonomous Communities bordering the Mediterranean side (red line), i.e. Catalonia, Valencia, Murcia, Andalucía, and Balearic Islands (Source: By Authors, from World Imagery[30])

The greatest part of the Spanish national territory is located in the Iberian Peninsula, at the South-Western end of Europe. It includes, in addition to, two archipelagos: the Canary and the Balearic Islands, other smaller islands and the cities of Ceuta and Melilla. The country's peninsular section covers an area of 493˙514 square kilometres, whereas that of the islands amounts to 12˙484 square kilometres. The whole area (506˙030 square kilometres) makes Spain one of the 50 largest countries in the world and the second largest in the EU-27, behind France (European Environment Agency , 2011).

The length of the coastline can reach 10˙099 kilometres, if the mouths of the rivers, up to the point where tides make themselves felt, are to be included. The orography is characterized by a high average altitude, as 57.7% of the territory rises more than 600 metres above sea level, which gives Spain second place among the highest countries in Europe (European Environment Agency, 2011).

[30] *World Imagery provides one meter or better satellite and aerial imagery in many parts of the world and lower resolution satellite imagery worldwide. The map includes NASA Blue Marble: Next Generation 500m resolution imagery at small scales (above 1:1˙000˙000), i-cubed 15m eSAT imagery at medium-to-large scales (down to 1:70˙000) for the world, and USGS 15m Landsat imagery for Antarctica. The map features 0.3m resolution imagery in the continental United States and 0.6m resolution imagery in parts of Western Europe from DigitalGlobe. In other parts of the world, 1 meter resolution imagery is available from GeoEye IKONOS, i-cubed Nationwide Prime, Getmapping, AeroGRID, IGN Spain, and IGP Portugal. Additionally, imagery at different resolutions has been contributed by the GIS User Community* (ESRI, ArcGIS Online).

According to the National Institute of Statistics of Spain (INE), in 2012, Spain had 47˙265˙321 inhabitants[31] (23˙966˙965 women, and 23˙298˙356 men), which define a territorial density of about 93.4 inhabitants per square kilometre[32].

The pie-charts in figure 2.12 show the extension, in terms of covering area (in square kilometres), of each Region along the Mediterranean side; the amount of total population, and the territorial densities, both for the Regions as well as for the Mediterranean side of Spain as a whole.

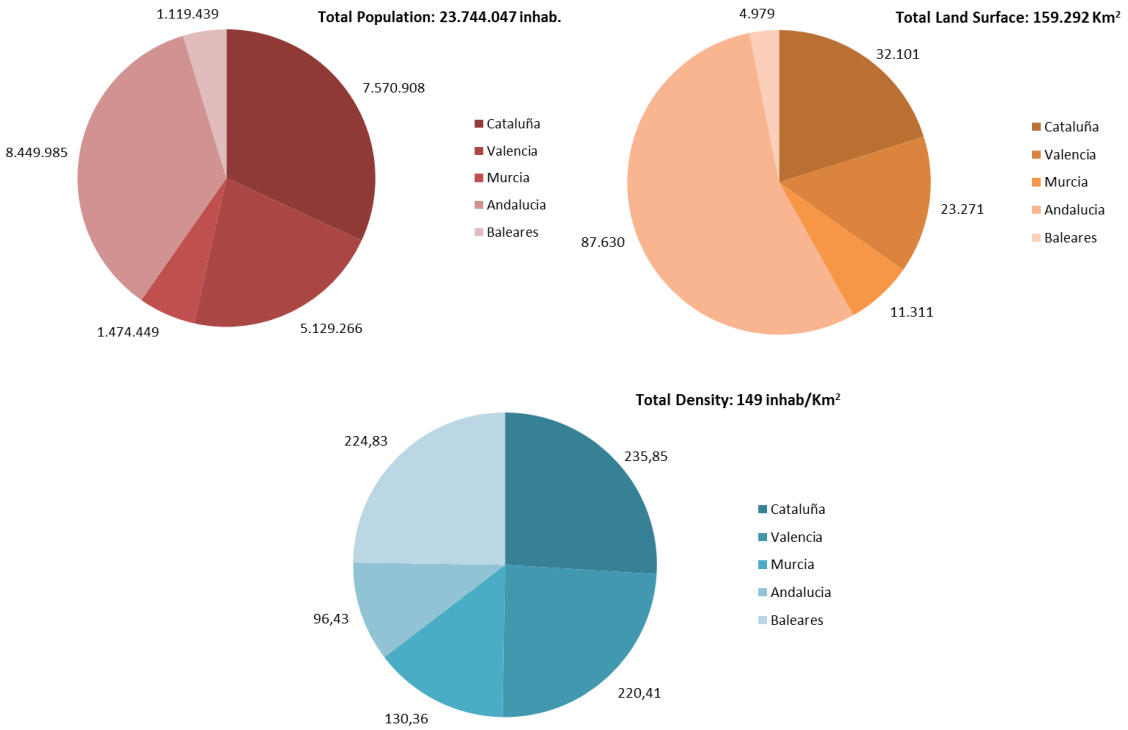

Fig 2.12: Population, Land Surface (covering area), and Territorial Density, for the Autonomous Communities of Catalonia, Valencia, Murcia, Andalucía, and the archipelago of Balearic Islands, at 2012[33] (Source: By Authors)

The five Mediterranean regions, together, cover a total amount of area of about 159˙300 square kilometres, which actually represents 31.5% of the entire national territory or almost a third of Spain. According to INE (2012), the population along the whole Mediterranean side reaches a total of 23˙744˙047 inhabitants, half of the entire national population, in which the results are distributed, in function of the regional administrative boundaries, as follows: 7˙570˙908 inhabitants in Catalonia; 5˙129˙266 in Valencia; 4˙474˙449 in Murcia; 8˙449˙985 in Andalucía, and 1˙119˙439 for the whole archipelago of the Balearic Islands.

Particular emphasis has to be placed when analysing urban expansion along the Mediterranean side of Spain, which, mostly during the last thirty years has been experiencing a special process of change in the classic paradigms of urban growth. In fact, the general concept of a Mediterranean city, as a synonym of compactness, relatively high density, functional variety and diversity, no longer finds a clear correspondence with urban and metropolitan agglomerates developed in this geographical area. Especially in large cities, only the central nucleus or nuclei preserve the aforementioned attributes of compactness.

[31] Official population figures resulting from the review of the Municipal Register, at 1st of January 2012

[32] As an example, think that Italy has 60˙813˙326 inhabitants (ISTAT-Italian National Institute of Statistics, 2011) and a land area of 301˙338 Km², reaching a density of 201.8 inhabitants per square kilometre, while France has 66˙007˙374 inhabitants (INSEE-National Institute of Statistics and Economic Studies of France, 2010) and 675˙417 Km² of land area, with a territorial density of about 97.7 inhabitants per square kilometre, and Germany with 81˙800˙000 inhabitants (DESTATIS-Federal Statistics Office of German, 2011) upon a land surface of 357˙104 Km² reach a territorial density of about 229 inhabitants per square kilometre

[33] Official population figures resulting from the review of the Municipal Register, at 1st of January 2012

2.2.1. Urban Development and Demography

The large increase in world population in the last century has produced an impressive pressure on natural resources, and the environment in general, and is currently threatening sustainable development within several geographical areas worldwide. Moreover, the pressure due to the population increase, often results in urban expansion dynamics, and at the expense of decreasing non-urban lands, such as agricultural land and/or forests.

Indeed, if we look at the spatial distribution of the most urbanized areas (calculated as the percentage of urban land upon municipal boundaries) along the Mediterranean side of Spain (figure 2013, right side), it is remarkable that land consumption in 2006 was mainly intense towards the immediate vicinity of the coastline, and around the most consolidated and populated urban nuclei (figure 2.13, left side) such as Barcelona, Valencia, and Sevilla, above all.

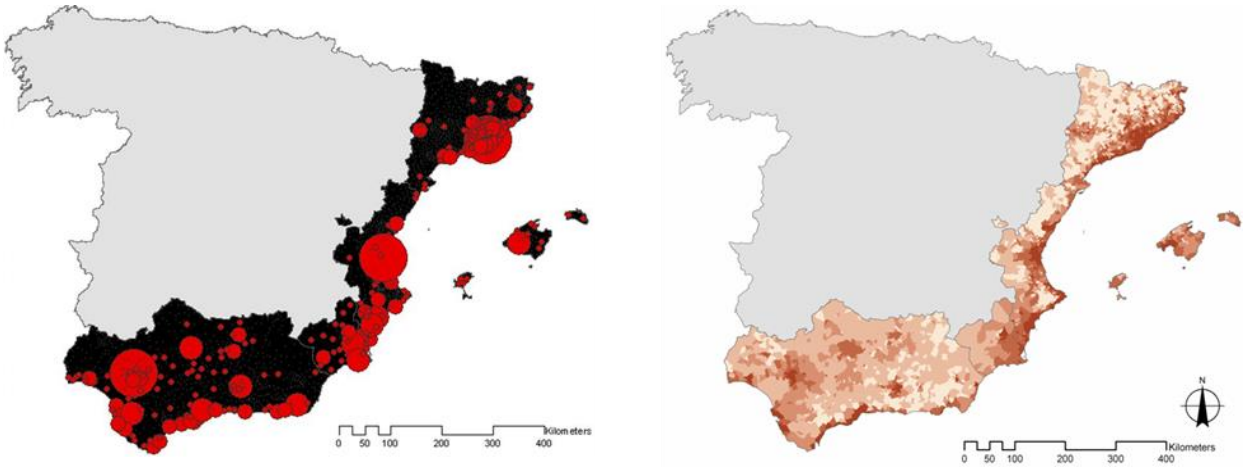

Fig 2.13: Spatial distribution of population and percentage of urbanized area, along the Mediterranean coast in 2006[34] (Source: By authors)

Certainly, the information about population is very important for purposes such as urban planning, resource management, and service allocation, hence suitable and accurate population estimation, at different levels, such as national, regional, and local, and its spatial distribution, become considerably significant data for understanding the effects of demographic trends on urban development (Weng, 2010). On the other hand, in order to objectively represent the main features and critical questions of urban development, further variables have to be taken into account in order to provide an effective quantitative analysis of the dynamics of urban growth. In particular, it could be achieved by means of a combination of fundamental variables such as the soil consumption rate and above all, the relation with the demographic curve over time[35].

Next, image 2.14 shows the comparison between the population growth rate[36] (left side), and the percentage of urbanized area (right side) over almost twenty years, i.e. between 1990 and 2006, and measured at three temporal steps: 1990, 2000, and 2006. The quantification of urbanized areas relies on our elaboration of the data provided by the European Project CORINE Land Cover (see section 3.2.1.1); while both population data and urbanization have been measured at each kilometre from the shoreline and over the first 80 kilometres from the coastline.

In 2006, the first kilometre of coastal territory, along the Spanish side of the Mediterranean, was around 30% urbanized. This percentage, which was 22% in 1990, and around 26% in 2000, drops sharply already in the

[34] CORINE Land Cover Project 2006

[35] Actually further variables need to be taken into account, mostly referring to the pattern of urban development in terms of urban forms, i.e. degree of fragmentation, dispersion, etc.

[36] For the data relative to the population, in the years 1990, 2000, and 2006, the database of the municipal register has been used, deriving from the survey of Spanish National Institute of Statistics (INE) for the years 1991 and 2001.

second kilometre (16% in 2006) to reach very low values at 20 or 40 kilometres[37]. The graphs in figure 2.14, also clearly shows how the first 10 km from the coastline is affected; both the rate of population as well as the amount of urbanized area, have reached very high levels. We also stress that the speed of the changes of both values, during the analysed period, is much more sensitive toward the coastline, and especially between 2000 and 2006, i.e. mostly in the last decade.

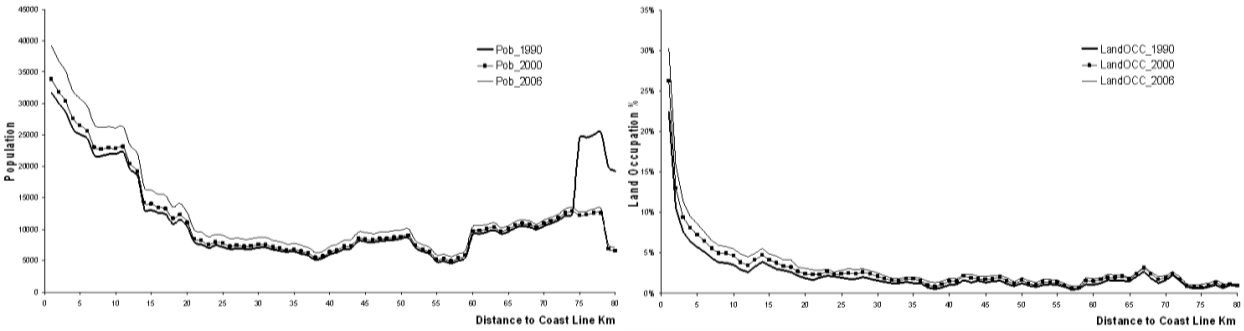

Fig 2.14: Population average[38], and percentage of artificialized area along the first 80 km from the coastline, and during the years 1990, 2000, 2006 (Source: By authors)

By reading the graph of population, it is possible to highlight that there has been a very sharp decline in the value of population, around the areas between the 70 to 80 kilometres from the coastline, and in particular during the decade between 1990 and 2000.

This occurrence could probably be a good argument for recognizing a starting point in the peak of the most speculative period, in the sector of construction, which the Mediterranean side of Spain has suffered, from Catalonia to Andalusia (even with some differences in the speed rate of growth). This is due to a strong tendency in the population to move toward the coast, which, when combined with mass tourism (i.e. seasonal demographic increments), represents important symptoms of increasing human pressure in this geographical area.

2.2.2. Overview of Main Characters and Drivers of Urban Growth

In general, during the last few decades, most of the major Spanish cities have lost population, typically in central areas, because of a demographic movement towards the metropolitan peripheries. The relative weight loss and "physical" dispersion of urban uses over the surrounding metropolitan area and the coastal area often has resulted in an exponential occupation of suburban areas based on low density residential settlements and the decentralization of urban facilities and industrial uses (Monclús, 1996).

The territorial transformation of a geographical area that has experienced a progressive increase of urbanized areas, and in particular in terms of secondary homes and seasonal housing, has produced a hybrid and heterogeneous system made up of an unplanned combination of natural and discontinuous urban areas. The production system traditionally associated with agriculture now mixes with the urban production system, and now occupies large areas of the coastal space (Vespere, 2008).

[37] We have evaluated here a difference in calculating the rate of urbanized land along the first kilometer, compared with data provided by the European Environment Agency, even if both are based on the same CORINE Land Cover Project. It is reported below the quantification made by the EEA: *In 2006, artificial surfaces accounted for 2.0% of Spain's total area. Their presence on the country's coastal strip is a phenomenon of particular concern— almost 45% of Spain's population live in coastal municipalities that account for just 7% of the country's territory. In 2006, artificial surfaces made up 22.7% of land area within the first kilometre of Spain's shoreline, while in 2000 they constituted 21%. In 2006, urban fabric accounted for 17% of land within one kilometre of the shoreline, port areas for 1.6%, and industrial or commercial areas for 1.5 %. In recent years, growth in the tourism and residential sectors has congested the shoreline on some parts of Spain's coast, particularly around the Mediterranean, and development has extended more than ten km inland. In 2006, artificial surfaces made up 9.4 % of this strip (8.5% in 2000), while urban fabric accounted for 6.5%* (European Environment Agency , 2011).
Some technical reasons could generate this difference between our measuring based on CORINE Land Cover and the data provided by the EEA.

[38] The value is calculated as the average of population between all the municipalities intersected by every strip of 1 km parallel to the coastline.

If we have a look at the urbanization rate in the entire Spanish territory, i.e. the increasing urbanized areas, measured using the CORINE Land Cover data at provincial level (figure 2.15), it should be pointed out that an impressive pressure has been undertaken mostly along the coastal provinces, and in particular along the Mediterranean side during the 2000-2006 period. Indeed, a part of the most striking cases in the provinces of Castellón, Malaga, and Cádiz which, during the period 2000-2006 have notably implemented the urbanized area; although some provinces in Spain have also decreased (as is the case of León or Salamanca, for instance). However, along the Mediterranean side a decrease in the urbanization rate has never been observed.

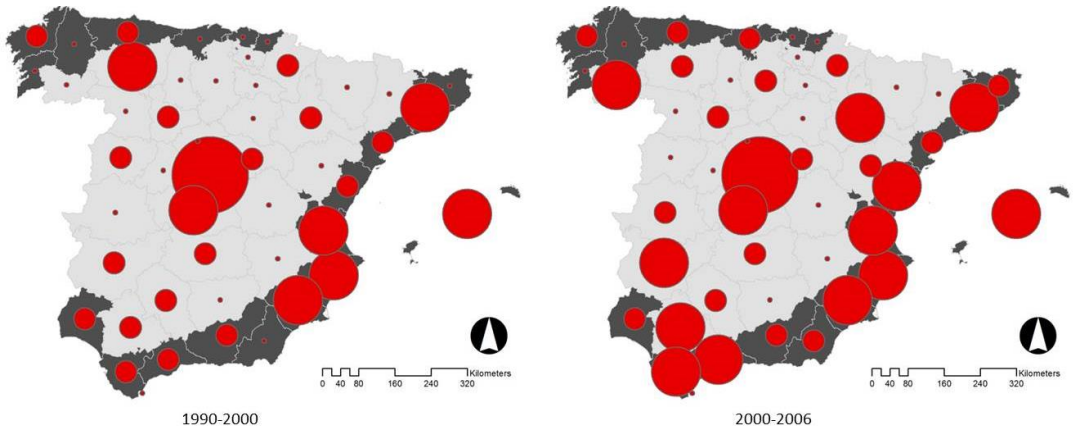

Fig 2.15: The increasing urbanized area, calculated from CORINE Land Cover at provincial level (provinces dark-grey colour, are those directly in contact with the sea) among 1990 and 2000, and between 2000 and 2006 (Source: By Authors)

If we take into account the demographic aspect and compute indices of urban density, i.e. the number of inhabitants per square kilometers of urbanized area, also at a provincial level, and again depending on the two temporal periods 1990-2000 (figure 2.16, left side) and 2000-2006 (figure 2.16, right side); we can see that almost all the provinces along the Mediterranean side have basically decreased in terms of density. This trend signifies that the increase in urbanization, at least since 1990, has been not at all consistent with demographic trends. Indeed, almost all of the Mediterranean provinces have experienced a remarkable decrease in urban density (dark-red colours) during the first period (1990-2000), except Gerona and Almeria (green colours). On the other hand, although a positive trend, i.e. a densification of the urban model, has occurred between 2000 and 2006 along the Catalan coastline (Gerona, Barcelona and Tarragona), and in the case of Alicante (probably due to an increase in population), the rest of the provinces, even in this second temporal stage are experiencing a decreasing trend, although minor, in urban density (figure 2.16).

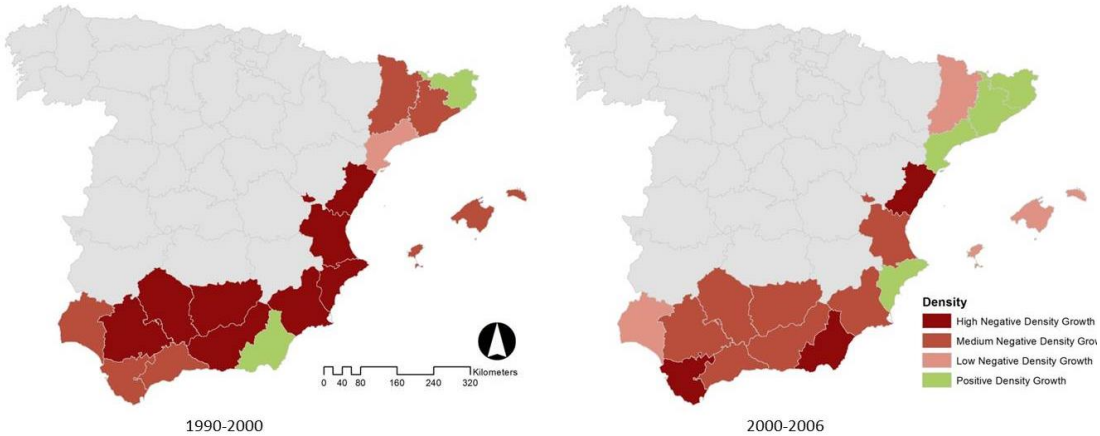

Fig. 2.16: Urban density along the Mediterranean side, at provincial level, for two temporal phases: 1990-2000, and 2000-2006 (green colour signifies positive values of density growth, dark-red signifies a decrease of urban density) (Source: By Authors)

Therefore, the amount of urbanized area along the Mediterranean side, between 1990 and 2000, was quite worrying mostly because it was not at all justified by an actual demand. At the level of Autonomous Communities, the graphs in image 2.17 show the growth of the urbanization phenomenon, in terms of percentage of land occupation, for each strip of 1 kilometre from the coastline and up to 80, for Catalunya (top right), Valencia (middle left), Murcia (middle right), Andalucía (bottom left), and the Balearic Islands (bottom right). The current situation, for the year 2006, is also provided (the top left graph) in a comparative analysis between the five regions at once. Here again, the analysis relies on (our own) quantification of data provided by the CORINE Land Cover project.

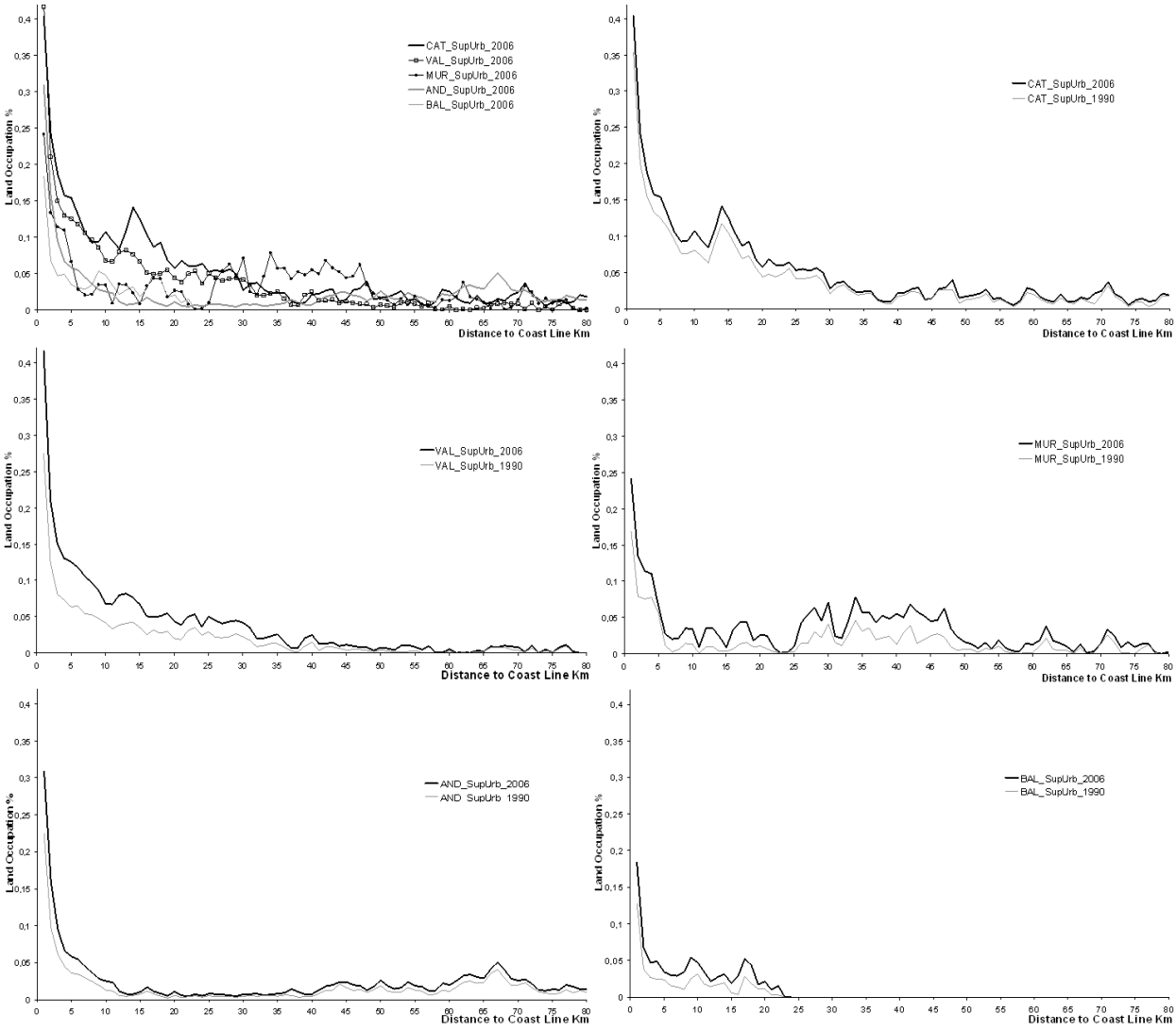

Fig. 2.17: Land occupation (%) at 2006 for the five Autonomous Communities along the Mediterranean (top left); and land occupation growth, for each Autonomous Community (top right until the end), experienced between 1990 and 2006 (Source: by Authors)

We emphasize that the Catalan coastline, compared to other regions along the Mediterranean coast, has grown at a slower rate, in relative terms of land consumption, from 35% in 1990 to about 40% in 2006[39]. The Autonomous Community of Valencia, for instance, failed in containing the explosion of urban developments along

[39] Data derived from analysis of CORINE Land Cover Project results

the coastline, thus raising the percentage of land occupation from a 28% in 1990 to 42% in 2006. In the Region of Murcia, we also witness a major leap in urban growth rate along the coastal area, from 18% to 25% (between 1990 and 2006), while along further inland areas, where the city of Murcia is located, the growth rate passes from 5% to 10%. In Andalusia, the growth rate is also considerable along the first kilometres of coastline, by increasing from 23% to 32%; while in the Balearic Islands, the rate of artificialized area increases from a 14% to almost 20%; even if, mostly in the case of the Archipelago one should consider that islands would need an *ad hoc* analysis (i.e. for separation).

In the same way, Marambio et al. (2011) points out that the impact of urban expansion along the Spanish Mediterranean coastline, when based on the analysis of the CORINE Land Cover data, reaches worrisome levels particularly in certain areas. In the case of the provinces of Castellón and Huelva, for example, urban growth has reached 40% in the last 20 years (urbanized soil has therefore almost doubled). Moreover, they remark that, in general, more than 40% of the urbanized surface is distributed at a distance of less than two kilometres from the coast.

The main drivers behind such a kind of urban phenomenon, which occurred in Spain, during the last few decades, and mostly in the coastal areas, have been well summarized by the European Environment Agency (2010), as follow:

- *Growing population density, though still below the EU average. In principle, this should produce less pressure on land. In 2000, Spain had a population density of 80 inhab/km^2 compared to the EU-15 average of 120 inhab/km^2. By 2006, Spain's population density had risen to 87.2 inhab/km^2, and by 2009 to 92.4 inhab/km^2.*
- *Economic development occurred later in Spain than in most other western and central European nations, but the country has seen strong growth in recent years.*
- *Spain's population has risen rapidly in recent years to reach a total of 46˙745˙807 inhabitants in 2009. Over the period 2000-2009, the population increased by 15.4 %. Immigrants account for a significant proportion of the population and in 2009 totalled over 5.6 million people (12 % of the resident population).*
- *Growing GDP, which reached 1˙053˙914 million €, in 2009 (current prices), though the rate of growth has slowed since 2006. Between 1995 and 2009 alone, Spain's net GDP rose by 135.7 % (current prices).*
- *One-third of the population lives on the coastal strip and in summer this area hosts four out of every five tourists travelling to Spain. This demographic pressure is a source of threat to many of Spain's natural coastal ecosystems.*
- *Since 1995, Spain has received growing numbers of foreign tourists (the total rose from 34.9 million in 1995 to 52.2 million in 2009). This process has taken place parallel to population growth. Air travel is the mode of transport most widely used by tourists visiting Spain. In 2009, the country received 1.12 foreign tourists per resident.*

2.2.3. Key Dimensions of Urban Sprawl: Magnitude, Density, Dispersion and Complexity

The analysis carried out in this section takes into account three of the main concepts of the urban growth process: the rate of population, the amount of land consumed for the urbanization, and the form of urban settlements, for around twenty years and across three temporal stages, i.e. 1990, 2000, and 2006. This allows us to detect the trend of urban development that occurred in Spain, placing particular attention on the Mediterranean side, which has suffered an important speculative process in the field of construction in the last few decades.

The data used to quantify the rate of urbanized land comes from the land cover/land use classification provided by the CORINE land cover project[40], which takes into account the aforementioned dates of 1990, 2000, and 2006. Indeed, according to many[41], the latter year represents a key date for the whole Spanish economy, as it was the beginning of the economic crisis, mainly caused by the real estate sector.

[40] CORINE Land Cover project is a joint initiative between the European Environment Agency and the European Commission and has affected 26 countries at European level, and includes the acquisition of data from ground cover classes through remote sensing techniques, using Landsat and SPOT satellite imagery, and photo interpretation. The categories employed in our analysis are those included in level 1 of the CORINE Land Cover Legend, which is named artificial surfaces (more details, about CORINE project, can be found in chapter 3).

[41] Fernando Gaja (2008) points out the necessity to find a starting point for an analysis of the speculative dynamics along the Spanish Mediterranean coast, and look at the final stage of the building boom between 1996 and 2006 and at the dynamics which generated it. The

Based on an investigation of the use of quantitative indices for analysing patterns of urban growth in Spain[42], four synthetic indices have been provided through the use of the factor analysis, and based on ten spatial metrics[43] capable of quantifying urban density and urban forms. In particular, firstly, the spatial distribution of the population density has been taken into account by using two different types of densities, i.e.: gross and net density. However, in order to provide an effective perspective about the form of the urban settlements, the main physical features of the urban profile have been taken into account, and the spatial relation between all the urban patches within the urban profile, in terms of distances. Depending on the input set of primary metrics, four synthetic indices have been defined, which are: *Magnitude*, *Density*, *Dispersion* and *Complexity*[44] (figure 2.18, and 2.19).

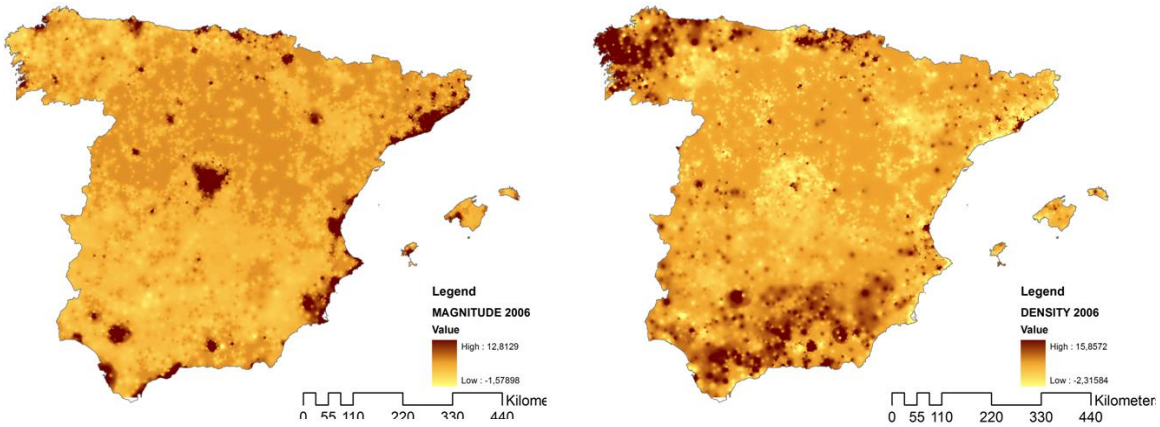

Fig 2.18: Spatial distribution of *Magnitude* and *Density* for Spain (Source: By Authors)

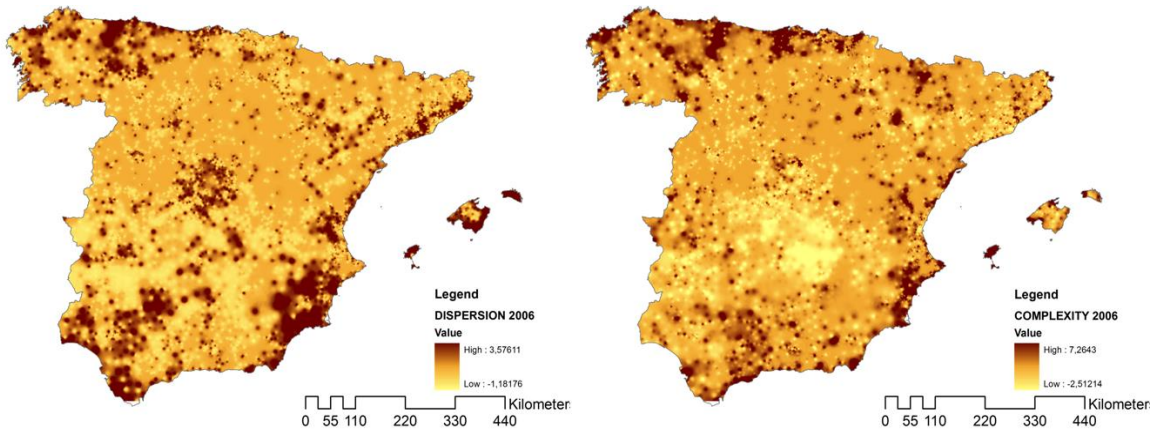

Fig 2.19: Spatial distribution of *Dispersion* and *Complexity* for Spain (Source: By Authors)

consequences deriving from this growth model should also be analysed and, above all, without forgetting that "real estate hyperproduction" reflects a model of real estate speculation developed to maximize profit, whilst leaving aside social and environmental concerns.

[42] Colaninno, N.; Cerda, J.; Roca, J. 2011. Spatial patterns of land use: morphology and demography, in a dynamic evaluation of urban sprawl phenomena along the Spanish Mediterranean coast. 51st ERSA congress, Barcelona, Spain.

[43] Land Occupation; Gross Density; Net Density; Shannon Diversity; Shannon Evenness; Degree of Landscape Division; Standard Distance; Gini Index of Concentration; Shape Index; Fractal Dimension

[44] It is critical to highlight a few of the limitations of the investigation, mostly concerning the database. The first problems were related to the data of population and the administrative boundaries. In fact, we found some faults in the database concerning the population: between the year 1990 and the 2006 the administrative boundaries of a number of municipalities changed. Moreover, due to the coarse spatial resolution of the outcomes of CORINE Land Cover, the urban areas of small municipalities were not detected, so we could only select 3500 cases out of 8000 municipalities. Another limitation derives from the generalization, provided by CORINE Land Cover, of the shape of the urban polygons. This produces less precision when measuring urban forms. Anyway, even with these limitations, we considered the outcomes of the experiment were certainly interesting and coherent, based on our empirical knowledge of the area under investigation (Colaninno, N.; Cerda, J.; Roca, J., 2011)

The synthetic index of *Magnitude* takes into account the percentage of urbanized land and the gross density of population[45], i.e. people within the administrative boundaries of a municipal area. Positive values of this index (or factor) are associated to high values (intensity) of human pressure, either for primary needs or speculative issues.

Density, instead, takes into account the net density of population, i.e. number of inhabitants per square kilometre of urbanized area within the administrative boundaries of the municipality. As previously stressed (section 2.2.2), this indicator provides a useful measurement for urban models. It means that, by keeping the number of inhabitants constant, if the built-up area is more continuous and made up of more intensive buildings (i.e. low proportion of detached houses), the net population density will be higher. Conversely, urban settlements formed by isolated and single-family homes will generally provide lower net density values.

The indices of *Dispersion*[46] and *Complexity* are based on a set of spatial indices that provide morphological measurements of the urban settlements, either in terms of structure (i.e. number of patches that make up the urban settlement and distances between them), as is the case of the dispersion index, as well as in terms of profile of the urban settlement, as is the case for the complexity index. In particular, positive values of *Dispersion* are associated with high values of fragmentation of the urban fabric and high values for distances between patches, i.e. lack of physical continuity. On the other hand, positive values of *Complexity* provide a model of land occupation made by a very "convoluted" or elongated profile.

In order to trace the trends of the indicators along the Mediterranean coast, and during the period between 1990 and 2006, the average value of each index has been estimated for each kilometre of strip parallel to the coastline, up to a distance of 80 km, and for three temporal stages: 1990, 2000, and 2006 (figure 2.20, and 2.21).

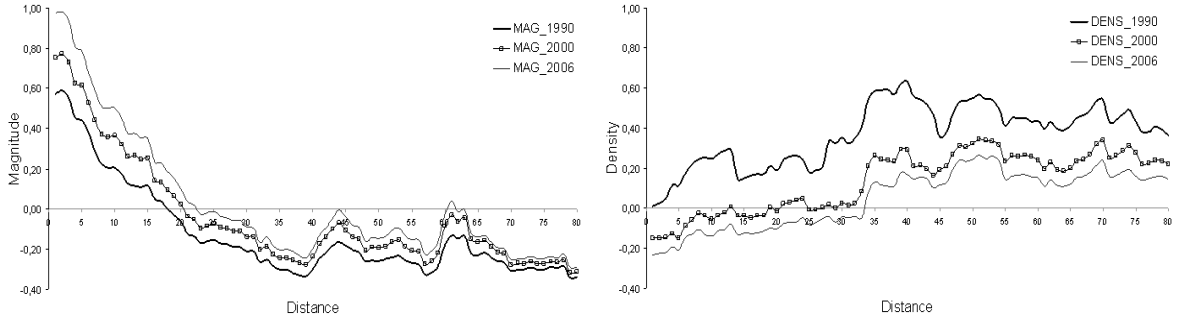

Fig 2.20: *Magnitude* and *Density* along the first 80 km from the coastline of the Mediterranean side (Source: By Authors)

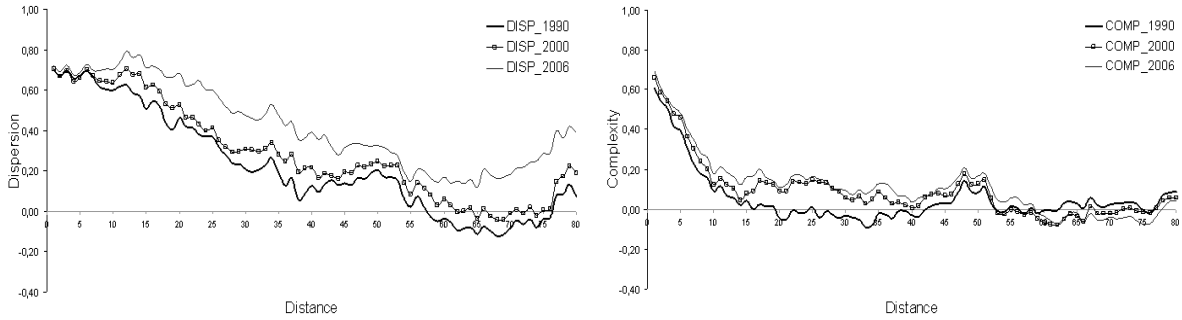

Fig 2.21: *Dispersion* and *Complexity* along the first 80 km from the coastline of the Mediterranean side (Source: By Authors)

[45] The density index might be gross or net, respectively depending on whether it refers to the number of inhabitants in a territorial unit, or the number of inhabitants in just the urbanized area within that territorial unit. Actually, both indicators place in perspective the number of people with an area; hence we speak about density. However, we emphasize here that both densities are static and not dynamic measurements, meaning that only the resident population is taken into account and not population flows.

[46] The dispersion index is a synthetic index, derived from the *Shannon* indices that account for the degree of fragmentation of an urban structure, the *Gini* index that calculates the level of concentration of urban areas in one or more polygons, and the *standard distance* that measures the distances between urban polygons weighted by the size of the polygon itself in terms of urban area.

The decrease in Density values is quite impressive, in particular, between 1990 and 2000. The inverse relationship between the increase in Magnitude and decrease of Density, mostly along the first 20 kilometres from the coastline, indicates different trends (actually opposite) in terms of population growth with respect to urban development. This means that there has been an important change in the pattern of urbanization that has shifted toward low density models during the last few decades. Dispersion and Complexity show a remarkably direct correlation with the increased rate of land occupation, while are inversely correlated with Density, mostly towards the coastline.

In general terms, it has been emphasized that a decrease in Density has taken place during the past two decades. However, the inverse correlation between the growing land consumption and human pressure (Magnitude), and the (decreasing) density (mainly along the first 20 kilometres from the coastline), is an index of the different speed in the population increase with respect to the urban expansion that, instead results in being more correlated with Dispersion and increasing Complexity of the urban fabric. Based on these variables, we could infer that the decrease in density accompanied by increasing values of magnitude, dispersion and complexity, which account for high levels of land consumption and the fragmentation of the urban texture excessively spread over the territory, often provide an effective point of view about the phenomena of urban sprawl.

An increasing trend in density accompanied by the drop in dispersion theoretically highlights a growth pattern based on the continuity of the urban texture often due to strategies of planning that rely on a fill-in kind of urban development. Indeed, this dynamic can be often observed in the central area of certain metropolitan systems that are currently experiencing a different phase of urban development, mostly based on filling in the gaps generated during the years of great expansion and economic boom, which occurred in Spain, and characterized by a "jumping-stains" type of urbanization. The central metropolitan area of Barcelona, for instance, seems to follow that direction[47].

Conversely, the mainly medium sized cities surrounding the main metropolitan center, often suffer the centrifugal movement of people and urban uses from the center to the periphery, thus experiencing a major change in expansion. Indeed, such a dynamic is followed by high levels of dispersion and fragmentation, besides the low density values. According to Dematteis (1998), the higher growth of minor and peripheral systems is the result of the balance of two movements: a decentralizing one, i.e. the moving of jobs from the central metropolitan system to the peripheral areas, or creating ex novo jobs in minor systems; and a centralizing one, with the development of new jobs in the metropolitan centre, jobs that are generally tied to highly qualified activities and services.

The analysis provided in this section was a previous approximation, made in 2011, for setting up an effective methodology for the analysis and quantification of different urban models, based on spatial metrics. Actually, the morphological part of that study has been rectified and enhanced here, by considering both the number of spatial metrics and the synthetic indices. Instead of using the CORINE Land Cover data, we have provided our own land cover data, obtained by using techniques of remote sensing (see chapters 4, and 5).

2.3. URBAN OVERPRODUCTION IN THE MEDITERRANEAN REGIONS: A “MISCONFIGURATION” OF THE ENVIRONMENT?

Without doubt, the urbanization process in Europe is currently experiencing a new phase of growth, which is not characterized by concentration but rather by the dispersion of both population and economic activities over the territory. The most visible result of this phenomenon is the migration from large metropolitan areas toward medium sized and/or smaller cities around the metropolitan core. In many cases, this phenomenon of diffusion has not been accompanied by a consistent development of services and infrastructures. This kind of urban development, which has arisen since the sixties, is often led by private needs and interests, and commonly appears in rural areas and coastal environments, as well as along main transport infrastructure routes (Vespere, 2008).

[47] In this way, an interesting point of view is provided by Marmolejo and Stallbohm: *En contra de la ciudad fragmentada: ¿hacia un cambio de paradigma urbanístico en la Región Metropolitana de Barcelona?* Scripta Nova, vol. XII, núm. 270 (65), 2008.

In particular, the suitability of flat areas for human installations, such as Industry, construction, or transport, and the availability of coastal areas that are often configured as tourist attractors[48], act as a modelling factors (or maybe "de-modelling") on the form of the cities. The recent phenomenon of urban speculation in place along the Mediterranean side of Spain, for instance, is a clear example that certain geographical conditions strongly impact the growth phenomena. Indeed, the increasing demand for coastal land for urbanization occurred during the last few decades, and has been one of the main problems concerning sustainability management and planning of coastal areas.

Under the umbrella of the XXI European Meeting of Architecture Students, EASA 2011[49], in which the issue of the "de-configuration" of the natural landscape along the Spanish Mediterranean coastline as a result of urban growth has been addressed, the Technical University of Valencia has promoted the publication of the book "*DeCOASTruction. La desconfiguración del litoral mediterráneo español*", edited by Fernando Gaja (2012) which, through the analysis provided by different scholars in the field of urbanism[50], delineates the main aspects that have characterized the process of urbanization along the Mediterranean side of Spain in the most recent decades.

In light of this, and based on the aforementioned work provided by Gaja, the following sections aim to examine in detail the phenomena of "uncontrolled" urban development through providing an analysis of the main growth dynamics, and their progression over time, which occurred in each of the administrative Mediterranean Regions, individually.

2.3.1. Catalonia between Urban Growth and Population Trends: Towards a Polycentric System?[51]

It is currently impossible not to speak about the Mediterranean cities along the Spanish coastline, without taking into account the phenomena of uncontrolled expansion, and the dispersion of artificial soil in rural areas in a discontinuous, but abundant way. Indeed, if it is true that, according to Gaja (2008), the Spanish model of economic development relies on three factors since its launch in the 1950's, these being: emigration, building and mass tourism; we could also state that building and tourism have most incisively conditioned political decisions in matters of urban growth in the last few decades. We face this kind of phenomena along the Catalan coast, although an inversion of the trend is perceivable, mainly around the Metropolitan Area of Barcelona (RMB). In fact, the dynamics of development which occurred in Catalonia in the last few decades, have been affected by strong speculative dynamics, mostly related to tourism and the construction sector, but some differences need to be stressed in relation to different geographical areas. Here, we must emphasize the idea of Font, et al. (1981), who argue that *there is no doubt that when trying to interpret the present urban Catalonia, the existence of the Barcelona metropolis appears as a predominant factor, as a directional center for all the system and summary of all the processes of concentrated urban growth. Starting from this confirmation of reality, a mechanical interpretation of the history of the confirmation of urban Catalonia from the sole point of view of the "capital-city" or the "industrial-city" cannot be inferred, as if all urbanizing processes should necessarily go through the sequence "industrial growth-urban dynamics", and as if the "urban project" were only possible in those prototype situations. On the contrary, the understanding of the diversity of situations and the close description of the small nuclei and regions, explains a process of formation which has been complex and heterogeneous, and can also help us to evaluate the capacity of some urban structures which exist in the rest of the Catalan territory to plan on their own their own urban role, up to a certain point "independently" from that of Barcelona* (Font, et al., 1981).

The northern Catalan coast, and in particular the area between Lloret de Mar (Gerona) and Calella de Mar (Barcelona), was a pioneering area for tourists visiting Spain. The construction sector, which transformed the Costa

[48] *In 2009, 86.8 % of foreign tourists (84.3 % in 2008 and 88.6 % in 2007) chose Spain's Mediterranean coast and its archipelagos as their destinations, resulting in an average of 5˙759 foreign tourists per kilometer of coastline (a 10.3 % decrease from 2008). This sector has not escaped the effects of the international economic crisis and in 2009 8.7 % fewer foreign tourists travelled to Spain than in 2008* (European Environment Agency, 2010).

[49] The European Architecture Student Assembly (EASA) 2011, was held in Cadiz (Spain) under the title DeCOASTruction

[50] The author and director of this thesis have participated in the redaction of the book by providing the first chapter about the urban development in the Autonomous Community of Catalonia

[51] This section is centred on the analysis about Catalonia included in the book "*DeCOASTruction. La desconfiguración del litoral mediterráneo español"*, edited by Frnando Gaja (2012)

Brava into a kind of "Spanish tourism Mecca", poses a threat to the territorial sustainability several decades later. Currently, from the Costa Brava to the Maresme, dozens of hotels, restaurants, apartments, buildings and campsites, built during the sixties and seventies, sometimes occupy even the smallest space between the beach and the train line (Blanchar & Pellicer, 2007).

Along the coastline of Catalonia, around 63% of the entire Catalan population is concentrated. Only between 2001 and 2006 the "Catalan coastal population" grew, as a whole, by 11.07%. The coastline extends nearly 700 km and consists of a variety of temperate coastal systems, of which 270 km are beaches. The industrial and commercial activities are strongly associated with the metropolitan areas of Barcelona (Central) and Tarragona (South), but are less dominant throughout the rest of the coastal area where other economic activities like tourism mainly dominate instead (Greenpeace, 2012).

The worrying state of conservation of Catalonia's coastal ecosystems, as is the case for much of Spain, is related to a process of uncontrolled coastal development and urbanization. In particular, think about the cases of the Costa Brava, El Maresme, the Central Coast, Costa Dorada and the Ebro delta, for instance. However, to get an idea of the touristic pressure, imagine that if along the whole coast of Spain each kilometre receives around 5˙759 foreign tourists annually (although the breakdown by region is quite uneven), Catalonia, which provides around 18˙868 tourists / km of coastline, leads these statistics[52] (Greenpeace, 2012).

The tourism sector, which has grown most rapidly in the last few decades along the coastal areas of Catalonia, has produced various patterns of fragmentation in the urban land uses, and an urban model that is strongly dependent on seasonal housing and services. In this sense, Marambio et al. (2011), in order to analyse the urban phenomenon along the Catalonian coast, proposed a *horizontal* section relative to the coastline (i.e. parallel to the coastline), analysing all 70 coastal municipalities, and emphasizing in particular the proportion of the secondary (often seasonal) residences with respect to the total number of residences along the Costa Dorada, the Costa Brava, and Metropolitan Region of Barcelona (RMB), as shown in figure 2.22.

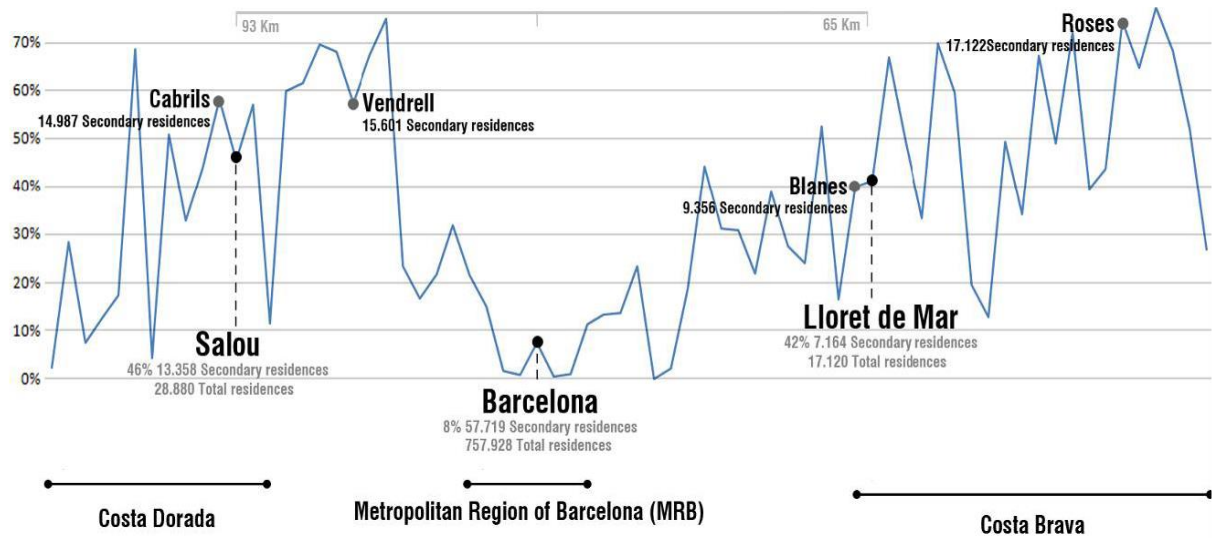

Fig 2.22: Percentage proportion between second homes and total residences (2010), for the 70 municipalities along the coastline of Catalonia (Source: Marambio et al., 2011).

The analysis provides an interesting outline, which shows that the highest number of second homes is in Barcelona (57˙719 units), a number representing, however, only 8% of total housing, i.e. the lowest percentage along the Catalonian coast. Lloret de Mar, in Costa Brava, for example, has 42% of second homes over total housing, which is well above the average value of 36.6%. The graphics, moreover, show that second housing is mainly concentrated in the areas of Cabrils (Costa Dorada), Vendrell and Roses.

[52] Ministerio de Medio Ambiente, Rural y Marino (2010) Perfil Ambiental de España. Report based on indicators.

The spatial distribution of the economic activity, as shown in figure 2.23, and in particular concerning the localization of second homes and the hotel market, provides a map of Catalonia where we corroborate the aforementioned concerns about the localization of second homes and hotels especially in certain zones of the coastline (Costa Brava, Costa Dorada and the surroundings of Tarragona). At the same time, we notice the presence of this kind of specialization in the Pyrenees. While, the area around Barcelona in particular specializes in services.

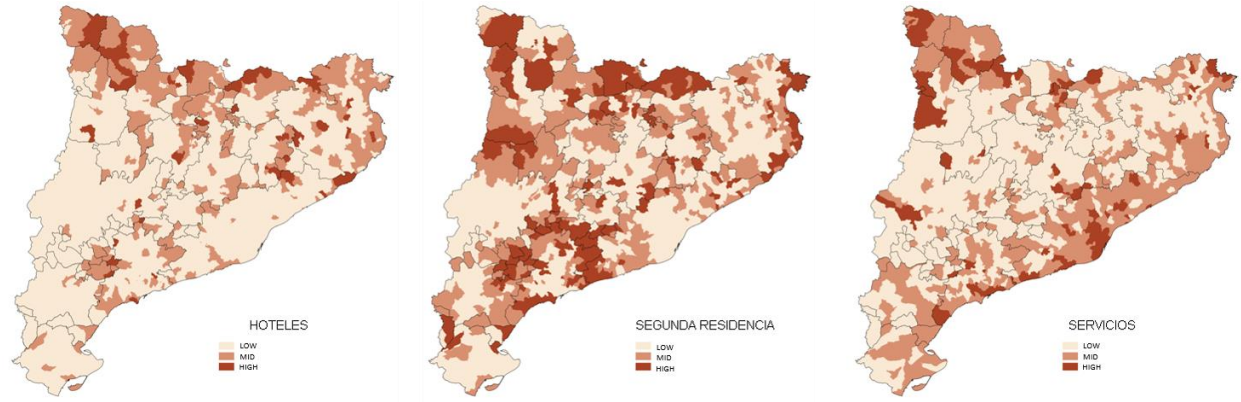

Fig 2.23: Economic specialization in second homes[53], hotels and services[54] in Catalonia (Source: by authors)

The case of the Costa Brava, in particular, is a prime example of the speculative logic that has occurred as a result of mass tourism. In fact, in the province of Gerona, unlike the provinces of Tarragona and Barcelona, there is currently a "bipolar" structure, due to the internal position of the capital (the city of Gerona is about 30 kilometres from the coastline), with respect to the coastal side, which is made up of a continuous linear system, along the coastline, competing with the consolidated structure of the central city. Hence, it is clear that the important (linear) urbanization occurring on the Costa Brava has been mainly pushed by extraordinary tourist flows often facilitated by economic and physical accessibility (consider the number of low cost flights).

This constant struggle between the traditional compact structure of Catalan cities, and new urban paradigms imposed by speculation dynamics mainly linked to massive tourism and seasonal residences, have provided an important variety in terms of urban syntax along the coastal side of Catalonia. Actually, if we have a look at the Catalan territory from above, it is possible to observe different morphological patterns of land occupation provided by coastal cities, and based on very different syntaxes. In particular, figure 2.24 shows a comparison of four main types of urban structures currently present along the Catalonian coastal area.

Fig 2.24: Examples of some main urban models along the Mediterranean side in Catalonia (Source: By authors)

The morphological profile of soil occupation, based on the continuity/discontinuity of the urban fabric, is the effect of different functional distributions, which *draw* urban structures that could be much more diverse in their composition or, perhaps, excessively specialized in specific functions, such as industry or residential type.

[53] CNAE, National Classification of Economic Activities.
[54] INE, National Institute of Statistics of Spain.

If we refer to the urban structure in the previous figure 2.24, Javier Monclús' words give us an interesting description about the change in urban structure occurring during the last few decades, passing from a more compact form (left side of figure 2.24) to a dispersed structure (right side of figure 2.24). He argues that more and more independent pieces are juxtaposed in a discontinuous fashion, and among which we find a proliferation of interstitial areas, urban vacuums and *vague terrains*, which produces a final effect of generalized loss in brute density. The growing protagonism of these new suburban landscapes is undeniable: it is necessary to acknowledge that, as J. L. Sert warned, they grow larger and larger and occupy increasingly larger portions of natural space (Monclús, 1996). A differential growth between population and urban density then arises, and this is a symptom of a low density urban growth.

In addition to this change of paradigm in the urban syntax, and the speculative dynamics related to tourism, the increase in population in Catalonia throughout the twentieth century has allowed its population to almost quadruple from 1˙966˙382 in 1900 to 7˙504˙881 in 2010 through not a linear evolution but continuously over time[55], which also represents a critical issue. At any rate, it has to be emphasized that, especially in the last thirty years, the demographic weight, along with the weight of urbanization has been redistributed throughout the whole Catalan territory, i.e. well beyond the city of Barcelona and the other provincial capitals. In fact, in the autonomous community as a whole, the population growth in recent decades, from the eighties, has suffered an important decline in the case of the central urban areas, although urban growth has followed different trajectories.

Nel·lo (2001) points out that if between 1960 and 1975 the resident population grew, passing from 2.5 to 4 million people, in the next twenty years the growth was just 200˙000 people. Moreover, between 1991 and 1996 there was even a small loss in population in absolute terms. Even the Metropolitan Region of Barcelona (the RMB) as a whole lost population relative to the total weight of Catalonia.

In addition, within the RMB, the development process generates an important *differential* growth, mainly due to changes of residence of the population, which particularly moves towards the second metropolitan ring. The municipality of Barcelona, between 1975 and 1996 has undergone a major reduction in population, from 1˙751˙136 to 1˙508˙805 inhabitants, with a negative migration balance compared to all the municipalities in the metropolitan area (although by 2010 the population in the city of Barcelona had again risen to 1˙619˙337[56]) (Figure 2.25).

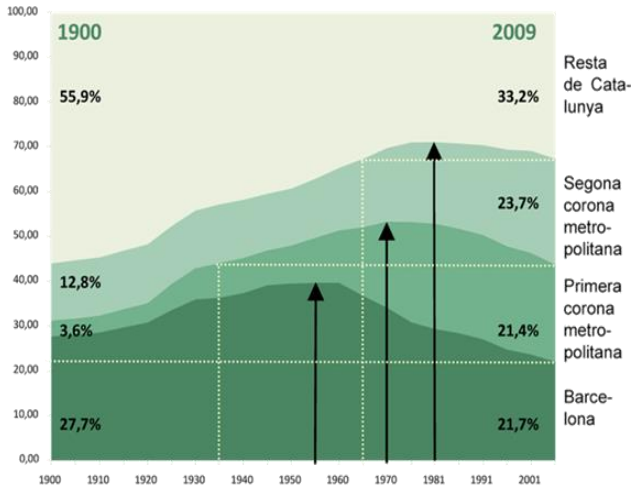

Fig 2.25: Evolution of the Catalan population by territorial ambits, 1900-2009 (Source: SERRA, J., Metropolitan Area of Barcelona)

For over two centuries, the main Catalan cities have experienced an almost incessant growth in population and an extraordinary increase in the relative weight (in terms of demography), urbanizing a considerable part of the rural areas. It has generated an asymmetry between the development of Barcelona and the rest of Catalonia,

[55] Institute of Territorial Studies. Slices of territorial information, number 5, July 2010.
[56] National Institute of Statistics, Municipal Census: Population at 1 January 2010 (23 December 2010).

producing large migratory movements towards the capital and a secular process of concentration that tends to gather people, activities and services in major cities in Catalonia and in particular Barcelona and its urban environment. Thanks to this, although the province of Barcelona, toward the coastline and around the capital, has had the highest growth in terms of area covered compared with other provinces, it has to be pointed out that in the space around Barcelona, and especially in the first 10 km from the coastline, the increase in urbanized land rate has maintained a more direct relationship with the population rate.

Actually, in the mid-seventies, other cities outside the Barcelona metropolitan area begin to build their own metropolitan structures, so gaining relative weight (Nel·lo, 2001). The *differential* growth rate, related to territorial distribution, often depends on the size of the municipalities, in terms of population, which shows that municipalities maintaining *positive* and relevant growth trends are the median, i.e. those municipalities from 5˙000 to 500˙000 (Figure 2.26).

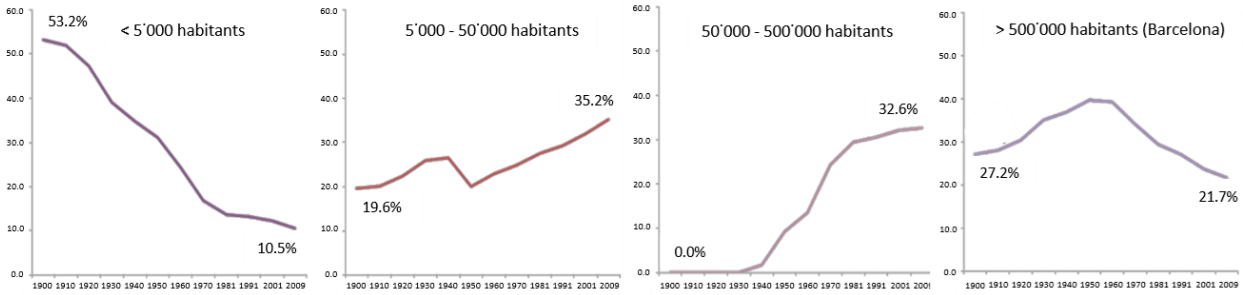

Fig 2.26: Evolution of the weight of the population by size of municipality, Catalonia 1900-2009 (Source: Institute of Territorial Studies. Sheets of territorial information, Number 5, July 2010)

The smallest municipalities have changed from retaining more than half of the population of Catalonia in 1900 (53.2%) to only one-tenth in 2009 (10.5%). In a context of overall growth of the Catalan population it is logical that many of the small municipalities have *jumped* to another category. Middle size municipalities have been over the last decade those which have shown a higher rate of growth, providing the category that collects a higher proportion of the population, with 35.2% of the total.

Large municipalities that experienced the most growth between 1940 and 1981 have seen stabilizing their share of the overall Catalan population, approximately one third (32.6%). The cities of Badalona, Terrassa, Sabadell and Lleida fell into this category in 1940 (L'Hospitalet had done it during the previous decade), while Tarragona, Mataró, Santa Coloma de Gramenet, Reus, Manresa Cornella de Llobregat did not until the decade of the 1950's, and others like Gerona in the 1960's. Barcelona, meanwhile, despite having regained positive growth rates that had been lost over the decades of the 1980's and 1990's, shows a growth rate below the average values of Catalonia, by losing weight to 21.7% of the total[57].

Currently, the regional hierarchical system, which historically was dependent mainly on the Barcelona metropolitan area, now appears to be structured by functional dynamics dependent upon the urban areas of Gerona, Tarragona, Lleida, Manresa, Tortosa, the Seu d'Urgell and other cities. Indeed, several authors have stressed how *intra-metropolitan* migration has origins and destinations much farther from the central municipality (Nel·lo, 2001). This provides a polycentric network, centred on Barcelona, which tends to expand its area of influence over the whole regional territory, thus generating phenomena of *tertiarization*, *decentralization* and *flexibility* of the economic structure (Nel·lo, 2001).

[57] Institute of Territorial Studies. Slices of territorial information, number 5, July 2010. Goerlich, F.J. MAS and M: The location of Spanish population on Territory. A century of changes. A study based on homogeneous series (1900-2001). BBVA Foundation. Bilbao, 2006, 2002-2009: INE: Census.

2.3.1.1. Regional Planning in Catalonia: a New Challenge

Particular emphasis has to be placed on the development of urban management in Catalonia, which is undoubtedly providing a new cycle of urban growth, by configuring a polycentric system model, mainly structured around the city of Barcelona, but based on multiple territorial systems.

In light of this, current territorial and urban planning, in recent years, has led to an empowerment of alternative and complementary urban centres, with the aim of providing a multipolar or polycentric structure. In fact, with the Master Plan of the Metropolitan Area of Barcelona[58] from the 1960's, the concept of City-Territory was already addressed, while in 1976 the Metropolitan General Plan raised the development of cities around Barcelona to compensate and make a counterweight to macro-cephalic development (Nel·lo, 2001).

As highlighted by Marmolejo y Stallbohm (2008), it is important to take into account that above the economic and social aspects that affect the processes of *spatial self-organization* of homes and businesses; there is the influence of public intervention which, in this case, has its highest realization in the territorial and urban planning policies.

The General Territorial Plan of Catalonia, approved by the Catalan Parliament in 1995, represents the instrument that defines the regional balance objectives of general interest to Catalonia and, at the same time, the guiding framework of actions to promote, through public interventions, the right conditions to attract economic activity in the appropriate spaces and allowing citizens to have high levels of quality of life regardless of the territory where they live.

The plan proposed, as one of its main objectives, *to slow down the present process of concentrations* in order to favour *those strength aspects of the areas with the capacity to rebalance the territory* inside and outside the metropolitan area (Nel·lo, 2001). From the implementation perspective, the General Territorial Plan of Catalonia defines a development model based on the *target image* of the demographic distribution projection in Catalonia for 2026. Moreover, the Plan is set to run seven areas, based on the territorial functionality, in which a Partial Territorial Plan must be developed: the Territorial Metropolitan Plan of Barcelona (approved 2010); the Partial Territorial Plan of the *Comarques Gironines* (approved 2010) Partial Territorial Plan of *Terres de l'Ebre* (approved 2010); the Partial Territorial Plan of *Camp de Tarragona* (approved 2010) the Partial Territorial Plan of *Comarques Centrals* (approved 2008); the Partial Territorial Plan of *Ponent* (approved 2007) and the Partial territorial Plan of *Alt Pirineu i Aran* (approved 2006).

The regional plan especially focuses on those territorial variables which could most strongly be affected, and in which there is a greater technical capacity to develop agreed proposals over a short period of time. These aspects are articulated in the three basic territorial systems: open spaces, urban system, and mobility infrastructure. In order to stop uncontrolled growth, a number of areas that are classified as being of scenic value are included within the *non-developable soil* category of the plan: such as natural heritage, ecological connectivity and agricultural values, geological heritage, and cultural goods of national interest (Source: Department of Planning and Sustainability, Government of Catalonia).

Difficulties in managing such a complex territory, and the fragmentation of the municipal map of Catalonia which has 947 municipalities for an area of 32˙118 km^2, often makes municipal urban planning a scale too small to develop effective strategies for management of land use (more than 156 municipalities are still without planning). Therefore, for realizing territorial planning purposes, the Department of Planning has considered the development of a set of Urban Master Plans to be of great importance, and which have accompanied and sometimes preceded the adoption of territorial plans. So, in the same period of the drafting and adoption of spatial plans, the Catalan

[58] The laws of the Catalan Parliament in 1987 obliterated the Barcelona Metropolitan Corporation that managed the Metropolitan General Plan from 1975 (27 municipalities affected), and created two metropolitan entities: the Environment Entity Ambient (18 municipalities) and the Metropolitan Transportation Authority (32 municipalities). In response to this policy carried out by the Catalunya Metropolitan Government of those years, a number of municipalities that had belonged to the former Metropolitan Corporation of Barcelona created the Association of Municipalities of the Metropolitan Area of Barcelona. At the time of its creation, the Commonwealth was formed by 24 municipalities. The area drawn by all the municipalities, included in some of these three new metropolitan institutions (36), sets the field that has been called the Barcelona Metropolitan Area or first metropolitan ring. During the first few years, this area did not have any kind of institutional recognition. The Comarcal Ley was approved in 1987, which established the Comarcas (41) as local government areas of Catalonia. The so-called Barcelona Metropolitan Area includes the entire region of Barcelona and part of the Baix Llobregat, Maresme and Vallès Occidental. Despite the complexity posed by the simultaneity of metropolitan institutions and new districts, such districts had and still have their own governing bodies and exercise the powers granted by Comarcal law (Haas & Riera Figueras, 2005).

government has promoted a total of 37 urban master plans, of which, at the end of 2010, 28 were finally approved, 3 had the initial approval, 3 were in development, and 3 other plans were waiting for award contest.

The Master plans are organized into six groups: coastal protection, mountain regions, preservation and management of heritage and landscape, urban areas, infrastructure, and strategic residential areas (Nel·lo, 2011), and are configured as a supra-municipal coordination tool, above all, to protect the territory, to manage mobility and implement infrastructure.

In accordance with the revised text of the Town Planning Act, the urban master plan is responsible, among other things, for the following tasks: to establish guidelines for coordinating the urban planning of a territory at a supra-municipal scale, set determinations for sustainable urban development, the mobility of people and goods and public transport, measurement of protection for undeveloped land, specify and delimitate land reserves for major infrastructure, and supra-municipal policy programming for soil and housing, agreed upon with the municipalities affected. In addition, in order to achieve these objectives, master plans include guidelines for municipal planning, which provide a useful tool for the coordination of municipal plans affected by common objectives and problems[59].

Among the master plans, the Urban Master Plan for the Coastal System (PDUSC)[60] is the instrument that aims to protect and add value to the Catalan coastal system, by ordering the development and avoiding the urbanization of the empty spaces (Burns et al., 2011).

The scope of the PDUSC affects a strip of 500 meters starting from the interior shore of the sea, and over the whole length of the Catalan coast. In this space, the Master Plan proceeded to suspend whatever was pending or any license which could involve moving towards the use of soils and that did not dispose of urban planning finally adopted. At the time of the writing of the PDUSC, 46.5% of the soil was classified as urban, 39.6% was protected, and 5.7% was developable while 8.2% was undevelopable. The intention of the plan was that almost all the undevelopable land, and much of the developable not delimited soil located on the coast, would be excluded from the urbanization process in order to ensure connectivity among the protected spaces, and to avoid the phenomena of conurbation in the urban nuclei, to open the inland protected spaces toward the sea and to ensure that no urbanization was situated on river mouths.

The Master Plan identifies little more than 24˙500 hectares (ha) of area, located on the prime Catalan coastline, which deserves to be preserved. If we consider that for 24˙500 ha, only 7˙000 ha were already protected previously, with the Plan of Natural Interest (PEIN), the importance of this intervention is clear to protect more than triple the area formerly defined (Burns et al., 2011).

The territorial policies in Catalonia, according to different local characteristics, and including the various structural components, provide, for the partial territorial plans, in addition to the provisions for urban planning, a themed content similar to the territorial general plan. The goal is to achieve a balanced distribution of growth between different areas bounded by the planning and the definition of specific nuclei capable of developing a so-called *nodal* role within the planned polycentric structure, in order to achieve an equal distribution of demographic weights, and urban and socio-economic development over the entire territory.

2.3.1.2. The Metropolitan Region of Barcelona (RMB)

Actually, economic activity within the region of Catalonia currently tends to be distinct and complementary between different urban systems. Each system creates its own cities, and thus its own capita. In turn, each city has its own territory, which is structured around a specific set of features. However, all of these

[59] Already within the coastal strategic plan of the RMB from 2005, promoted by the Government of Catalonia, Barcelona Provincial Council, Port Authority, municipalities of the AMB (Metropolitan Area of Barcelona), and coastal municipalities, were featured contents such as the recovery of the overall quality of the coastal landscape based on the protection and restoration of non-urban space, forming a continuous network for linking all protections local, district and metropolitan, ranging from urban parks and gardens to the natural areas; the reconstruction of urban fabrics in order to increase moderately the densities by integrating new economic intensive activities that increase the self-containment of workers. Also, to promote infrastructure and equipment and better urban integration of the industrial sites that would tend to provide more diverse activities, and generate new centers with tertiary activities in connection with new railway stations and public transport.

[60] Prepared in accordance with the Catalan urbanistic planning legislation - the Urban Planning Law 2/2002 of March 14, as amended by Law 10/2004 of 24 December.

systems ultimately refer to Barcelona, which indeed assumes the role of unifying the entire territory. This fact, on the other hand, causes the large relative weight that the city of Barcelona, with its metropolitan area, to represent an important position on the issue of the conceptual dichotomy between *policephaly-macrocephaly,* understood as a concern from a functional point of view above all.

In fact, among the regional plans, the Territorial Metropolitan Plan of Barcelona[61] (PTMB) which comprises 164 municipalities is of strong interest. The PTMB refers to a territory which, despite representing only 10% of the territory of Catalonia (3.236 km2), contains almost 70% of the population (4.8 million) and generates an equivalent proportion of Gross Domestic Product (GDP). The metropolitan area is thus the cornerstone of the Catalan regional structure. Regarding the system of settlements and, as highlighted in precedence, according to the Territorial General Plan, the PTMB aims for the configuration of a metropolitan region of Barcelona with a poly-nodal character with regional impact. That is, it rejects both excessive centralization and formless dispersion, and articulates the metropolitan space on a system of cities (Nel·lo, 2001).

A containment role in growth, due to urban "*mature"* centres, is currently particularly noticeable in the RMB, also due to Barcelona city; where in fact, as Marmolejo points out (2011), since the decade 1981-1991, the highest growth in the context of the RMB was in the second ring of the metropolitan area, which lies between 20 and 30 km (measured by road) from Barcelona, and today includes consolidated municipalities. In the decade from 1991 to 2001 the municipalities which experienced the greatest growth are those of the third metropolitan ring, 30 to 40 km from Barcelona, while in the last decade the municipalities with the highest growth are those within the more external ring that is located more than 40 km from Barcelona, where an *inside out* growth is clearly provided and where, the peripheral municipalities are now gradually obtaining a central role in metropolitan development.

In recent years, although significant and dramatic changes in the construction sector have already been generated, and most of the land consumption has been associated with industrial activity and housing production in discontinuous tissue, the RMB has gained in density, as previously stated, due to a process of filling-in of the gaps within the urban continuum, because the change in the planning and management has enabled a process of mending fragmented tissue caused by urban sprawl. A kind of inversion in the pattern of building, which leads to the existence of the first signs of a change in the use of the Catalan territory, which is directed at a process of reclassification of the peripheries and the possible beginning of the end of the fragmented city (Marmolejo & Stallbohm, 2008).

2.3.2. Valencia: "A Tsunami of Urbanization" [62]

In order to clarify the use of the term "real estate tsunami", Fernando Gaja explains that although the word tsunami fits with the strength of the image, with the description of what happened in the peninsular Mediterranean coast and in the Baleares Islands, it is misleading, because a tsunami is an unpredictable natural phenomenon, while what happened with the housing overproduction cycle along coastal areas has been definitely characterized by human development[63].

What happened during the period 1996-2007, was not the random effect of unexpected forces, disjointed from the "market". It was not an accident, or unforeseen catastrophe. Instead, it was the consequence of the combination of several factors that produced an explosion of unprecedented magnitude in the real estate sector (Gaja, 2012). Gaja attributes a good part of the responsibility to the wrong policies pursued, consciously, by

[61] On 20 April, 2010, the Government of the *Generalitat* of Catalonia approved the Territorial Plan of Barcelona.

[62] This section is mainly based on the analysis that Fernando Gaja proposed in the chapter entitled "*antes, durante y después del tsunami inmobiliario en el País Valenciano"*, in the context of the book "*DeCOASTruction. La desconfiguración del litoral mediterráneo español"*.

[63] In reference to the term tsunami, other authors have used that word to describe a phenomenon of uncontrolled massive urbanization. Javier Garcia Bellido, for example, speaks about an urban tsunami in a paper entitled "*Por una liberalización del paradigma urbanístico español (III): el tsunami urbanístico que arrasará el territorio*" published in 2005. In 2006, Ramón Fernández Durán also used that term in a high-impact paper (*El tsunami urbanizador español y mundial. Sobre sus causas y repercusiones devastadoras, y la necesidad de prepararse para el previsible estallido de la burbuja inmobiliaria*), later published as a book [Fernández Durán, 2006]. In 2003, the same Fernando Gaja published a previous paper (*El suelo como excusa: el desarrollismo rampante*), in which he suggested that at the beginning of the 21st century an exceptional juncture occurred by combining synergistic circumstances with the result of that boom of development, an urbanizing wave of unusual magnitudes, which from the coastal viewpoint could be graphically described as an urban tsunami. Even in the daily press, it has been widely used by Olmos [2005], Benlloch Perez [2005], Vázquez [2007], or Fernández [2007] (Gaja, 2012).

Universidad Politécnica de Cataluña, Barcelona TECH
Departamento de Tecnología de la Arquitectura
Centro de Políticas de Suelo y Valoraciones
Nicola Colaninno, Josep Roca Cladera

governments[64]. Actually, he spoke about a sort of agreement between public sector and private promotion to achieve the highest benefits, while minimizing the costs. In this way, a swollen real estate sector is strongly affecting the other economic sectors of the country. It is "funny", but the citation of Italo Calvino is extremely hypothesized, and in which Gaja proposes in "*La especulación inmobiliaria*", talks about a butcher in a village who leaves his own business to do real estate promotion, attracted by fast easy money.

It seems that the engine of growth in the real estate sector for the Autonomous Community of Valencia during the last few decades has been, without a doubt, tourism. A so-called tourism of "beach and sun", or as pointed out by Gaja, the tourism of the three S's: Sun, Sex and Sangria. But with some exceptions (one above all is the case of the city of Benidorm which covers more than half of all the hotel business in the region of Valencia[65]), the majority of tourism in Valencia is based on an "apartment tourism", through the promotion of residential housing. In fact, Vera Rebollo (1990), already in the early 90's, warned that the 74˙000 hotel beds in the coastal strip generate an important indicator if compared to the 1.45 million existing homes and tourist apartments.

In the Region of Valencia, between 1987 and 2000[66] the increase in artificial areas (which includes transport infrastructure, mines, and landfills) was estimated at 39˙948.40 hm^2, of which 16˙557.24 was destined to residential uses, 12˙376.36 for infrastructure and productive uses (industrial, commercial, etc.), 8˙487.26 were designated to mining, landfills and construction, and 2˙527.51 were used for green non-farm areas. However, looking at the growth patterns of urbanization, we find that the largest increase, both absolute and relative, is given by what the OSE[67] calls "exempt urbanizations or garden urbanizations", i.e. low-density residential development. While the commercial and industrial uses have also provided the basis for the phenomena of urban dispersion and fragmentation[68] (Gaja, 2012).

In the province of Castellón, for instance, the "brick" has replaced agriculture. Here, the "macro-urbanization" of Marina d'Or[69] is the clearest example of the paradigm shift from the urban development produced along the Spanish Mediterranean coast. Still, in 2007, the same Marina d'Or aimed at promoting a complex, which expected the population to increase up to 200˙000 inhabitants (from 10˙000), including 40˙000 homes, three golf courses, six hotels with 7˙500 beds, an artificial ski slope, a casino, private parking and public parking, and an aquatic park. Forecasts indicate that such a macro-urbanization will require 20 million cubic meters of water per year; slightly more than a city like Albacete consumes, for instance, (Fabra, 2007).

The coastline of the province of Valencia is an overloaded axle of road infrastructure, boardwalks, ports, apartments and villas with about 29% of its first kilometre of coastline completely urbanized. In recent years, the urban occupation has affected the beaches north and south of the province of Valencia as well, including the few surviving unspoiled stretches in the 126 kilometres of coastline. The proliferation of marinas along the coast of Valencia seems to have achieved an average of 10 facilities per 100 kilometres. Paradoxically, the V-21 motorway, which runs a few meters from the sea, and the national park of Albufera, have kept the advance of apartments in some parts of the coast in check (Vázquez, 2007).

The alarmism is more than justified. In fact, apart from the many complications from the social and economic standpoint; the environmental situation due to additional natural risks to which the coastal areas are generally subject is quite worrying. Imagine the phenomenon of coastal erosion. Indeed, the coastline of Valencia is one of the most eroded over the Iberian Peninsula: 14% is affected by serious erosion processes[70]. Nevertheless, of the entire shoreline of Valencia, which extends 470 km, only a third has been classified as undevelopable by municipal urban planning.

---

[64] In 1994, the Law Regulating Urban Activity (LRAU) was approved in order to "modernize" the sector, and to boost the "production" of urbanized land, by abolishing the exclusive attribution of the power to build to the land owner. With the LRAU the possibility that a third party, the "Urbanizer", was implanted and could undertake the development work without having any property, with the only requirement being that it was appointed by the public authority, upon submission and approval of a project called Integrated Action Programme (PAI)

[65] BALAGUER, A. [2011]: "Benidorm supone la mitad del turismo". *El Pais*, Wednesday, July 20, 2011, based on data from the study by the consulting firm Monitor Hosbec, 2011.05.
http://www.elpais.com/articulo/Comunidad/Valenciana/Benidorm/supone/mitad/turismo/elpepiespval/20110720elpval_17/Tes

[66] Data provided by the Observatory for Sustainability in Spain (OSE) in its Sustainability Report in Spain, 2007.

[67] Observatory on Sustainability in Spain.

[68] A reasonable urban standard density around 100-125 house/hm^2 is increased to 30-35 reaching, in some areas of single-family housing, values of 10-15.

[69] Marina d'Or is a Spanish business group, from Valencia, known for the resort "Ciudad de Vacaciones", located in the province of Castellon.

[70] ECOLOGISTAS EN ACCIÓN [2010.06]: Caos en la costa. Banderas Negras 2010. Ecologistas en acción, Madrid, pág. 44.

Among all the Spanish regions affected by sea, both on the Mediterranean and the Atlantic side, the Region of Valencia is the one with the lowest percentage of protected coastal area (figure 2.27), which is quite alarming. So, the soil which by its own nature is a limited resource, in some geographical areas is even more sensitive due to the character of scarcity.

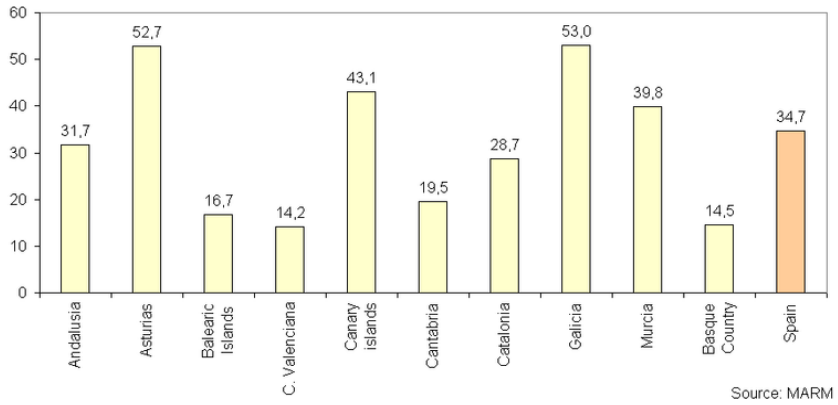

Fig 2.27: Percentage of protected coastline[71] (June, 2006) (Source: European Environment Agency , 2011)

All these concerns were officially confirmed by the local authorities, through the "Territorial Action Plan of the Coast"(PATL), published in 2006 (even though the Plan was yet to be processed), an instrument of supra-municipal planning that affected 60 municipalities directly affected by the relationship with the sea, and 17 more municipalities of influence. The Plan focused on the compulsory urbanization of the coastal strip, the densification and congestion in certain areas, the hegemony of an economic model with strong pressure on resources, particularly on the ground and the negative consequences of the model of diffuse urbanization[72].

According to Martí and Domínguez (2012), the metropolitan area of Madrid and the coastal regions on the Mediterranean side have been the most affected by the large phenomenon of territorial transformation. But, special attention, within the Region of Valencia, should be placed on the province of Alicante. They state that: *it is the Region of Valencia that has experienced the greatest increase in artificial surface at 50%, and the processes of intensive coastal urbanisation are largely determined by the "littoralisation" of urban development in Spain. As tourism is such a driving force behind the economy in many areas of eastern Spain* […]. *Of the three provinces in the Region of Valencia, Castellón, Valencia and Alicante, the latter has recorded the highest levels of coastal land transformation. According to the data, for the strip of land between 0 and 2 kilometres from the coast, Alicante is the third Spanish province (behind Castellón and Huelva) with the highest levels of artificial land transformation, but is the first province in the country for the strip from 2 to 5 kilometres, recording an increase of 92.2%, with all other Spanish provinces (including those on the Mediterranean and Atlantic coasts, and the islands) below 40%.*

Alicante province, therefore, has the highest level of artificial coastal land transformation, not just in the Region of Valencia but in the whole of Spain. The strong growth of both the continuous and particularly the discontinuous urban fabric has produced the greatest impact on the coastline of Alicante province, causing a major environmental burden in terms of resource consumption, emissions and waste. Furthermore, in recent decades these processes of intensive urbanisation along the coastline have transformed the landscape to a high degree, both on the coast itself and in immediately adjacent areas (Martí & Domínguez, 2012).

The early construction, between 1985 and 1989, of more than 70˙000 new houses in the Alicante coastal municipalities (which represented at that time almost 90% of the construction of the entire province), built

[71] *In June 2006, approximately 35 % of the country's coast was included in one of the available protection categories. The percentage protected varies widely between autonomous communities, with Galicia and Asturias having the highest proportion of protected coastline (over 50 %)* (European Environment Agency , 2011).

[72] The synthesis by Fernando Gaja about the PATL, actually is that of a plane of good analysis and good intentions, but a plan that in the end was placed in a position of continuity with the urban development happening until that moment in Valencia. In fact, according to estimates of the same Gaja, the PATL proposed a budget of 14,000 million euros, of which 87% was destined to infrastructures, 6% to Environment Management and 7% to Urbanism, and three quarters of this section was attributed to diversification of tourism as urban development.

primarily for tourism has brought unbridled growth in supply, and a restructuring of the offer itself, in relation to the dynamics of demand, already reaching in that moment higher values than the limits of tourism flows. This is an exorbitant growth phenomenon, manifested by a profound interweaving between investments and housing promotion. The central role attributed to the construction sector as an engine of economic growth in Valencia since the end of the 1990's (Vera Rebollo, 1990) is not surprising.

In the framework of a series of reports provided by the newspaper *El País*, Santiago Navarro (2007), reported that, according to the CORINE Land Cover report, in 2000, 49.38% of the first kilometre of coastline of the province of Alicante was already urbanized, and the invasion of private urbanizations, in some cases, has clearly crossed the 100 meter line of the public domain maritime-terrestrial. The most blatant examples of such runaway growth, are the urbanization of Bon Nou (seven bungalows 20 meters from the sea) in Villajoyosa, two towers of 22 floors on Levante beach, in Benidorm (the "vertical urban mecca" of tourism, along the Spanish Mediterranean coast), and a hotel with 24 floors, six meters from the shoreline in Calp.

It seems quite effective to conclude this section with the question, perhaps the most important one that Gaja emphasizes in the framework of his analysis about the region of Valencia. This could certainly be generalized for a bigger part of the whole country, and some suggestive images about a part of the urban landscape in Valencia (Figure 2.28), which justify the definition "European Florida" used to publicize tourism in Valencia. In particular, Gaja wonders about what to do with the huge stock of urbanized land and houses, whose digestion by the market seems impossible in the short and medium term, which is neither seen nor reused, and which have a tremendous impact on the ecosystem and the public purse.

Fig 2.28: The cities of Benidorm (top left) and Orpesa (top right), the resort of Marina Dór (bottom left), and the bay of Cullera (bottom right) (Source*: DeCOASTruction. La desconfiguración del litoral mediterráneo español*, 2012)

2.3.3. Murcia: "A Regular Inopia" [73]

Even in the region of Murcia which, with the exception of the area of the "*Manga de Mar Menor*", seemed to be safe from the Mediterranean trend of hyper-urbanization, the real estate tsunami has erased this illusion by generating a surprising strength in making an "innovative" model intended for mass tourism in an urban context defined as high-density, low quality and few provisions.

By reading these lines, we reveal the approach proposed by Juan Antonio Sánchez Morales (2012), in analysing the urban phenomenon that occurred in the region of Murcia, which is certainly an emotional approach tending to explain the loss of identity suffered by an area with a high value of natural scenery, which was subjected to a harsh and ruthless speculation, but most of all scarified in a meaningless way to create tourism; or at least inconsistent with the geographical context. The blind trust in an obtuse real estate development, and especially one directed at the tourism sector, is the inexcusable motivation of the current profound crisis, with its devastating effects on the sustainable development of the Region; a deep economic and identity crisis, which boosts a differentiated regional tourism model, and in which the cities are still immersed. It is a model which tried to incorporate "Resorts" in its development.

It seems to be a common sense, and a widely shared, idea that something went wrong in the urban management and planning of the last 20 years in Spain. In particular, various theorists set a milestone of urban developmentalism in 1998. Actually, according to Sánchez Morales (2012), passing from the Land Act of 1956 to the Law of Land Regime and Valuations of 1998, the concepts of developable and undevelopable soil were fully inverted. Until that time, the territory was "innocently" but fully protected.

Actually, it was undevelopable because, in order to classify as developable, explicit justification of need was required. With the new law, the opposite occurs: it was only necessary to declare the undevelopable, so in the practice all the remaining soil was automatically developable. As a result, and according to Martí & Domínguez (2012), *the increase of artificial land use carried out in the province of Murcia has been similar to the region of Valencia. In fact, between 1987 and 2000 the expansion of artificial surfaces is quantified in 14˙004 ha, which represents 62% of the artificial surface in 1987. This increase is the highest percentage in relative terms in Spain*.

This situation has fostered a speculative policy in Murcia, mostly related to the phenomenon of mass tourism, and especially from abroad. Actually, although the "new model" of development obviously comprises all the internal displacements, regional and national, mostly connected with the coastal side[74]; a long-haul displacement[75] model has been boosted particularly, on which the modern public and private tourism have been organized, and all connected dynamics of real estate speculation. The origins of this new model are to be found as far away as the north of Europe, where the means of transport is any of low-cost flight[76] to reach any golf course in any no-location.

The construction of airport infrastructure (the direct link to Europe), and the administrative limitless permissiveness, are synergistic factors that explain the emergence of the phenomena known as "Resorts", residential tourism based on closed urbanizations with unavoidable golf (Sánchez Morales, 2012). Indeed, if we only consider the connection between the United Kingdom as the origin and Murcia as the destination made by the Ryanair airline, as shown in figure 2.29[77], it is at least "curious" to note the number of available connections.

---

[73] This section is based on the examination Juan Antonio Sánchez Morales provides in the chapter entitled "*la Región de Murcia en su habitual inopia"*, in the framework of the book "*DeCOASTruction. La desconfiguración del litoral mediterráneo español"*.

[74] While the regional tourism movements have been redirected toward home ownership, the national movements, mainly originating from Madrid, move toward quite diversified destinations: home ownership, rental or hotel accommodation (Sánchez Morales, 2012).

[75] In the analysis and characterization of the urban areas, at a global level, cities acquire a "supranational or multinational status", like a consequence of the effect of the power that new technologies have to "connect" dispersed urban spaces, by constituting nodes through which the conditions of physical or geographical distance do not represent limits. From this overall vision of the urban network, it would be possible to define a new map of the world with a new system of cities, whose relevance would be determined by the degree of connections, so that the urban connectivity would be completely independent of the location or the physical size (Sánchez Morales, 2012).

[76] Despite the crisis, the airline companies are still operating, and are yet to inaugurate the new regional airport in Corvera, whose construction, is not without difficulty, look like advancing to its final completion (Sánchez Morales, 2012).

[77] Due to resolution issues, the original image, provided by Sánchez Morales (2012) in the book "DeCOASTruction. La desconfiguración del litoral mediterráneo español", has been redrawn here based on the 2016 map connections data provided by Ryanair. Actually, the connection between Murcia and Liverpool is no longer available.

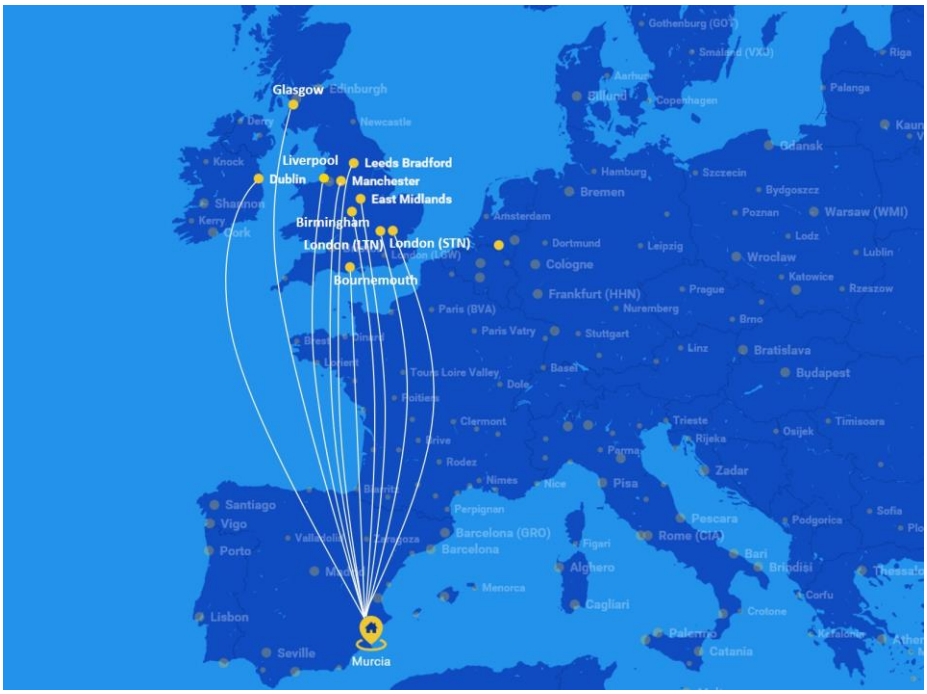

Fig 2.29: Ryanair connections between the United Kingdom and Murcia: Birmingham, Dublin, Bournemouth, East Midlands, Glasgow Prestwick, Leeds Bradford, Liverpool, London Luton, London Stansted, Manchester (Source: By Authors; adapted from 2016 ©Ryanair Ltd.|Map data - ©2016 GeoBasis-DE/BKG (©2009), Google, Inst. Geogr. Nacional, Mapa GISreal, ORION-ME)

The Region of Murcia is configured like an interstitial territory, a "residual" space between Castilla-La Mancha, Valencia and Andalusia (which in the framework of the Spanish administrative division, only obtained the Statute of Autonomy in 1982). So, for its dimensions, it could be argued that all the Region of Murcia is today “Mediterranean coast", and nothing remains outside the potential scope of the "predator" development of the tourism.

If we actually consider the isochrones, by car, and around the airports of San Javier and Alicante which allow access to the Region of Murcia, this space covers the entire regional extension, just considering one hour of driving. In this context, and due to the short distances needed to reach the beach, it was not necessary to directly destroy the coastal landscape (although in some areas, a kind of aberrational coastal urbanization occurred). It was "enough" just to contaminate, in a dispersed but generalized form, the rest of the region by “punctuating” the entire regional area with frequent episodes represented by resorts, which the architect Sánchez Morales defines as the oxymoron of residential tourism[78].

In most cases, these Resort exist, formally, only for their relationship with a golf course, which also generates another series of problems, that being that a golf course requires an important effort to provide continuity to their own existence in a completely inappropriate environment. Imagine the water consumption and maintenance costs in relation to the real demand of use. Throughout the twentieth century, before the arrival of the resorts and predominantly in the second half of the century, different tourism phenomena are recognizable on regional coastal development, in particular: *Mar Menor, La Manga, Puerto de Mazarron and Aguilas*, spotlights from which traditionally spread the on-going territorial transformation of the shoreline.

[78] The spread of the Resort phenomenon, similarly to that of a virus, all over the regional territory, during the first years of the last decade, was a true pandemic that only the "power" of the current crisis has dampened suddenly. It is perhaps the architect Enrique Nieto, in the ambit of the work "Murcia 2020", made a contribution to the Workshop for innovation and service development and sustainable architectural products, directed by Jose Maria Torres Nadal and the same Juan Antonio Sánchez Morales, who has come further in the study the state of affairs at the regional level, recording up to 100 resorts in different stages of development, about which he comments, "they are 100 incisions, 100 fractures, over our territory". Some of those Resorts are completed and in use, and others are reduced to mere commercial facades.

All these processes are similar in nature, but it is perhaps The *Manga del Mar Menor* which reaches the highest level of incompetence and disappointment, the complete transformation of a unique natural area in the Mediterranean space more than 30 km long[79] (Sánchez Morales, 2012).

In the 1960's, the promoter Tomás Maestre bought the tongue of land that marks the largest salt lake in the Mediterranean, builders and municipalities have done nothing more than build. In its 36 kilometers length, there is almost nothing of land free of urbanization (figure 2.30). This is the "first line of the coast" in Murcia which, according to the 1988 Coastal Act, is for public use. Moreover, the *Manga del Mar Menor* is threatened due to the predicted rise in sea level (15 centimetres by 2050, according to the Ministry of Environment) that discourages further cementing the "tongue" of land that separates the *Mar Menor*, from the Mediterranean (Méndez, 2007).

Fig 2.30: View of the southern section of the sleeve (*La Manga del Mar Menor*) at the beginning of the development works, and similar view today, after around 50 years (Source*:* Sánchez Morales, 2012; Gaja, 2012)

In parallel to the aforementioned, and maintaining the idea that speculation has greatly affected the natural landscape of Murcia, even so, it is significant to point out that the Region still maintains, in the framework of Spanish Mediterranean area, the lowest percentage of urbanization in the first kilometre of shoreline, 13.6% against the 49.38% of the neighbouring Alicante province[80].

In 2007, Rafael Mendez, warned that the urbanization of *Marina de Cope*, with 11˙000 homes, 22˙000 hotel rooms, five golf courses, inland marina with 2˙000 berths and an investment of 3˙800 millions of euros, would create a sort of Marina d'Or (like the one in the province of Castellon, Valencia), promoted by the same regional government in the context of a national park which was declared unprotected by law in 2001, and was threatening the region of Murcia. The same Rafael Mendez, in 2012, wrote in *El País*, that the Constitutional Court has annulled, almost 12 years later, an article of the land law by the regional government of Murcia, which declared 11˙000 hectares of unspoiled coastline unprotected from urbanization. With the bursting of the housing bubble, failure comes when, fortunately, Marina de Cope, the jewel of the unspoiled coastline of Murcia, is not yet built. Thus, in light of this, it seems appropriate to close this section by showing a few images from the landscape of Murcia (Figure 2.31), in order to demonstrate which kind of "values" have to be preserved, in the future, in a scenario like the one analysed in this research.

[79] It should be noted that for urbanizing "*La Manga*", a law was defined ad hoc, the Law of Centres and Tourism Zones of 1962, which allowed circumvention of the constraints established by the Land Act of 1956, and is still in vigour (Sánchez Morales, 2012)
[80] Strategy for Coastal Sustainability, Environment Ministry of Spain

Fig. 2.31: Murcia: Arenales y Salinas de San Pedro del Pinatar (top left), Calblanque (top right), Cabo Tiñoso (bottom left), Cuatro Calas (bottom right) (Source*: DeCOASTruction. La desconfiguración del litoral mediterráneo español*, 2012)

2.3.4. Andalucía: "Destruction at All Coast" [81]

In line with Marcos et al. (2012), here we aim to emphasize the effect of urban expansion in Andalucía, from an environmental point of view because, in order to measure the severity of the speculative phenomena of recent years, we need to observe the effects that it implies on the surrounding landscape.

The coastal system in Andalucía is defined by six major coastal units: mountains, coastal platforms, plains (coastal, alluvial and deltaic), dune systems, wetlands (marshes, estuaries, lagoon complexes) and waterfronts (cliffs, beaches and coastal lowlands). The geographic location of the Andalusian coast favours wealth of habitats and high levels of marine and terrestrial biodiversity. 40% of species of wild flora, located along the coast[82], are currently endangered, threatened by the high anthropic pressure[83] (Marcos Rodríguez, et al., 2012).

The region of Andalucía has the highest coastal extension in Spain, and a "leading" position in terms of visitors per year. The deterioration of coastal ecosystems is the other side of the coin in this overwhelming success, with a brilliant growth rate for the real estate sector, which has been accompanied by all kinds of infrastructure, leisure endowments, golf courses, etc. (Marcos, Jiménez, & Del Río, 2012).

The cities of Andalusia, mainly the most dynamic (in terms of urban development), i.e. those cities of over one hundred thousand inhabitants and those cities toward the coastline, have experienced strong growth in the artificialized areas and in the last ten years. Not even that kind of growth has been justified with the growth

[81] This section relies on the analysis that Pilar Marcos Rodríguez, Elvira Jiménez Navarro, and Sara del Río Paredes (members of Greenpeace), provide through the chapter entitled "*la urbanización en el litoral andaluz durante los últimos 10 años. Destrucción a toda costa*", in the framework of the book "*DeCOASTruction. La desconfiguración del litoral mediterráneo español*".

[82] Ministry of Environment. Junta de Andalucía. (2008). Andalusian Strategy Proposal for Integrated Coastal Zone Management.

[83] Road construction and urbanized areas so close to the sea, in the Malaga coast for example, leaves only very altered fragments of different vegetation and biological communities (Marcos et al., 2012).

experienced by the population living in them. This disproportionate growth has been well above the population growth, which all of the Andalusian municipalities have taken.

This is shown especially in the so-called medium-sized cities, 50˙000 to 100˙000, which have increased their population by 115.9% since 1956, but however, have a 593.6% increase in built area. In large cities, those with more than 100˙000 inhabitants, the population grew by 92.8%, while the urban area grew 353.3%. The built area growth has also been above 300% during this period in other populations of the Region, but it is the municipalities that occupy the coastal strip. It is home to 35% of the population of Andalusia, where there is a more intense population growth and therefore constructed area (Donaire, 2008).

The following table 2.2 shows the amount of artificial soil surfaces in 2000 and 2006, and its percentage change between these years, beside the population census in 2009 with the change occurring between 2001 and 2009. The data refers to the provincial capitals, except for Cadiz, as it is an "island" whose municipality is fully urbanized, so Jerez has been included as being the largest city in that province. Two cities (Ayamonte and Vera) have also been included due to their share of the "dubious honour" of occupying the top positions in increased percentage of artificialized soil (Zamorano Wisnes, 2011).

Population	*Artificial area in 2000 (ha)*	*Artificial area in 2006 (ha)*	*Variation 2006-2000 (%)*	*Population 2009*	*Variation 2009-2000 (%)*
Almería	1˙801	2˙283	26.8	188˙810	-2.9
Córdoba	6˙250	6˙707	7.3	328˙428	0.8
Granada	2˙027	2˙251	11.1	234˙325	-0.3
Huelva	2˙633	2˙955	12.2	148˙806	0.6
Jaén	980	1˙161	18.4	116˙557	0.4
Jerez	3˙305	3˙900	18.0	207˙532	1.6
Málaga	6˙253	6˙837	9.3	568˙305	1.0
Sevilla	7˙216	7˙453	3.3	703˙206	0.3
Ayamonte	336	852	153.0	20˙334	2.6
Vera	178	758	326.0	13˙985	-0.9
ANDALUCÍA	145˙748	168˙922	15.9	8˙302˙923	1.5

Tab. 2.2: Evolution of artificialized soil surface and population for some cities in Andalusia[84] (Source: Zamorano Wisnes, 2011)

According to Marcos Rodríguez, et al. (2012), the phenomenon of “urban overproduction” (which was actually unstoppable for four decades), has spread to the farthest and most well preserved corners of the Andalusian coast: Almeria, Cadiz and Huelva. In 2005, 34% of the first kilometre of coastline along the Mediterranean side was already urbanized; this figure rose to over 59% in Andalucía. Just a year later, in 2006, the number of homes planned on the coast doubled: 1,479 million new houses. The Regions of Valencia, Andalusia, and Murcia exceeded the amount of 300˙000 projected houses. Most of the new residential areas were focused around golf course projects. The case of Andalusia stands out, where there were more than 150 golf courses planned.

In 2007, in the peak of the urban madness, the "brick" in Andalusia was consuming an average of 12.81 hectares per day, of which 9.23 were located on the coastal provinces. Greenpeace catalogued about 683˙350 houses and planned tourist places, throughout its 817 kilometers of coastline, of which the highest percentage was for Almería, with 320˙000 houses, mostly belonging to the urban plans for Vera and *Cuevas del Almanzora*, followed by Malaga with 154˙600, Huelva with 126˙750, Granada with 54˙000, and Cadiz with 28˙000. Certainly some reasons could be found to justify this type of uncontrolled urban development, at least partially; such as the empowerment of young people, which even without assuming an increase in population has led to the need for new homes, or the reduction in number of persons per household, which also represents an increase in housing to accommodate the same people, or, finally, the increasing number of tourist residences in a country where tourism accounts for over ten per cent of GDP, and in Andalusia, as of 2007, accounted for 12.5%[85]. However, it is a fact that, in the whole of Andalusia, growth in the consumption of land that is more than ten times the population growth can be described in many ways, but in no way could be defined as rational or sustainable (Zamorano Wisnes, 2011).

[84] This is based on data from the Digital Atlas of the urban areas of Spain's Ministry of Housing.
[85] Exceltur (2009): Estudio de Impactur Andalucía 2007.

Universidad Politécnica de Cataluña, Barcelona TECH
Departamento de Tecnología de la Arquitectura
Centro de Políticas de Suelo y Valoraciones
Nicola Colaninno, Josep Roca Cladera

The coasts of Almeria and Granada are the least urbanized in Spain and, simultaneously, the most threatened. In fact, today, urban developers are focusing their attention on these areas, after exhausting the soil in other parts of the coast. Thus, Almería is currently experiencing, probably, the largest urban explosion on the Mediterranean side of Spain. However, the coast of Almeria was spared from the developmentalism of the 1960's and 1970's, but it seems that at present coastal municipalities have approved plans for tens of thousands of houses. Moreover, in Almeria, "the cranes today compete with the greenhouses". In fact, the current agro-tourism and industrial development on some parts of the coast is causing rapid deterioration of natural conditions that characterize this coastline. The plastic of the greenhouses, in some cases, reaches the edge of the sea.

The situation is no better in Granada, the coastal province with the smallest coastline. Its 81 kilometers of coastline host a "good" showcase of urban abuses: from hotels which invade the maritime-terrestrial public domain, to the greenhouses "that reach the waves", according to the words of Francisco Javier Egea, of Ecologists in Action. The difficult topography of the coast of Granada, full of cliffs and rocky beaches, is not an obstacle to urban promoters. Almuñécar's population, for instance, has grown 18% in its area in five years, and in other coastal towns, such as Rubite, with 468 inhabitants in 2006, it is planned to build 3˙500 homes in the next decade (Méndez and Pérez, 2007).

At present it is difficult to find a single meter of the coast of Malaga free of cement or brick. Indeed, the 208 kilometers of Málaga's coastline, especially those between the capital and Manilva, on the border of Cádiz, are a continuous wall of concrete and glass barely interrupted by the mouth of some rivers. In the whole province, the first kilometre from the sea to the interior is urbanized by 50.8% and in many points the buildings are located almost upon the sea. The area around the city of Marbella collects some of the most significant strategic urbanizations on the coast. Its 26 kilometers of coastline are some of the most abused of the province, and property development in recent decades has greatly "punished" the beaches, which are the real engine of the tourism in Malaga (Pérez, 2007).

In 2003, only 25% of the total coastline, in the province of Malaga, was free of buildings, and coastlines like Benalmádena were already completely urbanized by 2002. The number of hotel rooms on the Costa del Sol have grown by 54.8% between 2001 and 2010 (in just nine years), while overnight stays increased by only 17%. In 2004, in Costa del Sol, hotels began to be offered for sale, because of low profitability. Even so, in 2005, only in the Costa del Sol over 2˙681 hotel rooms were built. In Andalusia between 2000 and 2004 a 29% increase of their hotel rooms occurred, compared with the 14% of the national average[86].

In the province of Huelva in 2007, 10% of the coastline was already occupied by urbanization, although the growth rate in this area was somewhat slower and less intense with respect to the rest of Andalusia. At any rate, the growth rate between 1991 and 2002 was unstoppable, reaching an increase of around 60% in terms of housing along the coastline, according to the 2007 report about the "Destruction at all Coasts" made by Greenpeace. In particular, the urban model here was mainly based on the occupation of large portions of land for townhouses and single-family homes, instead of tall buildings[87]. In the municipality of Punta Umbria, for instance, several natural areas covered by forests were threatened in order to allow new construction along the coast. It was planned to replace 60˙000 m^2 of forest with "bricks", and in order to justify the project, the City stated the need for housing. However, it should be noted that half of the houses in the municipality remain empty during 9 or 10 months per year (Marcos Rodríguez, et al., 2012).

Ginés Donaire (2008) points out that, actually, the elevation of urban values has been critical to the loss of agricultural land and forests. Indeed, urban fabric has affected farmland (47%) and forests (33.2%) in order to satisfy the interest of speculators. Seville and Malaga are the provinces in which the rural extent has been most affected, losing respectively 16.66% and 19.66% of agricultural areas. On the other hand, the population of large cities grew by up to 92% and urban land up to 353%.

Marcos Rodríguez, et al. (2012), remark that this "exceptional" urban development has led to an exponential development of golf courses and marinas in Andalusia. Furthermore, golf courses are one of the clearest examples of urban development subject to speculative interest. According to the Counsel of Tourism and

[86] Greenpeace (2010). Destruction at all coasts.

[87] Actually, there are also good examples of the "traditional" model of development based on apartments and buildings, as in Isla Canela, The Portil or Matalascañas. Towards La Antilla and Lepe, to the east, it is possible to find blocks of apartments situated second and third beachline, preceded by a front of nailed houses, often, a few meters from where the waves break (Albert, 2007).

Sport of the “Junta de Andalucía”, golf tourism represents a small participation of 1.5% of total tourists visiting Andalucía.

In 2008, the Decree 43/2008 of 12 February was approved, regulating the conditions of implementation and operation for golf courses in Andalucía. This Decree contemplates the figure of "Golf Courses of tourist interest", which allows the construction of residential complexes associated, being actually an aspect that aligns with the original philosophy of this Decree that sought to end the binomial golf/urbanization.

Just as an example, we could have a look at the following figure 2.32, where, in about 14 kilometers of coastline, between Marbella y Mijas, in the Province of Malaga, and comprising the urbanizations of Albarizas, Las Chapas, Elviria, Artola, Sitio de Calahonda, Agua Marina, around 8-10 golf courses can be counted!

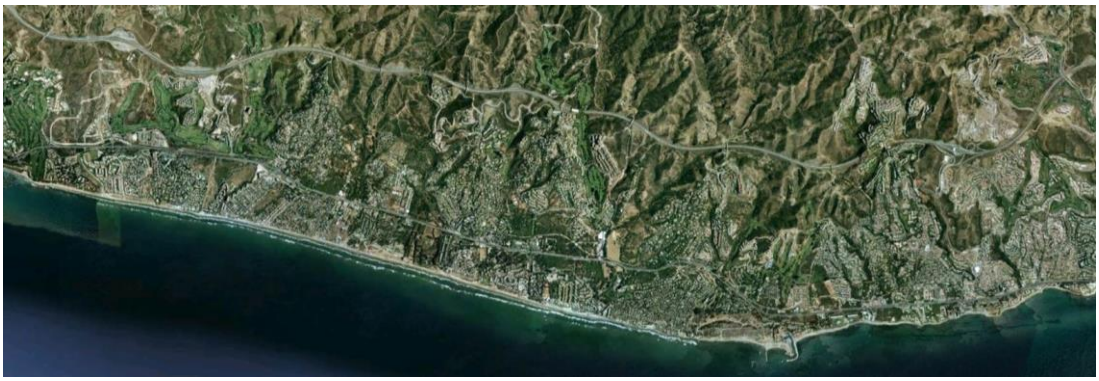

Fig. 2.32: A transect along the Andalusian coast, located between Marbella y Mijas, in the Province of Malaga (Source*:* Google Earth, Digital Globe Image, 2013)

Imagine that between the shoreline and the highway, there is no more than 2.5 km of fringe! It means that we are talking about 35 square kilometers, a space smaller than the municipality of Gerona, which is 39 square kilometers... Could we imagine the municipality of Gerona with that number of golf courses?! The image also shows clearly the whole discourse on the uncontrolled dispersion of the urban fabric, low density, at the expense of natural areas, which are also losing their direct relationship with the sea.

In the case of Andalucía, it seems a shared idea that unhealthy land management, both at regional as well as local levels, has incisively influenced the "special" combination between public and private interests. Actually, as stated by Marcos Rodríguez, et al. (2012), the Ministry of Environment, responsible for managing and preventing coastal degradation has not acted properly. In light of this, we should mention the amendment of Law 22/1988 of Costas which was camouflaged within the Accompanying Law of the State Budget, approved in late 2002. This change has encouraged more complete occupation of coastal areas (by allowing to build up to 20 meters from the coastline), thus subordinating the protection of the coasts to the urban development.

On November 27, 2008, the plenary Andalusian Parliament approved the new Law 1/2008, tax and financial measures to boost economic activity. An urgent text written to allow discretion for the Andalusian Junta, rather than streamline procedures and alleviate bureaucracy. Under the cellophane of the fight against the economic crisis, the Andalusian Government changed ten laws, seven of which relate to the environment. The new text approved, among other things, an amendment to the Law on Spatial Planning of Andalusia (LOUA) to enable the Junta to declare "regional interest" actions it deems appropriate, therefore forcing the sub-regional plans to adapt

Although in 2006, the Spatial Plan of Andalusia (POTA)[88] was approved, which limits the urban growth of municipalities to 30% of the population, and land occupation to 40% of the current urban area, over the next eight years. In 2007, only 9% of the Andalusian municipalities met these measures, and a look at the urban planning of that year, permitted checking the "urbanistic nonsense" spread along the coastline. The POTA, was lowered in January 2008 by the Government Council of the Junta de Andalucía, by cancelling the limit of 40% for the developable land of municipalities and 30% of population. The amendments allow these limits to be ignored if they

[88] Ureba, A. A. (2006). Código de Urbanismo en Andalucía: Normativa Autonómica y Estatal. Editorial La Ley. 969 pp.

are within sub-regional plans and, in practice, continue to allow the rezoning that has taken place so far. The "flexibilization" of POTA has also removed the limitation of growth for municipalities with fewer than 10˙000 inhabitants, the only useful measure which could allow the end of urban overproduction in small municipalities[89] (Marcos Rodríguez, et al., 2012).

This Region, which was a pioneer twenty years ago, for enacting a Law which approved the inventory of protected natural areas of Andalusia, and established measures for their protection (Law 2/1989 of Protected Natural Areas Inventory of Andalusia), has experienced a marked increase in artificial areas in recent years, mainly due to increased diffuse urbanization, and a 500% increase in areas dedicated to highways and motorways. The areas, assigned to sports and recreation, have grown more than 150%. Due to this soil loss, a 40% loss of its rivers and natural waterways is detectable in the last decade[90].

Currently, Andalusia has 53˙282 hectares of protected littoral-marine area. In other words, from the 979.5 kilometers of coastline, 286.2 kilometers are protected, at least on the map, which means almost 30% of its coastline. Even so, the data leaves no doubt: 59% of the Andalusia coastline is already urbanized. According to the Counsel of Environment of the Junta de Andalucía[91], between 1956 and 2003 Andalusian cities have increased five times its built-up area, an increase which occurred at the expense of agricultural land (by 76.40%) and forested areas (23.17%). Beaches, dunes, cliffs, and coastal pines live with an excessive number of marinas, golf courses and, worse still, with some of the most contaminated areas of the Iberian Peninsula, such as the chemical hole of Huelva and Algeciras Bay. Planning and land management in Andalusia are subjected to the pressures of construction, tourism, or chemical industry, which "shapes" the decisions of the Board, setting aside the environmental health of Andalusia and welfare of its citizens (Marcos Rodríguez, et al., 2012).

2.3.5. Balearic Islands: "Destruction and Protection" [92]

From a geographical point of view, the Balearic Islands provide a clear physical unit: the Archipelago. However, an archipelago is formed by single islands often independent and different[93]. The islands that make up the archipelago altogether cover an overall area of 4˙928 square kilometers[94]. The length of the coastline[95] is around 1˙723 km, and most of the length of the three major islands (Mallorca, Menorca, and Ibiza) is formed by high cliffs, high rocky coast and, in smaller part, low rocky coast. The beaches on the three largest islands cover a percentage of less than 3% of the length of the coast. Only in Formentera is it over 15% (Cabellos Barreiro, 2012).

It is possible to identify in the Balearic Islands a key representative of what is currently defined as the overproduction phenomenon of the real estate sector, mainly linked to the mass tourism dynamics along the Mediterranean coast of Spain. The islands have more than 360 beaches, and are populated with a million inhabitants and 11 million annual visitors. Most of the Balearic coast has been protected for decades against rampant urbanization, but, even so, many areas have already succumbed to private developments: hotels, pools and buildings constructed on the beach. In the bay of Palma, the tourism heart of the Balearics, there are sections of about 17 kilometers of the 62 km of shoreline, where you cannot access the beach (Manresa, 2007).

Despite its relative small dimensions, the Archipelago has the "merit" of driving the phenomenon of the "global Balearization[96]". Indeed, the headquarters of some of the most important European companies lie in the

[89] Ojeda Zújar, J. y Villar, A. 2006. Evolución del suelo urbano/alterado en el litoral de Andalucía (España): 1998-2002. GeoFocus (Artículos), nº7, p.73-99. ISSN: 1578-5157.

[90] Greenpeace (2008). Destruction at all coasts. Chapter: Andalusia. Based on data from the annual report of the Spanish Observatory for Sustainability 2008. Indicator: Territory.

[91] *El País* (28/08/2008). The built area in the region has increased fivefold in half a century.

[92] This section is mostly based on the analysis which Manuel Cabellos Barreiro provides through the chapter entitled "*islas baleares: tensión entre destrucción y protección"*, in the framework of the book "*DeCOASTruction. La desconfiguración del litoral mediterráneo español"*.

[93] It is vital to highlight the differences between the Islands, because the urban growth has actually been developed following patterns.

[94] The size of Mallorca is considerably greater than the others because it reaches 72% of the total; while Menorca, which provides 14% and Ibiza with 11.5% are almost similar. Formentera, despite its importance for tourism, is less than 1%, and the other islands, including the island of Dragonera and the sub-archipelago of Cabrera, barely exceed another 1%.

[95] Measured on digital cartography developed by SITIBSA at 1:5˙000 scale.

[96] The Balearic Islands hold the "honor" of having generated the word "Balearization", which is currently synonymous throughout Europe, with the uncontrolled urbanization built along the coastlines.

Balearic Islands, and has contributed to the phenomenon of the tourism transformation called "balearization", being synonymous of coastal destruction. Currently, seventeen hotel chains maintain their corporate headquarters in the Balearic Islands. In 2007, the countries which place the largest number of accommodations (figure 2.33) deriving from Balearic hotel chains are: Spain (437˙955 beds), Mexico (60˙047), Dominican Republic (54˙798), Cuba (34˙994), Tunisia (17˙802) and the USA (15˙692). However, Europe is the continent with a greater percentage of hotels, with 68.4% of total accommodations (Blázquez, Murray, & Artigues, 2011).

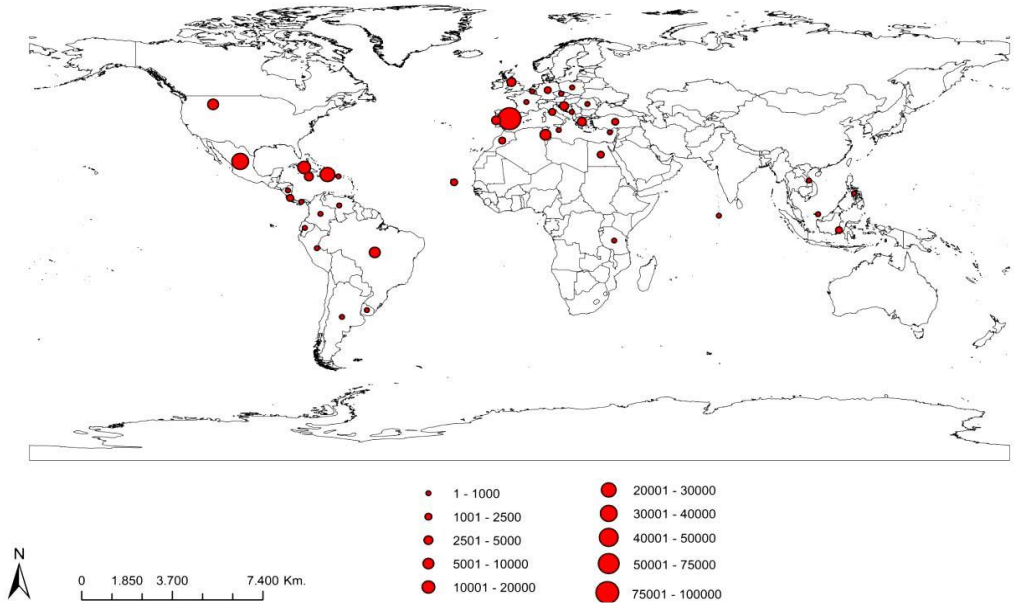

Fig. 2.33: Capacity of accommodations (2007) of the Balearic hotel chains in the world, by number of rooms (Source: Blázquez, Murray, & Artigues, 2011)

According to Blázquez et al. (2011), the Balearic trans-nationalization capital of tourism took place, through the mid-1980's, not only with the support and subsidies of the central and regional Spanish governments, but also with the consent and participant agreement of host states. Its dissemination and implementation involved the tourist commoditization of land and natural resources, leading to processes of "dispossession", for the local populations, and democratic decay.

Although the Balearic Islands emerged as a mass tourism destination around the mid twentieth century, the main tourism development experienced by Balearic Islands is often defined as a “fundamental asset” of that mass tourism of “sun and beach” in Spain. This can be defined by three main stages, covering the second half of the 1900’s, until the first decade of the 2000’s. Therefore, it is possible to identify a first phase, which ranges from 1950 to 1975, defined as the time of opportunities. A second phase, from 1975 to 1995, is the period which most affects the coastal areas of the Island, and is defined as urbanization at “all Coast”. Finally, the last phase, from 1995 to 2010, is the epoch of the main residential expansion until reaching the current crisis (Cabellos Barreiro, 2012).

The approach of Cabellos Barreiro (2012), to describe the first phase, and perhaps the most important of the Balearic tourism development, begins in an almost "romantic" way by telling us that in the nineteenth century there was not "a tourist" but rather "a traveller". Mallorca had travellers, but in reality, few. Actually, the inauguration of a steamboat line in 1837 allowed a regularity of schedules and assured travel times, eliminating the uncertainties of wind-driven ships.

In Palma de Mallorca, the century began with the opening of the Grand Hotel in 1903. This hotel, similar to two others in project, struggled for return on investment, as the first two decades were marked by economic depression until the end of the First World War [...]. With the economic momentum of the 20’s in Palma, seven luxury hotels with a total of 776 accommodations had already been built by 1934. The Archipelago was actually entering "tourism producing" in the 1950’s, with industrial development capable of producing 48.6% of gross domestic product.

The number of tourism establishments existing in 1950 was about 130 with a capacity of 4˙020 accommodations in the entire archipelago[97]. Figure 2.34 shows a picture from 1958, where, up on the right side, it is possible to see rising over the houses of the first row, the first hotel built in the Arenal[98]. It was the first tall building in the city, which was inserted in an environment of streets eight meters wide and surrounded by houses built using traditional typologies of one and two floors and a front porch. Unfortunately, the hotel served as a precedent, for future development. We can imagine that hotel as a symbol of the upcoming development!

Fig. 2.34: The Arenal of Llucmajor on the southern side of the great "Beach of Palma" (Source*:* Peter Canals[99])

Very often the beginning of the European tourism of "sun and beach" can be explained as the result of a set of circumstances that came together by chance over time. Surely one of them was the key around which governments and private companies came to formulate a development strategy: air transport. In the Balearics, most of the tourists in 1934 (61.9%) came from Spain and France. This percentage became 86.8% in 1950. Clearly, by having access to the islands by boat, it was only possible to attract French tourists, and not massively. The low percentage of 2.7% of British tourists or 0.2% of Germans who came this year confirms this statement[100]. In figure 2.35, the graph shows that the time of onset of mass tourism growth coincided with the inauguration of the airport runways suitable for reactors, with terminals able to satisfy ground services. This was achieved in 1960 in Mallorca, with the airport of Son Sant Joan, in 1966 for Ibiza, and in 1969 for Menorca (Cabellos Barreiro, 2012).

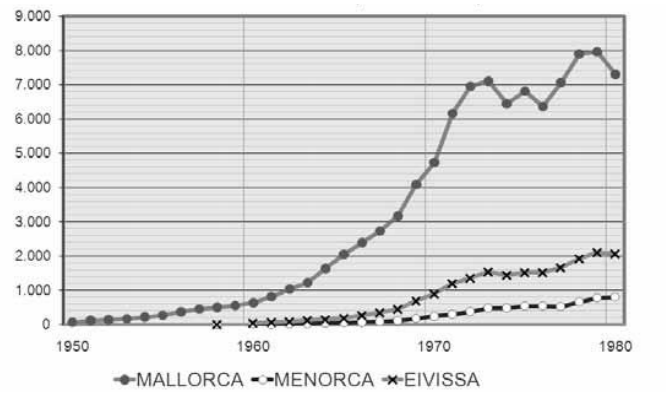

Fig. 2.35: Air travel figures, in the airports of Mallorca, Menorca, and Ibiza, from 1950 to 1980 and for number of travels (Source*:* Cabellos Barreiro, 2012)

[97] In the Balearic Islands, between 1950 and 1967, hotels had been built that contained 89˙265 accommodations, with 54˙611 in Mallorca, 10˙019 in Ibiza and 814 in Formentera. In Menorca, the growth had just started with only 1˙868 accommodations.

[98] El Arenal (officially and in Catalan s'Arenal) is a place in the island of Mallorca, situated between the cities of Llucmajor and Palma de Mallorca. The area on the northern side of the Jews torrent (Torrent dels Jueus), is in the municipality of Palma and is called Playa de Palma. Its proximity to Palma (15 km) and to the airport (7 km) makes it a place of easy access for tourists and residents. The old fishing village, is currently an eminent tourist district with great demographic expansion, which occurred especially from the 1970's. This change was due to tourism, mainly English and German. Source: Wikipedia, The Free Encyclopedia at http://es.wikipedia.org/wiki/El_Arenal_ (Mallorca)

[99] Canals Morro. S'Arenal que he Viscut.

[100] Cirer Costa. *La Invenció del Turisme* … Pág. 350, 351.

From the viewpoint of urban management, the Land Act of 1956 provided, as a key instrument of planning, the drafting of provincial plans, only two of which were approved. This instrument, as argued by Cabellos Barreiro (2012), was also adopted in order to rationalize the runaway growth of the use of land for tourism, by providing some key points, such as: the establishment of boundaries and conditions, although of minimal character, to safeguard protected landscapes, preserved places, and unique landscape elements; the establishment, for urban areas and new developments, of a catalogue for its zoning following residential uses, tourism, industrial, rural, and services, by establishing management and building standards, in each area; and the definition of urban parameters and a calculation system for the intensity of urban development and building.

From the point of view of the containment of the mass tourism phenomenon in particular, the establishment of maximum growth ceilings of hotel rooms by Comarca[101] and for the following 10 years[102] was provided. Moreover, it also limited the maximum area for urban developing for each Comarca (administrative division of municipalities), and again for the following 10 years (Mallorca 5˙000 ha; Menorca 693 ha; Pitiusas[103] Islands 1˙107 ha).

However, some aspects provided by the provincial plan were considered negative from the point of view of sustainable growth. That was not a real Territorial Plan because it did not solve the needs resulting from the growth allowed. It did not raise the question of the needs of location and access to housing for tourism workers, social facilities, or mobility which was already being generated at the time of drafting the Plan. Actually, and in practice, it was almost a plan to legitimize widespread tourism growth. The plan also allowed the trend of continuous occupation of the coast without assessing its impact. The Plan only limited the possibility of urbanizing the coastline in those areas of real development inability due to the extremely rugged terrain.

The basic numbers of the Balearic economy, and the speed of growth at the end of the "first phase" which ranged from 1950 to 1975, in just 25 years, were that the resident population increased from 419˙628 to 597˙715, with an average annual growth rate of 1.4%; hotel accommodations increased from 4˙021 to 213˙772 with an average annual growth rate of 17.2%. The number of passengers by air, and to the airports of the three Islands, increased from 74˙700 to 8˙874˙000 with an average annual growth rate of 21.1%. The number of tourists staying in hotels grew from 98˙000 to 3˙436˙000 with an average annual growth rate of 15.3%. However, it is important to note that the incidence of the service sector in GDP increased from 27.2% to 70%! (Cabellos Barreiro, 2012).

The second phase, starting in 1980 after the oil crisis (1973-1979), that had put a brake on growth, saw a new opportunity for growth dynamics, also coinciding with an opening of the market for air travel. This new phase (until the first half of 1990's) provided, above all, a major change in the model of hotel facility, which was mainly provided by the Provincial Plan and subsequently included in municipal planning. It means buildings with a height of 8-9 floors, sometimes more, with terraces, gardens and pools on the ground floor level, high above the ground and usually situated on the seafront; in places of difficult terrain shapes, or inside urban networks where the allowable intensity for building was high.

In fact, the growth of the construction sector, in general, was intense in the Balearic Islands. The resident population increased by 163˙000 people up to reaching 760˙000, implying an average annual growth rate of 1.2%. The tourist accommodations increased from 175˙000 up to 389˙000. This growth was 2.9% of the annual average. It is interesting to note that the process of tourism integration of Menorca was delayed (late 1960's), but at this stage it was the leader at an average rate of 6.3%. In fact, the first tourism boom of Menorca occurred during phase two, even without reaching the intensity of Mallorca and Ptiusas during phase one. For the three airports, the number of passengers increased at an average rate of 3.8% annually.

The third phase was identified, by Cabellos Barreiro (2012), with the phenomenon of residential expansion and the subsequent crisis, between the years 1995-2010, mostly connected with the dynamics of real estate speculation in Spain. The construction sector greatly increased the number of apartments and homes due to various financial circumstances that became the subject of housing investment. This development transformed the vicinity of the beach into the most important area of the Archipelago.

[101] A Comarca is a traditional local administrative division of municipalities in Spain.

[102] Mallorca could increase its number of hotel accommodations from 170˙950 in 1970, up to 388˙220 in 1980; Menorca from 5˙603 up to 27˙400; the Pitiusas Islands from 29˙042 up to 82˙100.

[103] The Pitiusas Islands is the name given collectively to the Balearic Islands of Ibiza, Formentera, S'Espalmador and other small islets in the Mediterranean Sea (Source: http://en.wikipedia.org/wiki/Pityusic_Islands).

This kind of development led, inexorably, to the explosion of an economic and financial crisis. In this phase, the number of tourism accommodations was stabilized, and even the size of tourist facilities decreased slightly[104]. Table 2.3 summarizes, in numbers, the intensity of the construction sector, through the number of homes built between the years 1996 and 2008[105] (both years included)[106].

1996-2008	Built Houses	Annual average	Average Annual Rate
Mallorca	104˙184	8˙014	2.0%
Menorca	15˙869	1˙220	2.3%
Pitiusas	22˙850	1˙758	2.6%
Balearic Islands	**142˙903**	**10˙992**	**2.1%**

Tab. 2.3: The number of homes built, between 1996 and 2008, for the three main Balearic Islands (Source: Cabellos Barreiro, 2012)

It is important to note that the 10˙992 annual homes built during this period exceeds 50.5%, the average of previous periods between 1900 and 1995! However, the most impressive result of the addition of vacant soils with a circumstance of great demand for housing has been that, in this phase, the equivalent of a "city" of 138˙500 homes as large as Palma de Mallorca has been built, and the crisis has now left us mortgaged, together with an amount of over 20˙000 houses for sale. The construction of such housing was basically within the huge bag of urbanized land, which had in the year 2000 a capacity of 824˙000 lots, that is, about 286˙000 houses. From 2002 to 2008, 82˙000 homes were built.

Now, assuming that each promotion could take three or four years to be sold during a "fast market period", we can infer that at least a quarter, and i.e. 20˙000 houses remained unsold when the crisis came. To this number, the houses finished in 2009 should be added, and those finished before 2000 which were 85˙135, were identified as "empty" according to the 2001 census once separating from the number of second homes (Cabellos Barreiro, 2012).

The tourism attraction in the Balearics added to the urban deregulation process, which started in the mid-90's, and facilitated the urbanization of the interior and expanding consolidation of some tourism areas, leading to what later became the property boom. All this was intimately connected with the construction of several "megaprojects" of transportation, and whose role was to catalyse investment toward pre-set zones, also coinciding with the proliferation of numerous cases of political corruption with business.

During the last period of growth, the Balearic Islands continued to increase its economic dependence on tourist arrivals and the construction of infrastructure, adding environmental impacts shaped on land consumption and resource consumption. Moreover, for further centralizing economic activity in construction and tourism, the Balearics accelerated the process of relocation of extraction and production centres abroad. The bursting of the housing bubble in mid-2008 not only highlighted the growth pattern of recent years, but also left the region the hardest hit by urban sprawl, mortgage debt and unemployment (Ginard Bosch & Murray Mas, 2012).

During this last phase, the resident population has increased by 340˙000 inhabitants up to 1˙106˙000, which implies a high average annual growth rate of 2.8%, well over double the previous phase[107].If we look at the relation between resident population and the tourism sector (figure 2.36), which is leading the current Balearic economy, it is clear that despite the increase in population, the main economic sector is now being affected by the crisis, so it is generating unsustainable patterns of growth.

[104] In April 1995, the POOT (Management Plan of Tourism) was approved, which provided important territorial provisions. On both sides of the coast, in each of the 37 coastal areas, strips of 1˙000 meters width were created that should be maintained as undevelopable; moreover it created an additional protection area 500 meters wide. By implementing these measures, the possibility of creating new neighbourhoods on the coast was limited. But, it is important to note that the general plans, of almost all coastal municipalities, were approved with huge tracts of land for development, so therefore actually wiping out the immediate effect of the POOT (Cabellos Barreiro, 2012).

[105] This period coincides with the expansion phase of construction, until the housing bubble burst in early 2008.

[106] Data is only provided for the residential construction sector, excluding industrial, leisure, tourism, administrative and equipment.

[107] In 160 years the Archipelago has increased its resident population by 5 times, passing from 228˙500 inhabitants in 1842 to 1˙106˙000 in 2010.

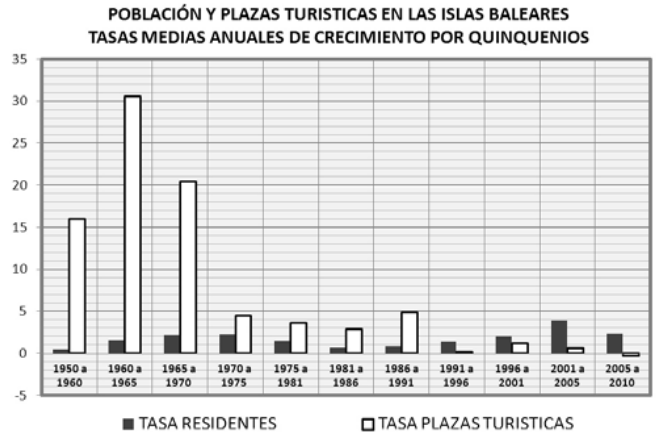

Fig. 2.36: Average annual growth rate of Population, and hotel accommodations in the Balearic Islands from 1950 to 2010 every five years (Source*:* Cabellos Barreiro, 2012)

The intense process of tourism specialization of the Balearic economy has meant an enormous pressure on both the primary sector and the industrial sector, by unstoppably attracting both human resources as well as their capital. In the Balearics, the presence of the tourism industry within the service sector has been estimated around 60%, well above the Canary Islands (20%), Catalonia (11%), Andalusia (15%) or Valencia (9%)[108] (Greenpeace, 2012).

In order to better explain the effects of tourist pressure on the growth dynamics of a territorial system, such as that of the Balearic Islands, but in general for any territorial area, Cabellos Barreiro (2012) uses the density as a fundamental aspect to measure the cultural and psychological impact of tourism on the local population. In order to analyse this effect, the same methodology used by Eurostat in the MEGRIN program (Multipurpose European Ground Related Information Network) through the REGIO database[109] has been used. The study calculated the ratio between available accommodations and the number of resident inhabitants. This ratio was applied to each Island (Mallorca, Menorca, Ibiza, and Formentera) and the data was grouped in 5 subjects for comparing the intensity of the effect of tourism on the population (figure 2.37). The fifth value on the chart is the last value of the MEGRIN range, which was greater than 320[110].

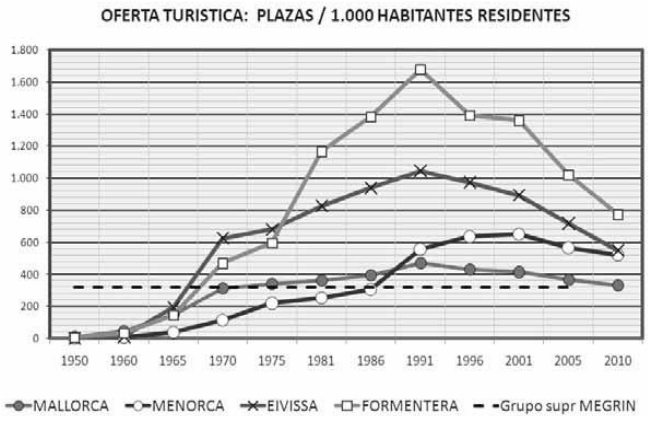

Fig. 2.37: Coefficient of touristic pressure, on the resident population (Source*:* Cabellos Barreiro, 2012)

[108] Olabe, A. (2000). Economía y Medio Ambiente: Hacia un desarrollo sostenible en les Illes Balears. Conselleria d'Economía i Hisenda: Direcció General d'Economia. Govern de les Illes Balears.

[109] Regional statistics collected by Eurostat are stored in the public database New Cronos, in Theme 1 "General Statistics", in the "Domain" REGIO. Eurostat's regional statistics cover the principal aspects of the economic and social life of the European Union, such as demography, economic accounts, employment, unemployment, and so on. The concepts and definitions used are as close as possible to those used by Eurostat for the production or collection of statistics at national level (REGIO database - User's guide, 2000).

[110] The MEGRIN program ranges, applied in its first season, 1998, were <20 <40 <90 <320, and >320.

In the graph we see that Ibiza (Eivissa) and Formentera reached the last value of MEGRIN already in the period from 1965 to 1970, then reached higher levels of 1˙400 and 1˙670 hotel accommodations per 1˙000 inhabitants, respectively. Mallorca and Menorca surpassed widely that level in the 80's before almost declining to a lower range. Interestingly, this decrease is due to the incorporation of migrants to the resident population, which probably had an important impact in Mallorca. To get an idea of what these figures mean, we could state that Pitiusas Islands during the summer are denser than any country in Europe, except Malta which is a country with a tiny surface area (less than half of Menorca). Mallorca is second in density after Holland. Only Menorca is saved, being the third after the Netherlands and Belgium. According to the MEGRIN program, when the intensity of the tourism economy is high in relation to the social and cultural basis, it is the moment at which the pressure of economic operators can be so involving that the citizens lose collective conscience, making it difficult to redirect the growth process (Cabellos Barreiro, 2012).

2.4. FIRST REMARKS

The complexity inherent in coastal planning, different sensibilities, priorities and visions, that local and regional authorities have in planning and urbanism, have led to a diversity of proposals along the coastline of Spain, ranging from the adoption of an Urban Master Plan for the Coastal System (PDUSC) in Catalonia, or the implementation of residential development plans in Murcia, or even to the bitter controversy between the EU and Valencia about the Town Planning Law of this region. An increased "sensitivity" to the role of tourism as an organizing and transforming activity of the territory also arises from land management policies as a phenomenon that results in the recent emergence of different plans for tourist management (González Reverté, 2008).

It does not seem an exaggeration to say that the main problem currently related to the relationship between tourism and territory is the identification or the confusion still prevalent in many areas, between the residential uses (reflected in second homes) and the more specifically tourism uses (i.e. those related to establishments or enterprises in tourism: hotels, campsites, apartments regulated, complementary offer, etc.), which often coexist in the same space of leisure. The same portion of land dedicated to coastal hotel uses would generate eight times more jobs, and twelve times more income than when it is dedicated to a second home[111] (Fernández Tabales & Santos Pavón, 2011).

In general, it is possible to state that Medium-sized cities are those which have undergone a major urban expansion, and especially those cities that are located around a large metropolis, or along the coastline (or both cases, such as the case of those cities around Barcelona or Valencia), and which tend to have a more pronounced dynamism. Apart from showing a high level of dispersion together with high levels of land consumption, they even tend to increase at a notable speed, while maintaining medium and sometimes low values of density.

The reading of the analysis provided in this section gives an interesting overview about the main causes and effects that have occurred during the last twenty years, with special attention toward the Mediterranean arc. This is basically due to an oversized type of growth in the construction sector, in part due to population growth, but primarily due to an increasing demand from tourism. In particular, the thrust due to an inflated tourism demand, derived from the euphoria of an exceptional economic growth which took place in Spain in recent decades, has generated an equally inflated offer in the construction sector, directed not only towards the hotel offering, but especially to residential tourism. In many cases, residential tourism, besides second or third homes, has come to accompany big tourism settlements around golf courses, thus in a lot of cases, creating those "famous" structures known as resorts.

In order to review, in a few words, the main trends of overproduction in the real estate sector across the five Mediterranean regions, we could summarize that Catalonia has partly offset the phenomenon of tourism along the coastline with a metropolitan type of growth around the city of Barcelona. Although, there is also a demographic curve linked to massive immigration that is not at all stable, which has created demand, but which at present is clearly in decline.

[111] According to calculations made in preparing the Development Plan of Territory of West Coast of Huelva (Council of Public Works and Transport of the Government of Andalusia, 2000: 70-73).

The Region of Valencia is probably the emblem of residential tourism, based on the second home dynamics, especially in the area around Valencia and in the province of Alicante, but we have also seen it recently in the province of Castellón. The special case of hotel tourism, such as the one of Benidorm or even the important contribution of the resorts such as Marina D'Or, is not to be forgotten of course.

There is no doubt that the greatest impact in the region of Murcia was due to the phenomenon of resorts. Indeed, as well as for Andalucía, the impressive increase in the number of golf courses has also accompanied residential tourism in areas such as the one of the province of Malaga. The Balearic Islands, depending on the region, have staged a sort of struggle between the push towards urbanization and conservation of the natural patrimony, even if in many areas the hotel tourism phenomenon has prevailed over the landscape. So, what is now of most concern facing the available property assets after this huge growth period which occurred, are the trends of changes of the demographic curves, currently and projected into the future, as well as trends and scenarios for the tourism sector.

Referring to the demographic trends and *according to the annual population census, the Spanish population in 2009 was 46.7 million, 15.4% higher than in 2000 with an average annual growth of 1.7%. Of this population, 5.7 million were foreign residents (mainly Romanian with 798˙892 residents, Morocco with 718˙055 and Ecuador with 421˙426). The most recent advances in population projections made by the INE ("Short term population projection in Spain from 2010 to 2020" Press Release of October 7, 2010) state that the population will grow by 2.7% until 2020 with the current demographic trends, compared with 14.8% growth over the last decade* (figure 2.38). *Spain will keep an annual rate of population growth in the coming years less than 0.35% with a slight downward trend. After some years of high population growth, Spain will reach just over 47 million people in 2020, with the current demographic trends. Thus, in the period 2010-2020 the resident population will grow by 1.2 million (2.7%) compared to the 5.9 million increase (14.8%) in the first decade of the century. Based on annual average, population growth would be 124˙591 inhabitants, lower than 593˙931 in the past decade. The foreign population input may diminish over the next few years due to the economic crisis and to the growth of unemployment, as well as a result of the immigration restriction measures enforced throughout Europe, but it is estimated to hold to around 250˙000 people annually in the next decade* (European Environment Agency , 2011).

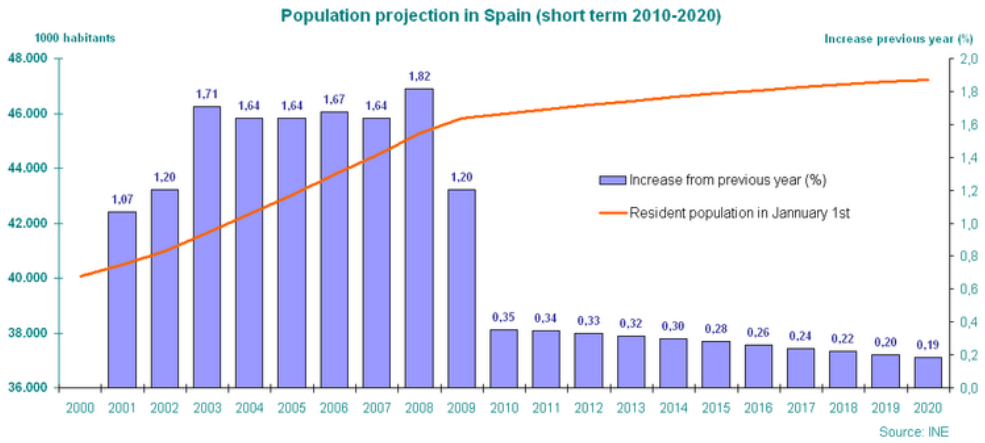

Fig. 2.38: Population trends of growth in Spain, between 2000 and 2010, and future projection to the year 2020 (Source: European Environment Agency 2011; INE, 2010)

In addition, the other important driver of the urban development in Spain has strongly decreased during the most recent years. Throughout the year 2009, the Spanish tourism industry was severely affected by the financial and economic crisis, both at national and international travels. Spanish tourism companies closed the year 2009 with double-digit widespread falls in profits, putting a growing number of them in loss situations. About 84.5% of Spanish tourism businesses have experienced a decline in profits. Declining profits recorded in 2009 were in addition to the trend of reduced profitability, which 75.3% of the entire Spanish tourist companies had experienced already in 2008. As shown in the following figure 2.39 the tourism sector suffers more intensely than the average

for the Spanish economy, the decline of activity, with a decrease of -5.6% of the tourism GDP in 2009 (EXCELTUR 2010).

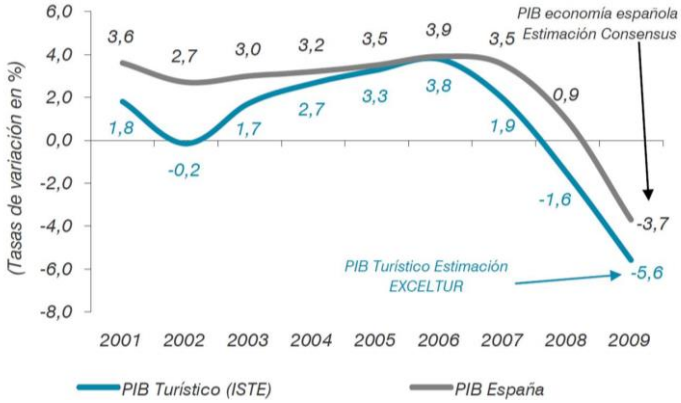

Fig. 2.39: Comparison of tourism GDP with the overall GDP of the Spanish economy between 2001 and 2009 (Source: Exceltur, INE y Consensus)

At the end of 2012, Europe came back from economic recession while Spain is facing its sixth year of economic crisis, so it will receive more tourism demand and this will affect the general trends of consumption. As reported by the European Travel Commission (ETC) during the third quarter of 201 there was only a very slight growth in both air transport indicators as well as for residential tourism, because the tourists continue to travel, using even more thrifty travel behaviour. In Germany, despite the good performance of the economy in 2012, there was no growth in outbound tourism, but on the contrary, the market stagnated, while from the UK the outbound travel only grew by 1% (World Travel Market 2013).

In spite of the economic crisis, and all of the aforementioned trends in population and economic growth which strongly emphasize a loss in the tourism sector and a decline in many areas of the demographic curve, and which could be defined as a fourth stage of urban development in Spain, it seems that even if the building sector has suffered in practice a clear loss of impetus (imagine the number of unsold houses or unfinished buildings) already in the period from 2007 to the actual date. There have been many signs in the same sector for continuing in the same direction, producing for at least the first years of this decade… Therefore, when facing the future, many more questions will need to be answered.

Chapter 3

URBAN MODELLING AND TECHNOLOGICAL APPROACH TO SPATIAL ANALYSIS: A STATE OF THE ART

Cities concentrate investment and employment opportunities, promoting economic growth and increased productivity. They provide higher-income jobs, as well as greater access to goods, services and facilities, and improved health, literacy and quality of life. These opportunities tempt rural residents to search for a better life and higher income in urban areas. However, in the absence of strong governance, rapid urban growth can cause major environmental challenges by increasing both consumption and urban poverty (EEA, 2013).

The study of the city (which is the "natural" habitat of the human being) includes the modelling of the physical space, the understanding of dynamics such as the distribution and agglomeration of economic activities, and the composition of social structure. This is a process historically associated with the research of formal rules that define different shapes of urban structure, both in terms of buildings and urban profiles as well.

The primordial necessity of concentrating human activities and the clustering of human beings into a well-defined area constituted, thousands of years ago, the first "civilizations". This is the case of civitas found in Mesopotamia, for instance, around the fourth millennium B.C.; or the tendency to structure the city on a regular mesh of axes (cardo and decumanus) as was the basic rule behind the typical ancient Roman cities and camps; both cases provide the first examples of urban management and planning, based on rules such as agglomeration, and spatial distribution of functions.

By making a big jump through time towards more recent eras, this chapter provides two main sections; the first one aims to trace an overview of the evolution of the main urban growth patterns during the past 20th century, and the current tendencies of development, mostly focused on the key theories about modern urbanism, seen through the investigations undertaken by relevant exponents in the field of urban studies and spatial planning of the modern scenario. The second part of the chapter focuses on some relevant approaches to urban and regional analysis, which rely on the use of new technologies for the detection and quantification of land cover composition. The latter part places particular emphasis on several ways of measuring urban phenomena, through the examination of a number of representative projects at a global level, as well as European and national level, which have particularly inspired the present research work.

Currently, many institutions, ranging from National to Regional Governments, as well as important research centres and governmental agencies in the international scenario, such as the National Aeronautics and Space Administration (NASA), the European Space Agency (ESA), the European Environment Agency (EEA), the Joint Research Centre (JRC) of the European Commission, among others, have undertaken many programs and projects focused on land cover monitoring and landscape analysis, This takes into account the varying aspects, both natural or artificial. In fact, although lots of approaches and techniques have been developed, there is still a challenge to find generalized and objective globally recognized methodologies, for detecting, measuring and comparing specific geographical phenomena.

3.1. URBAN MODELLING: AN OVERVIEW

By 2050, about 70% of us are likely to be urban dwellers, compared with less than 30% in 1950 (UNDESA, 2010). Cities are also reaching historically unprecedented sizes. The rising number of megacities across the globe puts enormous strain on their natural resource support systems. The even faster growth in small and medium-sized cities could eventually be even more important from an environmental perspective (European Environment Agency, 2013).

Mostly during the second half of the last century, an increasing range of urban accomplishments have appeared around the peripheral areas of the cities, with various levels of impact on the environment. This is due to an important process of urban expansion linked, basically, to technological development, which has facilitated urban connections by implementing transportation and its capabilities.

Actually by the late sixties, many European cities started to undergo an important change in their urban development. The most common phenomenon affecting big cities during these years has been a growing decentralization or de-urbanization of the urban fabric and the demographic weight, that is to say, a loss of population in the inner city, which now tends to move away towards more external areas.

The urban space expands and spreads over the territory giving rise to different dynamics of growth at different spatial scales. Hence, further instruments for spatial analysis are required in order to provide suitable land management. Indeed, several emerging fields, such as human geography, urban morphology or sciences for geographic information, have been seeing growing interest within scientific communities especially during the second half of the last century.

In 1976, Michael Batty argued that during the two decades between the 1950's and 1960's, two main topics summed up a new path in the field of spatial planning best known as "Quantitative Revolution" and "Systems Approach". It derived from an important change to approaching spatial analysis, which resulted in a sort of "revolution", and occurred during the late 1950's in the social sciences, also including geography and urban planning, raised from the idea that more rigorous theories about urban dynamics could improve the quality of information more than a "loose speculation".

The Quantitative Revolution attempted to define the "nature of geographical space", meaning the description of the geometrical features of the space, and the transformation phenomena which occur over time, through the use of mathematics and statistics. It gives rise to modern geography (Batty, 1976).

Even if it is impossible to question in detail the path of urban development, which has occurred throughout the last century and until today, or make an extended excursus about the history of modern urbanism in a few pages, neither it is the main objective of this study. The upcoming sections attempt to provide a summary (hopefully exhaustive) about the main phenomena and concepts of urban growth, which occurred mostly during the last half of the past century, up until current models of urban development, and in addition, the most common practices of modelling and measuring the extent of the phenomenon.

3.1.1. Main Theories and Approaches to Urban Modelling

Present-day dilemmas in urban planning are fundamentally directed at the analysis of three main themes: the urban form (compactness-diffusion), functionality (complexity-specialization) and equity (integration-segregation) (Nel·lo, 2001). However, the urban growth process is the result of a number of variables, such as the spatial distribution of population (demography), the location of economic activities, and the functional flows. These features, in turn, are strongly related to the physical (topography) and geographical features of the territory. Different combinations of such factors give rise to different models of urban expansion, both at local and territorial level.

According to Angel, et al. (2005), the *differences that arise in the form of urban expansion have been attributed to six different types of effects: the effects of the natural environment; the effects of demographics; the effects of the economy; the effects of the transport system; the effects of consumer preferences for proximity; and the effects of governance*. However, according to Camagni (2005), the main principles behind the generation of the urban environment are: agglomeration; accessibility; spatial interaction; hierarchy; competition; and land values. Actually, Camagni argues that agglomeration explains the existence of the city (i.e. why does a city exist?), the accessibility is the base of the urban organization (i.e. "where" in the city?) and spatial interaction is explanatory of the functioning of the parts which compose a city (i.e. "how" in the city?). However these three principles need to be read in conjunction with some extra principles that are hierarchy, competition and land values (Camagni, 2005).

Hierarchy defines the degree of dependency between different urban objects or functions; the competition between different economic activities is the attempt to ensure more advantageous locations (the competition is behind the principle of accessibility); while land values is cause and effect of the location of the activities.

Over the last century, several Scientists, from different disciplines, have faced the challenge of conceptually summarizing the most common theoretical models of urban expansion. In particular, the main approaches to spatial analysis of the urban models come from the field of landscape ecology, economics,

geography, statistics and urban morphology. In this section, we aim to provide a quick overview of the scientific development concerning the main theoretical models of urban development theorized during the last few decades.

Although several approaches to the analysis of urban models exist, a key topic common to almost all the approximations, although especially related to the urban economy, is the theory of the "central place". In particular, those approaches which derive from this line of investigation mostly focus on the study of the spatial position of the elements in the territory, the nature of their characteristics, their interrelationships within the system (location, proportionality and structure) and functional differentiation (Gomez Piñeiro, 1994).

One of the most important approaches to urban modelling derives from the field of human ecology. This approach originally arises from empirical observations of the configuration of the urban districts, so the approximation is clearly morphological because it analyses the spatial shape of distribution of urban activities. In fact, because these models analyse all activities at once, in an interrelated manner, they can be classified as models of urban structure. In particular, the first development of this model arose in 1925, from the School of Chicago, where Burgess suggested a conceptual model of radial distribution (concentric rings model), based on ecological relationships between activities, including the population distribution (Cerda, 2012).

Indeed, as argued by Camagni (2005), the urban model proposed by Burgess analyses both the location pattern of activities as well as the process of progressive physical expansion of the city, and relies on the hypothesis of an "ideal" trend to expand the physical space of the city radially and concentrically, by circles around the Central Business District[112] (CBD). The first circle after the CBD is represented by a transition area, composed of offices and industry[113], while the successive rings are occupied, respectively, by residential areas of skilled workers and generally formed by the lower-middle class that live closer to the industrial areas; a residential area of middle-high class (as people become wealthier, they move further out of the city center and live in bigger houses with gardens); and an outer zone at a distance between 30 and 60 minutes from the workplace.

In 1939, the economist Homer Hoyt proposed a radial model of urban land use, also known as Hoyt's sector model. This model is, basically, a modification of Burgess's concentric model but it allows for an outward progression of growth based on transport infrastructure in order to determine the location of the different sectors. Indeed, here, land-uses are distributed according to sectors, instead of rings. Although the model still assumes the existence of a transition zone formed by lower-middle class housing around the CBD, but industry now spreads out from the city centre towards peripheral areas, radially, by following major transport axes. The lower-middle class housing is still located close to industry, while the high class housing still holds its own sector of the city, following a radial axis directly connected to the CBD.

In 1933, the theories of Harris and Ullman arose, which proposed a multiple-nuclei structure instead of the radial model. Although here the CBD is still providing a central role, with respect to the structure of the city, now other smaller centres are performing specific functions related to business activities. Indeed, industrial suburbs and then residential suburbs also arise.

An important evolution of the ecological approach arose in 1965, when Berry introduced the use of the statistical technique of factor analysis in order to determine homogeneous areas of socio-ecologic relations, while in 1971 Murdie systematized the model of Berry (Cerda, 2012).

Figure 3.1 shows the conceptual schemes of the three most famous models about spatial distribution of urban activities, as treated here, i.e. Burgess's concentric model; Hoyt's sector model; and the Ullman and Harris's multiple nuclei model.

[112] The CBD is the central and most accessible point of the city, where retail shops, entertainment, financial services and other professional services are located. The CBD provides the highest land prices, and this commonly makes buildings tend to grow upwards in order to take advantage as much as possible of the value of accessibility. Such a dynamic, mostly in American cities, gives rise to tall skyscrapers.

[113] However, in most of the cases, modern urban developments (mostly since the second half of the XX century) have produced a movement of the industry out of the city center, towards more peripheral areas. In this way, the houses closest to the center, which originally were inhabited by local workers of the inner city industries, have been later used by immigrants, either national or international.

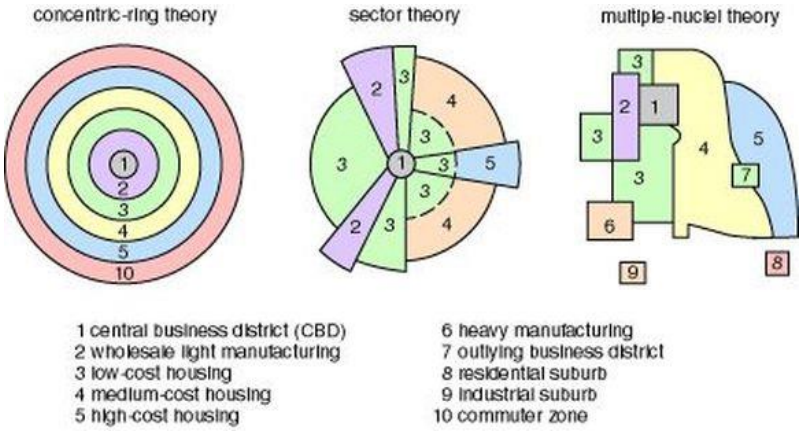

Fig. 3.1: Main conceptual models of spatial distribution of the urban activities, arising from human ecology: Burgess's concentric model; Hoyt's sector model; and Ullman and Harris's multiple-nuclei model (Source: Burdett, 2015)

Besides the models based on the field of human ecology, an additional key category of urban models is provided by those models related to spatial distribution (structure) of the economic activities, i.e. the location models of specific economic activities; such as industrial activity (for Weber) and services (for Christaller). Indeed, within this category we find Weber's model (1909) that, although based on economics, mainly deals with the spatial configuration of the different features of industrial activity, and the hierarchical model developed by Christaller (1933), which defines the spatial distribution of the economic activities (mainly services), based upon the theory of central places hierarchically arranged for optimizing client-service interactions. In 1940, Lösch formalized the Christaller model[114], and in 1958 Beckmann developed the gravitational aspect of activities, i.e. the interaction among different economic activities is directly proportional to the dimension and inversely proportional to the distance. The attractiveness of the approach is its structural essence, and the hierarchical relation between them, so these models gave rise to the development of many studies (Cerda, 2012).

Two further families of urban models are: the gravitational model (with economic base) and the model of urban economy. In particular, the first type of model arises from the famous model developed by Lowry in 1964, a conceptual model that provided a gravitational formulation of the location[115] and the relationship among housing (population) and workplace in the territory. The model makes a zoning of the space (nonlinear). In 1966, Garin made significant contributions to the model, introducing constraints based on availability of land, thus arose the model known as the Garin-Lowry model. This model locates all the activities at the same time, in order to consider the entire interaction between them. The results show the intensity of activities within, and between, the territories, hence the model can be classified as a model of urban structure (Cerda, 2012).

[114] The approaches of Christaller and Lösh, based on the theory of a central place, and which rely on the hypothesis of an isotropic space (i.e. homogeneous in all directions), both in terms of demographic density as well as physical characteristics and infrastructure provision, focus on the principle of hierarchy. The geographical approach of Christaller, based on physical distances, proposes hierarchical levels, of goods and services, organized according to three principles: the market, transportation and administrative organization. However, on the one hand, the Christaller perspective of the centres are considered rigorously equal in terms of structure and dimension, on the other hand, the Lösh model relies on an economic approach that proposes the possibility of a different composition of the productive structure of the centres, under a hierarchical structure. This offers the possibility of different productive specializations of the centres (Camagni, 2005).

[115] All activities located in a physical space develop a complex network of bidirectional relationships that take place at multiple levels, in conjunction with the surrounding environment. Around a specific activity arises a complex set of attraction, irradiation, repulsion, and cooperation forces, which provide the basic energy for the functioning, and even for the same existence of a territorial system. These relationships seem to be organized on the basis of gravitational fields, sensitive to the dimension of the activities on the territory and their relative distances. Each point in the space seems to receive, and exert, an influence which is directly dependent on the mass of each involved entity, while being inversely proportional to the distances that separate each entity from each other in space. Since more than a century ago, H. G. Carey expressed the idea that the area of influence of the city was proportional to its population, and that this influence, exerted on the other entities in the space, was decreasing as the distance increased. But especially in the second half of 1900, through the works of Zipf (1949), the gravity model was used to statistically interpret a wide range of territorial phenomena and spatial interaction between urban settlements (Camagni, 2005).

The second type of model, i.e. the model of urban economy, is characterized by having not just a conceptual base, but also an economic formulation of the equations. This type of model is what has had the greatest development in the scientific literature, and is also the one that has had the largest number of paradigm shifts. The most famous model emerged in 1826 with Von Thünen, who proposed a location model based on transport costs and land rental values. This modelling approach inspired many scientific studies until 1961, when Wingo formally analyzed the main question of this approach, i.e. by considering the same variables of income and transportation costs, he adds the variable of land consumption. The approach of Wingo, and especially the incorporation of the land consumption variable in the model is also taken into account by Alonso, who, in 1964, published his model of locational equilibrium based on an auction method and dependent upon the willingness to pay for different activities (Cerda, 2012).

Such approaches are based on the Bid Rent theory (figure 3.2), or land value model, which explains the variation in economic activity based on the competition for acquiring the most economically desirable (the "best") land. In particular, here the spatial distribution of three main urban uses is taken into account, i.e. residential, commercial and industrial (all economic activity is divided into the latter two categories).

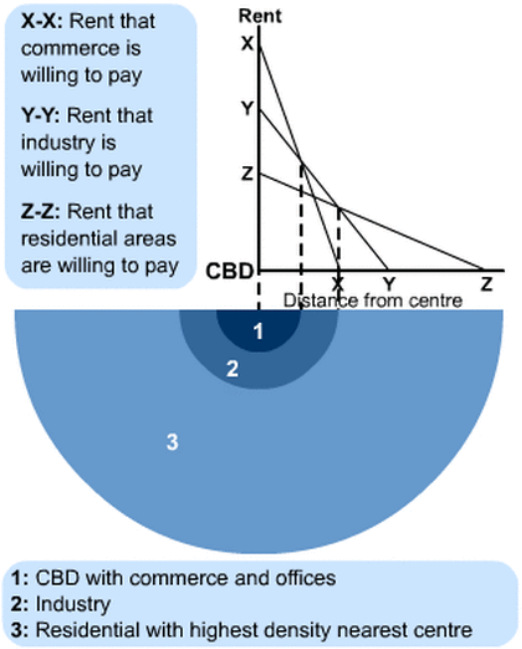

Fig. 3.2: The Bid Rent theory model (Source: Burdett, 2015)

The bid rent model is based on the idea that the land use configuration is the result of economic forces. Indeed, land users usually aim to reach a particular spatial location in order to maximise their profit. In particular, the model assumes that the CBD is the best location for economic activities, either for reasons of accessibility, because it is the converging point of transport networks (accessibility is the key to economic development), as well as for reasons of agglomeration, i.e. similar economic activities tend to be close to each other. Hence, generally speaking, the closer the land is to the CBD, the higher the economic value. Besides that, the model basically suggest that the value of land depends on the distance to certain central areas, therefore we can infer that similarly to the monocentric model, a number of secondary land value peaks are often generated depending on accessibility, competition and agglomeration, and according to a hierarchical structure. Although the dynamics behind the bid rent model are based on very general features, several aspects of the bid rent model can be observed in many cities[116] at a global level in developed and developing countries.

[116] According to Camagni (2005), the location model of agricultural activities provided by Von Thünen (the model from which it has been derived, directly or indirectly) and all modern urban models of economic activities location are based on the principle of accessibility. In particular, the model is a circular distribution of activities around a central market, from which the different level of incomes are calculated

In the 1980's, Fujita introduced a family of models known as models of the new urban economy. In particular, the original model from Fujita considered the distribution of housing around the CBD, but the novelty was the consideration of a territorial structure formed by subcenters of activities, connected together. This approach "broke" with the monocentric models imposed by classical models. Afterwards, Ogawa and Fujita (1980) generalized the polycentric model of location of activities, considering both companies and consumers. In this way, the model of Fujita and Krugman arose in 1995, which is a model of general equilibrium of activities. This new line has been named the "new economic geography" (Cerda, 2012).

Many other approaches have been proposed, which do not fall directly in some of the familiar models presented before. In particular, it has to be highlighted that those studies that are generally directed at territorial analysis (not only urban) are dependent on various scales of analysis. Within these models, it should be mentioned that the initial model of Clark (1951), which explained population density and exponential decay, with distance (Cerda, 2012). Indeed, *according to spatial economic Bid Rent models (Alonso, 1964; Muth, 1968; Mills, 1973), population density depends on accessibility (Muñiz, et al., 2005), while actually the Bid Rent Model, or Monocentric City Model, supports the assumption that population density declines with distance to the city center because bid rent declines to compensate for commuting costs. The population density gradient measures the proportional decline in population density per unit of distance. The lower the gradient, the higher the suburbanization* (Muñiz, et al., 2003).

According to Angel, et al. (2011), among the various theoretical results obtained from the classic economic models, one of the most important is the analysis of the relationship between the amount of space (and resources) used for urban uses (housing, transport, shopping, and recreational areas), number of inhabitants (and cars), levels of per capita income and land availability, with respect to the distance to the CBD.

In particular, in 2010, Angel, et al.[117], tested five hypotheses derived from the classic theory of urban spatial structure, using a set of multiple regression models:

- *the higher the population of the city, the larger its urban area*
- *the higher the average per capita income, the larger the urban area*
- *the higher the agricultural land rent around the city, the smaller its area*
- *the higher the cost of transport, the smaller the urban area*
- *the greater the share of informal settlements in the city, the larger its area*

The results of the proposed study have accepted and confirmed, the first four hypotheses, while for the fifth model, a negative and significant coefficient, indicates that *other things being equal, countries with greater shares of their urban populations living in informal settlements can be expected to have less, and not more, urban land cover than countries with fewer people living in informal settlements. In other words, in contrast to the theoretical discussion, the more people live in informal settlements, the more likely they are to be overcrowded, taking up less land. The coefficient indicates, in particular, that a 10 percent increase in the share of the urban population living in informal settlements is associated with a 0.8 percent increase in urban land cover* (Angel, et al., 2010).

Additionally, five other hypotheses have also been tested concerning the average population density of cities:

- *the higher the population of the city, the higher its average density*
- *the higher the average per capita income in the city, the lower its average density*
- *the higher the agricultural land rent, the higher its average density*
- *the greater the share of people informal settlements in the city, the lower its average density*
- *the higher the cost of transport in the city, the higher its average density*

The key result derived from the aforementioned study, now provide a set of models which, by accepting again the first four hypothesis and rejecting the last one, demonstrate a robust relationship between population, in terms of demography as well as in terms of socio-economic features and average density (Angel, et al., 2010).

---

depending on type of product and distance. However, the model assumes some simplified hypotheses; such as a single market centre with unlimited demand for products, and a homogeneous space with the same fertility, and infrastructure facilities consisting of a constant flow (Camagni, 2005).

[117] Angel, S.; Parent, J.; Civco, D.; Blei, A.; Potere, D. *A Planet of Cities: Urban Land Cover Estimates and Projections for All Countries, 2000-2050.* s.l. : Lincoln Institute of Land Policy, 2010. Working Paper WP10SA3.

According to Cerda (2012), within the density approach, four different methods for detecting structuring subcenters of activities in the territory should be highlighted, which are: first, the method provided by McDonald (1987), which is based on the identification of "peaks", in terms of density of employment, in relation to adjacent areas. In particular, the author suggests that a sub-center is a second "peak" of density, with respect to the central business district (CBD); the methodological line, originally suggested by Giuliano and Small (1991), which relies on the use of reference thresholds (cutoffs) that allow us to identify sub-centers; from an econometric perspective, and a third line seeks to identify the sub-centers using parametric models; while the last approach is based on non-parametric methods, such as locally or geographically weighted regression.

A more innovative approach, although less used, is based on the analysis of functional flows. This second method relies on the hypothesis that a sub-center, as well as affecting the density, is able to structure the surrounding territory through functional relationships. The works of Bourne (1989), Gordon & Richardson (1986), Burns, Moix & Roca (2001), and Marmolejo & Roca (2009) are some useful references in this area. In particular, the identification of functional areas as proposed by Burns, Moix & Roca, 2011, for instance, relies on the calculation of the value of interaction, an indicator that is calculated from the interaction matrix between residence and workplace in the territory (Cerda, 2012).

Finally, mathematical modelling of cities is a newly developed branch of science, due to the computational advances in recent years. While theoretical mathematical models have existed for several decades, the implementation and resolution thereof, in a practical way, has only been possible in recent decades. The developments that the city models have taken are based on the structural basis of the models of urban economy, which generate a series of lines of development, some of them in parallel, and others in a sequential way. In the framework of the current situation, we can identify three major groups of urban modelling, according to the mathematical techniques used. These groups are: the spatial interaction models, the discrete choice models (transport and land use), and the simulation models (cellular automata, and agent-based models). However, although there are other techniques used in urban modelling (such as optimization, econometrics (traditional and spatial), these applications are not massive, nor have representative and identifiable icons (Cerda, 2012).

3.1.2. The Morphological Approach: Local and Regional Viewpoint

Introducing the issue of urban form, it seems quite appropriate to cite a few lines from the work of Bernardo Secchi, *Le Forme della Città*, which first emphasized that the term "form" is difficult to imagine, while associated to the city. Actually, Secchi (2008) argued that the form of a city is not just a profile on the background of a landscape. The shape of a city, or some of its parts, is affected by a large number of concepts, which rely on spatial and social issues, thus including the forms of the landscape and territory, the forms of society in which they live, the social relationships that are there, the different forms of institutions, economics of politics and power; besides the forms of artistic expression, speech and imagination, without establishing any hierarchy and priorities between the different forms (Secchi, 2008). Therefore, the study of urban form is a key factor to understand, in order to be able to manage urban growth dynamics. It means understanding the physical complexities, at various scales of analysis, ranging from the buildings, to the street patterns that make up the structure of towns (Larkham, 2005), and the internal and external interaction that the city generates in the territory, thus giving rise to different typologies of spatial structures. So, besides traits, such as size and densities, and the dualistic relationship based on urban/rural functions, one of the most important features, considered for identifying and classifying different urban settlements and which has been investigated with particular emphasis during the last century, is the form of the city.

By using the words of Batty and Longley (1994) we could state that: a*s our immediate knowledge of the city is visual, it is perhaps explicable that urban problems which manifest themselves in cities are first associated with the destruction of visual order and harmony*. *We know instinctively that the physical form of cities is the ultimate result of a multitude of social and economic processes, constrained and shaped by the geometry of the natural and man-made world. We know that urban problems are manifested in the first instance in physical and spatial terms. We also know that many, if not most, of the instruments we have at our disposal for designing better cities are physical in form and intent. But there is still no widespread consensus as to the importance of form, geometry, layout, and configuration which characterize the physical city* (Batty and Longley, 1994).

The research about urban form relies on the field known as urban morphology, which lies at the intersection of several academic disciplines, such as architecture, urban planning, geography, statistics, and history. It aims to "explain" the city intended as a "natural" human habitat. In particular, urban morphology first assumes that urban shapes rely on modelling the surrounding space through dynamics of demographic movements and economic activities as well as social relationships over time[118].

Many contributions have supported this field of research for over half a century, through analysing the urban growth phenomenon from different perspectives of the spatial shape, as well as with different scale approaches. Besides the already cited Secchi, Batty and Longley, or Moudon; an important enquiry about urban morphology, at both regional and local scale, is provided by Gauthier, et al. (2006). It relies basically on "classifying" several of the most important contributions, according to different *theoretical or epistemological perspectives*, provided over the last few decades in this scientific ambit.

By using a "simple" Cartesian grid, they synthesize many representative studies in order to "improve intelligibility" in urban morphology, and through a *two-tiered examination of prevailing approaches in the field* (figure 3.3).

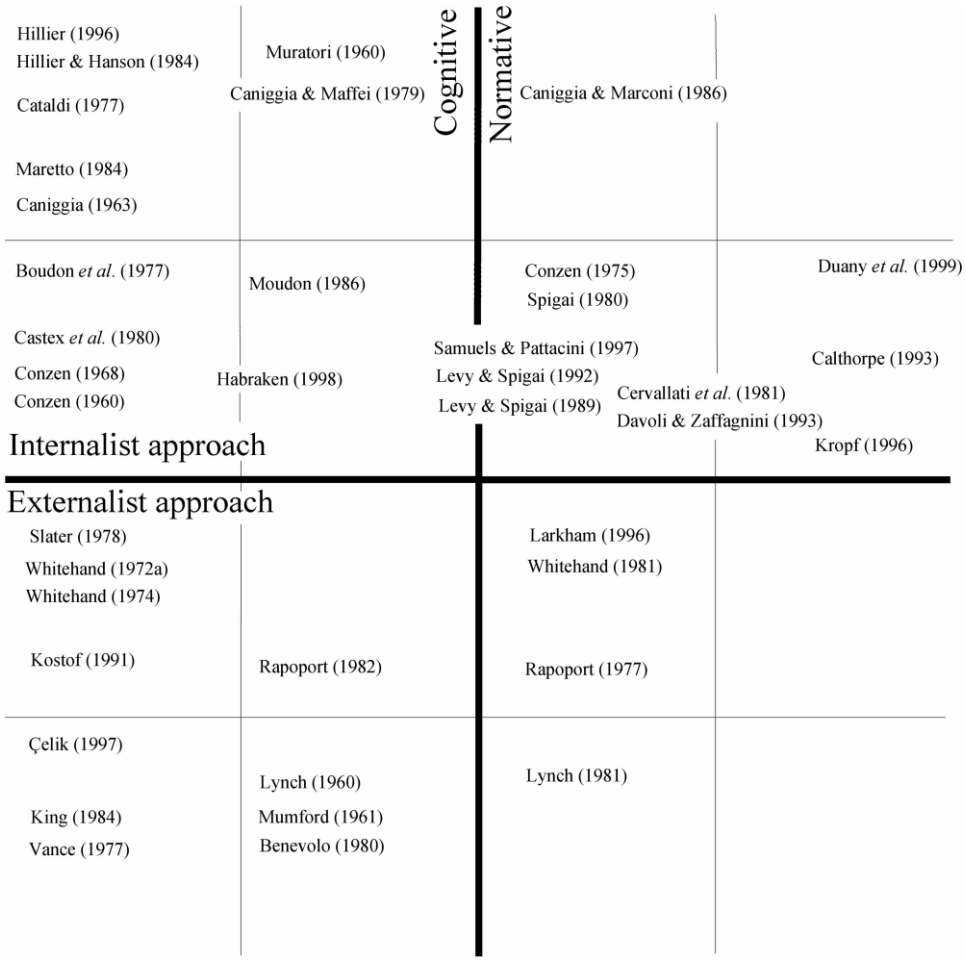

Fig. 3.3: Mapping of key contributions to the study of urban form (Source: Gauthier, et al., 2006)

[118] *Urban morphologists focus on the tangible results of social and economic forces: the study of outcomes of ideas and intentions as they take shape on the ground and mould our cities. Buildings, gardens, streets, parks and monuments, are among the main elements of morphological analysis* (Moudon, 1997)

The Cartesian space used for classifying relies on four items and two distinctions[119], which, first being between cognitive[120] and normative[121] approaches to the study of urban forms, while a second distinction focuses on concepts known as internalist[122] and externalist[123] (Gauthier, et al., 2006).

Currently, the use of geometrical rules and perspective, applied to urban design, was the basic principle on which Camillo Sitte founded his classical principles of urbanism and were already seen since the end of 19th century. The most famous work by Camillo Sitte relies on a morphological analysis of European cities, the urban space and its standards of "beauty". As argued by Sitte (1889), it is important aesthetically only what can be perceived by the senses and through the eyes, while walking through the streets (Milesi, 2006). This statement is a different way to express the aforementioned *"our immediate knowledge of the city is visual"* (Batty, et al., 1994). Pierre Lavedan during the first half of the 20th century used geometrical concepts for describing three main "archetypal" urban forms. By analysing the pattern of three cities, Kimolos, Saint Nicolas de la Greve and Brieve, Lavedan (1926) speaks about the "squared" city, the linear city, and the star-like city (Figure 3.4).

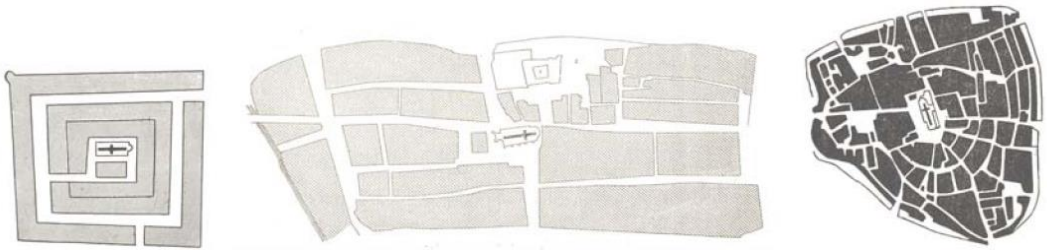

Fig. 3.4: Samples of Squared city, linear city, and star-like city: Kimolos, Saint Nicolas de la Greve, Brieve (Source: Lavedan, 1926; Milesi, 2006)

It was during the beginning of the 20th century that in England, the most famous movement of the garden city as a method for urban planning practice took place. It was under the umbrella of the theories and plans for ideal cities developed during the last part of the 19th century, such as the model of city for workers at Bourneville in Birmingham, or Port Sunlight (Liverpool) founded in 1886, that Ebenezer Howard, in harmony with the Utopian socialist movement, proposed his theories about the model of garden cities[124].

A new urban typology, arising from the decentralization of the metropolis, based on self-sufficient units made by single-family buildings surrounded by green areas, which collected the positive aspects of both city and countryside by making an urban environment available, with all the amenities and comforts that it implies, together with the characteristics of rural life[125]. Although, currently, it is seen as a sort of "aberration" that occurs in the use of the term garden city, as it is often synonymous of certain "formless" contemporaneous suburbs based on low

[119] Actually, *drawing upon the work of Lang (1987), Moudon (1994) proposed a similar distinction aimed at producing an epistemological map of substantive research related to urban design by using the terms normative-prescriptive and substantive-descriptive for describing each category*. While, *Levy (2005) suggested that the same distinction be made in the field of urban morphology, to distinguish between what he termed normative and cognitive approaches* (Gauthier, et al., 2006)

[120] *The expression "cognitive" reflects the heuristic nature of an intellectual enterprise concerned with producing knowledge, or at developing theoretical means, methods, techniques and analytical tools destined to produce such knowledge* (Gauthier, et al., 2006)

[121] *The term "normative" denotes an intellectual exercise accurately, which aims to articulate a view of what the future should look like, or at exposing a doctrine or specific sets of norms and prescriptions that would serve such a view, and thus for formulating an approach to planning practices* (Gauthier, et al., 2006)

[122] The "internalist" approach refers to the theoretical framework which finds the main explanation of morphogenesis based on constraints and potentialities for changes within the same urban system, i.e. basically by understanding the internal logic of the urban fabric (Gauthier, et al., 2006)

[123] "*Externalist" focuses on those approaches that primarily see the urban form as the end product of processes driven by political (e.g. Çelik, 1997), anthropological (e.g. Rapoport, 1977, 1982; Rykwert, 1988), geographical and economic (e.g. Vance, 1977, 1990), historical (e.g. Benevolo, 1980), and perceptual (e.g. Lynch and Rodwin, 1958; Lynch, 1960) determinants* (Gauthier, et al., 2006)

[124] Available in: *Tomorrow, a peaceful path to real reform* (1898), and *Garden cities of tomorrow* (1902)

[125] In 1904, the construction began of Letchworth, the first garden city, about 40 km north of London, on land purchased by the same Howard, and designed by architects R. Unwin and B. Parker.

density residential settlements. The original idea of Howard's garden city[126] involved the construction of new towns based on precise rules of density and form. In fact, the size was intended to be limited to 30˙000 inhabitants in an area of 1˙000 acres destined to the urban core, and 2˙000 inhabitants in the expected 5˙000 acres of farmland, surrounding the city by providing a sort of "farm belt". Once these numbers were reached, other cities were planned to be constructed in order to form a "network" of garden cities, all linked together by means of rapid communication pathways. A well-defined shape for a territorial system was set up, by harmoniously relating the town with the countryside, in a kind of "planned dispersion" (for using Mumford's statement[127]).

According to Mumford (1981), Howard understood that once the "optimum" equilibrium was reached, a city no longer needs to increase further in size and population, but form part of a broader context that has the advantages of large numbers of people and equipment on a large scale. The principles of design and aesthetics of the garden city, which were quite widespread in England during the 20th century, generated plans based on very "regular" forms. Applying those principles of regular geometric shapes, in an easier way, it conceptually allowed us to recognize the main structures on a territory (Milesi, 2006). This is where the garden city model provides an important example of morphological rules applied at a territorial level. On the other hand, it is to be acknowledged that the use of geometrical rules for city planning can already be found in the symmetrical plans typical of the nineteenth-century city, in which geometric squares and sequences form regular figures together (Milesi, 2006). Moreover, the research of the "ideal" form of the city can be also found in the ancient circular plan of the city, as first proposed by Vitruvius, and successively reproduced in the ideal city during the renaissance period, which could be recognized in the plan of Palma Nova (figure 3.5) and is usually accredited to the Italian architect Vincenzo Scamozzi (Morris, 1979; Batty, et al., 1994).

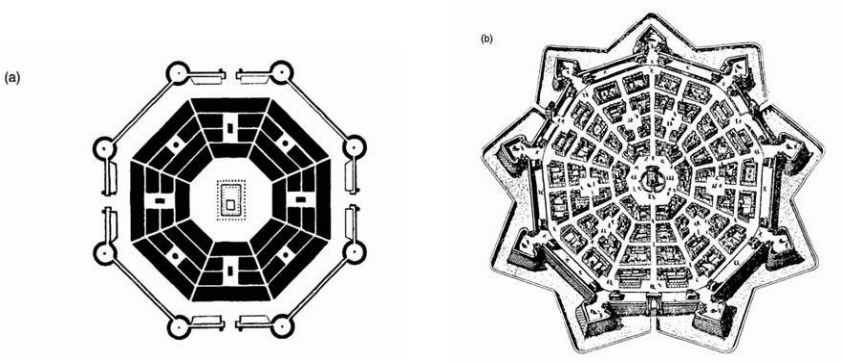

Fig. 3.5: The shape for an ideal city during the Renaissance: (a) from Vitruvius; (b) the plan for Palma Nova from Vincenzo Scamozzi (Source: Morris, 1979; Batty, et al., 1994)

Urban morphology, as an emerging interdisciplinary field (Moudon, 1997) supported by several scientists in the framework of spatial planning mainly during the 20th century (as shown in the previous scheme, figure 3.3), *primarily refers to the study of all those constraints and relationships which generate a specific land cover composition, the infrastructure network complexity, and the formal features of the built-up area* (Batty, et al., 1994).

It is generally and broadly recognized that there are three main schools of thought behind the field of urban morphology, which have gave rise to many followers and different perspectives since the second half of the past century. These are the Italian School, the British and the French. According to Gauthier, et al. (2006), these three seemingly different theoretical approaches are instead intrinsically similar, being that each one has contributed to the development of an *internalist* perspective on the development of urban form.

The Italian School focuses on the work pursued by Saverio Muratori, who attempted to provide an approach for integrating the architectural design within the syntax of the urban tissue. A second generation, within

[126] The Garden city model mostly relies on the idea of collecting the positive aspects of both city and countryside, by making an urban environment available and which arises from the decentralization of metropolitan functions. This is based on self-sufficient, and self-governed, units of single-family homes surrounded by green areas.
[127] Mumford, L. 1981. *La città nella storia.* [trans.] Italian. Milano : Bompiani, 1981

the Italian School, arises from the works of the "typologists" such as Caniggia[128], Maffei, Cataldi, and Maretto, which aim to strengthen the practice of analysing the built-up environment through the syntax of the building typologies, within an urban space intended as a dynamic environment that results from the interaction between political, social and economic forces. Actually, *various commentators have posited that the Muratorian tradition has developed a normative approach to the built-up environment* (Gauthier, et al., 2006), while Moudon (1994) states that the Italian school offers a renewed theoretical foundation for urban planning and design.

The British school mainly focuses on the work of M.R.G. Conzen, who attempts to *describe the integral role of urban landscapes in the early development of urban morphology, within the discipline of geography[129]. The morphogenetic method, cartographic representation and terminological precision, are the main topics on which Conzen put forward a sort of tripartite division of urban form, which first provides the town plan, or ground plan (comprising the site, streets, plots and block plans of the buildings); secondly, building fabric (the 3-dimensional form); and thirdly, land and building utilization* (Conzen, 1960; Whitehand, 2007). *More important than the proposed division of urban form, within the work of Conzen, are the concepts he developed, about the process of urban growth* (Whitehand, 2007), *which relies on a thorough, almost geological, examination of historical evidence, and became a powerful tool for elucidating the development of towns and cities in Britain, especially in the north east* (O'Sullivan, 2000). The model behind the method of the British School relies on the cognitive approach, instead of the normative approach of Gianfranco Caniggia, in the framework of the Italian School (Gauthier, et al., 2006). "Followers" of Conzen's work, such as J.W.R. Whitehand, have *pushed the limits of urban morphology into urban economics, by researching the relationship between the city, its habitat, and the dynamics of the building industry. In 1974, he formed the Urban Morphology Research Group at the University of Birmingham, which includes research on mediaeval cities that was notably conducted by T.R. Slater[130], as well as studies of twentieth-century suburban expansion and transformations* (Moudon, 1997).

The French *typo-morphological* approach emerging during the late 1960's, which had its major antecedents in the Italian Aymonino-Rossi branch of the Muratorian School, placed the attention on the dialectical interaction between the physical and historical evolution of the town and its building types. In particular, within the most famous *Ecole d'Architecture de Versalles*, the research in the urban morphology field was mainly pursued by the architects Jean Castex and Philippe Panerai, in addition to the sociologist Jean-Charles De Paule (Darin, 1998).

A significant contribution to urban morphology derives from the research tradition known as "space syntax" (Hillier, et al., 1984; Hillier, et al., 1993). This is based on a *graph representation* of spatial patterns and the understanding of the city as systems of open space, of which the organization can be described by *simple structural measurements of the resulting graphs* (Gauthier, et al., 2006). This approach relies on the idea that the layout of the road network, together with other urban open spaces, provides one of the main elements of urban morphology. In fact, a typical method within the space syntax derives from constructing an axial map for public spaces by drawing a set of axial lines, providing the *minimum number* of lines apt to cover the studied open space (Asami, et al., 2002). According to Hillier (1997), *because cities are essentially nonlocal[131] systems, the method leads to a powerful analysis of urban structures. The 'line-graph' internalizes geometric and metric properties into the structure of the graph, so it allows the analysis to pick up the non-local, or extrinsic, properties of spaces that are critical to the movement dynamics through which a city evolves its essential structures* (Hillier, 1997).

During the twentieth century, social scientists have largely questioned physical and functional models of cities, besides matters of the more suitable ways for identifying limits between the urban core area and the surrounding environment, and in order to better explain those forces which commonly links a city to its regional space. Two main groups of theoretical approaches about the analysis of *urban form and urban extension could be*

[128] *In Italy, Gianfranco Caniggia took up the mantle of Muratori which he called "procedural Topology" because of the focus on building types as the elemental root of urban form* (Moudon, 1997)

[129] *The origins of urban landscape management are intimately connected to the nature and development of an important part of urban morphology itself (Conzen, 1966). That part is concerned with tracing how the physical configurations of cities have developed over time. An important basis for urban landscape management was the urban landscape units (or morphological regions) identified from systematic survey and analysis of the historical development of towns and cities. But, linked to the social, economic and cultural forces driving the development of urban areas, systematic surveying and mapping of ground plans, building types, and land and building use became fundamental to the recognition of urban landscape units* (Whitehand, 2005)

[130] Slater, T.R. 1990. *The built form of Western cities.* Leicester : Leicester University Press, 1990

[131] *Nonlocal properties are those which are defined by the relation of elements to all others in the system, rather than intrinsic to the element itself* (Hillier, 1997)

discerned. In fact, while a first group of analysts, during the first decades of the century focused on the study of the internal structure of the city (as can be read in the previous paragraphs); an increasing interest towards regional perspectives of urban development grew later, mostly due to new dynamics of urban development, such as suburbanization and de-urbanization. *Towards the end of the century, these two groups seemingly came together in a new debate on the terms "city" and "urban region"* (Bontje, 2001). Actually, since the mid-20th century, the idea of examining urban form on a larger scale, i.e. the city and its region, has become well established. Urban morphology as an interdisciplinary field of analysis has been more and more implemented in studies concerning the form of urban pattern on the territory, in relation to all the causes and effects which it implies. Therefore, the approach provided by Hillier and Hanson's (1984), based on space syntax, provided a first change in the scale of analysis by aiming to analyse the spatial forms at a slightly higher scale than the architectural. So they intended to quantify *the actual network qualities of neighbourhoods and districts up to entire cities*, by using statistical measurement of *patterns of connectivity described using graph theory* (Batty, et al., 1994).

It is doubtless that the samples of shapes and geometries, and thus current urban forms, have strongly and rapidly changed, mostly during the second half of the past century due to the improvement in technology that has enhanced the capacity for the urban space to spread out over the territory. Therefore, the analysis of urban settlements must be adapted to "new" formal paradigms, by considering the cities as being more and more related to a huge surrounding environment, which is not only the built-up area, but rather the space between the networks of urban centres.

According to Lewis Mumford, *in our time, new forces have appeared, that threaten to shatter the historic urban forms and to scatter the contents of the city at random over the landscape. The overfilled urban container has burst. The central core has become demagnetized. All roads still lead to Rome, only to find that our new "Romes" have become faceless and formless*[132]. According to Benni, et al. (2007), the territorial systems following this logic of growth have experienced major changes during the last few decades, especially in the zones extending outside the compact urban structure, generally defined as peri-urban. These have given the landscape certain features quite different from the typical urban structure of the traditional compact nuclei or of rural areas.

These spatial dynamics, at a territorial scale, make it more difficult to quantify the urban form and this tends to develop by following a more "organic" and irregular way. Therefore, in light of this, the main approach proposed by Batty & Longley (1994) should be mentioned, which relies on the use of fractal geometry for measuring complex models of urban growth, as a link among more dynamic urban modelling approaches based on mathematical modelling of cities, for simulating possible urban growth scenarios and more purely morphological concerns (O'Sullivan, 2000).

In this scenario, Michael Batty (2008) states that *cities are highly organized with respect to their form, displaying in terms of city size, clusters of activity on all scales, in short, fractal*, and that *fractal geometry enables us to search out functions and processes which give rise to the man-made and natural patterns we observe in the real world, thus helping us not only to describe and understand reality a little better, but to progress our forecasts and predictions of how the real world might evolve* (Batty, et al., 1994)[133].

An earlier effort for analytically defining the complexity of urban dynamics on the territory, and an attempt at providing a morphological description of urban form based on the use of mathematical tools was provided by Christopher Alexander in a famous paper entitled "A city is not a tree" (1965). In his work he pursued the *idea that any concept of the city must necessarily involve breaking it down into units. These units, in turn, may be grouped into sets of related elements. A semi-lattice arrangement,* not a tree-structure*, of such elements is formed when any intersection of two sets of elements is also a potentially meaningful set of elements* (O'Sullivan, 2000).

In 1994, Batty & Longley spoke about the organic city, as mentioned from the Alexander theories, for identifying *not only cities which display an 'irregular' geometry, but also cities where that underlying structure of the*

[132] Lewis Mumford, *The City*. New York, 1939. Documentary film

[133] *There is a great deal of work investigating urban form using more recently developed mathematical tools, particularly cellular automata and fractal geometry. A direct connection between discretized cellular or grid-based simulations of urban growth processes and resultant fractal forms was established in earlier work by Batty & Longley (1986). The use of fractal geometry applied to urban morphology is thoroughly discussed by Batty & Longley (1994). The crucial insight here is the direct applicability of measures of fractal dimensionality to urban systems represented in various ways. Given the origin of fractal forms in processes operating across a range of scales, but in generally local ways, this is a suggestive result* (O'Sullivan, 2000)

geometry of its relationships is also 'irregular', or at least asymmetric in the sense of the difference between a lattice and tree (figure 3.6).

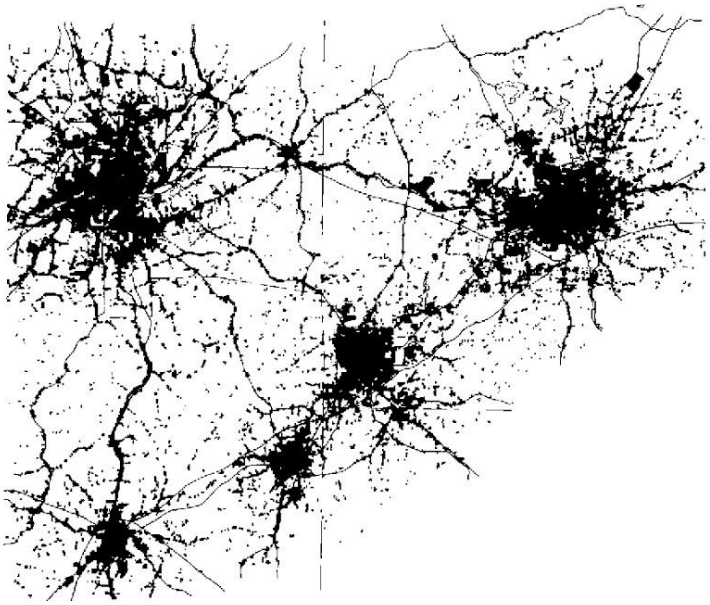

Fig. 3.6: Contemporary urban growth patterns (Source: Chapin, et al., 1962; Batty, et al., 1994)

Actually, the incipient evolution of new technologies applied to spatial analysis (such as Geographical Information Systems (GIS), and Remote Sensing through aerial and satellite imagery, besides the improvements in computational capacities) now allows not only to record spatial characteristics about the environment including the land cover composition, but also to link spatial features to quantitative data for implementing powerful statistical examinations and measuring the physical space in relation to the socio-economic dynamics that shape it (Moudon, 1997). It provides the possibility of analysing huge areas as complex urban systems spread over the territory, ranging from a parcel level to a regional scale. Besides this, the geographical description of fundamental spatial characteristics of urban shapes has required the implementation of specific metrics for a mathematical definition of measurements: such as symmetry, elongation, linearity, compactness or dispersion of the urban profile.

In this context, the work undertaken by the Landscape Ecology Lab at the University of Massachusetts in Amherst directed by Kevin McGarigal needs to be mentioned, which relies on research studies about sustainable landscape management within the wider discipline of landscape ecology[134]. Through the implementation of a computer software program (FRAGSTATS), as a research tool for spatial analysis purposes, the Landscape Ecology Lab has developed an effective information technology platform for computing a wide variety of landscape metrics for categorical map patterns. The software in particular allows us to calculate several indices, grouped by following general concepts: such as area metrics, density, size and variability, shape metrics, as well as nearest-neighbourhood, diversity, and contagion metrics. This is focused on analysing the environment at three different levels of detail: patch, class and landscape[135] (McGarigal, et al., 1994).

Another interesting approach to the analysis of dynamics of urban development at a territorial scale (i.e. the urban profile as a whole, not at building level), relies on comparing the growth which occurred since the early 1990's in 120 urban areas around the world, both in terms of land consumption, as well as in terms of population growth, is provided by the Lincoln Institute of Land Policy. By using new technologies for computing objective

[134] *Landscape ecology, as the name implies, is the study of landscapes; specifically, the study of landscape patterns, the interactions among the elements of pattern, how patterns and interactions change over time, and the consequences (ecological and socio-economic) of these patterns and changes. In addition, landscape ecology involves the application of these principles in the formulation and solving of real-world problems. Landscape ecology is perhaps best distinguished from other ecological disciplines by its focus on: 1) spatial heterogeneity, 2) broader spatial extents than those traditionally studied in ecology, and 3) the role of humans in creating and affecting landscape patterns and process. The central unifying theme of landscape ecology is the interplay of spatial pattern and process. In other words, landscape ecology seeks to understand how spatial patterns affect and is affected by ecological and socio-economic processes* (UMass Landscape Ecology Lab)

[135] Detailed information about FRAGSTATS and employed metrics at: http://www.umass.edu/landeco/research/fragstats/fragstats.html

metrics about the form of development, such as area metrics, besides indices of compactness, fragmentation, and densities, the work aims to "explain" phenomena such as urban dispersion, inter alia, for different geographical ambits (see paragraph 3.2.3.3).

Morphological criteria have often been used also for delimiting the urban extension and measuring the impact of built-up areas on the environment. In Europe, for instance, an important approach to the morphological delimitation of urban agglomerations, defined as Urban Morphological Zones (UMZ), derives from the methodology provided by the CORINE Land Cover project. It was implemented by the European Commission in conjunction with the European Environment Agency, and for three main temporal stages since the early 1990's: 1990, 2000, and 2006 (see paragraph 3.2.1.1). Furthermore, the method provided by the Network on Urban Research in the European Community (N.U.R.E.C.), in the framework of the *Atlas of Agglomerations in the European Union* published in 1994, delivers a significant contribution to the morphological approach for defining urban areas. In particular, the method delimits a continuous settlement when the distance between built-up polygons is less than 200 m, and the inside green areas have a diameter smaller than 500 m, or the area is less than 25 ha. The primary detection of urbanization relies on photo-interpretation techniques by employing satellite imagery (Landsat 7 ETM+) in addition to ancillary topographic maps and the whole process has been applied to many municipalities, with at least 100˙000 inhabitants within the European space by using the administrative boundaries of communes as a basic unit of measurement. In the context of the European Research Project COMET[136], the addition of a fringe area has been proposed in order to avoid the exclusion of important areas, and this is done by calculating the fringe as an ambit within a distance of 10 km from the N.U.R.E.C delimitation. Maintaining the same administrative boundaries as a basic unit, the communes "touched" by the fringe are included in the same urban agglomeration *if either more than 50% of their area is located inside the belt, or if more than 50% of their inhabitants live inside the 10 km belt* (COMET).

3.1.3. From Compactness to Urban Sprawl: Aberration or Natural Progression?

As we have seen in the previous sections, a number of important and rigorous theories concerning the dynamics of urban growth and several approaches to spatial analysis have been proposed since the last century. Actually, from the analysis based on precepts of human ecology, to strictly economic approaches, to the study of the forms of the city based on the urban morphology field, all these approaches are not alternatives, but rather complementary, because the urban space is the result of several dynamics that act simultaneously.

The action of such dynamics throughout history has generated different models of growth, but with the evolution of transport technology, which has occurred since the early decades of last century, the urban space began to grow much more rapidly and to expand more and more over the surrounding landscape, thus giving rise to much more complex urban forms that now need to be examined, not just at the urban level but at a territorial level. Indeed, the widespread use of the car has led to exacerbation of that phenomenon of centrifugal movement of the population, which now moves towards to urban areas farther and farther from the city center, looking for less congested and less urban spaces. In fact, as argued by Arellano & Roca (2010), *the expansion of the cities had its origin in the model of suburban life, which began with the generalized use of the automobile. A lifestyle based on the "American dream", one single family-home, one (or more) car (s).*

Around the metropolis, the automobile, because it had more freedom of movement, scattered the fragments of the city at random over the whole countryside, flinging ever larger numbers of people into ever more distant suburban dormitories, much thinly scattered and populated to be served by public transportation. These fragments can be served only by the automobile. The more the city has scattered, the more the need for the automobile (Mumford, 1939). Actually, this model of city makes typologies of settlements very demanding, in terms of mobility, being difficult to deal with mass transport and therefore induces intensive use of private cars for urban journeys (Pozuea, 2000; Cerda and Marmolejo, 2007). *But it has been since the late 1970's of last century, when it has had a more dramatic development, as a consequence of the crisis of metropolitan areas linked to what is called Post-Fordism economy and some authors have characterized as counter-urbanization (Berry, 1980), desurbanization*

[136] *COMET Competitive Metropolises* is a research project supported by the European Commission under the Fifth Framework Programme, which included 16 European participants within 7 countries/cities, developed between 2001 and 2004

(Berg, et al., 1982), edge-cities (Garreau, 1991), metapolis (Ascher, 1995), or diffuse city (Indovina, 1990). Despite the diversity of urban development, the increasing consumption of land, the excessive use of land as a scarce resource, it is a constant in the urbanization process in the early twenty-first century (Arellano & Roca, 2010).

Berry (1976) described urban development until the 1970's through four sequences, which are: the absolute centralization, which occurs when the population growth derives from the concentration in urban centres, at the expense of growth in the rest of a region; the relative centralization, in which both center and periphery grow together; the relative decentralization, which is when the suburbs grow faster than the inner city; and the absolute decentralization, or the "counter-urbanization"[137], which affects either the metropolitan area, as a whole, non-metropolitan areas or isolated urban nuclei as well as the rural area (Cerda and Marmolejo, 2007).

Such a (absolute) decentralization process of the population and functions that, in a generalized way, occurred principally since the seventies, has given rise to the phenomena of urban dispersion and fragmentation, in most of the cases following a low density development based on a different speed between urban growth rate and demographic trend. The space of the city has increased and spread mainly by invading nearby territories, an uncontrolled consumption of land, incorporating neighbouring towns and merging more cities within a continuous urban development. Conurbations, metropolitan areas, megalopolis, urban corridors, diffuse urbanizations are all included in the next phase of the urban development process. This has not been taken into account at all, either politically or culturally, even if it is currently spreading worldwide and whose future developments are not yet exactly known (Equip Redactor del PTMB, 1999). However, the global nature of such urban expansion has led the scientific community worldwide, during the last few decades, to devote increasing attention to the study and quantification of this phenomenon which, nowadays, is widely recognized by the term "urban sprawl". Indeed, many approaches and theories are currently available concerning the matter.

As argued by Angel, et al., 2010, *there is an almost universal consensus, with a few minor exceptions, on what the key manifestations of the urban sprawl phenomenon are: endless cities, low densities, fuzzy boundaries between city and countryside, a polycentric urban structure, large expanses of single-use zones, ribbons and commercial strips, scattered development, leapfrogging development, and the excessive fragmentation of open space, among others*. In particular, some key topics on which several researchers focus the measurement of the urban sprawl are: the growth rate, or expansion, of the built-up area over time, beside the decongestion, suburbanization, fragmentation and dispersion of the urban outline over the territory.

Indeed, some scholars *define and measure sprawl as the quantity of land converted to urban use* (Sinclair, 1967; Brueckner, et al., 1983; Lowry, 1988; Hasse, et al., 2003). This is the *expansion, or the formation of 'endless' cities, typically measured by the increase over time of the total built-up area (or impervious surface) of cities, sometimes including the open spaces captured by the built-up area or the open spaces on the urban fringe affected by urban development* (Angel, et al., 2010).

Others (Brueckner, et al., 1983; Brueckner, 2000; Civco, et al., 2000; Ewing, et al., 2002; Fulton, et al., 2001; El Nasser, et al., 2001) *define and measure sprawl as low density or density decline, i.e. the decongestion, or the decline of urban densities, typically measured as the decline over time of the ratio of the total urban population and the total built-up area it occupies* (Angel, et al., 2010).

There are also scholars that define and measure sprawl as *the increasing share of the urban population living in suburbs* (Self, 1961; Gottmann, et al., 1967; Jackson, 1972; Kasarda, et al., 1975; Hall, 1997), i.e. the *suburbanization, or the decentralization of metropolitan areas, which is typically measured by the decline in both parameters of the density curve, i.e. its intercept and its gradient, where the first corresponds to maximum densities at the urban center, and the second to the rate of decline in density as distance from the city center increases* (Angel, et al., 2010).

Further scholars (Clawson, 1962; Peiser, 1989; Carruthers, et al., 2001; Heim, 2001; Weitz, et al., 1998; Burchfield, et al., 2006) *define and measure sprawl as non-contiguous development, also known as fragmentation, or scattered development, which is typically measured by the relative amount and the spatial structure of the open spaces that are fragmented by the non-contiguous and non-compact expansion of cities into the surrounding countryside* (Angel, et al., 2010).

[137] The term *counterurbanization*, was coined by Berry in 1976, for defining *a process of population deconcentration, which occurred in the United States after the process of population concentration known as urbanization, and characterized by smaller sizes, decreasing densities, and increasing local homogeneity* (Berry, 1980)

Finally, some scholars also define *urban sprawl as dispersion, or the reduced interconnection of the urban footprint, which is typically measured by compactness metrics or by some of the accessibility metrics found in the literature and reviewed by Ewing who claims that "[u]ltimately what distinguished sprawl from alternative development patterns is poor accessibility of related land uses to one another"* (Ewing, 1994; Angel, et al., 2010).

Wilson et al. (2003) identified three categories of urban growth: infill, expansion, and outlying; with outlying urban growth further separated into isolated, linear branch and clustered branch growth. The relation (or distance) to existing developed areas is important when determining what kind of urban growth has occurred (Bhatta, 2012). However, according to Cerda, et al. (2007), an analytical compilation of definitions of urban sprawl, in social science and territorial planning literature (Galster, et al., 2001), allows us to identify various broad types which define the phenomenon from different standpoints. In particular, urban sprawl is often defined as:

- An "example" of a low density discontinuous urban development (the cities of Los Angeles and Atlanta are the most cited in that sense);
- A phenomenon related to sustainable development, i.e. as a cause of certain externality, such as a high reliance on automobiles, transport congestion, residential segregation, poor spatial relationship between residence and work, environmental pollution, among others. In this way, the phenomenon is understood as what it produces, and not for what it is;
- A consequence, or effect, of any independent variable such as the fragmentation of local government, poor planning or restrictive zoning. With respect to this, the explicit intentionality of such variables for producing a discontinuous expansion of the urban areas is not clear [138];
- A spatial pattern of urban development measured as the different spatial shapes that the phenomenon produces: such as, for instance, the discontinuous urban expansion, patterns of low-density development, randomly urbanized settlement, large tracts of housing, etc.

At any rate, *there is the oft-repeated lament that sprawl, as an overarching characteristic common to all these manifestations, is ill defined and therefore difficult to measure in a convincing and systematic way.* Following Galster et al (2001), Angel, et al. (2010) defined and measured sprawl both *as a pattern of urban land use (that is, a spatial configuration of a metropolitan area at a point in time) and as a process, namely as the change in the spatial structure of cities over time. Sprawl as a pattern or a process is to be distinguished from the causes that bring about such a pattern, or from the consequences of such patterns* (Angel, et al., 2010).

However, specialized literature also focuses on demonstrating the effects and impacts of urban sprawl by maintaining an explicitly negative position. The first positions are more radical and are reactions to the loss of agricultural land, or rather, the replacement of natural soil with artificial uses, by increasing the degree of land imperviousness. This is followed by approaches seeking to evaluate, from several points of view, the environmental implications, energy consumption and economic implications of urban sprawl, in comparison with what is known as the compact city. From a functional standpoint, urban sprawl is a relocation of part of a city into isolated settlements, formed by low-density residential uses and surrounded by a rural context, where the car is the main conveyance that allows interaction with suburbs or the city center (Cerda, 2012).

As argued by Bhatta (2012), *it is worth mentioning that opinions on sprawl held by researchers, policy makers, activists, and the public differ sharply, and the lack of agreement over how to define sprawl certainly complicates the efforts to characterize and restrict this type of land development*. On the other hand, *although accurate definition of urban sprawl is debated, a general consensus is that urban sprawl is characterized by an unplanned and uneven pattern of growth* (Bhatta, 2012).

Cerda (2012) highlights that while there is disagreement about what is meant by "urban sprawl", this phenomenon is broadly recognized as dispersed uncoordinated urban development not taking into account the social and environmental effects produced. One of the many lines of understanding and explanation of this phenomenon has to do with the so-called centrifugal and centripetal forces of urban development. This view of urban sprawl, allows the assumption of various combinations of these forces, which cause different types of expansion depending on the predominant force.

[138] *Downs (1998), among others (Black, 1996; Burchell, et al., 1998; Moskowitz, et al., 1993; Orfield, 1997), argued that sprawl occurs as a consequence of the fragmentation of control over land use in metropolitan areas. It is unclear whether sprawl is an intentional, necessary, or inadvertent consequence of fragmented governance of growth* (Galster, et al., 2001).

Nonetheless, although the definition of sprawl relies on broad and multidimensional analysis, and *a relative rather than an absolute characterization of the urban landscape should be provided* (Angel, et al., 2010); usually one of the biggest and widely recognized factors that identify this phenomenon is the territorial discontinuity of urban developments (Cerda, 2012). That said, it should be stressed that the discontinuous development, both in terms of urban shapes as well as densities, gives rise to different forms of sprawl. This means that, also following the previous assumptions, it is not feasible to us to speak about urban sprawl by taking into account a single type of pattern of development. In fact, the sprawl phenomena has a common matrix, which could be identified by an important dispersion of the urban texture over the territory. This is best characterized by low levels of population density, among others. In accordance with Cerda (2012), we should take into account at least four different kinds of urban sprawl. In particular, some of the main types of spatial shapes, which can be recognized as providing sprawled typologies of urban settlements, are:

- Low density continuous development, which is the model that "consumes" the largest amounts of land, mainly located on the urban fringe areas around the consolidated metropolitan structures;
- Linear development, which mostly occurs along the axis of great transport corridors which radiate from the central areas of the cities, thus generating an important urban/rural mixing phenomenon;
- Discontinuous development, often identified as the leapfrog phenomenon, that relies on marginal fragmented urban developments, and provides discontinuous and remote conurbations around metropolitan structures that requires great investments in urban services and infrastructures;
- Extra-urban dispersed development (known as low-density spread development), which is associated with the concept of low density housing within natural environments (agricultural, forestry, etc.), which goes even beyond the suburban agglomerations, by not providing suburbs nor rural patterns (Cerda, et al., 2007).

Although the term urban sprawl has been coined, and it is often used, for identifying a kind of urban growth typical of American metropolises, as in the case of Los Angeles, for instance (see transect at figure 3.7), we wonder what the common features are among the "American sprawl" and the model of dispersed urban expansion that has occurred over certain geographical areas in Europe.

Fig. 3.7: An American sprawl sample: transect of the city of Los Angeles (Source: By Authors, from Google Earth)

Actually, the next transects, provided by images 3.8, 3.9, and 3.10, illustrate three further urban textures that could reasonably be identified as phenomena of urban sprawl commonly found in Europe. In particular, image 3.8 shows an urban development typical of the north-east of Italy, normally identified by the concept of "*città diffusa*", as proposed by Francesco Indovina (1990)[139].

[139] According to Indovina (1990), the city should be considered primarily for its functionalities and social relations. This view does not deny that the physical/morphological character of the city (density, intensity, and lack of continuity) is significant, so that the concept of "*città diffusa*" does not reject a-priori the analysis of the physical transformation of the urban landscape, but mostly emphasizes the absolute importance of the connotation of "urban condition", i.e. functionality, and social relations. The meaning of "*città diffusa*" would be justified only under the assumption of such a point of view. Indeed, the *città diffusa* is not formed by only low density single-family housing but, instead this model foresees the existence of different residential forms and urban uses simultaneously, i.e. infrastructure, urban equipment, services (collective, private and public), business, and public spaces. On the other hand, all the components are not concentrated but mostly widespread according

Fig. 3.8: The "Città Diffusa": transect of Veneto, between Venice and Padua, Italy (Source: By Authors, from Google Earth)

Images 3.9 and 3.10, instead, show two examples of possible sprawl phenomena along the Mediterranean side of Spain. In particular, the first model (figure 3.9) is composed of an almost continuous and disorderly agglomeration front of low density housing along the coastline and towards the interior for several kilometers. Such a pattern empties the traditional model of a Mediterranean city of meaning. Indeed, as is the case of the main transport infrastructure, the coastline here acts as a catalyst for urban development that tends to follow a longitudinal model, often giving rise to contemporary models of linear cities basically produced by economic interests linked to the industry of tourism.

Fig. 3.9: Urbanization along the coastline of Alicante (Valencia), between Carrio and Moraira, Spain (Source: By Authors, from Google Earth)

Finally, the pattern in transect in figure 3.10 shows an urban structure made by several "leapfrogging" urbanizations, which mostly rely on just low-density residential uses. This model is often caused by a centrifugal force that pushes local people towards the suburbs from the center of metropolitan settlements, although maintaining strong functional relationships in terms of employment. Often these suburban settlements assume the essence of mere dormitory towns.

---

to a low-density continuity. The functional hierarchy is not as strong, because the structural elements do not seem driven by agglomeration but, rather, they follow dynamics of accessibility.

Fig. 3.10: Sample of suburban structure in Catalonia, within the municipal boundaries of Corbera de Llobregat, Spain (Source: By Authors, from Google Earth)

Although there have been, and still are, debates as to which degree compact urban form is more sustainable than a fragmented and sprawling city (Williams, 2000), there is a relatively wide consensus among planners and researchers that compactness is desirable from the point of view of sustainable development (Newton, 2000; Kasanko, et al., 2007). However, the question is if all the different types of urban expansion can be classified as urban sprawl (understood as a negative phenomenon) or, instead, certain growth processes are the natural evolution of the urban development. Kasanko et al. (2007) stress the idea that *there are a large number of drivers which have made urban areas less compact during the past decades. Macro and micro economic factors, such as economic growth, rising living standards and intra-municipal competition are the underlying triggers for urban sprawl. It is also affected by transport issues and housing preferences*. As remarked by Finley, 2011, *urban development is a growing phenomenon fuelled by the need to accommodate growing populations with housing, work space and efficient means of transportation*.

At the core, and concerning the territories, it seems that there are two opposing views. Urban development has always favoured a kind of organization based on zoning, borders and boundaries, but the "new" typologies of urban expansion seem to be an opposing concept, being based on the idea of a reticular territoriality, which goes beyond zoning and barriers, and in which other “forces” are exerted. In new developments of modern urban planning, it is fundamental to recognize the territorial networks as a new paradigm for better understanding and modelling urban growth dynamics (Cerda, et al., 2007).

The new periphery is a complex space: at the macro scale, it appears to be a large diffuse structure and net-like, whereas at the micro scale each *node* of this network reveals specific characteristics and individual identities, and therefore the main principles of spatial organizing (Dematteis, 1998). Since the industrial revolution, the urban peripheries have been the sites of innovation and change, but only recently have they begun this vocation to be considered as a positive value and essential attribute of a metropolitan area. Large metropolitan areas are rich and complex spaces where the real city goes beyond administrative boundaries and urban space that becomes a network of municipalities that establish joint strategies for economic and social development for their territory and strategies for linking them to global networks. (Cerda, et al., 2007).

Currently, the contemporary trends in urban development such as the Città Diffusa theorized by Indovina, for instance, or the peri-urbanization defined as the process of dispersion of urban zones usually following suburbanization and counter-urbanization (Racine, 1967; Berry, 1976; Dematteis, 2003), are summed up by the concept of “metropolization” as theorized by Camagni (1999). He interprets the urban growth dynamics observed in the European scenario according to three different patterns of metropolization, i.e.: diffused metropolization, concentrated metropolization, and a set of urban and regional networks (Benni, et al., 2007). The same Francesco Indovina defines the structural changes happening in the urban forms in Veneto, and the metropolitan area of Milan, and as an expected consequence of the intense phenomena of decentralization occurring during the previous decades. Due to this, Bernardo Secchi (2007) argued that, the dispersion, not only in the European diffuse

city, is actually not the result of a centrifugal movement or "explosive" escape from the city, but rather the opposite. It is often the result of a progressive densification of a much older pattern of settlement, and indicates a radical change in the modern condition, a change that involves forms of social and political organization, the relationship between society and objects, and between society and territory.

Benni, et al. (2007) also highlight that some scholars like Hall, Cheshire, Berg and Drewett, among others[140], perceive these changes as successive phases of an *urban life cycle* which, starting with the concentration of population in the central nucleus or core (urbanization), goes on with the growth of the *rings* (suburbanization), followed by a demographic decline (de-urbanization) and a hypothetical recovery of the core (re-urbanization) (Dematteis, 1998). Nel·lo (2001) draws attention to the fact that the present process of urban diffusion over the territory could also have positive effects, mostly when the decrease of density in central urban areas could favour the progressive relative homogenization of urban functions all over the territory, such as work, infrastructure and services. On the other hand, he also points out that, being largely regulated by the filters of soil and the housing market, the old and large social contraposition, i.e. centre vs. metropolitan periphery, this gives rise to a much more complex “kaleidoscope” where barriers do not disappear but are multiplied in smaller and smaller units.

3.2. LAND COVER MONITORING AND SPATIAL ANALYSIS: MAIN PROJECTS ANALYZED

Land Cover/Land Use information is primary information for spatial analysis. Its quantification delivers an important measurement of human activities within the natural environment, such that the consumption of natural resources in most cases, is derived from urban development and is one of the principal drivers of environmental changes (Lobley & Winter, 2009, European Environment Agency, 2010). *Extensive urbanization and increasing population growth – especially in the megacities[141] of developing countries – were recognized as being of major concern in 1992, when the United Nations Conference on Environment and Development (UNCED) recommended redressing the various environmental problems caused by urbanization, and promoting economic, social, and ecological dynamics that would enhance the contribution of the city to sustainable development. More recent evidence has heightened the urgency of monitoring and understanding urban dynamics* (Lavalle, et al., 2002).

The solution to the problems of contemporary cities obliges us to reconsider the conventional urbanistic theories, but above all, the way of managing suitable spatial information about urban growth phenomena and the interaction with the environment. The need for standardized information about land use/land cover is more and more evident when assessing and managing areas such as floodplains and wetlands, wildlife habitats, or the main sites of residential and industrial development, for instance. These represent the main aspects for environmental control, from the standpoint of sustainable development (Anderson, et al., 1976).

The best planning practice is necessarily linked to a better prior knowledge of the territory, so indirect methods for generating thematic cartography through photo-interpretation of aerial or satellite imagery for classifying and quantification of land cover classes, provide the main tool for gathering such knowledge. In particular, it is based on three fundamental topics: precision and homogenization of the information at large scales, rapidity in collecting information which allows continuous monitoring over time and an effective cost-time balance. The improvement in new technologies linked to the field of geomatics, such as remote sensing and GIS, provide tools for “quickly” acquiring and analysing spatial information, although the use of automatic processes requires a reduction in subjective interpretations and arbitrary interventions by analysts, as much as is possible.

As early as the 1970’s, Anderson et al. (1976), emphasized that *recent developments in data processing and remote sensing technology make the need for similar cooperation in land use inventories even more evident and more pressing. Development and acceptance of a system for classifying land use data obtained primarily by use of remote sensing techniques, but reasonably compatible with existing classification systems, are the urgently needed first steps*.

[140] See HALL, P. and HAY, D., Growth Centers in the European Urban System, Heinemann, London 1980; BERG Van Den, L., DREWETT, L. (et al.), Urban Europe: a study of growth and decline, Pergamon, Oxford 1982; and CHESHIRE, P. and HAY, D., Urban Problems in Western Europe: An Economic Analysis, Unwin Hyman 1989

[141] Large and fast-growing urban areas (Lavalle, et al., 2002)

At present, in Europe for instance, a directive (DIRECTIVE 2007/2/EC), was approved in 2007 to establish Infrastructure for Spatial Information in the European Community (INSPIRE)[142], which included a great variety of topical and technical themes and came into force on 15 May 2007. This had the prevision of performing various sequential stages, and with full implementation required by 2019 in order to enable the sharing of environmental spatial information among public sector organizations in Europe, and for better assessing policy-making across administrative boundaries.

In 1985, the European Commission launched the CORINE Program, and within it, the CORINE Land Cover (CLC) Project, which is one of the most important projects for producing a homogeneous database of land cover for the whole of Europe, and covering around 20 years in three main temporal stages: 1990, 2000, and 2006. A key objective of this project, in line with other projects such as MURBANDY and MOLAND, is producing a consistent and standardized nomenclature of land cover typologies at the European level, together with effective indices for spatial analysis of the environment. The same effort has been pursued during the past few decades in other countries, where other LC Nomenclatures have been developed and used. E.g.: 1976 USA's USGS Anderson´s Nomenclature (Villa, et al., 2008). This is the reason why more recent projects, such as GlobCOVER (2006), are currently following the objective of providing a global generalization and homogenization of an effective nomenclature which focuses on the different land cover classifications.

Quite a lot of useful techniques, based on remote sensing and GIS technologies and methodologies for automatic classification and analysis of the environment for both urban landscapes as well as for natural landscapes, have been developed in the last few decades due to the undoubted acceleration of the urban growth phenomenon experienced at a global scale.

Earth observation, by aerial photographs or satellite imagery, offers primary tools for global monitoring of land cover, due to an increasing provision of digital and homogeneous information from sensors on-board several remote platforms. Digital imagery derived from sensors able to capture the land reflectance in different ranges of the electromagnetic spectrum are used for extracting thematic cartography basically through two different approaches: visual photo-interpretation of landscape features, by using techniques of image enhancement and computer-assisted digitalization; and automatic classification based on spectral information stored in a multispectral raster format (see chapter 4). In both cases, the extracted objects are mapped and labelled, according to specific nomenclature (Weber, 2009).

A quite representative sampling of projects aimed at the classification of land cover based on both photo interpretation techniques as well as on automatic classification procedures, besides spatial analysis objectives, are highlighted below, according to a division which relies on three geographic scenarios: the European framework, the national level for Spain (with a detailed case for the region of Catalonia), and an "international" outline covering projects developed in North America.

3.2.1. European Viewpoint

In Europe, the main land cover changes in relation to economic drivers and ecological impacts are: urban sprawl, agriculture internal conversion/arable land, agriculture internal conversion/fallow land and set asides, conversion of natural land to agriculture, withdrawal of farming, afforestation, deforestation, forest rotations. They make more than 80% of total land cover change in Europe. The number may look small but when crossed with the various land cover types impacted, it gives a fairly good picture of the processes (Weber, 2009).

Urban development, industry and energy, transportation and agriculture all need amounts of land cover for being placed, but in a harmonious coexistence with the natural environment. At present, political decisions that affect different developments of land use over time, also involve many sectorial interests and thus could produce important changes in an ideal equilibrium between them.

The European Member States, as recently as during 2005-2006, indicated an increasing need for real and quantitative spatio-temporal information about the state of the environment, and in particular, the current state of land cover/land use structure across the European territory. Strategic considerations have been undertaken between the European Parliament and the main EU institutions supporting environmental policy, reporting and

[142] http://inspire.jrc.ec.europa.eu/index.cfm/pageid/48

evaluations (such as the DG for Environment, the European Environment Agency, Eurostat and the joint Research Centre) in order to provide updated information about landscape monitoring (European Environment Agency, 2007).

In reality, a good balance among different needs could be achieved through the implementation of integrated programs for land use management and spatial planning, as well as through sectorial policies and instruments, such as the definition of protected areas networks. In the framework of the EU, integrated programs like the Territorial Cohesion and Water Framework Directive have been set up in addition to the guidelines of the Common Agricultural Policy (CAP) and the employment of renewable energy objectives, which will have significant impacts on forest and agricultural land uses mainly. The management of natural resources is also founded on the role of the so called "green infrastructures", as well as on the network of protected spaces provided by Natura 2000[143]. While the main tools for evaluating programs and projects that have an impact on land resources are the Strategic Environmental Assessment (SEA) and the Environmental Impact Assessment (EIA).

Undoubtedly, the most important instrument for land monitoring in Europe is the CORINE Land Cover (CLC) project inventory, developed over three temporal stages; the first one in 1990, then in 2000, and the last version was in the year 2006, which was basically an update of the 2000 results (a CLC 2012 is also available but not yet validated). The CORINE data, in combination with land statistics, currently supports the European ability for spatial analysis and monitoring of land-use changes as a robust basis for policy making (European Environment Agency, 2010).

3.2.1.1. CORINE LAND COVER (CLC) Project

From 1985 to 1990, the European Commission implemented the first CORINE program (coordination of information on the environment), thus giving rise to an information system (the CORINE system) for monitoring the actual state of the European environment, supported by standardized nomenclatures and methodologies developed and agreed on at EU level. CORINE land cover is currently recognized, from local to international decision-makers, as one of the key reference data sets for spatial and territorial analysis[144] at different levels. This is because many of the European entities, such as Regional Policy DG, Environment DG and Agriculture DG, as well as the European Environment Agency and its European Topic Centres (ETCs), need precise and easily accessible spatial information at one's disposition for providing integrated environmental assessment on land cover in Europe and is a growing necessity (European Environment Agency, 2002).

Setting up the European Environment Agency (EEA) and the establishment of the European Environment Information and Observation Network (Eionet), the CORINE land cover (CLC) project has been realized in most of the EU countries as well as in Central and Eastern European states. The coordination and generation of the CORINE database, with updating, is undertaken by the same EEA. Following the first CLC inventory (CLC 1990), the first update was implemented in 2000, in the framework of the I&CLC2000 project[145], with the overall objective of producing an updated, so called CLC 2000, in addition to the database of land cover changes between the two CLC projects 1990-2000 (European Environment Agency, 2007).

The CLC classification describes land cover (and partly land use) according to a standardized nomenclature which includes 44 land cover/use classes (Level III), hierarchically grouped in three levels. The five main categories,

[143] Natura 2000 is an ecological network of protected spaces throughout the whole European Union territory. In May 1992, European Union governments adopted legislation designed to protect the most seriously threatened habitats and species across Europe. This legislation is called the Habitats Directive and complements the Birds Directive adopted in 1979. At the heart of both these Directives is the creation of a network of sites called Natura 2000. The Birds Directive requires the establishment of Special Protection Areas (SPAs) for birds. The Habitats Directive similarly requires Special Areas of Conservation (SACs) to be designated for other species, and for habitats. Together, SPAs and SACs make up the Natura 2000 series. All EU Member States contribute to the network of sites in a Europe-wide partnership from the Canaries to Crete and from Sicily to Finnish Lapland (Source: http://www.natura.org/)

[144] There are two international land cover classification systems, the FAO/UNEP/GLCN (LCCS) and CORINE Land Cover (CLC), about the European Union territory

[145] The I&CLC2000 (IMAGE 2000 and CORINE Land Cover 2000) are two joint projects, developed in conjunction between the EEA and the Joint Research Centre, and co-funded by the Member States, which have been focused on two main components: providing an orthorectified satellite imagery mosaic, covering the whole European territory, to be used as the basic reference for CORINE updating (IMAGE 2000); classifying land cover categories, detecting and interpreting land cover changes between 1990 and 2000 (CLC 2000)

which result in the first CLC level (level I) are: Artificial Surfaces, Agricultural Areas, Forests and Semi-natural Areas, Wetlands, and Water Bodies (Heymann et al., 1994). The second level (Level II) covers physical and physiognomic entities at a higher level of detail (urban zones, forests, lakes) and is composed of 15 categories. A detailed scheme of all 44 classes divided by the three levels is provided in the following table 3.1.

Level 1	Level 2	Level 3
1. ARTIFICIAL SURFACES	1.1 Urban fabric	1.1.1 Continuous urban fabric
		1.1.2 Discontinuous urban fabric
	1.2 Industrial, commercial and transport units	1.2.1 Industrial or commercial units
		1.2.2 Road and rail networks and associated land
		1.2.3 Port areas
		1.2.4 Airports
	1.3 Mine, dump and construction sites	1.3.1 Mineral extraction sites
		1.3.2 Dump sites
		1.3.3 Construction sites
	1.4 Artificial, non-agricultural vegetation areas	1.4.1 Green urban areas
		1.4.2 Sport and leisure facilities
2. AGRICULTURAL AREAS	2.1 Arable land	2.1.1 Non-irrigated arable land
		2.1.2 Permanently irrigated land
		2.1.3 Rice fields
	2.2 Permanent crops	2.2.1 Vineyards
		2.2.2 Fruit trees and berry plantations
		2.2.3 Olive groves
	2.3 Pastures	2.3.1 Pastures
	2.4 Heterogeneous agricultural areas	2.4.1 Annual crops associated with permanent crops
		2.4.2 Complex cultivation patterns
		2.4.3 Principally agriculture, with significant areas of natural vegetation
		2.4.4 Agro-forestry areas
3. FOREST AND SEMI NATURAL AREAS	3.1 Forests	3.1.1 Broad-leaved forest
		3.1.2 Coniferous forest
		3.1.3 Mixed forest
	3.2 Scrub and/or herbaceous vegetation	3.2.1 Natural grasslands
		3.2.2 Moors and heathland
		3.2.3 Sclerophyllous vegetation
		3.2.4 Transitional woodland-shrub
	3.3 Open spaces with little or no vegetation	3.3.1 Beaches, dunes, sands
		3.3.2 Bare rocks
		3.3.3 Sparsely vegetated areas
		3.3.4 Burnt areas
		3.3.5 Glaciers and perpetual snow
4. WETLANDS	4.1 Inland wetlands	4.1.1 Inland marshes
		4.1.2 Peat bogs
	4.2 Maritime wetlands	4.2.1 Salt marshes
		4.2.2 Salines
		4.2.3 Intertidal flats
5. WATER BODIES	5.1 Inland waters	5.1.1 Water courses
		5.1.2 Water bodies
	5.2 Marine waters	5.2.1 Coastal lagoons
		5.2.2 Estuaries
		5.2.3 Sea and ocean

Tab. 3.1: CORINE Land Cover Nomenclature (Source: European Environment Agency, 1995)

Urban uses, which are the main reasons for landscape fragmentation, as well as for the consumption of natural resources, are defined by the first category of level 1 of the CLC legend, i.e. artificial surfaces. Level two is detailed by urban fabric, intended as areas mainly occupied by dwellings and buildings, including their connected areas. These include industrial, commercial and transport units, which are those areas mainly occupied by industrial activities of transformation and manufacturing, trade, financial activities and services, transport infrastructures for road traffic and rail networks, airport installations, river and sea port installations, also including their associated lands and access infrastructures, as well as industrial livestock rearing facilities; mine, dump and construction sites,

which are those artificial areas mainly occupied by extractive activities, construction sites, man-made waste dump sites and their associated lands; and artificial, non-agricultural vegetated areas, which are those artificial areas voluntarily created for recreational use, including green, recreational and leisure urban parks and sports and leisure facilities[146] (Bossard, et al., 2000).

The approach behind the CLC mapping methodology is a computer assisted visual interpretation of satellite images, at medium-resolution, so that the main source of data for deriving land cover information comes from earth observation satellites. In particular, CLC is elaborated based on the interpretation of SPOT-XS and Landsat (Landsat TM, and Landsat MSS) satellite imagery. Multi-temporal satellite images are selected, for each area to be mapped, in order to achieve high quality photo-interpretation. Moreover, pre-processing and enhancement of satellite imagery are realized for providing geometric correction, improvement of visualization and projection of primary data using the European geographical coordinates system. While in IMAGE 90 only a polynomial correction was applied, and GCPs were mostly selected from 1:100˙000 scale maps, for CLC 2000, ortho-corrected Landsat-7 ETM satellite images were provided, by the IMAGE 2000 component, with an RMS (root-mean-square) error below 25 meters (European Environment Agency, 2007). Besides satellite information, ancillary data such as aerial photographs, topographic or vegetation maps, statistics and local knowledge are used to refine interpretation and the following assignment of land portions into the different categories of CORINE land cover nomenclature.

The smallest mapping units to be classified correspond to 25 hectares, while linear objects of width less than 100m are not separated. The scale of the output product for CLC classifications has been fixed at an operational scale of 1:100˙000, thus reaching a location precision of the CLC database around 100m (Vidal, et al., 2001). *The choice of scale (1:100˙000), minimum mapping unit (MMU[147]) (25 hectares) and minimum width of linear elements (100 meters) for CLC mapping represents a trade-off between production costs and level of detail of land cover information (Heymann, et al., 1994). These two basic parameters are the same for CLC 1990, CLC 2000 and the subsequent CLC 2006* (European Environment Agency, 2007).

After the first CLC project in 1990, improvements in methodology were made also from the standpoint of the automatization of the process. In fact, while during the first CLC inventory the photo-interpretation was carried out through hardcopies by using transparent overlays, fixed on top of satellite images, on which were drawn polygons associated to different CLC codes; CLC 2000 was based on computer-assisted image interpretation, discarding the method of drawing on transparencies, thus avoiding several types of errors in geometry as well as in thematic content, which also had to be corrected within the context of the I&CLC2000 project (Büttner, et al., 2002; European Environment Agency, 2007).

The incoming CLC 2006 database was generated by following a mainly automatic process, through the use of GIS platforms, and by basically combining CLC 2000 results with CLC-Changes detected between 2000 and 2006. Consequently, the errors found within CLC 2000, both thematic as well as geometric, were corrected, thus providing a CLC 2000 reviewed dataset. The final result of CLC 2006 classification, resulting from a semi-automatic process, is founded on two main parts (European Environment Agency, 2007) as follow:

1. Computerized processing:

- *Integration of changes > 25 ha*
- *Generalization of small (< e.g. 23 ha) changes (amalgamation). The threshold of amalgamation could be slightly lower than 25 ha to allow for 'intelligent' exaggeration*
- *Generalization of small changes to one of the neighbors (if generalisation situation is clear).*

2. Non-automated processing (requires a photo-interpreter decision):

- *Handling polygons just under the 25 ha limit (e.g. between 23 and 25 ha)*
- *Generalization of small changes to one of the neighbors*

[146] *In case of cultivated areas inter-mixed with built-up areas within a patchwork system, the minimum threshold to be considered to classify in discontinuous urban fabric is 30 % (at least 30 % of the small parcels are urban fabric). Otherwise the area should be classified as complex cultivation patterns* (Bossard, et al., 2000)

[147] The Minimum Mapping Unit defines the smallest patch, intended as a continuous area having the same land cover type, and being recognizable within the satellite image, so that a patch becomes a valid CLC polygon only if its size exceeds the MMU (European Environment Agency, 2007)

The main technical characteristics of CLC projects, for each temporal stage (1990, 2000, and 2006), and the evolution of specific aspects, mostly related to the enhancement of the methodology over the last 20 years are schematically represented in the next table 3.2.

	CLC 1990 Specifications	CLC 2000 Specifications	CLC 2006 Specifications
Satellite data	Landsat-4/5 TM single date (in a few cases Landsat MSS, as well)	Landsat-7 ETM single date	SPOT-4 and/or IRS LISS III two dates
Time consistency	1986–1998	2000 +/– 1 year	2006+/– 1 year
Geometric accuracy satellite images	≤ 50 m	≤ 25 m	≤ 25 m
CLC minimum mapping unit	25 ha	25 ha	25 ha
Geometric accuracy of CLC data	100 m	Better than 100 m	Better than 100 m
Thematic accuracy	≥ 85 % (not validated)	≥ 85 % (validated, see Büttner, G., Maucha, G., 2006)	≥ 85 %
Change mapping	N.A.	Boundary displacement min. 100 m; change area for existing polygons ≥ 5 ha; isolated changes ≥ 25 ha	Boundary displacement min. 100 m; all changes >5 ha have to be mapped
Production time	10 years	4 years	1.5 years
Documentation	Incomplete metadata	Standard metadata	Standard metadata
Access to the data	Unclear dissemination policy	Free access	Free access
Number of European countries involved	26	32	38

Tab. 3.2: Evolution of CORINE Land Cover Projects: 1990-2000-2006 (Source: European Environment Agency, 2007)

The landscape, which includes lots of aspects ranging from the natural to the artificial, is the main backdrop for all human activities, thus it is constantly changing due to the dynamism of human necessities, which in recent decades, has developed often without taking into account the cumulative impact and the speed of change that has undoubtedly been exceptional, at least in the European territory. Moreover, decision-making still misses certain sensitivity towards landscapes, mainly in urban planning, considering that urban settlement and infrastructures are one of the most important agents in landscape fragmentation phenomena.

The detailed map of land cover composition in Europe, which covered 36 European countries and temporal monitoring since 1990, provides a useful database for setting a lot of spatial analysis about the actual state and the dynamics of changes of European landscapes. At present, the European Environment Agency provides a series of assessments based on CLC outcomes, under the title “10 messages for 2010”, where each message affords a valuation focused on a specific ecosystem, and in particular those of: Climate change and biodiversity; Protected areas; Freshwater ecosystems; Marine ecosystems; Forest ecosystems; Urban ecosystems; Agricultural ecosystems; Mountain ecosystems; Coastal ecosystems; Cultural landscapes and Biodiversity heritage.

The spatial distribution of the 44 aggregated land cover classes, for the whole European Territory is provided by the map in the next figure 3.11.

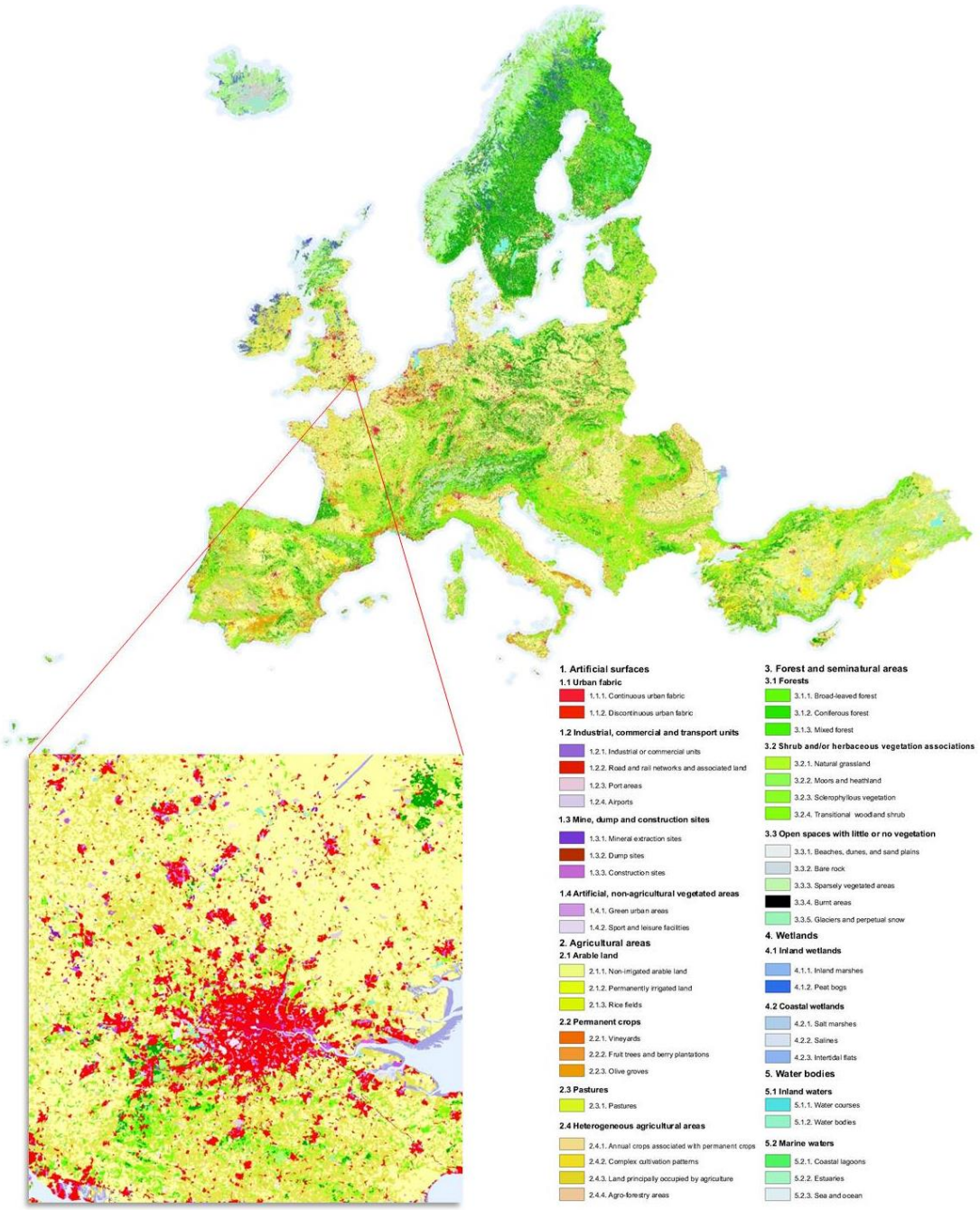

Fig. 3.11: CORINE Land Cover Map for Europe (Source: By Authors, from European Environment Agency, 2010[148])

EEA analysis of land-cover change shows a change in land-cover type for 1.3 % of the total land stock (68,353 km2 of 5.42 million km2) from 2000–2006. The annual rate of these changes has slowed compared to the period 1990–2000. However, land-use specialization (urbanization, agricultural intensification and abandonment plus natural afforestation) is still a very strong trend and is expected to continue in the future, depending on many interacting drivers (European Environment Agency, 2010).

[148] Downloadable at: http://www.eea.europa.eu/data-and-maps/data/corine-land-cover-2006-raster

For outlining the boundaries of city areas, which are often the main cause of landscape fragmentation and therefore the area of influence, the main way provided by the EEA is the so-called Urban Morphological Zones (UMZ), defined as a set of built-up areas lying less than 200m from each other, and primarily focused on four CLC urban core classes:

- *Continuous urban fabric comprises buildings, roads and artificially surfaced area covering almost all ground; non-linear areas of vegetation and bare soil are exceptional.*
- *Discontinuous urban fabric comprises buildings, roads and artificially surfaced areas with vegetation and bare soil occupying discontinuous but significant surfaces.*
- *Industrial or commercial units primarily comprise artificial surfaces (concrete, asphalt) devoid of vegetation but also contain buildings and/or areas of vegetation.*
- *Green urban areas, as patches of vegetation within urban fabric including parks and cemeteries with vegetation.*

In addition, port areas, airports, and sports and leisure facilities are included within UMZs if they are neighbors of the core classes. Road and rail networks and water courses are considered part of a UMZ if they are located within 300 m. Forest and scrub areas belong to the UMZ if they are completely encircled by one or more of the four core classes. Furthermore, as UMZs are based on CORINE Land Cover databases updated in 1990, 2000 and 2006, changes to UMZs can be calculated between those years (European Environment Agency, 2011).

Although CORINE Land Cover is one of the most homogeneous land cover maps currently available, and covers most of the European countries, a few limitations of the projects must be mentioned. Some differences, for example, could occur from one country, or even region, to another, due to technical choices or the use of different resolution of satellite imagery (SPOT XS, Landsat TM, Landsat MSS) or different photo-interpretation criteria. An additional restriction is well explained by Gallego, et al. (2001), which states that *a large number of communes*[149] *appear as not having any urban area (class 1.1) according to CORINE Land Cover*, and that even if this category of urban settlement represents a small part of all of the urban areas categorized for the municipalities, it is a significant part of the rural population, or corresponds to areas with very scattered settlements. Possible reasons for the lack of urban area for several municipalities could be, for instance, that the area of the built-up surface is smaller than the CORINE Land Cover threshold (25 ha), and this would be the explanation for the great majority of cases; but geometric inconsistencies could also occur due to location inaccuracy, between CLC and administrative boundaries (Gallego, et al., 2001).

3.2.1.2. GlobCOVER and GlobCORINE

In 2008, the European Space Agency (ESA) provided the first map for global land cover classification, with a resolution of 300 meters and based on pixel-based automatic classification of monthly coverage of the earth, by using Envisat MERIS[150] (Medium Resolution Imaging Spectrometer Instrument) Fine Resolution (FR) surface reflectance mosaics satellite imagery, and based on the LCCS[151] system. It was called GlobCOVER 2006, derived from the ESA-GlobCOVER 2005 project, which intended to update the classification every year or two years (Weber, 2009). The ESA-GlobCOVER 2005 project provided a key role in the field of earth exploration, as it clearly demonstrates the possibility to improve automated services for spatial investigation and in a reasonable timeframe.

In 2009, following the same direction as the ESA-GlobCOVER 2005 project, the ESA's 2009 global land cover map was generated (figure 3.12), by using data collected through the same Envisat/MERIS sensor, and covering a temporal stage of twelve months ranging from 1 January to 31 December 2009. Although the classification process carried out for the 2009 land cover map has benefited from the pre-classifications made by GlobCOVER 2006. It was mainly aimed at re-labelling the previous classification (Weber, 2009), the GlobCOVER 2009 result again clearly demonstrated the possibility of using automatic land cover detection, and in addition to that, a global land cover map can be created within a short period, such as a year (Arino, et al., 2011).

[149] NUTS 5 (Nomenclature of territorial units for statistics)
[150] More details about the MERIS sensor can be found in Chapter 4, paragraph 4.2.2
[151] FAO/UNEP/GLCN international land cover classification systems

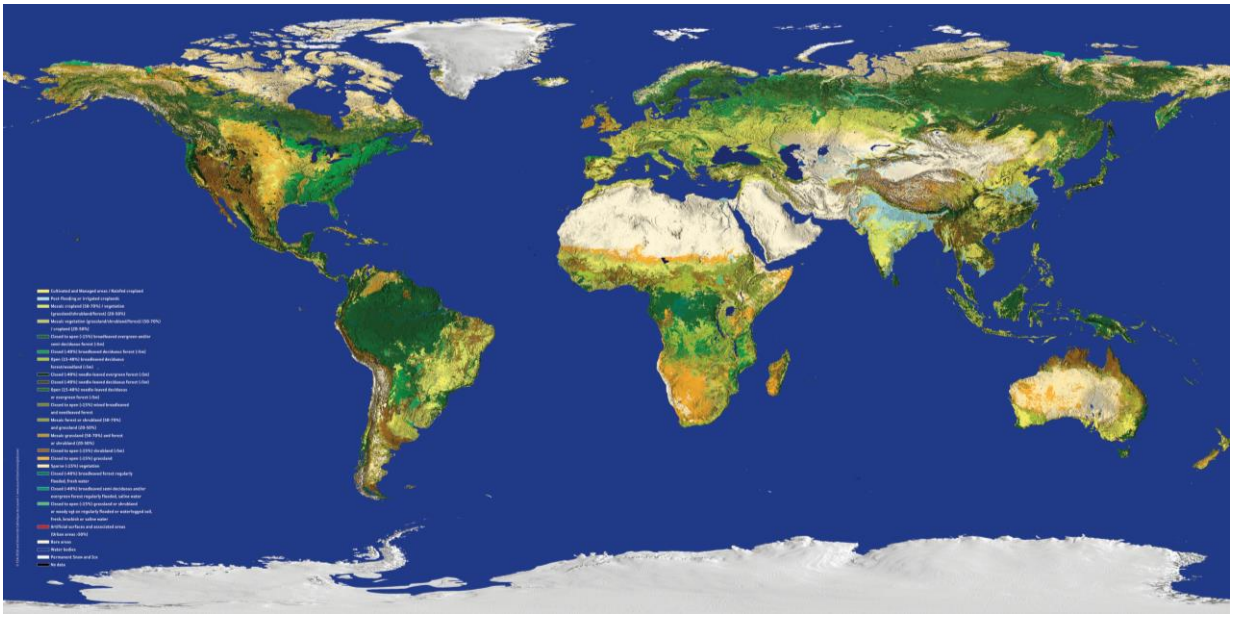

Fig. 3.12: ESA's 2009 Global Land Cover Map. GlobCOVER 2009|MERIS 300m (Source: European Space Agency)

Due to the fact that the LCCS legend was evaluated to be too complex for providing automatic classification, due to great difficulties for homogenizing Land Use/Land Cover across large territories, a simplified legend has been provided. This is compatible even with LCCS and CORINE classification systems, in order to match as closely as possible the minimum requirements in terms of change monitoring. In order to achieve this generalization of Land Use/Land Cover concepts, the legend of GlobCOVER has been based on some key modifications, as follows: *urban as a single class; pasture and semi-natural/natural grassland are grouped; Forested wetlands are separated (as could be savannah or tundra for the time being). Forests are not detailed, which means that it remains open for adopting LCCS breakdown. A particularity introduced is bringing forests and transitional woodland closer. This is important for change assessment as long as new felling and new plantation are the most important part of this category; without this grouping, a gap with forest statistics would open up, which consider as forest the forest territory as a whole* (Weber, 2009).

The GlobCOVER project is actually based on two main objectives. The first one is an automated pre-processing of time series MERIS imagery for achieving global mosaics of land surface reflectance at a resolution of 300m/pixel. In particular, the project provides two global mosaics (a bimonthly mosaic) for which the average values of reflectance in four MERIS spectral bands, and between correspondent suitable images, are calculated every two months, and therefore over an entire year an annual GlobCOVER surface reflectance mosaic for which average values of reflectance are calculated. Pre-processing operations depend on some specific actions, such as geometric correction of imagery; atmospheric correction (which include aerosol correction); cloud screening and shadow detection; land/water reclassification; projection; and BRDF[152] effect reduction and temporal compositing. The second objective of the project is to provide an automatic regionally-tuned classification of land cover categories, at a resolution of 300m/pixel, which delivers a global land cover map based on a 22-class legend, and defined in accordance with the United Nations (UN) Land Cover Classification System (LCCS) (Arino, et al., 2011).

Apart from the GlobCOVER project, the European Environment Agency, together with the ESA, have set up another land cover project called GlobCORINE, in order to support environmental assessments and spatial planning and is focused on three main objectives: providing rapid updating for the CORINE project to meet the needs of policymakers for new data that correspond to the political cycles; increasing the range of land cover monitoring to other European adjacent areas such as Eastern Europe and the Southern Mediterranean; and performing global assessments about ecosystems. Again, as for the GlobCOVER projects, the land cover categories have been reduced

[152] Bidirectional Reflectance Distribution Function

to a more generalized legend, as shown in table 3.3, in order to reduce complexity, and thus allows us to achieve the best results for automatic classifications (Weber, 2009).

Level 1	Level 2
1. Artificial areas	1.1. Artificial areas
2. Arable land and permanent crops	2.1. Non-irrigated arable land 2.2. Irrigated or post-flooded agriculture 2.3. Permanent crops and associations
3. Pasture, grassland and mosaic farmland	3.1. Pastures and grassland 3.2. Mosaic farmland
4. Forest and transitional woodland shrub	4.1. Standing forest 4.2. Transitional woodland and shrub
5. Heathland and Sclerophyllous vegetation	5.1. Heathland and Sclerophyllous vegetation
6. Open space with little or no vegetation	6.1. Beaches, dunes, sand plains and bare rocks 6.2. Sparsely vegetated areas 6.3. Glaciers and perpetual snow
7. Wetlands	7.1. Forested wetlands 7.2. Low vegetation and bare wetlands
8. Water bodies	8.1. Inland water bodies 8.2. Coastal water bodies

Tab. 3.3: The working legend for GlobCORINE (Weber, 2009)

"The map, based on ESA's Envisat MERIS data from 1 January to 31 December 2009, is the first of its kind to be produced in such a short time – nine months as opposed to years. [...] The map, providing a resolution of 300m, was delivered to the European Environmental Agency (EEA), the project's main user, in October. [...] "GlobCorine is much more than a project aimed at delivering a European land cover map. It is the scientific and technical demonstration that a description of the state of land surface on a continental scale can be provided within a year."[153]

3.2.1.3. MURBANDY and MOLAND

Despite the important achievements that the CORINE project have provided, *few studies in Europe have analysed the urban growth phenomenon in terms of spatial expansion of built up areas, rather than from the population changes* (Fricke & Wolff, 2002).

In the context of developing urban analysis, modelling techniques and simulations and for supporting policy makers to better allocate appropriate decisions in spatial planning and funding, two additional key projects need to be mentioned (also related to the CORINE Land Cover project) and were undertaken by the European Commission, through the Joint Research Centre (JRC): MURBANDY and MOLAND.

The binomial MURBANDY/MOLAND projects attempt to fill a gap in the existing lack of reliable spatial data and offer new points of view. A Europe-wide data set for urban areas was created based on natural and artificial land cover characteristics. Under the European Commission's fourth framework program (1995-98) for research and technological development and demonstration (RTD), the Centre for Earth Observation (CEO) of the Directorate General Joint Research Centre was responsible for promoting the overall use of Earth Observation (EO), particularly by demonstrating its potential applications and by favouring the exploration and expansion of the EO market (Lavalle, et al., 2002).

Under the umbrella of the 4th framework program, the MURBANDY (Monitoring Urban Dynamics) project was launched in 1998 as a pilot project in the context of Earth Observation (EO) science and was undertaken by the Directorate General Joint Research Centre of the European Commission. It was focused on measuring, analysing,

[153] GlobCORINE 2009 Land Use Land Cover Data for Europe (Source: http://www.slashgeo.org/2010/11/25/GlobCorine-2009-Land-Use-Land-Cover-Data-Europe-Available)

understanding and forecasting the urban expansion dynamics of several European cities[154], by taking into account four urban land use categories and the transportation network, with their evolution over time from the 1950's to 1997 (Fricke, et al., 2002).

The adopted working scale for MURBANDY was 1:25˙000, which is, according to Fricke, et al. (2002), *a good intermediate scale between a fine scale needed for the intensive urban land use of the city (1:5˙000 or 1:10˙000) and the necessity to cover a large study area to monitor urban sprawl*. The methodology behind MURBANDY land cover classification is based on computer assisted photo-interpretation of satellite images and aerial photographs, and provides information about selected cities and urban areas, over a period of 50 years since the mid-50's, and measuring urban development in the 60's, 80's, and 90's until 1997.

The reference land use database was interpreted on screen, according to the MURBANDY legend, using an approximate scale of 1:10˙000 in GIS software. The satellite imagery and the ortho-photos were displayed alternately under the edited coverage: the first one for an up-to-date image and the second for a precise delineation. A numerical copy of the survey maps was also available for the interpreter (Fricke, et al., 2002).

The project focuses, in particular, on identifying and analysing growth dynamics of four categories of land uses for urban and peri-urban areas, which rely on the CORINE "artificial surfaces" class, by detailing urban fabric in dense, medium, discontinuous and sparse, together with an also more detailed classification of the CORINE "industrial or commercial units" class, in three categories, as they result in an additional level (level 4), as shown in table 3.4.

CORINE third level	MURBANDY (fourth level)
1.1.1 Continuous urban fabric	1.1.1.1 Residential continuous dense urban fabric
	1.1.1.2 Residential continuous medium dense urban fabric
1.1.2 Discontinuous urban fabric	1.1.2.1 Residential discontinuous urban fabric
	1.1.2.2 Residential discontinuous sparse urban fabric
1.2.1 Industrial, commercial, public and private units	1.2.1.1 Industrial areas
	1.2.1.2 Commercial areas
	1.2.1.3 Public and private services
1.2.2 Road and rail networks and associated land	1.2.2.1 Toll-Ways
	1.2.2.2 Other roads
	1.2.2.3 Railways

Tab. 3.4: Sample of new classes for level 4 (used in the Belgian MURBANDY Project), introduced for the MURBANDY for detailing the CORINE artificial surfaces (Level 1) class (Source: Fricke, et al., 2002)

As the MURBANDY project drew important interest from European and other countries as well, as a consequence, the number of study areas was extended and the project overview broadened, together with its objectives. In fact, in 1999 under the 5th framework program, a new project called MOLAND (Monitoring Land Use/Cover Change Dynamics) was launched with the aim of extending the field of the research outside urban areas, to define and validate the methodology in support of sectorial policies with territorial and environmental impacts. Actually, MURBANDY itself suggested the need for the new MOLAND, based on the project MURBANDY-Munich in which it was stated that: *The result of the MURBANDY-Munich project shows that further urban growth will not be within the limits defined by the central polygon approach but along the major traffic routes (motorways and public transport network). It seems to be advisable to extend the analysis to the "Region of Munich" (e.g. in the framework of MOLAND project) or – as a minimum solution – to analyse urban growth along the development axis stretching towards the new Munich airport north of the city*[155] (Lavalle, et al., 2002).

Therefore, the MOLAND project, initiated in 1999 under MURBANDY, provides a broader project which also aimed at defining a specific comparative methodology for monitoring and analysing the spatial evolution of urban growth, and the resulting effect on the environment, based on morphological and structural changes, for a

[154] The studied cities are: Helsinki (Finland), Tallinn (Estonia), Göteborg (Sweden), Copenhagen (Denmark), Sunderland (England), Dublin (Northern Ireland), Brussels (Belgium), Essen, Dresden and Munich (Germany), Praha (Czech Republic), Bratislava (Slovakia), Vienna (Austria), Lyon, Grenoble and Marseille (France), Milan, Padova-Mestre and Palermo (Italy), Bilbao (Spain), Porto and Setubal (Portugal), Iraklion (Greece) and Nicosia (Cyprus)

[155] From MURBANDY-Munich final report

representative number of geographical areas in Europe, together with a group of so-called megacities situated in developing countries[156]. Moreover, the project provided models for past, present and future scenarios of growth based on the analysis of different temporal satellite imagery and aerial photography, through the use of Remote Sensing and GIS techniques (Lavalle, et al., 2002).

The methodology behind MOLAND is focused on earth observation and multi-temporal analysis of geographical datasets processed through photo-interpretation technique based on standardized rules for digitalizing land cover/land use categories. This is combined with geoprocessing tools and statistical data for monitoring environmental and morphological changes in urban areas by using GIS platforms. As well as for MURBANDY, the land cover/land use classification is based on visual interpretation of satellite imagery, in particular by using an on-screen analysis of the Indian Remote Sensing satellite (IRS), SPOT, Quickbird and IKONOS data for more recent observations, while for the historical database, in addition to satellite imagery, geo-coded aerial photography from the mid-50's, late-60's, and 1980's is used (Lavalle, et al., 2002; Shahumyan, et al., 2009). The project covers around 40 urban areas in EU countries and includes three transport corridors, and two extended regions in Europe, together with seven urban areas outside Europe. It relies on providing databases about land cover inventory at urban and regional level, with one present reference (generally at the end of the 1990's) and three historical observations since the 1950's, with the aim of supporting spatial analysis and planning by producing specific indicators for modelling future scenarios of urban growth as well.

MOLAND provides three main sections of analysis. The first one is defined as the "Change Module" and is directed at measuring changes in urban expansion by comparing current and previous datasets on land uses and transportation. The so called "Understand Module" aims to analyse those changes by applying spatial indices at a socio-economic and physical level, which is the morphological dimension of the city. The last part of the project, the "Forecast Module", provides the projection of future scenarios about possible urban growth models (Clarke, et al., 1998; Fricke, et al., 2002).

MOLAND works on two spatial scales. At regional level, the project provides detailed territorial information about the spatial composition of the landscape. While at local level, it matches the urban area, and it aims to assign a land use category to each grid cell. The project delivers detailed GIS datasets about land cover/use types and transport networks for urban areas, together with definite indicators about land-use changes of the three main classes (i.e. artificial surfaces, agriculture and natural areas) over a 50-year period, at a mapping scale of 1:25˙000 and in particular for four main periods, in line with MURBANDY, i.e. early 1950's, late 1960's, 1980's, and late 1990's; while in the case of larger areas two temporal stages are analysed (mid 1980's and late 1990's).

In order to model the development of urban and regional environments, and the improvement in scenarios of territorial evolution for urban and peri-urban areas, i.e. the estimation of possible future changes of land cover categories (Forecast Module) for any one of the cells of a geographical spatial grid, an integrated model of regional spatial dynamics consisting of a Cellular Automata (CA) land-use model is employed. This is linked to both GIS and regional, economic and demographic models (Lavalle, et al., 2002), and whose application, for predicting the evolution of every land cover cell is based on information and constraints derived from the neighbouring cells.

Cellular automata are computer simulations that try to emulate the ways the laws of nature are supposed to work in nature (Lavalle, et al., 2002). The methods of spatial analysis based in CA may be defined as a relatively simple dynamic system, but is really effective for modelling complex spatio-temporal processes consisting of the analysis of individual cells and their neighbourhoods in a matrix, whose future state, within a spatial area, depend on its previous and actual state, and according to a set of simple and determinable transitional rules (White, et al., 1999; Barredo, et al., 2003).

In the framework of the MOLAND project, the cities have been studied as dynamic systems and their spatial complexity characteristics have been modelled by using CA. This is done through a digital space model based on a rectangular grid of square cells with each one representing an area of 100m×100m (1 ha), which is consistent with the size of the minimum mapping area for urban uses in MOLAND. The datasets about land cover/use delivered by MOLAND reach an accuracy which refers to a scale of 1:25˙000, while the object-oriented digitalization relies on a minimum mapping unit for a polygon, which ranges from 1 ha (100 m x 100 m) for the artificial surfaces,

[156] Buenos Aires, Chongqing, New Delhi, Bangkok, Johannesburg/Pretoria, Mexico City, and Seoul

up to 3 ha for non-artificial surfaces. In addition, the road and rail networks, and rivers and canal networks are digitalized as linear features and as polygons when they are broader than 25 meters (Barredo, et al., 2003).

In order to define suitable spatial analysis, the produced databases are combined with associated socio-economic datasets and statistical ancillary data, such as demography, transportation and commuting information, environmental data (pollution, for instance). This is for computing various types of indicators about urban and regional development, from the point of view of sustainability growth. The goal is the development of comparable data series over time and between different locations, to allow the use of such data in planning, by using data on population evolution, mobility and security, environmental impact assessment and urban sprawl measurements (Barredo, et al., 2003).

The MOLAND land use nomenclature, following the same logic used for MURBANDY, relies on an extended and more detailed version of the CORINE land cover legend particularly by providing a level 4, which details the level 3 of CORINE in approximately 100 land use classes (or sub-classes). The following table 3.5 shows a sample of the MOLAND legend for level 4, and for the category "artificial surfaces" in the CORINE legend.

CORINE third level	MOLAND legend
1.1.1 Continuous urban fabric	1.1.1.1 Residential continuous dense urban fabric
	1.1.1.2 Residential continuous medium dense urban fabric
	1.1.1.3 Informal settlements
1.1.2 Discontinuous urban fabric	1.1.2.1 Residential discontinuous urban fabric
	1.1.2.2 Residential discontinuous sparse urban fabric
	1.1.2.3 Residential urban blocks
	1.1.2.4 Informal discontinuous residential structures
1.2.1 Industrial, commercial, public and private units	1.2.1.1 Industrial areas
	1.2.1.2 Commercial areas
	1.2.1.3 Public and private services
	1.2.1.4 Technological infrastructures for public service
	1.2.1.5 Archaeological sites
	1.2.1.6 Places of worship
	1.2.1.7 Cemeteries with no vegetation
	1.2.1.8 Hospitals
	1.2.1.9 Restricted access services
	1.2.1.10 Agro-industrial complexes
	1.2.1.11 Surface pipelines
1.2.2 Road and rail networks and associated land	1.2.2.1 Fast transit roads and associated land
	1.2.2.2 Other roads and associated land
	1.2.2.3 Railways and associated land
	1.2.2.4 Other rails
	1.2.2.5 Additional transport structures
	1.2.2.6 Parking sites for private vehicles
	1.2.2.7 Parking sites for public vehicles
1.2.3 Port areas	1.2.3.1 Civilian ports
	1.2.3.2 Military ports
1.2.4 Airports	1.2.4.1 Civilian airports
	1.2.4.2 Military airports
1.3.1 Mineral extraction sites	1.3.1 Mineral extraction sites
1.3.2 Dump sites	1.3.2 Dump sites
1.3.3 Construction sites	1.3.3 Construction sites
1.3.4 Abandoned land	1.3.4.1 Bombed areas
1.4.1 Green urban areas	1.4.1.1 Cemeteries with vegetation
1.4.2 Sport and leisure facilities	1.4.2 Sport and leisure facilities

Tab. 3.5: *Codes and headings of the third level of CORINE and the fourth level of the MOLAND legend for class 1* (Source: Barredo, et al., 2003)

If compared with CORINE land cover classification, which is based on a scale of 1:100˙000 and a Minimum Mapping Unit (MMU) of 25 ha, the results derived from MOLAND, and mainly for the artificial surface classes as they are digitalized according to a MMU of 1 ha, deliver polygons which are actually more detailed and defined according to further categories of land covers, due to the enhanced taxonomy, as shown in figure 3.13.

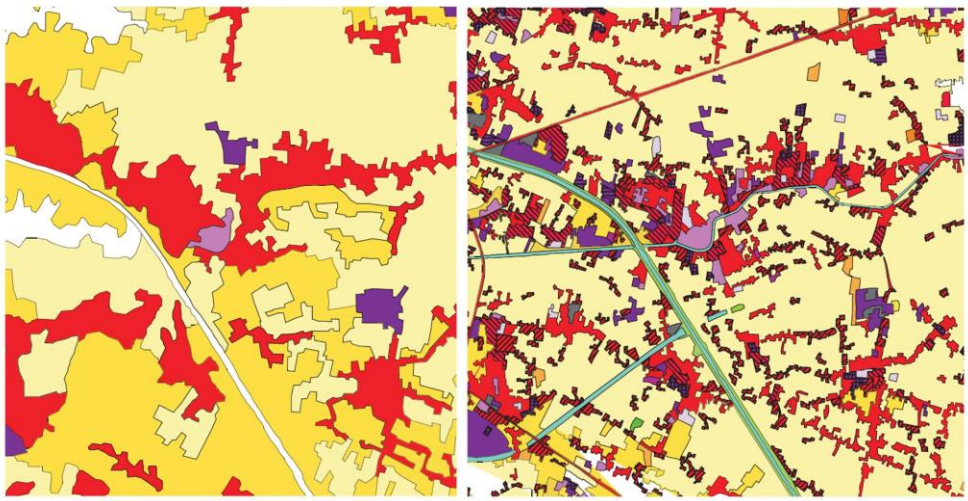

Fig. 3.13: Sample of the same area mapped by CORINE land cover (left side) and MURBANDY/MOLAND (right side) (Source: Lavalle, et al., 2002)

The MOLAND indicators, which rely in particular on urban and regional sustainability, are designed to be robust and sufficiently standardized, as well as flexible enough and cross-sectorial spatially referenced, in order to evaluate even more complex processes for landscape changes (e.g. fragmentation). This is so that changes in the structure of urban landscape and the level of fragmentation are being measured and analysed by using landscape structural analysis software such as FRAGSTATS[157], based on various fragmentation metrics (e.g. edge metrics, core area metrics, nearest neighbour metrics, diversity metrics).

The urban area to be analysed for MOLAND for all the cities is dependent on the inner urban area; it means the core area, which corresponds to all of the artificial uses. A buffer around the core area is calculated by using a standardized formula [3.1] which allows a suitable comparison between different urban areas, due to the fact that this relationship provides a constant proportion between urbanization and its surrounding space.

$$\text{Buffer Area} = 0.25 * \sqrt{\text{Urban Core Area}} \qquad [3.1]$$

The following figure 3.14 shows two example of urban areas, for the case study of Bratislava and Milan, analysed through the use of MOLAND methodology, and the surrounding areas calculated by using the aforementioned formula. The samples form part of an urban atlas provided by Lavalle, et al. (2002)[158], which examined a set of 25 cities throughout the European territory.

[157] FRAGSTATS is a computer software program designed to compute a wide variety of landscape metrics for categorical map patterns. The original version of FRAGSTATS, published in 1995, was developed by Dr. McGarigal and Barbara Marks of Oregon State University. More details about FRAGSTATS at http://www.umass.edu/landeco/research/fragstats/fragstats.html

[158] Lavalle, C., Demicheli, L., Kasanko, M., McCormick, N., Barredo, J., & Turchini, M. (2002). *Towards an urban atlas. Assessment of spatial data on 25 European cities and urban areas.* European Commission, Directorate General Joint Research Centre. Copenhagen: European Environment Agency

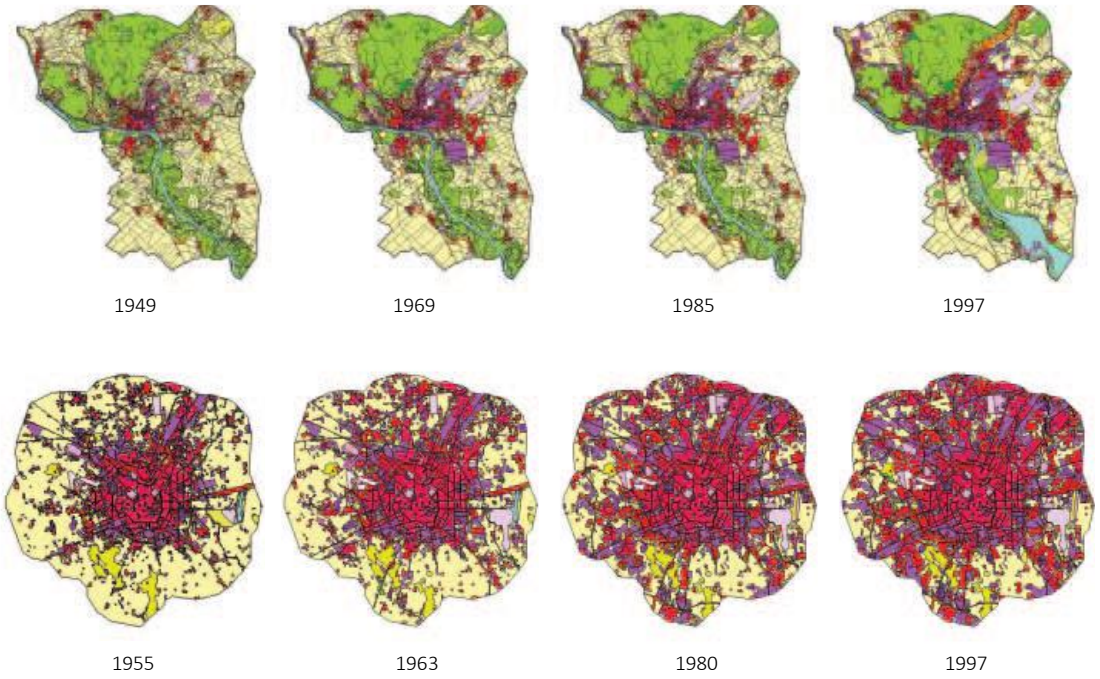

Fig. 3.14: Samples from the MURBANDY/MOLAND database: Bratislava and Milan (Source: Lavalle, et al., 2002)

MOLAND matches several topics and actions of environmental policies, at the EU level, on sustainable growth, land use management and urban development in the framework of the initiatives on Environmental Impact Assessment and on Strategic Environmental Assessment. This involves the further implementation of the ESDP (European Spatial Development Perspective), also including the establishment of the European Spatial Planning Observation Network/ESPON.

3.2.2. Spain: National and Regional Perspectives

Depending on the path set at the European level, promoted by the European Commission through the JRC and EEA, a series of research projects have been undertaken at national level in several member countries in order to transpose the results of projects such as CORINE land cover, but also to propose alternative methodologies, even compatible ones, to adapt the spatial analysis to a more detailed scale that would cover the whole country evenly. The most important effort at a national level that needs to be mentioned is provided by the Spanish government, through the Ministry of Environment and the National Geographic Institute[159] (IGN). It is establishing a national geographic information infrastructure (the Information System about Land Cover in Spain – SIOSE), in order to meet the needs of national and regional administration regarding land use/land cover mapping. While at a regional level, a program developed for land cover classifying and landscape analysis purposes, mostly cited for the robustness of the proposed methodology and the level of details of the results, is the land cover map of Catalonia (MCSC) pursued by the Regional Government of Catalonia.

[159] The IGN (*Instituto Geográfico Nacional*), the Spanish Mapping Agency, is the EIONET's Land Cover National Reference Centre, which has coordinated the CLC projects and updates for Spain: CLC 90, I&CLC2000, CLC 06. Since 2005, the IGN, as National Reference Centre for Land Cover Classification, in the performance of its duties, has participated in the coordination and generation of CLC 2006 database, and CLC-Changes 2000-2006 for Spain. To do this, as reference the same images used in SIOSE2005 were used, thus maintaining maximum compatibility between the two projects (even within the differences in terms of scale resolution and thematic details of the two projects)

3.2.2.1. Land Cover/Land Use Information System in Spain: SIOSE[160]

The Information System about Land Cover in Spain (SIOSE), which relies on the EIONET system (European Environment Information and Observation Network) of the European Environment Agency (EEA), is a project that is part of the National Plan of Territory Observing in Spain (PNOT), coordinated and managed by the Directorate General of the IGN of the Ministry of Development (General Sub-Division of Cartographic Production and National Geographic Information Centre). This forms part of its role as National Reference Centre on Land Cover/Land Use and Spatial Planning (CNR-OS) in Spain; the Ministry of Environment through the Secretariat General for Territory and Biodiversity; and the National Centre of Geographic Information (CNIG). The project stems from a protocol signed in October 2005 between the Ministries of Defence, Development and Environment for obtaining the coverage of the Spanish territory through satellite images of high and medium resolution, within the framework of the National Remote Sensing Plan (PNT)[161].

In 1990, based on the European CORINE Land Cover project, a database of land use for the entire national territory at a scale of 1:100˙000 was generated for the first time in Spain. The availability of homogeneous information for all of Europe and its effectiveness for spatial analyses and the need for establishing European policies meant that in 2000, the previous database of land cover classification was updated, according to the second CORINE Land Cover project (I&CLC2000), together with the analysis of the changes that occurred between 1990 and 2000. However, as the need for national information was much larger than the one provided by the CLC project, the so-called Land Cover Information System in Spain (SIOSE) was launched in 2005 by integrating the information available for the Autonomous Communities (CCAA) and the General Administration of State (AGE). This generated a database of land cover for all of Spain at a scale of 1:25˙000 together with reference imagery for the year 2005 (SIOSE2005).

The overall objectives of the project were the production and coordination of a multidisciplinary geographic information infrastructure, regularly updatable, by allowing its integration into other databases of land use, both at a European (such as CORINE Land Cover) and global scale (e.g. the GlobCOVER), and for meeting the needs of the Central Government and all of the Spanish Autonomous Regions in the field of land use (and land cover). In particular, the project pretended to:

- Avoid duplication of data and reduce costs in generating periodical geographical information about land cover/use
- Integrate the information proceeding from the Autonomous Communities, in terms of production, control and management of final databases
- Comply with European Union requirements regarding land use issues
- Integrate and harmonize existing databases at national and regional levels
- Define agreed and harmonized methodologies for spatial analysis
- Create a normalized data model (OGC, ISO), object-oriented, in UML language
- Distribute costs and promote cooperation in European and global policies

Among the specific objectives, the project proposes to provide a basic tool for planning and management of environmental resources and relies on several thematic working teams: such as urban, rural, forestal, aerospace imagery management, methodology (GIS and Reference Imagery) and data dissemination. This was done through the following actions:

- Dynamic analysis of land occupation
- Causes and consequences of natural and/or artificial change processes
- Environmental impact evaluations
- Obtaining agro-environmental indicators
- Monitoring and maintaining the ecological equilibrium

[160] This section is based on the SIOSE 2005 Technical Document: Information System about Land Cover in Spain (version 2). The report describes the objectives, organization, features, methodology and products of the project SIOSE2005, managed by the Directorate General National Geographic Institute of Spain (IGN), Land Cover Service, General Secretary of Cartography (Ministry of Development, 2011). More information can be found on the website of SIOSE: http://www.siose.es/siose/

[161] The reference agencies for the SIOSE project are: EEA (European Environment Agency), ESA (European Space Agency), ETC / TE (European Topic Centre on Terrestrial Environment), JRC (Joint Research Centre), Eurostat (European Statistical System), DG Environment of the European Commission, DG Agriculture, DG Enterprise and Industry, DG Regional Policy

- Spatial Planning
- Data integration in environmental models
- New strategies for coastal zone management
- Promotion of sustainable development

From a technical aspect, the SIOSE project for the production of thematic maps of land cover at a scale of 1:25˙000 relied on the use of multispectral satellite imagery of SPOT 5, at medium resolution (10 meters), implemented through pan-sharpening operations by using SPOT panchromatic imagery at high spatial resolution of 2.5 m, for the year 2005, together with coverage provided by Landsat 5 TM imagery (spring and fall) for 2005, and high-resolution ortho-photos (pixel size ≤ 1 m) from 2004 and 2006, as ancillary data. Additional ancillary data, for supporting the photo-interpretation of imagery, were provided (where available and updated) by cartographic information at a scale of 1:25˙000 from the National Geographic Institute, vector data from cadastral mapping of the DG Registry of the Ministry of Economy and Finance (urban limits and urban street axes), crop and exploitation maps (MCA) from the Ministry of Agriculture, Fisheries and Food, Forestry maps of Spain (MFE) from the Ministry of Environment, Geological maps (MAGNA) of the Canary Islands provided by the Geological and Mining Institute of Spain (IGME), Ministry of Education and Science; as well as other topographic and/or thematic databases, regarding land occupation, in vector or raster format, which may be available in each Autonomous Community.

The methodology, according to the CLC project (even if with a different spatial scale to the outcomes), is aimed at computer-assisted photo interpretation, supported by the use of tools for performing basic operations; such as:

- Basic functions of image processing
- Overlaying of vector data on raster datasets
- Topologically consistent editing of vector data
- Multi-window displaying for allowing the simultaneous analysis of data from different data sources

The Geodetic Reference System for SIOSE is the ETRS 89, while the projection is UTM for the zones 28, 29, 30, and 31, north hemisphere. The minimum unit of area classified for artificial surfaces and water bodies is 1 ha; for beaches, riparian vegetation, wetlands and forced crops (greenhouses and under plastic) is 0.5 ha; while for agricultural, forest and natural areas it is 2 ha. All updating is planned to be done with a frequency of 5 years.

Each classified unit area is defined by a polygon, and each polygon provides a spatial entity that represents a portion of land occupied by a homogeneous type of land cover. Two super-classes are associated with the polygons which are defined according to "Use" and "Cover". *Cover* directly refers to the type of surface covering the ground or to the items that stand on such surfaces, and therefore can be classified by their own biophysical properties; while the *Use* is a concept relating to socio-economic activities that take place on that land.

The SIOSE Data Model allows the assignment of one or more uses and cover to a single polygon, so the polygon represents a simple cover type when it is a unique class, and composite coverage when the polygon is formed by two or more single, or even composite, classes of coverage (such as mixed urban uses for instance). Depending on the type of combination, the composite coverage will be an association of classes or a mosaic. The association is the combination of coverage without fixed distribution, when they are interchangeably intertwined. The mosaic is the combination of coverage, whose geometric distribution and spacing between them is clearly perceptible[162]. In other words, a significant difference in this classification system, in comparison with CLC, is that SIOSE focuses on a sort of parametric classification for defining each polygon of land cover. In fact, once a continuum polygon is digitalized, it is analysed according to the percentage of the most relevant elements present in it, and the defined information is stored in a specific database which actually "describes" the polygon more than classify it; so the classification can be realized according to successive queries. As an example, a continuous urban fabric class could be defined by trees covering 5% of the area of a polygon, buildings 85%, and roads 10%, thus these numbers are those stored in the polygon in the database.

The following image (Figure 3.15) provides a direct comparison between the outcomes of SIOSE project, at the aforementioned spatial scale of 1:25˙000 and using the described technical characteristics, and the classification results of the CLC project (discussed in paragraph 3.2.1.1) at the spatial scaling of 1:100˙000.

[162] More details about the SIOSE data model structure, together with the specific nomenclature as adopted by the project can be found in the "SIOSE2005 Photointerpretation Manual" at http://www.siose.es/siose/documentacion.jsp

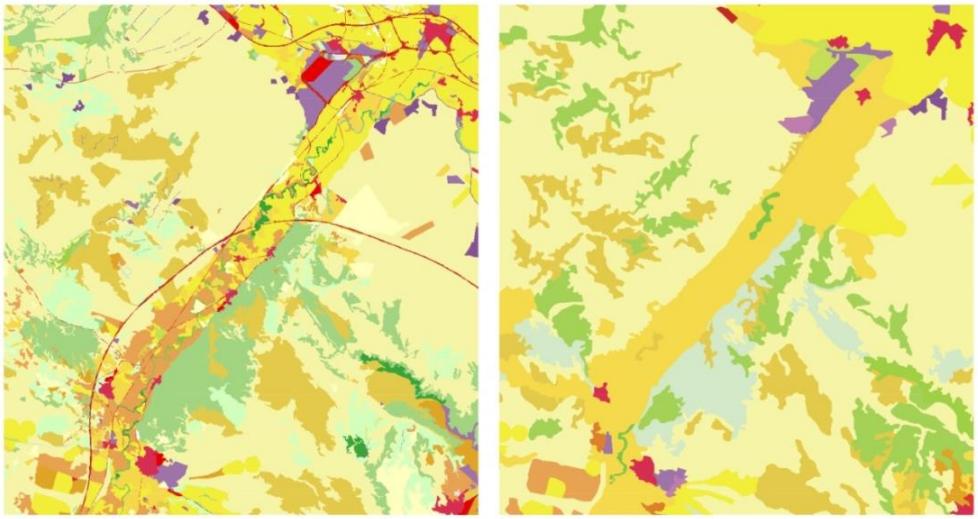

Fig 3.15: Differences between SIOSE outcomes and CLC outcomes for thematic map classification (Source: SIOSE 2011, provided by © IGN)

Despite the changes in the data model adopted for the SIOSE project (with respect to other approaches) and the specific minimum mapping unit used for digitalizing, the classification results keep the interoperability between the SIOSE databases and other European projects nationally and regionally. These include CORINE Land Cover (1990, 2000, and 2006), for instance, or the national crop and exploitation maps, the Forestry maps of Spain, Cadastre, the National Cartographic base and the regional databases about Land cover composition.

After the digitalization through photo-interpretation, the project provides a check, in situ, by taking georeferenced digital pictures of geographical areas, using GPS. In addition, a local specialized team for each region must ensure the geometric, topological, and thematic quality of produced data, following the specifications defined by the same SIOSE project.

3.2.2.2. Land Cover/Land Use in Catalonia: CREAF and ICC

In recent decades, changes in land cover and land uses have accelerated, so much so that even in Catalonia the impact of development has been considerable on natural resources, environment and landscape. Thus, whatever planning action or territorial management that seeks to avoid or even solve these problems, not only requires precise cartography, satellite or aerial image series, but also the evolution of land use and land cover and changes in landscape structure over time. In order to provide useful information concerning the actual status of regional landscapes and plan future territorial developments in Catalonia, the Regional Government of Catalonia (*Generalitat de Catalunya*) has financed the land cover map of Catalonia (MCSC[163]), carried out by the Centre for Ecological Research and Forestry Applications (CREAF).

The MCSC currently offers primary, high-resolution, digital thematic cartography of the main land cover types within the whole regional territory and their spatial distribution, such as forests, crops, urban areas, etc. Actually, because of its high detail, the MCSC is of great interest to the knowledge of the territory, as well as for the assessment and management of land cover, both from the ecological and economic standpoint. The MCSC allows us to measure the available forest areas, crop lands or natural parks, as well as the amount of urban areas at various administrative levels, up to the municipal. We can then extract the corresponding maps in digital format, so it provides good instruments for urban and regional planning, infrastructure, or preserving natural connectors, irrigation plans, environmental impact assessments, etc.

[163] *Mapa de Cubiertas de Suelo de Cataluña* (MCSC), at: www.creaf.uab.cat/mcsc

The MCSC project relies on four consecutive editions. The first edition of this digital information was carried out based on the first series of digital ortho-photos, in natural colour, produced by the Cartographic Institute of Catalonia (ICC) and entirely captured during the summer period of 1993, with a spatial resolution of 2.5 meters per pixel. For the second and third editions, the adopted ortho-photos (again derived from the ICC) had a pixel of 0.5 meter, while the fourth edition relies on ortho-photos (ICC 2009) with a pixel of 0.25 meters (figure 3.16).

Fig 3.16: From left to right, the ortho-photos, provided by the ICC, and employed for producing the four editions of MCSC, with spatial resolution of respectively 2.5; 0.5; and 0.25 m/pixel (Source: Ibàñez, et al., 2009)

The first MCSC produced in 1995 was completed in 2003 and counts 21 land cover types. The process used to classify is by photo-interpretation and digitalizing in a GIS platform, at a scale of 1:25˙000, and was based on a minimum mapping unit of 500 m^2.

In late 2003, the second edition of MCSC began (unfinished) following the same protocol, but with images in natural colour visualized at 1:5˙000, and with a resolution of 0.5 m/pixel, for the period 2000-2003. The legend was also enhanced by including 61 categories[164] (for a new level 3), hierarchically structured, where level 2 and higher were compatible with the first edition[165].

In 2009, the third edition was finished, based partly on the updating part developed in the 2nd edition, and also based on the same technical characteristics, but for the period 2005-2007. A further enhancement of the legend allowed inclusion of more than two hundred categories, even maintaining the correspondence of the first two levels of the legend with the first edition and the first three levels with the second edition.

Actually in the making of the MCSC projects, the compatibility between editions has always been maintained, and that is why the cover map legend has a hierarchical structure with levels of aggregation ranging from the maximum possible, which is level 1 in all editions, up to the minimum level of aggregation (the most detailed), represented by level 5, which is exclusive to MCSC-3.

The MCSC nomenclature also provides an extra level 1, called level 1F, which aims to detail the four key categories (Forest land, inland waters, Crops, Unproductive artificial), that correspond to the main types of land covers in the main thematic sub-levels, composed of 9 categories, 6 of which are subdivisions of the forest land category of level 1.

To resume, the legends of the MCSC ranging from level 1 to level 2 for the MCSC-1, up to level 3 for the MCSC-2, and level 4 and 5, for the MCSC-3. Thus, the MCSC-1, and 2 share the same legend until level 2, and MCSC-2 and 3 have the same legend up to level 3 (table 3.6).

Level 4, which is available for the MCSC-3, is not considered an original level of the MCSC hierarchical legend, but mostly a gateway between MCSC and SIOSE, as it is derived from the Land Cover Information System of Spain.

[164] The legend, in level 3, corresponds essentially to the level 3 of CORINE Land Cover, even if this product has more categories and it is derived from a resolution 50 times higher.

[165] Level 2, in the second edition, provides 24 categories, essentially the same as the first edition, even if previously there were 21.

Nivell 1	Nivell 1F	Nivell 2	Nivell 3
Improductiu artificial	Improductiu artificial	Zones urbanitzades	Urbà residencial compacte
			Urbà residencial lax
			Zones industrials i comercials
			Cementiris
			Zones verdes urbanes
			Granges
			Preses
		Basses urbanes	Basses urbanes
		Vies de comunicació	Aeroports
			Autopistes i autovies
			Carreteres
			Vies de ferrocarril
			Zones portuàries
			Zones verdes viàries
		Zones esportives i lúdiques	Càmpings
			Camps de golf
			Altres zones esportives i lúdiques
		Zones d'extracció minera	Zones d'extracció minera
			Salines
			Abocadors
		Sòls nus urbans	Sòls nus urbans

Tab 3.6: Sample of the hierarchical Legend of the Land Cover Map of Catalonia (MCSC), for the category "artificial unproductive" of the level 1 and for the first three levels (1, 1F, 2, and 3)[166]

In 2010 the fourth edition began, by using ortho-imagery at a spatial resolution of 0.25 m/pixel, and visualized at a scale of 1:2˙500, both natural colour imagery as well as infrared colour images were employed for enhancing the quality of interpretation. The legend is the same as that of the third edition, while the result of the classification refers to the year 2009.

Anyway, the MCSC-3 represents an important evolution for reference cartography for the Catalan land cover mapping program, based on land cover information captured by photo-interpretation methodology, and digitalizing onscreen through GIS platforms. In the 3rd edition, in particular, in order to achieve a more homogeneous temporal series, natural colour ortho-photos were used besides the photo-interpretation and also takes into account SPOT-5 images from 2005 (basically used to support the interpretation of forest systems, habitat, crops and urban areas), and was provided by the IGN (National Geographic Institute of Spain), which were used for conducting SIOSE in Catalonia[167]. Additionally, for urban area interpretation, the topographic maps at a scale of 1:5˙000 provided by the ICC are used together with ancillary specialized thematic data. Ground testing could also be required in some cases (Ibàñez, et al., 2009).

The photo interpretation onscreen procedure, based on ortho-photomaps with a pixel of 0.5 meters (as mentioned before), is made by working at a scale of around 1:1˙500 (it was at 1:3˙000 for the previous editions), so achieving a digital map in vector format at 1:5,000. The minimum area for information captures (MMU) has been maintained at 500 m^2, for each version of MCSC, which means that any land cover surface, is diversified from neighbouring areas by digitalizing only when it covers a surface of at least 500 m^2. Homogeneous areas, in terms of land cover, are delineated through photo-interpretation as polygons, by digitalizing vectored objects, and considering diverse ancillary information, such as the previous editions of MCSC essentially, some 1:5˙000 topographic layers, lakes and lagoons, reservoirs, axes of streets, etc..; as well as other databases such as the SIGPAC[168], for instance. Linear elements (roads, rivers, linear vegetation, etc.) in the first edition were digitalized only when measured as being 10 meters wide and over 50 meters long, while in further editions, they are digitalized when more than 8 meters wide and 62.5 meters long.

[166] The whole legend can be found at: http://www.creaf.uab.cat/mcsc/descriptiu.htm#significat
[167] In Catalonia, the SIOSE database is obtained by a process of generalization relying on the 3rd edition of the MCSC
[168] Geographic Information System of Farming Land, Ministry of Agriculture, Food and Environment, Government of Spain

The vector format is topologically structured (polygons) and is based on several rules, such as the elimination of topological and thematic errors, as well as the provision for spatial relationships between objects, enabling complex analysis, such as recognizing multiple holes inside polygons, the spatial neighbourhood, as well as linking groups of patches, etc. Moreover, the vector format is associated with several extra databases and other statistical information concerning the structure of the landscape. The result is also converted to raster format (a sample is shown in figure 3.17), at a planimetric resolution of 2 meters per pixel. The raster images also allow, as well as the vectored database, interactive queries by attribute and location and calculation of the area of one or more covers, apart from being a very manageable format to analyse in GIS (Ibàñez, et al., 2009).

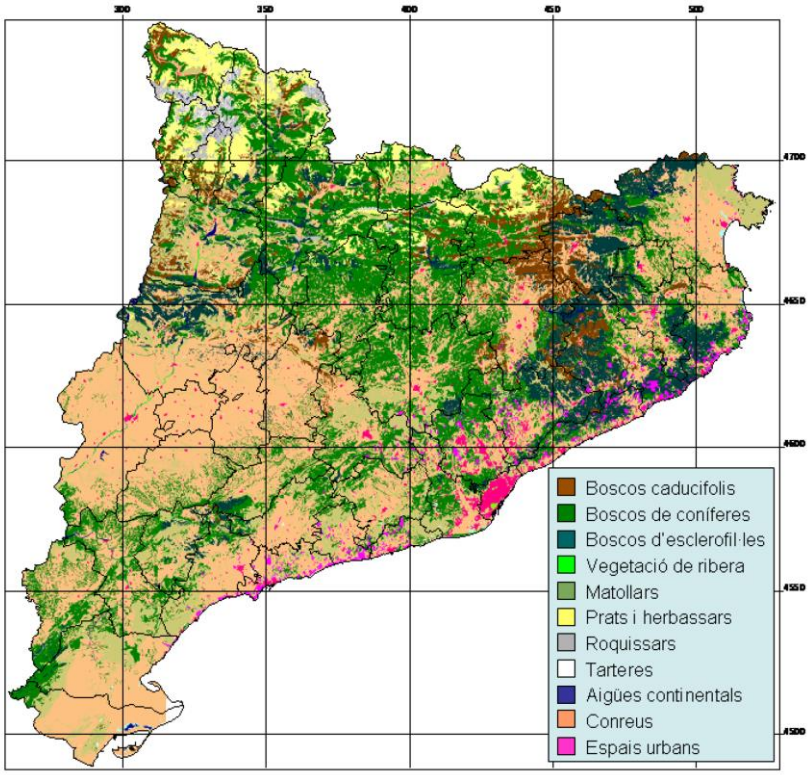

Fig 3.17: Sample of a thematic map of the spatial distribution of main land cover classes in Catalonia, aggregated based on key concepts of the legend, and derived from the MCSC-3 project

3.2.3. An International Overview: North America

From the viewpoint of land cover monitoring and spatial analysis, some of the key studies and projects are provided by important North American organizations, such as the National Aeronautics and Space Administration (NASA), the U.S. Geological Survey (USGS), and the Multi-Resolution Land Characteristics Consortium (MRLC). Many of the products provided, mostly by US institutions, have represented the main engine for pursuing more and more methodologies and tools for Earth Observing techniques since the early 1950's.

As early as during the mid-1940's, Francis J. Marschner (Marschner, 1950) provided a relevant land use map for the whole Country which was based on aerial photographs of the United States territory during the late 1930's and the early 1940's. It was a set of State land use maps at the scale of 1:1˙000˙000 from which a map was then compiled about the major land uses, at a scale of 1:5˙000˙000.

Early in 1971, the formation of an interagency Steering Committee on Land Use information and Classification was created. It was set up due to the necessities revealed by the Federal agencies for producing extensive and overall national land use and land cover information, together with development trends and

environmental indices addressed at analysing levels of sustainability. The work of the committee, composed of representatives from the Geological Survey of the U.S. Department of the Interior, NASA, the Soil Conservation Service of the U.S. Department of Agriculture, the Association of American Geographers, and the International Geographical Union, was coordinated by the USGS for producing suitable land cover maps, as well as reliable spatial analysis over the last few decades (Anderson, et al., 1976).

3.2.3.1. USGS: NLCD & NALCMS

The U.S. Geological Survey science agency provides information about ecosystems and environment, by focusing in particular on natural hazards and natural resources, as well as on the impacts of climate and land-use change. One of the most important products, from USGS, at least of key importance for this research, is undoubtedly the National Land Cover Database (NLCD).

This database delivers spatial reference and descriptive data about the main characteristics of land surface, such as thematic classes including urban, agriculture, forest, and water. In particular, it is aimed at the analysis of two key systems: the impervious surface and the tree canopy cover. In fact, even if there is a globally recognized requirement for urban-oriented analysis within the whole land cover system, there is also a clear need for a rigorous natural resource-oriented quantification, which in the United States for instance, represents around 95 percent of the whole territory, once the number of urbanized areas is subtracted (Anderson, et al., 1976)

The *NLCD supports a wide variety of Federal, State, local, and nongovernmental applications that seek to assess ecosystem status and health, understand the spatial patterns of biodiversity, predict effects of climate change, and develop land management policy. The NLCD products are created by the Multi-Resolution Land Characteristics (MRLC) Consortium in partnership with Federal agencies, led by the U.S. Geological Survey*[169] (USGS, 2012).

The NLCD program relies on three major data releases based over a 10-year production cycle. Before the NLCD 2006 release, a circa 1992 conterminous U.S. land cover dataset was produced, followed by a circa 2001 land cover database for the United States and this time also including Puerto Rico (the NLCD 2001).

An extra version of NLCD 2001, called the 2.0 version was also produced to allow the best comparison between the different temporal versions of the databases, which for around twenty years have been seeing changes in the detection methodology, due to the enhancement of both the technology as well as for the primary information derived from satellites. In fact, with the NLCD 2001 a 1992/2001 Land Cover Change Retrofit (LCCR) product was released.

The release of NLCD 2006 represents the first product which marks the objective of producing a 5-year repeat cycle, with additional products specifically designed for land cover monitoring. In addition, the change monitoring products, also for comparing 2006 with 2001 and 1992 provides us with a national capability to assess land cover changes across the conterminous United States since the early 1990's.

The current digital land cover thematic cartography available, at a resolution of 30 meters per pixel derived from Landsat satellite imagery, is for the 2006 land cover dataset for the conterminous U.S.A. (figure 3.18).

[169] All NLCD data products are available for download from the MRLC Web site: http://www.mrlc.gov

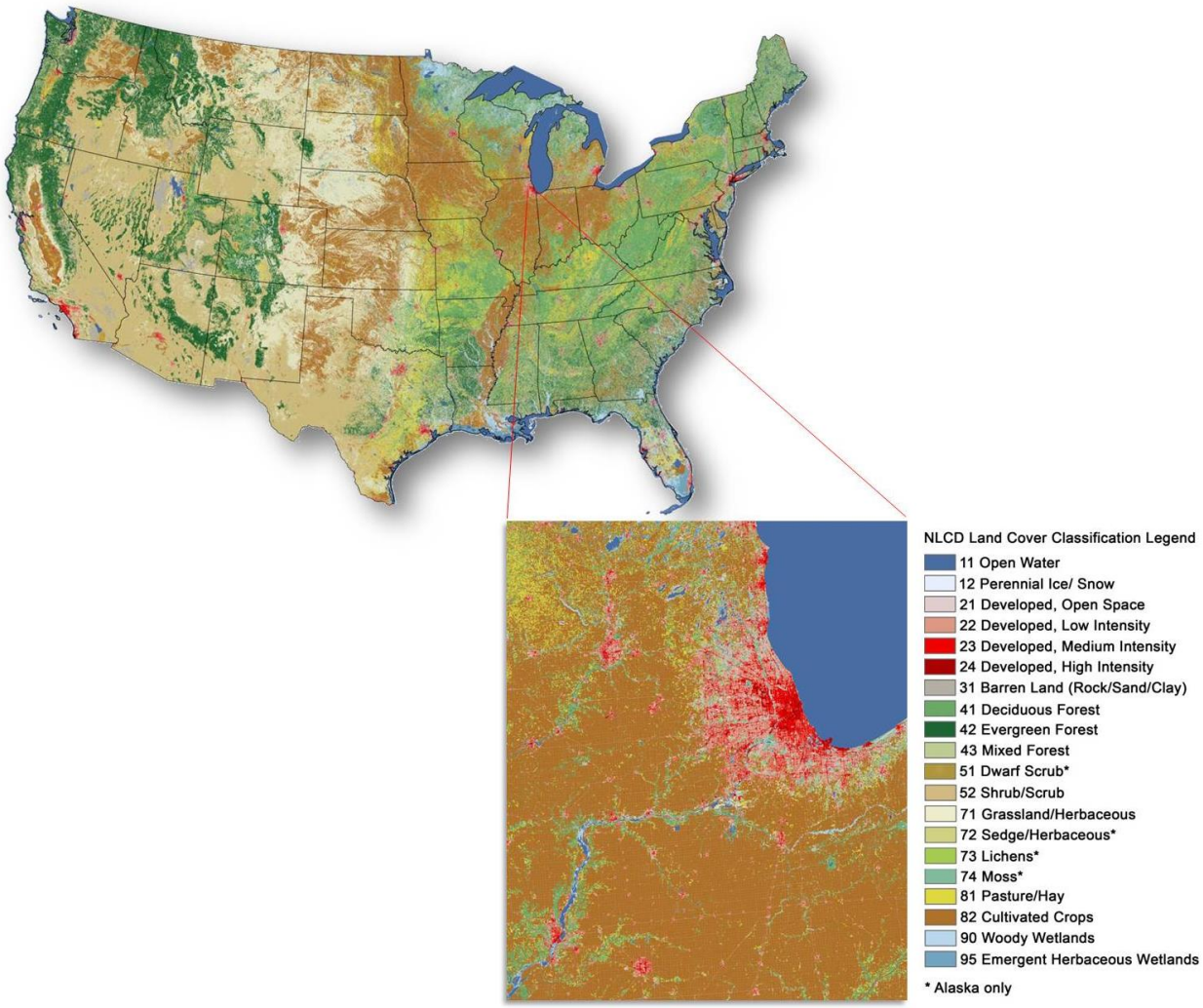

Fig 3.18: The National Land Cover Database (NLCD) 2006. The most recent 30-meter, seamless, wall-to-wall land cover database for the conterminous United States (Source: USGS, 2012)

The NLCD products attempt to be the main land cover change monitoring "wall-to-wall" databases for the whole United States and are aimed at measuring the magnitudes, impacts and future effects of land cover changes on the environment, by comparing several temporal stages since the first edition of NLCD-1992, up until the most actualized base map[170] (USGS, 2012).

A post-processing homogenization of the NLCD outcomes has been undertaken between the different editions, but some differences have occurred since the first NLCD-1992 between the applied methodologies for mapping land cover categories and need to be mentioned. A first circa 1992 National Land Cover Data set, based on the use of Landsat 5 Thematic Mapper (TM) imagery for the early 1990's, and which provides intermediate-scale land cover cartography, was carried out by the U.S. Geological Survey (USGS) EROS Data Center (EDC) and

[170] *Rigorous thematic land cover product accuracy assessments have been completed for NLCD 1992 and 2001 (Stehman, et al., 2003; Wickham, et al., 2004; Wickham, et al., 2010) with a similar assessment in progress (2012) for NLCD 2006. Results of land cover product accuracy assessments have indicated that NLCD 1992 has an overall Anderson Level I (Anderson and others, 1976) class accuracy of 80.4 per cent and an Anderson Level II class accuracy of 55.7 per cent (Stehman, et al., 2003; Wickham, et al., 2004). For the conterminous United States, NLCD 2001 has an improved Anderson Level I class accuracy of 85.3 per cent and an Anderson Level II class accuracy of 78.7 per cent (Wickham, et al., 2010). For the NLCD 2001 Alaskan land cover classification, the overall thematic accuracy was 83.9 per cent at Anderson Level I and 76.2 per cent at Anderson Level II* (Selkowitz, et al., 2011)

completed in the year 2000. The *NLCD 1992 classification was based on a several-stage method of unsupervised clustering, using both pre-classification and post-classification stratification with ancillary spatial data, and manual editing to complete the work…the need for visual inspection and "heads up" on-screen corrections of the preliminary land cover persisted* (Vogelmann, et al., 2001).

This thematic cartography is a "reasonable" and consistent 30-meter resolution product of land cover classification for the conterminous United States and is particularly based on primarily pre-processing steps applied on Landsat imagery, such as terrain-correction using 3-arc-second digital terrain elevation data; geo-registration to the Albers Equal Area projection grid by using ground control points, resulting in a root mean square registration error of less than one pixel (30 meters). However, the classification process relies on two or more TM images acquired from different seasons, and in addition, a variety of other intermediate-scale spatial data has been used for enhancing the results, including Digital Terrain Elevation Data (DTED) and derivative DTED products such as slope, aspect, and shaded relief, besides the population density data at the census block level. Moreover, the classification process for the whole United States is applied by dividing the entire territory in 31 regional units, based on political administrative divisions, contiguity of Landsat scenes and data volume. For each unit, imagery mosaics have been generated of leaf-on (i.e. summer) and leaf-off (i.e. spring) and then classified separately[171]. According to Vogelmann, et al. (2001), the main steps for generating the NLCD classification product can be summarized as follow:

- *Cluster the baseline mosaic using unsupervised classification (spectral clustering)*
- *Interpret and label clusters using aerial photographs*
- *Resolve confused clusters by constructing logical or threshold models that utilize appropriate ancillary data, and an approach based on decision trees modelling, based on threshold using non-parametric techniques*
- *Develop and incorporate information from onscreen digitalizing (e.g. quarries, transitional bare areas)*

The NLCD final classification system provided a consistent hierarchical legend which defines 21 classes of land cover, but the resulting thematic cartography is recommended to be used mostly for analysis at both regional and national scale, due to the primary imagery resolution used and the spatial resolution of the outcomes, as well as for the accuracy of the methodology, it is not recommended for local scale investigation (Vogelmann, et al., 2001).

In 1999, a new NLCD was initiated with the aim of expanding and updating NLCD 1992 and producing a land cover database for all 50 states, plus Puerto Rico. The NLCD 2001[172] cartography took around 6 years to finish, delivering a land cover classification based on a nomenclature of 16 types, plus the percent tree canopy and the percent urban imperviousness, in a raster format with a spatial resolution again of 30 meters per pixel. NLCD 2001 was generated based on 65 mosaicked mapping zones for the conterminous United States, and by using a standardized process spanning data preparation, classification and quality control (Homer, et al., 2007).

The standard set of mosaicked zonal layers to be classified rely on around 18 or more levels, which, among others, includes cloud-free multi-season Landsat 5 and Landsat 7 imagery. This was also selected by using multi-temporal greenness degree measurement derived from the average of multi-temporal Normalized Difference Vegetation Index (NDVI); normalized tasseled cap (TC) transformations of Landsat 7 imagery plus the thermal band calibrated to temperature; a 30m Digital Elevation Model (DEM), and derived terrain models such as slope, aspect, positional index and extra ancillary data (as shown in figure 3.19). All of the layers are geo-registered to the Albers equal area projection grid and resampled to 30m grid cells to achieve a homogeneous database (Homer, et al., 2007).

[171] *In most cases, the general thematic approach was to designate either mosaic (leaf-on or leaf-off) as the "baseline" data set, and to use that spectral information as the primary source of information from which to derive the classification product…Many land cover features are much easier to map accurately using remotely sensed data sets from the appropriate time of year. For instance, hay/pasture is easier to discriminate from other types of land cover in early spring rather than mid-summer* (Vogelmann, et al., 2001)

[172] The NLCD 2001 refers to the nominal year from which most of the Landsat 5 and Landsat 7 imagery was acquired

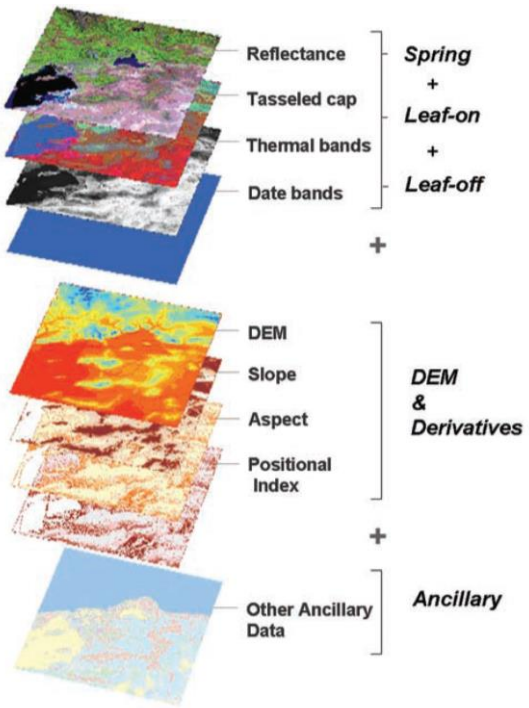

Fig 3.19: Mapping Zone Input Layers used to Derive NLCD 2001 Products (Source: Homer, et al., 2007)

The land cover classification methodology implemented in the NLCD-2001 relies on the use of a Decision Tree (DT) classification method, which provides a supervised classification technique based on a large amount of training region of interest collected by using several data sources; such as high-resolution ortho-imagery, local datasets, field collected points and existing regional land cover maps (ancillary) in order to improve classification efficiency. Advantages of using the Decision tree classification method include: *(1) it is non-parametric and therefore independent of the distribution of class signature, (2) it can handle both continuous and nominal data, (3) it generates interpretable classification rules, and (4) it is fast to train and often as accurate as, or even slightly more accurate than many other classifiers. It was estimated the new NLCD 2001 method produced about a 50% gain in mapping efficiency with comparable or improved accuracies over NLCD 1992 methods* (Homer, et al., 2007).

Impervious areas and continuous tree canopy were classified by using Regression Tree (RT) models, through the use of training data mostly derived from 1m resolution Digital Ortho-image Quarter Quadrangles (DOQQs), and classified categorically into canopy/non-canopy, or impervious/non-impervious for each 1m pixel. Additionally, the main urban categories have been defined by thresholding different degrees of classified imperviousness. Final results both for impervious areas and tree canopy have been resampled to a 30m grid format.

A successive masking approach has been employed to reduce errors in estimating areas with similar spectral characteristics (e.g. shrub and grassy areas for canopy, and bare agriculture fields for imperviousness). For impervious areas masks were produced by employing GIS layers of road density buffers, city lights, spectral classifications and image segmentation-based classifications. *When land cover modelling was completed, the final product* (figure 3.20) *was aggregated to a one acre minimum mapping unit (5 TM pixels) using a "smart eliminate" aggregation algorithm. This algorithm uses eight-corner connectivity from a central pixel to allow non-linear features like roads and streams to remain intact, and accesses a weighting table to allow "smart" decisions on a dissolve protocol. In a few land cover zones, higher minimum mapping unit thresholds were applied to agricultural classes to reduce commission errors in problematic areas. Canopy and imperviousness products underwent no aggregation* (Homer, et al., 2007).

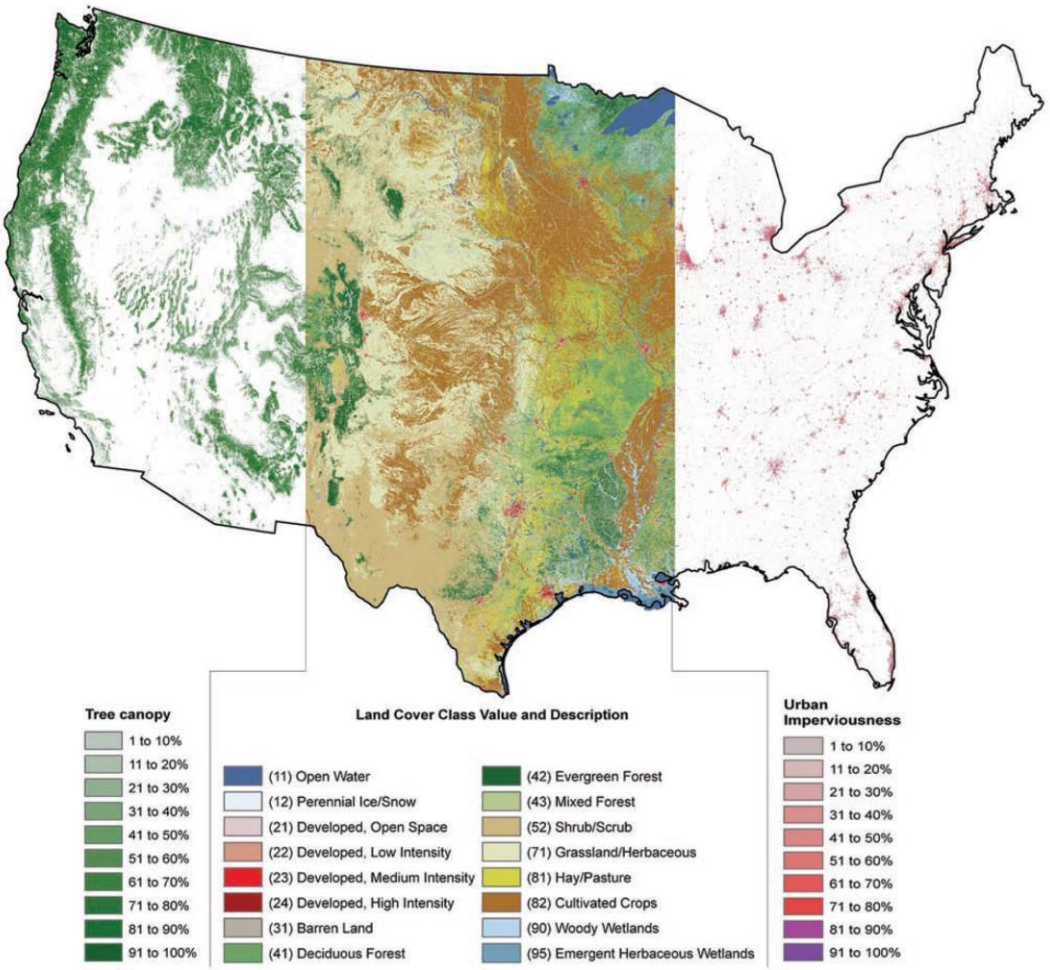

Fig 3.20: NLCD 2001 Tree Canopy, Land Cover and Urban Imperviousness Products (Source: Homer, et al., 2007)

Regarding the aforementioned technical differences in classification methodology, which occurred between NLCD-1992 and NLCD-2001, great inconsistencies could occur while directly comparing results and quantifying changes produced over nearly 10 years. Therefore a "bridge product", which was scheduled to be produced by the end of 2007, was set up for allowing suitable land cover change analysis between the two different stages, and was derived at the more achievable Anderson Level I scale through 8 broad land cover classes[173], for both the 1992 and 2001 classification (Homer, et al., 2007).

The land-cover thematic accuracy of NLCD 2001 was assessed from a probability-sample of 15˙000 pixels (Wickham, et al., 2010), and *results from three initial mapping zones show single-pixel land cover accuracies ranging from 73-77%, imperviousness accuracies ranging from 83-91%, tree canopy accuracies ranging from 78-93% and an estimated 50% increase in mapping efficiency over previous methods* (Homer, et al., 2007).

The same USGS Earth Resources Observation and Science (EROS) Center was responsible for developing change detection protocols used for generating the last current version of NLCD-2006, which has the objective of characterizing a more continuous land cover classification for monitoring and measuring landscape changes over time.

Actually, a change in the mapping interval, from 10 years to 5 years, was planned in order to provide more frequent updates for land cover information at regional and national level. Landsat 7 Enhanced Thematic Mapper

[173] More details about Anderson Level I classification can be found in: Anderson, J., Hardy, E., Roach, J., & Witmer, R. (1976). A Land Use And Land Cover Classification System For Use With Remote Sensor Data. United States Department of the Interior. Washington: United States Government Printing Office

Plus (ETM+) and Landsat 5 Thematic Mapper (TM) imagery collected between 2001 and 2006 was used to provide the three primary Landsat-based products, which are: spectral land cover change analysis; the land cover classification; and imperviousness modelling available for NLCD 2006 (Fry, et al., 2011). *The protocols behind NLCD-2006 are built upon the NLCD 1992 (Vogelmann et al., 2001), NLCD 2001 (Homer et al., 2004, 2007), and NLCD 1992-2001 Retrofit (Fry, et al., 2009) mapping projects and include: (1) data source preparation, (2) change analysis, (3) impervious estimation, (4) land cover characterization of change pixels, and (5) post-processing*.

Ancillary data, such as the National Elevation Dataset (NED) Digital Elevation Model (DEM) and night-time stable-light satellite imagery from the National Oceanic and Atmospheric Administration (NOAA) Defence Meteorological Satellite Program (DMSP), were used to produce the NLCD-2006, and all layers are geo-registered to the Albers Equal Area projection grid, and resampled using a raster format at a resolution of 30 meters per pixel. As well as for the 2001 land cover classification, the impervious areas for 2006 are classified by using Regression Tree (RT) software. Again to allow suitable and accurate comparison between 2001 and 2006 product, the "bridge product" NLCD-2001, known as NLCD 2001 Land Cover Version 2.0 was used (released from 2002 to 2007). This version in particular relies on a homogenization of the MMU, which for the “old” version presented some inconsistencies in several MRLC zones. Version 2.0 is based on the same 5-pixel (0.45 hectare) MMU applied to all areas (Fry, et al., 2011).

The next version of NLCD, entitled NLCD 2011, updates the NLCD products to a nominal year of 2011 in all 50 States and Puerto Rico, and will continue to provide a national assessment of land cover change back to either 2001 or 2006. NLCD 2011 was scheduled for public release in December 2013 based on 2011 Landsat imagery (USGS, 2012).

National Land Cover Database 2011 (NLCD 2011) is the most recent national land cover product created by the Multi-Resolution Land Characteristics (MRLC) Consortium[174]*. NLCD 2011 provides - for the first time - the capability to assess wall-to-wall, spatially explicit, national land cover changes and trends across the United States from 2001 to 2011. As with the two previous NLCD land cover products, NLCD 2011 keeps the same 16-class land cover classification scheme that has been applied consistently across the United States at a spatial resolution of 30 meters. NLCD 2011 is based primarily on a decision-tree classification of circa 2011 Landsat satellite data* (U.S. Department of the Interior | U.S.G.S., 2015).

The objective of developing a large consistent multi-scale land cover monitoring program, to apply across the whole of North America, for harmonizing the information about land cover dynamics and in order to meet high accuracy for each specific requirement of the included countries meant that a joint project was needed between: Natural Resources Canada/Canada Center for Remote Sensing (NRCan/CCRS); the United States Geological Survey (USGS); and three Mexican organizations: the National Institute of Statistics and Geography (*Instituto Nacional de Estadística y Geografía-INEGI*); National Commission for the Knowledge and Use of Biodiversity (*Comisión Nacional para el Conocimiento y Uso de la Biodiversidad-CONABIO*); and the National Forestry Commission of Mexico (*Comisión Nacional Forestal-CONAFOR*). The project was facilitated by the Commission for Environmental Cooperation (CEC), and an international organization created under the North American Agreement on Environmental Cooperation (NAAEC) by Canada, Mexico and the United States was undertaken in 2005.

The North American Land Change Monitoring System (NALCMS) for 2005 at a spatial resolution of 250 meters per pixel (figure 3.21) is the first step towards achieving the objective of forwarding the concept and methodology behind the NLCD program to a bigger scenario. *The product is based on observations acquired by the Moderate Resolution Imaging Spectro-radiometer (MODIS). Mapping was performed by each country using unique data pre-processing and information extraction methodologies. These national products were subsequently used to assemble an integrated North America land cover database. The classification legend is designed in three*

[174] For NLCD 2011, two major change detection advancements over previous NLCD methods were implemented. First, unlike NLCD 2006 (Fry et al, 2011), two pairs rather than one pair of Landsat images between 2006 and 2011 (one leaf-on pair and one leaf-off pair) were utilized for spectral change analysis. Use of an additional image pair for land cover change detection reduced commission errors caused by seasonal phenology in agriculture and wetland dominant areas, and reduced omission errors due to limitations of using one image pair in areas with clouds and shadows, fire disturbance, forest cutting, and urban development. Secondly, the core spectral change detection method used for NLCD 2011 was an enhanced and improved version over NLCD 1992, 2001, and 2006 methods (Homer C. , et al., 2015).

hierarchical levels using the Food and Agriculture Organization (FOA) Land Classification System. Level I and II are common for North America while level III is country specific[175].

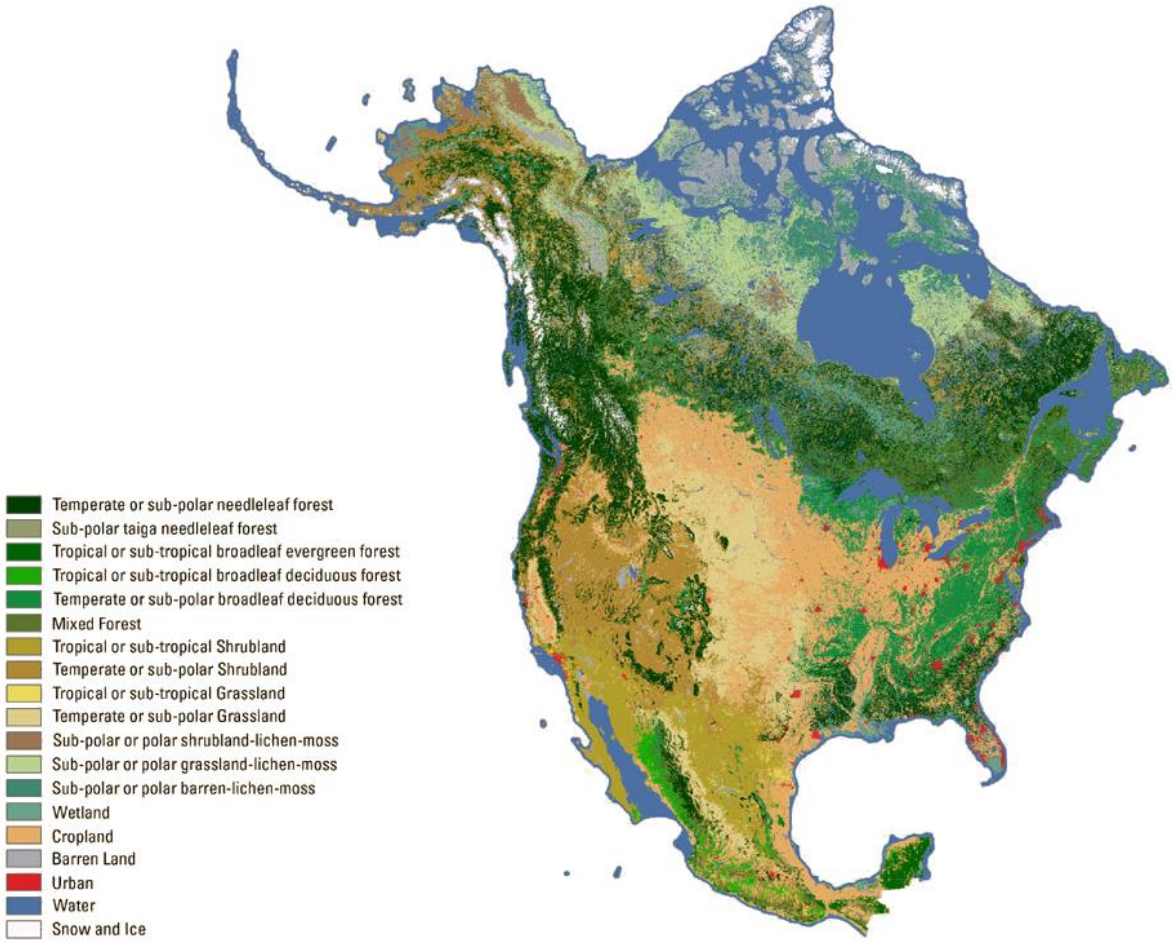

Fig 3.21: NALCMS: The North American Land Change Monitoring System (Source: USGS Land Cover Institute-LCI, 2012)

3.2.3.2. ISA: Different Approaches for Impervious Surface Area Classification

Research suggests that man-made impervious surfaces[176] *can decrease the quality of surrounding natural resources. For this reason, environmental analysts have traditionally used aerial photographs to create maps of impervious surface area (as a good measure of environment quality), which are in turn used to study how increasing amounts of impervious surfaces are impacting the environment.* So based on this concept, many decision-makers at different spatial levels, ranging from the local to the regional and up to the national level, have implemented various methods for evaluating the impact of the evolution of Impervious Surface Areas (ISA) on natural resources, and on the sustainable development of cities by producing ISA maps, through satellite imagery processing (Finley, 2011).

[175] "2005 North American Land Cover at 250 m spatial resolution". Produced by Natural Resources Canada/Canadian Center for Remote Sensing (NRCan/CCRS), United States Geological Survey (USGS); Instituto Nacional de Estadística y Geografía (INEGI), Comisión Nacional para el Conocimiento y Uso de la Biodiversidad (CONABIO) and Comisión Nacional Forestal (CONAFOR). At: http://landcover.usgs.gov/nalcms.php

[176] *Impervious surface area is a term that refers to artificial surface cover through which water cannot evaporate to the atmosphere or infiltrate into the soil, such as buildings, roads, sidewalks and parking lots* (Hebble, et al., 2001)

The classification of ISA relies on three main approaches based on remote sensing techniques, of which, the first is centred on the use of high spatial resolution imagery of about one meter, and which is usually implemented for covering small geographical areas. This method has the limitation of not being standardized, so managing data from different data sources causes several difficulties (Slonecker, et al., 2001; Goetz, et al., 2003; Yang, et al., 2003; Slonecker, et al., 2004; Elvidge, et al., 2007).

A second method relies on the use of medium spatial resolution multispectral imagery, such as Landsat, which is the case of the ISA density grid for the USA, at 30 meters of spatial resolution, provided by the U.S. Geological Survey (USGS) in the framework of the National Land Cover Database (NLCD), which is actually derived from processing Landsat TM imagery (Yang, et al., 2003; Elvidge, et al., 2007). The third commonly used approach is based on the use of demographic indicators, such as population numbers, and is collected by government agencies in order to estimate the density of ISA (Stankowski, 1972; Elvidge, et al., 2007).

In light of this, according to Finley (2011), we could state that a "traditional" approach for detecting impervious surfaces derives from measuring artificial areas (based on the degree of ISA in relation to percentage of imperviousness) by ground surveys and in conjunction with aerial photographs; even if ground cover maps resulting from aerial photographs could form part of the current spatial source of ISA, aerial photographs are still an important source of land use/land cover.

This methodology, which mainly focuses on photo-interpretation of land cover classes, provides a not at all practicable approach, due to excessively expansive costs and increased times when analysing huge geographical areas. Consequently, a “new” approach has been broadly established which relies on the use of digital imagery derived from sensors on board Earth Observing (EO) satellites, and which offer several advantages: such as complete coverage, both for small or large geographic areas; relatively lower costs for generating land cover maps; as well as digital formats compatible with GIS platforms.

An “integrated” approach, based on the joint use of ISA classification through aerial photograph measurements, in addition to a classification which relies on spectral-radiometric characteristics of satellite imagery proposed by the Remote Sensing and Geospatial Laboratory of the University of Minnesota for the Twin Cities Metropolitan Area (TCMA), has provided good results for allowing analysts to create suitable maps of ISA[177] (Finley, 2011).

The first global inventory of the spatial distribution and density of constructed Impervious Surface Area was based on night-time light intensities as captured by satellite platforms and population count (LandScan) and made for the years 2000-01, since both data sources are from those two years[178]. As reported by Elvidge, et al. (2007)[179], the final result of the ISA map delivers the estimated density over a one-km^2 grid, which relies on a model that was calibrated using 30 meter resolution ISA of the USA provided by the U.S. Geological Survey[180]. The night-time light intensities, as the first milestone for the Global ISA, derives from a radiance calibrated product composed by using data provided by the U.S. Air Force Defense Meteorological Satellite Program (DMSP) Operational Linescan System (OLS)[181], which collects global data in two broad spectral bands, i.e. visible and thermal[182].

Then, the NGDC[183] serves as the long-term archive for DMSP data, and has data holding extending from 1992 to the present collected in three overlapping fixed gain[184] settings (low, medium and high[185]), at alternating 24-hour periods.

---

[177] More details about an example of ISA classification, of the Twin Cities Metropolitan Area (TCMA) in Minnesota, based on the integrated approach, can be found in the Fact Sheet 1: *Impervious Surface Mapping Using Satellite Remote Sensing*, provided by the Remote Sensing and Geospatial Analysis Laboratory, Department of Forest Resources, University of Minnesota, and edited by Finley, S. R. (2011). Available at: http://rsl.gis.umn.edu/factsheet.html

[178] The methodology behind the global inventory relies on the methods used by NOAA in 2004, which produced a one km2 grid of ISA densities for the conterminous USA using indirect data sources to estimate ISA (Elvidge, et al., 2004; Elvidge, et al., 2007)

[179] Christopher D. Elvidge, Benjamin T. Tuttle, Paul S. Sutton, Kimberly E. Baugh, Ara T. Howard, Cristina Milesi, Budhendra L. Bhaduri and Ramakrishna Nemani, “Global Distribution and Density of Constructed Impervious Surfaces,” *Sensors,* no. 7, pp. 1962-1979, 2007

[180] A global ISA map at a resolution of one-km^2 grid can be downloaded in various format and coordinate systems at: http://ngdc.noaa.gov/eog/dmsp/download_global_isa.html

[181] *The DMSP satellites fly in polar orbits and each collects fourteen orbits per day. With a 3000 km swath width, each OLS is capable of collecting a complete set of images of the earth twice a day* (Elvidge, et al., 2007)

[182] *At night, a photomultiplier tube (PMT) intensifies the visible band signal to enable the detection of moonlit clouds. The boost in gain enables the detection of lights present at the earth’s surface* (Elvidge, et al., 2007)

183 National Geophysical Data Center.

According to Elvidge, et al. (2007), the lights detected are mainly derived from urban settlements, even if ephemeral episodes, such as areas on fire or lights from gas flares can also be detected, which can be readily identified (and masked) offshore or in isolated areas anyway, so it avoids an important influence on the urban light detection which relies on several criteria for identifying the best night-time lights data from the set of fixed gain collections, as follows:

- *Center half of orbital swath (best geo-location and sharpest features).*
- *No sunlight present.*
- *No moonlight present.*
- *No solar glare contamination.*
- *Cloud-free (based on thermal detection of clouds)*
- *No contamination from aurora emissions*

Besides the night-time light intensities, the methodology behind ISA also relies on an evolving series of spatially disaggregated global population count[186] data sets, known as LandScan, produced by the U.S. Department of Energy, Oak Ridge National Laboratory, and are centred on models developed by taking into account the spatial allocation of disaggregated data from population census numbers. The final model, of estimated ISA (2001), was derived from both the 30 meter USGS Landsat impervious surfaces aggregated to a one-kilometre equal area, together with the LandScan data projected to the same one kilometre grid, by applying a linear regression for defining an equation to calculate the density of ISA.

Only grid cells with population count values of three or greater were included in the regression. This excluded airport lands from the regression. Also excluded from the regression were outliers having extremely high population counts (greater than 3˙000 persons/km^2) and extremely bright lights (digital numbers greater than 800). The regression included 470˙894 grid cells. The equation [3.2] is the one developed through the regression, which *had an r^2 squared of 0.59 and is highly significant $p < .0001$* (Elvidge, et al., 2007).

$$\text{Percent cover of ISA} = 0.0795\ (\text{radiance}) + 0.00868\ (\text{population count}) \qquad [3.2]$$

The results of the work, for the ISA grid of the USA (as an example), are shown in figures 3.22, by displaying the USGS Landsat derived ISA, aggregated at 1 Km^2, the radiance calibrated night-time lights image, LandScan, and the final ISA map[187].

---

[184] *In the standard collection mode, the OLS gain is turned up quite high for the detection of moonlit clouds. Under these operating conditions the night-time visible data are saturated (DN=63) in urban centres. In addition, during the operational collections, the system gain can vary, modified by on-board algorithms* (Elvidge, et al., 2007)

[185] *The low gain collections provide unsaturated data of bright urban cores. The high gain setting data provide detection of dim lights – but has saturation in the bright urban cores. The medium gain setting covers the gap between the detections achieved with the high and low gain settings. The digital numbers from the low and medium gain settings were converted to the radiance units of the high gain data based on the sensor's pre-flight calibration* (Elvidge, et al., 2007)

[186] *The term population count is used instead of population density - which is based on residence. On a population density grid, commercial centres and airports have very low numbers, despite the fact that there are substantial numbers of people present during certain hours. Population count products, also referred to as ambient population, attempt to represent the spatial distribution of population based on person hours. The Landscan 2004 product has substantial ambient population numbers in commercial centres and even along some major transportation routes, such as interstate highways. The Landscan 2004 product assigns population values of "zero" to airport lands* (Elvidge, et al., 2007)

[187] *A threshold of 0.4 percent was applied to eliminate the salt and pepper noise present at the very low end of the ISA scale. ISA values over 100 were reset to 100. Extractions of the digital values were run to tally the quantity of ISA for countries, sub-national units (states / provinces) and major watersheds. 1.05% of the United States land area is impervious surface (83˙337 km^2) and 0.43 % of the world's land surface (579˙703 km^2) is constructed impervious surface. China has more ISA than any other country (87˙182 km^2), but has only 67 m2 of ISA per person, compared to 297 m^2 per person in the USA. Moreover, the ISA cover present in the major watersheds of the world was analysed to tally the percent area of each watershed that was pristine (zero ISA), stressed (1-10% ISA), impacted (10-25%), and damaged (more than 25% ISA)* (Elvidge, et al., 2007)

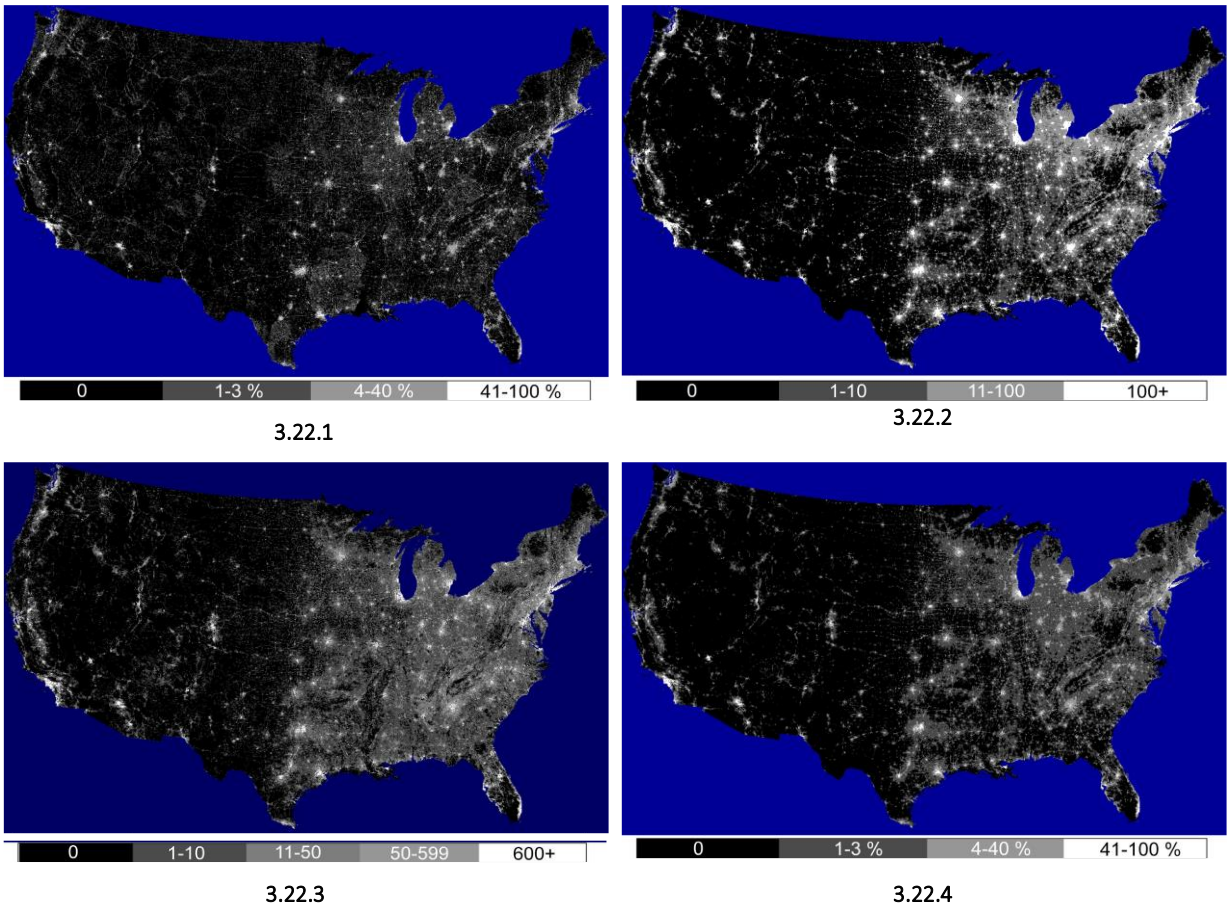

Fig 3.22: .1) The 30 meter resolution USGS' Landsat derived ISA density data for the conterminous USA, aggregated to a one km^2 Albers equal area grid; .**2)** Radiance calibrated DMSP (Defense Meteorological Satellite Program) night-time lights data for the conterminous USA from the years 2000-01; .**3)** Landscan 2004 population count data of the conterminous USA; .**4)** NGDC's ISA grid of the conterminous USA (Source: Elvidge, et al., 2007)

Besides the above analysed approaches for detecting ISA, many important studies could also be mentioned, most of which are based on the same concepts and methodologies and directed at analysing the interaction between ISA and the natural environment. Ridd (1995), for instance, *demonstrated that impervious surface area is a surrogate for population density, mean income, housing values, social conditions and other factors that reflect human living conditions*.

Arnold and Gibbons (1996) highlight the effect of ISA as a degrading factor on water resources. Actually they state that *diffuse sources of pollution associated with peak storm runoff over impervious surfaces are the second leading cause of water pollution in the United States and threaten the quality of wetlands as well as the efficacy of existing clean water regulations*.

Civco and Hurd (1997) *stress the need for using satellite data to identify non-point sources of water pollution*. Hebble, et al. (2001), apply advanced remote sensing techniques and indices, such as the NDVI (Normalized Different Vegetation Index) for estimating ISA, based *on Ridd's observation that impervious surface area is inversely related to vegetation cover in urban areas* (Hebble, et al., 2001).

3.2.3.3. Lincoln Institute: Atlas of Urban Expansion

It deserves to be cited, in the ambit of this research work, the important analysis focused on urban growth dynamics at a global scale that have been carried out since 2005, which derived from the joint work of the World

Bank, the National Science Foundation, NASA, Cities Alliance, and the Lincoln Institute of Land Policy. A five-year study of urban expansion resulted in a report which aimed to compare urban development, both in terms of land consumption and population growth, by analysing 120 cities and metropolitan areas around the world. These 120 global samples derive from a stratified structure which relies on nine geographic regions, four population size classes and four per capita income classes; the analysis is developed through four main stages. The first part of the study is focused on analysing and comparing data sets of digital maps based on satellite imagery, and urban population information for the whole group of the 120 sampled urban areas in two temporal periods which are circa 1990 and 2000. A second stage, based on a survey carried out by local consultants in 2006–2007, provides an investigation about housing conditions and the policies that regulate urban growth. The following third and fourth phases, *involved several additional stages and resulted in three Institute-sponsored working papers. They present historical research on urban expansion in 20 U.S. cities from 1910 to 2000; historical analysis of a representative global sample of 30 cities from 1800 to 2000; and the analysis of a new global urban land cover map of all 3˙646 named large cities with 100˙000 people or more in the year 2000. The complete data sets, with their associated maps and spread sheets, are available in The Atlas of Urban Expansion on the Lincoln Institute*[188] (Angel, et al., 2011).

The urban atlas is derived in particular through the use of remote sensing techniques by employing Landsat imagery at a 30 meter/pixel resolution and Mod500 imagery at 463 meter/pixel resolution, for creating maps of urban land cover and the affected open space, both inside and the close surrounding urban areas. Actually, the information derived by satellite imagery allows identification of the built-up areas of a city by defining impervious surfaces (such as pavements, rooftops, and compacted soils), due to the fact that this kind of information is *a much more precise, consistent and comparable measure* of an urban area. The resulting digital maps have been used in combination with demographic data associated with administrative boundaries relative to the sampled urban areas in order to compute consistent spatial metrics by using Geographic Information Systems platforms. Of interest, the population figures have been collected for two census periods (circa 1990 and 2000) and then interpolated consistent with the satellite images, assuming a constant rate of population growth between census periods (Angel, et al., 2011).

The methodology behind the classification process for the 120 analysed cities, which the Atlas of Urban Expansion is based on, relies on a rigorous, innovative and cost-effective remote-sensing approach. A computer-assisted processing of medium-resolution satellite imagery using the Landsat Thematic Mapper (TM) and Enhanced Thematic Mapper (ETM+) in particular as optimal sensors for this purpose was employed for classifying urban land cover classes into built-up and non-built-up areas at a resolution of 30 meter per pixel. This was done by using a thematic extraction algorithm, (Angel et al. 2005, chapter 3) for all of the cities in the global sample, with a temporal interval of approximately a decade, which allows for accurate and detailed measurement of changes in the built-up area over time.

The Iterative Self-Organizing Data Analysis (ISODATA) algorithm is used for providing an unsupervised classification approach, which focuses on partitioning a multispectral image into self-defining spectral clusters by using minimum spectral distance for assigning a cluster for each candidate pixel. The process begins by first assigning a specified number of arbitrary cluster means, for then deriving final cluster centres through a number of iterative computations. Once the cluster formation has been completed, each pixel in the multispectral image is subjected to a minimum Euclidean distance to means classifier, using the final spectral cluster centroids. Each pixel is classified into the spectral cluster when their mean is the closest to the pixel value, depending on a nearest neighbors approach and in the n-dimensional spectral space.

Due to possible mistakes, which can often be generated by “confusion” in discriminating certain type of land covers reflectance (urban and bare land cover types, for instance) when applying a pixel based automatic classification centred on a spectral data-alone examination, the resulting classification is subject to a post-process phase. This phase is when an analyst, after assigning a meaningful land cover class label to each spectral cluster through photo-interpretation and on-screen editing of regions of pixels, also provides an “a posteriori” inspection for detecting obvious misclassifications by comparing the classification results with a “section-by-section” examination of the Landsat source imagery.

[188] Available at: www.lincolninst.edu/subcenters/atlas-urban-expansion

The final result achieved relies on land cover classifications, which especially focuses on enhancing the classification of built-up areas by providing two main classes: urban and non-urban. Special emphasis is placed on defining water bodies by using a "water index" derived from spectral algebra, as water is considered an important constraint to urban growth (Angel, et al., 2005).

The following figure (3.23) shows a sample of urban classification, taken from the Atlas of Urban Expansion, for the case study of Madrid (Spain), and for the two analysed temporal stages T^1 (1990) and T^2 (2000), in which a clear increase in urban areas can be noticed over a ten year period.

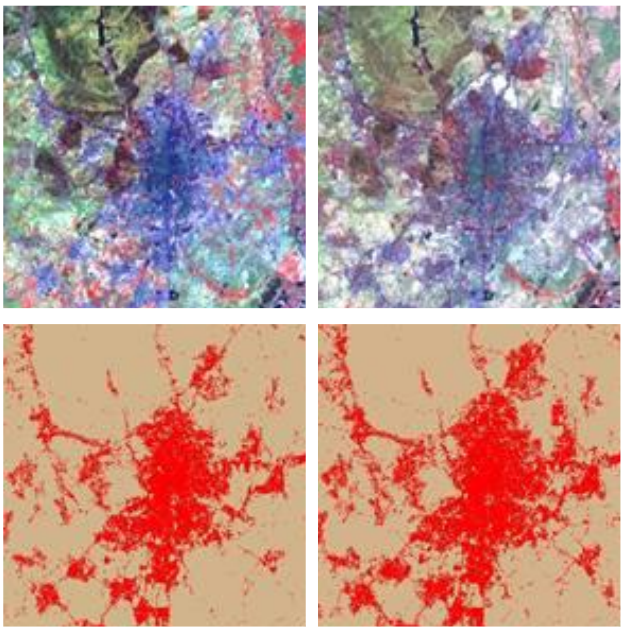

Fig 3.23: Classification sample for the case study of Madrid: Landsat TM Image taken on 25-May-89, and Landsat TM Image at 22-Aug-00; and respectively T^1 (1990) urban land cover classification, and T^2 (2000) urban land cover classification (Source: Angel, et al., 2005)

Using 10˙000 Google Earth validation sites, Potere et al. (2009) reported that pixels identified as "built-up" in our sample were found to be built-up in Google Earth 91% of the time and those identified as urban were identified in our sample 89 % of the time, confirming a relatively high level of accuracy (Angel, et al., 2011). Angel, et al. (2011), also describe that *the land cover estimates, used in the projections, were obtained from our Mod500 global map of large cities, which has a 463 meter pixel resolution. These larger pixels contain significant amounts of urbanized open space. For the global sample of 120 cities, the built-up area calculated from the Landsat 30 meter pixel imagery was 0.71 the Mod500 urban land cover (R2 = 0.97), and the city footprint was 1.16 the Mod500 urban land cover (R2 = 0.92). The Mod500 estimates are therefore not unrealistic estimates of the land needed to accommodate the projected fragmentation in city footprints*.

Spatial metrics, applied on previous urban land cover classification, are used in GIS platforms in order to measure urban growth dynamics based on key concepts, such as urban sprawl or compactness. A lot of urban indices have been developed and applied during the last decades for quantifying urban phenomena, but it is often difficult to provide homogenous comparative analysis among different geographical areas. Due to several limitations for comparing urban areas, the analysis undertaken in the framework of this study relies on five conceptual and general indicators which, according to the authors, allow for quite suitable comparison between the analysed case studies. Angel et al. (2011), state that *five discrete attributes of urban spatial structure can be*

measured and analysed systematically in all cities and countries: Urban land cover, Density, Centrality, Fragmentation and Compactness[189].

Due to the fact that the key data commonly used for measuring urban spatial structure is the built-up area and the affected open space, three main types of urban structures are defined according to the percentage of urbanized area within a fixed distance. The urban built-up area is classified like that, when there is a majority of built-up pixels within a 1 km^2 circle (the walking distance circle) around every urban pixel; suburban areas have between 10 and 50 percent of built-up pixels within the walking distance circle around an urban pixel; while rural areas have less than 10 percent of built-up pixels within the walking distance. From a morphological standpoint, the study also provides a methodology based on standardized spatial indices for discriminating different urban structures in the ambit of all of the built-up areas: such as the main core urban area, the secondary core, the urban fringe, the urban ribbon, and the urban scattered structure.

Moreover, due to the availability of different temporal stages (T^1 and T^2) the *Atlas* also offers an important examination of new urban developments that have occurred over a 10 year period roughly, in particular by classifying three different types of growth, which are: infill, *defined as all new development that occurred between two time periods within all the open spaces in the city footprint of the earlier period excluding exterior open space*; extension, as in all those *new developments that occurred between two time periods in contiguous clusters that contained exterior open space in the earlier period and that were not infill*; leapfrog developments, defined as *all new constructions that occurred between two prescribed time periods and were built entirely outside the exterior open space of the earlier period* (Angel, et al., 2011).

[189] A detailed description of the indices used for defining the five discrete attributes about urban spatial structures can be found in: Angel, S.; Parent, J.; Civco, L.; Blei, A.M. 2011. *Making Room for a Planet of Cities*. Cambridge: Lincoln Institute of Land Policy, 2011. Policy Focus Report Series

Chapter 4

LAND COVER CLASSIFICATION THROUGH REMOTE SENSING TECHNIQUES

The urban environment is a heterogeneous space, hence often it is necessary to simplify such a space into a combination of basic land cover and land use elements, in order to allow quantitative studies (Rocha, et al. 2007).

Indeed, spatial planning is greatly improved by the availability of thematic cartography of land cover/land use as a key contribution to sustainable development, regardless of whichever procedure of spatial monitoring and land management used. The provision of such thematic maps is maybe one of the most important applications of remote sensing techniques. The classification, which relies on meaningful categories or classes, aims to ascertain specific characteristics of various land cover/use patterns within a landscape. It could be used to define different factors, such as vegetation typologies, or describe man-made structures, or for providing water resource inventory and flood control.

The VIS model, proposed by Ridd (1995), for instance, is a conceptual model that simplifies the urban environment through the combination of three basic components: vegetation (V), impervious surface (I), and soil (S). Most urban uses can be interpreted through different combinations of these three basic components (Rocha, et al. 2007).

Moreover, *urban land use and land cover (LULC) datasets are very important sources for many applications, such as socioeconomic studies, urban management and planning, and urban environmental evaluation. The increasing population and economic growth have resulted in rapid urban expansion in the past decades. Therefore, timely and accurate mapping of urban LULC is often required* (Weng, 2010).

Unfortunately, collecting primary data for spatial planning and environmental monitoring is often an expensive "luxury" (from several standpoints). This was only plausibly possible for relatively small geographical areas around the world, mostly characterized for being rather densely populated, and consequently for having high levels of G.N.P. per capita. *The vast majority of the world is not like this* (Meaden, et al., 1991). Therefore, during the second half of the past century, aerial and space platforms were employed using advanced technological sensors, capable of collecting useful primary information about the current land cover status of the whole surface of the earth, and at regular time intervals.

The challenge of providing useful data for monitoring and managing the environment is becoming more effective and accessible for almost all of the world. Due to these needs, the relatively new discipline of Remote Sensing (RS) has been developing, in particular during the last decades, in parallel with those technological advances linked to the practices of aerial and space monitoring.

Currently, even though there are plenty of approaches for remote sensing image classification which have been advancing until now, Land Cover/Land Use classification is still an exciting challenge. This is principally because of the complexity of the landscape, or limitations within remote sensing data (Weng, 2010), but it also probably due to a lack of standardization and an effective clarity of the questions RS products can answer. Moreover, new scenarios are opening up in the huge RS field and inevitably are evolving ever more rapidly with technological advances and knowledge. Therefore, increasing efforts are required to develop standardized, widely available, and worldwide shared, methodologies for collecting RS data.

It is important to state that this chapter does not pretend to provide a significant (even if quick) overview of remote sensing issues, but is mostly based on the procedures used in this work. It does not aim to cover the entire scenario regarding the subject matter, but rather to provide an instrument for better understanding of the steps used for defining the upcoming methodology for land cover classification.

4.1. REMOTE SENSING: OVERVIEW AND MAIN THEMES

Some basics should be briefly explained to better understand the discipline that we are about to approach. Unfortunately, it will be not possible to more thoroughly explore the specific scientific fields which the remote sensing relies on, such as physics, statistics and geography. Although, further information on the subject matter can be found and extra knowledge could be provided.

Remote Sensing (RS), as a scientific field, is currently recognized as an interdisciplinary approach for observing and measuring objects and phenomena on the surface of the earth and in the atmosphere. This remote sensing is done from a distance by using instruments capable of collecting information without being in direct contact with the subject matter under investigation. Usually, the sensor devices are placed on aerial or orbiting space platforms and allow measurement of certain types of energy released from the earth. In particular, remote sensing processes aim to classify and quantify certain physical features within the earth environment. This is based upon the measurement of electromagnetic radiation (energy), naturally or artificially produced, and the interaction between the incident radiation and an object (target) under investigation.

The sun provides one of the main suitable sources of energy, through radiating electromagnetic energy. Commonly, when it encounters an object or surface, it is either transmitted through different strata, reflected (or scattered), such as in the case of visible light, or absorbed by objects and then emitted, such as is the case of thermal energy (figure 4.1).

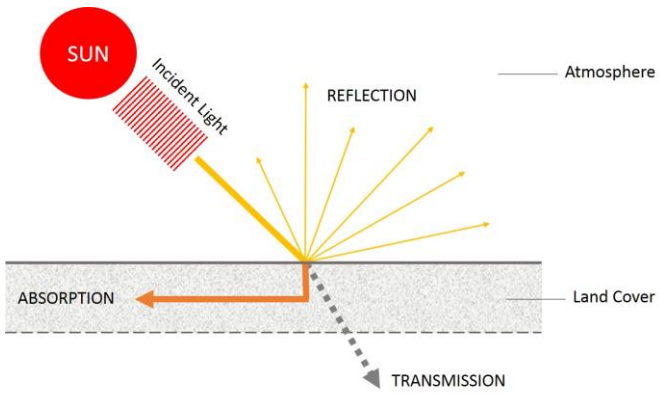

Fig. 4.1: Extinction of Incident radiation: absorption, transmission, and reflection (Source: By Authors)

The remote sensing process relies especially on sensing and recording of the reflected and emitted part of the incident energy, which can be measured, processed and stored as digital information. Then, the information about landscape and environment can be collected both in forms of digital image, as well as photographic outputs, more or less approximated, depending on the type of employed devices.

Actually, the overall process can be reduced to a few main components: a) the energy source; b) the interaction between energy radiation and the atmosphere; c) the succeeding interaction between energy radiation and ground targets (or the land surface); d) the recording of energy response, through the use of sensors; e) the processing, display, and interpretation of the derived information, in digital format.

Remote sensing, as a discipline, arose mainly with the development of flight. The original use of hot air balloons during the second half of the XIX century, was substituted during the course of the 20th century, primarily by aerial photography, which was mainly developed for military purposes, and for delineating topographic maps. While the development of space platforms (artificial satellites), during the second half of the 20th century, has provided us with an important inopportunity to improve this scientific field, by allowing the possibility of using technological sensors for monitoring land cover areas and earth's atmosphere, on a global scale.

As reported by Meaden, et al. (1991), *the period from the late 1950's has been extremely active for RS, with developments in the whole applications field occurring at an exponential rate. With satellite launches occurring regularly, following SPUTNIK 1 in 1957, the interest in RS concentrated on the use of this new and unique platform. In 1959 the first earth images were transmitted from EXPLORER 6 and the first meteorological satellite, TIROS-1, was launched in 1960. The next major advance for RS occurred with the launch of the Earth Resources Technology Satellite (ERTS-1, later renamed Landsat 1) in 1972. This was the first satellite designed to provide long-term, uniform global coverage, having the ability to transmit data gathered on a variety of instruments, for eventual mapping at scales of 1:250˙000 to 1:1˙000˙000. Since Landsat 1 there has been a succession of earth monitoring satellites launched, first by the U.S.A. and the U.S.S.R., but more recently by other countries. Their equipment has*

become progressively more sophisticated allowing a greater range of imaged data to be interpreted at a more detailed spatial resolution (Travaglia, 1989; Meaden, et al., 1991).

The remotely sensed data, which relies on satellite photography, is currently the basis for systematic earth observation and environmental sciences providing several chief improvements over ground exploration. In fact, satellite imagery allows us to capture images of huge landscape areas in one image, and monitor them. It also allows us the possibility to clearly discriminate different land cover patterns, thanks to the capability of capturing images in multispectral or hyperspectral resolution, within certain ranges of the electromagnetic spectrum, depending on the sensor type. Moreover, the ability to repetitively cover those areas, i.e. the possibility of taking pictures of the same specific area, at regular intervals (days, months, years), provides useful data for monitoring land cover changes over time. As pointed out before, *the concept of remote sensing covers a huge field. A field within science and technology, which encompasses a vast "applications domain", i.e. in the sense of inputs of applied science, applications in the processing field, and in the sense of the ways in which RS outputs can be applied* (Meaden, et al., 1991).

Perhaps one of the most familiar practises of remote sensing is photography, but other methods deserve to be mentioned, even if we are going to focus the discussion and experiments basically on the remote sensing of optical signals reflected by the surface of the earth, stored in a two-dimensional spatial grid. In fact, as claims Schowengerdt (2007), in order *to meet the needs of different data users, many remote-sensing systems have been developed, offering a wide range of spatial, spectral, and temporal parameters. Some users may require frequent, repetitive coverage with relatively low spatial resolution (meteorology). Others may desire the highest possible spatial resolution with repeat coverage only infrequently (mapping); while some users need both high spatial resolution and frequent coverage, plus rapid image delivery (military surveillance). Properly calibrated remote-sensing data can be used to initialize and validate large computer models, such as Global Climate Models (GCMs) that attempt to simulate and predict the earth's environment*.

Each different RS system relies on a different technology. The use of Interferometric synthetic aperture radar (SAR), for instance, allows the delineation of topographic maps of land surface, which are often used to produce digital elevation models (DEM) on a large scale. While stereographic pairs of aerial photographs, following the principles of photogrammetry, are employed to provide topographic maps at a more detailed scale.

Light detection and ranging (LIDAR) is used to measure the position of points, objects, and physical features on the ground, at a very high spatial resolution.

Radiometry is used for physical measurement of a wide range of radiation from x-ray to radio wave, while photometry corresponds to the human perception of visible light based on the human eye's sensitivity (Japan Association of Remote Sensing, 1999). Radiometers and photometers instruments are thus used for collecting reflected and/or emitted radiation in a wide range of frequencies. Multi-spectral sensors, which capture a limited amount of spectral information, are the basis for maps of land cover and land use, which allow the monitoring of earth surface status; while hyperspectral sensors provide imagery of wide and continuous spectral information, within a specific contiguous spectral range.

All of these techniques rely on detecting the electromagnetic energy emitted or reflected from the earth's surface, from a distance. Therefore, it is widely recognized that the starting point for a better understanding of the remote sensing discipline is a good knowledge of the electromagnetic (EM) spectrum, including the form and the way energy moves through space or matter.

4.1.1. Electromagnetic Radiation and Main Spectral Features

As was mentioned in the previous section, the purpose of the environmental remote sensing is to measure certain physical parameters of objects or surfaces, according to the variations of the electromagnetic radiation (EMR) emitted or reflected by the target, through the use of technological sensors on board aerial or space platforms. To do so, the primary condition is for the existence of a source of energy to hit the target.

A common source of energy used for remote sensing, is the electromagnetic radiation emitted by the sun, and this radiation moves through the vacuum of space at a constant speed[190] of $3x10^8$ m/s. This journey implicates

[190] The speed of light in the vacuum is commonly represented with the symbol *c*, and it is a universal constant in physics.

the transfer of certain amounts of energy to the surrounding space or matter. In fact, every object or surface, once touched by radiation, reflects or radiates a part of the energy, depending on the molecular composition of the matter, and the type of radiation. In practice, the electromagnetic radiation involves an electric field (E), which moves perpendicularly to the direction in which the radiation propagates, and a magnetic field (M), in turn oriented perpendicularly to the electric field. Both fields move, perpendicular to the propagation of the radiation, and in the form of waves which rely on two main physical features: wavelength and frequency (figure 4.2). Therefore, depending on the physical features of the waves, the matter can absorb or release more or less quantities of energy, and in different forms, thus returning varying types of information that specific sensors are capable of capturing[191].

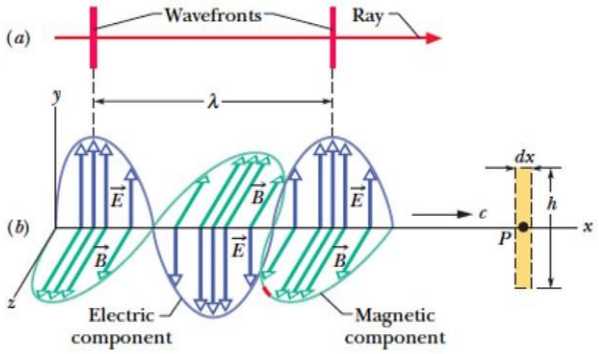

Fig. 4.2: *(a) An electromagnetic wave represented with a ray and two wavefronts; the wavefronts are separated by one wavelength ʎ. (b) The same wave represented in a "snapshot" of its electric field* $\vec{E}$ *and magnetic field* $\vec{B}$ *at points on the x axis, along which the wave travels at speed c* (Source: Halliday, D.; Resnick, R.; Walker, J. Fundamentals of Physics, 9th Edition)

The wavelength (ʎ) is the distance over which the wave's shape repeats (Hecht, 1987). It measures the distance between two consecutive and corresponding points of a wave segment (cycle), which could be two crests, or alternatively two troughs of the sinusoidal form of the waves. Being actually a physical distance between two points, the wavelength is measured in meters (m). Fractions of meter are then used when extremely small distances are considered, such as the centimetre (cm), millimetre (mm), or the micrometer (µm) which equals 10^{-6} m, and the nanometer (nm) which equals 10^{-9} m.

Frequency (ƒ) measures the number of repeated events which occur, for certain phenomenon, in a determinate interval (unit) of time. In the case of electromagnetic waves, for instance, the frequency is the number of cycles of a wave which repeat during a specific time interval. It is measured in hertz (HZ) which equals one cycle per unit of time, which within the International System of Units (SI) is established as one second.

The relation between wavelength and frequency is expressed in the following equation [4.1]

$$v = \lambda f \qquad [4.1]$$

With v Propagation speed (which is $c = 3x10^8$ m/s in the case of the speed of light)
ʎ Wavelength (m)
ƒ Frequency (Hz)

Therefore, wavelength and frequency are inversely related to each other, that is to say the shorter the wavelength, the higher the frequency, and vice versa. The understanding of these measurements of energy is central to the comprehension of the information provided by the remote sensing methods. In fact, all the ranges of all possible frequencies of electromagnetic radiation captured by remote sensors is termed the electromagnetic spectrum and is commonly classified according to wavelengths.

[191] The amount and type of radiation emitted or reflected depends upon incident energy (mainly from incoming solar radiation), the nature of the earth's surface and on the interaction with the earth's atmosphere (Meaden, et al., 1991)

There are a whole family of waves which collectively are called electromagnetic vibrations and which vary in their wavelength, and hence (since their speed is constant in space) their frequency. This family may be displayed as a spectrum of energies, hierarchically arranged by wave frequency or wave length. The spectrum covers a vast continuum of wavelengths (Meaden, et al., 1991). In particular, the electromagnetic spectrum, ranges from long wavelengths, and hence low frequencies, which include microwaves and broadcast radio waves, to the shorter wavelengths, and therefore high frequencies, which comprise gamma and x-rays. In fact, in terms of wavelength dimensions, the whole spectrum provides lengths which vary between thousands of kilometers down to a few nanometers. Figure 4.3 shows the main forms, and correspondent wavelengths, of the electromagnetic radiation which include:

- Gamma rays
- X-rays
- Ultraviolet (UV) rays
- Visible Light
- Infrared radiation
- Microwaves
- Radio waves

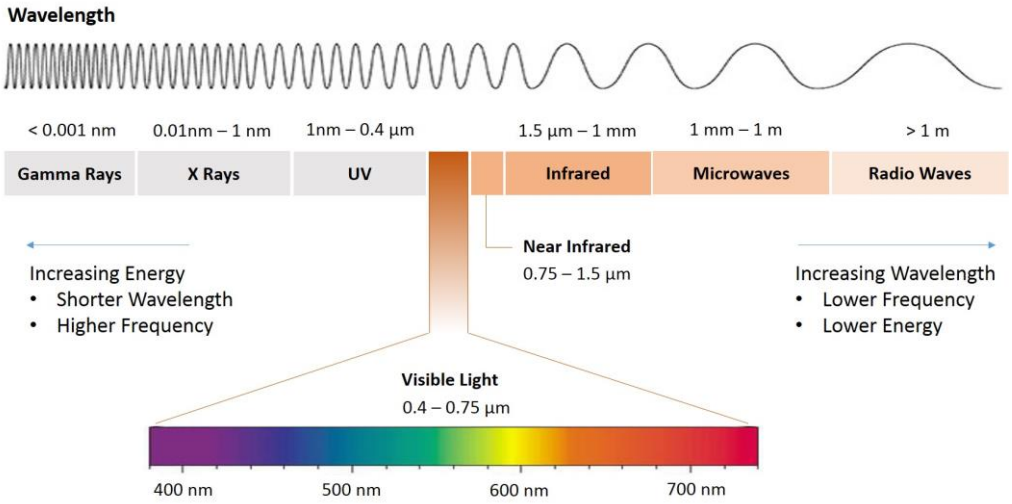

Fig. 4.3: Major wavelengths distribution across the electromagnetic spectrum (Source: By Authors)

Several of the aforementioned regions of wavelength, within the electromagnetic spectrum, are suitable for remote sensing, which is actually possible because matter (objects and surfaces) reflects, absorbs, and emits measurable forms of energy in certain specific ranges of those wavelengths. In particular, the portion of the electromagnetic spectrum suitable for remote sensing is the one found between UV rays and microwaves.

The ultraviolet part of the spectrum (0.01 to 0.4 µm), beyond the violet portion of visible light, provides the shortest wavelengths useful for remote sensing. Within the visible light portion falls the only part of the electromagnetic radiation which the human eye can perceive. Moreover, this is the portion of wavelengths which are commonly associated with the concept of colour. This section of spectrum is actually quite small, if compared to the other bands. That is why the use of technological instruments (sensors) is required for detecting those other types of radiation beyond this range which is invisible to our eyes. Visible wavelengths range from about 0.4 µm (violet light) to 0.75 µm (red light), and comprises the following main portions, or colours:

Violet	Blue	Green	Yellow	Orange	Red
0.400 - 0.450 µm	0.450 - 0.495 µm	0.495 - 0.570 µm	0.570 - 0.590 µm	0.590 - 0.620 µm	0.620 - 0.750 µm

The infrared (IR) region which ranges from about 0.75 µm to 1˙000 µm can be subdivided into two main regions, depending on their radiation properties. In fact the IR part, from approximately 0.7 µm to 3.0 µm, which is commonly termed Near Infrared (NIR) is used as a reflecting infrared in remote sensing, because this special radiation appears to be more similar to radiation in the visible portion.

On the other hand, the region between 3.0 µm to 1˙000 µm, is actually quite different, in comparison to the NIR, being that this kind of energy is derived from the radiation emitted by matter in the form of heat. It is effectively an emitting infrared region, commonly known as Thermal IR. Actually, in a more detailed way, we could differentiate the IR slice in three sub-regions based on their wavelengths: NIR (Near-Infrared) and SWIR (Short Wave Infrared) around 0.75 to 3.0 µm; mid-IR (MIR) with medium waves between 3.0 and 50 µm, and far-IR (FIR) with long waves, from 50 to 1˙000 µm.

The microwave region, which spans from 1 mm to around 1 m, involves all the intervals of wavelengths employed in remote sensing through the use of radar systems. These devices are capable of producing their own active radiation (pulses) that hit surfaces and then return to the instrument, thus collecting different types of information. The longest wavelength region within microwaves, i.e. further than 1 m, is commonly associated with radio waves.

High frequencies generate highly energetic radiation, so therefore the shorter the wavelength, the higher the energy of radiation. In fact, on the other side of the electromagnetic spectrum (with respect to microwaves), the most energetic emissions that can be found are x-rays and gamma rays.

Sunlight is the main source of energy which radiates the surface of the earth. The majority of this energy is distributed across the ultraviolet, visible, infrared, and short infrared areas within the EM spectrum. Wavelengths encompassed between 0.01 and 3.0 µm provide mainly reflected solar energy. While mid-infrared to microwave are radiations basically emitted by the earth's surface. In remote sensing, optical sensors are used to "capture" the solar radiation which is reflected or scattered by the earth's surface, and this extends from the visible and near infrared to short-wave infrared (SWIR).

Different types of sensors are then used for thermal and microwave RS. In any case, the intensity of that reflected or emitted energy is usually collected in digital formats for successive processing. In the following table (4.1), this is detailed for each specific range of wavelength of interest for RS, including the main detectors used to capture the reflected or emitted energy along with some of the main features related to the interaction between the radiation and the environment.

WAVE BAND NAME	WAVELENGTH	RADIATION SOURCE	DETECTORS	SOME CHARACTERISTICS
Visible (V)	**0.4 – 0.7 µm**	Solar	• Black & white plus colour photography • T.V. camera • Optical scanner	• High atmospheric scattering effect • Most EMR is reflected; solar radiation therefore is only used in day-light • Penetrates water
Near Infrared (NIR) **Short Wave InfraRed (SWIR)**	**0.7 – 1.1 µm** **1.1 – 3.0 µm**	Solar	• Infrared scanner • Infrared thermography • Multi-spectral scanner • Photography • Optical scanner	• High reflectance of vegetation • Solar energy reflected by surfaces
Med-Wave InfraRed (MWIR)	**3.0 – 8.0 µm**	Solar, Thermal	As above	As above
Thermal InfraRed (TIR) **Long-Wave InfraRed (LWIR)**	**8.0 – 9.5 µm** **10 – 14 µm**	Thermal	• Radar • Side Looking Air-borne Radar (SLAR) • Optical scanner	• Predominantly radiation emitted by the earth and atmosphere • Does not penetrate clouds
Microwave; Radar	**1 mm – 1 m**	Thermal (Passive) Artificial (Active)	• Radar • SLAR • Scanning radiometer	• Can penetrate clouds • Imagery acquired in active or passive mode - daytime or night-time

Tab. 4.1: Wave band main ranges, and primary features, of Interest for RS (Source: Meaden, et al., 1991; Schowengerdt, 2007)

4.1.2. Active Remote Sensing and Passive Remote Sensing

Within the field of remote sensing, it is central to distinguish the two main types of procedures, related to different technologies (sensors), as well as to different ranges of the EM spectrum. We refer to active remote sensing and passive remote sensing[192].

In order to scan objects when no natural energy is available, either reflected or emitted, an artificial source of radiation is required. That is why special devices are employed, capable of providing an artificial, proper radiation source that strikes a target under investigation, which consequently then reflects back, or scatters, a certain amount of energy. The energy is then measured and stored in the device. Active remote sensing is also termed microwave RS (most of the microwave sensors are actually active sensors, able to provide their own sources of energy), because it relies on the detection of those waves, not provided by natural light, which cover a range between approximately 1mm to 1m; precisely, the microwave portion of the EM spectrum.

In practice, the illumination caused by active sensors, obliges an object either to emit, or reflect the radiation produced by the sensor, so that no natural light is required for recording digital imagery, which thus could be made at any time, i.e. during day or night-time, or with clouds or rain. It is because of the long wavelengths that characterize the microwave radiation that therefore are not affected by atmospheric scattering, as happens on the contrary, with shorter optical wavelengths. Generally, microwave energy pulses are emitted at regular intervals in the form of radar beams and directed towards a target. The radar beam illuminates surfaces, or objects on the ground, which in turn reflect back the energy, depending on various factors such as surface roughness, for instance. The measurement of time delay, between the emission of pulses and the detection of the backscattered radiation is stored then as information, in digital data, thus making it possible to generate two-dimensional imagery of scanned areas.

Some active sensor systems are surface-based, e.g. sonar, others could be carried in aircraft, e.g. Side Looking Airborne Radar (SLAR) whilst others can be mounted in satellites, e.g. Synthetic Aperture Radar (SAR). A further type of active sensor is the laser radar (LIDAR[193]). LIDARs use lasers to generate short, high power light pulses. These can be used to measure the intensity of light back-scattered by the target as a function of the distance from the sensor[194] (Meaden, et al., 1991). In general, the RADAR (RAdio Detection And Ranging) and LIDAR systems measure time delay between emission and return of pulses that permit us to determine location, speed, and direction of objects[195].

Microwave sensors, for active RS, can be commonly classified into two main categories: imaging sensors (that build up a digital image of the area under investigation) and non-imaging sensors. The RADAR is an example of an active imaging microwave sensor; while non-imaging sensors such as altimeters, for instance, are used for altitude determination and topographic mapping. Instead, the main difference between airborne RADAR, and space-borne RADAR (the Canadian satellite RADARSAT, for example), is that the first one must use a wide incident angle of radiation for covering huge areas, while the second one needs smaller ranges of incident angles, to cover the same area under investigation. Understanding that the angle of incidence of the radar beam, is a key variable in defining the digital outcomes because it affects the degree of distortion that could occur during land scanning.

Then we have passive remote sensing, also termed optical and thermal RS, which relies on detecting the available background electromagnetic energy produced by natural sources (the sunlight), within the visible, near infrared, and thermal infrared portion of the spectrum. In fact, passive sensors are only capable of detecting natural radiation coming from the sun and back to the sensor, emitted or reflected by the environment. It is because the sensor actually does not emit energy itself. Visible and short to middle infrared wavelengths can only be captured by passive sensors during daylight hours. However, the energy which is naturally emitted by the earth's

[192] An intuitive sample for easily describe both passive, as well as active sensors, is the photo camera. In fact, when taking a picture, if adequate sunlight irradiates the environment, such that certain energy is reflected, the camera is capable of recording the information of all wavelengths reflected by the different matter. It is actually a passive mode. On the other hand, when not enough natural light is radiating the environment (during night-time for instance, or very cloudy days), a photo camera can provide its own source of energy by using the flash, which illuminates the targets and then collects the radiation reflected by the objects and surfaces. It is, in reality, an example of active RS

[193] Laser Interferometry Detection And Ranging

[194] Brightness or darkness values for imagery, derived through microwave RS, depend on the share of energy returned back to the radar, after stricken an object. Bright areas depend on a strong radar response, while dark areas result from a weak radar response

[195] *Because of their size LIDARs are presently limited to airborne craft* (Meaden, et al., 1991)

surface after absorbing natural radiation or due to the physical characteristics of the matter generating thermal infrared wavelengths, can be detected during the daytime or night-time. Obviously, the quantity of energy would be large enough to be recorded. Such as for the active RS, the information derived by the reflection of natural energy is then stored in digital format for providing two-dimensional imagery of the earth's surface.

Therefore, whatever the type of platform or sensor employed, the procedure for obtaining landscape maps relies mainly on the following key steps (the data flow): an emergent radiation from the land surface is collected by a sensor aboard a remote platform, the revealed data is transmitted towards ground instrumentations, then pre-processed, stored in digital formats and thus ready for use. Advanced image processing techniques and several software programs, are employed for extracting further information and creating maps of the geographical areas under investigation.

Moreover, radar and optical remotely sensed data can be complementary to each other as they offer different information about the earth environment. The image below (figure 4.4) shows, schematically, how active (airborne radar) and passive remote sensing operate, and the main features on which both are based.

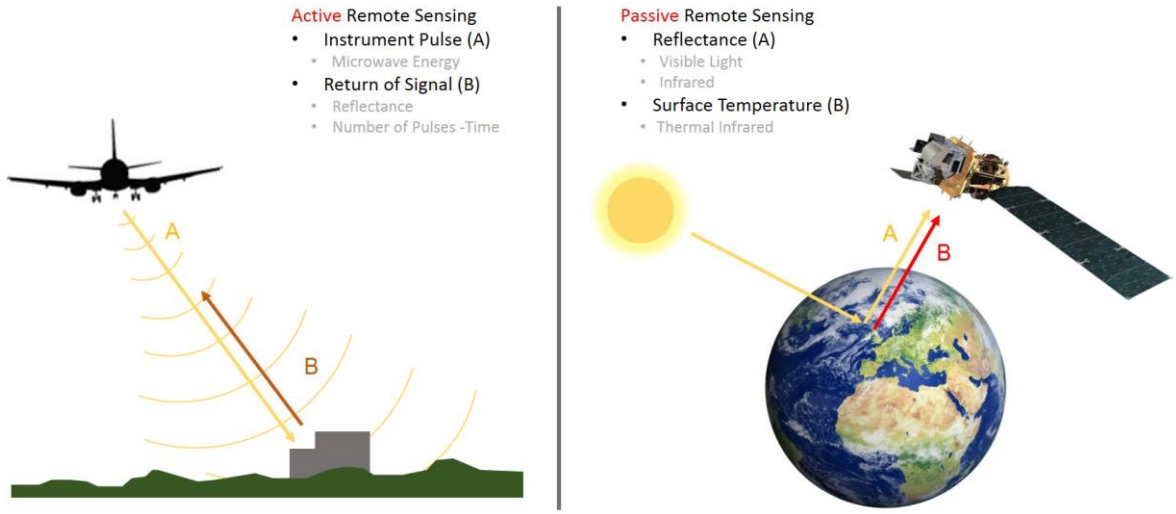

Fig. 4.4: Types of Remote Sensing and main features: Active RS and Passive RS (Source: By Authors)

In the framework of the present research work, we will limit our investigation in particular to the use of optical RS. While the experiments will particularly rely on the digital information derived from a specific type of sensor aboard the US space platform known as Landsat. Further details will be provided during the following part.

4.2. FORMAT AND CHIEF FEATURES OF THE REMOTELY SENSED INFORMATION: DIGITAL MAPS

The collection of data about the spatial distribution of the significant features of the earth's surface has long been an important part of the activities of organized societies. From the earliest civilizations to modern times, spatial data have been collected by navigators, geographers and surveyors, and rendered into pictorial form by map makers or cartographers (Anji Reddy, 2008).

Regardless of the type of technology used for remote sensing, the end result of a process of graphic restitution aimed at representing a certain phenomenon of the Earth's surface or simply the status of the current composition of the land pattern, is called a map. As Anji Reddy (2008) also claims, *maps are thus the starting point in any analysis. Whether it is remote sensing, photogrammetry, cartography, or GIS, the ultimate output will be the production of high quality, more accurate and clearer map, so that the user finds it easy to make appropriate decisions*.

A digital map is a two-dimensional form for representing spatial data, in terms of location (as the geographical position of a certain object in the space) and attributes (as qualitative or quantitative measurement of

it) and it relies on some key features; such as, the matrix distribution of information, geographical projections, and a variable degree of generalization, which generally depends on the type of technological sensor employed for detection. In optical RS, spectral measurements and relative spatial position are recorded in every cell of the matrix. This form of storing information is quite useful from the standpoint of computer-based data handling and analysis.

Currently, according to Richards, et al. (2006), *the great advantage of having data available digitally is that it can be processed by computer either for machine assisted information extraction or for enhancement of its visual qualities in order to make it more interpretable by a human analyst*.

4.2.1. Digital Image Data: Format and Resolution

An image may be defined as a two-dimensional function, f(x, y), where x and y are spatial (plane) coordinates, and the amplitude of f at any pair of coordinates (x, y) is called the intensity or grey level of the image at that point. When x, y, and the amplitude values of f are all finite, discrete quantities, we call the image a digital image…A digital image is composed of a finite number of elements, each of which has a particular location and value. These elements are referred to as picture elements, image elements, pels, and pixels. Pixel is the term most widely used to denote the elements of a digital image (Gonzalez, et al., 2002).

The remotely sensed data (mostly EM radiation), acquired through the use of electronic sensors[196], is commonly stored in such a format (digital imagery), i.e. two dimensional array of discrete elements, or pixels henceforth, organised in columns and rows. Each pixel within the array encompasses a portion of the area from the scanned surface. The value provided by each pixel is the intensity (or brightness) of the captured signal in that specific location inside the plane image. The intensity detected signifies the physical quantity of radiance, reflected or emitted from the ground according to a given wavelength. Actually, the final value of brightness, captured in each pixel is an averaged estimation of all intensities radiated by the various objects encompassed in that specific portion (pixel) of land. Therefore, the bigger the pixel, the more objects can potentially be involved, and therefore the bigger the generalization of reflectance values will be.

The averaged brightness of each pixel is represented by a number, as shown in figure 4.5, which is commonly termed Digital Number (DN). The DNs are positive integer numbers, coded according to a finite number of bits (binary digits), and *resulting from quantizing the original electrical signal from the sensor into positive integer values using a process called analog-to-digital signal conversion*. Therefore, a digital image (also known as *Raster Image*) can be now defined as a matrix of digital numbers (Anji Reddy, 2008).

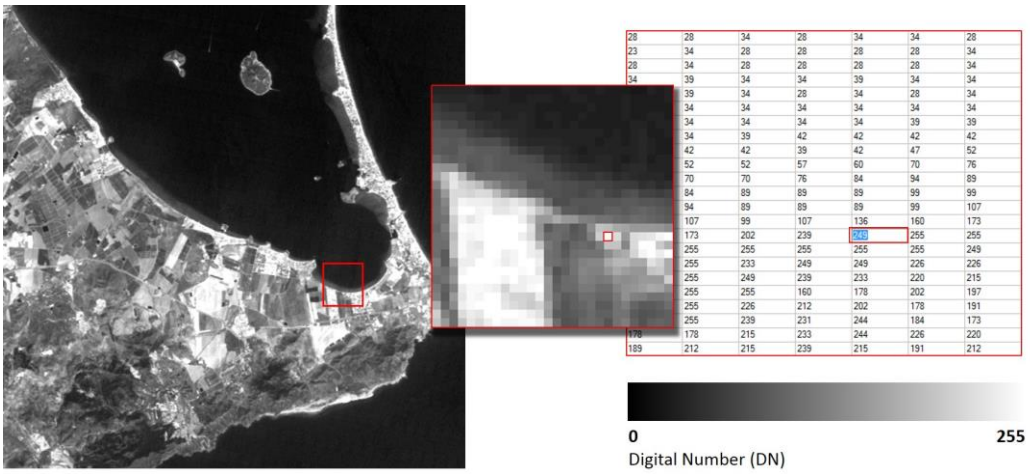

Fig. 4.5: Spectral reflectance values for digital numbers (DN) in 8-bit grayscale (Source: By Authors)

[196] Electronic sensors, or detectors, are employed in scanning systems, which cover geographical areas by arranging the detected information in a series of consecutive parallel lines, thus collecting data suitable for returning a two-dimensional digital image of that scene.

Specifically in optical RS, the values stored in the pixel provide the so called "spectral reflectance" of the matter, according to the spectral bands (wavelengths) being recorded. It is, in practice, the ratio between the incident light and the amount of reflected energy after deducting the amount of transmitted and absorbed energy. Therefore, reflectance values range from 0 to 1, where 0 means total absorption of energy by the matter, whereas a value of 1 means total reflection of the energy.

In order to classify the level of definition (and precision) of digital information provided by different RS systems, four key features have to be considered:

- Spatial Resolution
- Radiometric Resolution
- Spectral Resolution
- Temporal Resolution

Spatial resolution refers to that area of land surface encompassed in a pixel, i.e. the size of the smallest possible unit that can be stored within the raster image. It depends on the Instantaneous Field Of View (IFOV) allowed by the sensor. Generally, a pixel refers to squared areas and we define the pixel depending on the length of its sides, measured in meters. Therefore, the level of detail provided by an image is defined by the spatial resolution allowed by the employed sensor, in terms of meters per pixel[197].

Radiometric resolution is the number of different intensities of EM radiation which can be discriminated, by a sensor, for each pixel within the raster image. For every image, this value varies, usually between 8 to 16 bits of digital numbers (DN), i.e. 2^8 (256) or 2^{16} (65˙536) different values. These values, correspondent to the number of intensities, are displayed in a grayscale, for each wavelength. The greater the radiometric resolution, the more sensitive will be the detection of different degrees of reflected or emitted energy.

A sensor can allow us to collect multiple bands (or channels) of wavelength at once from the same geographical area, the *spectral resolution* defines the maximum number of bands that each sensor can collect during the scanning[198] (i.e. the capacity to detect more or less wavelength intervals). At higher spectral resolution, the finer will be the wavelength range provided by the bands. The sample in figure 4.6 shows, graphically, the meaning of spatial resolution, radiometric resolution, and spectral resolution, for a multispectral raster image.

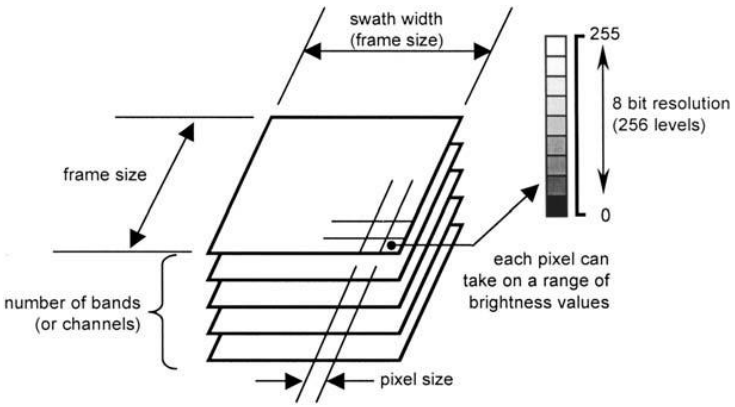

Fig. 4.6: Main technical characteristics of digital image data: image size, spatial resolution, spectral resolution, and radiometric resolution (Source: Richards, et al., 2006)

Depending on the degree of spectral resolution (i.e. number of spectral bands detected), optical and thermal RS systems can basically provide three main typologies of digital imagery:

[197] *The area covered by a pixel (the resolution) is a function of the height of the sensor, the focal length of the lens or focusing system, the wavelength of the radiation and other inherent characteristics of the sensor itself. Each pixel will be allocated a co-ordinate in a grid referencing system* (Meaden, et al., 1991)

[198] *Several bands of the EMR spectrum, either from the ultraviolet to infrared regions (multispectral scanners) or the microwave bands (radiometers), may be scanned simultaneously by optically splitting the collected radiation and diverting each part to a separate detector element. Final image products can be photographs or computer compatible tapes containing digital data* (Meaden, et al., 1991)

- *Panchromatic imagery*, which is derived by sensors capable of detecting levels of brightness in one single channel within a wide range of wavelength; this interval commonly spans the whole visible slice of the EM spectrum. It is, in practice, a black-and-white image.
- *Multi-spectral imagery*, which relies on multi-channel sensors capable of detecting more than one band at once. Commonly, it is a small number of spectral bands (in general less than ten), and each channel is suitable for collecting one specific radiation, within a narrow wavelength interval. Thus, the obtained digital data contains multiple bands from the "spectral colours", infrared reflectance and thermal emission, from the same area of interest.
- *Hyper-spectral imagery* provides, spectral information within a scan based on up to hundreds of bands, therefore allowing more precise spectral information and then enabling a better discrimination and classification of different objects in a scene.

Additionally, based on spectral resolution, cameras will require different types of film for different purposes. The main types, according to their range of spectral sensitivity, are: orthochromatic film; panchromatic; black and white Infrared; natural colour; and false colour films[199] (Meaden, et al., 1991).

Finally, *temporal resolution* is the minimum interval of time (or the frequency) between two consecutive observations of the same area of interest. It is due to the period of time a satellite requires to complete an entire orbiting cycle around the earth, which could generally take several days. The temporal resolution is mainly significant in circumstances such as: time-series analysis, averaged imagery of the same area; landscape mosaics; large percentage of cloud cover over an area under investigation, which thus requires repeating the observation.

4.2.2. Remote Sensing Platforms: Satellites

The imagery detection procedure through remote sensing relies on the use of two main types of platforms carrying the various types of available sensors: airborne platforms (balloons, helicopters and aircraft[200]) and space platforms (satellites). Besides the variations in terms of spatial, spectral, and radiometric resolution; the differences, in terms of altitude and stability, due to the type of orbit that each platform performs over the earth's surface can offer extra differences in the image properties. Currently, diverse orbits often affect the temporal resolution of imagery, and the size of the maximum coverage area per scan.

Due to the fact that the study carried out in the framework of this research is based on passive remote sensing through satellite platforms, we will address the main features of satellite orbits. Additionally, some important Earth Observation (EO) programmes using RS technologies will be briefly discussed in this section.

Satellites probably provide the majority of remotely sensed data. *Their primary capability is to carry sensors which can monitor the entire earth surface on a periodic basis, sensing a large area during each revolution. They all operate at an altitude which is sufficient to escape from the earth's atmospheric drag but still remain within the dominant gravitational field, i.e. between 150 kilometers and 40˙000 kilometers* (Meaden, et al., 1991).

Each satellite revolves in a specific orbit, following certain synchronism with respect to the Earth. The orbit can vary mainly in terms of altitude, orientation and rotation, and depending on these parameters, a satellite can capture different portions of the Earth's surface. As claimed by Meaden, et al. (1991), the primary advantages of using satellite RS systems relies on the possibility to provide a cost-effective repetitive monitoring of the huge surface of the earth, over time, at various scales and resolutions (*often satellite-sensed data is the only information available for large tracts of ocean, mountain, desert or tropical forest areas*). On the other hand, there are some disadvantages that also need to be underlined, which basically includes large capital costs for allowing permanent

[199] More details about the mentioned framing system films can be found in: Meaden, G., & Kapetsky, J. (1991). Geographical information systems and remote sensing in inland fisheries and aquaculture. FAO Fisheries Technical Paper No. 318, FAO, Fisheries Department, Rome

[200] According to Meaden, et al. (1991), there are several sub-categories of aircraft platforms, depending on the flight altitude:

- *High altitude aircraft - these usually operate at over 8˙000 meters allowing for photography at about a 1:100˙000 scale, or the use of multi-spectral scanners and Radar systems*
- *Medium altitude aircraft - which operate at 3˙000 to 8˙000 meters and can take photographs at a 1:20˙000 to 1:80˙000 scale or carry multi-spectral scanners*
- *Light aircraft - which fly below 3˙000 meters and can do aerial reconnaissance, take large-scale photographs and can supplement missing or uncertain satellite imagery*

monitoring and providing receiving stations, besides the technical limitations due to a relatively poor resolution for environmental analysis, and copious percentages of cloud cover for passive RS Systems (depending on the season).

Satellites generally follow different elliptical or circular orbits around the earth, by cyclically repeating the path employed for carrying out one entire revolution, following a known temporal interval. *There are essentially two broad classes of satellite program: those satellites that sit at geostationary altitudes above the earth's surface* (Geostationary Orbit) *and which are generally associated with weather and climate studies, and those which orbit much closer to the earth's surface and that are generally used for earth surface and oceanographic observations. Usually, the low earth orbiting satellites are in a sun-synchronous orbit* (Near Polar Orbit)*, in that their orbital plane processes around the earth at the same rate that the sun appears to move across the earth's surface. In this manner the satellite acquires data at about the same local time on each orbit* (Richards, et al., 2006).

In *Geostationary Orbit*, a satellite traces a path parallel to the equator, following the same direction and time period (24 hours) as the earth's rotation. That is why the satellite actually appears to be "stationary" with regard to the earth surface. Due to their stationarity (geosynchronous orbit), satellites, which are also generally positioned at high altitudes around 36˙000 kilometers above the equator (*at this altitude the speed of the satellite can exactly match the speed of the earth's rotation*), are able to cover huge areas of the earth's surface by always monitoring the same geographical portion. The geostationary orbit permits reaching high temporal resolution, even if the great distance to the surface implies a spatial resolution which normally spans between no more than 2 and 5 Kilometers, depending on the wavelengths[201] (Meaden, et al., 1991).

In *Near Polar and Sun-Synchronous Orbits*, the inclination angle between the plane of satellite revolution, and the axis of earth's rotation, is relatively small. Instead, with respect to the equator plane, the angle reaches nearly 90 degrees (*the satellite crosses the equator at the same sun time each day*), so that the satellite orbit almost intersects both the north and south poles, tracing half of its whole orbit along the northern side of the Earth and the other half across the southern side. The orbit height ranges between 270 km and 1˙600 km, and these altitudes allow detection of one specific location, at a given latitude, at the same local solar time. *In this way, the same solar illumination condition (except for seasonal variation) can be achieved for the images of a given location taken by the satellite* (Japan Association of Remote Sensing, 1999). It is particularly useful for providing comparative analysis of multi-temporal data. The specific *inclination of the flight path will determine the time period between re-visits to any specific location, but it is commonly once every 16 to 20 days* (Meaden, et al., 1991).

Even if most of the remote sensing satellites for Earth observation use near-polar and sun-synchronous orbits, a major distinction in the image data provided by different orbits is mostly related to the specific purpose for which the information is intended. As Richards, et al. emphasize (2006), *whereas data acquired for earth resources purposes generally has pixel sizes of less than 100 m, that used for meteorological purposes (both at geostationary and lower altitudes) has a much coarser pixel, often of the order of 1 km*.

Many programmes for Earth Observation are currently available (These rely on different technology, and platforms provided by various governmental monitoring programs), and a large amount of data has been acquired up until now, since the second half of the XX century. It would actually be quite difficult to make a full inventory of the satellites orbiting around the Earth and also provide the different technical characteristics about the on-board cameras. Therefore due to this, only a few satellites (as samples), and their relevant sensors (that are currently providing data), will be briefly treated in this essay; mostly because they are related to those technologies which have been analysed during the development of this research work in some way.

The following land observation satellites are used for passive remote sensing (for both optical and thermal imaging, and either for multispectral or hyper-spectral systems) and are categorized into three main groups, depending on their spatial resolution. It is actually possible to distinguish low resolution systems with a pixel size generally greater than 30 m (MODIS, for instance); medium resolution systems with a pixel size between 30 m to 5 m (ASTER, Landsat, SPOT 5 or earlier); and high resolution systems using a pixel size smaller than 5 m (GeoEye, IKONOS, QuickBird, SPOT 6, Pleiades).

MODIS (Moderate Resolution Imaging Spectroradiometer) is a sensor aboard two Earth Observing Systems (EOS) satellites termed Terra and Aqua, launched in 1999, which started acquiring data in February of 2000. Terra

[201] *This type of satellite was first launched in 1966 and there are currently five geostationary satellites with each covering a different portion of the earth: METEOSAT (ESA); GOES-East (USA); GOES-West (USA); GMS (Japan); and INSAT (India). They can image the earth's surface between latitudes 80N and 80S and they are able to image and transmit data of their whole viewable area every 30 minutes* (Meaden, et al., 1991)

orbits around the Earth passing from north to south across the equator during the morning (AM), while Aqua moves south to north, over the equator, in the afternoon (PM). Terra and Aqua MODIS monitor the entire Earth's surface every 1 to 2 days, acquiring data in 36 spectral bands. The satellites orbit at 705 km, following a sun-synchronous, near-polar, circular path. The spatial resolution varies depending on wavelength, i.e. 250 m for bands 1 and 2; 500 m for bands 3 to 7; and 1˙000 m for bands 8 up to 36. The radiometric resolution relies on imaging of 12 bits (NASA).

ASTER (Advanced Space borne Thermal Emission and Reflection Radiometer) is a medium-resolution sensor (built by a consortium of Japanese government, industry, and research groups), on-board of Terra satellite, mainly used for monitoring cloud cover, glaciers, land temperature, land use, natural disasters, sea ice, snow cover and vegetation patterns, at a spatial resolution of 90 to 15 meters.

The instrument is able to collect data in 14 different wavelength bands, ranging from visible and near infrared, to thermal infrared, besides producing stereoscopic (three-dimensional) images, and detailed terrain height models (Digital Elevation Models). In particular, visible and NIR, bands 1 to 3, rely on a spatial resolution of 15 m and a radiometric resolution of 8 bits; short wave infrared (SWIR), bands 4 to 9 are detected at a spatial resolution of 30 m and the same radiometric resolution as visible and NIR; thermal infrared bands 10 to 14, rely on 90 m spatial resolution and 12 bits of radiometric resolution. The grounding track repeat cycle is 16 days (Satellite Imaging Corporation - SIC).

SPOT (*Satellite Pour l'Observation de la Terre)* is a French satellite which provides various resolutions for high quality satellite images, and it was first launched in 1986 (SPOT 1). Thus the wide range of observations allow many applications that rely on time series analysis, in terms of temporal resolution. All SPOT (1 to 5) satellites orbit according to a sun-synchronous trajectory in an orbital cycle of 26 days. SPOT 1, 2, and 3 (respectively 1986, 1990, and 1993) carry HRV (Visible High-Resolution) optical instruments able to record a multispectral image in three bands (XS-mode), green (0.50-0.59 µm), red (0.61-0.68 µm), and NIR (0.78-0.89 µm), at a spatial resolution of 20 m and a panchromatic image (0.51-0.73 µm) at 10 m (P-mode). The SPOT 4 satellite (1998), which orbits at 822 km of altitude, is fitted with HRVIR (Visible & Infrared High-Resolution) sensors, capable of detecting a multispectral image of four bands, allowing an extra middle-IR band (1.58 -1.75 µm) at 20 m of spatial resolution (the other three bands of the multispectral image, and the panchromatic image, have the same characteristics as the previous satellites).

On SPOT 5 (2002), the HRG (High Resolution Geometric) instrument is capable of collecting a multispectral image of four bands at the same wavelengths as the HRVIR, but at a higher resolution up to 10 m and a panchromatic image at 5 m up to 2.5 m. Its HRS (High-Resolution Stereoscopic) sensor can acquire stereo pair imagery at 10 m of spatial resolution, in the panchromatic spectral band, providing Digital Elevation Model (DEM). The SPOT systems generally has a swath width of 60 x 60 km (up to 80), and 8 bits radiometric resolution. Additionally, it allows coverage of specific areas of interest every day because the sensors can be programmed.

There are numerous Earth Observation systems that have been launched during the past years, and have a spatial resolution better than 5 m. IKONOS, QuickBird and GeoEye are some of the most high-resolution satellites currently orbiting. *IKONOS is a commercial satellite that collects high-resolution imagery at 1- and 4-meter resolution. It offers multi-spectral (MS) and panchromatic (PAN) imagery. IKONOS was launched in 1999. The QuickBird satellite was launched on October 18, 2001. QuickBird offers panchromatic (PAN) imagery at 60- and 70-centimeter resolutions and multi-spectral (MS) imagery at 2.4 - and 2.8-meter resolutions. GeoEye is equipped with the most sophisticated technology ever used in a commercial satellite system. It offers spatial resolution by simultaneously acquiring 0.41-meter panchromatic and 1.65-meter multi-spectral imagery* (Malgorzata, 2010).

Besides the cited high-resolution satellites, the same SPOT system, with mission 6 (SPOT 6, 2012) and 7 (launched in 2014), provide optical imaging satellites capable of reaching spatial resolution of 1.5 meter for panchromatic and 6 meter for multispectral imagery (Blue, Green, Red, Near-IR). While in conjunction with the Pleiades satellites, Pleiades 1A (2011) and 1B (2012), the SPOT system is capable of providing orthorectified panchromatic, and colour data at 0,5-meter resolution in four spectral bands (blue, green, red, and IR).

The methodology for automatic land cover classification (which relies on the use of optical remote sensing), provided in the framework of the present research work is set up on Landsat multispectral imagery. The upcoming section 4.2.3 aims to specify in detail the main features of this remote sensing system.

4.2.3. Landsat Mission and the Thematic Mapper (TM) Multispectral Imagery

Within EO programs using space platforms, Landsat (managed by the USA) is probably the longest running system and provides multi-spectral information (optical and thermal) about the earth's surface. The first mission was launched[202] in 1972 and was named the Earth Resources Technology Satellite (ERTS 1), but later renamed Landsat 1. The Landsat system, which represents one of the major advances within passive RS procedures, is designed to deliver uniform long-term global coverage with the ability to generate digital data for several mapping purposes at operation scales of 1:250˙000 to 1:1˙000˙000.

The program has been operating continuously since the 1970's, with 8 consecutive missions. Actually, only seven satellites have been successful launched, since Landsat 6 which was launched on October 5th, 1993, failed to reach orbit. Of particular interest, Landsat 2 was launched in 1975 and expired in 1981; Landsat 3, 1978 to 1983; Landsat 4, 1982 to 1993; while Landsat 5, launched in 1984 remained functioning until 2012, when the USGS (United States Geological Survey) announced its decommission. Landsat 7 was launched in 1999 with notable improvements, and is still functioning, even if the scan line corrector was damaged in 2003, thus providing imagery with missing information since then. Landsat 8 was launched on February 11, 2013.

All Landsat satellites follow a (repetitive) circular sun-synchronous near-polar orbit, scanning a ground 185 km wide swath width. Other technical features have characterized the sensors aboard the various satellites, since the first mission. In fact, Landsat satellites 1 to 5 were equipped with a moderate-resolution scanner, termed Multispectral Scanner System (MSS), capable of acquiring images at a temporal resolution of 18 days, in four spectral bands (named band 4, 5, 6, and 7) between 0.50 and 1.11 µm (two within the green and red visible side of the spectrum, and two within the near infrared portion). The spatial resolution was of 68 m x 83 m, then resampled to a squared pixel at 60 meters. Landsat 3 carried an MSS sensor with an additional band, designated band 8, that responded to thermal (heat) infrared radiation (NASA). Landsat 4 and 5 were equipped with two cameras: the MSS (like the previous satellites) and a new sensor termed Thematic Mapper (TM) (which is the one this research is based on). Both satellites were inclined at 98° and repeated a complete cycle in 16 days[203], at an altitude of 705 km from the earth's surface (instead of the 900 Km of Landsat 1 to 3); while the imaging detection was maintained at a width of 185 km for the ground swath. Landsat TM provides multi-spectral imagery at resolution of 30 meters, based on six bands ranging from 0.45 to 2.35 µm, i.e. from the visible to the mid-infrared portion of the electromagnetic spectrum. In particular, the multi-spectral image is composed of one blue, one green, and one red band, within the visible region, and three infra-red bands which are; one near infrared (NIR), and two shortwave infrared (SWIR) bands (Figure 4.7).

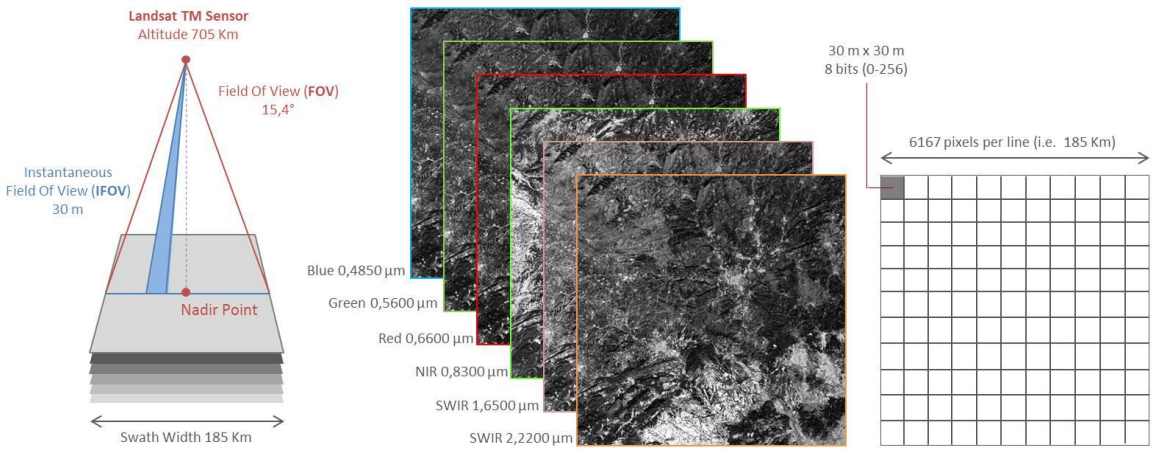

Fig. 4.7: Structure of Landsat TM Optical Multispectral Imagery (Source: By Authors)

[202] Landsat 1 stopped operating on January 6, 1978
[203] Both Landsat 4 and 5 make 14 or 15 revolutions per day, and it takes 16 days before a revisit track is made (Meaden, et al., 1991)

Besides the (six bands) multispectral images[204] with enhanced spatial resolution, the TM sensor is also able to collect thermal-infrared (termed band 6) at spatial resolution of 120 meters, and between 10.40 and 12.50 µm. All seven bands rely on an 8-bit quantization derived from the analogic-to-digital conversion process which provides 256 grey levels. The following figure 4.8 shows the spectral sensitivity, and the colour tonality appearing, for the bands detected through the use of the Landsat TM sensor.

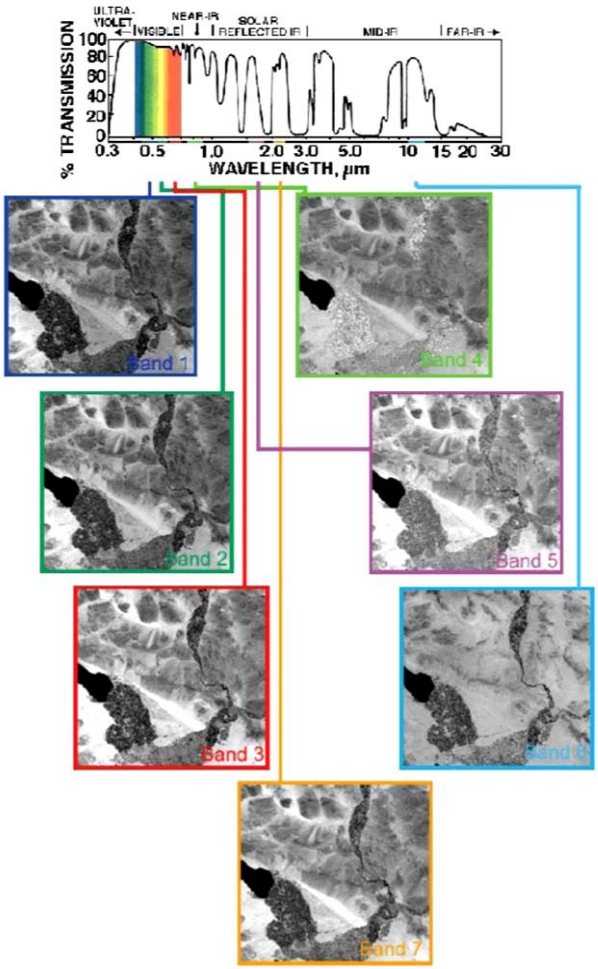

Fig. 4.8: Landsat Spectral sensitivity[205] (Source: NASA)

Landsat 7 (successfully launched in 1999, and still operating) carries an improved passive sensor for remote sensing, termed Enhanced Thematic Mapper Plus (ETM+). This new sensor which holds the legacy of Landsat moderate-resolution satellite imagery since the 70's, again provides multispectral imagery at 30 meters in six spectral bands with approximately the same wavelengths as for the TM sensor. Moreover, temporal resolution (16 days), as well as radiometric resolution (8 bits), are also maintained the same as for the TM; while, basically, two main enhancements occur for the ETM+ sensor: a pair of thermal images, band 6.1 and 6.2, are now available (instead of only one), at an effective greater spatial resolution of 60 meters; and a panchromatic image at 15 m of resolution, often employed for better interpretation of the multispectral information using several image enhancement procedures. Thus, 8 spectral bands are now available. The altitude of the satellite is maintained at 705 km offering a slightly smaller swath width of 183 km (NASA).

[204] The six bands are designated as band 1 (blue band), band 2 (green), band 3 (red), band 4 (NIR), band 5 (SWIR), and band 7 (SWIR)

[205] NASA-National Aeronautics and Space Administration, and Goddard Space Flight Center: The Landsat 7 Compositor. Consulting at: http://landsat.gsfc.nasa.gov/education/compositor/em.html

In addition to the three primary sensors (which are the MSS, TM and ETM+ and employed within the Landsat missions until Landsat 7), two new sensors are now available aboard the Landsat 8 satellite launched in 2013. These are: the Operational Land Imager (OLI), and the Thermal Infrared Sensor (TIRS). Landsat OLI image data consists of nine spectral bands with a spatial resolution of 30 meters for Bands 1 through 7 and Band 9, and a wavelength range between 0.43 and 2.30 µm[206]. The resolution of Band 8 (panchromatic) is 15 meters with a wavelength between 0.50 and 0.680 µm. Landsat TIRS image data consists of two thermal bands with a spatial resolution of 100 meters (re-sampled to 30) for Bands 10 and 11 (between 10.30-12.50 µm). *The TIRS data are packaged with the OLI for data distribution the majority of the time. The satellite collects images of the Earth with a 16-day repeat cycle, referenced to the Worldwide Reference System-2, and has an 8-day offset to Landsat 7. The approximate scene size will be 170 km north-south by 183 km east-west* (USGS). The following table (4.2) shows the main characteristics for all of the Landsat missions since 1972 (Landsat 1) until the most recent Landsat 8, detailing the different features available for the sensors.

LANDSAT MISSION SATELLITE	Sensor	Band Number	Spectral Range µm	Scene Size km	Spatial Resolution meter/pixel	Temporal Resolution
L 1-5	MSS multi-spectral	4,5,6,7	0.50 - 1.1 1	≈ 185 X 185	60	18 days
L 3	MSS thermal	8	10.41 - 12.60		60	
L 4-5	TM multi-spectral	1,2,3,4,5,7	0.45 - 2.35		30	16 days
L 4-5	TM thermal	6	10.40 - 12.50		120	
L 7	ETM+ multi-spectral	1,2,3,4,5,7	0.450 - 2.35		30	16 days
L 7	ETM+ thermal	6.1, 6.2	10.40 - 12.50		60	
L 8	OLI spectral bands	1,2,3,4,5, 6, 7, 9	0.43 - 2.30		30	16 days
L 8	TIRS Thermal	10, 11	10.30 - 12.50		100 (resampled 30)	
Panchromatic L7	ETM+	8	0.52 - 0.90		15	16 days
Panchromatic L8	OLI	8	0.50 - 0.68		15	

Tab. 4.2: Summary of main technical features for all sensors aboard Landsat satellites, 1 to 8 (Source: Authors)

4.2.4. Spectral Signature: The Curve of Reflectance for Main Land Cover Types

A basic assumption made in remote sensing is that a specific target has an individual and characteristic manner of interacting with incident radiation (Anji Reddy, 2008). In fact, all matter composing the earth's surface (and the objects found on it), provide different quantities of reflected or emitted energy which can be differently measured depending on the technical characteristics of the instrument employed for remote sensing. The remote sensor aims to acquire an energetic response which, in turn, depends on *what the target consists of, and the thickness of it…So all targets (or objects) in the environment emit and reflect different intensities and types of EMR in different portions of the spectrum, i.e. they have a so-called spectral signature which is predictable and repeatable* (Meaden, et al., 1991).

In optical RS, the spectral signature for each land cover element is drawn by collecting the value of reflected energy (reflectance) which varies between 0 and 1 being detected in each of the spectral channels provided by the sensor, as seen before. The more available spectral bands, the more detailed the signature. If we draw a Cartesian graph in which the abscissa axis represents the wavelength, and the ordinate axis provides values of reflectance (0-1) and we place the relative value of detected reflectance corresponding to each wavelength value (permitted by the employed sensor), the union of all the points derived from those observations will provide the profile of a continuous line which commonly takes the name of reflectance (or spectral) curve. In the case of measuring the reflectance for a single pixel (as the smallest portion of surface detected), the value placed in the graph will be exactly the one captured by the camera in that pixel (and for that wavelength). If we attempt to measure the reflectance value for a continuous object, defined through more than one pixel at a time, then the value placed on the graph will be the average reflectance for all the pixels which define that object under investigation.

[206] In particular, band 1 ranges between 0.433–0.453 µm; band 2: 0.450–0.515 µm; band 3: 0.525–0.600 µm; band 4: 0.630–0.680 µm; band 5: 0.845–0.885 µm; band 6: 1.560–1.660 µm; band 7: 2.100–2.300 µm; and band 9: 1.360–1.390 µm

Every object on the earth's surface has a unique spectral curve, depending on the type of technology employed, and notwithstanding, the physical and biological properties of the matter. This affects the shapes of the curve. As pointed out by Anji Reddy (2008), *the spectral curves describe the energetic response, in a particular wavelength region of electromagnetic spectrum, which, in turn depends upon certain factors, namely, orientation of the sun (solar azimuth), the height of the Sun in the sky (solar elevation angle), the direction in which the sensor is pointing relative to nadir (the look angle), and nature of the target*.

On the other hand, Meaden, et al. (1991), claim that the curve profiles also depend on the interactions between the incident radiation and the micro and macro-structure of the matter itself, so that *spectral signatures may vary temporally; e.g. as plants grow, or spatially with different types of vegetation, different soil conditions, water availability, effect of topography, etc*. Actually, as claimed by Richards, et al. (2006), *in the visible/infrared range the energy measured by a sensor depends upon properties such as the pigmentation, moisture content and cellular structure of vegetation, the mineral and moisture contents of soils and the level of sedimentation of water*. Therefore, according to technological restrictions and the physical characteristics of materials, a spectral signature can provide a set of measurements within a given range of wavelengths, by which a specific land cover, at a specific time can be quantified using satellite imagery. Different land cover types; such as water, soil, vegetation, buildings and roads, for instance, reflect visible and infrared light in certain specific "colours" (wavelengths) and brightness (reflectance), so the interpretation of remotely sensed data requires a good knowledge of spectral signatures of targets.

Figure 4.9 specifies the spectral reflectance curves for typically representative land cover features including the typical reflectance of vegetation (lawn grass), bare soil, water and two of which are man-made cover types, such as bricks and types of metal. The wavelength ranges, for the six bands provided by the multispectral Landsat TM sensor, are also indicated on the graph, in order to understand the TM sensitivity, in relation to these main land cover types.

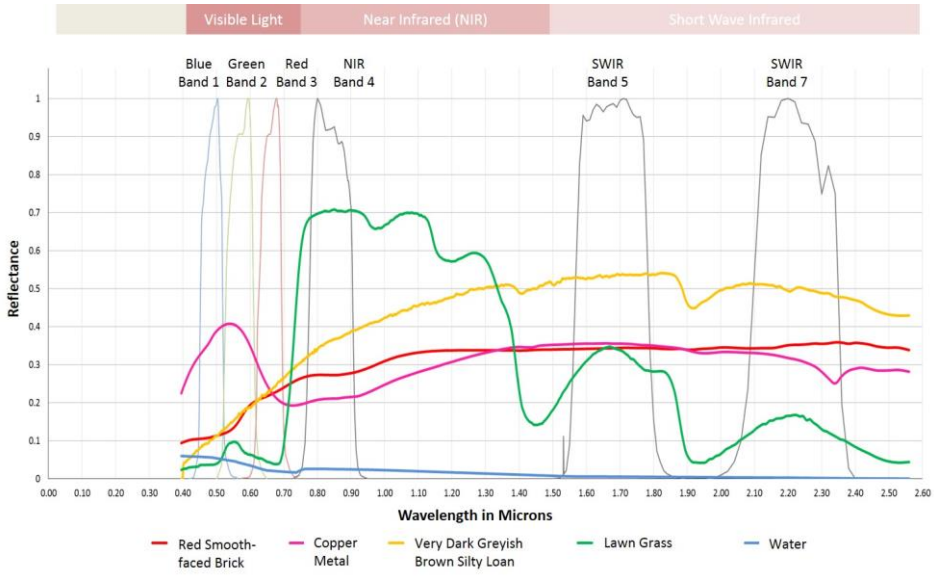

Fig. 4.9: Spectral signature for some main land cover surfaces (either natural or artificial), and wavelength intervals for Landsat TM sensitivity (Source: by Authors)

As shown in the graph, for each wavelength, the different materials provide a characteristic response to the incident light (in the visible and infrared range), which is measured in terms of reflectance and through typical spectral signatures. The vegetation, water and soil curves are maybe the most typically shown spectral signatures. A representative soil curve, for instance, usually provides a regular increasing reflectance which tends to grow by passing from the visible to infrared regions. This is because soils generally reflect more energy in the short-wave infrared region and the soil reflectance is decidedly affected by factors such as the moisture content, texture or

organic substances. Some of the depressions within the curve profile along the SWIR portion are probably due to increasing moisture content. SWIR bands suggest strong water absorption, which instead would not be appreciable for dry or sandy soils. A kind of brick, such as the one depicted in the graph, reveals a spectral profile which appears to be quite similar to the one provided by soil, although essentially lower toward the NIR and SWIR side and is caused by a higher absorption of energy. Additionally, there are no important depressions in the shape of the curve at SWIR level, probably due to a lower moisture content. The copper metal seems to be brighter along the blue/green visible side, and with high absorption between the red and NIR sides.

Water absorbs a lot of energy across the whole EM spectrum, which the optical RS covers. The typical spectral signature for water (generally clean water) shows higher reflectance values within the blue and green visible bands (around 0.10 or less, i.e. just 10% of energy is reflected); while from around a wavelength of 0.5 µm, a gradual but important decrease in reflectance is seen and reaches the lowest values towards the SWIR bands, then tending almost to zero.

The spectral curve for the healthy green vegetation (lawn grass in this case), depicts a quite complex profile with respect to the others previously analysed. A strong absorption, due to the water content, is provided along the SWIR portion of the EM spectrum and is mostly caused by the plant pigmentation (chlorophyll). This kind of vegetation provides absorption within the blue and red portions of the spectrum, and an important reflection of energy in the green band of the visible light (this is why we see plants as green). The highest values of reflectance are provided along the NIR slice, and in particular between 0.7 µm and 1.3 µm, also due to the molecular structure of plants[207].

Hence, when attempting to classify the land cover composition within a landscape, we could state that a key purpose of obtaining remotely sensed data is the capability to identify different spectral behaviours depending on the level of generalization pursued. Currently, a better *cover type identification should be possible if the sensor gathers data at several wavelengths* (Richards, et al., 2006). Moreover, as pointed out before, with more spectral observations, the ability to discriminate among different land cover categories increases. In fact, if we take a look at the graph below (figure 4.10), in which the spectral curve of vegetation detected by using a hyperspectral sensor, as compared with the one defined according to a six band multispectral image obtained with the Landsat TM sensor, the variation of precision provided by the different information is quite obvious.

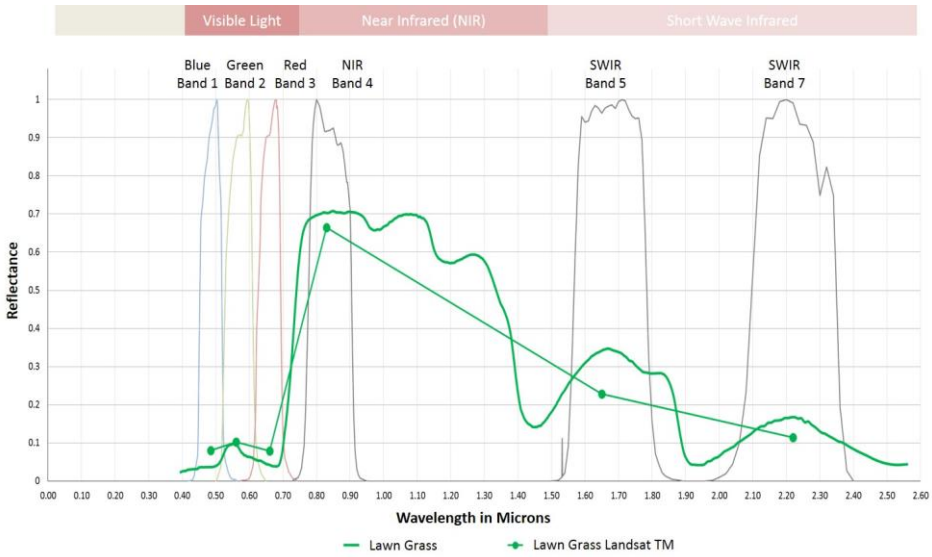

Fig. 4.10: Vegetation spectrum recorded through Hyperspectral camera, and vegetation spectrum defined by Landsat TM multispectral sensor in six spectral channels (Source: Authors)

[207] *The plant leaves exhibit a strong absorption property in the red band and a strong reflectance in the NIR. The reflection reduces slightly from the green band to red band and then a reflection valley is generated. The reflection rose sharply in the NIR and a reflection peak is formed; a valley again in the SWIR for the reflection weakens rapidly* (Lin, et al., 2010)

4.2.5. Digital Elevation Model and Topographic Modelling

As specified during the previous chapters, the use of remote sensing technologies allows us to acquire data about the earth's surface and environment, by gathering certain physical information and registering it in a minimum unit of detection; i.e. the use of a digital format. Once again, by using airborne or space platforms, it is possible to detect information about the earth's surface topography through measuring the elevation of specific points on the surface from a base reference level. The resulting information is a digital image known as Digital Elevation Model (DEM) which is a data file containing the altitude of every detected point in a terrain over specific areas, *usually at a fixed grid interval over the "Bare Earth"*. A Digital Elevation Model provides the z-values of height above the bare earth, at regularly spaced intervals along a 2D spatial plane (x and y). Therefore, a DEM is essentially a raster image where every pixel value provides the ground elevation height above a reference level, which is commonly assumed to be sea level (Satellite Imaging Corporation - SIC).

Spatial interval among pixels is referenced to some geographical coordinate system, which is usually either latitude-longitude or the UTM (Universal Transverse Mercator) coordinate systems. Obviously, the smaller the grid spacing, the more detailed the topographic information. *The details of the peaks and valleys in the terrain will be better modelled with small grid spacing than when the grid intervals are very large. Elevations other than at the specific grid point locations are not contained in the file. As a result, peak points and valley points not coincident with the grid will not be recorded in the file* (Satellite Imaging Corporation - SIC). Apart from the aspects regarding grid resolution or pixel size, other factors affect the quality of DEM-derived products; such as the terrain roughness, the sampling density (i.e. the elevation data collection method), the vertical resolution of z-values, and the algorithms employed either for interpolation of measurements and terrain analysis (SIC).

Digital Elevation Models can be generated by using a variety of technologies. A DEM can be derived from aerial or satellite imagery (in passive mode), for instance, when the employed cameras allow capturing stereo-pair images and following the principles of photogrammetry. This is the case with satellites such as IKONOS, SPOT (and Pleiades) or ASTER. On the other hand, active RS systems, such as RADAR, collect elevation data by using its own incident radiation (microwaves) which bring back the information to the sensor, measured depending on the time delay between the emission and the detection of the backscattered radiation (chapter 4.1.2). This concerns the DEM dataset engaged in the framework of this research work, which derives from the Shuttle Radar Topography Mission (SRTM), and is available from the collection held in the USGS EROS archive[208].

The SRTM instrument[209] was aboard the Space Shuttle Endeavour (launched during 2000) for an international project promoted by the National Aeronautics and Space Administration (NASA) and the National Geospatial-Intelligence Agency (NGA), and was aimed at acquiring radar data which could be used to create detailed topographic maps[210]. The Endeavour was operating at an altitude of 233 Km, with an inclination angle of 57°, and an orbiting period of 89.2 minutes. The shuttle actually revolved around the Earth about 16 times each day, thus completing 176 orbits during the 11-day mission. *SRTM successfully collected radar data covering 80% of the Earth's land surface between 60° north and 56° south latitude with data points posted every 1 arc-second (approximately 30 meters). The SRTM data, processed from raw radar signals spaced at intervals of 1 arc-second, were then edited or finished to delineate and flatten water bodies, better define coastlines, remove spikes and wells, and fill small voids* (USGS).

SRTM data is available through the USGS EROS archive, which provides two resolutions of processed datasets: high resolution elevation data at 1 arc-second (approximately 30-meter) for United States only; and a medium resolution elevation data at 3 arc-second (approximately 90-meter), for global coverage. Additionally, a 30-m resolution DEM in GeoTIFF format at a radiometric resolution of 16 bits per pixel (like the sample in figure 4.11)

[208] http://eros.usgs.gov/elevation-products

[209] *SRTM made use of a technique called radar interferometry, in which two radar images are taken from slightly different locations. Differences between these images allow for the calculation of surface elevation, or change* (USGS)

[210] *The radars used during the SRTM mission were actually developed and flown on two Endeavour missions in 1994. The Space borne Imaging Radar-C (SIR-C) and the X-Band Synthetic Aperture Radar (X-SAR) hardware were used on board the space shuttle in April and October 1994 to gather data about Earth's environment. A key SRTM technology was radar interferometry, which compared two radar images or signals taken at slightly different angles. This mission used single-pass interferometry, which acquired two signals at the same time by using two different radar antennas. An antenna located on board the space shuttle collected one dataset and the other dataset was collected by an antenna located at the end of a 60-meter mast that extended from the shuttle. Differences between the two signals allowed for the calculation of surface elevation* (USGS)

is also available through the USGS Global Visualization Viewer[211] (Glovis) or the Earth Explorer[212], at a global level[213] and is derived from resampling the high resolution dataset using a cubic convolution interpolation (USGS).

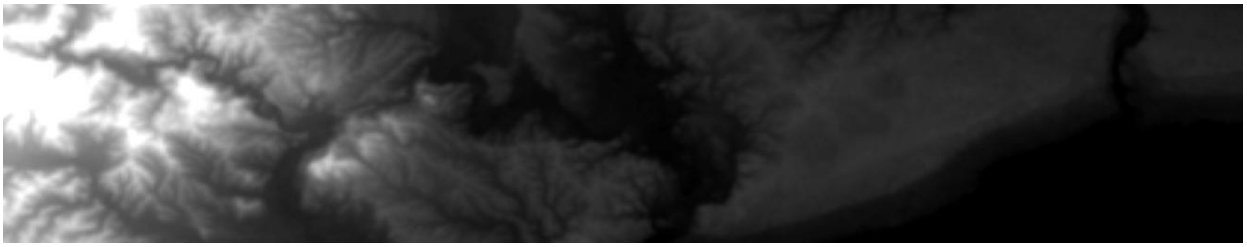

Fig. 4.11: Digital Elevation Model example, at 30-meters spatial resolution, and 16 bits. The brighter the pixel, the higher the elevation value (Source: Authors, from USGS-GLS 2010 collection)

When speaking about elevation models, it is critical to distinguish between the two main datasets: DTM and DSM. The DTM, or Digital Terrain Model, defines only the spatial geometric distribution of the terrain topography; i.e. the bare ground surface without including any objects on it (trees or buildings, for instance). On the other hand, the DSM, or Digital Surface Model, represents the reflective surfaces of all objects on the Earth's surface. It actually provides a model which includes height values for all types of vegetation and buildings within the area under investigation.

Even if DEM, DTM and DSM all refer to various types of continuous 3D topological data, in general, an Elevation Model provides basic information about the morphological structure of territories (topographic maps). Exhaustive environmental analysis can be conducted by modelling such digital data and allowing essential tasks; such as 3D visualization and ortho-rectification of aerial photography or satellite imagery. An extra set of analytical procedures is possible through DEM manipulating for improving the control over terrain and spatial management. In fact, some key parameters can be extracted from a DEM by creating physical models; such as slope maps, aspect, relief and contours (level curves). Water flow or mass movement can be modelled, for providing risk assessment protocols, while the quantification of surface areas can be assessed through generating the Triangulated Irregular Network (TIN) models, which turns the raster information of DEM into vector maps.

Moreover, from the standpoint of the land cover classification procedure, the understanding of terrain topology provides a useful tool for improving the discernment of certain categories. It is also important to remember that human activities and the natural landscape depend on the geomorphology of the land surface.

4.3. IMAGE PROCESSING AND INTERPRETATION

Digital image processing and interpretation procedures, through machine assessment, essentially aim to store, characterize and improve certain primary digital data features to allow the best information extraction. Currently, according to Gonzalez, et al. (2002), digital image processing through the use of imaging technologies involves a wide range of purposes, stating that, *unlike humans, who are limited to the visual band of the electromagnetic (EM) spectrum, they cover almost the entire EM spectrum, ranging from gamma to radio waves. It allows us to operate on images that can be generated using sources that humans are not accustomed to associating with images.*

Varying opinions exist among scientists about the operational field of interest for image processing, with respect to other related disciplines such as image analysis and computer vision. Anyway, as argued by Gonzalez, et al. (2002), it would be possible to establish three main types of computerized processes, common to all three

[211] http://glovis.usgs.gov/

[212] http://earthexplorer.usgs.gov/

[213] This spatial data collection was made possible by the development of more accurate elevation models with global or regional coverage, including the National Elevation Dataset (NED) of the USA, the Canadian Digital Elevation Dataset (CDED) of Canada and the Shuttle Radar Topography Mission (SRTM) covering most of the globe (Global Land Cover Facility - GLCF)

disciplines, which are low-, mid-, and high-level processes. *Low-level processes involve primitive operations such as image preprocessing to reduce noise, contrast enhancement, and image sharpening. A low-level process is characterized by the fact that both its inputs and outputs are images. Mid-level processing on images involves tasks such as segmentation (partitioning an image into regions or objects), description of those objects to reduce them to a form suitable for computer processing, and classification (recognition) of individual objects. A mid-level process is characterized by the fact that its inputs generally are images, but its outputs are attributes extracted from those images (e.g., edges, contours, and the identity of individual objects). Finally, higher-level processing involves "making sense" of an ensemble of recognized objects, as in image analysis, and, at the far end of the continuum, performing the cognitive functions normally associated with vision* (Gonzalez, et al., 2002).

This section is mostly centred on analysing pre-processing procedures for RS-derived data, and enhancement techniques for improving digital imagery information, particularly based on the case study of Landsat products. Classification methodologies, within the image processing (or analysis) field, will be discussed in subchapter 4.4.

4.3.1. Image Pre-Processing: Radiometric and Geometric Correction

The obtaining of digital data, through RS devices, represents the first phase within a complex process aimed at providing a continuous flow of information. In fact, the primary data which is stored in the form of pixel values is digitally coded in a finite number of bits and spatially allocated according to a coordinate system in a referencing grid. Several subsequent steps are required to obtain the desired useful and reliable information. In order to avoid important inaccuracies when the digital imagery is sensed by satellites (or aircrafts), at least two central issues firstly need rectification, and these are geometrical and radiometric inaccuracies (i.e. the brightness values of pixels). This impacts many applications within image understanding procedures, either for visual interpretation or through automated processes.

In general, and according to Meaden, et al. (1991), geometry errors and radiometric errors are mainly due to *a number of factors inherent in the RS system which contribute to the images being distorted in some way*:

- *Changes in the attitude, velocity and altitude of the sensing platform*
- *The forward motion of the platform causes scan skew*
- *The scanners (in Landsat) do not have a constant scan velocity*
- *The area covered by one pixel will have its shape distorted when viewing at an oblique angle*
- *The geometry of the images is affected by the earth's rotation, its curvature and atmospheric refraction*
- *Radiometry is affected by the sensor, e.g. sensor "noise" and poor calibration between detectors, by the atmosphere, e.g. presence of aerosols and scattering effect, and by the scene itself, e.g. effect of relief on reflection and type of reflection of the object.*

The matters that particularly effect the measurement of brightness values are mostly linked to the system and instrumentation employed to record the data, notwithstanding the environmental effects due to certain atmospheric properties which can affect solar radiation. As argued by Richards, et al. (2006), there are *two broad types of radiometric distortion*: when the relative distribution of brightness values, for a certain bandwidth in the image is different from the actual distribution of reflectance from the surface in the scene for that channel, and when the relative brightness for one given pixel results in bias between different bands of the multispectral image, thus giving altered reflectance values when compared to those on the ground. As pointed out, these types of distortion are mostly dependent on the effect exerted by the atmosphere during the transmission of energy, which travels from the earth's surface to the sensors (atmospheric scattering), in combination with the technological limitations of the same instrumentation (Richards, et al., 2006). Therefore, when trying to quantify certain features within a landscape[214], or attempting to compare different scenes within a temporal cut, the atmospheric effect on the radiometric values has to be corrected.

[214] *Correction for atmospheric attenuation is especially important for dark targets, such as water bodies. With relatively clear, deep and, therefore, dark water targets, together with somewhat hazy atmospheric conditions, the total radiance reaching the sensor may be composed of only 20% water-leaving radiance and 80% atmospheric path radiance. Although this is an extreme case, useful signals over water targets tend to be overwhelmed by atmosphere-generated noise* (Butler, et al., 1988)

Several techniques are generally employed for atmospheric correction and these range from simple methods, such as dark pixel subtraction and histogram handling, to more complex methods that involve the mathematical modelling of atmospheric properties. An example of atmospheric correction (for Landsat imagery) is provided in the following section (4.3.2); while further information about radiometric correction techniques can be found in Butler, et al. (1988); and Richards, et al. (2006).

However, according to Richards, et al. (2006), many more skew errors for image geometry can potentially arise due to additional sources of geometric distortion, which also lead to further critical effects. The main factors related to geometric alteration can be explained as follow:

- *The rotation of the earth during image acquisition*
- *The finite scan rate of some sensors*
- *The wide field of view of some sensors*
- *The curvature of the earth*
- *Sensor non-idealities*
- *Variations in platform altitude, attitude and velocity, and*
- *Panoramic effects related to the imaging geometry*

The Geometric Correction procedure involves several steps to be applied when rectifying a digital image. Firstly, errors due to earth curvature, earth rotation and satellite attitude need to be effectively fixed, whenever the nature of distortion is well known. Further approaches aim to determine mathematical relationships between the spatial position of the pixels in the image, and the corresponding geographical coordinates on the ground. *These relationships can be used to correct the image geometry irrespective of the analyst's knowledge of the source and type of distortion* (Richards, et al., 2006).

To do that, a suitable, and well spatially distributed, number of Ground Control Points (GCP) are chosen for converting the captured data to "real world" information, i.e. adjusting the image depending on standard coordinate systems. This process is commonly known as georeferencing, which implies a transformation of the digital image to match the terrain coordinates, thus obtaining a "new" image in which all the pixels are now properly geographically positioned, according to the terrain coordinate system (through the use of a Digital Elevation Model). An additional resampling process (which commonly relies on methods such as nearest neighbourhood, bilinear interpolation, or cubic convolution), is applied in order to derive the actual digital values from the original pixels of the primary image, once the image has been geo-referenced.

In the case of Landsat products, which is the data source employed for this study, all scenes are normally processed to Standard Terrain Correction (Level 1T-precision and terrain correction). If this is not possible due to missing GCPs or DEM, the best level of correction is applied, which could come from the Level 1G Systematic Correction[215] or the Level 1Gt Systematic Terrain Correction[216]. The Standard Terrain Correction (Level 1T) *provides systematic radiometric and geometric accuracy by incorporating ground control points while employing a Digital Elevation Model (DEM) for topographic accuracy. Geodetic accuracy of the product depends on the accuracy of the ground control points and the resolution of the DEM used* (USGS). All Landsat standard data products[217] are processed at Level 1 Product Generation System (LPGS) with the following parameters applied:

- GeoTIFF output format
- Cubic Convolution (CC) resampling method
- 30-meter (TM, ETM+) and 60-meter (MSS) pixel size (reflective bands)
- Universal Transverse Mercator (UTM) map projection (Polar Stereographic projection for Antarctica)
- World Geodetic System (WGS) 84 datum
- MAP (North-up) image orientation

[215] *Systematic Correction (Level 1G) provides systematic radiometric and geometric accuracy, which is derived from data collected by the sensor and spacecraft. Geometric accuracy of the systematically corrected product should be within 250 meters (1 sigma) for low-relief areas at sea level* (USGS)

[216] *Systematic Terrain Correction (Level 1Gt) provides systematic, radiometric, and geometric accuracy, while employing a Digital Elevation Model (DEM) for topographic accuracy. Landsat 7 scenes over Antarctica are the only data processed to an L1Gt* (USGS)

[217] Landsat 8 (2013-present), Landsat 7 ETM+ (1999 -present), most Landsat 4-5 TM (1982 -present) and all Landsat MSS 1-5 (1972-1983 and 2012-2013)

4.3.2. Radiometric Calibration and Atmospheric Correction

Remote sensing detectors collect the response of incoming radiance (L_λ), propagated by the Earth's surface and the raw quantized voltage, or response (Q), is converted to at-sensor spectral radiance by using instrument rescaling factors: Gain (G) and Bias (B) on board the satellite. The resulting information is then stored in a raster format (as pointed out in the previous section 4.2.1) based on an 8-bit brightness value commonly called Digital Numbers (DN).

Nevertheless, the information directly captured by satellites are noisy, mostly due to internal restrictions of the instruments, and to external atmospheric factors. Therefore, in order to obtain useful remotely sensed information, the detectors must always give the same, or at least similar, DN for a given amount of energy received. Therefore, Gain and Bias should remain a constant for as long as the sensor is working just as they have been measured before the launch (prelaunch radiances). However, once the satellite is launched, the sensor gain and bias can experience certain changes, a kind of sensor degradation.

Since it would be impossible to validate lamp radiances once the satellite is in orbit, prelaunch measured radiances are used to avoid internal noise. Therefore, the algorithm used for the on-board calibration employs a regression of the values collected by detectors, according to the prelaunch radiance values. Obviously, the method assumes that irradiance values remain constant over time. The slope of the regression, which relates DN to physically meaningful units of radiance, provides the Gain; while the intercept provides the Bias (or Offset), as shown in figure 4.12 (Chander, et al., 2009).

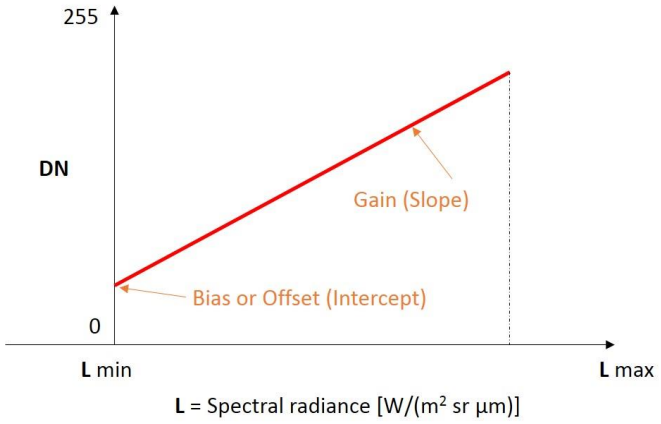

Fig. 4.12: Regression equation which relates DN with Spectral Radiance (Source: By Authors)

Due to the fact that the on-board process implies rescaling the raw digital numbers (Q), to calibrated digital numbers (Q_{cal}) in order to obtain actual physical units, such as at-sensor radiance, or Top-Of-Atmosphere (TOA) reflectance for each pixel, which in the case of Landsat products, these are the DNs that users receive with Level 1 of data processing. Therefore, instead of a monochromatic scale of 0 to 255 values of intensity, a radiometric calibration of satellite imagery has to be undertaken (Chander, et al., 2009). Actually, the calculation of at-sensor spectral radiance or reflectance is a key step within the satellite imagery processing, and is aimed at converting image data into physically meaningful measurements[218].

According to Chander, et al., 2007, the values of radiance, for each pixel in the image, can be derived from the Digital Number (DN) by using the following equation [4.2]. The resulting radiance (L_λ) is measured in units of watts per square meter per steradian per micrometer ($W/(m^2*sr*\mu m)$).

[218] According to Butler, et al., 1988, the calibration process is fundamental when quantitative, or multi-image analysis is to be performed; while photointerpretation procedures can rely on 8-bit imagery

$$L_\lambda = \left(\frac{LMAX_\lambda - LMIN_\lambda}{Q_{calmax} - Q_{calmin}} \right) * \left(Q_{cal} - Q_{calmin} \right) + LMIN_\lambda \quad [4.2]$$

With
- L_λ Spectral radiance at the sensor's aperture (for each wavelength λ) [W/(m² sr µm)]
- Q_{cal} Quantized calibrated pixel value [DN]
- Q_{calmin} Minimum quantized calibrated pixel value corresponding to $LMIN_\lambda$ [DN]
- Q_{calmax} Maximum quantized calibrated pixel value corresponding to $LMAX_\lambda$ [DN]
- $LMIN_\lambda$ Spectral at-sensor radiance that is scaled to Q_{calmin} [W/(m² sr µm)]
- $LMAX_\lambda$ Spectral at-sensor radiance that is scaled to Q_{calmax} [W/(m² sr µm)]

If we take into account that for 8-bit imagery Q_{calmax} equals 255 and Q_{calmin} is 0, then the spectral radiance can be calculated according to the equation [4.3], or [4.4].

$$L_\lambda = \left(\frac{LMAX_\lambda - LMIN_\lambda}{255} \right) * Q_{cal} + LMIN_\lambda \quad [4.3]$$

$$L_\lambda = G_{rescale} * Q_{cal} + B_{rescale} \quad [4.4]$$

With
- $G_{rescale} = \frac{LMAX_\lambda - LMIN_\lambda}{255}$ Band-specific rescaling Gain factor [(W/(m² sr µm))/DN]
- $B_{rescale} = LMIN_\lambda$ Band-specific rescaling Bias factor [W/(m² sr µm)]

The spectral radiance, as calculated above, can be converted to exoatmospheric TOA reflectance values. The exoatmospheric reflectance (ρ_ρ), which provides values on a scale of 0 to 1 for each DNs of the pixels, is the ratio between the incident light (see section 4.1) and the amount of reflected energy by surfaces, once the absorption and transmission effects have been discounted. It is computed according to the equation [4.5].

$$\rho_\rho = \frac{\pi * L_\lambda * d^2}{ESUN_\lambda * \cos\vartheta_s} \quad [4.5]$$

With
- ρ_ρ Planetary TOA reflectance [unitless]
- L_λ Spectral radiance
- d Earth-Sun distance in astronomical units
- $ESUN_\lambda$ Mean solar exoatmospheric irradiance [W/(m² µm)]
- ϑ_s Solar zenith angle in degrees[219]

According to Chander, et al., 2009, several advantages must be highlighted concerning the use of TOA reflectance, instead of at-sensor spectral radiance, mostly when comparing images from different sensors:

- *TOA reflectance removes the cosine effect of different solar zenith angles due to the time difference between data acquisitions;*
- *Compensates for different values of the exoatmospheric solar irradiance arising from spectral band differences;*
- *Corrects for the variation in the Earth–Sun distance between different data acquisition dates. These variations can be significant geographically and temporally.*

Another key issue to take into account when working with satellite imagery is the noise produced by the aforementioned external atmospheric factors. In fact, the electromagnetic radiation travels through the Earth's

[219] *The cosine of the solar zenith angle is equal to the sine of the solar elevation angle. The solar elevation angle at the Landsat scene center is typically stored in the Level 1 product header file (.MTL or .WO)* (Chander, et al., 2009); Earth-Sun distance and Mean Solar Exoatmospheric Irradiance for Landsat products can be found on: Chander, G.; Markham, B.L.; Helder, D.L. *Summary of current radiometric calibration coefficients for Landsat MSS, TM, ETM+, and EO-1 ALI sensors*. Remote Sensing of Environment, 113, pp. 893-903, 2009

atmosphere covering certain distances before being sensed by the satellites. Thus, the heterogeneous composition of the atmosphere, because of the presence of several gases, particles and other impurities, "disturbs" the flow of radiation captured by the sensors in some way, once reflected by the objects. The most commonly derived phenomena is the scattering of light within the visible range of the EM spectrum (*it depends on the ratio of the wavelength to the size of the particles*), and the absorption in the ultraviolet and infrared regions[220]. Due to the scattering effect, the signal captured by the satellites encompasses both the reflection from the atmosphere, as well as the one from the Earth's surface (Meaden, et al., 1991). The entire transmittance of energy, within the EM spectrum, partially includes the effect of scattering, which is important mainly within the shorter wavelengths (visible light). The effect of atmospheric absorption depicts a "real" spectral curve of transmittance (as shown in figure 4.13), in which the low parts of the curve show the effect of absorption due to specific molecules[221] (Japan Association of Remote Sensing - JARS, 1999).

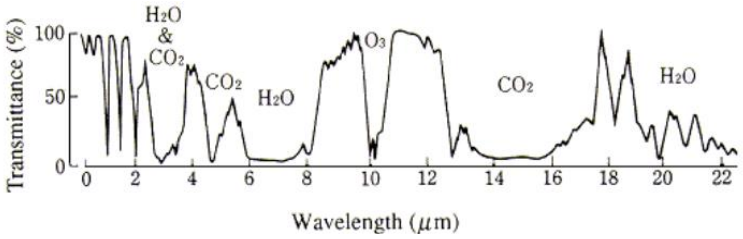

Fig. 4.13: *Characteristic of atmospheric spectral transmittance* (Source: Japan Association of Remote Sensing - JARS, 1999)

The variation of scattered energy depends on several factors; such as wavelength, the abundance and dimensions of particles or gases, and the distance covered by the radiation through the atmosphere before reaching the satellite. The scattering effect is, thus, a sort of redirection of radiation flows, with respect to the normal path, which occurs when the energy interacts with the atmospheric components[222].

Therefore, in order to retrieve actual ground reflectance values, the atmospheric effects need to be removed, or at least greatly reduced. Atmospheric correction is certainly an essential step within the pre-processing techniques for improving remotely sensed data from satellites, and a critical phase within quantitative analysis directed at measuring land cover features. Atmospheric noise, for instance, particularly affects certain kinds of land cover categories such as water bodies[223] or vegetation. Due to the fact that satellite sensors measure either the Earth's reflectance (or radiance) as well as the atmosphere's reflectance simultaneously, the process of calibration alone does not provide data solely about land surface, but a complex signal depending on atmospheric conditions. That is why it is essential to run suitable and effective atmospheric correction algorithms to identify the ground reflectance data.

Complex algorithms are required to rectify atmospheric effects and doubtless there has been extensive research on the necessity and techniques for satellite rectifying during the last few years. Some methods, such as the Radiative Transfer Code (RTC) computer models, focus on simulating the physical behaviour of solar radiation on the atmosphere, thus allowing the possibility of approximating the observed brightness to actual ground reflectance values. Other approaches concentrate on observing the *spectra of objects of known or assumed*

[220] *About 18% of the incident radiation in the atmosphere is absorbed or scattered and about 35% of the incoming solar energy is reflected by the earth and the atmosphere, including clouds* (Meaden, et al., 1991)

[221] The phenomenon of absorption causes the particles within the atmosphere to capture energy at various wavelengths. In particular, some important atmospheric elements such as ozone (O_3), carbon dioxide (CO_2), and water vapour (H_2O) absorb electromagnetic energy in very specific regions of the spectrum

[222] Various types of scattering effect could be mentioned, which are basically a function of the size of particles in the atmosphere. When particles are very small, in comparison to the wavelength of the radiation, for instance, the shorter wavelengths tend to be scattered much more than the long ones (Rayleigh scattering). This effect makes the sky appear blue because, within the visible range of the electromagnetic spectrum, the blue slice provides the shorter wavelengths. Within lower portions of the atmosphere, where elements of greater size such as dust, smoke, or water vapour can be more copious, the longer wavelength tend to be scattered (Mie scattering). When all wavelengths within the visible spectrum range are scattered in about equal quantities, it makes objects appear white, such as in the case of fog or clouds

[223] *In the infrared portion of the spectrum, both water bodies and shadows should have brightness at or very near zero, because clear water absorbs strongly in the near infrared spectrum and because very little infrared energy is scattered to the sensor from shadowed pixels* (Campbell, et al., 2011)

brightness recorded by multispectral imagery. This method relies on a basic knowledge of principles of atmospheric scattering, according to which, *we know that scattering is related to wavelength, size of atmospheric particles, and their abundance. This approach is often known as "image-based atmospheric correction" because it aspires to adjust for atmospheric effect solely, or mainly, from evidence available within the image itself. This strategy is a direct methods for adjusting digital values for atmospheric degradation known sometimes as the histogram minimum method (HMM) or the dark object subtraction (DOS) technique* (Campbell, et al., 2011).

In the framework of this work we employed the Dark Object Subtraction (DOS) approach in order to retrieve rectified visible-to-near infrared and shortwave infrared (VNIR-SWIR) information for Landsat TM imagery. Actually, the DOS, which removes, or at least reduce significantly the effects of atmospheric perturbations, is perhaps the simplest yet most widely used image-based absolute atmospheric correction approach (Song, et al., 2001). In particular, the DOS relies on the assumption of the existence of objects that provide values of reflectance equal or very close to zero (dark objects). According to this approach, the minimum values in the histogram derived from the entire scene is due to the atmospheric effect thus it is subtracted from all the pixels (Chavez, 1989).

This is a direct method based on primary knowledge about atmospheric scattering, i.e. it puts in relation the scattering with wavelength, size of atmospheric particles, and their abundance. Basically, the correction is mainly realized from data available within the image itself (Campbell, et al., 2011).

The effect of the DOS on Landsat TM, in the particular case of cropland, is appreciable in the next table 4.3, which shows how the values of reflectance vary after applying radiometric calibration and atmospheric correction, and image 4.14 which displays the same effect in terms of spectral curves.

Landsat TM		Wavelength (μm)	Radiometric Values 8 bits	Reflectance Values (Calibration)	DOS Reflectance Values (Dark Object Subtraction - Atmospheric Correction)
Band 1	Blue	0.4850	66	0.0899	0.0271
Band 2	Green	0.5600	30	0.0839	0.0294
Band 3	Red	0.6600	23	0.0608	0.0160
Band 4	NIR	0.8300	130	0.4593	0.4881
Band 5	$SWIR_1$	1.6500	72	0.1578	0.1717
Band 7	$SWIR_2$	2.2200	21	0.0593	0.0729

Tab. 4.3: DOS Atmospheric Correction effect on the digital information in the case of a generic cropland class, and for Landsat TM imagery (Source: by Authors)

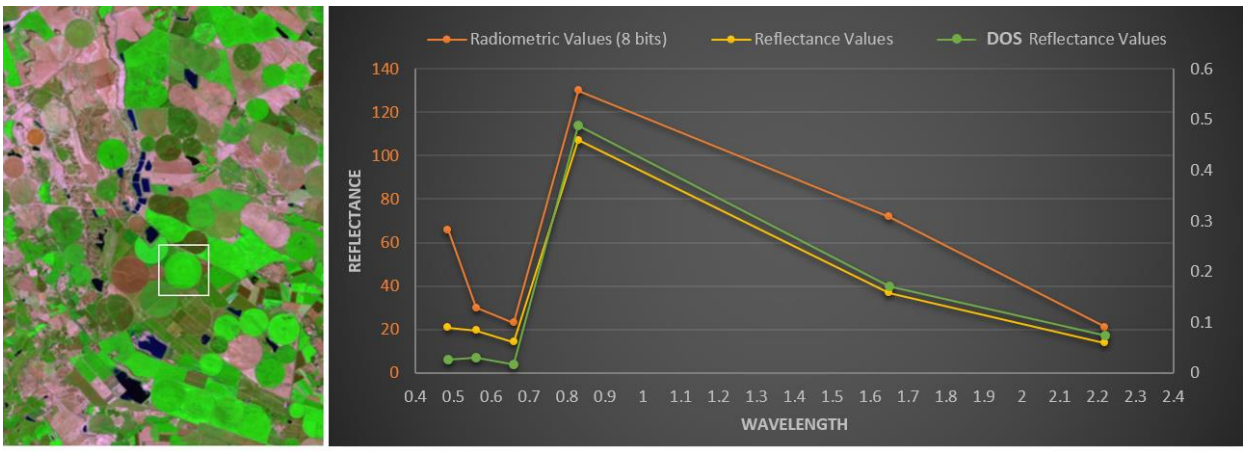

Fig. 4.14: Spectral behaviour, for a cropland class according to Landsat TM bands, shown in 8-bits brightness scale, and reflectance values before and after DOS atmospheric correction (Source: by Authors)

4.3.3. Image Display and Enhancement Techniques

The image enhancement procedures belong to those primary and significant actions within the field of digital image processing, apt for emphasizing or providing better understanding of certain features of interest in a digital image. Notwithstanding, being that the enhancement mostly depends on visual matters, in most of the cases the enhancement results could be determined by subjective criteria derived by the "sensitivity" of the analyst.

When working with multispectral (or hyperspectral) imagery, the most basic option is the possibility of displaying a different combination of colours for one image, depending on the purpose of the study. The effectiveness of arranging more than one wavelength, and then the possibility of displaying colours rather than grey tones, is that the images allow a better discrimination of the different land cover types.

At present, a single digital image is commonly displayed using a grey scale (which ranges from 0 to 255 brightness values, for instance, or 0 to 1 in the case of reflectance), but being that standard computers support three-dimensional colour systems, different "pseudo-colour" images can be revealed, in the case of multispectral imagery, by assigning colours to the different DN values (Bakker, et al., 2009).

Similarly to geometrical data, a three-dimensional colour system relies on a solid space which provides its own coordinate structure. The main colour systems, as shown in figure 4.15, are the RGB (Red, Green, and Blue), CMY (Cyan, Magenta, and Yellow), and HIS (Intensity, Hue, and Saturation) models[224]. *Due to their definitions, it is possible to convert images lossless from one colour model to the other* (Neteler, et al., 2008).

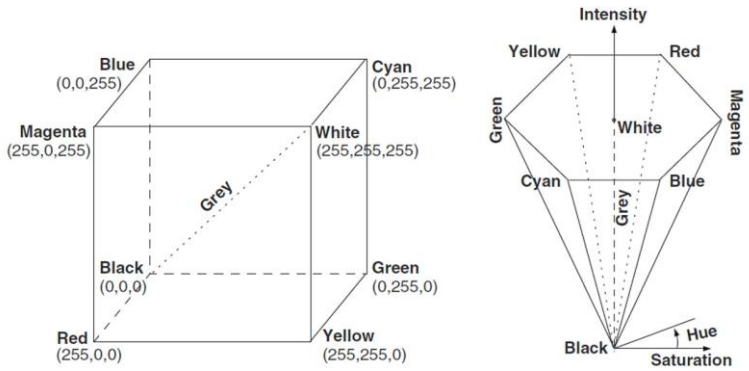

Fig. 4.15: Red-Green-Blue (RGB) and Cyan-Magenta-Yellow (CMY) cubic colour space; and Intensity-Hue-Saturation (HIS) hexcone colour space (Source: Neteler, et al., 2008; adapted from Mather, 1999)

When working with multispectral imagery, it is possible to use any combination of three bands, as input to the RGB channels employed as the colour model by the monitor. A so called True Colour image is displayed when the red, green and blue wavelength bands fit the RGB channels respectively. Another popular RGB combination, for multispectral imagery, is known as false colour composite, or Colour Infra-Red (CIR), and is the combination of the NIR Band (for the Red channel), Red Band (Green channel), and Green Band (Blue channel). This combination shows whatever kind of vegetation area through a red-purple scale of colour. This is because while within the visible part of the spectrum, plants reflect mostly green light, and alternatively, through the infrared slice, vegetation reflects even higher. That is why vegetation, in this false colour composite, appears as *a combination of some blue and a lot of red*, thus resulting in that typical reddish tint of purple. Sequences that display the NIR band in the green channel

[224] The RGB is defined as an additive colour model, which derives actual colours by adding the three base colours at different levels (yellow = red + green, for instance), and it is mostly used by computer screens. On the other hand, the CMY system, which is the one commonly employed for hardcopy printing, provides a subtractive model which displays colour by subtracting the three components from the incident light (magenta subtracts green wavelengths, cyan subtracts red wavelengths, and yellow subtracts blue wavelengths from the light). *The IHS model is different; here, the Intensity (sometimes also called "value") is a measure of color brightness, the Hue corresponds with the dominant wavelength (which is related to colour names), and the Saturation describes degree of colour purity. A pixel in the RGB colour space has a specific position within the cube spanned by the coordinate axes, while the IHS colour space forms a hexcone. The main advantage of RGB is that it is easy to understand; however, intensity changes are dependent on colour settings. Thus, in the RGB model, a change in intensity always leads to a change in colours. The IHS colour model preserves colours in case of intensity changes which is a major advantage for this model* (Neteler, et al., 2008)

of the RGB model, provide images in which vegetation is shown according to different green tones, thus giving rise to different kinds of pseudo-natural colour composites (Bakker, et al., 2009).

The next two pictures show respectively: the blue, green, and red band, of a Landsat TM image, combined in a natural colour composite (figure 4.16); and some of the most common RGB colour combinations which are, from left to right side: Natural Colour, Colour Infrared (CIR), a Pseudo-Natural Colour, and an Infrared based combination (figure 4.17). Clearly, each band and their different combinations provide specific features which allow a better interpretation of different land cover classes (see section 4.4.2).

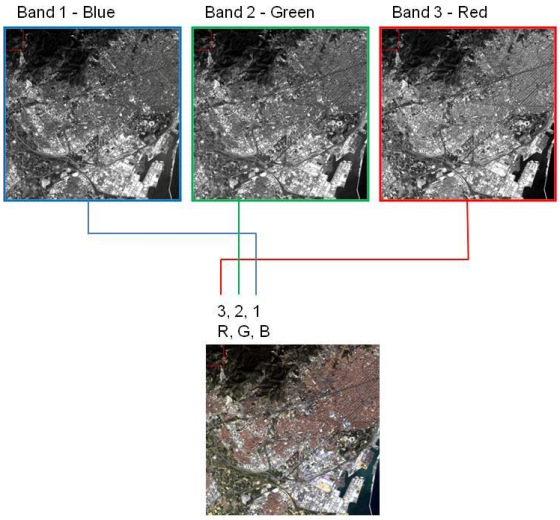

Fig. 4.16: Natural Colour combination sample, for Landsat TM imagery (Source: By Authors)

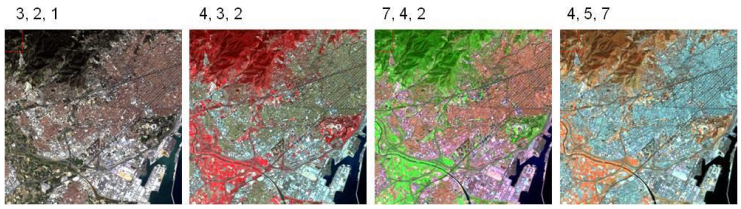

Fig. 4.17: Some of the most common band combinations, for Landsat TM multispectral imagery: Natural Colour; Colour Infra-red (CIR); Pseudo-Natural Colour; and Infrared based combination (Source: by Authors)

Further procedures for image enhancement can be performed, in order to obtain the best results for photo-interpretation. Two chief categories of image processing, for enhancing data information, rely on histogram operations and filtering, which, in turn, provide several operational techniques. In general, *in order to increase the visual distinction between features, histogram operations aim at global contrast enhancement, while filter operations aim at enhancing brightness edges and suppressing unwanted image detail. Histogram operations look at pixels without considering where they are in the image and assign a new value to a pixel by making use of a look-up table, which is set up from image statistics. Filtering is a "local operation", computing the new value for a pixel based on the values of the pixels in the local neighbourhood* (Bakker, et al., 2009).

The histogram refers to how the pixel values are distributed in relation to the total number of pixels which comprise the whole digital image; i.e. it reveals the radiometric properties of the image. In practice, the histogram provides the number of pixels for each value (within a specific range), which is actually the frequency distribution of the DNs. Thus, if we change the distribution of radiometric values, by increasing or decreasing the number of pixels in a specific DN, the visual aspect of the image will be modified, and the visual understanding enhanced. The result of enhancement can be just “temporary”, i.e. we do not change the original data but we only obtain an improved visualization; or, alternatively, new values can be generated by saving the modified histogram. The histogram,

which is generally displayed as a bar graph, can be summarized by using descriptive statistics, i.e. mean, standard deviation, minimum and maximum amounts. In particular, the mean provides the average of all the pixel values within the image, and *it does not often coincide with the DN that appears most frequently. The standard deviation indicates the spread of the DNs around the mean. A narrow histogram (thus, a small standard deviation) represents an image of low contrast, because all the DNs are very similar and mapped to only a few grey values* (Bakker, et al., 2009).

Some common techniques for contrast stretching, used for adjusting the brightness values of a digital image, are the linear stretch, Gaussian, or equalization, for instance, which actually provide a grey scale transformation of the input DNs. This then returns an output stretch of the selected slice of DNs, adjusted within the range 0-255. The linear stretch provides a simple transformation by converting the lowest DN value of interest to 0 and the highest to 255. A common linear transformation is 2% linear stretching, which takes into account just a smaller interval of the input values, usually arranged around the higher frequencies, in order to avoid very small and very large DNs which often correspond to noisy information. Histogram equalization, which aims at achieving a more uniform histogram, and Gaussian transformation are non-linear methods also used to achieve any desired colour adjustment for digital information (figure 4.18).

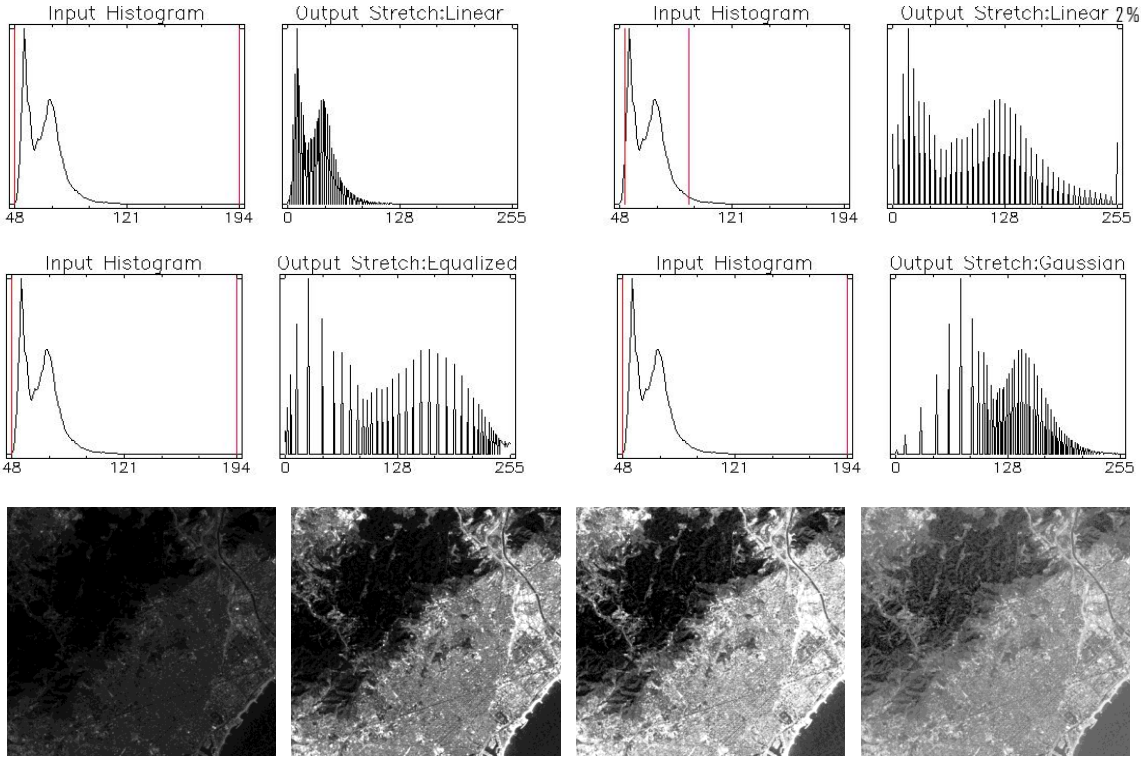

Fig. 4.18: Bar graphs show, from the upper left to the lower right side, in that order, a linear stretch sample, a linear stretch at 2%, an equalized, and a Gaussian stretch. While the Images, from left to the right side, show the visual results of the different stretches respectively: linear, linear at 2%, equalized, and Gaussian (Source: By Authors)

Another approach for providing optimal images for photo-interpretation, is to run spatial filtering procedures (typically carried out on single bands), which actually also include several methods that rely on deriving a specific pixel value, from a set of spatially related pixels. Filtering offers different results; such as smoothing (to reduce noise), or sharpening of blurred images, as well as edge enhancement for automatic pattern recognition, and object extraction. A simple example of a filtering procedure is when *"low pass" filters assign to each pixel of the radiance, values to be suppressed. On the other hand, "high pass" filters can enhance differences of reflectance values in the image* (Meaden, et al., 1991); *a smoothing filter sample is to compute the average of the pixel values of a 3 by 3 neighbourhood and assign it as new value to the central pixel; while an edge enhancing filter, which*

calculates the differences between the central pixel and its neighbours, is implemented using negative values for the non-central kernel elements, in order to emphasize local differences in grey values, for example related to linear features such as roads, canals, geological faults, etc. (Bakker, et al., 2009).

Besides the two mentioned image enhancement techniques, it is also necessary to emphasize the procedures of image fusion, apt for combining a low resolution image (multispectral) with a high resolution image (panchromatic[225]). This is done by applying mathematical functions to the pixels, after both images are previously geometrically co-registered. This technique is known as pan-sharpening (figure 4.19).

Fig. 4.19: Pan-Sharpening transformation result (Right side) for a multispectral Landsat image, at 30m resolution (left side), combined with a Landsat 15m panchromatic image (Source: By Authors)

Statistical transformations, such as principal components (see section 4.3.4.2) *and regression analysis, have been frequently used in image fusion, since they have the theoretical advantage of being able to combine a large number of images and compresses multi-spectral data sets as an aid to image classification and pattern recognition* (Meaden, et al., 1991).

4.3.4. Image Arithmetics, and Advanced Transformations

Similarly to what we have discussed during the previous section, this paragraph aims to explore some advanced techniques which also focus on the enhancement of image information, by transforming the raw data scanned by satellites.

Several methods are actually available for the analysis of multispectral satellite data, which rely on the manipulation of the spectral characteristics of the images. Without doubt, a powerful method for quick feature extraction procedures is provided by image arithmetics, in which two or more spectral bands are combined by applying basic calculations; such as addition, subtraction, multiplication, or division, between brightness values (computed pixel by pixel), in order to obtain new images with different spectral meanings.

The basis of simple algebraic operations employed for feature extraction is the band ratio, which is useful for reducing topographic effects or emphasizing slight differences in spectral reflectance characteristics. Meanwhile, improved variations on simple arithmetic operations between bands are also used for providing thematic indices. An example of the use of image arithmetics is the setting up of vegetation indices (VI), by combining infrared bands with visible data. This data reduction transformation allows vegetation classifications to be performed quickly (Richards, et al., 2006).

[225] *Most of the cameras use a spatial resolution for the panchromatic channel that is about a factor four higher than the resolution of the RGB and IR channels* (Bakker, et al., 2009)

Apart from image arithmetics, further advanced transformations; such as the Tasseled Cap and principal components analysis (PCA), also rely on the essential understanding of the reflectance curves and the spectral feature space in order to reduce and synthesize raw data into factors, thus eliminating redundant information and improving the interpretation and classification of land cover.

4.3.4.1. Band Ratios and Vegetation Indices: Simple Ratio (SR) and NDVI

Through band ratio operations, it is possible to directly discriminate specific areas of interest (land cover types, for instance), where a certain kind of material is dominant. The ratio will produce a new image which provides a change in the emissivity spectrum[226], with respect to raw images employed for undertaking the process. *Band ratios are quotients between measurements of reflectance in separate portions of the spectrum. Ratios are effective in enhancing or revealing latent information when there is an inverse relationship between two spectral responses to the same biophysical phenomenon. If two features have the same spectral behaviour, ratios provide little additional information; but if they have quite different spectral responses, the ratio between the two values provides a single value that concisely expresses the contrast between the two reflectances* (Campbell, et al., 2011).

While working with Landsat TM data, some useful band ratios are the combinations band 5/band 7, and band 3/band 1. In particular, the ratio 5/7 gives useful results for detecting various mineral groups; such as clays, micas, carbonates, and sulphates, as well as dense vegetated areas which should appear as light grey to white tones (Knepper, et al., 1992). Dry soils and artificial areas, together with water, in this ratio appear as dark tones and bare croplands show middle grey shades. A band ratio 3/1 emphasizes iron oxides (Knepper, et al., 1992), which should appear as light grey to white tones. Dry land also tends towards light greys, while water and forest exhibit dark shades. Significant results can also be achieved by combining band 4 with band 5. For instance, the 4/5 ratio, which is also known as the Moisture Stress Index (Rock, et al., 1985), enhances vegetation and moisture areas which appear in lighter tones; on the other hand, the 5/4 ratio separates water bodies and vegetation (mainly forest) from barren lands. In this ratio, water and forests show dark tones, while barren lands and bare croplands exhibit brighter tones.

A key role, within the image arithmetics ambit, is covered by bands 3 (Red Band) and 4 (NIR Band) of Landsat TM imagery. In terms of band ratios, a 3/4 combination, even if not very diagnostic for mapping minerals, can be used to identify areas where vegetation dominates the spectral response (Knepper, et al., 1992). The vegetation appears in very dark tones, thus being quite well separated from water which shows very light tones. This ratio also separates barren lands and urban areas from dense vegetation. Conversely, the ratio 4/3 heightens the brightness of forests and dense vegetation, which now appear in very light shades. It is because vegetation exhibits higher reflectance in the Near IR region (green leaf scattering), and strong chlorophyll absorption in the red region. This ratio, which well defines the distribution of vegetation is also known as Simple Ratio (SR) Vegetation Index (Birth and McVey, 1968), and forms part of a wide range of vegetation indices (VI) that rely on the use of these bands (the pixel values provided by this index ranges from 0 to more than 30, while the common range for green vegetation varies between 2 and 8).

In general, the Vegetation Indices (VIs), which are combinations of several surface reflectance measurements at different wavelengths (particularly sensitive to the effect of chlorophyll concentration, canopy leaf area and architecture, and foliage clumping), aim to quantify biomass or vegetative vigour dependent on the brightness values of pixels. They are actually designed to highlight the amount of healthy vegetation, i.e. the brighter the VI value is, the higher the vegetative vigour. The pixel value of a VI is derived by adding, dividing or multiplying the reflectance of specific bands and each VI is designed to emphasize particular characteristics linked to plant foliage chlorophyll distribution (Campbell, et al., 2011).

The Vegetation Indices, discussed in the framework of this investigation, belong to the category of indices known as broadband greenness VIs, which provide the simplest measurements of the general quantity and vigour

[226] In order to visualize the spectral signature of a specific land cover, according to more band ratios, it is required to combine a color-ratio-composite (CRC) image. This composite image will be also useful during photointerpretation procedures, to be used like ancillary data for complementing the raw satellite images

of green vegetation[227]. These VIs do not provide quantitative information directly, but mainly deliver measurements concerning the overall amount of chlorophyll and quality of photosynthetic processes[228]. They compare measurements of reflectance peak for vegetation and detect the presence and relative abundance of pigments, water and carbon. This is based on wavelengths between 400 nm to 2500 nm, collected from broadband multispectral sensors, such as Landsat or SPOT (more precise VIs could be computed by using hyperspectral imagery which allow more than one band for each slice of the electromagnetic spectrum).

Undoubtedly, one of the most "famous" and frequently employed Vegetation Indices is the Normalized Difference Vegetation Index (NDVI), introduced by Rouse, et al. (1974), which provides effective mapping over a wide range of conditions, due to a good balance between the normalized difference formulation, and the use of the highest regions of chlorophyll absorption, and reflectance, within the electromagnetic spectrum. In particular, when the sunlight hits any vegetation objects (see next figure 4.20), *the pigment in plant leaves, chlorophyll, strongly absorbs visible light (from 0.4 to 0.7 µm) for use in photosynthesis. The cell structure of the leaves, on the other hand, strongly reflects near-infrared light (from 0.7 to 1.1 µm). In general, if there is much more reflected radiation in near-infrared wavelengths than in visible wavelengths, then the vegetation in that pixel is likely to be dense and may contain some type of forest. If there is very little difference in the intensity of visible and near-infrared wavelengths reflected, then the vegetation is probably sparse and may consist of grassland, tundra, or desert* (Weier, et al., 2000).

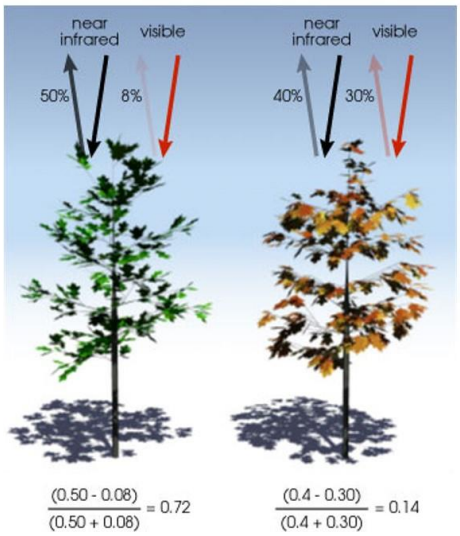

Fig. 4.20: *NDVI is calculated from the visible and near-infrared light reflected by vegetation. Healthy vegetation (left) absorbs most of the visible light that hits it, and reflects a large portion of the near-infrared light. Unhealthy or sparse vegetation (right) reflects more visible light and less near-infrared light. The numbers on the figure above are representative of actual values, but real vegetation is much more varied* (Illustration by Robert Simmon; Source: Weier, et al., 2000)

According to the previous concepts, the NDVI is mathematically calculated (as shown in the formula [4.6]) as the near-infrared (NIR) radiation minus the visible red radiation (RED), divided by near-infrared radiation plus visible radiation, where the radiations are those reflected back by the objects.

$$NDVI = \frac{NIR - RED}{NIR + RED} \qquad [4.6]$$

[227] A clear correspondence exists between the broadband greenness VIs and the canopy LAI (Leaf Area Index)

[228] Further applications include vegetation phenology (growth) studies, land-use and climatological impact assessments, and vegetation productivity modeling

A photo of synthetically active vegetation shows a typical reflectance of less than 20%, in the narrow visible red band (≈ 0.6 to 0.75 µm), with a much higher reflectance which can reach 60% within the near IR slice (≈ 0.75 to 1.5 µm). *Calculations of NDVI for a given pixel always result in a number that ranges from minus one (-1) to plus one (+1); however, no green leaves give a value close to zero. A zero means no vegetation and close to +1 (0.8 - 0.9) indicates the highest possible density of green leaves* (Weier, et al., 2000). When pixel values within the near-infrared slice are greater than those of red wavelengths, the NDVI is positive. Actually, the common range for green vegetation varies between 0.2 and 0.9, due to the increase in canopy density. Instead, clouds, water and snow (and, in general, also built-up areas) have negative NDVI, since they are more reflective through the visible red slice than through the NIR. Barren soils and rocks are those land cover classes which give NDVI values close to "0".

The computation of NDVI transforms multispectral data into a new single band image (according to a shade of greys which ranges from -1 to +1), and represents the vegetation distribution within a landscape. This new digital image, if combined with NIR and Green Band based on a RGB model (NIR, NDVI, and Green Band respectively) in order to display a composite image (see previous section 4.3.3 about multispectral imagery displaying), provides a combination which is a pseudo-colour NDVI composition, as revealed in figure 4.21.

The NDVI combination generally shows sparse crop vegetation and some forest areas in moderate shades of green. Other areas of vegetation, such as river grasslands, dense croplands and forests, produce high NDVI values and in this combination appear as intense green and yellow tones because of the increased photosynthetic activity and greater density of canopy. Arable bare fields, pavement and bare ground appear to exhibit pink/purplish kinds of shades, whilst water bodies provide dark blue/green tones.

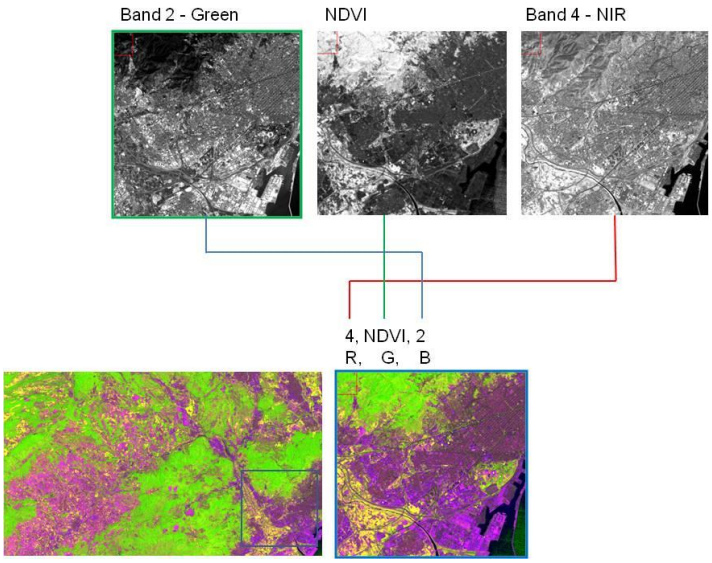

Fig. 4.21: A Pseudo-Colour NDVI composite, according to a RGB model (Source: By Authors)

At present, remote sensing data is being extensively used for mapping and monitoring (over time) of vegetation, and over huge areas of interest. Moreover, almost all broadband satellites capture the necessary wavelengths for generating Vegetation Indices, such as the NDVI, which allows us to quantify the density of plant growth over the whole Earth during a given period[229].

In fact, Weier, J. and Herring, D. (2000), report that *in an effort to monitor major fluctuations in vegetation and understand how they affect the environment, 20 years ago Earth scientists began using satellite remote sensors to measure and map the density of green vegetation over the Earth. Using NOAA's Advanced Very High Resolution Radiometer (AVHRR), scientists have been collecting images of our planet's surface. By carefully measuring the*

[229] *The NDVI values can be averaged, over time, to establish the "normal" growing conditions for the vegetation in a given region for a given time of the year. A region's absorption and reflection of photosynthetically active radiation over a given period of time can be used to characterize the health of the vegetation there, relative to the norm* (Weier, et al., 2000)

wavelengths and intensity of visible and near-infrared light reflected by the land surface back up into space, scientists use an algorithm called a "Vegetation Index" to quantify the concentrations of green leaf vegetation around the globe. Then by combining the daily Vegetation Indices into 8-, 16-, or 30-day composites, scientists create detailed maps of the Earth's green vegetation density that identify where plants are thriving and where they are under stress (i.e., due to lack of water). Following this direction since February 2000, the National Aeronautics and Space Administration (NASA) has been producing monthly maps about the global-scale patterns of vegetation around the Earth, by using the NDVI[230], based on measurements taken by the Moderate Resolution Imaging Spectroradiometer (MODIS) on NASA's Terra satellite (figure 4.22).

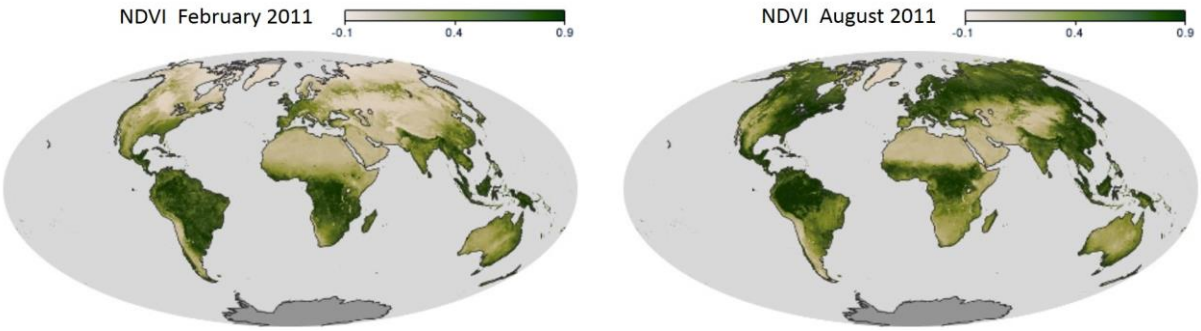

Fig. 4.22: The Normalized Difference Vegetation Index (NDVI), computed over the entire globe through the use of satellite imagery, displays the density of plant growth in February 2011 and August 2011. Low values of NDVI (0.1 and below) refer to barren areas of rock, sand or snow. Moderate values identify shrub and grassland (0.2 to 0.3), and high values of NDVI (0.6 to 0.8) signify temperate and tropical rainforests (Source: NASA)

As well as for the NDVI, advanced indices apt for measuring specific characteristics of green vegetation, have been provided during the last decades. They also rely on the use of the typical spectral bands employed for computing VIs, or in conjunction with auxiliary bands, allowing several mathematical combinations. Some further samples of broadband greenness VIs are provided in section 4.5.5.1.

4.3.4.2. The Principal Components Analysis (PCA)

The multispectral or multidimensional nature of remote sensing image data can be accommodated by constructing a vector space with as many axes or dimensions as there are spectral components associated with each pixel (Richards, et al., 2006). Multispectral data commonly shows an important correlation between the stacked images provided at different wavelengths (the visible bands of Landsat TM, are highly correlated between them, for instance). Actually, the high correlation, which is both visual as well as numerical between spectral bands, often depends on a combination of factors, such as:

- Similarities of the spectral response of certain land covers (vegetation, for instance, shows a relatively low reflectance within the visible spectrum, thus producing similar signatures in visible bands);
- Topographic effect, which produces the same shaded areas at any wavelength (except for thermal bands), thus the reflective region could not depend on the effective interested land surface. *The shaded effect can even be the dominant image component in mountainous areas and at low sun angles*;
- Sensor band overlapping effect, which even if typically small and minimized during the sensor design stage, cannot be completely avoided (Schowengerdt, 2007).

This band correlation produces redundancies within the data set. Therefore, the processing of the raw spectral information could be inefficient for certain advanced purposes of image analysis. A variety of methods do exist that are suitable for transforming raw multispectral imagery, in order to reduce the original information and obtain new uncorrelated images by using only significant parts of the data. The Principal Components Analysis

[230] http://earthobservatory.nasa.gov/GlobalMaps/view.php?d1=MOD13A2_M_NDVI

(PCA), applied to the field of Remote Sensing (Jensen and Waltz, 1979) and Tasseled Cap transformation (Kauth and Thomas, 1976), are maybe two of the most recognized and widely investigated standard techniques, which are employed in multispectral data reduction procedures.

According to Schowengerdt (2007), the PCA is a transformation of the feature space, and it aims to reduce spectral redundancy by applying a linear transformation; as shown in the equation [4.7], which relies on an image-specific matrix W_{PC} and zero bias.

$$PCA = W_{PC} * DN \qquad [4.7]$$

The images, defined through PCA, result from a projection of raw pixel values, i.e. those of the initial bands, onto new orthogonal axes (or new bands) by defining a new coordinate system. This new space, which is drawn by a rigid rotation of the original coordinate system, aims to intercept the major data concentration and thus find the maximum variability of information. The highly correlated spectral bands now give rise to a new set of uncorrelated images which concentrates the whole image information in fewer bands (or dimensions), and more effectively characterises the variance of the data set. *This is achieved by maximising the projected variance onto mutually orthogonal eigenvectors along the directions of higher eigenvalues through iterative algorithms that minimise information losses* (González, et al., 2009; Bishop, 2006).

Once a PCA transformation (also known as Principal Components (PCs)) has been performed, the amount of new independent image data is the same as the number of input bands. In general, the first PC image encompasses the major percentage of variance of the original images, while the second PC provides the following largest part of the remaining data variance, as it is orthogonal to the first PC. Consequently, the succeeding PC images cover, proportionally, the remaining amount of variance, since it decreases from the first to the last PC. This provides an increase in noisy information towards the final PCs, because they contain very small variance of information (Weng, 2010; Neteler, et al., 2008; Schowengerdt, 2007; Richards, 1994).

Figure 4.23 displays a theoretical transformation of a co-ordinate system, into new uncorrelated components. For simplicity, the example is based on a two dimensional space, which relies on the visible red and NIR bands of a generic multispectral Landsat TM image. Moreover, the scatter-plots in the figure show the original spectral axes, and the spatial position of each pixel value within a two-dimensional representative space (TM3, and TM4) of a specific Landsat 5 TM image; as well as the new rotated orthogonal axes and spatial position of pixel values after PCA transformation. The first PC provides 79.46% of explained variance, thus leaving an important part of useful information stored in the second PC.

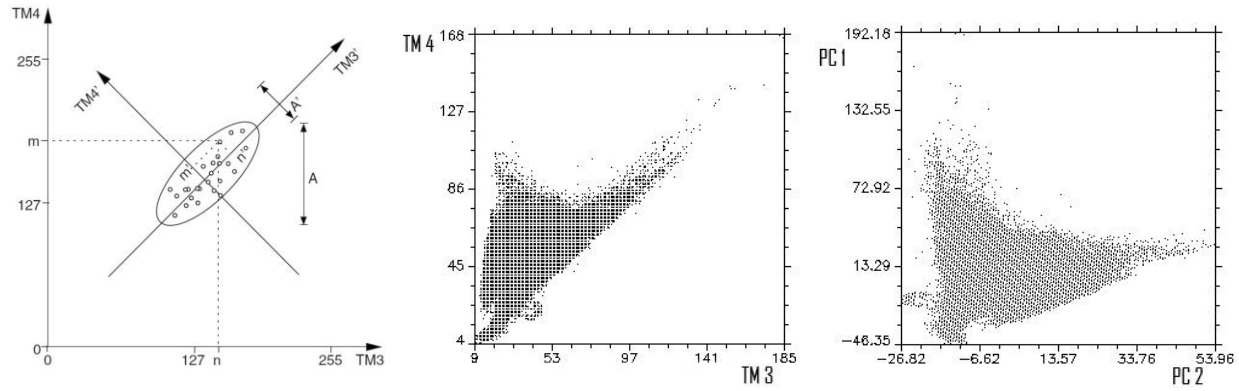

Fig. 4.23: A theoretical sample of a PCA transformation, for band TM3 and TM4, of a Landsat data set (left side), which shows the original spectral axes, and the PC axes TM3^{I}, and TM4^{I} (Source: Neteler, et al., 2008); as well as a real sample of a two-dimensional PCA transformation, applied to band TM3, and TM4, of a Landsat 5 data set, with the resulting PC1 and PC2 spectral space (Source: By Authors)

For imagery with more than two bands, as is the case for Landsat Thematic Mapper multispectral images, this provides a six-dimensional spectral space (hyperspectral data are expected to define several hundred axes, for

instance), the PCA will produce six uncorrelated Principal Components. The following figure 4.24 shows a TM multispectral image, composed of six bands (1 to 5 and 7), on which a PCA transformation has been performed. Six Principal Components have been obtained, where the first two PCs account, respectively, for over 89% and 97% of the original variance. Although lower order components could contain extra image details, the examination of the dataset of principal component images reveals, in this case, only few possible useful details provided by the fifth and sixth components. Actually, most noisy information is often stored in the two last PCs.

If we create a colour display of remotely sensed data, by allocating the PCs in a RGB model space, the first four PCs are probably the best components to be used for visualizing pseudo-colour composite images, because they account for 99,79 percent of total variance[231]. Moreover, even the analysis of the eigenvalues, reveals a flattening of the linear graph after the fourth eigenvalue (figure 4.24).

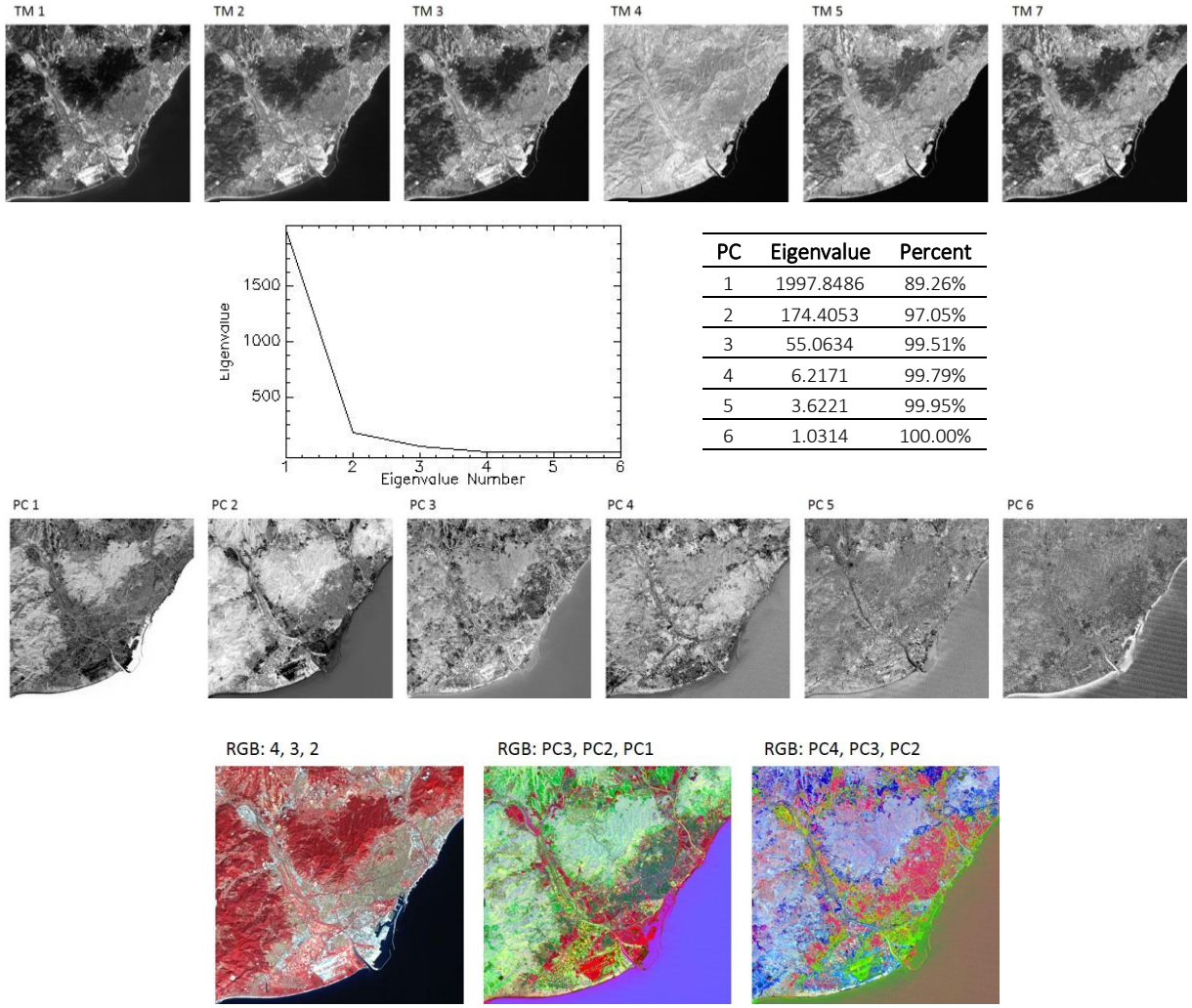

PC	Eigenvalue	Percent
1	1997.8486	89.26%
2	174.4053	97.05%
3	55.0634	99.51%
4	6.2171	99.79%
5	3.6221	99.95%
6	1.0314	100.00%

Fig. 4.24: Principal Component Analysis applied to highly correlated TM image bands. From top to bottom of the figure: 1) the initial TM bands; 2) eigenvalues graph and values, and percent of variance explained for each PC; 3) the six resulting Principal Components; 4) pseudo-colour composite images which involve TM bands 4, 3, 2; and the first four PCs (Source: By Authors)

[231] *A difficulty with principal components colour display, however, is that there is no longer one to one mapping between sensor wavelength bands and colours. Rather, each colour now represents a linear combination of spectral components, making photointerpretation difficult for many applications* (Richards, et al., 2006)

The PCA, which is a technique widely used for several applications such as data compression (as it allows us to "synthesize" the image information in fewer channels), feature extraction, and visual enhancement; can also serve for generating additional information useful for improving classification processes, by providing more variables to be analysed (Neteler, et al., 2008).

4.3.4.3. The Tasseled Cap Transformation

The principal components transformation (discussed in the previous section 4.3.4.2), is a technique able to generate a new spectral space based on uncorrelated axes. It works by applying a linear transformation on the initial spectral bands, and through the use of the covariance matrix of the system. During the last few decades, several methods for data synthesizing have been developed along the same lines as the PCA, in order to process remotely sensed information, since satellite data have always been increasing their availability and potentialities.

The Tasseled Cap (TC) transformation, developed by Kauth and Thomas (1976), provides another chief technique for data reduction, which aims to emphasise some important features within multispectral imagery. In particular, the work undertaken by Kauth and Thomas[232] focused on highlighting the behaviour of crop pixels, dependent on certain specific spectral subspaces of Landsat MSS multispectral imagery. These spectral observations about crop development, monitored over time, were aimed at recognizing reflectance of different crop patches based on different vegetation covers. This objective was pursued through developing a special linear transformation, provided by PCA, which would be suitable for crop discrimination. Based on Landsat MSS data, the proposed TC transformation produced four new orthogonal axes, which were adjusted to extract the best spectral components and maximise the information concerning croplands (Richards, et al., 2006).

According to Schowengerdt (2007), the Tasseled Cap Transformation (TCT), which is a "special" case for PCA, is also calculated based on a similar equation to the one described below [4.8]; but unlike the PCA, a predetermined transformation matrix (W_{TC}) is provided, independently of the scene configuration[233].

$$TCT = W_{TC} * DN + B \qquad [4.8]$$

In this equation, DN represents the original brightness values collected by the satellite, while B (Bias) is a constant vector built ad-hoc for a given sensor, used to avoid negative values in TCT. In the case of Landsat 5 TM, *the additive vector must also be applied (to the computed Tasseled Cap features) in order to obtain signal range equivalence (*with respect to Landsat 4*, Ed.). Note also that without the additive vector, the features are not technically orthogonal* (Crist, et al., 1986).

The TCT, as designed by Kauth and Thomas for Landsat MSS imagery, yields four new axis: of which the first one is named soil brightness and is most useful for identifying areas of no vegetation; the second coordinate axis, which is orthogonal to the soil brightness, defines different vegetation signatures well and is known as greenness; the third dimension, which increases its signature values when vegetation brightness decreases (when *crops mature and become senescent*), is the so-called yellow stuff dimension; while the fourth axis is known as the non-such element[234].

Third and fourth axes were drawn as orthogonal to the first two, and both have also demonstrated a degree of sensitivity for defining alterations in atmospheric haze conditions (Schowengerdt, 2007). Similarly to the

[232] Kauth, R., & Thomas, G. (1976). The Tasseled Cap - A graphic description of the spectral temporal development of agricultural crops as seen by Landsat. Proceedings of LARS Symposium on Machine Processing of Remotely Sensed Data, Purdue University

[233] *The PCT (*Principal Components Transformation*, Ed.) is data dependent; the coefficients of the transformation are a function of the data spectral covariance matrix. While this feature allows the PCT to adapt to a given dataset and produce the best transformation from a compression standpoint, it makes the comparison of PCTs from different images difficult. The PCs can usually be interpreted in terms of the physical characteristics of a given scene, but the interpretation must change from scene to scene. Early in the Landsat era, it was recognized that a fixed transformation, based on physical features, would be useful for data analysis* (Schowengerdt, 2007)

[234] For all Landsat MSS imagery, independently of the scene composition, soil brightness, greenness, yellowness and non-such dimension are achievable by applying the same W_{TC} transformation matrix to each pixel within the multispectral image (Richards, et al., 2006)

Vegetation Indices, these four new uncorrelated images can, as a result, be used as thematic indices to quickly extract specific land cover features.

The coefficients, which compose TC transformation matrices, are currently fixed for all Landsat sensors, from the L-1 MSS (Kauth, et al., 1976) up to the L-7 ETM+ (Huang, et al., 2002). The images employed in the framework of this study refer to Landsat TM 4 and 5. The table 4.4 provides the coefficients set up for both sensors, i.e., L-4 TM (Crist, et al., 1984), and L-5 TM (Crist, et al., 1986).

Sensor	Axis Name	W_{TC}						Bias
		B1	B2	B3	B4	B5	B7	
L-4 TM	Soil Brightness	0.3037	0.2793	0.4743	0.5585	0.5082	0.1863	
	Greenness	-0.2848	-0.2435	-0.5436	0.7243	0.0840	-0.1800	
	Wetness	0.1509	0.1973	0.3279	0.3406	-0.7112	-0.4572	
	Haze	0.8242	-0.0849	-0.4392	-0.0580	0.2012	-0.2768	
	TC5	-0.3280	0.0594	0.1075	0.1855	-0.4357	0.8085	
	TC6	0.1084	-0.9022	0.4120	0.0573	-0.0251	0.0238	
L-5 TM	Soil Brightness	0.2909	0.2493	0.4806	0.5568	0.4438	0.1706	10.3695
	Greenness	-0.2728	-0.2174	-0.5508	0.7221	0.0733	-0.1648	-0.7310
	Wetness	0.1446	0.1761	0.3322	0.3396	-0.6210	-0.4186	-3.3828
	Haze	0.8461	-0.0731	-0.4640	-0.0032	-0.0492	0.0119	0.7879
	TC5	0.0549	-0.0232	0.0339	-0.1937	0.4162	-0.7823	-2.4750
	TC6	0.1186	-0.8069	0.4094	0.0571	-0.0228	0.0220	-0.0336

Tab. 4.4: Coefficients used for the Tasseled Cap transformation matrices (W_{TC}), in the case of sensors on Landsat TM 4 (Crist, et al., 1984), and Landsat TM 5 (Crist, et al., 1986). *The Landsat-5 TM coefficients were derived by reference to the Landsat-4 coefficients; they include extra additive terms that must be used to compare the TC features from the two sensors* (Crist et al., 1986; Schowengerdt, 2007)

The TC transformation uses the same coefficients every time to redefine the new orthogonal axes, just depending on the sensor. In the case of Landsat TM, a 6x6 transformation matrix has been set up, which actually provides six independent axes (as shown in table 4.4), instead of four components, as is the case of the MSS sensor. At any rate, the first three axes are commonly used for analysing Landsat TM imagery. Of interest, the brightness axis consists of a soil brightness index (SBI), greenness is a green vegetation index (GVI), while the third component, is known to be useful for discriminating moisture content for land cover types and is also recognized as a wetness index, related to certain soil features, but in particular with moisture status. These components are often combined in order to provide a Tasseled Cap pseudo-colour image through the use of a RGB model (figure 4.25).

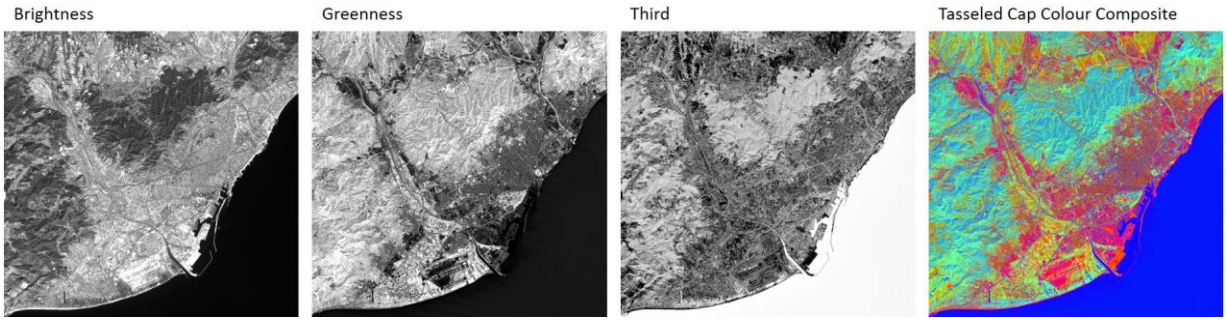

Fig. 4.25: Tasseled Cap Transformation for a Landsat TM multispectral image. From left to right side, Brightness, Greenness, and the Third component, as well as a TC pseudo-colour composite image according to a RGB model (Source: By Authors)

4.4. PATTERN RECOGNITION AND IMAGE CLASSIFICATION

Pattern recognition refers to a set of techniques for monitoring and change detection along the Earth's surface and atmosphere. These include measuring and categorization of certain specific features, such as vegetation, land cover inventory or atmospheric phenomena. Being linked to digital data (satellite or aerial), these techniques rely on three dimensions, which are the spatial, the spectral, and the temporal; of which image classification provides an example of spectral pattern recognition. The field of pattern recognition is supported by the use of computer algorithms in order to provide standardized procedures for data enhancement and automatic extraction of information. Thus, logically encompasses both image processing practices[235] (strictly speaking), where inputs and outputs are images; and image analysis aims to extract attributes from images (such as the land cover classification, for instance) which can yield categorical or thematic maps[236].

Land cover classification, which is an important part within the field of remote sensing, is a procedure which aims to identify certain patterns within an image that is associated to a specific pixel location, both in terms of spectral as well as spatial position. The final objective of thematic classification is the automatic categorization of all pixels into actual land cover classes. This process is therefore a pixel-by-pixel analysis, which relies on spectral information as the basis for automated grouping, and commonly depends on multispectral measurements, which actually provides each pixel with a vector of numerical values according to the number of available bands[237].

There are basically two different approaches to land cover classification: through photo-interpretation and on-screen digitalization, or by automatic recognition of specific reflectances for sets of pixels. In remote sensing, numerous algorithms for automatically classifying satellite imagery are provided, such as spectral clustering, decision tree classifiers, or neural networks, for instance. There are two broad types of automatic classification procedure, alternatively used, or combined into hybrid methodologies: the unsupervised classification (see section 4.4.4), and the supervised classification (see section 4.4.5).

According to Schowengerdt (2007), three main steps are commonly involved in thematic classification procedures. These are: the feature extraction phase, which relies on processing digital data through spectral transformation for data dimensionality reduction (Principal Components, and Tasseled Cap Transformation, for instance), or spatial transformation based on filtering operations[238]; the training step, which is directed at selecting the best pixels, or Regions of Interest (ROI henceforth), suitable *for training the classifier to recognize the desired themes, or classes*; and labelling, which relies on the *application of the feature space decision boundaries to the entire image to label all pixels*[239]. If the training process relies on a supervised approach, labels of land covers are already associated with the feature space regions; while, if training follows an unsupervised method, it is necessary for an analyst to assign labels to the regions. Anyway, output maps consist of one label for each pixel group (or class). *The end result is a transformation of the numerical image data into descriptive labels that categorize different surface materials or conditions. By virtue of the labelling process, we have presumably converted the data into a form that has informational value* (Schowengerdt, 2007).

Photo-interpretation in remote sensing is an effective procedure for feature recognition, usually for a general assessment of ground cover types. It is often used at a primary stage for information analysis, both for image enhancement as well as for classification approaches. Additionally, it can be used as a post-evaluation

---

[235] In general, the term image processing indicates a whole scientific field and also includes image analysis procedures. According to Gonzalez and Woods (2002), *interest in digital image processing methods stems from two principal application areas: improvement of pictorial information for human interpretation; and processing of image data for storage, transmission, and representation for autonomous machine perception* (Gonzalez, et al., 2002)

[236] *A thematic map shows the spatial distribution of identifiable earth surface features; it provides an informational description over a given area, rather than a data description. Image classification is the process used to produce thematic maps from imagery. The themes can range, for example, from categories such as soil, vegetation, and surface water in a general description of a rural area, to different types of soil, vegetation, and water depth or clarity for a more detailed description. It is implied in the construction of a thematic map from remote-sensing imagery that the categories selected for the map are distinguishable in the image data* (Schowengerdt, 2007)

[237] A pattern, within a digital image, is nothing more than a set of pixels themselves, with similar characteristics; or more precisely mathematical vectors of pixels, which contain a set of brightness values related to each spectral band (Richards, et al., 2006)

[238] *This step is optional, i.e., the multispectral image can be used directly, if desired* (Schowengerdt, 2007)

[239] Bishop (2006) speaks about two separate phases of classification process, the inference, in which training data are used *to learn a model*, and a following decision stage, in which *posterior probabilities are used to make optimal class assignments*. An alternative possibility is the use of a discriminant function to handle both problems at once. This function actually maps each input pixel directly onto a class label.

instrument for evaluating the goodness of automatic processes of classification. However, as pointed out by Richards and Xiuping (2006), the photo-interpretive approach is little suitable when handling huge datasets. When a classification process is intended to be undertaken at pixel level, it is practicable only if a handful of pixels is of interest; otherwise this procedure could actually be very costly and expansive in terms of time and resources. An additional restriction is provided by the limitative use of the spectral information, while working through photo-interpretation. In fact, since this approach relies on the ability of human interpreters (the analyst), only three bands of the whole available multispectral data can be analysed at once through colour models; therefore, an analyst will be not able to discriminate objects based on the actual radiometric resolution, as there are seven bands in Landsat TM imagery, for instance.

The recognition of specific ground cover types, by managing multispectral vectors of pixel values, (*image data exists in sets of spectral classes*), is possible only by using mathematical pattern recognition techniques. The automatic computer understanding, which refers to quantitative analysis of digital data, is able to take full account of multidimensional qualities of remotely sensed data and to recognise pixels depending on numerical attributes. This makes it possible to examine the full radiometric resolution (Richards, et al., 2006).

If a RS user wishes to classify all the tones on an image which have a certain range of, for instance, crop categories, then by finding out the typical pixel values for each crop (using field investigations), the findings can be applied to the rest of the image, i.e. the computer can be "trained" to seek out various spectral signatures for one small area and then apply it across the image. The automatic image classification will become more effective as more spectral variability is provided by digital data, i.e. if the objects of interest are spectrally very different (Meaden, et al., 1991).

In remote sensing, several statistical techniques are available for automatically classifying pixel values in different spectral classes, dependent on numerical features. Some of those approaches are examined in the following sections of this chapter.

4.4.1. Land Use and Land Cover (LULC): What is the Matter?

Before going on to discuss some of the key techniques for automatic classification, it is essential to clarify two concepts of interest for this investigation about remote sensing outcomes: Land Use and Land Cover. Frequently, it occurs that the terms land use and land cover are used indistinctly, or interchangeably, within classification systems; instead, a fundamental distinction is necessary to avoid confusion and ambiguity between these two different issues, especially if data from different dimensions need to be matched, compared and/or combined (EUROSTAT, 2001). Even if both terms are closely related, it is essential to highlight that remote sensing devices do not record functions directly, but detect physical attributes for different types of land cover, to which human activities are commonly associated (agriculture, residential or industrial, for instance). Thus, while land cover can be defined through photo-interpretation or automatic image processing, the land use cannot be ascertained so readily.

It is said that Land Cover is "observed". This means that observation can be made from various "sources of observation" at different distances between the source and the earth's surface: the human eye, aerial photographs, and satellite sensors. Contrary to land cover, land use is difficult to "observe". For example, it is often difficult to decide if grasslands are used or not for agricultural purposes. The information coming from the source of observation may not be sufficient and may require additional information (EUROSTAT, 2001). Therefore, the analyst should derive further information regarding land use activities mainly by interpreting patterns, tones, textures, shapes, and site associations from the remotely sensed data (Anderson, et al., 1976); by using whatever ancillary data available about a specific geographic area; or through physical measurement on the ground[240]. A strict theoretical distinction between land use and land cover is actually quite complex to implement and the relationship is not generally that clear and direct either. In fact, as depicted by Weber (2009), land uses could be multiple and

[240] *Often, land use is deduced from land cover (e.g. crop assessment from surface yield). Often land cover is shaped from land use (e.g. a vegetated area within a city is generally considered as an urban park and not an agriculture area)* (Weber, 2009)

inconsistent within the same land cover[241]; on the other hand, homogeneous portions of land cover can be generally established, *although classification may vary – to some extent – according to the attributes chosen or seasonal variability* (Weber, 2009), and even if, in some cases, a single land use may also involve the existence of several distinct land cover types; such as certain farming systems which combine cultivated land, wood lots, improved pasture, and settlements (Meyer, et al., 1994; Weng, 2010). At any rate, it is critical to define both concepts as well as possible in order to set up a proper classification system as an objective of this study.

Therefore, it has to be understood that land use is the anthropic use of the soil, i.e. the various types of urban settlements, such as residential or industrial, for instance; the different types of cultivation and pastures; or timber production, in the case of forests. In other words, whichever way the biophysical attributes of the land and the functions for which the land is used. In contrast, the term land cover is intended to delineate the reflectance of either the natural cover types or the generalized manmade surfaces, i.e. all those materials, which are currently covering the ground. It thus comprises both the biophysical state of soil, such as forests, grassland, cropland, or wetland, as well as human structures, such as cities (Turner et al., 1995; Weng, 2010).

According to Weng (2010), in many cases, changes that occur upon land cover are a direct consequence of changes related to land use, which means that any anthropic manipulation of the soil generally has a direct effect on the physical characteristics of the land cover. However, the relationship between land use and land cover is not one-way, in fact, as a change in the physical characteristics of ground cover often leads to changes in the environment, which in turn, may have effects not only on the same land cover but may also affect the intensity and variability of uses related to human activity within a portion of land cover.

Most of the common classification systems (some examples are provided in chapter 2) employ a first level of generalized classes (for mapping the Earth surface), which rely on four main land cover types that are usually: Forest (evergreen, deciduous, or mixed) and natural areas (grassland, barren land, and rocks); crop lands (flat plantations or row of crops); water bodies (rivers, lakes and seas); and urbanized areas (cities, towns, parks, roads). In most cases, further levels of categorization are required to define types of land cover and land uses, dependent on the purposes of the work being undertaken.

4.4.2. The Photointerpretation Approach for Image Understanding and Classification

The primary understanding and interpretation of images are probably the most significant procedures aimed at extracting sensible information from digital data, regardless of the analysis approach undertaken. At present, the procedures for analysing and extracting information from remotely sensed data follow two main paths: a traditional image-centred approach, which focuses mainly on the spatial relationships within features on the ground (Schowengerdt, 2007); and a computer based analysis, which aims to measure spectral pixel attributes, when image data is radio-metrically quantised into discrete brightness levels. This latter approach is referred to as quantitative analysis (Richards, et al., 2006).

The "traditional" approach, also known as photo-interpretation, directly involves a qualified experienced human analyst, generally referred to as a photo-interpreter. He visually detects, recognizes and labels features of interest on the ground by observing digital or hardcopies of photographs. Once specific features are located and characterized according to a predetermined classification system, they are geocoded in order to be transferred to GIS platforms, and then used to provide thematic maps (Schowengerdt, 2007). If digital data is available, the process of photo-interpretation is commonly undertaken directly by using GIS platforms and on-screen analysis and digitalization.

Extracting information by visual assessment is generally a method suitable for defining large scale features (i.e. to delimit a finite set of pixels, with similar texture), not at the single pixel level, and it is often independent of the spectral measurement of the imagery. Even so, the success of the process depends upon the effective exploration of the spatial, spectral and temporal dimensions of the imagery, whilst taking into account that the spatial dimension signifies the set of feature qualities; such as shape, size, orientation and texture (which can be

[241] *Forest, a land cover dominated by woody species, may be exploited for uses as varied as recreation, timber production and wildlife conservation* (Turner, et al., 1993). *Moreover, a land-cover type may be used for contrasting activities during different seasons of the year. Some farmland might be employed alternatively as cropland and as pasture at different times in an agricultural calendar* (Campell, 1983; Weng, 2010)

improved by applying geometric, radiometric or contrast enhancements). The spectral dimension in photo-interpretation is instead referred to as the degree of the analyst's experience to visually recognize typical brightness characteristics of different land cover types, dependent on the available captured bands and their combinations according to the various colour composites (Richards, et al., 2006).

The next image, 4.26, depicts a typical example of on-screen photo-interpretation, digitizing and labelling different land cover classes, based on an orthophoto. Each of the polygons generated (using a defined classification system and their associated information) provide the final geo-referenced thematic map available for GIS platforms.

Fig. 4.26: Photo-interpretation on orthophoto and digitalization results from the land cover map of Catalonia (MCSC)[242] provided by the Centre for Ecological Research and Forestry Applications (CREAF) (Source: Ibàñez, et al., 2009)

Historically, photo-interpretation was mostly suitable for aerial photographs and hardcopies, but with the introduction and increasing development of digital data and satellite imagery, several additional potentialities and better information gathering have been added to this approach.

Multispectral sensors (such as those aboard the Landsat satellites and in particular the Thematic Mapper (TM) sensor which was used for this study) provide land cover brightness at different wavelengths of light, and can be stored as digital data. In fact, in addition to the standard "natural" colour images (i.e. those images captured only using the visible slice of the energy spectrum range), satellites are able to provide information through the infrared and even the thermal slice of the electromagnetic spectrum. It is fundamental that analysts are able to interpret each one of these grey scale images, and therefore detect different objects of interests by analysing single brightness features (according to the specific wavelength of the information collected). They must also be able to combine the images in order to obtain the best sequence of the different wavelengths through an image displayed in a three dimensional colour model.

It is useful to draw your attention to some of the main features highlighted by the different bands provided by a Landsat TM sensor, and their derived RGB combinations. As also summarized in table 4.5, each band can be suitable for detecting different land surface characteristics, as follows:

Band 1 (0.45-0.52 µm), also known as the blue band, is a short-wave band which penetrates the Earth surface much better than longer wave Landsat bands. This allows a better emphasis of shaded areas, and water which reflects these wavelengths more than other land covers. It is also useful for discriminating soil and vegetation, as well as for mapping different forest types. At these wavelengths, vegetation does not appear very brightly as the energy is absorbed by chlorophyll. This band is the "noisiest" Landsat sensor band, because it is the most susceptible to the atmospheric scattering phenomena.

Band 2 (0.52-0.60 µm), the green band, has similar qualities to the blue band and is within the visible slice of the electromagnetic spectrum, which better reflects the vegetation land covers, i.e. the band which shows the typical green colour we see when looking at vegetation. This band allows a good discrimination between vegetation and bare soils including manmade features.

Band 3, the red band, which ranges from 0.63 to 0.69 microns, is almost completely absorbed by green vegetation (rich in chlorophyll), while it reflects from dead foliage. This band also provides good information in order to discriminate vegetation (also for monitoring vegetation health) from bare soils, and for identifying some types of urban features.

[242] Technical details about the MCSC classification system can be found in chapter 3, section 3.2.2.2

Band 4 is the Near Infrared (NIR) band, which ranges from 0.76 to 0.90 microns. This band, which is almost completely absorbed by water bodies, makes water appear very dark. The bright reflectance of soils and vegetation therefore allows a good discrimination of water/land boundaries. Moreover, this is the most reflective Landsat TM band for vegetation land covers which are rich in chlorophyll (much more than the visible green band), thus showing vegetation very brightly, and with several differentiated shades of brightness. This wavelength is particularly suitable for analysing vegetation and biomass contents.

Bands 5 and 7 are two Short Wave Infra-Red (SWIR) bands which range respectively between 1.55 and 1.75 microns, and 2.08 and 2.35 µm. Both bands provide good contrast between different types of vegetation, and are quite sensitive to moisture, thus allowing suitable images for measuring moisture contents of soils and vegetation. Moreover, band 7 yields important support for analysing soil and geological characteristics, while band 5 could be most appropriate for detecting snow and clouds.

Additionally, the Landsat TM sensor delivers one long-wave infrared (LWIR) band (band 6), also known as the Thermal band (10.40-12.50 µm) at 60 meters of spatial resolution (instead of 30 like the previous bands). This band is mostly used to measure land surface temperature, and the effect of temperatures depending on the daily and seasonal variations. Moreover, band 6 could also be useful to identify vegetation densities and measure plant heat stress. It detects moisture content and differentiates clouds (since clouds tend to be very cold) from bright soils.

Landsat TM Band	Main Applications
1 Blue	Bathymetric mapping; bare soil and vegetation discrimination; forest mapping (deciduous and coniferous discernment)
2 Green	Emphasizing vegetation peaks and vegetation health monitoring; bare land and man-made feature discrimination
3 Red	Plant species identification and vegetation classifying; man-made settlements and bare soils mapping
4 NIR	Water/Land boundaries detection; soil moisture; vegetation monitoring and classification; biomass contents
5 $SWIR_1$	Moisture contents monitoring; vegetation analysis; snow and cloud detection
6 Thermal	Surface temperature mapping; vegetation stress monitoring; clouds and bright soils differentiation
7 $SWIR_2$	Moisture content monitoring; vegetation analysis; mineral and rock discrimination

Tab. 4.5: A summary of the main emphasized features by each Landsat TM band (Source: By Authors)

Besides the capability of each single band to reveal certain specific land cover attributes, perhaps the best way of understanding surface features is provided by the possibility of composing several colour images by using a computer screen colour model for allocating all satellite bands, alternately in the Red, Green and Blue channels. An appropriate selection of bands, for making colour composite images, can have a critical impact on the understanding of specific feature types to be digitalized and then labelled within a landscape under investigation.

It is reasonable to state that three main typologies of colour composite images can be set up based on multispectral sensors (such as for SPOT, QuickBird, Ikonos or Landsat). These are: Natural Colour (or True Colour) image composite; Colour Infra-Red (CIR) images; and Pseudo-Natural Colour Images (see figure 4.17, in section 4.3.3, of this essay).

The natural colour composite image, which relies on the use of bands 3, 2 and 1 (the Red, Green, and Blue channels respectively) in the case of Landsat TM imagery, best reproduces the "real" appearance of the surrounding environment as perceived by the human eye. This image combines the main characteristics of the three visible light bands, as previously illustrated, thus providing a good chlorophyll absorption index in vegetation (band 3), high reflectance values from green vegetation (band 2), as well as good water reflectance (band 1). Even if this combination produces a “quite opaque” image, *those are the colours that people unfamiliar with remote sensing expect to see, and for those people, representing features with reasonably life-like colours helps them interpret the image* (Horning).

The most typical colour infrared composite (or false colour) uses bands 4, 3 and 2 in a RGB model. Since this combination includes the NIR band, which provides high reflectance peaks from vegetation features and a

strong absorption for water, the land/water boundaries appear sharper and differences in vegetation types are enhanced. The CIR image shows vegetation in red tones (instead of green tones), where the brighter reds reveal higher chlorophyll content. Barren or sandy soils, including sparsely vegetated surfaces, are displayed by ranging from white to green shades. Water appears dark blue and tends towards black, the more limpid the water is. Urban areas appear in bluish/greyish tones[243].

Amongst the various pseudo-natural colour combinations, maybe one of the most famous is the 7/4/2 band composite, which is the combination commonly employed by NASA to produce global Landsat mosaics. This image shows vegetation in various green shades (similar to natural colour), but the green tones appear much more brilliant and diversified, because band 4, i.e. the most reflective band for vegetation, is allocated in the green channel of the RGB model; and band 2, which is the green band, in the blue channel. Moreover, band 7 is particularly indicated to highlight minerals, rocks and moisture contents. Band 7 is the SWIR closest to the thermal slice of the spectrum, and is also sensitive to heat sources to a certain extent. When it is allocated in the red channel, it allows good variability for discriminating various barren and sandy soils, as well as differentiating artificial land cover types. These categories appear in various shades of reddish to brown tones, not to mention; white, mostly for soils; while orange, pink and white to light blue for artificial land covers. Water again appears dark blue to black.

The first applications of photo-interpretation procedures used hardcopies of aerial imagery, and the concepts behind this method are the basis for the modern (and increasing) development of automated computer-aided applications based on multispectral and hyperspectral image analysis. When attempting to classify digital imagery, it is important to take into account the advantages and disadvantages provided by both approaches. Regarding this, Richards and Xiuping (2006), offer this helpful point of view (also shown in table 4.6): *photo-interpretation, involving direct human interaction and therefore high level decisions, is good for spatial assessment but poor in quantitative accuracy. Area estimates by photo-interpretation, for instance, would involve planimetric measurement of regions identified visually; in this, boundary definition errors will prejudice area accuracy. By contrast, quantitative analysis, requiring little human interaction, has poor spatial ability but high quantitative accuracy. Its high accuracy comes from the ability of a computer, if required, to process every pixel in a given image and to take account of the full range of spectral, spatial and radiometric detail present. Its poor spatial properties come from the relative difficulty with which decisions about shape, size, orientation and texture can be made using standard sequential computing techniques* (Richards, et al., 2006).

Photo-interpretation (Human Analyst/Interpreter)	Quantitative Analysis (Computer)
On a large scale relative to pixel size	At individual pixel level
Inaccurate area estimates	Accurate area estimates possible
Only limited multispectral analysis	Can perform true multispectral (multi-dimensional) analysis
Can assimilate only a limited number of distinct brightness levels (say 16 levels in each feature)	Can make use quantitatively of all available brightness levels in all features (e.g. 256, 1024, 4096)
Shape determination is easy	Shape determination involves complex software decisions
Spatial information is easy to use in a qualitative sense	Limited techniques available for making use of spatial data

Tab. 4.6: *A comparison of photo-interpretation and quantitative analysis* (Source: Richards, et al., 2006)

In other words, human eyes are not able to detect spectral patterns well, while computers have major limitations for interpreting spatial patterns. Anyway, both approaches (visual and numerical) provide their own effectiveness, and are often complementary. In fact, automatic classification is strictly dependent on visual interpretation of land cover types using the knowledge of expert analysts, who understand the radiometric significance of pixels. They can use it just like an accuracy tool for results assessment or for identifying and selecting specific land cover samples, in order to extract the relative spectral information and then run automatic processes based on it. At present, what we do is therefore a combination of the two approaches.

[243] *This is a band combination popular with remote sensing specialists largely for historical reasons, as this appears similar to what you would get if you took a picture using a camera with colour infrared film. Since infrared film was very popular for monitoring vegetation before the advent of digital remote sensing devices, there is a tendency to continue simulating this effect* (Horning)

4.4.3. Density Slice and Decision Tree: A Basic Approach to Automatic Classification

Computer-based quantitative analysis, which provides automatic classification of different land cover classes and is one of the most investigated techniques, focuses on numerical measurement of the spectral attributes for each pixel in a scene and at each available wavelength. Therefore, it makes it possible to automatically label one pixel, or set of pixels, as belonging to a specific class.

Several approaches, algorithms and software types are currently available for classifying digital data, but maybe one of the simplest approaches for categorising pixels in an image relies on thresholding operations. Thresholding is a contrast manipulation procedure which *segments* the digital information into two or more categories based on the digital number of the pixels. The use of binary or multiple thresholds provides *sharply-defined spatial boundaries that may be used for masking portions of the image* (Schowengerdt, 2007). An example of a thresholding technique is one known as density slicing, which is a process of quick image classification, based on assigning different colours (or even black and white shades), to the brightness ranges of a single band image. The density slice approach, which converts the brightness levels of images to specific sets of colours, aims to arbitrarily allocate the total number of pixels into a predefined number of intervals, dependent on a certain threshold, in order to emphasize specific land cover features. However, this process does not add any extra information to the original image, but just categorizes the pixel values.

It is possible to define the most appropriate thresholds for separating individual colours by using either automatic slicing (i.e. by assigning patches of pixels with similar reflectance values to the same colour) or histogram manipulation. Then the different ground features are coded by colour and quantified by whatever approach adopted. As an example, the greenness degree of an NDVI (from -1 to 1), could be quickly classified into discrete classes of chlorophyll abundance by slicing the whole range of values into logical fixed thresholds; for instance: -1 to 0.2, no vegetation; 0.2 to 0.4, sparse vegetation; 0.4 to 0.7, moderate vegetation; and 0.7 up to 1, dense vegetation areas. Figure 4.27 shows a Landsat TM SWIR band portion graphically (on the left side), with the corresponding histogram that defines frequencies of brightness values; and on the right side, we can see the same image after applying a density slicing operation based on eight categories, with its corresponding coloured histogram. *The analyst can adjust the levels represented by colours to emphasize those features of greatest interest* (Campbell, et al., 2011).

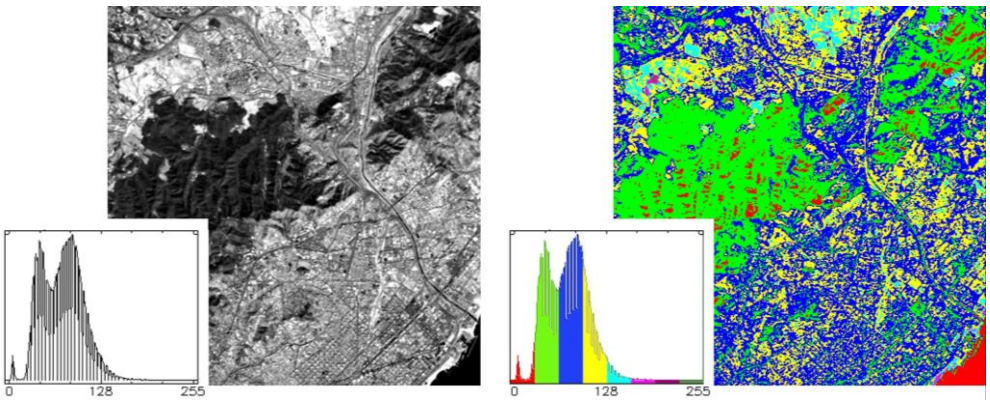

Fig. 4.27: Density slice example, for a Landsat TM SWIR band portion, classified into eight classes of brightness values (Source: By Authors)

Another classification technique, based on thresholding operations, employs binary decisions in order to place pixels into defined classes instead. This is called the decision tree algorithm. Actually, the classification process behind this method can mainly be described as a sequence of binary decisions (conditions), in which every decision, or node, fits inside a tree structure. Each node distributes the total number of pixels (within a set of images), into two classes (0 if data do not match the condition, or 1 if it matches the condition), dependent on an expression based on mathematical functions, or relational and logical operations. Therefore, the decision tree classifier provides a multi-stage classification, where each node is trained separately, and in which the first decision

node provides a selection of pixels based on only one attribute (vegetation or no-vegetation, for instance), while the following nodes will provide further differentiation of the previously classified binary image, according to other attributes (such as the slope greater than 20%, for instance). This means that each node generates one class and each class can then be further divided into two, or more classes, depending on the numbers of nodes and decisions needed for the analysis.

The input data can come from different imagery and information. In fact, data from different bands of multispectral imagery can be combined, between them and/or together with digital elevation data (DEM) or thematic indices such as NDVI, for instance.

4.4.4. The Unsupervised Classification: An Advanced Method

Alternatively to the previous computer-based classification methods which rely on "simple" thresholding operations, two broad classes of advanced automatic classification procedures commonly used in the analysis of remotely sensed data, are referred to as the supervised classification and the unsupervised classification. *These can be used as alternative approaches but are often combined into hybrid methodologies* (Richards, et al., 2006).

Unsupervised classification can generally be understood as a method which relies on identifying, labelling and mapping certain kinds of "natural" groups of pixels[244] (or clusters), essentially dependent on the vectors of spectral values of pixels within a multispectral image, and requires no previous user training or foreknowledge of existing spectral classes. This step of automatic identification of a number of (spectrally coherent) land covers in a landscape is a purely computer-based process used to identify each pixel within an N-dimensional spectral space, belonging to a predetermined cluster dependent on spectral features and distance to the cluster centre. In order to make an effective segmentation of images into classes, the classifier requires previous specification of a suitable expected number of clusters[245]. This entered number provides the starting positions, or centres of the clusters, around which all the pixels within the data will be grouped at first. Then, the algorithms employed to allocate pixels will follow an iterative process in order to progressively optimize the spatial position of the initial centres, and thus changing the final class groupings for the pixels.

Once the final classification of the pixels has been obtained, the analyst then firstly has to label the resulting classes, by comparing samples of pixels from each class through photo-interpretation. This is done using the available ground reference data, which could be from the same original multispectral image or platforms such as Google Earth or even on the ground verification, if possible. Consequently, a series of class merging operations and filtering are often required in order to deliver effective and logical information concerning the land cover composition. This is stored in thematic maps, as the final result of the unsupervised classification.

According to Campbell and Wynne (2011), some advantages of undertaking this kind of classification is that it does not require an extensive prior knowledge of the area under investigation, for instance. Moreover, this technique tends to minimize human subjectivities and also allows us to identify those classes with a very small area, which the human eye would not be able to detect[246]. On the other hand, unsupervised classification can classify certain spectrally homogeneous classes that are not necessarily of interest for the analyst, who often *has limited control over the menu of classes and their specific identities* (Campbell, et al., 2011).

Unsupervised classification relies on different algorithms and is performed by automatically assigning pixels to spectral classes by using clustering methods[247]. In particular, two of the main clustering approaches are discussed here: the K-Means algorithm (Duda and Hart, 1973), and the ISODATA (Ball and Hall, 1967). The K-Means

[244] *The notion of the existence of natural inherent groupings of spectral values within a scene may not be intuitively obvious, but it can be demonstrated that remotely sensed images are usually composed of spectral classes that are reasonably uniform internally in respect to brightnesses in several spectral channels* (Campbell, et al., 2011)

[245] *In practice, the actual or optimum number of clusters to choose will not be known. Therefore, it is often chosen conservatively high, having in mind that resulting inseparable clusters can be consolidated after the process is completed, or at intervening iterations, if a merging operation is available* (Richards, et al., 2006)

[246] *To conduct unsupervised classification, the operator may perhaps specify only the number of categories desired (or, possibly, minimum and maximum limits on the number of categories) and sometimes constraints governing the distinctness and uniformity of groups* (Campbell, et al., 2011)

[247] *The clustering methods, even if generally computationally expensive, provide a key technique for analysing remotely sensed imagery* (Richards, et al., 2006)

algorithm is maybe one of the most recognized clustering and non-probabilistic methods employed in RS. This technique works by calculating the initial mean vectors for a certain number of pixel groups, based on a uniform distribution of the values within the multispectral space. Consequently, the algorithm designates those mean vectors as initial centres of the clusters. In practice, the initial mean vectors (also known as "seeds" or "attractors") are arbitrarily defined for each of the "K" pre-established clusters during this stage. Each pixel in the image is therefore firstly allocated into the class whose mean vector (or seed) is the closest to the pixel vector to be classified. This delineates the first set of decision boundaries. After this initial classification, a new set of cluster mean vectors is calculated, to which the pixels are consequently re-assigned. Thus, an iterative process is undertaken and each subsequent iteration recalculates class means and then reclassifies pixels into the nearest mean vector, based on the minimum Euclidean distance. *All pixels are classified to the nearest class unless a standard deviation or distance threshold is specified, in which case some pixels may be unclassified if they do not meet the selected criteria* (Exelis Visual Information Solutions). *In each iteration, the K means will tend to gravitate toward concentrations of data within their currently-assigned region of feature space*, and this iterative process continues until there is no more significant changes in pixel assignment between successive iterations (Schowengerdt, 2007), or the maximum assigned number of iterations is reached. Figure 4.28 shows a K-means algorithm for a set of data, classified into two classes, in a 2-D space.

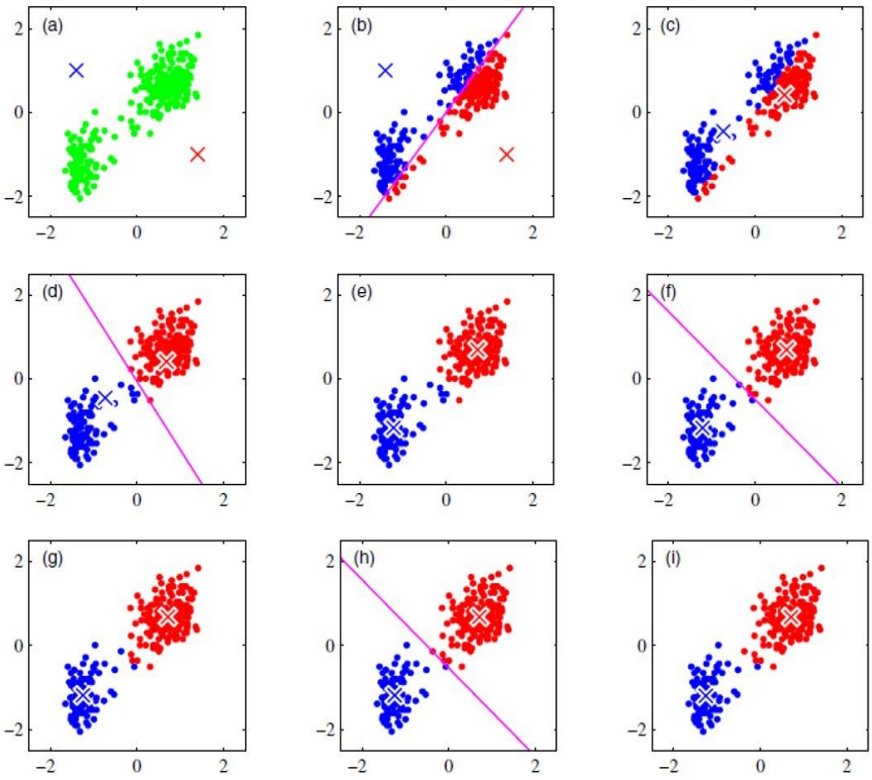

Fig. 4.28: A K-Means algorithm example, in which the pixel values in a 2-D spectral space are first classified depending on two initial cluster centres that are afterwards reallocated following several iterative stages, to finally achieve an effective classification of the pixels into two classes, the blue and the red one (Source: Bishop, 2006)

A detailed description for each stage depicted in figure 4.28, which schematically summarizes the process of unsupervised classification using the K-Mean algorithm, is provided by the same author, as follows: *(a) Green points denote the data set in a two-dimensional Euclidean space. The initial choices for centres μ1 and μ2 are shown by the red and blue crosses, respectively. (b) In the initial E (expectation) step, each data point is assigned either to the red cluster or to the blue cluster, depending on which cluster centre is nearer. This is equivalent to classifying the points according to which side of the perpendicular bisector of the two cluster centres, shown by the magenta line,*

they lie on. (c) In the subsequent M (maximization) step, each cluster centre is re-computed to be the mean of the points assigned to the corresponding cluster. (d) to (i) show successive E and M steps through to final convergence of the algorithm (Bishop, 2006).

The ISODATA classifier is also a method based on minimum distances and actually provides a modification of the K-means algorithm. In fact, during the first stage, this technique also calculates the class mean values for data evenly distributed within the N-Dimensional spectral space, and then it iteratively groups the residual pixels by using minimum distance. However, the following iterative clustering optimization phase (also known as the migrating means technique), *is based upon estimating some reasonable assignment of the pixel vectors into candidate clusters and then moving them from one cluster to another in such a way that the SSE (Sum of Squared Error) measurement of the preceding section is reduced* (Richards, et al., 2006).

In other words, each iteration recalculates mean values and reclassifies pixels with respect to the new means, dependent on the SSE (as depicted in figure 4.29). Iterative class merging, splitting or deleting of clusters also occurs depending on a fixed threshold. Merging of clusters, for instance, depends on values smaller than the threshold, while splitting into two clusters happens if the threshold is too large (Schowengerdt, 2007). The process continues until the pixel values in each class change by less than the selected threshold, or the maximum number of iterations is reached (Exelis).

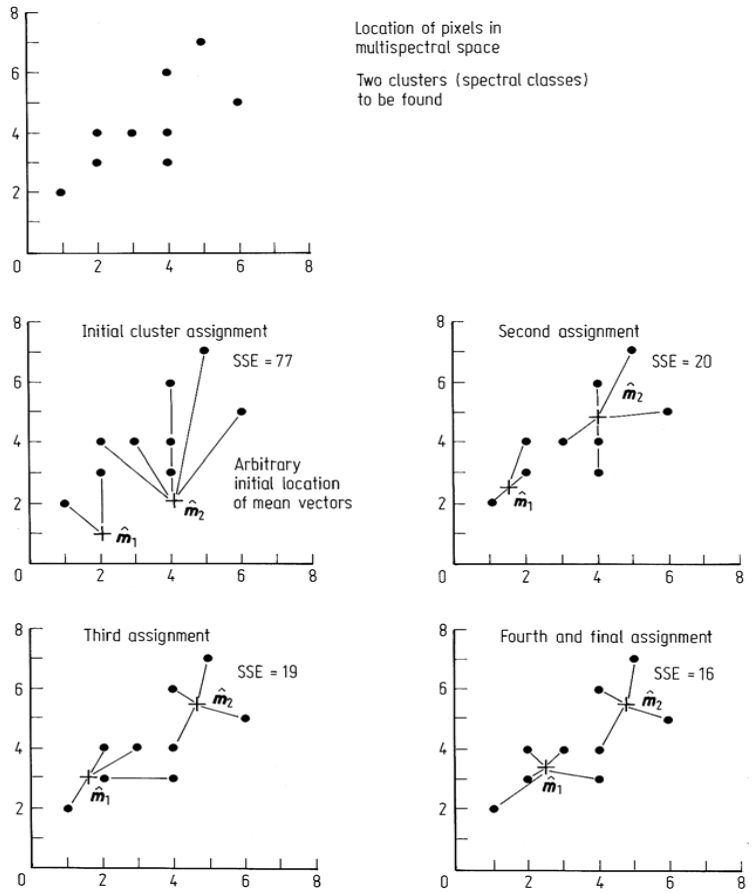

Fig. 4.29: A clustering process for automatic classification, according to iterative optimization (ISODATA algorithm), in which the method leads to a progressive reduction of the Sum of Squared Error (SSE) (Source: Richards, et al., 2006)

With reference to the ISODATA classifier, Campbell and Wynne (2011), argue that despite what certain descriptions imply, the distinction between unsupervised and supervised classification (see section 4.4.5) is not that clear. Instead, this technique is often intended as a form of supervised classification, although it differs appreciably from the classical model of supervised classification. However, from a conceptual standpoint, unsupervised

classification could provide a good example of the coexistence of both methodological approaches, thus making it a sort of "hybrid" classification (Campbell, et al., 2011).

The main difference, with respect to a supervised classification for the K-Means algorithm, is that the latter technique provides the possibility of introducing training data sets (previously defined) in the analysis. These can be designed as the initial cluster centres, with the added possibility of applying advanced algorithms of clustering, such as those based on the use of covariance matrices.

On the other hand, the final cluster mean vectors derived from an unsupervised classification could be employed in supervised processes by applying further algorithms in additional stages, thus keeping those cluster centres as training samples.

4.4.5. Supervised Classification approach: Main Algorithms

The automatic process for digital data classification actually relies on a variety of approaches, but without doubt, the two most explored techniques are supervised and unsupervised classification. The most important difference between these approaches is basically that in unsupervised classification, a clustering algorithm automatically delineates a certain number of clusters based on similar characteristics within the multispectral space[248] (the interaction of analysts in searching for natural groups of pixels is quite minimal or mainly used for reviewing the results, and for post-processing stages for grouping classes, if necessary). Supervised classification requires significant interaction with the analyst, who previously defines (during a so-called training process) a number of groups of known pixels, also named Regions Of Interest (ROI), which correspond to the ground truth information used to undertake the classification process (Campbell, et al., 2011).

The sample groups of pixels or classes, defined by the analysts, are vectors of values within the multispectral space detected prior to executing a clustering algorithm. These regions of interest, which attempt to describe the most effective land cover composition in the scene, provide average vector values of reflectance for each sampled class. Hence the process of classification will assign each pixel, in the image, to the closest previously defined (average) cluster value based on statistical algorithms, as is depicted in figure 4.30.

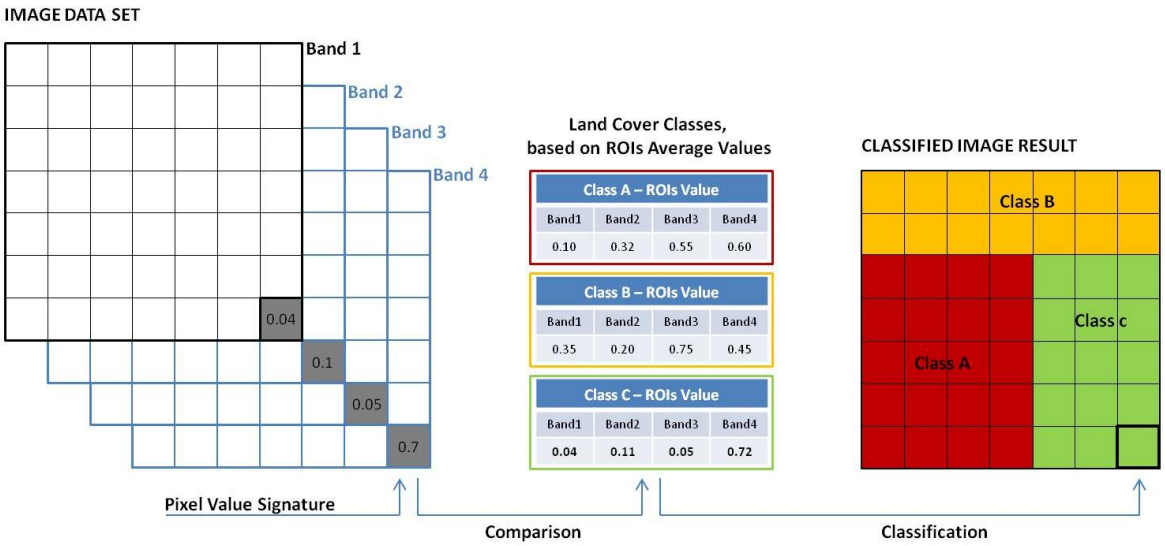

Fig. 4.30: Graphical characterization for a generic supervised classification process (Source: By Authors)

[248] According to Richards and Xiuping (2006), unsupervised classification could be useful for determining a more consistent composition of the spectral classes, within the image data, prior to providing a detailed analysis based on methods of supervised classification. Actually, suitable regions of interest may arise from previous unsupervised classification

The sample classes are commonly defined by on-screen digitalization and labelling, following a photo-interpretation protocol, and are then stored in a sort of training map. Consequently, a suitable selection of samples mainly depends on the analyst's skills and knowledge of the investigated geographical area[249] (on-ground direct observations, apart from other ancillary data, are often employed in order to improve the training map setup).

In practice, the spectral information (or signature) which is extracted through averaging the pixel reflectance values for each homogeneous sampled class, is used for training the computer to recognize pixels with similar spectral signatures. Each pixel is then classified and labelled based on the input training area labels.

According to Richards and Xiuping (2006), the general supervised classification process could be summarized in a few main stages, as follows:

- *Decide the set of ground cover types into which the image is to be segmented*
- *Choose representative or prototype pixels from each of the desired set of classes, i.e. the training data*
- *Use the training data to estimate the parameters of the particular classifying algorithm to be used; these parameters will be the properties of the probability model used or will be equations that define partitions in the multispectral space*
- *Using the trained classifier, label or classify each pixel in the image into one of the desired ground cover types (information classes)*
- *Produce tabular summaries or thematic (class) maps which summarise the results of the classification*
- *Assess the accuracy of the final product using a labelled testing data set* (Richards, et al., 2006).

Supervised classification is strictly related to the use of a variety of algorithms, which can be generally assigned to two broad categories of statistical analysis. These are either based on probability distribution models or on the division of the multispectral space into different areas, dependent on the number of classes to be classified and on distances between pixel values and cluster centres. Four of the most significant statistical algorithms employed for developing the classification method provided in this investigation are discussed in the following sections: the Parallelepiped classifier, the Minimum and Mahalanobis Distance and the Maximum Likelihood[250].

4.4.5.1. Parallelepiped Classification

Parallelepiped classification relies on a simple decision rule to train the computer that basically analyses the histogram of brightness values for each ROI and for each spectral component. An n-dimensional (depending on the multispectral space and a standard deviation threshold from the mean) parallelepiped boundary is drawn for each sample class. The range of values within the training data in each band defines the multidimensional box (or parallelepiped) which will be used to classify all the pixels in the image. Actually, pixels “captured” in a specific parallelepiped are labelled as belonging to that class. The parallelepiped classification is also known as box decision rule, or level-slice procedures (Campbell, et al., 2011).

This method can be useful when quick extraction of classes is needed, for instance, but in many cases it provides a low accuracy of results and a large number of unclassified or erroneously classified pixels. At present, the most relevant disadvantages derived from this technique, as reported by Richards and Xiuping (2006), are, *first of all, the existence of considerable gaps between parallelepipeds, for instance, hence pixels in those regions will be not classified. Previous probabilities of class membership are not taken into account; moreover, overlapping of parallelepipeds will occur with correlated data, since the box sides are parallel to the spectral axes, hence a not effective discrimination of pixels is achieved in that case* (Richards, et al., 2006). Figure 4.31 graphically illustrates the process behind the parallelepiped algorithm, in the case of a two-dimensional pattern space.

[249] *The objective is to identify a set of pixels that accurately represent spectral variation present within each informational region* (Campbell, et al., 2011).

[250] Additional classification methods (not argued in the framework of this investigation) such as the Spectral Angle Mapper (SAM) and the Spectral Information Divergence (SID) classifiers, employ a physically-based spectral classification process by using an n-dimensional spectral angle which classifies pixels (treated as vectors in a space with dimensionality equal to the number of bands), either depending on spectral similarity between spectra (SAM) or based on a divergence measurement among spectra (SID). Besides these, learning algorithms are also available, such as the Neural Net technique, which employs a back propagation process, in order to minimize errors by adjusting the weights in the nodes through a recursive method.

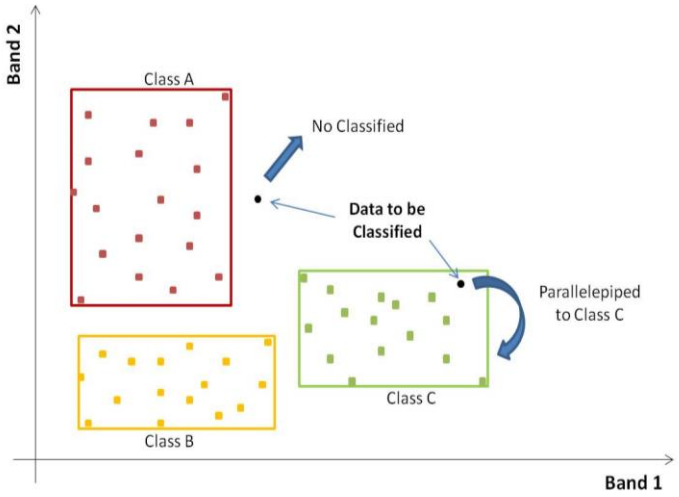

Fig. 4.31: Conceptual scheme of a Parallelepiped classifier, in a two-dimensional spectral space (Source: By Authors)

4.4.5.2. Minimum Distance

The minimum distance classification or more precisely, minimum distance to class means classifier (Richards, et al., 2006), is used to automatically classify unknown pixels in an image as belonging to specific land cover classes in a multispectral space by minimizing the distance between the image data and the class. Actually, the distance is defined as an index of similarity (Japan Association of Remote Sensing, 1999) between group-mean vectors and unknown pixels. This classification method calculates the Euclidean Distance[251], as defined in equation [4.9], between each unknown pixel and the mean vector value of a specific region of interest (or class). All pixels are then classified to the nearest class depending on such a distance, measured in each dimension of the multispectral space at once. Generally, the shorter the distance, the more the similarity.

$$d\,(X_i, m_i) = \sqrt{(X_i - m_i)^t (X_i - m_i)} \qquad [4.9]$$

Where: d = Euclidean Distance
X_i = Data to be classified
m_i = Mean value for a class i
i = 1,....., n
t = Transposed matrix

The clusters calculated using a minimum distance algorithm may appear to be the same as those defined for unsupervised classification. *However, in unsupervised classification, these clusters of pixels were defined according to the "natural" structure of the data. Now, for supervised classification, these groups are formed by values of pixels within the training fields defined by the analyst* (Campbell, et al., 2011). In fact, each class is defined through the use of training data (ROI instrument) and average values of spectral reflectance are calculated in a multidimensional space. The vectors of sampled average values then provide the cluster centres, to which Euclidean distance of the pixels is calculated. Hence, image data will be assigned to the class whose centre provides the shortest distance to the pixels (Figure 4.32). Due to the fact that the minimum distance classifier does not make use of covariance between different spectral bands, but mainly depends on the spatial position of the pixel values in the multidimensional space, the method appears to be especially precise when the variance between land cover

[251] The Euclidean Distance corresponds to the geometric concept of distance, here applied in a multidimensional space.

classes is significant. This provides an efficient classification, however, it does not work so well when the variance of some classes is highly correlated to others.

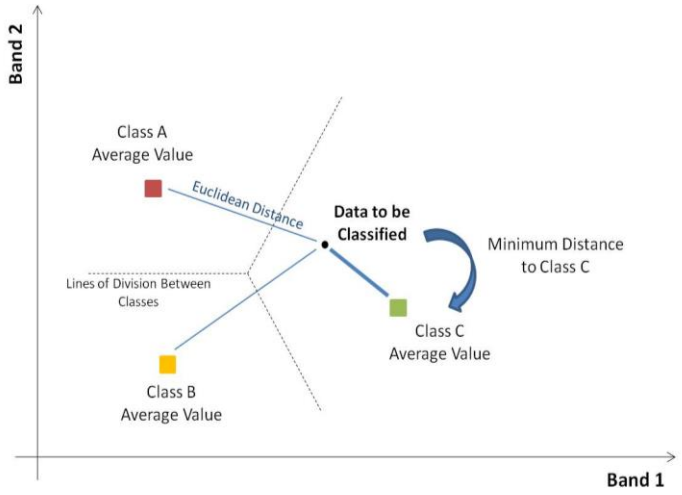

Fig. 4.32: Conceptual scheme of a Minimum Distance classifier, in a two-dimensional spectral space (Source: By Authors)

4.4.5.3. Mahalanobis Distance

Similarly to the Minimum Distance, the Mahalanobis Distance is defined as an index of similarity between sampled cluster vectors and image data. Therefore, the criterion of assigning pixels to a specific class is also based on the smallest Euclidean distance. However, in the case of the Mahalanobis classifier, the distance measured by using the covariance matrix [4.11] between bands is calculated as defined by equation [4.10], for a multivariate vector X and the mean value of a selected class i.

$$d_M(X_i, m_i) = \sqrt{(X_i - m_i)^t \Sigma_i^{-1} (X_i - m_i)} \qquad [4.10]$$

With

$$\Sigma_i = \begin{vmatrix} \sigma^2_{11} & \sigma^2_{12} & \dots & \sigma^2_{1n} \\ \sigma^2_{21} & \sigma^2_{22} & \dots & \sigma^2_{21} \\ \vdots & \vdots & \ddots & \vdots \\ \sigma^2_{n1} & \sigma^2_{n2} & \dots & \sigma^2_{nn} \end{vmatrix} \qquad [4.11]$$

Where: d_M = Mahalanobis Distance
X_i = data to be classified
m_i = mean value for a class i
$\sum_i$ = covariance matrix
t = transposed matrix
i = 1,....., n
σ^2 = variance

For both the Minimum and Mahalanobis Distances, the objective is to estimate the distance from an unknown pixel in an n-dimensional Euclidean space to a set of points which provide centre values of prior defined sampled areas (ROIs). Again, the closer the pixel is to the centre, the greater will be the likelihood that a pixel belongs to that class. However, it is important to keep in mind that when data are strongly correlated between them, the use of minimum distance could provide little accuracy. Hence, the use of the Mahalanobis Distance could

provide an improved instrument to complement the process of classification[252]. Actually, this algorithm, which works with covariance between variables, takes into account all the interdependences and weighs the data depending on the redundancy of information.

4.4.5.4. Maximum Likelihood

An important assumption in statistical supervised classification usually adopted in remote sensing is that each spectral class can be described by a probability distribution in multispectral space: this will be a multivariable distribution with as many variables as dimensions of the space. Such a distribution describes the chance of finding a pixel belonging to that class at any given location in multispectral space (Richards, et al., 2006).

The Maximum likelihood classification is perhaps the most common supervised classification method used in remote sensing and is based on probabilistic computation in order to decide that a pixel belongs to a certain class. In particular, *the Maximum Likelihood (ML) is a standard, pixel based approach that classifies pixel according to the multivariate probability density functions of the classes of interest. Statistical properties of training data sets from ground reference data are typically used to estimate the probability density functions of the classes. Each unknown pixel is then assigned to the class with the highest probability at the pixel location*[253] (Santos, Tenedório, & Rocha, 2006).

This algorithm (based on multivariate normal distribution theory) has been used in the framework of social sciences and in the field of pattern recognition since the late 1940s and has been employed increasingly during the following decades. This is due to the capacity of providing a probabilistic method for recognizing similarities between measurements (Chow, 1957; Sebestyen, 1962; Nilsson, 1965). In remote sensing, the development and improvement of multispectral scanning technology that allows us to collect multispectral digital images (either from aircraft or satellites), has provided the opportunity to employ the maximum likelihood criterion to produce thematic classification maps concerning the land cover composition of large geographical areas (Schell, 1972; Reeves et al., 1975; Strahler, 1980).

The process used behind the maximum likelihood classifier depends on the probability for image data to belong to a predefined land cover class. Therefore, the pixel is assigned to the class with maximum probability (or likelihood). If we take into account two land cover classes i and j, for instance, the decision rule employed to assign a pixel at position X, to the correct class w_i, relies on the following assumption:

$$X \in w_i \quad \text{if} \quad p(X|w_i)\,p(w_i) > p(X|w_j)\,p(w_j) \quad \text{for all} \quad j \neq i \qquad [4.12]$$

Therefore, the likelihood depends on the $p(X|w_i)$, that is, the conditional probability to observe the pixel X in the class w_i (it is also defined as the probability density function), and which is a value known from training data[254]; and $p(w_i)$, which is the (a priori) probability that a class w_i occurs in the image, i.e. the probability with which the class membership of a pixel could be predicted before classification. This prior probability is also plausible to be known, or it can be estimated, based on the analyst's knowledge of the image (Richards, et al., 2006).

The discriminant function $g_i(x)$, employed in maximum likelihood classification, which is applied to each pixel in the image, is calculated as the natural logarithm of the product between the probability density function and the prior probability $p(w_i)$, using the equation [4.13]:

$$g_i(X) = \ln\left\{p(X|w_i) * p(w_i)\right\} = \ln p(X|w_i) + \ln p(w_i) \qquad [4.13]$$

[252] Both classification approaches, i.e. Minimum Distance and Mahalanobis Distance, label all pixels in an image, unless thresholding methods are used (Richards, et al., 2006).

[253] *Some classes requested more samples then others due to its spectral diversity and seasonal differencing* (Santos, Tenedório, & Rocha, 2006).

[254] *There will be as many p(X|wi) as there are ground cover classes. In other words, for a pixel at position X in multispectral space a set of probabilities can be computed that give the relative likelihoods that the pixel belongs to each available class* (Richards, et al., 2006).

For mathematical reasons, the algorithm assumes a multivariate normal distribution of the probability density function for the training classes, which means that the statistics for each sampled class provide a Gaussian distribution of the values in each band, (figure 4.33). Even if it is just a hypothesis, rather than a demonstrable property of natural spectra, it actually leads to certain useful mathematical simplifications (Richards, et al., 2006).

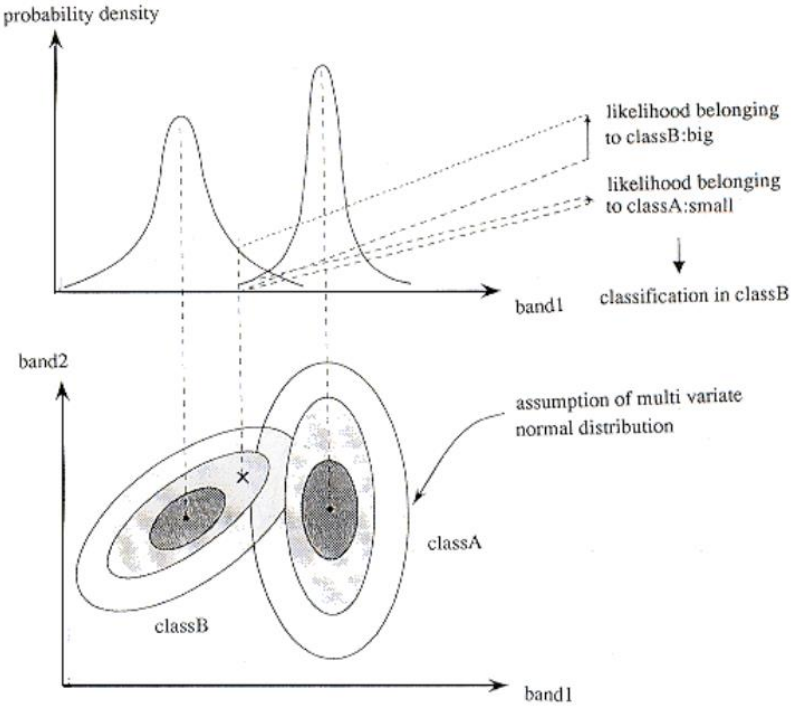

Fig. 4.33: Concept of Maximum Likelihood classifier, in a two-dimensional spectral space (Source: Japan Association of Remote Sensing, 1999)

In the hypothesis of normal distributions for multispectral image data, it is considered an n-dimensional multivariate normal density function using the number of available bands. Thus, the estimated probability density function, which relies on mean vectors and the covariance matrix of the classes, is computed using the formula expressed by the next equation [4.14]:

$$p(X|w_i) = (2\pi\pi^{-N/2} \left| \Sigma_i \right|^{-1/2} \exp\left\{ -\frac{1}{2} (X - m_i)^t \Sigma_i^{-1} (X - m_i) \right\} \qquad [4.14]$$

Where: X = N-dimensional vector data (where N is the number of bands)
p (X|w_i) = conditional probability that a vector X, randomly selected, belongs to class w_i
$|\sum_i|$ = determinant of the covariance matrix of the data in class w_i
m_i = mean vector of data in class w_i
$\sum_i^{-1}$ = inverse matrix of covariance
t = transposed matrix

As reported by Richards and Xiuping (2006), *the resulting term −N/2 ln (2π) is common to all $g_i(x)$ and does not aid discrimination. Consequently it is ignored and the final form of the discriminant function for maximum likelihood classification, based upon the assumption of normal statistics*, and applied to each pixel in the image, is expressed in the equation [4.15]. All pixels in the image will be classified, unless a probability threshold is specified. A thresholding operation should be undertaken in order to avoid misclassification of pixels in the case of

overlooked spectral classes, for instance, or if insufficient training data is available for estimating the parameters of their distributions with any degree of accuracy (Richards, et al., 2006).

$$g_i(X) = \ln p(w_i) - \frac{1}{2} \ln \left| \Sigma_i \right| - \frac{1}{2}(X - m_i)^t \Sigma_i^{-1}(X - m_i) \quad [4.15]$$

Where: i = class
x = *n*-dimensional data
$p(w_i)$ = probability (*a priori*) that class w_i occurs in the image and is assumed the same for all classes
$|\sum_i|$ = determinant of the covariance matrix of the data in class w_i
$\sum_i^{-1}$ = inverse covariance matrix
m_i = mean vector

In cases concerning a symmetrical covariance matrix, the maximum likelihood will just depend upon the Euclidian distance. While in cases where the determinants of covariance matrix are equal to each other, the maximum likelihood will be the same as the Mahalanobis distances classifier (Japan Association of Remote Sensing, 1999).

When applying maximum likelihood classification, a sufficient amount of training data should be selected in order to allow an effective estimation of mean vectors and covariance matrixes (see section 4.5.4.1). Moreover, to achieve the best results, it would be appropriate to reduce the number of bands as this would produce a biased covariance matrix. This could be done by using principal component analysis in order to avoid high correlation between bands, or excessive homogeneity between training data. Bands with little or no variance will produce mistakes in the classification because it becomes a near-perfect linear combination of other bands (Japan Association of Remote Sensing, 1999).

4.5. TOWARDS SETTING UP A SUITABLE CLASSIFICATION METHODOLOGY

In this section, the main objective is to formulate a methodology of land cover classification calibrated using Landsat multispectral imagery (in particular Landsat 5 TM at 30 meters/pixel spatial resolution, and a spectral resolution based on six bands, of which three are visible and three are infrared). It should be able to provide a quick and generalized tool, as objectively as possible, for automatic extraction of digital information regarding land cover over large geographical areas.

The approach will rely on the use of several techniques discussed in the previous chapters in order to set up a system of actions for automatic extraction of information on land cover composition. Later, by employing the process of photo-interpretation mainly in a post-classification stage, we can enhance the results obtained of certain land cover classes by using a sort of semi-automatic process. Actually, several effective algorithms and methodologies already exist for digital data classification, and for plenty of applications, but there is no "ideal" classification for land use/land cover extraction, *and it is unlikely that one could ever be developed* (Anderson, et al., 1976). However, that said, the effectiveness of a classification can be evaluated depending on the aims of the study and the temporal stage to which it refers, not to mention, the employed imagery and the pre-processing robustness.

In fact, as argued by Anderson, et al. (1976), *there are different perspectives in the classification process, and the process itself tends to be subjective, even when an objective numerical approach is used. There is, in fact, no logical reason to expect that one detailed inventory should be adequate for more than a short time, since land use and land cover patterns change in keeping with demands for natural resources*.

Certainly, a key role is played by the analysts and their knowledge for understanding and manipulating digital data prior to applying any classification process. Moreover, various accuracy assessment tests are recognized and provide a degree of goodness for classification results.

At any rate, a set of basic criteria need to be established in order to obtain a suitable classification system, which can effectively rely on satellite or aerial data and that matches the requirements of a certain number of users. A few criteria were suggested by Anderson, et al. (1976):

- *The minimum level of interpretation accuracy in the identification of land use and land cover categories from remote sensor data should be at least 85 percent.*
- *The accuracy interpretation for the several categories should be about equal.*
- *Repeatable or repetitive results should be obtainable from one interpreter to another and from one time of sensing to another.*
- *The classification system should be applicable over extensive areas.*
- *The categorization should permit vegetation and other types of land cover to be used as surrogates for activity.*
- *The classification system should be suitable for use with remote sensor data obtained at different times of the year*
- *Effective use of subcategories that can be obtained from ground surveys or from the use of larger scale or enhanced remote sensor data should be possible*
- *Aggregation of categories must be possible*
- *Comparison with future land use data should be possible*
- *Multiple uses of land should be recognized when possible*

There is an additional concern with reference to the operational scale of analysis which should be taken into account when setting up a classification system. Satellite data sets which rely on low or middle resolution, such as those derived from the Advanced Very High Resolution Radiometer (AVHRR) or Landsat, for instance, are usually best suited for global or regional analysis, but these become quite inaccurate for land use/land cover investigations at a local scale. *Similarly, fine resolution land cover data sets (e.g. four meter or less spatial resolution) are very appropriate for local land use planning, but are generally inappropriate for regional to global analyses*[255] (Vogelmann, et al., 2001).

4.5.1. A Pixel-Based Classification Approach

The amount of radiation reflected by matter (found within a certain range of the electromagnetic spectrum) is recorded in each pixel of a digital image and provides a numerical value of brightness (Digital Number) that identifies different physical features of objects. Therefore, depending on those values, it is possible to cluster together several pixels with similar characteristics by using two broad classification approaches: the pixel-based classification and the object-based classification.

While the traditional pixel-based classification classifies each pixel according to certain statistical values, the object-based classification first sorts pixels into object primitives, builds so called segments and then assigns each segment to a class[256] (Santos, Tenedório, & Rocha, 2006).

Perhaps one of the most significant differences between the two approaches is that the pixel-based analysis measures the brightness information stored in each pixel individually; while the object-based analysis, which is a rather newly developed technique with respect to the pixel-based one, focuses on prior subdivision of RS imagery into different image-objects. This is defined as a set of pixels with similar spectral features, thus allowing further measurement of attributes; such as the size of the objects (area, or length), shape (compactness, rectangular fit, elongation, etc.), texture (range, mean, variance, homogeneity, entropy) and spatial relationships surrounding the pixels. Synthetically, we could define the process behind the object-based analysis as being based on two main stages: image segmentation, which aims to delimit objects using homogeneity criteria and spatial contingency; and then subsequent classification, which relies on finding objects with similar features, either spectral or spatial.

A pixel-based clustering method, which is the one employed in the framework of this investigation for classifying Landsat 5 TM imagery, classifies depending on spectral similarities using a pre-defined taxonomic system of land cover classes, without taking into account spatial relationships between objects (Blaschke, et al., 2001).

[255] A detailed scheme of the spatial relation between pixel size (and thus different sensor types), and the operational scale of analysis is provided in chapter 4.5.7.2

[256] According to Santos, Tenedório, & Rocha (2006) for coarse spatial resolutions (they speak about a spatial resolution of 300m pixel), *land cover characteristics such as texture or form that can be of great use in an object-oriented context, are not very explicit and, therefore, could not be explored*. They argue that *in objects with a minimum mapping unit of 9ha, the form is not clearly present*.

In practice, the spectral pattern most commonly provided by each pixel (averaging values of a set of sampled pixels depending on a hyperspectral or multispectral space) is used as a numerical basis for the categorization of different classes with similar characteristics in each available spectral band. This automated technique, which links a label to a pixel representing certain physical features of a particular land cover type, relies on the use of some classical pixel-based methods (such as the minimum distance, parallelepiped or the maximum likelihood classifiers), as discussed during the previous section 4.4.5.

Therefore, *the purpose of acquiring remote sensing image data is to be able to identify and assess, by some means, surface materials and their spatial properties* (Richards, et al., 2006). Many scientific studies, besides those based on field and laboratory measurements, demonstrate that specific objects on the ground provide singular spectral responses, which can be captured by using remote sensors, as shown by image 4.34 for Landsat 5 TM imagery. Based on these spectral characteristics, it is possible to detect similar objects within certain geographical areas stored in a digital dataset (Anji Reddy, 2008).

For example, as argued by Richards and Xiuping (2006), *if for each pixel, measurements of reflection at 0.65 μm and 1.0 μm were available (i.e. we had a two band imaging system) then it should be a relatively easy matter to discriminate between the three fundamental cover types based on the relative values in the two bands. For example, vegetation would be bright at 1.0 μm and very dark at 0.65 μm whereas soil would be bright in both ranges. Water on the other hand would be black at 1.0 μm and dull at 0.65 μm. Clearly if more than two measurement wavelengths were used more precise discrimination should be possible, even with cover types spectrally similar to each other* (Richards, et al., 2006). In reality, the successful development of remote sensing of the environment over the past decade bears witness to the validity of the aforementioned capability of recording and measuring certain physical properties of matter from a remote distance (Anji Reddy, 2008).

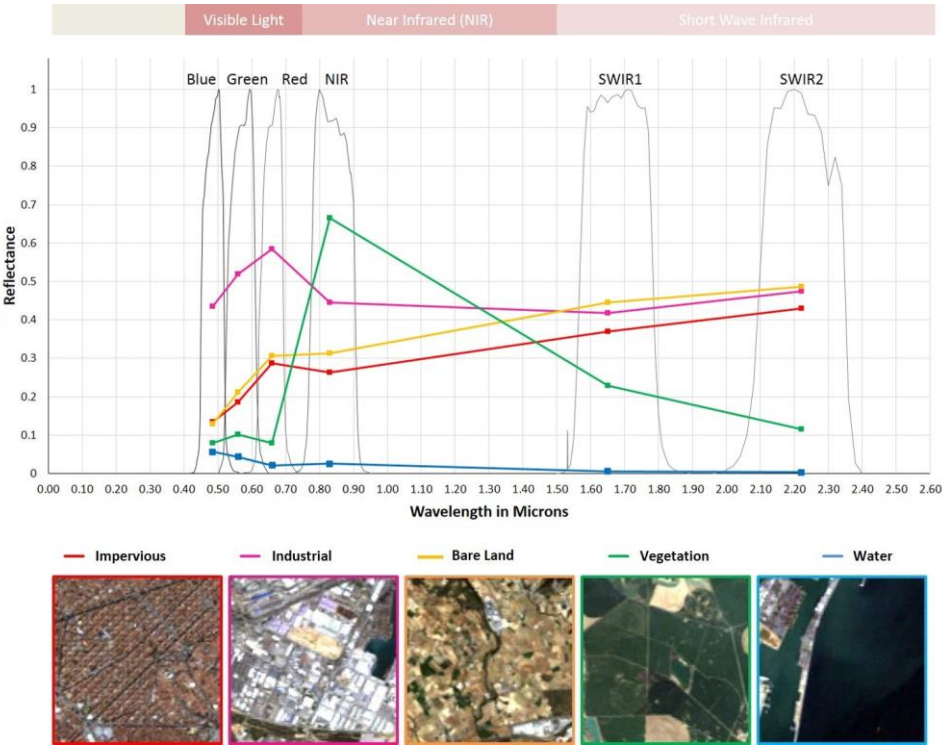

Fig. 4.34: Spectral response sample for some (key) generalized land cover classes, based on a six band multispectral image, as captured by a Landsat 5 TM sensor (Source: By Authors)

Certain criticism is due when applying automatic processes to digital data classification, whether using a pixel-based or object-based approach. First of all, it is vital to take into account the relationship between spatial resolution and classification method. In fact, object-oriented methods are more suitable when classifying high-

resolution imagery, i.e. when the merging of single pixels into an object provides a reasonable solution for delineating entities on the ground and which best correspond to different physical features, even if the segmentation follows certain mathematical abstraction when grouping similar pixels into objects. On the other hand, when working with low or medium resolution imagery, as in our case, it does not make sense to identify objects by summing up pixels prior to applying clustering algorithms. This is because each pixel of 30 meters of spatial resolution can allocate more than one object at once, and this generates a certain mixing of information, due to the averaging of different brightness values. Instead, it would be much more effective to use prior procedures for the un-mixing of spectral information, to obtain the best separation of general land cover categories, such as vegetation, water, etc. The Venn diagram in figure 4.35, as depicted by Potere, et al. (2009), provides an interesting representation of those theoretical areas where overlapping of information could occur (i.e., in which spectral information tends to mix) when a per-pixel automatic classification process, mainly for low-to-medium spatial resolution data, is undertaken to identify all the pixels as belonging to certain main land cover classes (such as the built, the cultivated and the natural environment).

Within this generalized land cover structure, based on the three comprehensive land cover types, it is also described how the urbanized areas (which are the main target of this investigation) supposedly tend to spread across other classes when using automatic classification[257]. *The red oval represents urban areas, a subset of the built environment that includes: (a) areas of contiguous built land, (b and d) areas of interspersed built and cultivated or built and natural land, and (c) areas that contain a mosaic of all three types. This classification system reflects the fact that measurement of urban areas is sensitive to the effects of resolution: a reduction in the size of the minimum mapping unit generally reduces the proportion of landscape elements (e.g. pixels) that are classified as mixtures of the three land-use categories* (Ozdogan, et al., 2006; Potere, et al., 2009).

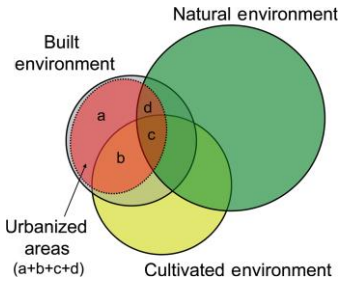

Fig. 4.35: A Venn diagram which describes how pixels of urbanized areas (red) behave within a land cover structure based on three main land cover classes: natural (green), built (grey) and cultivated (yellow) environments (Source: Potere, et al., 2009)

Even if the purpose of this study is to provide an automated process, based on a per-pixel approach for classifying medium resolution digital data, it is critical to take into account the actual effectiveness of automation (consistent with the above assumptions). This study aims to provide a relatively fast, as-accurate-as-possible standardized classification of those comprehensive (and generalized) categories, fundamental for describing landscape composition. However, human efforts should always be employed for final reviewing, label editing and if necessary, re-classifying those areas not reliably labelled. Actually, *any type of digital image classification, be it pixel-based or object-based, will be at best semi-automated* (Congalton, et al., 1999).

4.5.2. Effectiveness of Making a Generalized Nomenclature of Land Cover Composition

Land cover products have often been developed according to specific project needs, with methods and results generally not designed to extrapolate to other areas or to crosswalk to different land cover schemes. These

[257] *Within a land cover framework composed of natural (green), built (grey) and cultivated (yellow) environments, each coarse-resolution pixel belongs to one or more of the three environments. Urbanized areas are pixels completely dominated by the built environment (a), or pixels containing mixtures of several environments but are majority-built (b, c, d)* (Potere, et al., 2009)

approaches have often resulted in remote sensing datasets and methods that develop categories that are difficult to compare (spatially and temporally) and have limited flexibility for other uses (Homer, et al., 2007).

In order to avoid the above mentioned problems of data comparison and flexibility of remote sensing results, a major part of a classification system should involve the setting up of a recognized and standardized nomenclature[258] (prior to beginning an automatic process of pixel clustering) suitable for effectively defining the major structure of a landscape at a global level.

For a classification system to be suitable at a global level, it should be highly compatible with other existing information systems (or at least the main ones). This would make it possible to undertake several broadly acknowledged, relevant, spatial analyses over time, and this could possibly be linked to other critical global socio-economic variables. Therefore, the structure of the nomenclature, which will rely on a list of homogeneous land cover categories, needs to accurately summarize the main required information in a *highly reduced form while attempting to maintain a maximum information content* (EUROSTAT, 2001). Moreover, a hierarchical structure of nomenclature is often required for achieving the best simplification of the complexity of interactions between land cover types. The organisation of categories in hierarchical levels of classes and sub-classes allows us to convert the real complexity of the environment into a conceptual tree of linkages based on accepted terminology. Thus, reflecting the significance of a landscape composition as well as possible through the use of a common language.

A simplified nomenclature of 20 categories, based on two levels of generalization[259], as depicted in table 4.7, is provided for the land cover classification system in this study. Actually, the first level is based on four overall categories, using other principal land cover/land use classification systems (as was discussed in Chapter 2); while an advanced second level of generalization relies on twenty land cover sub-classes.

LEVEL I		LEVEL II			RGB
ARTIFICIAL AREAS	1.0	1.1	Urban Areas and Main Transport Units	1	255,0,0
		1.2	Large Industrial and Commercial Parks	2	255,0,255
		1.3	Land Movements, Extraction and Dumpsites	3	85,26,139
PLANTED/ CULTIVATED	2.0	2.1	Dense Crop Vegetation	4	255,255,0
		2.2	Moderate Crop Vegetation	5	238,238,0
		2.3	Row Crop	6	205,205,0
		2.4	Arable Land	7	139,139,0
		2.5	Wet Crop	8	255,165,0
		2.6	Greenhouses	9	205,41,144
FOREST AND NATURAL AREAS	3.0	3.1	Dense Forest	10	0,139,0
		3.2	Moderate Forest	11	0,205,0
		3.3	Scrubland	12	0,238,0
		3.4	Natural Areas with Sparse Vegetation	13	0,255,0
		3.5	Sandy Areas	14	205,104,57
		3.6	Bare Land	15	160,82,45
		3.7	Snow	16	255,255,255
WATER AND WETLANDS	4.0	4.1	Deep Water	17	0,205,205
		4.2	Medium-depth Water	18	0,238,238
		4.3	Shallow Water	19	127,255,212
		4.4	Wetlands	20	0,139,139
NO DATA	5.0	5.1	No DATA		0,0,0

Tab. 4.7: The nomenclature structure of the Land Cover classification system (Source: By Authors)

[258] The term nomenclature, which labels all of the possible detectable land cover classes that compose a landscape, is not to be confused with a legend. The legend actually provides a display of categories derived from the nomenclature and arranged for a specific purpose, such as thematic mapping. In most cases, the legend represents a sub-set of the nomenclature dependent on the aim and the scale of analysis. However, a classification system should be a whole and generalized representation of the landscape, independent from scale and thematic exemplifications.

[259] Further third and fourth levels, such as the case of CORINE Land Cover, SIOSE, or the MCSC system for Catalonia, should provide more advanced details of land uses

As stated in a previous section, 4.4.1, the terms land use and land cover are frequently used indistinctly or interchangeably within classification systems. In the framework of this investigation, the proposed classification system relies on the use of nomenclature essentially derived from the analysis of ground reflectance, i.e. from an automated process of pixel-based classification. Therefore, what is detected is mainly land cover types which are observed by satellites, and not land uses, except those cases in which the use is strictly related to physical characteristics, thus producing a clear differentiation in the cover types[260].

The category 1.0, at level I, named Artificial Areas, refers to the urban environment. This class mainly comprises all of the urbanised surfaces, thus including those areas with much of the land covered by built-up structures: Residential areas, industrial and commercial complexes, transportation and strip developments alongside main roads (Anderson, et al., 1976), ports and airports, as well as land movements and extraction sites, form part of this category of land cover. At level II, class 1.0 has been separated into three sub-classes based on different roof reflectance: Urban Areas and Main Transport Units (class 1.1); Main Industrial Estates, and Commercial Parks (class 1.2); Land Movements, Extraction and Dumpsites (class 1.3).

At this level of class generalization, some criteria is required to explain the choice of the sub-categories. In fact, when we speak about urban, industrial or extraction areas, we refer to specific uses. Therefore, in the case of higher spatial resolution imagery, some more advanced methods and data could be developed to better detect them or obtain further details. Anyway, in order to avoid misclassifications as much as possible, the choice of sub-classes has basically been created from the physical differentiation provided by diverse cover reflectance values, as the only available discriminating factor. The geographical area under investigation provides certain peculiarities in terms of urbanization processes, mainly due to local building practices and planning as well. The use of zoning, for instance, allows us to segregate important industrial complexes which tend to have buildings covered by metallic roofs. It is not a strict rule, of course, as other materials are employed, but usually the mix of reflectance from a pixel of 30 meters within industrial areas may be isolated from urban areas. Actually, not only for this geographical localization, industrial areas are not necessarily directly in contact with urban areas. Class 1.2 may include, besides industrial buildings, a wide array of other types of land uses; such as large parking lots, electric power generating stations, oil refineries, ports and airport facilities.

Within an urban area, roofing tiles, bricks and asphalt are commonly used to cover buildings, squares, streets or parking lots. This makes it possible to detect the main urban settlements to a certain extent. However, at this spatial resolution of the imagery, several difficulties greatly reduce the capability of differentiating the road network from the residential sector (except in the case of big transportation corridors such as highways). Even if vegetation and water on the fringe of an urban area are not be generally included in class 1.1, those natural areas surrounded and/or dominated by urban development form part of this category.

Finally, class 1.3 comprises those anthropized areas that rely on reflectance values of uses related to materials, such as bare dry soil. This is the case of structures associated with mining operations, certain extraction uses and areas designated for future urban development[261].

With regard to the following categories of level I, the subclasses now do not strictly rely on uses, but instead, the nomenclature mostly reflects the degree of intensity of pixel brightness, thus classifying the different spectral responses coming from the ground.

The Planted/Cultivated class at level I, for instance, broadly identifies farming activities and those uses primarily targeting food production, but at level II, the taxonomy discriminates different degrees of greenness provided by the pixels. In fact, while dense and moderate crop vegetation classes reflect different amounts of grass abundance, row crops and arable lands depend on the partial or total absence of grass cover within agricultural areas. Wet crops depend on the presence of water that modifies the normal degree of energy absorption of croplands, by mixing the spectral information of both water and lawn (such as rice fields, for instance). Actually, where farming activities adjoin wet areas, the exact boundary of crops may be difficult to distinguish, thus agricultural land could fall into a wetland category. Anyway, *when wetlands are drained for agricultural purposes, they should be included in the Agricultural Land category* (Anderson, et al., 1976). *The interface of Agricultural Land with other categories of land use may sometimes be a transition zone in which there is an intermixture of land uses*

[260] Commonly, detailed land use discrimination relies on photo-interpretation techniques and the use of ancillary data

[261] Although it is extremely difficult to detect these categories from remotely sensed data, and by using automatic processes of classification, mainly due to the mixing of information that occurs with other types of natural soils, but some main settlements can be discriminated.

Universidad Politécnica de Cataluña, Barcelona TECH
Departamento de Tecnología de la Arquitectura
Centro de Políticas de Suelo y Valoraciones
Nicola Colaninno, Josep Roca Cladera

*(*even*) at first and second levels of categorization*. Pasture, for instance, is really difficult to be separated from croplands based on reflectance values, and scrublands may be confused with some crop activities. This is also true for some urban land uses covered by grass, such as parks and large cemeteries, which often need further processes to be classified as urban green areas (Anderson, et al., 1976). The "artificial" covers of greenhouses, separated in class 2.6, are detected based on a different reflectance response, with respect to both crop and urban uses, although this kind of land cover may produce similarities with industrial uses.

The Forest and Natural Areas class, at level I, attempts to provide exhaustive mapping of areas generally untouched by human intervention. Even if several productive activities (or uses) are forest related, it is extremely difficult to detect them through remote sensors based on spectral response only. Similarly, at Level II, in order to effectively differentiate this category in subclasses like deciduous, evergreen, or mixed forest, for instance, one should have at one's disposition further image data acquired during a different time interval at least[262]. Therefore, based on tree-crown areal density and then only in relation to the spectral response of pixels, forest areas are detailed in dense and moderate forest, scrubland and natural areas with sparse vegetation. Although *forests generally can be identified rather easily on high-altitude imagery* (Anderson, et al., 1976), enhanced results, for discriminating these classes from crop lands, have been achieved by using further information, such as vegetation indices and slope. Similarly, sandy areas, bare land and snow, which are included in the generalized class of Forest and Natural Areas, would also need advanced information (specific indices, thermal images, as well as topological features) in order to avoid misclassifications. In particular, sandy areas may mix with land movement or extraction sites, for instance, or bare land may mix with urban areas, while snow could be confused with some metals or clouds. Moreover, likewise for crop lands, often the boundary between forest/natural areas and urban settlements may be difficult to delineate precisely. According to Anderson, et al. (1976), *lands that meet the requirements for both forest/natural, and urban areas, should be placed in the latter category, by using effective post-classification procedures.*

The delineation of water depends, to a certain extent, on the spatial and spectral resolution of imagery (besides the scale of analysis the thematic information is aimed at). For many investigations, the purpose would be a precise detection of size and number of water bodies, for instance, and this should be obtainable from small-scale remote sensor data with considerable accuracy (Anderson, et al., 1976). This is not the case. Therefore, the proposed classification procedure for mapping water, which relies on the use of Landsat imagery at medium resolution and six spectral bands, has been based on measuring the different spectral responses from different degrees of light absorption. Further information has been provided by using topographic data and specific indices, such as water indices and wetness. This approach has facilitated the use of four subclasses, at level II; Deep, Medium-depth, Shallow Water and Wetlands, for detailing the class Water and Wetlands of level I. The wetlands have been kept in this class when few or no agricultural use exists.

4.5.3. Data download, Pre-Processing Steps and Mosaicing of Multispectral Imagery

The main objective of this section is to provide a proper method for automated classification of huge geographical areas, achieving a reasonable degree of accuracy and in a relatively brief time period. To do so, the multispectral imagery from the Landsat program, at 30 metres of spatial resolution, has been employed for several reasons. Firstly, in the framework of The Earth Observation programs through space platforms, Landsat is perhaps one of the longest running systems and the first satellite, named Landsat 1, was launched in 1972. Thenceforth, the program has been operating continuously counting 8 consecutive missions (Landsat 8 was launched in 2013). This provides a crucial instrument for undertaking several highly accurate land monitoring analyses. Moreover, the medium spatial resolution, effectively meets the objective of producing thematic maps of the entire Mediterranean side of Spain, by maintaining a suitable level of details for spatial analysis at a regional scale. Finally, the possibility of freely accessing and downloading Landsat imagery offers the opportunity to undertake plenty of experiments for various users, thus allowing knowledge to be increasingly in the public domain.

[262] Land cover maps should be as much accurate as possible, therefore if two forest types (such as evergreen and deciduous, for instance) are relatively inaccurate, it could be more useful to combine them into a single forest class, thus providing much higher accuracy. This could generate a significant increase in the utility of the information.

Landsat imagery is currently held and managed by the United States Geological Survey[263] (USGS), and is freely downloadable through two main platforms: GloVis at http://glovis.usgs.gov/, and EarthExplorer at http://earthexplorer.usgs.gov. Many scenes are ready for immediate download because they are already pre-processed at primary levels of correction, and unprocessed downloadable scenes can be requested.

The USGS Global Visualization Viewer (GloVis), which was used in this study, is a quick online search and order instrument for selecting and downloading satellite data. The platform allows access and interactive selection of all available imagery from the Landsat program; i.e. Landsat 7 ETM+, Landsat 4/5 TM, and Landsat 1-5 MSS, besides EO-1 ALI, EO-1 Hyperion, MRLC, and Tri-Decadal data sets, as well as Aster TIR, Aster VNIR and MODIS. A graphic map display, as shown in figure 4.36, allows the user to select any area of interest and immediately view all available browser images, within the USGS inventory, for the specified location.

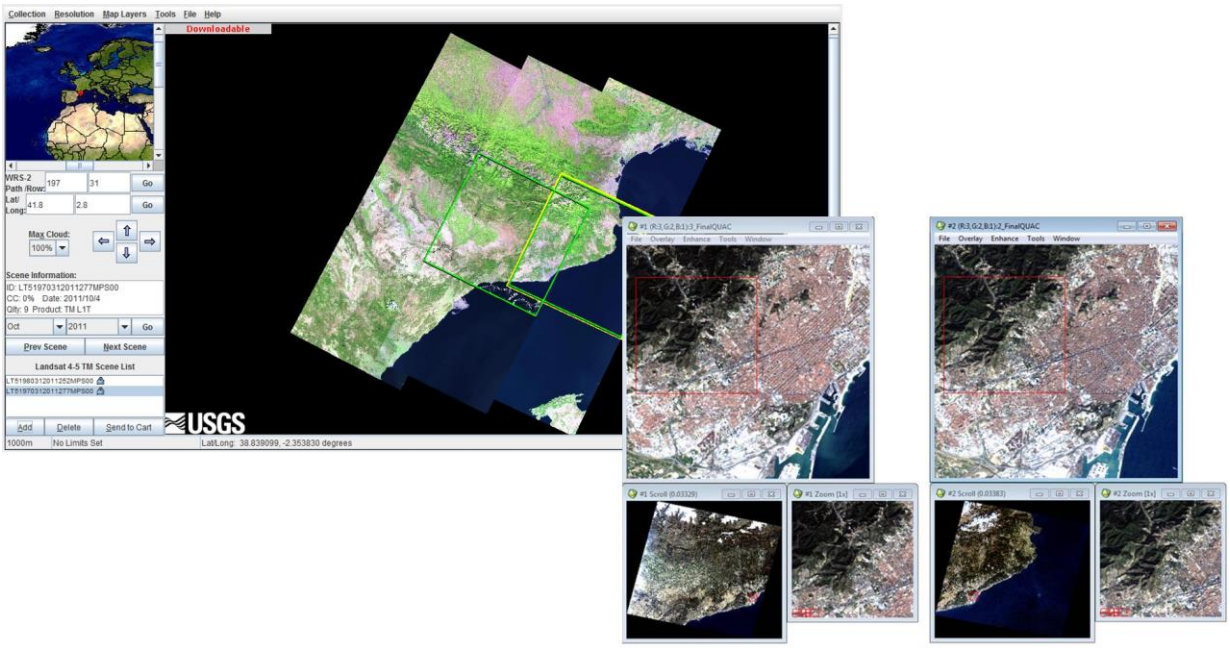

Fig. 4.36: The USGS GloVis platform; and two Landsat TM image samples[264] of Catalonia, loaded in RS software (Source: By Authors)

The image above shows a mosaic of Landsat 4-5 TM scenes, around the region of Catalonia, observed by the use of the USGS GloVis interface. Two images have been selected and downloaded, as an example, and then handled through the use specific software suitable for advanced Remote Sensing procedures.

The GloVis interface provides a user friendly tool for downloading digital imagery (either aerial or satellite and from various datasets). All the available data is listed under the “Collection” menu, on the menu bar. Furthermore, through the "Map Layers" menu, advanced information can be obtained about administrative boundaries, country boundaries, the collection grid, roads, water, north arrow, cities and other layers, such as protected areas. Several tools and search options allow better exploration of images available from the archive, and selection of the desired scenes and data. The arrow buttons or the global locator map near the top left of the display both allow navigation around the earth's surface, to obtain imagery of the geographical area to be analysed. It is also possible to directly specify a location by entering the desired WRS-2 "path" and "row" or, alternatively, latitude and longitude. Advanced search options are available by limiting the scene parameters. It is possible, for

[263] The USGS is the Nation's largest water, earth and biological science and civilian mapping agency. It is a science organization that collects, monitors, analyses and provides scientific understanding of the Earth’s environment and ecosystems, natural hazards and resources at a global level. The USGS carries out large-scale, multi-disciplinary investigations and provides impartial scientific information, also concerning impacts of change on climate and land-use. It is directed at resource managers, planners and other customers.

[264] © LANDSAT Image Copyright 2011, from USGS

example, to set search limits (in the tools on the menu bar), depending on year (start and end), month (start and end), and percentage of cloud cover (minimum and maximum), as well as by entering the location name. The maximum admissible cloud cover percentage can also be selected by using the "Max Cloud" drop-down selector.

The "Prev. Scene" and "Next Scene" buttons facilitate temporal navigation for one selected (highlighted) scene. Otherwise, a specific date can be entered by specifying month and year (depends on the sensor collection dates). Moreover, in order to better visualize the selected scenes, a limited "zoom in" and "zoom out" can be achieved through the "Resolution" menu on the menu bar (USGS). Generally, all Landsat standard data products (as downloaded) are already pre-processed according to the Standard Terrain Correction (Level 1T), and delivered at Level 1 Product Generation System (LPGS), as detailed in the previous section 4.3.1.

The Mediterranean side of Spain is administratively separated in five Autonomous Communities: Catalonia, Valencia, Murcia, Andalucía and the Balearic archipelago and this covers an area of about 159˙300 Km^2 that accounts for 31.5% of the whole national territory of Spain. Twenty-three Landsat TM scenes were employed to cover this geographical area, for the nominal period of the year 2011. However, “optimal” images are often not available for the time period under investigation due to various “impurities”; such as clouds or haze, or the smoke from bushfires, for instance. Occasionally, the lack of data for the appropriate period, and an additional lack of previous knowledge of the “optimal” period for the best land cover separability for each scene (Vogelmann, et al., 2001), as shown in figure 4.37, required extra effort during the scene-selection phase of the study.

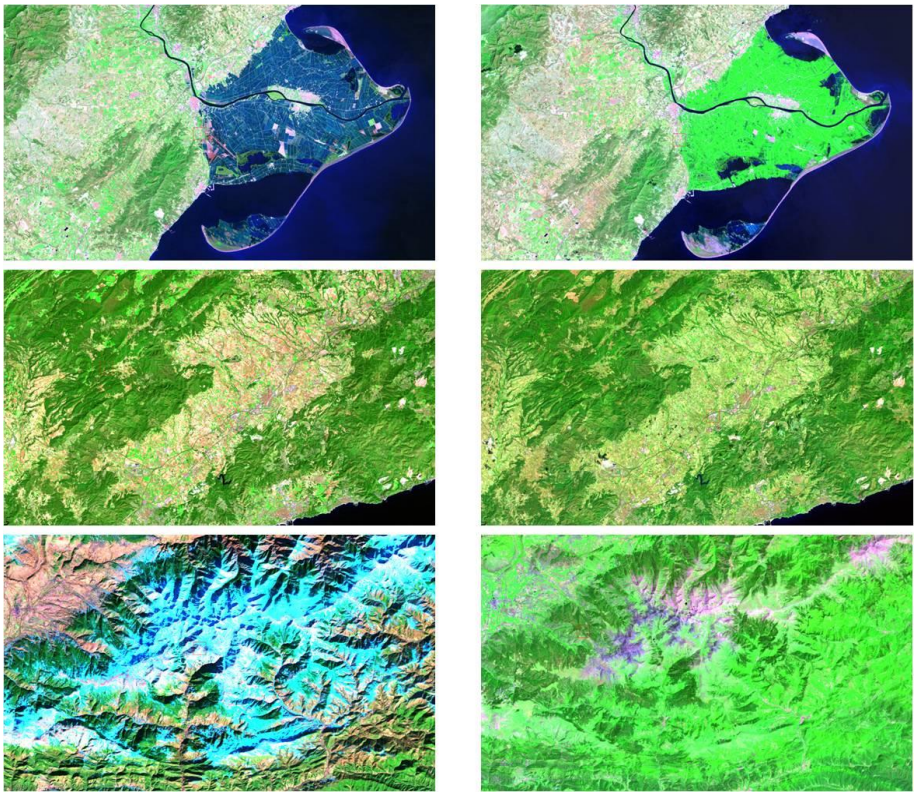

Fig. 4.37: Samples of seasonal differences of reflectance values, for different land cover types, and cloud covering variation, within the same geographical areas (Source: By Authors)

In order to compensate for the above mentioned restrictions, the year 2011 is intended as a nominal period based on the use of Landsat TM imagery, which refers to a time period that ranges from one year before

(2010) to one year after (2012) with respect to the analysed time period[265]. This approach allows us to have several images for each scene at our disposal, thus allowing the possibility of selecting the "best" information available during that time. Consequently, one single scene can be the result of merging different temporal information by employing arithmetic operations within the digital data. In this way, three main approaches could be used to combine imagery. In fact, based on a stack of image scenes, it is possible to average all reflectance values of the stack, pixel-by-pixel, once outlier values, such as clouds, have been removed (by masking, for example). Similarly, it would also be possible to directly select required pixel values which fall in an average range of values for the stack. Finally, the undesired masked values from one image could be directly substituted with "valid" data from another image.

Several studies rely on the use of averaging methods; such as, for instance, the Mean Compositing method which consists of averaging (for each pixel and in each spectral band) all the valid reflectance values acquired during the chosen compositing period (Vancutsem, et al., 2007); or the GlobCOVER 2009 temporal reflectance compositing, in which an iterative procedure is first applied for detecting "valid" surface reflectance values, and the mean is then applied over the "valid" values at several temporal frequencies (Arino, et al., 2011).

Within this research, thermal images have been first employed for quickly masking clouds using the ACCA (Automatic Cloud Cover Assessment) algorithm. A threshold between 295 and 300K is used for detecting all potential cloud pixels. *If a pixel value exceeds 300K, a realistic cloud temperature maximum, it is excluded and labelled as non-cloud in the mask. All pixels with temperature values less than 300K are masked as clouds*[266] (Irish, et al., 2006). Additionally, the minimum image derived as a composite image of the minimum values within the entire stack is used to mask potential shadow pixels. No other filter has been applied for selecting "valid" values from a scene because a relatively suitable number of cloud-free images, or a low percentage of cloud cover, are available within the geographical area under investigation for the Landsat TM sensor and during the selected period. Once clouds and shadows are masked, and before averaging all the available valid data, a multi-date effect correction procedure has to be undertaken on all image scenes, in order to minimize the differences of brightness values between images caused by seasonal changes. To do so, one main image is first selected from the stack of all Landsat TM images collected for the same scene between 2010 and 2012. The remaining information provides secondary images, used to enhance the main one. *The main image refers to the principal image to be used in subsequent analysis, and which possesses less cloud and shadow area than the secondary image, used to supplement the values for cloud and shadow areas of the main image. Because of the time difference, and assuming no significant phonological difference, the brightness of the secondary image should be adjusted to the same level as main image* (Song and Civco, 2002).

This statistical approach, as developed by Caselles (1989), relies on the use of statistical characteristics of multi-date images, such as mean and standard deviation, by maintaining a main reference image. The following equation [4.16] has been applied to the stack of images for each scene.

$$DN_{corr} = Mean_{main} + (DN_{secd} - Mean_{secd}) * SD_{main} / SD_{secd} \qquad [4.16]$$

Where: DN_{corr} = corrected brightness of the secondary image
DN_{secd} = original brightness of the secondary image
$Mean_{main}$ = mean of pixel values of the reference (main) image
$Mean_{secd}$ = mean of pixel values of the secondary image
SD_{main} = standard deviation of pixel values for the reference (main) image
SD_{secd} = standard deviation of pixel values for the secondary image

However, as argued by Song and Civco (2002), *when using this method in the multi-date images with substantial amounts of cloud and shadow present, the statistical parameters of image features can be severely*

[265] This kind of flexibility is also employed for setting up the Global Land Survey collections provided by USGS (and available in GloVis) for the nominal dates of 1975, 1990, 2000 and 2010, even if those cases assume an average margin of two years either before or after the selected time period.

[266] Actually the ACCA algorithm relies on the use of eight different filters to achieve the purpose of a better cloud isolating result. The Thermal band, within the algorithm, just provides one of those filters.

Universidad Politécnica de Cataluña, Barcelona TECH
Departamento de Tecnología de la Arquitectura
Centro de Políticas de Suelo y Valoraciones
Nicola Colaninno, Josep Roca Cladera

affected by their presence. Therefore, a prior cloud and shadow masking operation is needed in order to avoid biased values in the calculation of statistical measurements. This process of masking and averaging "valid" image data is quite operative for obtaining an image scene effectively representative for one selected year (2011 in our case), especially if the investigation focuses on measuring urban areas, for example, these supposedly do not experience significant changes during such a period and at a regional scale of analysis. When investigating other kinds of land cover types which are more affected by seasonal changes (such as crops, forests or water), monthly monitoring could be required, and thus a process of image averaging over longer periods is less suitable.

Once the final image scene of the whole Mediterranean side of Spain has been obtained, a digital mosaicing operation has to be undertaken, combining the minimum number of scenes required to cover the administrative boundaries of the Autonomous Communities. Additional statistic colour balancing is provided during mosaicing between the different adjacent geographical scenes in order to avoid multi-date effect on brightness values. In fact, the patch-working of images from the same sensor over large areas could contain radiometric and geometric problems[267] due to the fact that the selected scenes may have been sensed in different seasons of the year or at different latitudes (Meaden, et al., 1991).

Image 4.38 shows the final mosaic of four multispectral images, taken from the administrative area of Catalonia, in a Pseudo-Natural colour composite (742 in RGB model).

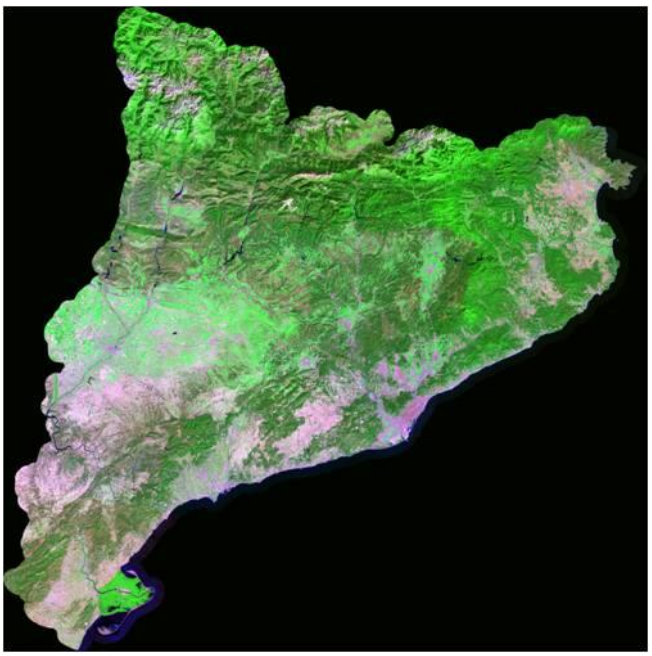

Fig. 4.38: Landsat TM image mosaic of Catalonia, displayed in a Pseudo-Natural colour combination (742) from the (nominal) year 2011 (Source: By Authors)

Independently from the approach for combining images, the challenge of pre-processing and digital mosaicing is obtaining the best enhancement of land cover classification results, whilst taking into account that all pre-processing procedures are key stages when the aim is, not only visualizing, but mainly measuring ground reflectance values. Actually, according to Homer, et al. (2007), c*hallenges to large-scale, multi frame, satellite-based land cover characterization include consistent geometric correction, normalizing noise arising from atmospheric effect, adjusting for changing illumination geometry, and minimizing instrument errors inherent when using multiple frames of imagery. Such geometric and radiometric error can hinder the ability to derive land surface*

[267] Landsat standard data products are normally pre-processed using the Standard Terrain Correction (Level 1T), but when mosaicing different adjacent scenes, it is critical to ensure that all match the same coordinate system.

information reliably and consistently[268]. Moreover, cloud-free images and statistical homogenization of reflectance values would be necessary when combining different images, either for the same scene or for mosaics.

All of the processes, which were carried out in the framework of our investigation for achieving improved Landsat TM imagery bounded at the level of Autonomous Communities, are summarized following the steps depicted in the following workflow diagram in figure 4.39. This was done prior to providing a more effective land cover classification.

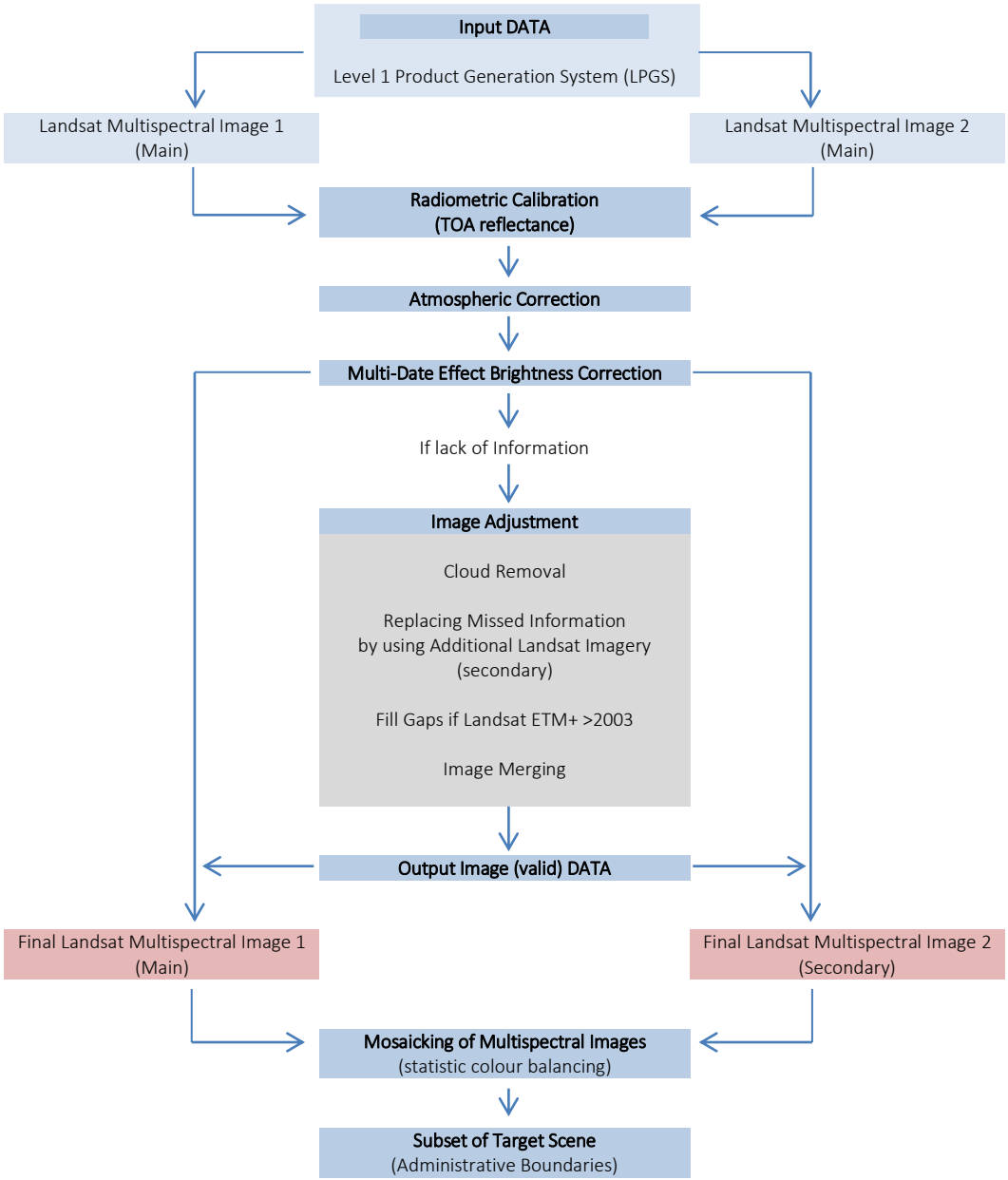

Fig. 4.39: Workflow of the main pre-processing steps undertaken on Landsat TM imagery, prior to proceeding with the land cover classification phase (Source: By Authors)

[268] See previous sections 4.3.1 and 4.3.2

4.5.4. Setting up a Spectral Library for Landsat Imagery Classification

A well-known way to extract information from an image is the classification, which is the process of assigning each pixel to a class (Campbell, 1996). Each pixel provides a set of measurements, in terms of reflectance stored in different spectral bands, about a given portion of land. Many of these pixels form groups of similar radiometric level in the different spectral bands. These groups are called spectral classes and each class is characterized by a spectral signature that corresponds to the typical land cover reflectance (Rocha, et al. 2007).

The reflectance of specific materials can be coded in spectral curves, by recording reflectance values at all available wavelengths. The shape of spectra is defined according to the absorption features detected in each of the spectral regions. It can identify specific falls along the spectral curve depending on the physical properties of the materials. Thus, the peculiarities of the spectra in terms of absorption provide useful information for discriminating several objects in the Earth's environment. Consequently, remote-sensing measurements (either made in situ by using spectroscopy, but also from airborne or spaceborne platforms) basically rely on acquiring and estimating those absorption or reflectance values and are benefitted by storing the material response in reference archives, known as spectral libraries. Actually, *libraries provide a useful tool for comparing spectral signatures and then determining whether, and in what spectral regions, surface features are distinct* (US Army Corps of Engineers, 2003).

Having a well-defined spectrum of land cover types provides the possibility of carrying out a scientific approach to interpretation and quantitative identification at pixel level. The spectrum of an unknown pixel recorded by a sensor can be identified by *comparing it against a data base of pre-recorded spectra and labelled as belonging to a given class, if the properties of its diagnostically significant absorption features match those of the spectrum for that class held in a spectral feature library* (Richards, et al., 2006). In the same way, the analyst can examine regions of pixels and attempt to match them to entries from spectral libraries.

This kind of approach is effective, if used with information sensed by repetitive circular sun-synchronous satellites, as it is based on the use of reflectance curves and the reflectance is theoretically an unvarying physical property of a material. So, according to this assumption and under conditions of unvaried illumination, the spectra of specific materials stored in a spectral library should always match the spectra of the corresponding materials on the ground, even if recorded at different periods, or places (US Army Corps of Engineers, 2003). As claimed by Richards and Xiuping (2006), it is critical that searching and matching processes must be efficient in such a procedure. Actually, full spectral matching using original radiometric data is not practical. Instead, an increasing effectiveness in spectral comparison operations aimed at pixel identification is achieved, either with previously recorded data or with laboratory spectra[269], by using digital data corrected for atmospheric and solar distortions.

Currently, many software programs permit the setting up and management of customized spectral libraries by recording spectral signatures for objects of interest and storing curves of reflectance response in a digital format, which can then be employed for identifying unknown pixels in image data. *In the particular case of hyperspectral data, because of the high spectral definition available, pixel identification and thus classification is possible using knowledge of the spectroscopic properties of earth surface materials* (Richards, et al., 2006). At present, several spectral libraries are available which provide spectral reflectance curves for many materials, and for hyperspectral data. USGS, for instance, provides a spectral library based on reflectance values at hyperspectral resolution for hundreds of materials, measured by researchers at the USGS Denver Spectroscopy Lab through a custom-modified computer-controlled Beckman spectrometer. Wavelength accuracy is in the order of 0.0005 µm (0.5 nm) in the near-IR and µm micron (0.2 nm) in the visible. Different subsets, such as the USGS vegetation spectra, minerals, or soils, are extracted from the main spectral library[270] as reference for materials identification for application in remote sensing analysis (Clark, et al., 1993). *A library of over 2˙000 spectra of natural and man-made materials was compiled as the ASTER (Advanced Spaceborne Thermal Emission Reflection Radiometer) Spectral Library[271]. The library includes contributions from the Jet Propulsion Laboratory (JPL), Johns Hopkins University (JHU) and the USGS. The library includes spectra of rocks, minerals, lunar soils, terrestrial soils, manmade*

[269] *Given the degree of redundancy spectrally and radiometrically that one would anticipate with the data recorded by an imaging spectrometer, coding techniques can be employed to represent a pixel spectrum in a simple and effective manner so that fast library searching and matching can be achieved* (Richards, et al., 2006)

[270] Further details and specifications of the USGS Spectroscopy Lab, and the existing spectral libraries, are available at http://speclab.cr.usgs.gov/

[271] Available from http://speclib.jpl.nasa.gov

materials, meteorites, vegetation, snow and ice covering the visible through thermal infrared wavelength region (0.4–15.4 μm) (Baldridge, et al., 2009).

Resampling procedures can be undertaken on the spectral responses collected in such libraries, based on hyperspectral information, in order to match digital data recorded from remote sensors at different spectral resolutions if within the same range of the electromagnetic spectrum (even multispectral). At any rate, a number of technical hitches can arise when seeking to match spectral curves from libraries to the absorption features stored in remotely sensed images. In particular, a mixture of spectral responses is often stored in a pixel and the mixture progressively increases depending on the pixel's dimensions. According to the US Army Corps of Engineers (2003), *while spectral libraries have known targets that are "pure types", a pixel in a remote sensing image very often includes a mixture of pure types: along edges of types (e.g., water and land along shoreline), or interspersed within a type (e.g., shadows in a tree canopy, or soil background behind an agricultural crop)*. Moreover, some materials have very similar spectral features (Richards, et al., 2006), as represented by the five soil types sampled in figure 4.40, and it can produce certain misclassifications.

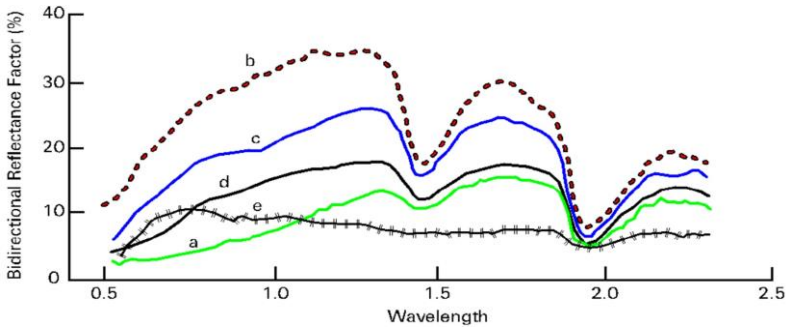

Fig. 4.40: *Reflectance spectra of five soil types: a) soil having > 2% organic matter content (OMC and fine texture; b) soil having < 2% OMC and low iron content; c) soils having < 2% OMC and medium iron content; d) soils having > 2% OMC, and coarse texture; and e) soil having fine texture and high iron-oxide content (> 4%)* (Source: US Army Corps of Engineers, 2003)

Beyond the criticism of the aforementioned complications which can arise when working with spectral libraries, the main effort of this investigation is to provide a spectral library suitable for dealing with coarse resolution imagery (either spatial or spectral). This is based on several generalized features of interest and the nomenclature system, as detailed in the previous table 4.7.

Consistent with the purpose of the investigation and due to the relatively coarse resolution, a limited number of classes have been defined through drawing spectral curves based on six wavelengths provided by Landsat TM multispectral sensors. A spectral library of 250 generalized land cover types was built by collecting several sets of training pixels (as homogeneous as possible) for each spectral class within the geographical area under investigation. This measured reflectance values of such pixel groups depending on final Landsat imagery mosaics, once radiometric, atmospheric and multi-date brightness corrections were applied, as depicted before.

Two approaches, based on the principles of physics, photo-interpretation and statistics, have been employed for collecting homogeneous groups of pixels and measuring their basic stats; such as minimum, maximum, mean and standard deviation of reflectance values. One approach is based on analysing the multispectral space of imagery (for the understanding and selection of specific land cover features) through the use of 2D scatter plots that visualize the spatial distribution of reflectance values for all pixels. Additionally, the ROI (Region Of Interests) tool has been used for digitalizing groups of pixels directly on the image. For both approaches, the curve of mean values for any training samples has been extracted and used as the curve of reflectance stored in the final spectral library.

4.5.4.1. The Multispectral Space for Spectral Understanding and Selection of Land Cover Training Samples

The bands of a multispectral satellite sensor provide a multi-dimensional coordinate system known as feature space. The most effective tool for understanding multispectral data with the purpose of formulating algorithms for quantitative analysis and land cover classification is provided by a multispectral vector space (or feature space), where each axis is characterized by a spectral component, or band. Thus, each plot will be made by as many dimensions as the number of bands provided by the sensor. In the case of Landsat TM imagery, for instance, the multidimensional space relies on six axes and each axis spans from 0 to 1 reflectance values. Within this plot, each image pixel is defined as a point and the spatial coordinates are given by the brightness values (or reflectance) for each band (Richards, et al., 2006).

Within a feature space formed from a three-dimensional coordinate system, for instance, such as the one covering the visible light slice (blue, green and red), the pixel position can be considered as a vector defined by three values of brightness. Considering the three values at once, a pixel can be labelled as belonging to a specific land cover class. Similarly, for a two-dimensional feature space, the pixel position depends on the vector defined by brightness values on band 1 and band 2. Figure 4.41 depicts the theoretical position of a pixel, both in a two-dimensional and three-dimensional feature space, within a digital image.

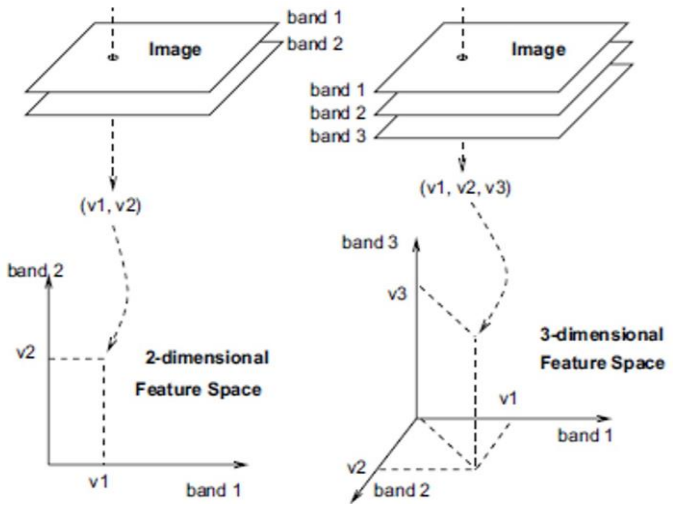

Fig. 4.41: The spectral significance of an image pixel, within the multidimensional space of brightness values, as defined both for a two-dimensional and three-dimensional feature space (Source: Bakker, et al., 2009)

The concept of feature space plays an important role in image classifications that are used to derive land use maps from satellite data. Classification methods are based on the idea that pixels containing the same land use are close to each other within the multi-dimensional feature space (Neteler, et al., 2008). Therefore, groups of pixel points (or clusters) with similar spectral characteristics (also referred to as information classes) are actually the data that the computer-based classification procedures attempt to discriminate and label. In fact, in quantitative analysis, the main assumption is that a finite number of pixels in image data can be clustered together, dependent on physical features of reflectance and the distance between pixels in a multispectral space. Each cluster will provide different spectral classes corresponding to as many ground cover types as are present. It is these *spectral classes that a computer will be asked to work with since they are the "natural" groupings or clusters in the data. After quantitative analysis is complete the analyst simply associates all the relevant spectral classes with the one appropriate information class* (Richards, et al., 2006).

According to Richards and Xiuping (2006), for statistical approaches aimed at land cover classification, *while single spectral classes are expected to be based on unimodal probability distributions, on the other hand the information classes usually involve multimodal distributions that need to be resolved in individual groups of models,*

for "convenience" and "accuracy" in the analysis. In fact, most of the time, the information classes depend on several spectral groups in the feature space. Imagine different soil classes (as depicted in the previous figure 4.40) or vegetation, for instance, which could be affected by differences in moisture content, soil types under vegetation and topographic influences. Moreover, the degrees of chlorophyll content variation in vegetation cover types provide quite a lot of canopy mixtures rather than well-defined subclasses. That is why, during pixel-based classification processes, it is not practical to directly separate coarse spectral types of cover, such as vegetation/no-vegetation, but instead, it is necessary to determine appropriate sets of spectral sub-classes before further generalization in order to represent the information classes effectively[272] (Richards, et al., 2006). Therefore, when applying methods of classification based on a clustering algorithm, the process first aims to cluster adjacent pixels within the multi-dimensional feature space, in groups of pixels, then more groups are assigned to the same land cover class. *For example, a number of multispectral pixels which cover a forest will show similar spectral signatures and therefore should be assigned to land use class "forest"* (Neteler, et al., 2008).

The following figure 4.42, shows the relationship between the spectral responses of some common generalized land cover types; such as water, sandy soil, and green vegetation. In particular, the Landsat TM spectrum depicts the typical spectral response for three pixels of each observed generalized class in the red (TM3) and near-infrared (TM4) slice of the spectrum, and the feature space scatter plot represents the spatial position of the pixel's reflection, per channel, in a two-dimensional graph of brightness values, again for the red and the NIR bands.

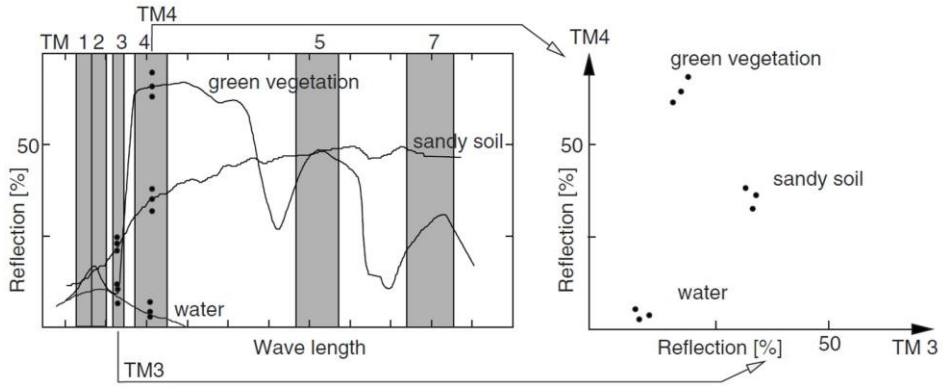

Fig. 4.42: Typical spectral response of common objects, such as water, sandy soil and green vegetation, through Landsat 5 TM, for band 3 (red) and 4 (NIR); and the approximate pixel brightness values within the two-dimensional feature space based on the same channels, 3 and 4 (Source: Neteler, et al., 2008)

During a classification procedure, the whole multi-dimensional feature space will be partitioned depending on the mean vector of pixel clouds in order to separate homogeneous spectral classes (as discussed during the previous sections 4.4.4 and 4.4.5 about unsupervised and supervised methods of classification). Consequently, since it is impractical to work with a space with more than three dimensions, for this reason it is critical that the selection of spectral classes (based on the two-dimensional feature space) should rely on the simultaneous analysis of several combinations of bands to achieve the best result. Moreover, bi-dimensional scatter plots should be provided for a certain number of image windows, moving through small areas of the entire scene, in order to decrease the difficulties of understanding clustered areas. For that reason, several combinations of 2D scatter plots (such as band 3 with band 4, 3 with 5, and 2 with 7) have been simultaneously used for interactively understanding and selecting image data with similar spectral features[273], and from different image subsets of the scene (because a two-dimensional scatter plot only provides the spatial distribution of data for an image window, not for the whole

[272] Actually, even if the final thematic maps resulting from this investigation will only rely on twenty categories as depicted in the nomenclature system, the spectral library employed for classification has been taken from 250 spectral classes.

[273] Some band combinations, such as band 2 with band 3, or band 5 with 7, are less practical because they are highly correlated. This makes the clouds of points strictly distribute in a linear direction, thus providing a quite narrow shape of the cloud and a number of complications could arise during selection operations.

scene). This procedure allows direct drawing of a polygon on the scatter graph, and quick visualizing of the automatically selected resulting land cover portions in the image window.

Before selecting a pixel cluster on the graph and saving it as a possible spectral class, a "dancing" pixels option provides the possibility of observing how the distribution of the spectral information changes, by interactively moving around the image window. Additionally, it is possible to export and import the features of selected groups of pixel from one scatter plot to another. The selected areas can be saved as ROIs (both from the image window or the scatter plot) from which the main statistics regarding reflectance values can be derived and then the spectral curve of the objects can be extracted.

Figure 4.43 shows a transept of a Landsat TM image from the region of Murcia, displayed using a Pseudo-Natural colour composite, and based on a 742 RGB combination. Additionally, the scatter plots of the feature space, which characterise the cloud of pixel values of reflectance through the 2D spectral spaces of band 3 relative to bands 4 and 5, and band 2 relative to band 7. Seven generalized land cover classes are typified and colour coded according to the spatial position of data points within the scatter plots, as indicated on the image. In particular, the graphs provide spectral features for the following land cover types:

A). Urban (red)
B). Croplands (yellow)
C). Arable Land (orange)
D). Undeveloped Land (brown)
E). Forest (green)
F). Deep Water (blue)
G). Shallow Water (cyan)

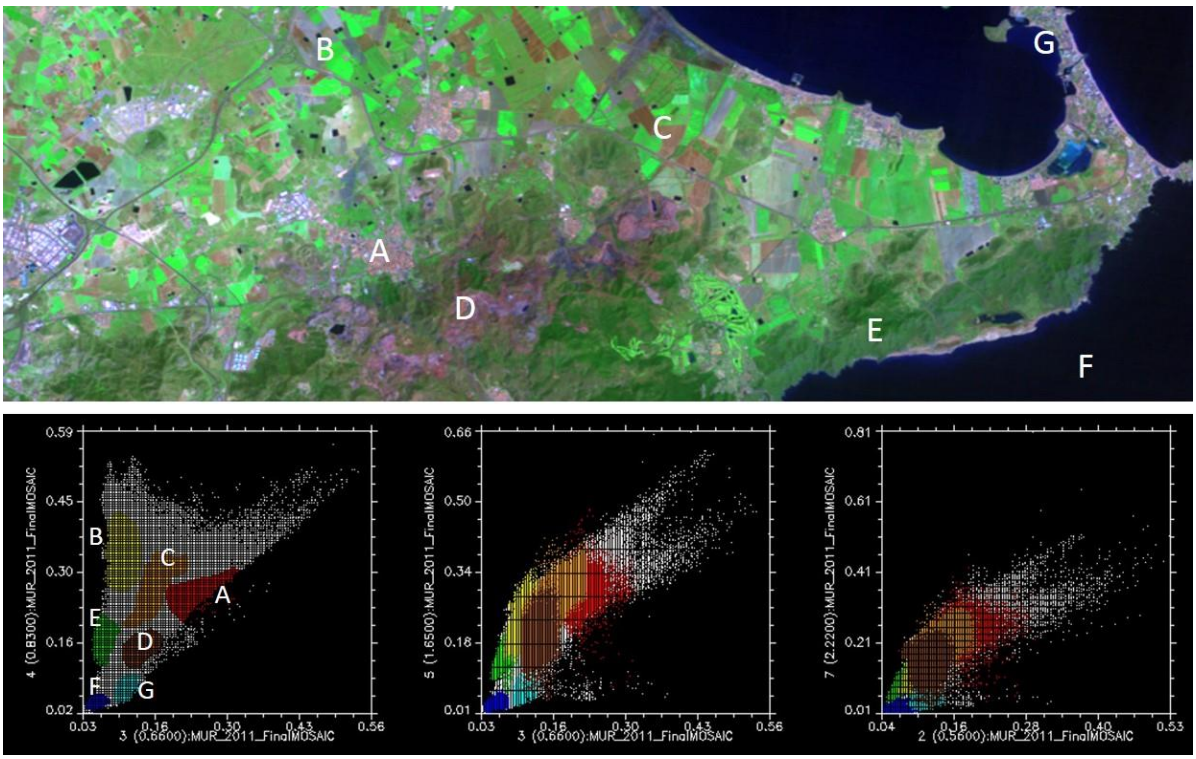

Fig. 4.43: Typical spatial position of reflectance values, for the pixels of a Landsat TM multispectral data, within the two-dimensional feature spaces of band 3 relative to band 4, band 3 relative to band 5, and band 2 relative to 7, and for seven generalized land cover classes, such as: A) Urban; B) Croplands; C) Arable Land; D) Undeveloped Land; E) Forest; F) Deep Water; and G) Shallow Water (Source: By Authors)

4.5.4.2. The ROI Tool: Digitalizing Training Samples

Within the pattern recognition field, as claimed by Anji Reddy (2008), *selecting a good set of training points* (or Regions Of Interest) *is one of the most critical aspects of the classification procedure*. A training dataset for multispectral imagery is usually understood as a set of points, whose spectral measurements and category membership for the entire multidimensional space, and are known by the analyst. Every point within a dataset is therefore a mathematical pixel vector X, that contains sets of N brightness values arranged in column form (and within square brackets for mathematical convention), for as many as the number of bands available for the sensor.

As depicted by the example in figure 4.44, the vector X is formed from four brightness values (in this case) for the same selected pixel x_n, one for each band from 1 to 4 respectively. Consequently, the training dataset for each land cover class consists of a set of input vectors X. Therefore, the first goal in image learning issues aimed at classification is to discover groups of similar vector values. From this the mean vector of reflectance for one spectral class can be derived, prior to running automatic clustering algorithms for the entire data.

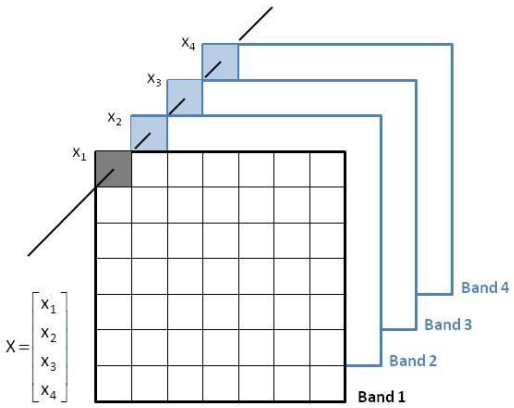

Fig. 4.44: A vector sample X for a generic four band digital image, normally formed from N pixel brightness values dependent on spectral resolution (Source: By Authors)

If no additional information is available (such as existing maps, field surveys or aerial photographs) to support the selection process of ROIs, the training dataset will be selected dependent only on the analyst's knowledge of typical spectral signatures (Anji Reddy, 2008), and the image aspect for the different land cover classes. However, certain basic rules have to be taken into account when undertaking the digitalization of specific training pixels on imagery, when using polygons, lines or points.

Firstly, changing the band composite combination for the RGB model interactively while digitalizing ROIs (as well as the use of image enhancement techniques), improves the ability of the analyst for image interpretation and class separability[274]. Therefore, once the best interpretability of the image has been reached, it is critical to attempt to select the most representative training data sets for each class. This means those regions of interest which show both the typical average feature values and a typical degree of variability. Actually, a unimodal distribution of the values in the histogram for the selected areas is desirable, because *a bimodal histogram suggests that pixels from two different classes may be included in the training sample*. To do so, it is favourable to select training samples from areas which provide a high density of the pixels from the same class. Moreover, for each class, select several training areas, instead of just one, possibly widely and spatially distributed across the full image. It is vital that each training area should contain a moderately large number of pixels (Anji Reddy, 2008). In fact, as argued by Richards and Xiuping (2006), a *sufficient number of training pixels for each spectral class must be available to allow reasonable estimates to be obtained of the elements of the class conditional mean vector and covariance matrix*. Signifying that each N-dimensional measurement vector is formed from N sample pixels, one pixel for each band of the multispectral space (as depicted in the previous figure 4.44); thus, the minimum required

[274] Because, several classes are likely to overlap, the less the overlap between classes the lower the chance of misclassifying a given pixel. On the other hand, those classes that have little overlap are said to be highly separable (Anji Reddy, 2008)

number of independent training pixels suitable for best estimating one land cover class equals the number of bands (N) plus one[275]. However, due to certain practical difficulties with achieving the desired independence, many more pixels than the minimum allowable number need to be selected in order to achieve the most significant mean value of the class especially when the selected area for one class shows high variability (i.e. the training points of the class are significantly dispersed within a scatter plot). Theoretically, the more points, the more accurate the classification will be, but the most practical recommendation suggests selecting at least 10*N training pixels per spectral class, and up to 100*N per class, even if this threshold is reasonable mainly for data with low dimensionality, such as multispectral data. On the other hand, *for hyperspectral data sets finding enough training pixels per class is extremely difficult* (Swain, et al., 1978; Richards, et al., 2006).

As used within this study, a suitable method for selecting training data should be to follow a sort of iterative process, i.e. classifying depending on a primary set of training points, and then depending on the results, come back and modify training sets and class definitions, if necessary. Moreover, classes from previous quick classifications, based on the use of the parallelepiped algorithm, have been used for assisting the selection of the most effective training samples.

4.5.5. Enhancing the Image Information

Certainly one of the most important uses of remote sensing, within the context of environmental observation, management and planning, is the detection and quantitative assessment of specific land cover features. This includes: vegetation, either agriculture or forestry; water, for assessing both inland water and the marine environment; as well as specific soil types. To achieve the best detection and analysis of patterns and structure of such key natural resources, several indices have been developed for enhancing specific feature extraction operations which are intended to automatically estimate certain ground cover types in a digital image.

These indices can be obtained by using mathematical equations between spectral bands and transformations, as discussed in the previous chapter 4.3.4. They are based on the fact that vegetation, water or soil absorb or reflect a certain amount of energy, at specific wavelengths, depending on the physical characteristics of the matter. Besides the detection improvement of particular physical features, the usefulness of these indices also relies on an important reduction of sensitivity to topographic and atmospheric effects, without altering the spectral sensitivity of the types of cover (Philpot, 2011).

However, it should be taken into account that for a more effective use of the indices, the original input variables need to be pre-processed, and often normalized using a common range of values to transform them into a comparable space of variables. Moreover, either for multispectral or hyperspectral data, the bands employed for computing indices require high-quality reflectance measurements. Therefore, digital imagery that has not previously been calibrated for reflectance values and atmospherically corrected, are unsuitable and typically provide inadequate results.

The main objective of this section is to provide a suitable set of indices, specifically for vegetation, water, and soil features (as detailed in the following sections) in order to improve the original information provided by the multispectral Landsat imagery. As a lot of indices exist, with each one providing different attributes of the same feature, and usually highly correlated between them. A synthetic index will be calculated for each one of the analysed environment (i.e. vegetation, water, and soil), employing a principal component analysis. Then, the synthetic indices, together with the original Landsat bands, will provide an enhanced stack of information and a "multi-index" image. Henceforth, used for achieving a better discrimination of pixels from different spectral classes when applying clustering algorithms (see 4.5.7.1).

[275] *For an N dimensional multispectral space the covariance matrix is symmetric of size N*N. It has, therefore, 1/2N*(N + 1) distinct elements that need to be estimated from the training data. To avoid the matrix being singular at least N*(N + 1) independent samples is needed* (Richards, et al., 2006)

4.5.5.1. Vegetation Indices

Many vegetation indices (VIs) have been developed during the past decades, both for hyperspectral and multispectral data, in order to measure the general health status and vigour of vegetation. The simplest measurements are referred to as the broadband greenness Vegetation Indices, and are derived basically from multispectral information.

Taking into account that healthy vegetation absorbs the energy provided by red wavelengths (chlorophyll absorbs photons that are stored as energy through the photosynthesis process), while efficiently reflecting the energy from the near infrared slice of the spectrum. The broadband VIs are obtained by combining those reflectance features most sensitive to the effects of foliage chlorophyll concentration, canopy leaf area, foliage clumping and canopy architecture. Nevertheless, these VIs are not designed to quantify the concentration or abundance of any given vegetation component; instead, their use is generally intended to measure the quality of photosynthetic material in vegetation, and for mapping the overall amount of vegetation components[276] (Exelis) Jackson and Huete (1991), recognised two main groups of broadband greenness VIs, which are: the slope-based VIs, which provide *simple arithmetic combinations aimed at emphasizing the contrast between the spectral response patterns of vegetation, in the red and near-infrared portions of the electromagnetic spectrum*; and the distance-based VIs, *which measure the degree of vegetation present by gauging the difference of any pixel's reflectance from the reflectance of bare soil* (Jackson, et al., 1991; Silleos, et al., 2006).

The spatial distribution of bare soil pixels within the RED/NIR feature space (figure 4.45), which ranges from wet bare soil pixels (bottom left in the 2D scatter plot) up to the dry bare soil pixels (upper right) depending on the degree of moisture content, tends to display a stripe of pixels known as the soil line. Bare soil classes are commonly placed along this line. On the other hand, as the degree of vegetation on the ground increases, the pixels in the scatter plot move increasingly further from the soil line in a perpendicular direction. The greater the biomass and/or canopy cover, the greater the NIR values of pixels will be in the graph (Silleos, et al., 2006).

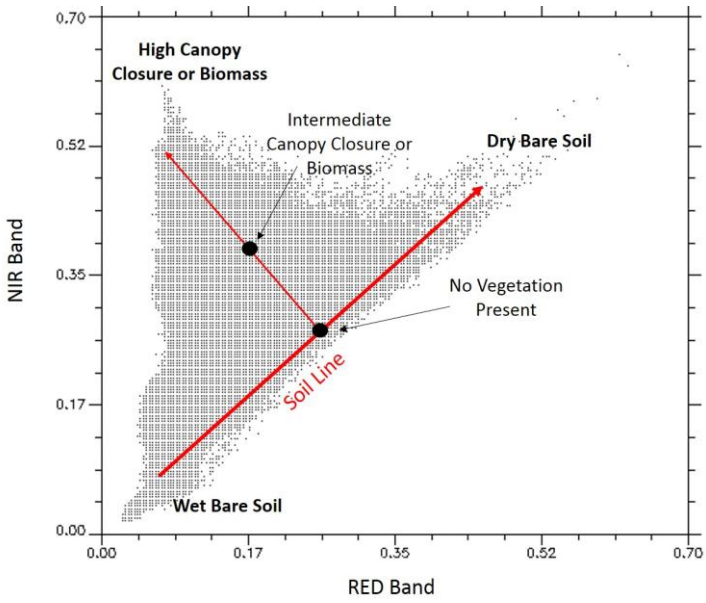

Fig. 4.45: Spatial distribution of all pixels in an image scene within a two-dimensional feature space based on Red and NIR bands. Pixels ranging from wet bare soils to dry bare soils define the so called soil line (Source: By Authors; adapted from Silleos, et al., 2006)

[276] *These VIs are well correlated with the fractional absorption of photosynthetically active radiation (fAPAR) in plant canopies and vegetated pixels. They do not provide quantitative information on any one biological or environmental factor contributing to the fAPAR, but broad correlations have been found between the broadband VIs and canopy LAI (Leaf Area Index)* (Exelis)

The Red-NIR feature space, as depicted in the 2D scatter plot in figure 4.45, is the key to the huge investigation undertaken in the discipline of RS behind the setting up of the most famous VIs (both slope-based and distance-based). Actually, a third group of VIs is provided by the orthogonal transformation indices which are based on the modification of the available spectral bands in order to achieve a new set of uncorrelated bands. Perhaps one of the most recognised vegetation indices (based on an orthogonal transformation and employed within this research) for improving the original Landsat information, is the Greenness index or green vegetation index (GVI). It is derived from the Tasseled Cap Transformation (Silleos, et al., 2006), as discussed during the previous section 4.3.4.3.

The Slope-based VIs, which rely mainly on the mathematical combination of the visible red and the near infrared bands, measure both the state and abundance of green vegetation cover and biomass. In particular, in the case of this group of indices, the position of each pixel value in the 2D Red-NIR feature space is *geometrically equivalent to the slope (tangent) of the line connecting the origin of reference and this particular point on a scatter-gram* (Mróz, et al., 2004). Alongside the Greenness index, some of the most common slope-based VIs have been included in this research as factors for improving the classification results, including: the Simple Ratio (SR); the Normalized Difference Vegetation Index (NDVI); the Enhanced Vegetation Index (EVI); and the Atmospherically Resistant Vegetation Index (ARVI).

The Simple Ratio (already mentioned in section 4.3.4.1, together with the NDVI), also known as Ratio Vegetation Index (RATIO), was originally described by Birth and McVey (1968), and is calculated by simply dividing the reflectance values of the NIR band by those of the red band. The resulting values, which range from 0 to more than 30, emphasise the contrast between the red band absorption and the NIR reflection for pixels of vegetation. In fact, high index values depend on the high infrared values divided by the low red values of reflectance, with a common range for green vegetation which varies between 2 and 8. *Because the index is constructed as a ratio, problems of variable illumination as a result of topography are minimized. However, the index is susceptible to division by zero errors and the resulting measurement scale is not linear* (Silleos, et al., 2006).

The Normalized Difference Vegetation Index (NDVI), introduced by Rouse et al. (1974) and based on Landsat MSS digital data, is obtained from NIR-RED/NIR+RED and provides a measurement of the amount of green vegetation present in a pixel. Thus, allowing separation of green vegetation from its background soil brightness. It is without doubt the most employed VI as it provides a good minimization of topographic effects while producing a statistically normal distribution. Moreover, division by zero means errors are significantly reduced with respect to the SR index, and a desirable property ranging from -1 to 1 is achieved, in which 0 is the approximate value of non-vegetation areas. Negative values indicate no vegetation; while, the higher the value of NDVI, the denser the vegetation concentration.

The Enhanced Vegetation Index (EVI), developed by the MODIS Science Team[277], is a modified NDVI defined using the equation below [4.17]. This improves the quality of the index by optimizing the vegetation signal in Leaf Area Index (LAI)[278] through the use of the BLUE reflectance. Additionally, there is a soil adjustment factor L, and two coefficients C_1 and C_2, in order to correct for some distortion caused by atmospheric influences, including haze and aerosol scattering, and the soil background signals (Huete, et al., 1997; Weier, et al., 2000).

$$EVI = G * \frac{NIR - RED}{NIR + (C_1 * RED) - (C_2 * BLUE) + L} \qquad [4.17]$$

Where: L = canopy background adjustment
C_1 = coefficient of the aerosol resistance
C_2 = coefficient of the aerosol resistance
G = gain factor

[277] *In December 1999, NASA launched the Terra spacecraft, the flagship in the agency's Earth Observing System (EOS) program. Aboard Terra there is a sensor called the Moderate-resolution Imaging Spectroradiometer, or MODIS that greatly improves scientists' ability to measure plant growth on a global scale* (Weier, et al., 2000)

[278] The EVI is most useful in LAI regions, where the NDVI may be saturated. In fact, *whereas the Normalized Difference Vegetation Index (NDVI) is chlorophyll sensitive, the EVI is more responsive to canopy structural variations, including leaf area index (LAI), canopy type, plant physiognomy, and canopy architecture. The two vegetation indices complement each other in global vegetation studies and improve upon the detection of vegetation changes and extraction of canopy biophysical parameters* (Huete et al., 1999; Huete, et al., 2002)

The NIR, RED, and BLUE are the atmospherically-corrected surface reflectance values, while L is *the canopy background adjustment that addresses the non-linear, differential NIR, and RED radiant transfer through a canopy. The coefficients C_1 and C_2 are the aerosol resistance factors, which use the BLUE band to correct for aerosol influences in the RED band*. The coefficients adopted in the MODIS-EVI algorithm are: L=1.00, C_1=6.00, C_2=7.50, and G is 2.50. The value of this index ranges from -1 to 1, while the common range for green vegetation is 0.2 to 0.8 (Huete, et al., 1997; Huete, et al., 2002).

The Atmospherically Resistant Vegetation Index (ARVI), was developed by Kaufman and Tanré (1992), as an enhancement to the NDVI, for minimizing atmospheric-induced variations in the VI, on a pixel by pixel basis. The ARVI is a VI relatively resistant to atmospheric factors, such as aerosols. It utilizes the difference between the BLUE and RED channels in order to correct the reflectance of the RED band for atmospheric scattering and stabilizes the index to temporal and spatial variations in the atmospheric aerosol content (Huete, et al., 1997). ARVI is defined by the following equation [4.18], and the value of this index ranges from -1 to 1. As for the case of the EVI, the common range for green vegetation is 0.2 to 0.8 (Kaufman, et al., 1996; Exelis).

$$ARVI = \frac{NIR - 2*RED - BLUE}{NIR + 2*RED - BLUE} \qquad [4.18]$$

Hence, the slope-based VIs are linear combinations of the visible RED and NIR bands and they rely on emphasising the differences between reflectance values at these wavelengths for each pixel into digital images. The Distance-based vegetation indices are intended to remove, or at least reduce, the effect of the background soil brightness when vegetation sparsely covers the ground, thus providing a combination of vegetation and soil features into the spectral signal of the pixels.

In particular, the distance-based VIs focus on measuring the perpendicular distance of each pixel value from the soil line that is derived through a linear regression between the NIR and the RED reflectance values (as depicted in the previous figure 4.45). Actually, the use of the soil line is particularly significant in arid and semi-arid environments because it provides the typical spectral signatures of bare soils within the RED/NIR feature space. *Pixels falling near the soil line are assumed to be soil, while those far away are assumed to be vegetation* (Silleos, et al., 2006). If we consider the linear regression $Y = a*X + b$ for the digital image under consideration, where the RED band is the independent variable *X*, and the NIR is the dependent variable *Y*. All of the distance-based VIs which involve the use of the soil line will require the coefficients *a* and *b* (respectively slope and intercept of the line) as chief inputs to the calculation.

Although several distance-based VIs are currently available, the indices employed for this investigation for improving the original image information are the Soil-Adjusted Vegetation Index (SAVI); the Modified Soil-Adjusted Vegetation Index; the Transformed Soil-Adjusted Vegetation Index (TSAVI); and the Perpendicular Vegetation Index (PVI).

The Soil Adjusted Vegetation Index (SAVI), proposed by Huete (1988) as a modification of the NDVI, is one of the major VIs developed for minimizing the influence of soil brightness in those areas where little vegetation cover is present. This index is mostly useful when comparisons are needed between soils that provide significant variations of reflectance values in the RED and NIR slice of the spectrum. Actually, the SAVI is mathematically structured similar to the NDVI and also based on Red and NIR bands but with the addition of a constant soil correction factor "L", as depicted by equation [4.19], which varies between zero and one.

$$SAVI = \frac{NIR - RED}{NIR + RED + L} * (1 + L) \qquad [4.19]$$

The lines of equal vegetation intensity (or vegetation isolines, in the case of the SAVI) do not converge at the origin of the RED/NIR feature space[279], as happens in the case of the NDVI, for instance, nor are they parallel to

[279] *Another difference between distance-based and slope-based VIs is the orientation of lines of equal vegetation intensity/vividness (isovegetation lines), regardless of moisture conditions. In slope-based Vis, isolines converge at the origin, whereas in distance-based VIs, all isolines remain parallel to the soil line. SAVI family VIs are also classified into this group, although isolines for these VIs are neither parallel nor convergent at the origin* (Mróz, et al., 2004).

the soil line, as is the case of PVI (see figure 4.46). Huete (1988) assumes the converging point of the isolines to be at a distance (OE) from the origin of the Cartesian system, and develops the SAVI by adding the soil adjustment factor *L* which is equals to l_1+l_2 (Qi, et al., 1994), where l_1 and l_2 are, respectively, the components *X* and *Y* of the distance OE.

According to Silleos et al. (2006), *L* varies with the reflectance characteristics of the soil (e.g., colour and brightness), and the values depend on the degree of vegetation density. In particular, for areas of high vegetation, the value of *L* can be assumed to be 0.00, or 0.25; while, when low vegetation cover is present, the value of 1.00 can be used as a correction factor. In the case of intermediate vegetation cover, the factor *L* is calibrated at a value of 0.50, which is the most widely used (Mróz, et al., 2004). Actually, the same Huete (1988) demonstrated that optimal values of *L* depend on different vegetation amounts present, but, on the other hand, a value of 0.50 provides an effective minimization of soil background effects for a wide range of conditions[280]. *The (1+L) term in SAVI equation* [4.19] *is meant to restore the loss in "dynamic range" of the SAVI resulting from the addition of the L factor to the denominator as well as to bound the SAVI within the range of ± 1* (Qi, et al., 1994).

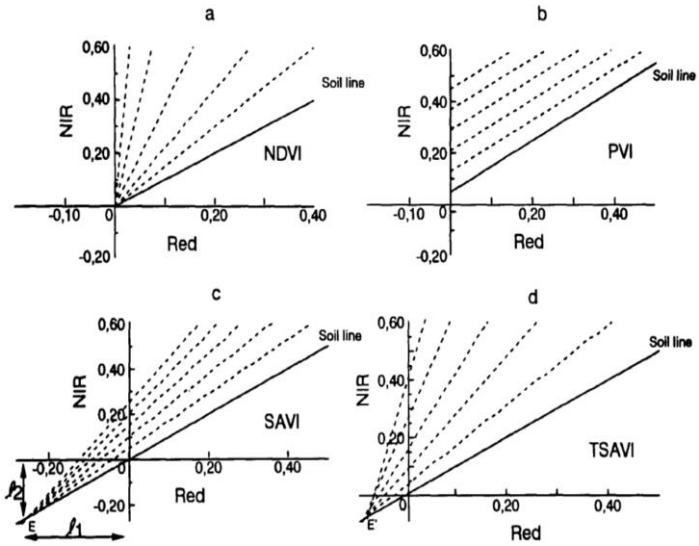

Fig. 4.46: *Concepts of vegetation isolines for various vegetation indices* (Source: Qi, et al., 1994)

Two Modified Soil-Adjusted Vegetation Indices, $MSAVI_1$ and $MSAVI_2$, both based on a dynamic adjustment of the factor *L*, were developed by Qi et al. (1994) in order to further reduce the effect of the soil background brightness on vegetation, with respect to the SAVI.

Based on the assumption that *L* decreases with an increase in vegetation cover, the factor *L* for the $MSAVi_1$ is selected as an empirical function[281]. In order to annul (or further minimize) the soil brightness effect through decreasing the sensitivity to soil noise, *L* is calculated as the product of NDVI and Weighted Difference Vegetation Index (WDVI)[282]. In particular, Qi et al. (1994) suggested a "self-adjustable" *L* according to equation [4.20]:

$$L = 1 - 2 * a * NDVI * WDVI \qquad [4.20]$$

Where *a* signifies the slope of soil line, and factor 2 serves for increasing the dynamic range of *L*. The resulting $MSAVI_1$ is then calculated as SAVI [4.19], with the factor L given in equation [4.20], instead of a constant. *The proposed empirical L function utilized the advantages of the opposite trends of NDVI and WDVI with the soil*

[280] As argued by Silleos et al. (2006), for L = 0.00, SAVI equals NDVI; while for L = 1.00, SAVI approximates the Perpendicular Vegetation Index (PVI).

[281] *There are many functions for L that would satisfy the criteria of L decreasing with increasing vegetation cover. A simple approach would be to use 1-NDVI. However, because NDVI is influenced by soil backgrounds, especially by the soil brightness, the L would contain soil noise* (Qi, et al., 1994)

[282] WDVI is calculated as *NIR - a*RED*, where *a* is the slope of the soil line (Clevers, 1988; Richardson and Wiegand, 1977)

background variations. Both the NDVI and WDVI vary with the soil brightness, but in an opposite manner, that is, darker (or wet) backgrounds result in higher NDVI values, but lower WDVI values than brighter (or dry) backgrounds for identical amounts of vegetation (Qi, et al., 1994).

However, the $MSAVI_1$ does not completely remove the soil noise, due to the fact that several soil effects exist. Therefore, Qi et al. (1994), also provided an iterated version of the first adjusted SAVI, known as $MSAVI_2$, which employs an inductive method to derive *L*, which can be demonstrated satisfactory for removing the soil noise not annulled by the $MSAVI_1$. It can correct the values greater than 1 that $MSAVI_1$ may have due to the low negative value of NDVI*WDVI (Silleos, et al., 2006).

Qi et al. (1994) argued that the use of "any seed value" L_0, would minimize the soil background effects upon an $MSAVI_0$, calculated using the equation [4.19], which consequently could be used for obtaining a new *L* function able to further minimize the soil effect. This new function *L* will be $L_1=1-MSAVI_0$ which then will result in a new $MSAVI_1$ again employed to further minimize the soil effect. This process is iteratively repeated *n* times, thus obtaining the function $L_n=1-MSAVI_{n-1}$, and $MSAVI_n$ as a result of equation [4.19].

Continuing with this iterative process, a time will be reached when *N* is such that $MSAVI_N= MSAVI_{N-1}$, in which the soil effects cannot be minimized further and the resulting equation appears as follow:

$$MSAVI_N = \frac{NIR - RED}{NIR+RED + 1-MSAVI_N} * (2 - MSAVI_N) \qquad [4.21]$$

One of the two solutions for Eq. [4.21] within the range of 0 and 1 is:

$$MSAVI_N = \frac{-b - \sqrt{b^2 - 4c}}{2} \qquad [4.22]$$

Where: $b = -(2*NIR +1)$
$c = 2*(NIR - RED)$

Therefore, with an inductive L function of $L=1-MSAVI_2$; the resultant MSAVI by induction, $MSAVI_2$, becomes:

$$MSAVI_2 = \frac{2*NIR+ 1 - \sqrt{(2*NIR+1)^2 - 8*(NIR-RED)}}{2} \qquad [4.23]$$

According to Qi et al. (1994), both modified SAVIs generally appear to be more sensitive indicators of the amount of vegetation by raising the vegetation signal and, at the same time, reducing the soil-induced variations. Actually, in relation to the SAVI, the $MSAVI_1$ shows a reduction of soil noise influences, as well as a more linear response to the percentage of green cover. Moreover, the variable *L* function improves the vegetation sensitivity, particularly at high vegetation densities, and *the vegetation estimate uncertainty is reduced from +2.5% (SAVI) to +1.6% ($MSAVI_1$). However, at 60 % green cover, and above, the vegetation signal to soil noise ratio (S/N) for the $MSAVI_1$ dropped below that of the SAVI.* Although, the $MSAVI_2$, in comparison with $MSAVI_1$ and the original SAVI, further increase the dynamic range, while maintaining minimal levels of the soil noise, it results in a higher vegetation signal to soil noise ratio (S/N), with respect to the SAVI. Instead, with respect to the $MSAVI_1$ the S/N ratio is slightly lower at low vegetation cover and slightly higher at a high vegetation density[283].

Possibly the best known of the distance-based VIs (from which several other indices of this group have been derived) is the Perpendicular Vegetation Index (PVI) proposed by Richardson and Wiegand (1977). The PVI measures the perpendicular distance between any point within the RED/NIR feature space, and its orthogonal projection upon the soil line. In other words, considering RED_{veg} and NIR_{veg} as the spatial coordinates (X, Y) of the reflectance values for one vegetation point in the scatter plot, and RED_{soil} and NIR_{soil} the coordinates of the

[283] An exhaustive dissertation about the MSAVI can be found in: Qi, J.; Chehbouni, A.; Huete, A.R.; Kerr, Y.H.; Sorooshian, S. 1994. *A Modified Soil Adjusted Vegetation Index*. Remote Sensing of Environment, 48, pp. 119-126. Elsevier Science Inc.

orthogonal projection of that point along the soil line (i.e. the reflectance of the soil background at that point). The PVI is calculated using the Pythagorean Theorem, as follows:

$$PVI = \sqrt{(RED_{soil} - RED_{veg})^2 + (NIR_{soil} - NIR_{veg})^2} \quad [4.24]$$

PVI for bare soils equals 0, regardless of the soil surface status, while values less than 0 account for a water environment, and values greater than 0 signify areas of vegetation (Leblon). The PVI corrects for soil reflectance and provides a more linear and less-scattered relationship with the fraction of intercepted photosynthetically active radiation (Casanova, et al., 1998). However, slope-based VIs, such as the NDVI for instance, do not abundantly minimize the soil optical effect on canopy reflectance (Richardson and Wiegand, 1977; Silleos, et al., 2006).

Three further PVIs have been suggested during the last few decades, also based on the use of the soil line as was the original one, to be able to achieve certain improvements over the performance of this index. The PVI_1 is the one employed in our investigation, proposed by Perry and Lautenschlager (1984); the PVI_2 developed by Bannari et al., (1996); and the PVI_3, developed by Qi et al. (1994). Anyway, Perry and Lautenschlager (1984) *argued that the original PVI equation is computationally intensive, and does not discriminate between pixels that fall to the right or to left side of the soil line (i.e., water from vegetation). Given the spectral response pattern of vegetation, in which the infrared reflectance is higher than the red reflectance, all vegetation pixels will fall along the right side of the soil line* (Silleos, et al., 2006). Therefore, to solve this problem and taking into account that NIR_{soil} depends on the linear regression $a*RED_{soil}+b$, they suggested a modified Perpendicular Vegetation Index (PVI_1) using equation [4.25]:

$$PVI_1 = \frac{a*NIR - RED + b}{\sqrt{a^2 + 1}} \quad [4.25]$$

Where: a = slope of soil line
b = intercept of soil line

An additional improvement to the PVI has been provided by Baret et al. (1989), and Baret and Guyot (1991), which proposed a Transformed Soil Adjusted Vegetation Index (TSAVI), as a transformation of the SAVI, employing two different formulations respectively: $TSAVI_1$, and $TSAVI_2$. The resulting convergence point of the vegetation isolines for the TSAVI is closer to the origin of the Cartesian system, with respect to the SAVI, but not coincident with the origin as is for the NDVI (see previous figure 4.46). The $TSAVI_1$ was defined under the assumption that all the reasoning behind the SAVI is exact only if the constants of the soil line are *a=1* and *b=0*. However, this is not generally the case. Therefore by taking into account the PVI concept, the first transformation of the SAVI was designated, specifically for semi-arid regions (Silleos, et al., 2006), using the following equation [4.26]:

$$TSAVI_1 = \frac{a*(NIR - a)*(RED - b)}{RED + aNIR - ab} \quad [4.26]$$

Due to the fact that the index maintains some resistance for high soil moisture and does not perform well in areas with full vegetation cover, it was readjusted by Baret and Guyot (1991), with an additional correction factor of 0.08 to minimize the effects of the background soil brightness (Silleos, et al., 2006). The $TSAVI_2$, which also requires the values *a* and *b* (slope and intercept respectively) of the soil line, is defined with the following equation:

$$TSAVI_2 = \frac{a*(NIR - aRED - b)}{RED + aNIR - ab + 0.08(1 + a^2)} \quad [4.27]$$

4.5.5.2. Water Indices

Remotely sensed imagery has long been used in water resources assessment and coastal management. Similar to the vegetation analysis, these applications rely on an effective delineation of the water environment by *using thematic information extraction techniques, for quickly and accurately discriminating water from non-water features*. Even if a band ratio approach between multispectral bands can be undertaken, by using visible and near-infrared (NIR) wavelengths, for "suppressing" vegetation and land presences while enhancing water cover, this method does not completely remove non-water features (Xu, 2006).

In order to solve this problem, McFeeters (1996) proposed a Normalized Difference Water Index (NDWI) derived using an approach similar to the one used for defining the NDVI[284]. In fact, by reversing the variables NIR and RED employed in the NDVI equation (either for numerator and denominator), and substituting the RED band with the GREEN band, as indicated in equation [4.28], it is possible to effectively emphasize water features by obtaining a single grey-scale image where water is brighter.

$$NDWI = \frac{GREEN - NIR}{GREEN + NIR} \qquad [4.28]$$

Of particular interest, the result of the index provides positive values for water features, while soil and vegetation move around zero and negative values. *The selection of these wavelengths was done to: (1) maximize the typical reflectance of water features by using green light wavelengths; (2) minimize the low reflectance of NIR by water features; and (3) take advantage of the high reflectance of NIR by terrestrial vegetation and soil features* (McFeeters, 1996). In fact, the NDWI will enhance those features that have higher reflectance towards the GREEN/BLUE side of the electromagnetic spectrum, while being highly absorbent at NIR wavelengths (such as water).

On the other hand, areas of vegetation and soil, which provide high reflectance on the NIR side of the spectrum and higher absorption in wavelengths of visible light, will be minimised or even eliminated. Nevertheless, the NDWI has an important limitation in differentiating the spectral signal from the built-up environment and the one from water. Actually, as argued by Xu (2006), in the same way as for water, urbanized areas also reflect higher in the green band than in NIR wavelengths. This produces values of NDWI greater than 0 for the built-up environment too[285], thus making its minimization not very effective. Consequently, when using the NDWI in areas with a built-up background, water features will be mixed with other land cover types, so a noisy discrimination and an overestimation of the water surfaces will result from it.

Principally based on these assumptions, Xu (2006) suggests an improvement of the index by substituting the NIR band with a Short Wave Infrared (SWIR), which in the case of Landsat imagery is provided by band 5 (TM5). The Modified Normalized Difference Water Index (MNDWI), calculated using equation [4.29], enhances open water features while efficiently suppressing and even removing built-up land noise as well as vegetation and soil noise (Xu, 2006).

$$MNDWI = \frac{GREEN - SWIR_1}{GREEN + SWIR_1} \qquad [4.29]$$

Therefore, while the NDWI works with Landsat bands 2 (TM2) and 4 (TM4), the modified NDWI (MNDWI) employs band 2 (TM2) and band 5 (TM5). The use of the SWIR (band 5 of Landsat Thematic Mapper), instead of the NIR, forces the built-up environment to reach negative values. Indeed, done this way, the computation of the MNDWI will produce three results: water will have greater positive values than in the NDWI as it absorbs more SWIR[286] light than NIR; built-up land will have negative values; soil and vegetation will keep negative values as soil

[284] The NDVI *is satisfactory when the desired goal is to assess above-ground biomass because the presence of vegetation is greatly enhanced, but does nothing to provide information regarding open water* (McFeeters, 1996)

[285] *The reflectance pattern of built-up land in the green band (TM 2) and NIR band (TM 4) is similar with that of water, i.e. they both reflect green light more than they reflect near infrared light. As a result, the computation of the NDWI also produces a positive value for built-up land just as for water* (Xu, 2006)

[286] Actually, Jensen (2004), and Xu (2006) speak about the Landsat TM band 5 as a Middle Infrared (MIR) instead of a Short Wave Infrared (SWIR). Within this study we have taken into account the designation of Landsat bands provided by USGS (Landsat - A Global Land-Imaging

reflects SWIR more than NIR (Jensen 2004), and vegetation reflects SWIR more than green light. *In addition, owing to the normalization algorithm, the MNDWI can reduce shadow noise without using sophisticated procedures* (Xu, 2006).

At any rate, both NDWI and MNDWI images clearly emphasize the three major water features, i.e. rivers, lakes and sea, even if with certain variations on the land environment. The objective of this study is to provide an overall classification of land cover composition, instead of a detailed analysis of the water environment. Therefore, both indices have been used for improving the digital information provided by Landsat imagery, in addition to the Wetness index, as defined by the Tasseled Cap transformation (see section 4.3.4.3).

4.5.5.3. Soil Indices

The spectral signal reflected back from the Earth's surface combines a variety of land cover types, which for most purposes and for practical reasons, can be generally classified into three main categories: vegetation, water and soils. The latter broad class normally includes natural categories (such as bare land, sand or clay) but most of the time can also identify artificial materials (such as concrete or asphalt).

Bare soil areas play an important role in environmental analysis without doubt and are strongly affected by seasonal variations, so seasonal or permanent bare soils have to be taken into account when classifying. This variability makes the extraction procedure less than ideal for bare soil areas by using clustering methods (such as maximum likelihood or minimum distance, for instance) directly applied on the multispectral data of an image. In most cases, an averaged image of reflectance values over a year could improve the detection of areas of permanent bare soils.

On the other hand, the spectral indices, based on arithmetics of the reflective information, were proved to be a good way to recognize different land cover types (Zha, et al., 2003). Therefore, by extending the idea of using NDVI for vegetation and NDWI for water, spectral indices for enhancing soil features have been provided based on the use of a Short Wave Infrared[287] (SWIR). This is in addition to MNDWI, because SWIR channels provide better effectiveness for monitoring various moisture conditions.

A Normalized Difference Soil Index (NDSI), formulated according to equation [4.30], was used because it *gives a more reliable estimation in a case of exposed soil conditions. This index is formulated to portray the characteristic of responses from soil other than vegetation or water* (Kasimu, et al., 2010), thus showing enhanced sensitivity to discriminate deciduous broad-leaved forest or sparsely vegetated areas, from dry land.

$$NDSI = \frac{SWIR_1 - NIR}{SWIR_1 + NIR} \qquad [4.30]$$

Optical wavelengths cannot penetrate objects, therefore optical RS can only detect surface conditions and not underground moisture content. Consequently, the NDSI has more potentialities to detect degrees of water amounts in soils, as short wave infrared enhances the monitoring of moisture contents on the ground. Actually, Rogers (2004) used the Normalized Difference Soil Index (NDSI) to reduce signature variability in un-mixing coastal marsh, for instance. Apart from that, it achieved the objective of better discrimination of different areas of vegetation both rural or forest (which range from dense canopy to sparse canopy with differing degrees of soil background) up to completely bare soils.

An advanced normalized index, known as the Bare Soil Index (BI), was proposed by Chen, et al. (2004). Similarly to the ARVI and in the same way as the discussed NDSI, the BI also employs the BLUE band to reduce some atmospheric effects and the $SWIR_1$ band for enhancing moisture content analysis. In fact, the Bare Soil Index is able to emphasize fallow lands or even vegetation with a marked soil background response. It is calculated as the ratio between the sum of band TM5 ($SWIR_1$) and band TM3 (RED), which provide two highly reflective bands for bare

Mission, 2013), in which band 5 (TM5) which ranges from 1.55 to 1.75 µm, and band 7 (TM7) which ranges from 2.08 to 2.35 µm, are defined as "Reflected IR" in the case of TM and ETM+ sensors. In the case of the OLI sensor on board Landsat 8, bands 6 and 7, which range respectively from 1.57 to 1.65 µm, and from 2.11 to 2.29 µm, thus providing wavelengths intervals similar to band TM5 and TM7, are designated as Short Wave Infrared (SWIR).

[287] Also in this case the $SWIR_1$, (i.e. band 5 of Landsat Thematic Mapper) has been used.

soils, minus the sum of band TM4 (NIR) and band TM1 (BLUE), which contrarily provide two highly reflective bands for vegetation; all divided by the sum of TM5+TM3 and TM4+TM1, as depicted in equation [4.31], in order to achieve the normalization of the results.

$$BI = \frac{[(SWIR_1 + RED) - (NIR + BLUE)]}{[(SWIR_1 + RED) + (NIR + BLUE)]} \qquad [4.31]$$

Similarly for water, both the NDSI and BI indices have been used in addition to the Brightness index (SBI) defined using the Tasseled Cap transformation (see section 4.3.4.3) in order to enhance soil features from the original information provided by Landsat imagery. All indices, obtained as discussed above, will form part of a "multi-index" image based on the reflective information of the Thematic Mapper bands and on the spectral indices derived from them.

4.5.6. The "Multi-Index" Image

In order to obtain the finest results when classifying satellite imagery, aspects such as spatial and spectral resolution play an essential role within a process configured as a complex sequence of tasks. These include operations like atmospheric correction and advanced enhancement techniques. Actually, the use of clustering algorithms is just the final stage of the process which will provide better or worse results depending on the quality of the pre-processing operations as well as the effectiveness of the improving techniques applied on the set of digital data.

The spatial resolution of imagery (i.e. the dimensions of the pixel) is directly related to the purposes of the study. In other words, if we attempt to provide analysis on a territorial scale (regional planning, for instance), middle resolution imagery (such as Landsat) is practical. However, we will require higher spatial resolutions when spatial analysis focuses on an urban or local scale. Similarly, higher spectral resolutions (hyperspectral imagery) allow advanced thematic analysis; such as computing further vegetation indices or providing detailed mineral analysis, broad water quality monitoring, etc.

At any rate, Landsat multispectral imagery can definitely supply effective information for the purposes of providing an overall classification of land cover suitable for spatial analysis and planning on a regional scale. However, in addition to the pre-processing procedures (such as geometric correction, radiometric calibration, and atmospheric correction[288]), in most cases cloud cleaning and brightness adjustment are required for reducing seasonal variations when mosaicking imagery[289].

Digital imagery is formed from multiple layers, with each one giving information about different physical aspects of the ground. One of the main objectives of this study, once Landsat data is pre-processed, is to increase spectral information by generating a "new" digital image based on several additional layers. These layers should be co-registered between them in order to multiply the information stored in each pixel (in addition to the original Landsat data).

To do so, transformation procedures and several band arithmetics (as discussed during the previous chapter 4.5.5) have been used to extract single image bands, or indices, that emphasise the abundance of specific land cover types (within a pixel). These include: vegetation, both natural and croplands; water and wet lands; soils and bare lands. Such indices allow significantly reduced environmental effects and the "noise" of information due to the similarity which can occur between different spectral responses at certain wavelengths and for certain land cover classes when working with coarse resolution data.

Thirteen spectral indices, as summarized in table 4.8, have been selected to be involved in the image enhancement procedure.

[288] See chapters 4.3.1, and 4.3.2
[289] See chapter 4.5.3

	INDEX	SYMBOL	EQUATION	AUTHOR
VEGETATION INDICES	Greenness (Green Vegetation Index)	GVI	-0.2848(BLUE) - 0.2435(GREEN) - 0.5436(RED) + 0.7243(NIR) + 0.0840($SWIR_1$) - 0.1800($SWIR_2$)	Crist, et al. (1984); Crist, et al. (1986)
	Normalized Difference Vegetation Index	NDVI	$\frac{NIR-RED}{NIR+RED}$	Rouse, et al. (1974)
	Enhanced Vegetation Index	EVI	$G * \frac{NIR-RED}{NIR+(C_1 * RED)-(C_2 * BLUE)+L}$	Huete, et al. (1997)
	Atmospherically Resistant Vegetation Index	ARVI	$\frac{NIR-2*RED-BLUE}{NIR+2*RED-BLUE}$	Kaufman, et al. (1992)
	Modified Soil-Adjusted Vegetation Index	$MSAVI_2$	$\frac{2*NIR+1-\sqrt{(2*NIR+1)^2-8*(NIR-RED)}}{2}$	Qi, et al. (1994)
	Perpendicular Vegetation Index	PVI_1	$\frac{b*NIR-RED+a}{\sqrt{b^2+1}}$	Perry, et al. (1984)
	Transformed Soil-Adjusted Vegetation Index	$TSAVI_2$	$\frac{a*(NIR-aRED-b)}{RED+aNIR-ab+0.08*(1+a^2)}$	Baret, et al. (1989)
WATER INDICES	Wetness	Third	0.1509(BLUE) + 0.1973(GREEN) + 0.3279(RED) + 0.3406(NIR) - 0.7112($SWIR_1$) - 0.4572($SWIR_2$)	Crist, et al. (1984); Crist, et al. (1986)
	Normalized Difference Water Index	NDWI	$\frac{GREEN-NIR}{GREEN+NIR}$	McFeeters (1996)
	Modified Normalized Difference Water Index	MNDWI	$\frac{GREEN-SWIR_1}{GREEN+SWIR_1}$	Xu (2006)
SOIL INDICES	Brightness (Soil Brightness Index)	SBI	0.3037(BLUE) + 0.2793(GREEN) + 0.4743(RED) + 0.5585(NIR) + 0.5082($SWIR_1$) + 0.1863($SWIR_2$)	Crist, et al. (1984); Crist, et al. (1986)
	Normalized Difference Soil Index	NDSI	$\frac{SWIR_1-NIR}{SWIR_1+NIR}$	Rogers, et al. (2004) Kasimu, et al. (2010)
	Bare Soil Index	BI	$\frac{(SWIR_1+RED)-(NIR+BLUE)}{(SWIR_1+RED)+(NIR+BLUE)}$	Chen, et al. (2004)

Where: BLUE, GREEN, RED, NIR, and $SWIR_1$ are, respectively, the Landsat TM spectral bands 1,2,3,4, and 5;
a and *b* are, respectively, the slope and intercept of the soil line identified by the RED-NIR feature space;
L is the canopy background adjustment factor; C_1 and C_2 the coefficients of aerosol resistance, and *G* is the gain factor

Tab. 4.8: Summary of spectral indices involved in the "multi-index" image for enhancing Landsat data (Source: By Authors)

Not all of the vegetation indices have been used for our purpose, with respect to those discussed in section 4.5.5.1. Some of them have actually been discarded and in particular, the Simple Ratio (SR) because it is sensitive to division by zero errors and the resulting measurement scale is not linear (Silleos, et al., 2006). The NDVI provides a statistically normal distribution, the property of ranging from -1 to 1, and division by zero errors are significantly reduced with respect to the SR.

The Soil Adjusted Vegetation Index (SAVI) is not included because it requires an arbitrary factor L, chosen among the values 0, 0.5 and 1.0. Meanwhile the MSAVI employs a more realistic L, and also provides a reduction of soil noise influences and a more linear response to the percentage of green cover with respect to the SAVI.

The Modified Perpendicular Vegetation Index (PVI_1) has been preferred because the original PVI does not discriminate between pixels from the right side of the soil line (i.e. mainly vegetation) and pixels on the left side of the soil line that are more inclined to be water (Perry and Lautenschlager, 1984; Silleos, et al., 2006). Finally, $TSAVI_2$ has been preferred basically because it appears to be more effective for mapping different degrees of deepness in water, as opposed to the $TSAVI_1$ which seems to be less suitable for water environments.

When computing spectral indices, one critical concern has to been taken into account, prior to setting up the final multi-index image. This is that in most cases, the mathematical form of the equation induces the arising of outliers within the values of the resulting image. Besides, when calibrating a multispectral image some zero values can occur, although an atmospheric correction is undertaken. In such a case, the division by 0, in the formulation of the NDVI for instance, induce no-data values in the image. These values can significantly affect statistical calculations, and can alter the results of image classification procedures. Therefore, it is essential to solve this issue before applying any transformation (Principal Component analysis, for instance) or clustering.

Consider, as an example, the NDVI image calculated for the Autonomous Community of Murcia, one of our case studies. Although the common range for an NDVI should not exceed the interval comprised between -1 and 1, in this case, minimum and maximum values for the NDVI have given respectively, -1 and 25. A value in the image is exceeding the normal maximum value for an NDVI, so this suggests the existence of outliers. However, if we plot the histogram of all the NDVI values, as depicted in image 4.47, we observe that almost one hundred percent of the values are concentrated into a small portion (a peak) of the histogram, which is actually found within the common range of the NDVI.

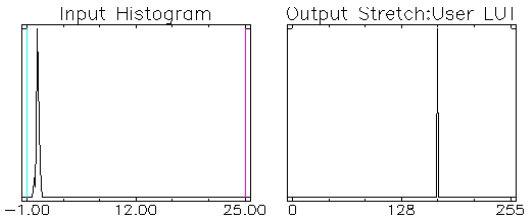

Fig. 4.47: Histogram for the NDVI, full band no stretched, as calculated for the case of Murcia (Source: By Authors)

In order to solve the problem, and therefore discard all the outliers, it is necessary to reduce the whole range of the histogram (i.e. -1 to 25), so that the resulting minimum and maximum values in the image should match the most significant interval of the NDVI, which is the one represented by the peak in the previous graph. This is achieved by applying a linear stretching using the subsampled set of values within the peak.

The ENVI software provides three windows for image visualization: Scroll, Image (which is a subset of the Scroll) and Zoom. The linear stretch is applied in the Scroll window and arranges the most suitable subsampled set of the values in the histogram, thus automatically discarding the outliers (in some cases a linear stretch at 2% could be desirable). The outcome of the stretch is displayed in the histogram in image 4.48, showing the resulting interval of values for the NDVI, i.e. the NDVI[1], now ranges from -0.52 to 0.87.

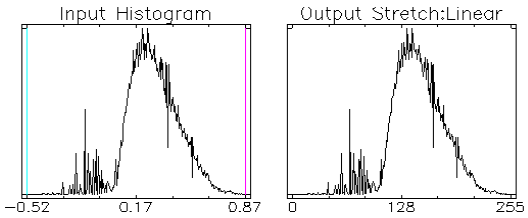

Fig. 4.48: Histogram of the linear stretched NDVI, i.e. the NDVI[1], as calculated for the case of Murcia (Source: By Authors)

Once minimum and maximum NDVI values are fixed at -0.52 and 0.87, respectively, as derived from the histogram of the stretched NDVI, all values smaller than the minimum are forced to match -0.52, and all values greater than the maximum are forced to match 0.87, by applying the relational operations, as follow:

- NDVI Less Than MINIMUM, then NDVI Equals the MINIMUM;
- NDVI Greater Than MAXIMUM, then NDVI Equals the MAXIMUM;
- NDVI Equals or Comprised between MINIMUM and MAXIMUM, then NDVI Equals the NDVI.

In this way, we obtain the NDVI[1], but the general significance of the index is kept unchanged. In fact, if we look at the basic statistics calculated both for NDVI and NDVI[1], as shown in table 4.9, although minimum and maximum values are different because we constrain them. Mean and Standard Deviation are practically the same,

except for a small variation. This means that the frequency distribution of Digital Values (DN) (i.e. the number of pixels for each DN) is similar, but outliers are rejected.

	Minimum	*Maximum*	*Mean*	*Standard Deviation*
NDVI: Full Band	-1.000000	25.000004	0.274805	0.169432
NDVI[1]: Linear Stretch	-0.520000	0.870000	0.274804	0.169308

Tab. 4.9: Basic statistics for NDVI, and NDVI[1] which are derived by linear stretching of a subsampled set of NDVI (Source: By Authors)

Instead, when no-data occurs along images, an automatic algorithm of "fill no-data" can be applied as provided by the Quantum GIS (QGIS) software for instance. The algorithm calculates values for the no-data pixels by interpolating from valid pixels surrounding the edges of the missing values, and based on an inverse distance weighting[290] (QGIS Development Team, 2015).

Depending on the "undesired" values, different correction procedures, as described above, has been applied to all of the spectral indices summarized in the previous table 4.8, thus finalising the Vegetation Indices[1], Water Indices[1], and Soil Indices[1], which form part of the multi-index image. This also presented the possibility of improving the spectral information of the sensor through the use of advanced spectral indices.

Further enhancements were allowed by a multi-index image derived from the possibility of internalizing some topographic features within the digital information, prior to applying a clustering process. In particular, if we attempt to find certain patterns within land cover types when analysing the Earth's surface, a relevant correlation is clearly observable between the land cover composition and the topography of the ground.

With this in mind, a Digital Elevation Model (DEM), discussed in chapter 4.2.5, provides a useful instrument for deriving topographic models. The DEM employed in this investigation is derived from the Shuttle Radar Topography Mission (SRTM), which offers a raster image of the ground elevation heights (or altitude), at a resolution of 1 arc-second (approximately 30-meter). Although altitude definitely affects the land cover composition, we found the use of the slope more reliable for improving land cover classification results, instead of the DEM. Observe figure 4.49, even if a significant correlation does exist between them, high values of DEM (from which the slope is obtained) (left side of the image) do not always correspond to high degrees of slope (right side).

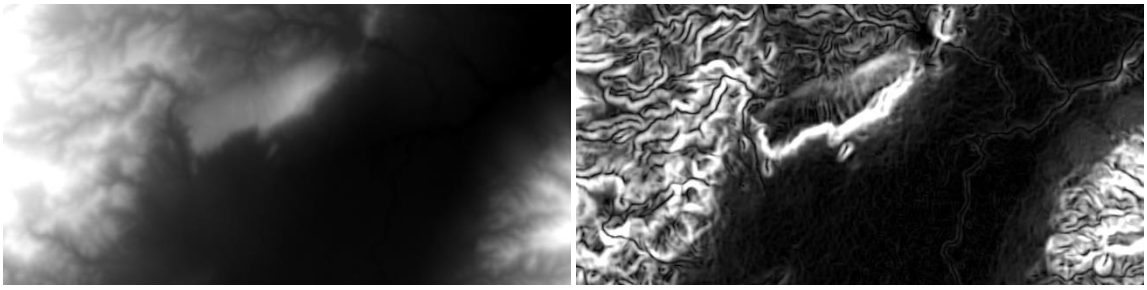

Fig. 4.49: Input elevation raster (left side); and output slope (right side), at 30 meters of spatial resolution (Source: By Authors)

Water bodies, for instance, can be found at any altitude as there are lakes or rivers on mountains, as well as on plains. However, water generally provides slope values equal (or close) to zero and at certain wavelengths water absorbs (or reflects) light in a similar way to shadow. Therefore, the use of the slope increases the capability of discriminating between water and steep shaded areas (such as the shaded side of mountains).

Similarly, areas of dense vegetation (such as croplands, grasslands, or forests) are also quite independent with respect to elevation. Moreover, they can provide similar reflectance values depending on the wavelengths. Areas of green vegetation on steep mountains can be detected with difference from grasslands and croplands, if slope features are taken into account. Imagine how difficult it is to plant crops on a high slope. This also concerns bare soils and even more so for urban areas. The degree of the slope shows a higher correlation with these land

[290] This algorithm is generally suitable for interpolating missing regions of fairly continuously varying rasters (such as elevation models for instance). It is also suitable for filling small holes and cracks in more irregularly varying images (QGIS Development Team, 2015).

cover classes than the altitude, and it therefore improves the possibility of avoiding classification mistakes due to similar reflectance values. The density of urbanization generally decreases as the slope increases, and the same is true for croplands,

The slope is the main derivative of a DEM and it signifies the degree of change of elevation values for each pixel in the raster. For each pixel, the extraction of the slope value is done by employing a plane which depends on the z-values of a 3x3 cell neighbourhood around a centre cell. The slope value of the plane is then calculated using the average maximum technique. In other words, the slope value is calculated from the maximum degree of elevation change over the distances from one pixel to its eight neighbours. Therefore, it identifies the shortest path between the central pixel and those in the analysed neighbourhood. Simply put, the lower the slope value, the flatter the terrain, and the higher the slope value, the steeper the terrain.

Slope, which can be measured either in percentages or in degrees, is conventionally fixed as zero (degrees or percent) for a horizontal plane. Slope is calculated in percentages as 100*rise/run, or can be derived from the slope in degrees using the relation 100*tan (degrees). The slope values range from 0 to 90 in degrees, while the percentage values range from 0 to infinite. As the slope angle approaches vertical, i.e. 90 degrees, the percentage approaches infinity.

As depicted in figure 4.50, the Landsat TM multispectral image, the derived spectral indices and the slope (co-registered) have been arranged within a multi-layer image. Henceforth, termed multi-index image, which relies on twenty digital images with each providing different information about the land cover composition at a spatial resolution of 30 meters per pixel.

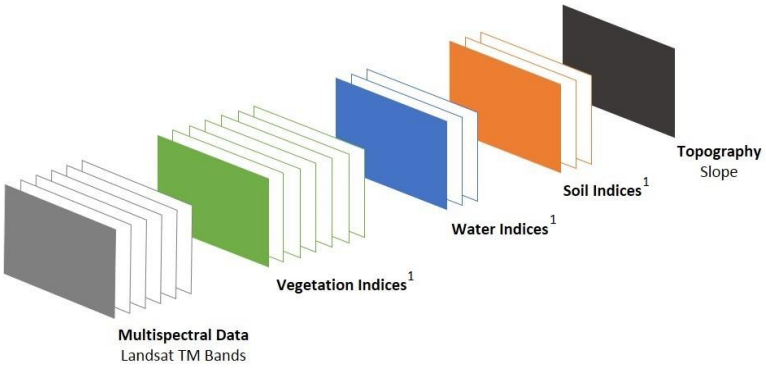

Fig. 4.50: The multi-Index digital image structure (Source: By Authors)

The layers are based on different ranges of values, so it is critical to homogenize the whole stack in order to make comparisons between the multi-index images and the information stored in them. It would also be advantageous to visualize the different behaviours of the land cover types for different indices. Moreover, the homogenization of the scale of values would ensure the same weight of the pixel response for each image layer during the classification process, thus increasing the divisibility between the different land cover types. This can be achieved by normalizing the range of values for all the images, by scaling the input Digital Numbers (DNx) using the equation [4.32], and consequently obtaining data at a common scale that ranges from 0 to 255. *This greatly reduces the variability within each digit class, because the location and scale of all the digits are now the same, which makes it much easier for a subsequent pattern recognition algorithm to distinguish between the different classes* (Bishop, 2006).

$$DN^* = \frac{DN_x - X_{min}}{X_{max} - X_{min}} * 255 \qquad [4.32]$$

Where: DN^* = Normalized Digital Number
DN_x = Digital Number of image data X
X_{min} = Minimum value of image data X
X_{max} = Maximum value of image data X

Normalization is the last task applied to the multi-index image, of which a sample is depicted in the next figure 4.51. In the case of Murcia, a subset of the whole geographical area has been detailed through visualizing the various indices including a pseudo-natural colour composite of Landsat TM imagery, in order to better understand the significance of the different layers that compose the enhanced digital information.

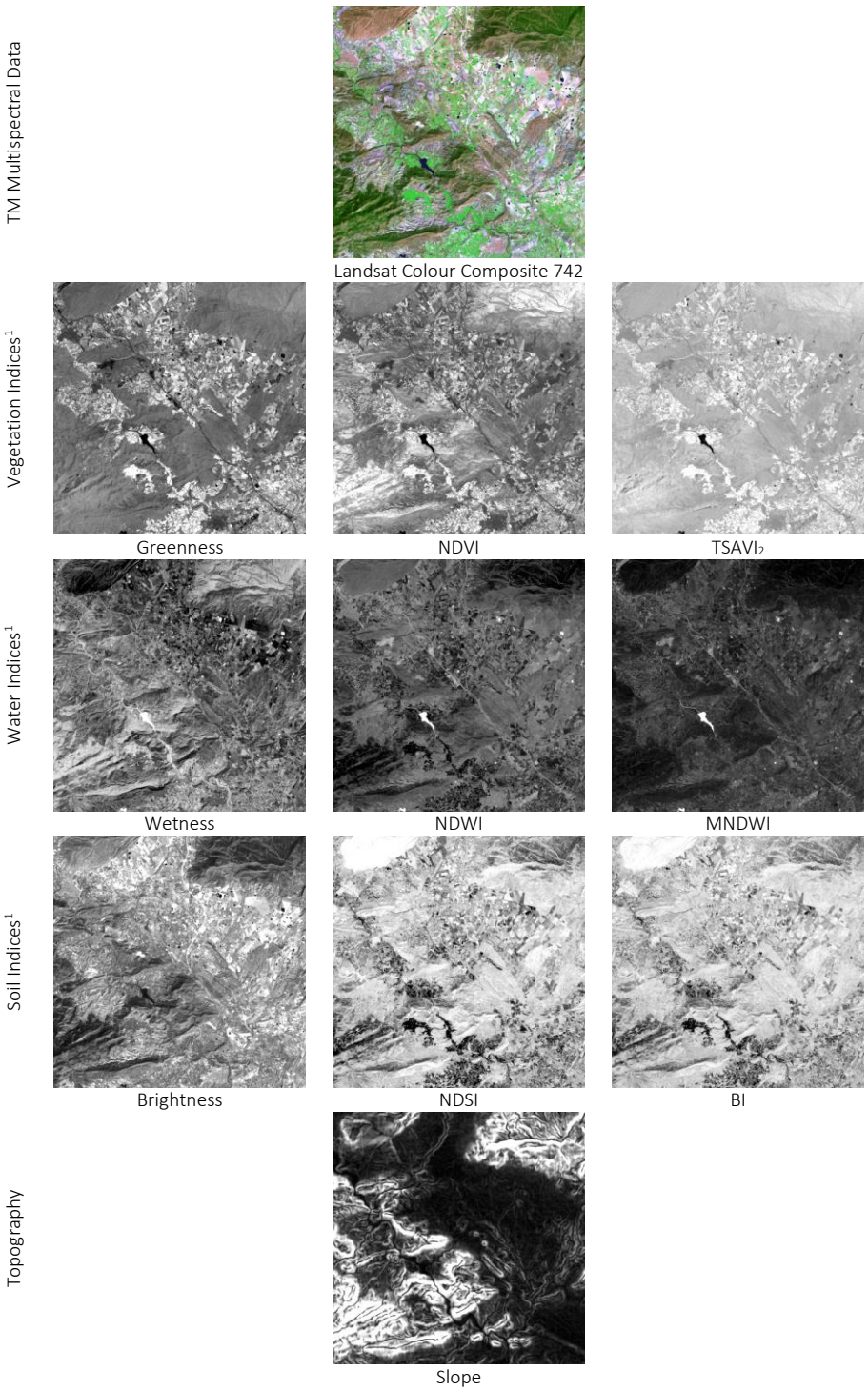

Fig. 4.51: A sample of the final layers which compose the multi-Index digital image: a subset of Murcia (Source: By Authors)

4.5.7. Classification and Post-Classification: Defining an Effective Land Cover Mapping Process

Depending on image resolutions, some important applications of Remote Sensing focus on: urban growth assessment and environmental monitoring; forestry, agriculture and water analysis; natural hazard management; global change detection, in particular, atmospheric ozone depletion, deforestation, global warming, etc. In most cases, land cover mapping is fundamental information to have prior to undertaking an analysis. Land cover mapping relies on certain generalized rules and assumptions which form part of a classification procedure that pursues the main objective of providing the most effective inventory possible of land cover composition covering specific portions of the Earth's surface. To do that, a number of issues need to be dealt with in order to set up a suitable and widely recognised classification scheme.

Firstly, the imagery used for undertaking land cover classification should be the most suitable possible. Image classification is based on the assumption that any variation in land cover composition has to be detected in the imagery and mapped. It is actually assumed that "true" variations on the land surface will correspond to changes in the spectral information contained within the digital data, but several factors may affect the spectral response. *There may be variation in the imagery caused by the sensor (an extreme case would be the SLC-off gaps in Landsat 7 imagery), by the atmosphere (clouds, for example), or by lighting conditions which cause shadows across an otherwise uniform surface. There may be important variations on the ground surface that are not easily detected in the imagery due simply to insufficient spatial resolution*. That is why all the possible, and appropriate, pre-processing steps have to be provided in order to reduce variation in the image caused by sources other than the ground surface reflectance values (Schuckman, et al., 2014).

Based on the aforementioned statements, and prior to undertaking the classification algorithm planned within this investigation, several pre-processing steps have already been applied to the imagery. This was detailed during the previous chapters and covers from the calibration stage (section 4.3.2) up to the normalization of the images which compose the multi-index image (section 4.5.6). Once all the possible variations are reduced and derived by "external" factors, the classification system needs to meet some chief requirements. According to Congalton, et al. (2009), a classification scheme must first require both hierarchical labels, i.e. the class names are organized by following a logical tree structure, as well as containing rules for defining the labels[291]. Moreover, it should:

- *Meet the user's needs*
- *Consist of classes that are:*
  - *mutually exclusive (an object/target should belong to one and only one class)*
  - *totally exhaustive (all objects/targets in the study area can be assigned to a class)*
  - *hierarchical (high level general classes further subdivided into more specific subclasses)*
- *Include a minimum mapping unit which defines the smallest size area to be classified (which should never be as small as a single image pixel)* (Schuckman, et al., 2014).

Therefore, preparing and understanding[292] images is the key to obtaining better results. Compliance with the aforementioned requirements for a classification scheme increases the consistency of the results of classifications (either for photo-interpretation or automatic clustering processes, as used in this investigation). The consistency of land cover classifications also depends on the relationship between the pixel size of the employed images and the operational scale to which the information will be analysed. Generally, the bigger the pixel size, the smaller the operational scale[293]. At any rate, post-classification merging operations, dependent on the expected level of details and filtering stages (such as sieving and/or clumping), are required for achieving more homogeneous classes and effective results. However, photo-interpretation criteria should always be applied to the final results which will be compared with the original satellite imagery in addition to other available ancillary data, in order to rectify possible misclassifications.

[291] This task was developed in section 4.5.2

[292] According to Congalton and Green (2009), an effective classification scheme should firstly rely on some key points, such as: understanding the real variations on the ground; linking those variations to the spectral response of digital data, once possible external alterations to the ground response are discarded; transforming these linkages between variations on the ground and variations in the imagery into a suitable land cover map.

[293] See next section 4.5.7.2

4.5.7.1. A Classification Algorithm

The process of land cover extraction that we have suggested within this study relies on an assisted automatic pixel-based method effectively calibrated on Landsat TM multispectral imagery at 30 meters of spatial resolution. The algorithm (as depicted in figure 4.52) relies on five main computational steps, three of which are clustering analysis and two are class statistics. The input data is provided by the pre-processed six band multispectral Landsat TM imagery; and used in relation with the relative spectral library based on 250 generalized land cover categories extracted from a series of pre-processed imagery, as described during chapter 4.5.4. Moreover, the multi-index image and the derived Principal Component Analysis are involved.

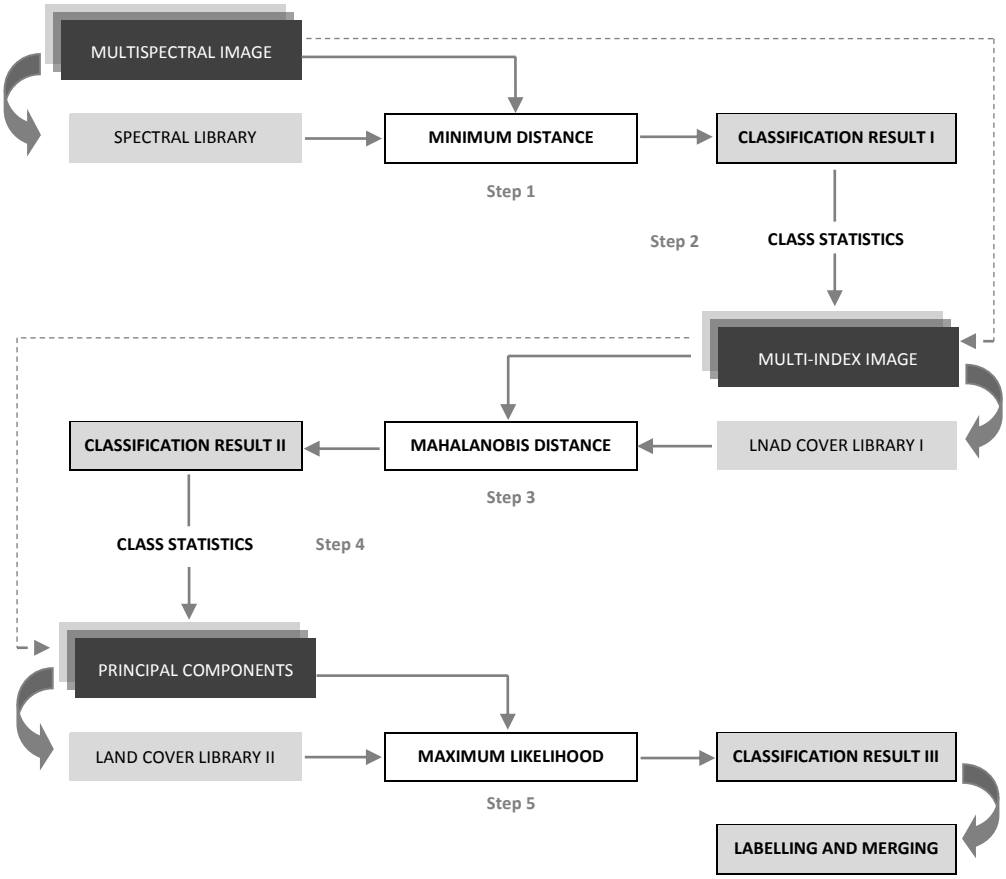

Fig. 4.52: Algorithm for an assisted automatic land cover classification built on Landsat TM multispectral data (Source: By Authors)

The methodology requires the use of a pre-constituted spectral library containing the physical characteristics of reflectance for several codified land cover types, dependent on the number of spectral bands provided by the sensor. The direct use of ROIs is discarded as a tool for the contingent collection of class statistics, thus reducing the subjectivity that could be derived from photo-interpretation practises during this phase.

Conceptually, the classification relies on an iterative process, in which the values of the spectral library provide the first cluster centres used for classifying Landsat multispectral data. After the first classification, new cluster centres are extracted from the enhanced image data and further clustering processes are undertaken. This approach, based on the use of automatically generated class statistics values, has the advantage of allowing classification of unknown pixels strictly according to the "nature" of materials and the maximum physical difference between them. This is a sort of machine learning process which, at each iteration, reduces the probability of misclassification through re-calculating the class mean values, dependent on improved information.

In particular, at step 1, the minimum distance clustering method is used for classifying Landsat TM scenes, dependent on the previously collected spectral library.

The classification result I, at step 2, is used to derive basic statistics with covariance[294], from the normalized multi-index image (section 4.5.6). This is done in order to generate an improved library of land cover types, now based on Digital Numbers (DN), ranging from 0 to 255. The averaged DN value of all the pixels which form one class is used to generate a new cluster centre vector comprising all of the class mean values, measured at each level of the multi-index image.

Thus, 250 vectors are collected in the land cover library I which, at step three, is used for classifying the multi-index image, using the Mahalanobis distance classifier to obtain the classification result II.

At this point, a principal components analysis (PCA) is undertaken on the multi-index image, prior to running the following classification step based on the maximum likelihood classifier. This kind of processing represents a form of dimensionality reduction, which is useful for discarding redundant information which can occur between the twenty layers of the multi-index image.

This process is required in order to avoid correlation between bands because the maximum likelihood classifier can produce zero eigenvalues if high correlation occurs or no covariance is present (eigenvalues in basic stats need to be greater than 0), this can reduce the accuracy of results. The PCA allows us to keep almost all of the original information of the multi-index data or at least a high percentage of it and in fewer bands which are uncorrelated between them.

At step four, class statistics is then computed for the obtained principal components, which provide a multi-layer image that generally does not exceed a stack of about nine or ten layers. It is requested to provide at least 98% of variability of the input data. This stage delivers the class mean values, extracted from the PCA image dependent on the classification result II, which will be collected in the land cover type library II.

The maximum likelihood classification is then applied[295] to the PCA data at step 5, by employing library II to obtain the final classification result III. When clustering is complete, class merging and labelling operations are undertaken based on the twenty land cover categories listed at level II of the nomenclature provided in chapter 4.5.2.

Merging sets of clusters is actually necessary for reducing the number of final land cover classes in order to make a more intelligible, useful and consistent map with the effective potentialities provided by the spatial resolution of the input data. As argued by Richards and Xiuping (2006), decisions about merging could be made on the basis of separability measures; however, here we opted for proceeding with photo-interpretation techniques based on the original satellite imagery and all the available ancillary data as a reference.

Therefore, relying on the analyst's skills and knowledge of the geographical areas under investigation. The final classes are verified and associated with ground truth information by labelling, and then colouring, in accordance with level II of the nomenclature. Hence, despite an important part of the methodology relying on automatic processes, the fundamental work of interpretation is necessary after the classification algorithm is performed. Both the clustering phase and subsequent post-classification steps, all require a high degree of expertise essential for obtaining the best result possible.

The land cover classification for year 2011 has been repeated for the five Autonomous Communities on the Spanish Mediterranean coast and organized in eight geographical areas due to the fact that Andalucía's huge dimensions has been divided into four smaller geographical ambits by joining provinces two by two. The same spectral library was built on Landsat TM data 2011 at 30 meters of spatial resolution and based on 250 spectral categories. It has been used to undertake the assisted automatic classification eight times (using the algorithm

[294] With difference to the minimum distance classifier, which only requires mean vectors for clustering, the Mahalanobis distance classifier, as well as the maximum likelihood, also require covariance values of one class between different bands in order to run a classification process.

[295] In order to achieve the best results when applying maximum likelihood classification, it would be appropriate to reduce the number of bands by using principal component analysis for avoiding high correlation between bands. Actually, bands with little or no variance will produce mistakes in the classification, because in such a case one band becomes a near-perfect linear combination of other bands (Japan Association of Remote Sensing, 1999). Moreover, Richards and Xiuping (2006) argue that *classification cost increases with the number of features used to describe pixel vectors in multispectral space – i.e. with the number of spectral bands associated with a pixel. For classifiers, such as the parallelepiped and minimum distance procedures, this is a linear increase with features; however for maximum likelihood classification, the procedure most often preferred, the cost increase with features is quadratic. Therefore it is sensible economically to ensure that no more features than necessary are utilized when performing a classification* (Richards, et al., 2006)

depicted in the previous figure 4.52) and we obtained a significant homogeneity of results between the different land cover maps[296].

Moreover, figure 4.53 shows the consistency between the classification system set up within this investigation and two widely recognized reference data such as Corine Land Cover 2006, and the MCSC (*Mapa de Cubiertas de Suelo de Cataluña*) 2009, provided by the Centre for Ecological Research and Forestry Applications.

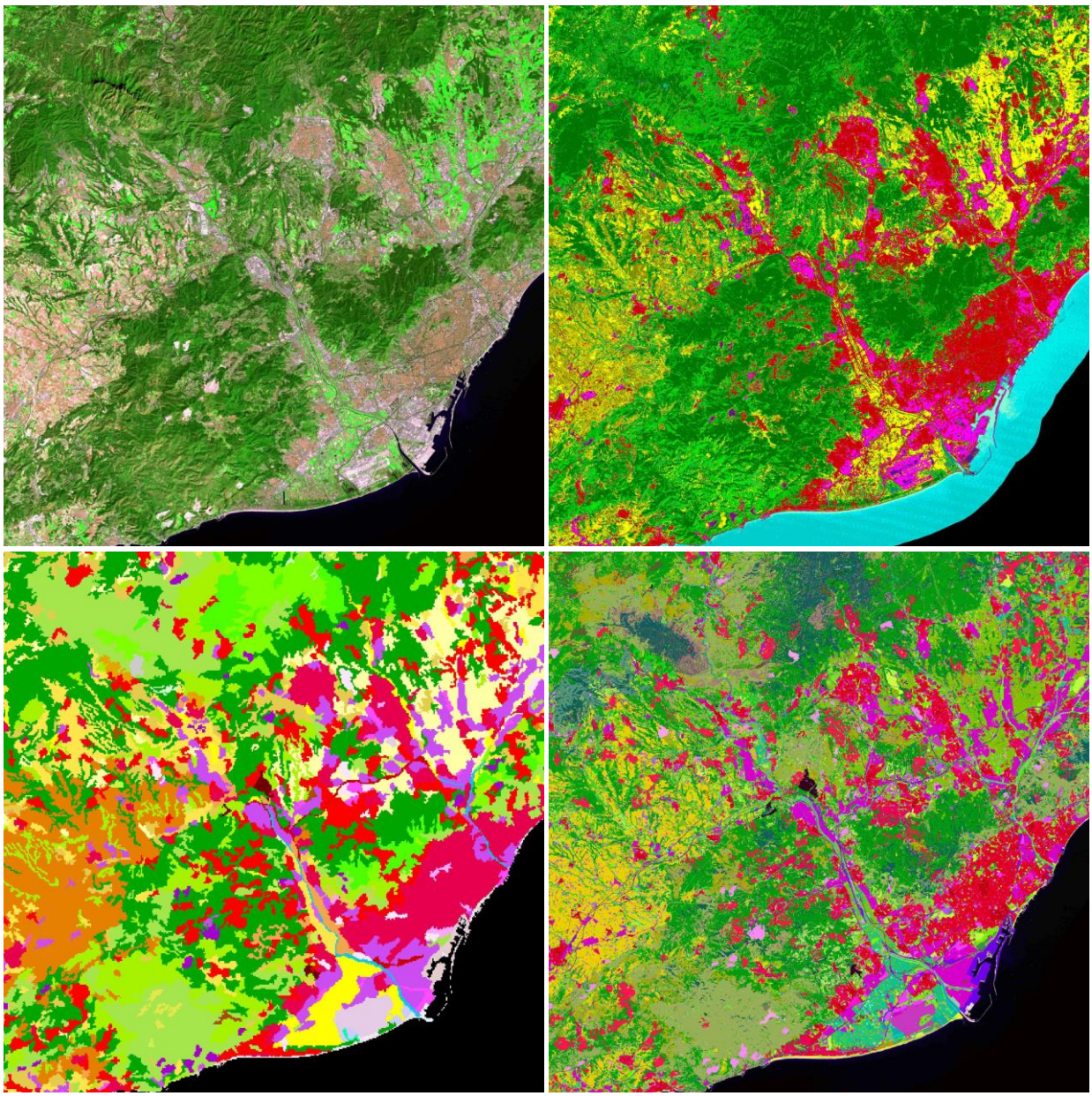

Fig. 4.53: Landsat pseudo-natural colour composite 2011 (upper left) and classification result (III), after class merging and labelling, according to level II of the proposed nomenclature (upper right); Corine Land Cover 2006 (bottom left); and *Mapa de Cubiertas de Suelo de Cataluña* (MCSC) 2009 by Centre for Ecological Research and Forestry Applications (bottom right) (Source: By Authors)

[296] All classifications results (for the eight geographical ambits) can be found in the section addendum at Annex I which provides an atlas of land cover, at provincial level, for the Mediterranean side of Spain at the year 2011.

Having a wide range of spectral classes at one's disposition at the beginning of the clustering process increases effectiveness as each material can provide certain variations of reflectance features, dependent on several factors which may affect the model of light absorption. If we consider the spectral properties of forests, for instance, besides the obvious variability due to a multitude of species of vegetation, the forest class can vary greatly depending on the exposure. In other words, the vegetation on the sloped side of a mountain, if in a shaded area, reflects differently when compared with the same vegetation on the sunny side.

At this spatial resolution it is also extremely complicated to discern urban settlements from certain bare soils. The coarse spatial resolution of the imagery contributes to a mixing of different reflectance features within a pixel, thus generating a certain number of transitional values quite difficult to label.

Hence, it is desirable to firstly define different subcategories in order to cover the spectral variability within a landscape as much as possible. Actually, the selection of a considerable number of spectral subcategories and the improvement of the original satellite data through the use of additional information (such as vegetation indices or topographical features, for instance) provides a variability level that is more representative of reality and greatly increases the capability of obtaining much more consistent results.

4.5.7.2. Post-Classification and Final Land Cover Maps: A Question of Operational Scale

Applying the proposed methodology produces remarkable outcomes, mainly for quickly discriminating artificial surfaces and natural land cover classes; such as vegetation, water, croplands or bare lands. The process also demonstrates goodness in identifying different vegetation categories for both agriculture and forest, as well as separating (to some extent) the key typologies of impervious areas (such as residential and industrial settlements). Although, impervious areas often tend to mix with certain categories of bare soils at this spatial resolution. Therefore, in order to reduce the automated classification mistakes and "noise" as much as possible due to the mixing of classes, the final step of the methodology foresees a filtering operation. This filtering operation is designed to fill small holes. In particular, removing or at least reducing islands of pixels and narrow elements smaller than the fixed structural element (kernel). This will provide a useful homogenization of results.

Two filters have been applied here: the Clump and Majority analysis, used respectively to fix lack of spatial coherence (speckle or holes in classified areas) and to remove salt and pepper noise or speckle. In particular, the first filter was particularly useful to ensure most coherence to urban areas, and clumps together adjacent similarly classified areas, by employing morphological operators[297]. The majority filter changes spurious pixels within a large single class to that class, dependent on kernel dimensions. Edges larger than the specified kernel dimensions are preserved.

Finally, the twenty land cover classes (as specified at level II of the nomenclature) are merged into the four generalized classes of level I, using the hierarchical relationships depicted by the nomenclature scheme in the previous table 4.7. At this point, final reviewing and manual corrections are undertaken through photo-interpretation and on screen digitization, which is aimed at rectifying important mistakes occurring between the four main classes. The analysis of the results is carried out by overlapping a regular grid on the original multispectral image as well as upon the final classification. These are linked together in order to improve the reviewing capabilities. A detailed example of the results is shown by the images in figure 4.54.

[297] The selected classes are clumped together by first performing a dilate operation, followed by an erode operation on the classified image using a kernel of the size (Exelis)

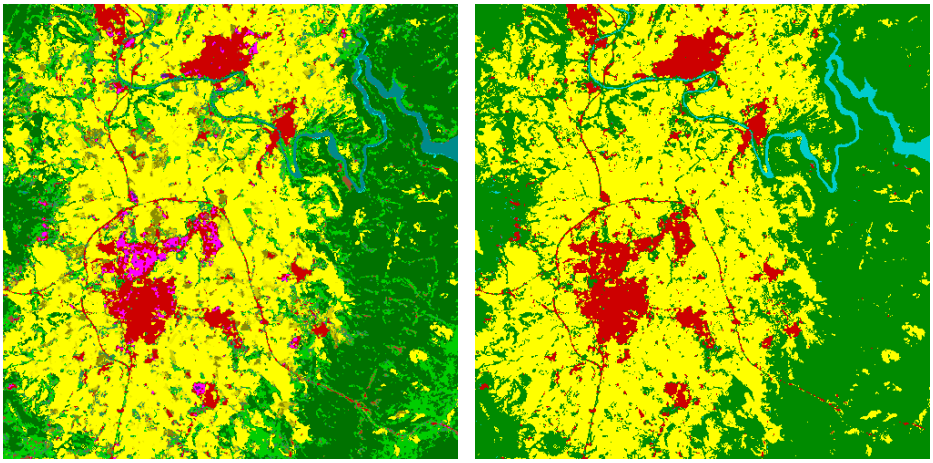

Fig. 4.54: Detailed example of land cover classification result in twenty categories after filtering (left side); and final result after merging the twenty filtered classes into four categories (right side) according to level I of the nomenclature (Source: By Authors)

Theoretically, there is no "perfect" classification, nor a single correct methodology, instead, several algorithms and methodologies can be properly applied to achieve reliable thematic cartography. This is the reason why a protocol of accuracy assessment has to be provided as a fundamental stage for every classification process, in order to guarantee the goodness of thematic maps.

Prior to undertaking the accuracy assessment, as discussed in the following chapter 4.6; a key question must be addressed in order to understand to what extent a land cover classification can be really useful. We are referring to the scale factor. Depending on the image spatial resolution (pixel dimension), the remote sensing sensors provide digital images at various scales of representation. Each time we take into account a land cover map, we need to clarify what the relationship is between the spatial resolution of the image and the operational scale for which we intend to use such information, to derive all required spatial analyses. Actually, according to Vogelmann, et al. (2001), general land cover information is often required for many environmental, land management and modelling applications, but this information may be derived at a range of spatial scales which derives the appropriate usage of the data. Therefore, the quality of a classification result is always relative to an operational scale, which could be broadly organised into three levels: a large scale, between 1:1˙250 and 1:25˙000; a medium scale, greater than 1:25˙000 and up to 1:200˙000; and a small scale, from 1:200˙000 onwards (Meaden, et al., 1991).

The following tables 4.10 and 4.11 summarize the relationship between the spatial resolution of common sensors, and the related scale. In particular, in table 4.10, which is provided by Richards and Xiuping (2006), *the relation has been derived somewhat simplistically, by considering an image pixel to be too coarse if it approaches 0.1 mm in size on a photographic product at a given scale. Thus, for example, Landsat MSS data is suggested as being suitable for scales smaller than about 1:500˙000 (Richards, et al., 2006), while it is reasonable to assume that the results of the classification based on Landsat TM, can match a scale of representation of around 1:250˙000.*

Sensor (nominal)	Approx. Pixel Size (m)	Scale
Ikonos panchromatic	1	1:10˙000
aircraft MSS, Ikonos XS	5	1:50˙000
Spot HRG	10	1:100˙000
Spot HRVIR, Landsat TM	25	1:250˙000
Landsat MSS, LISS	50	1:500˙000
OCTS, OCM	500	1:5˙000˙000
NOAA AVHRR, MODIS	1000	1:10˙000˙000
GMS thermal IR band	5000	1:50˙000˙000

Table 4.10. Suggested maximum scales of photographic products as a function of effective ground pixel size (based on 0.1 mm printed pixel) (Richards, et al., 2006)

Table 4.11 also lists other currently leading sensors by specifying the spatial resolution for both multispectral as well as for panchromatic data, and is derived from the technical fact-sheets provided by Geoimage[298], an international company specialized in satellite imagery and geospatial solutions.

Resolution	Sensor	Approx. Pixel Size (m)		Largest operational Scale
		Panchromatic	Multispectral	
Very High	WorldView-3	0.3	1.24	1:1˙000
	WorldView-2	0.5	2	1:2˙000
	WorldView-1	0.5	-	1:2˙000
	Pleiades	0.5	2	1:2˙000
	GeoEye-1	0.5	2	1:2˙000
	QuickBird	0.61	2.44	1:2˙000
	IKONOS	0.82	3.2	1:2˙500
High	RapidEye	-	5	1:15˙000
	SPOT-6/7	1.5	6	1:5˙000
	SPOT-5	2.5/5	10	1:10˙000/1:25˙000
	SPOT-4	10	20	1:40˙000
Mid	Landsat-7/8	15	30	1:50˙000
	Landsat-4/5	-	30	1:100˙000

Table 4.11. The largest allowable operational scale in relation to the image pixel size, as suggested by the Geoimage Company for some common satellites[299] (Source: By Authors, from Geoimage company)

4.6. CLASSIFICATION ACCURACY ASSESSMENT

First of all, it is important to keep in mind that thematic cartography is a representation of reality, not reality itself. Therefore, the goal is to reproduce the state of the land cover composition at a given temporal stage as faithfully as possible. Thus, the classification process which leads to detection of a specific land cover status must be validated and this requires a control of the goodness of the results.

This is done in order to assess the accuracy and degree of confidence, and consequently for supporting the validity and objectivity of any measurements and quantifications made on the derived thematic cartography. Even if there is an increasing need for standardized methods for accuracy assessments, it is also important to highlight the multiplicity of needs and uses in existence for the remotely sensed information. *There is, therefore, no single universally acceptable measurement of accuracy, but instead a variety of indices, each sensitive to different features* (Stehman, 1997a; Foody, 2002). *In reality, it is probably impossible to specify a single, all-purpose measurement of classification accuracy* (Foody, 2002).

Thematic accuracy generally focuses on measuring the correspondence between the class labelled by a classifier and the one observed in reality, as many mistakes can be committed during image classification processes. According to Weber (2009), while making a classification based on multispectral imagery, the sources of errors can be reduced to four main types:

- *confusion of spectral classes (overlap of spectral distributions)*
- *mixed pixels (pixels containing 2 or more land cover types)*
- *system errors (recording, geometry)*
- *conceptual errors (coherence between land cover classes and separability in the feature space, and internal variability within one class)*

The accuracy assessment procedure implies the comparison of the classification results with geographical data that is supposed to be truly representative of reality. Thus, a protocol for accuracy assessment should form a vital stage in any land cover classification process. A quantitative analysis is commonly required for reporting the precision of land cover classifications. This should be achieved by comparing a sample of pixels from the final classification with *some form of* reference data, the ground truth information. *Preferably, when available, these*

[298] http://www.geoimage.com.au/

[299] Further satellite and sensors specifications can be found at: http://www.geoimage.com.au/satellites/satellite-overview

reference data should: (a) be of a higher spatial resolution than that of the classifications being assessed, (b) be contemporaneous with the dates of the classifications' source remote sensing imagery, (c) possess a known (and acceptably high) classification accuracy themselves (Angel, et al., 2005).

Generally, the quantitative procedure for reporting the accuracy of a classification is calculated through statistical comparison of pixels labelled in each class of the obtained thematic map. This is done with the corresponding classes defined in the reference data commonly derived from the ground truth information (previously mentioned).

The use of a so called "confusion (or error) matrix", or contingency table, is the typical method for computing the degree of accuracy for a given land cover classification result. It is essential for providing most of the measurements of thematic map accuracy (Story, et al., 1986; Liu, et al., 2007). In fact, the use of an error matrix as the standard protocol for assessments of classification accuracy has been clearly demonstrated by Congalton (1991). It is recommended by many researchers to be adopted as a standard reporting convention[300].

Table 4.12 is the confusion matrix which reports the results of the accuracy assessment for the case study of Catalonia. It compares the classification resulting from level I of the LCBC 2011, with the land cover classification realized by CREAF in 2009[301]. A per-pixel accuracy assessment for the four main grouped classes of level I is provided and a spatial resize of the CREAF classification (MCSC) has been undertaken in order to achieve the same minimum sample size (the comparing unit). In the case of this study, this is a pixel of 30 meters as provided by the Landsat TM multispectral imagery. Moreover, some merging operations have been conducted for level I of CREAF classification system to achieve a comparable four category classification[302].

ACCURACY ASSESSMENT						
		Ground Truth Class (CREAF-MCSC 2009)				
Thematic Map Class (LCBC 2011, Level I)		100	200	300	400	Total of Classified Pixels
Artificial Areas	100	958˙808*	177˙766	104˙698	3˙396	1˙244˙668
Planted/Cultivated	200	456˙107	8˙081˙739*	1˙638˙290	19˙983	10˙196˙119
Forest and Natural Areas	300	484˙019	2˙474˙128	20˙976˙047*	81˙557	24˙015˙751
Water and Wetlands	400	10˙494	11˙022	47˙087	146˙245*	214˙848
Number of Ground Truth Pixels		1˙909˙428	10˙744˙655	22˙766˙122	251˙181	**35˙671˙386**
						* Number of pixels per class, correctly classified

Tab. 4.12: Confusion matrix sample for the case of Catalonia: LCBC 2011 vs. CREAF-MCSC 2009 (Source: By Authors)

The error matrix can be used as a starting point for a series of descriptive and analytical statistical techniques (Congalton, 1991). In fact, through combining the values provided by the contingency table, it is possible to calculate a set of items which offer a general report concerning the accuracy of a classification result. In particular, six main indices are computed and reported in the framework of this investigation that are:

- Overall Accuracy
- Kappa Coefficient
- Errors of commission
- Errors of omission
- Producer Accuracy
- User Accuracy

[300] An extensive, and effective review of procedures and indices for assessing classification accuracy based on error matrices, both for category-level accuracy as well as for map-level accuracy, is provided by Canran Liu, Paul Frazier, and Lalit Kumar (2007) in "*Comparative assessment of the measurements of thematic classification accuracy*", Remote Sensing of Environment 107, pp. 606–616. About 14 category-level accuracy measurements, and 20 map-level accuracy measurements are provided and analyzed in the paper.

[301] Technical details about the MCSC land cover classification are reported in section 3.2.2.2.

[302] Following the MCSC classification system provided by CREAF, the four classes named *improductiu artificial* (100), *conreus* (200), *terrenys forestalls* (300), and *aigües continentals* (400) of level I have been maintained.

The Overall Accuracy (O_A), is one of the most common measurements to quantify the goodness of land cover classifications and it relies on the average of the percentage of exact classifications[303]. It is obtained by summing the number of pixels in the diagonal line of table 4.12, which comprehends the correctly classified pixels, and then the resulting value is divided by the total number of classified pixels, as follows in equation [4.33]:

$$O_A = \frac{\sum_{i=1}^{n} x_{ii}}{N} * 100 \qquad [4.33]$$

With n number of land cover classes which appear in the rows of the matrix
x_{ii} number of observations in row i and column i
N total number of observations

If we introduce the appropriate values of the contingency table in the equation, so that x_{ii} is equal to 958˙808+8˙081˙739+20˙976˙047+146˙245, and *N* is equal to 35˙671˙386, we obtain an overall accuracy value of about 84.56 percent[304].

The overall accuracy, as a measurement of total classification precision, can be interpreted as the probability for a reference pixel being correctly classified. In other words, it is the probability that a classifier has labelled an image pixel as belonging to a certain land cover class, using the corresponding land cover class, as defined by the ground truth information. Therefore, obviously, a high level of accuracy is desirable in order to make the land cover data comparable to those obtained in other classifications. According to Anderson (1971), and Anderson, et al. (1976), the minimum level for classification accuracy in the detection of land use and land cover through remote sensing techniques should be at least 85 percent; for both the classification as a whole (i.e. considering all the classes together), as well as for the single categories considered individually.

The thematic cartography for urban planning and management should achieve an accuracy of interpretation ranging from at least 85 to 90 percent (at any generalized level of classification). Actually, greater levels of accuracy are generally attained at much higher costs (Anderson, et al., 1976). Although, given the complexity of digital classification, Mather (1999), and Weng (2010), argue that even if *remote sensing technology has been applied widely in urban land-use, land-cover classification and change detection; however, it is rare that a classification accuracy of greater than 80 percent can be achieved using per-pixel classification (so-called "hard classification") algorithms*.

The Kappa coefficient (Cohen, 1960; Hudson, et al., 1987; Congalton, et al., 1999) is an additional index for assessing thematic map accuracy which relies on discrete multivariate techniques. Actually, according to Congalton (1991), discrete multivariate procedures are suitable because remotely sensed data is discrete rather than continuous information. The Kappa coefficient is computed following the equation [4.35], which gives a value of around 0.68 for the case study provided by the sample in table 4.12.

---

[303] Richards, et al. (2006), state that a better measurement globally would be to weight the average according to the areas of the classes in the map. Actually, in the framework of the GlobCOVER project (see section 3.2.1.2) a weighted overall accuracy has also been provided, by using the area of the land cover classes and the correspondent user accuracy values (Arino, et al., 2011), according to the equation [4.34]

$$\text{Global Accuracy} = \frac{\sum_{i=1}^{i=n} S_i * ua_i}{\sum_{i=1}^{i=n} S_i} \qquad [4.34]$$

With S_i the surface of land cover type i
ua_i the user's accuracy of land cover type i
n the total number of land cover classes of the product

[304] In order to make a comparison, we should mention that the accuracy assessment for the land cover classification results provided by the National Land Cover Database (NLCD) for conterminous United Sates, for instance, have indicated that NLCD 1992 reached an overall accuracy for the Anderson Level I (Anderson, et al., 1976) of 80.4 percent (Stehman, et al., 2003; Wickham, et al., 2004). The NLCD 2001 has an improved Anderson Level I class accuracy of 85.3 percent (Wickham, et al., 2010)

$$K = \frac{N \sum_{i=1}^{n} x_{ii} - \sum_{i=1}^{n} (x_{i+} * x_{+i})}{N^2 - \sum_{i=1}^{n} (x_{i+} * x_{+i})} \quad [4.35]$$

With
- n number of land cover classes which appear in the rows of the matrix
- x_{ii} number of observations in row i and column i
- N total number of observations
- x_{i+}; x_{+i} the marginal totals of row i and column i, respectively[305]

The overall accuracy measures the number of pixels correctly classified, but it only takes into account the major diagonal and excludes errors of omission and commission. However, the kappa coefficient measures the degree of incoherence between the classification results and the ground truth data. Therefore, the kappa accuracy *indirectly incorporates the off-diagonal* elements, derived by the row and column (marginal) totals of the error matrix (Congalton, 1991). Congalton and Green (1999), pointed out that a Kappa value greater than 0.80 indicates strong agreement, while values between 0.40 and 0.80 represent moderate agreement, and values smaller than 0.40 indicate poor agreement[306].

Errors of commission and omission measure the degree of spectral confusion between classes. In particular, the errors of commission measure the number of pixels wrongly labelled as belonging to a specific class of interest although they actually belong to a different class according to the ground truth data. Whereas, the errors of omission measure the number of pixels belonging to the ground truth data class of interest and that the analyst fails to classify in the proper class. In practice, the errors of commission appear in the rows of the confusion matrix. If we consider the sample shown in table 4.12, and the class termed as Planted/Cultivated, for instance, there is a total number of 10˙196˙119 pixels classified as such, of which 8˙081˙739 were properly classified and 2˙114˙380 wrongly classified. This is derived from the sum of those pixels in the Planted/Cultivated row, but which fall in the column of a different class. The error of commission for the Planted/Cultivated class is the result of the ratio between the number of pixels wrongly classified and the total number of pixels (2˙114˙380/10˙196˙119), which equals 0.207, i.e. 20.7%.

The errors of omission are derived from the values in the columns of the confusion matrix. For the previous sample of Planted/Cultivated class (table 4.12), a total of 10˙744˙655 ground truth pixels are now classified, where 8˙081˙739 are pixels properly labelled and 2˙662˙916 ground truth pixels are wrongly labelled (which is 177˙766 + 2˙474˙128 + 11˙022) . Therefore now, the ratio between the number of wrong pixels and the total number of pixels in the ground truth column (2˙662˙916/10˙744˙655), provides the error of omission for the Planted/Cultivated class, which equals 0.247, i.e. 24.7 %. The following table (4.13) shows, as a sample, both errors of commission and omission for all classes at level I of classification LCBC 2011 in comparison with CREAF-MCSC 2009 used as ground truth information.

ACCURACY ASSESSMENT			
		CREAF-MCSC 2009	
Thematic Map Class (LCBC 2011, Level I)		Errors of Commission (%)	Errors of Omission (%)
Artificial Areas	100	22.97	49.79
Planted/Cultivated	200	20.74	24.78
Forest and Natural Areas	300	12.66	7.86
Water and Wetlands	400	31.93	41.78

Tab. 4.13: Errors of Commission/Omission for the case of Catalonia: LCBC 2011 vs. CREAF-MCSC 2009 (Source: By Authors)

[305] For the sample in table 4.12, the terms $\sum_{i=1}^{n} (x_{i+} * x_{+i})$, of the equation used for computing the Kappa coefficient, is calculated as follow:
(1˙244˙668 x 1˙909˙428) + (10˙196˙119 x 10˙744˙655) + (24˙015˙751 x 22˙766˙122) + (214˙848 * 251˙181)

[306] Mainigi, et al. (2002), based on SPSS software guidelines (1998) state that *values of KAPPA greater than 0.75 indicate strong agreement beyond chance, values between 0.40 and 0.79 indicate fair to good, and values below 0.40 indicate poor agreement.*

The producer accuracy (pa_i) measures the likelihood that a given pixel labelled in a certain land cover class by the classifier effectively corresponds to a pixel classified in the same class by the ground truth data. This means the probability that a pixel classified as Planted/cultivated, for example, is actually classified as such in the ground truth image. Therefore, this results in the ratio between pixels correctly classified in a class and the number of pixels classified in the same class by the ground truth information, as shown in the equation [4.36].

$$pa_i = \frac{x_{ii}}{x_{+i}} \qquad [4.36]$$

With x_{ii} number of observations in row i and column i
X_{+i} the marginal totals of column i

This index is an expression of errors of omission, or false dismissals (Angel, et al., 2005), of how well a certain area has been classified. In the confusion matrix sample (table 4.12), the Planted/Cultivated class has a total of 10˙744˙655 ground truth pixels, of which 8˙081˙739 are correctly classified. The producer accuracy is computed as the ratio between 8˙081˙739 and 10˙744˙655, which equals 0.752, i.e. 75.2%.

User accuracy (ua_i) indicates the reliability that a pixel classified in a certain land cover class on the thematic map effectively represents that category on the ground (Story, et al., 1986). Actually, user accuracy expresses the errors of commission or false alarms (Angel, et al., 2005). In other words, with the sample of Planted/Cultivated class in mind, the user accuracy is the ratio between pixels correctly classified and the total number of pixels classified as Planted/Cultivated by the classifier (as expressed by the equation [4.37]), which then includes those pixels that, according to the ground truth image, effectively correspond to a different class.

$$ua_i = \frac{x_{ii}}{x_{i+}} \qquad [4.37]$$

With x_{ii} number of observations in row i and column i
X_{i+} the marginal totals of row i

In the confusion matrix (table 4.12) 10˙196˙119 pixels are classified as Planted/Cultivated, of which 8˙081˙739 pixels are properly classified. The user accuracy is derived from the ratio between 8˙081˙739 and 10˙196˙119, which equals 0.792, i.e. 79.2%.

The next table (4.14) shows Producer Accuracy and User Accuracy for all classes at level I of LCBC 2011 classification, used in comparison with the CREAF-MCSC 2009 classification (as ground truth information).

ACCURACY ASSESSMENT			
		CREAF-MCSC 2009	
Thematic Map Class (LCBC 2011, Level I)		Producer Accuracy (%)	User Accuracy (%)
Artificial Areas	100	50.21	77.03
Planted/Cultivated	200	75.22	79.26
Forest and Natural Areas	300	92.14	87.34
Water and Wetlands	400	58.22	68.07

Tab. 4.14: Producer and User Accuracy for the case of Catalonia: LCBC 2011 vs. CREAF-MCSC 2009 (Source: By Authors)

A key point to remember when providing the accuracy assessment, as emerged during the previous assumptions, is the choice of the ground truth data. This question is essential as the degree of consensus greatly depends on what the final thematic map can achieve derived through the classification process. In keeping, it is basically possible to focus the accuracy assessment on two different approaches: the use of *Ground Truth ROIs* (Region of Interests) and the use of a *Ground Truth Image*. The land cover classification can be compared and then evaluated by generating the error matrix and derived indices.

4.6.1. Ground Truth ROIs Approach

The scheme for accuracy assessment procedures involves several elements, also including the definition of a proper sampling design, both in terms of size and spatial distribution of samples. *Samples for which accuracy is to be assessed can be in the form of either regions or individual groups of pixels. Furthermore, these samples can be selected using several different strategies* (Angel, et al., 2005). If, for instance, the same training pixels (ROIs) used for classifying are also employed as ground truth data for running the validation procedure, the classification will certainly result in an excessively optimistic accuracy degree (Congalton, 1991). This is due to the accuracy analysis not being independent of the training pixels. Thus, in order to avoid biased reference information the selected ground reference test pixels or polygons labelled through human visual interpretation, preferably should not be the same ones used to develop the classification process. Therefore, one should collect extra ground reference data by using the ROI instrument prior to the classification, or a different database, if collected at the same time of assembling training data for processing the classification procedure.

A sort of "conflict of interest" could also occur if the classifier is the same person that collects data for accuracy assessment. This again would provide an overly optimistic degree of accuracy. Therefore, it would be desirable that at least a couple of analysts without prior knowledge of the analysed area could examine the same set of sample pixels for validating the land cover classification in order to minimize human errors during the photo-interpretation process. Clearly, the wrong interpretation of sampling points or spatially poorly precise reference data could result in a reduced degree of goodness and then provide an incorrect evaluation of the classification. Perhaps it would be better to obtain fewer, but more precise references. Moreover, since the whole inventory of mapped areas for verification is impossible (Mainigi, et al., 2002), the effort of covering huge areas is sometimes useless because of allocating too many points of interests and this could lead to a costly process which can be avoided by setting up a smarter sampling design. To achieve a balanced set of ground reference information for the confusion matrix, and then evaluate the classification results through rigorous statistical testing of the land cover accuracy, we believe it is necessary to design the minimum and most suitable sample size. Additionally, we require the most representative spatial distribution scheme for locating the sample points across the landscape (Congalton, et al., 1999; Mainigi, et al., 2002).

Usually, the magnitude of pixel samples depends on several factors, such as the area extension or number of classes considered in the nomenclature. An overly reduced set of sample pixels, smaller than the "minimum suitable" for sampling, due to both cost and time constraints as well as other practical restrictions, could provide a less than sufficient sampling design for achieving an effective goodness evaluation. In general, it could be argued that about 100 samples for each class in an image can be a reliable sample size.

Congalton (1991) argues that at least 50 samples, and in large area at least 75 to 100 samples per class, should be collected. While Hashemian, et al. (2004), in the framework of research work[307], the goal is to reach overall accuracies which *go towards stability and the best results*, by collecting 50 to 70 samples for each class in all images used for the study.

When ground data collection is unsuitable or because physical access to sites is impractical and restricted, high-quality fine spatial resolution imagery, if available, has to be used for ground truth data as a surrogate for direct ground observation (Foody, 2002). Worth bearing in mind, *spatially clustering the reference sample pixels lowers the overall cost of data collection, either by reducing travel time in the case of ground visits, or by reducing the total number and processing time of aerial photographs, high resolution satellite images, or videography used in the response design protocol* (Strahler, et al., 2006). The use of random sampling, based on general estimation theory of probability sampling, instead of manual collection of ROIs, becomes desirable for storing the minimum suitable set of unbiased observations per category. It is commonly assumed that five main sampling methods could be used for the automatic collection of reference data to conduct a land cover accuracy assessment:

- Simple random sampling: no rules are used for collecting sample points
- Systematic sampling: uniformity/regularity in the spatial or temporal distribution of sample points
- Stratified random sampling: random selection of data within non-overlapping sub-samples, commonly defined as "strata"

[307] Hashemian, M.; Abkar, A.; & Fatemi, S. (2004). Study of sampling methods for accuracy assessment of classified remotely sensed data. Proceedings of the 20th International Society for Photogrammetry and Remote Sensing (ISPRS) Congress

- Stratified systematic unaligned sampling: hybrid technique which incorporates elements of the simple random sample and systematic methods for collecting points within strata
- Cluster sampling: sample units are not single pixels, but groups (clusters) of pixels[308]

A suitable procedure for using ground truth ROIs for accuracy assessment is expected to provide the following steps: the sampling design definition for extracting reference points from the thematic map; labelling of detected points through photo-interpretation of high-resolution imagery (Google Earth, for instance), or ground visits if possible; conversion of sampling points into Region Of Interests; building of the confusion matrix for computing the accuracy degrees by using the obtained ROIs.

Within the ambit of NLCD projects (see section 3.2.3.1), the main elements for the report scheme provided for the accuracy assessments have been: *1) the use of a pixel as the* (minimum) *spatial unit for the accuracy assessment; 2) a blind collection (i.e. interpreters have no a priori knowledge of map land cover labels) of primary and alternate reference labels for the sample pixels, and; 3) nominal confidence rating for the reference land cover labels. More teams are involved in the process of land cover label assignment and in order to avoid biased interpretation, a certain degree of consistency is expected to be achieved, within and across teams, for reference label assignments* (Wickham, et al., 2013).

The accuracy assessment procedure has been based on the stratified random sample method for selecting reference points, while ground truth labels have been obtained for each reference land cover data by using photo-interpretation based on multi-temporal high resolution digital imagery[309]. Digital Orthophoto Quarter Quadrangles (DOQQ), other high-resolution aerial photographic sources and the Google Earth platform,[310] have been used as primary sources of reference data imagery (Wickham, et al., 2013).

Potere et al. (2009), by using 10˙000 Google Earth validation sites, provided an accuracy assessment which reaches a *relatively high level of accuracy* (Angel, et al., 2011), for validating urban areas. It focused on a five-year study of global urban expansion based on the use of satellite imagery for a global sample of 120 cities and for two "circa" temporal stages of 1990 and 2000 (see section 3.2.3.3).

To validate the LCBC 2011 land cover classification outcomes for the present study, certain restrictions in terms of human resources, besides cost and time issues, have led us to provide an extra accuracy assessment based on widely recognized land cover classifications, such as the CORINE Land Cover, SIOSE, and the MCSC systems, i.e. a ground truth image approach, besides the building of a proper protocol for accuracy assessment based on the sampling collection of testing points, i.e. a ground truth ROI approach.

4.6.2. Ground Truth Image Approach

It is crucial in Remote Sensing to recognize errors and their derivation by precisely reporting the degree of confidence of the thematic information in order to minimize their magnitude through applying enhanced methods as much as possible. Therefore, a *classification accuracy assessment is necessary for comparing the performance of various classification techniques, algorithms or interpreters* (Congalton and Green, 1998).

As pointed out before, the assessment of accuracy for land cover maps generated through remotely sensed techniques is often expensive both in terms of time and costs. Moreover, clearly, the validation of the whole inventory of the classified areas is impossible, so a sampling scheme is required to derive a suitable validation assessment (Hashemian, et al., 2004).

The assumption of finding an effective solution for adequately assessing the accuracy of land cover classifications based on accurate ground reference data is that an existing reference data set is correct. The possibility of using already existing validated information of land cover derived from official environmental monitoring programs (produced for the same geographical areas under investigation) would be a less costly and time effective procedure than carrying out extra database testing for accuracy evaluation. Actually, according to

[308] The whole group of pixels (cluster) is generally defined as the primary sampling, and the pixel itself represent the secondary sampling unit, as the smallest reference unit

[309] The NLCD Level II (16 classes) overall accuracies for the 2001 and 2006 land cover were 79% and 78%, respectively, while Level I (8 classes) accuracies were 85% for NLCD 2001 and 84% for NLCD 2006 (Wickham, et al., 2013)

[310] Recommended reference data for classification accuracy assessment, when ground truth data is unavailable, is large scale (1:12.000 or larger) colour aerial photography (Congalton, et al., 1999; Mainigi, et al., 2002)

Strahler, et al. (2006), existing reference data, available for processing an accuracy assessment, theoretically would not require *expending resources for field visits, imagery, or other reference data materials*. However, some extra effort may be required to homogenize data to be compared using the technical features within the land cover maps. For example, it could be necessary to reclassify the existing data to match the classification nomenclatures; a resizing of the maps would be required if different spatial resolutions occur; or re-projecting the geographical coordinates would be essential when comparing data based on different coordinate systems.

In any case, having the possibility to rely on an existing official database leads the accuracy assessment, provided in this study. Therefore, we have used a ground truth image approach instead of using a region of interests approach derived from a sampling design method. Thus, while maintaining the idea of planning an extra validation procedure based on ROIs truth collection in future developments (for validating the classifications results obtained through the proposed methodology), we now provide a pixel-based accuracy assessment which relies on existing officially recognized reference data provided by government monitoring programs for whole or part of the Spanish territory.

Three land cover/use databases are employed as ground truth images for evaluating the degree of goodness achieved by the Land Cover Base Classification (LCBC) methodology: Corine Land Cover (CLC); Information System about Land Cover in Spain (SIOSE); and the land cover map of Catalonia (MCSC).

Before generating the error matrix between LCBC and the three aforementioned land cover/use maps, for extracting the accuracy indices, some technical concerns and derived limitations should be highlighted for better comprehension of the level of goodness achieved by the LCBC 2011 classification.

First of all, particular emphasis has to be placed on the natural changes that occur over the earth's surface due to seasonal variations[311], not to mention directional deviations and intensity variability of the ground reflectance caused by different sun elevation degrees and atmospheric effects. These kinds of phenomena are particularly marked even after only a few months for certain types of land cover classes; such as vegetation, either natural or cultivated, or rivers, which provide quite important variations even over short time periods.

Consider this effect over several years. Actually, relevant changes also affect urbanized areas or large water bodies as well as the coast line, depending on the scale of analysis. If the classification relies on high resolution imagery, urban areas and water could show changes even in a few months, while for middle-low resolution imagery important variations in these classes can be detected over a few years. Therefore, it is highly relevant to point out the obvious differences arising between the maps of certain land cover composition to be analysed and compared, when detected in different years: LCBC 2011; CLC 2006; SIOSE 2005; and MCSC 2009.

In order to reduce the more sensitive differences between land cover types as much as possible, it has been decided to run the accuracy analysis for level I of classification. This provides the more generalized land cover level based on four classes, as shown in the sample in figure 4.55: *Artificial Areas; Planted/Cultivated; Forest and Natural Areas; Water and Wetlands*.

[311] Actually, seasonal differences also occur while interpreting reference points collected by sampling design procedures through the use of high resolution imagery. Therefore, these kinds of issues have to be taken into account, even if the accuracy analysis relies on the use of ROIs on Google earth platform.

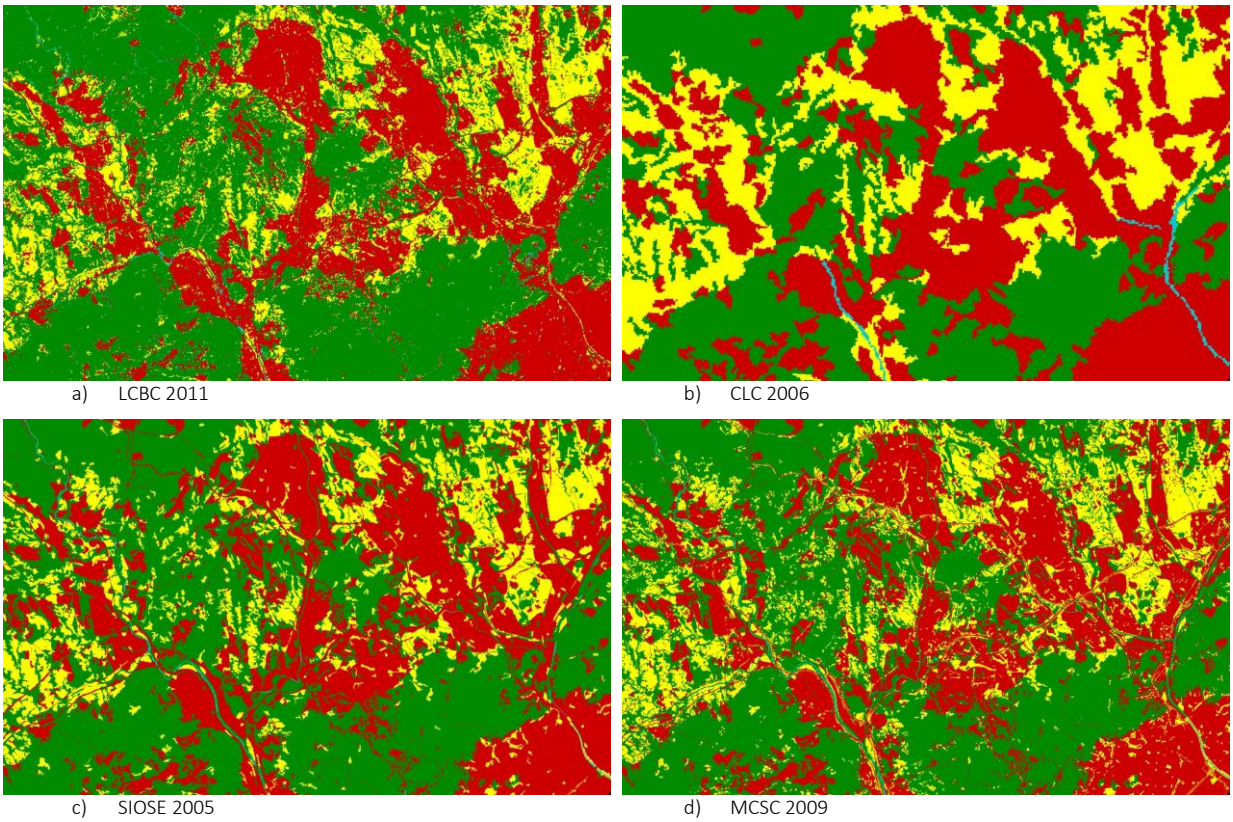

Fig. 4.55: Samples of the generalized level I of land cover classification for LCBC 2011 (a), compared with CLC 2006 (b), SIOSE 2005 (c), and MCSC 2009 (d) classification systems used as ground truth images for accuracy assessment (Source: By Authors)

The choice of working with level I only is also due to greater difficulties in homogenizing the different nomenclatures, even though we are conscious that the accuracy degree for level I of classification does not have the same value as the accuracy for levels II or III which would require extra validation analyses. Actually, a lack of global standardization of nomenclatures generates certain discrepancies within land cover typologies used for building a legend. This is both in terms of number of categories as well as labelling. Some relevant efforts have been made to produce global standardized nomenclature (CLC, GlobCOVER, USGS), but it would be desirable to obtain a largely accepted standard nomenclature for each classification system as soon as possible.

Prior to building the error matrix, other chief aspects should be highlighted. These are: the differences in spatial resolution and scale of analysis that elapse between the different reference data and the LCBC classification. The LCBC system relies on Landsat TM imagery with a resolution of 30m/pixel, which then provides a minimum mapping unit of 0.09 ha, so according to Richards, et al. (2006), we achieve thematic cartography at an operational scale of 1:250˙000. The scale of the output maps for the CLC system has been fixed at 1:100˙000, while the smallest mapping unit corresponds to 25ha and linear objects with a width less than 100m are not separated. This classification scheme (as well as the SIOSE and MCSC systems) is based on photo-interpretation and on-screen digitalization of satellite imagery, instead of automatic classification. For the SIOSE system, the major percentage of coverage has been used as criterion for selecting land cover types within polygons when more than one use, or cover type, is assigned to a single polygon. The SIOSE classification methodology provides thematic maps at a scale of 1:25˙000 with a minimum mapping unit of; 1ha for artificial areas and water bodies; 0.5 ha for beaches, riparian vegetation, wetlands and forced crops; and 2 ha for agricultural areas, forest and natural surfaces. Finally, the MCSC classification system provided by CREAF creates a digital map in vector format at a scale of 1:5˙000, with a minimum mapping unit of 500m, thus achieving very detailed cartography[312].

[312] More details about CLC, SIOSE and MCSC are provided in chapter 3

Firstly, all the maps have been converted to raster format and resized due to these differences. This was done in order to match the same 30x30m resolution as the LCBC. Geographic projections have also been changed to UTM WGS 84 for all ground truth images. Therefore, due to the data generalization in the assessment procedure, some positional errors are assumed to occur because of this homogenization of different spatial resolutions[313].

Once comparable thematic cartography of the four land cover classes (defined by the generalized level I of classification) has been obtained at the same geographical projection and spatial resolution, the error matrix can be built for computing *Overall Accuracy* (O_A) and *Kappa Coefficient* (K_C). Firstly, the three ground truth reference data between them (table 4.15) and then, following that, each reference image has been compared with the LCBC classification results (table 4.16). Administrative boundaries have been used for defining sub-sets on the Mediterranean side of Spain, as was done at the previous classification stage. The Autonomous Communities of Catalonia, Valencia, Murcia, and Balearic Islands have been considered using the regional administrative limit, while provincial administrative boundaries are used in the case of the Region of Andalucía, for providing four sub-regional ambits by grouping provinces two-by-two. Thus, finally, eight case studies have been evaluated according to the classification scheme.

			ACCURACY ANALYSIS					
	ADMINISTRATIVE AREA UNDER INVESTIGATION		SIOSE 2005* CLC 2006		MCSC 2009* SIOSE 2005		MCSC 2009* CLC 2006	
			O_A	K_C	O_A	K_C	O_A	K_C
1	**1. CATALUÑA**		83.1325 %	0.6794	93.7734 %	0.8756	81.7641 %	0.6529
2	**2. VALENCIA**		79.4986 %	0.6279	-	-	-	-
3	**3. MURCIA**		84.0152 %	0.7019	-	-	-	-
4	**4. BALEARES**		76.7231 %	0.5934	-	-	-	-
5	**5. ANDALUCÍA**	5.1. Almería-Granada	82.6506 %	0.6581	-	-	-	-
6		5.2. Jaén-Córdoba	81.2343 %	0.6374	-	-	-	-
7		5.3. Málaga-Jerez de la Frontera	82.6058 %	0.6924	-	-	-	-
8		5.4. Sevilla-Huelva	80.0341 %	0.6473	-	-	-	-

* Ground Truth Image

Tab. 4.15: Overall Accuracy and Kappa Coefficient computed for the truth reference maps, between them: CLC 2006, SIOSE 2005, and MCSC 2009 (Source: By Authors)

			ACCURACY ANALYSIS					
	ADMINISTRATIVE AREA UNDER INVESTIGATION		CLC 2006* LCBC 2011		SIOSE 2005* LCBC 2011		MCSC 2009* LCBC 2011	
			O_A	K_C	O_A	K_C	O_A	K_C
1	**1. CATALUÑA**		80.0228 %	0.6105	85.0355 %	0.6910	84.5575 %	0.6798
2	**2. VALENCIA**		78.9138 %	0.6088	82.7164 %	0.6574	-	-
3	**3. MURCIA**		75.2589 %	0.5493	80.8794 %	0.6454	-	-
4	**4. BALEARES**		77.0686 %	0.5878	83.4929 %	0.7020	-	-
5	**5. ANDALUCÍA**	5.1. Almería-Granada	78.2594 %	0.5677	81.3871 %	0.6087	-	-
6		5.2. Jaén-Córdoba	73.5856 %	0.5014	80.6996 %	0.6319	-	-
7		5.3. Málaga-Jerez de la Frontera	76.5709 %	0.5779	82.2307 %	0.6794	-	-
8		5.4. Sevilla-Huelva	71.3153 %	0.5033	86.1332 %	0.7441	-	-

* Ground Truth Image

Tab. 4.16: Overall Accuracy and Kappa Coefficient computed for the LCBC 2011 classification system, in comparison with CLC 2006, SIOSE 2005, and MCSC 2009 used as ground truth images (Source: By Authors)

[313] Actually, according to Weber (2009), the generalization, due to the change in scale of the data, is one of the most relevant properties affecting the quality of assessment. It reduces the complexity of the data structure, and automatically adds errors in the database, thus scarifying part of the quality of classification results in favour of simplicity and legibility.

Besides the cited limitations concerning the generalization of the reference data which certainly leads to criticism in the evaluation of results of overall accuracy and kappa coefficient, other sources of errors could contribute to reducing the values of accuracy depicted in the error matrix. This could be due to possible mistakes at any stage of the classification process. In fact, errors also depend on collecting primary data, for instance. The use of images with relevant seasonal differences or atmospheric constraints could produce an inaccurate mosaic due to the colour balancing of incongruous overlapping regions (see section 4.3). During the classification stage when using medium-resolution imagery, the process often suffers an important spectral mixture within the pixels. Other common aspects that decrease the degree of classification accuracy (see section 4.5) can include: mixtures of impervious areas, for instance, typically low-density residential texture which can mix with natural vegetation (trees) or grass, or the mixture between grass and croplands.

It should be pointed out that the degree of accuracy is not calculated based on a sampling test, but it takes into account the whole image, so the per-pixel assessment is developed for each pixel, one by one. This procedure requires more precision and then is more demanding during the accuracy analysis. Moreover, the validation is processed by evaluating thematic cartography derived from an automatic process, as is the LCBC. This is in comparison to ground truth reference maps which resulted from an on-screen photo-interpretation process that is assumed to be more accurate than purely automatic processes, especially if high resolution imagery is used for digitalizing. In fact, Congalton (1991), claims that *digital classifications are often assessed with reference to photo-interpretation because, traditionally, the accuracy of photo-interpretation has been accepted as correct without any confirmation*.

In light of this, in our opinion, it is quite appreciable reaching values around 80% (or greater) for the overall accuracy, as well as values between 0.6 and 0.7 for the Kappa coefficient for almost all of the ambits under investigation. This is when compared against the SIOSE, and MCSC in the case of Catalonia only. In fact, an increase in both values (O_A and K_C), was desirable as an extra index of goodness by passing from comparing LCBC with SIOSE, to comparing LCBC with CLC. This is because the 1:100˙000 operational scale provided by CORINE gives a higher degree of simplification for the thematic maps, but is probably more appropriate for analysis at national level (i.e. Countries); whereas the more detailed classification system of SIOSE at a scale of 1:25˙000 (or the MCSC for Catalonia at a scale of 1:5˙000,) offers improved maps with less generalization of parts within each land cover class. These maps are more suitable for regional studies.

Significant emphasis has to be placed on the accuracy analysis per-class. One of the main objectives of this study is the analysis of the morphology of urban settlements. Thus, among the four indices provided by the accuracy assessment, it must be apt to evaluate the degree of goodness for single land cover classes (Errors of Omission/Commission, Producer, and User Accuracy), the results for User Accuracy are represented in the following tables 4.17, 4.18, and 4.19, for the eight cases analysed with the four land cover classes of level I.

According to Richards, et al. (2006), *as a user of a thematic map produced by a classifier, we are more interested in the probability that the actual class is B, given that the pixel has been labelled B (on the thematic map) by the classifier*. Therefore, if we take into account the class of artificial areas, for instance, which merges together all the impervious categories, we see a user accuracy of around 77% between the LCBC system in comparison to MCSC. This relates to the number of pixels classified as urban, which similarly matches the areas classified as such by the MCSC system as well (table 4.17).

USER ACCURACY				
ADMINISTRATIVE AREA UNDER INVESTIGATION	MCSC 2009* / LCBC 2011			
	Artificial Areas	Planted Cultivated	Forest and Natural Areas	Water and Wetlands
CATALUÑA	77.03 %	79.26 %	87.34 %	68.07 %
				* Ground Truth Image

Tab. 4.17: User Accuracy for the region of Catalonia, at the generalized level I of classification, between LCBC 2011 and MCSC 2009 as ground truth image (Source: By Authors)

Universidad Politécnica de Cataluña, Barcelona TECH
Departamento de Tecnología de la Arquitectura
Centro de Políticas de Suelo y Valoraciones
Nicola Colaninno, Josep Roca Cladera

	ADMINISTRATIVE AREA UNDER INVESTIGATION		USER ACCURACY CLC 2006* / LCBC 2011			
			Artificial Areas	Planted Cultivated	Forest and Natural Areas	Water and Wetlands
1	**1. CATALUÑA**		68.00 %	87.26 %	77.80 %	55.11 %
2	**2. VALENCIA**		66.98 %	89.54 %	74.48 %	63.24 %
3	**3. MURCIA**		55.19 %	93.76 %	64.19 %	33.56 %
4	**4. BALEARES**		68.57 %	88.76 %	66.32 %	49.75 %
5	**5. ANDALUCÍA**	5.1. Almería-Granada	48.91 %	84.54 %	75.53 %	75.11 %
6		5.2. Jaén-Córdoba	59.48 %	93.40 %	57.22 %	46.76 %
7		5.3. Málaga-Jerez de la Frontera	52.24 %	82.88 %	73.19 %	76.37 %
8		5.4. Sevilla-Huelva	58,69 %	95.59 %	58.74 %	64.71 %

* Ground Truth Image

Tab. 4.18: User Accuracy for the generalized level I of classification, between LCBC 2011 and CLC 2006 (Source: By Authors)

	ADMINISTRATIVE AREA UNDER INVESTIGATION		USER ACCURACY SIOSE 2005* / LCBC 2011			
			Artificial Areas	Planted Cultivated	Forest and Natural Areas	Water and Wetlands
1	**1. CATALUÑA**		78.21 %	81.10 %	87.25 %	63.49 %
2	**2. VALENCIA**		77.94 %	74.86 %	87.20 %	60.15 %
3	**3. MURCIA**		66.29 %	90.71 %	75.30 %	30.91 %
4	**4. BALEARES**		73.90 %	80.10 %	88.34 %	46.74 %
5	**5. ANDALUCÍA**	5.1. Almería-Granada	66.56 %	73.25 %	86.06 %	88.16 %
6		5.2. Jaén-Córdoba	80.99 %	84.35 %	77.86 %	65.29 %
7		5.3. Málaga-Jerez de la Frontera	60.06 %	78.56 %	86.70 %	83.41 %
8		5.4. Sevilla-Huelva	67.68 %	95.82 %	82,21 %	70.64 %

* Ground Truth Image

Tab. 4.19: User Accuracy for the generalized level I of classification, between LCBC 2011 and SIOSE 2005 (Source: By Authors)

The complete outcome of accuracy assessment is provided in the Annex II within the addendum section. This is detailed for all eight administrative ambits under investigation and all the indices of validation, as previously cited (overall accuracy, kappa coefficient, errors of commission and omission, producer and user accuracy).

4.6.3. A Proper Accuracy Assessment: The Ground Truth ROI Approach for Catalonia

Since, in general, a recognized database about land cover/use classification to which may refer the accuracy assessment analysis is not always available, the most common approach relies on providing a proper sampling design by collecting an appropriate amount of random ground truth points, both in terms of number and spatial distribution of the samples[314], in order to verify if there exist relatively high levels of goodness.

As argued in the previous section 4.6.1, since the whole inventory of mapped areas for verification is impossible (Mainigi, et al., 2002), the effort of covering huge areas is sometimes useless because of allocating too many points and this could be avoided by setting up a smarter sampling design. Indeed it would be better to obtain fewer, but more precise references. In this sense, as a reference we could take into account that, generally, about 100 samples for each class could be a reliable sample size. Actually, Congalton (1991) argues that at least 50, and up to 75 or 100 samples should be collected, depending on the dimension of the area under investigation.

Here, for storing a suitable set of unbiased observations per category, an automatic random sampling approach instead of manual collection of points has been used. In particular, although various sampling approaches are commonly recognized we employed two different methods, i.e. a stratified random sample with a point density

[314] Further details about the truth ROI approach can be found in the previous section 4.6.1

of 0.1% is used for selecting reference points for urban class; while equalized sample approach is used for the other classes based on 100 sample points consistent with the previous statements.

The choice of using different approaches mainly depends on practical reasons. In fact, if a stratified random approach with a point density of 0.1% is undertaken for the whole image, i.e. calculated for the four classes at once, we reach a total amount of 35˙673 random points, where 1˙245 refers to the urban class, 10˙196 for cropland, 24˙016 for forest and natural, and 216 for water. It is a "proportionate" stratification and all the sample points represent the 0.1% of each class. Actually, it is a difficult stuff and quite expansive, in terms of time, to provide the examination of 35˙673 points. Hence, also because our study mainly focuses on the analysis of the urban areas, we used 1˙245 random points for the urban class according to the stratified approach and 100 points for the rest of the classes.

Once obtained the dataset of the random points, a labelling operation has been undertaken through photo-interpretation of high-resolution imagery in order to achieve the most suitable ground truth data, as a surrogate for direct ground observation (Foody, 2002). Here, in particular, the analysis has been provided only for the case of Catalonia as a further analysis for completing the accuracy assessment provided in section 4.6.2; while satellite imagery of Google maps as provided by the QGIS platform[315] have been used as primary sources for photo-interpretation. Regarding this, it has to be emphasized the different spatial resolution while labelling, since a 30m/pixel is compared with high resolution imagery, which could lead to some questionable choice.

Finally, a confusion matrix has been built based on the classification and the labelled random pixels in order to compute the accuracy, and depending on the overall accuracy, the kappa coefficient, errors of commission/omission, and producer/user accuracy, as shown in table 4.20.

OVERALL ACCURACY = (1342/1545) 86.86%

KAPPA COEFFICIENT = 0.6784

					Ground Truth (Pixels)	
	Class	100	200	300	400	Total
URBAN	100	1˙085	59	94	7	1˙245
CROPLAND	200	3	92	5	0	100
FOREST/NATURAL	300	4	7	89	0	100
WATER	400	6	4	14	76	100
	Total	1˙098	162	202	83	**1˙545**

					Ground Truth (Percent)	
	Class	100	200	300	400	Total
URBAN	100	98.82	36.42	46.53	8.43	80.58
CROPLAND	200	0.27	56.79	2.48	0	6.47
FOREST/NATURAL	300	0.36	4.32	44.06	0	6.47
WATER	400	0.55	2.47	6.93	91.57	6.47
	Total	100	100	100	100	**100**

	Class	**Commission** (Percent)	**Omission** (Percent)	**Commission** (Pixels)	**Omission** (Pixels)
URBAN	100	12.85	1.18	160/1˙245	13/1˙098
CROPLAND	200	8	43.21	8/100	70/162
FOREST/NATURAL	300	11	55.94	11/100	113/202
WATER	400	24	8.43	24/100	7/83

	Class	**Producer Accuracy** (Percent)	**User Accuracy** (Percent)	**Producer Accuracy** (Pixels)	**User Accuracy** (Pixels)
URBAN	100	98.82	87.15	1˙085/1˙098	1˙085/1˙245
CROPLAND	200	56.79	92	92/162	92/100
FOREST/NATURAL	300	44.06	89	89/202	89/100
WATER	400	91.57	76	76/83	76/100

Tab. 4.20: Summary of the accuracy assessment for the case of Catalonia based on a sample set of ground truth points (Source: By Authors)

[315] QGIS 2.8.1 Wien, Google Satellite imagery, Imagery © 2015, DigitalGlobe, *Institut Cartografic de Catalunya*

Chapter 5

URBAN MORPHOLOGY: DEFINING MODELS OF LAND OCCUPATION

The word 'form' has many meanings, such as shape, configuration, structure, pattern, organization, and system of relations. We are here interested in these properties only in so far as they are clearly set in space (Whyte, 1968; Batty, et al., 1994).

Understanding urban dynamics is one of the most complex tasks in spatial planning (Lavalle, et al., 2002). Currently, the present-day dilemma in urbanism is mainly directed at three themes: urban form (compactness-diffusion), functionality (complexity-specialization) and equity (integration-segregation) (Nel·lo, 2001).

Urban morphology[316], as mentioned in Chapter 3, aims to analyse and measure all the formal aspects of human settlements (urban form) by understanding the syntax of spatial structure in relation to both patterns of movement and land occupation at different levels of detail (scale). This includes streets, buildings, lots, neighbourhoods, cities and territories.

The urban environment is made by patterns of full and empty spaces. We look at it on a micro-scale, i.e. the relation between buildings and streets (or squares), or as multiple agglomerations that draw circumscribed geometrical forms on the territory. In the latter case, it is significant to measure and understand the causes and effects of the final outline of such urban agglomerations (due to the internal dualism of full/empty space), and the spatial relation between them, in order to provide effective tools for land management and planning. In other words, we need to define the form and structure of urban land coverage by establishing hierarchical relationships between settlements: within a territory, in terms of size, shape, continuity, and distance to each other.

Here, the focus is not on emphasizing the relationships between the smallest components of a city (buildings or lots), but rather applying morphological techniques to investigate the entire built landscape as a whole, and the geometrical aspects that define the shape of land occupation. Special attention is given to understanding how the overall layout of the physical form of a city can be measured and compared with other cities within the geographical area under investigation.

5.1. REMOTE SENSING & GEOGRAPHIC INFORMATION SYSTEMS FOR SPATIAL ANALYSIS

There is no doubt that, during the last decades, geospatial technologies have completely changed the way we deal with environment analysis, as well as the manner of approaching questions of land management and spatial planning. Currently, the combination of Remote Sensing (RS) technologies, and derived data, with Geographic Information Systems (GIS) provides powerful and effective tools for understanding spatial dynamics along the Earth's surface.

As previously mentioned, Remote Sensing is aimed at obtaining information and measurements regarding the Earth's environment. This is based on physical features captured by sensors on-board aircrafts or spacecraft, allowing land monitoring without being directly in contact with the matter. On the other hand, a GIS can be used as a rigorous instrument for storing, organizing, manipulating and analysing geographically referenced information, either in raster or vector format. This allows you to extract further spatial features that are otherwise difficult to emphasize through other means, allowing the data combinations to create new information.

With the proliferation of GIS in both industry and government for numerous applications, there has been a tremendous increase in demand for remote sensing as a data input source to spatial database development. Products derived from remote sensing are particularly attractive for GIS database development because they can provide cost-effective, large area coverage in a digital format that can be input directly into a GIS. Because remote

[316] *The term morphology was first used by Goethe in 1827 as 'the study of unity of type of organic form' (noted in March and Steadman, 1971). Morphology is thus the study of form and process, growth and form, form and functions and as Goethe stated: "The formative process is the supreme process, indeed the only one, alike in nature and art"* (Whyte, 1968). *Form too is always more than shape, and we will follow Whyte (1968) who speaks of spatial form which he defines as comprising external form or visible shape, and internal form which is structure* (Batty, et al., 1994)

sensing data are typically collected in a raster data format, the data can be cost-effectively converted to a vector or quadtree format for subsequent analysis or modelling applications (Lee, 1991; Ross, et al., 1991).

Consequently, the combination of remote sensing and GIS technologies allows for complex processes of data management and analysis designed for observing, outlining, and modelling spatial phenomena of the Earth's surface. In other words, GIS is necessary for obtaining comprehensive understanding of remote sensing results.

Regardless of the degree of integration, a trend towards the convergence of both technologies is evident in the development of applications capable of solving land management problems, either at a local, regional, or even coarser scale. In particular, the joint use of both technologies in the field of spatial planning, in addition to the use of statistical models, provides a recognized solution for critical questions such as urban development, resources management, and natural hazard assessments, among others.

Moreover, *Land use and Land cover maps are able to capture the combined effects of environmental and socio-economic policies on the territory and therefore are fundamental indicator for integrated coastal zone management* (Freire, Santos, & Tenedório, 2009).

Here, remote sensing techniques have been used to carry out land cover classifications at the regional level, along the Mediterranean side of Spain. This is based on Landsat Thematic Mapper multispectral data in order to separate urbanized areas from croplands and other undeveloped land cover classes such as forest and waters, for example. On the other hand, the spatial patterns of urban settlements have been analysed by using a GIS-based modelling approach.

5.1.1. Geographic Information Systems (GIS): An Overview

A Geographic Information System, or GIS, is an "integrated collection of computer software and data used to view and manage information about geographic places, analyse spatial relationships, and model spatial processes. A GIS provides a framework for gathering and organizing spatial data and related information so that it can be displayed and analysed" (ESRI, 2006).

Currently, in a broader sense, the term GIS refers to a number of different technologies, processes, and methods, mainly used within fields such as engineering, planning, management, transport and logistics, among others, for manipulating and displaying georeferenced[317] information. GIS applications generally provide a graphical interface that allows users to visualize, create interactive queries, analyse, edit, and interpret the spatial information stored in a map in order to understand and display relationships, patterns, and trends within a territory, in terms of either physical, social, or economic dynamics.

According to Huisman, et al. (2009), a GIS is a computer-based system that supports the study of both natural and man-made phenomena, with an explicit location in space. It mainly provides four sets of capabilities to handle georeferenced data, which are:

- Data capture and preparation;
- Data management, including storage and maintenance;
- Data manipulation and analysis;
- Data presentation.

The appearance of geographic information systems in the mid-1960s mostly revealed a progress in computer technology and the emergence of a quantitative approach in geography. Currently, GIS have developed dramatically since the late 1970's, in terms of both technical and processing capabilities (Huisman, et al., 2009). It has evolved from a tool for mapping and data management, during the first phase, into *an efficient spatial data-handling and analysis technology and, more recently, into geographic information science (GISc*).

The commercial success of GIS that occurred around the early 1980s has greatly increased the fields of application, potentialities (Weng, 2010), and end-users. Hence, since in the 1990's there has been an increasing trend in applications that use GIS technologies for spatial analysis, as well as databases for storage. In more recent years, spatial databases, also known as geodatabases, have emerged for storing GIS data (Huisman, et al., 2009).

[317] *Georeferencing means aligning geographic data to a known coordinate system so it can be viewed, queried, and analysed with other geographic data. Georeferencing may involve shifting, rotating, scaling, skewing, and in some cases warping, rubber sheeting, or orthorectifying the data* (ESRI, 2006)

GIS are currently widely used all over the world for a wide range of purposes[318] (Huisman, et al., 2009). Nowadays, GIS is considered to be the nerve centre that handles geographic information because it can integrate all sorts of spatial data such as RS, cartography, census data and GPS, among others (Chuvieco and Huete, 2010). In particular, as argued by Konecny (2003), geographic information systems arose from activities in four different fields (figure 5.1) as follows:

- *Cartography, which attempted to automate the manually dependent map-making process by substituting the drawing work by vector digitization.*
- *Computer graphics, which had many applications of digital vector data apart from cartography, particularly in the design of buildings, machines and facilities.*
- *Databases, which created a general mathematical structure according to which the problems of computer graphics and computer cartography could be handled.*
- *Remote Sensing, which created immense amounts of digital image data in need of geocoded rectification and analysis.*

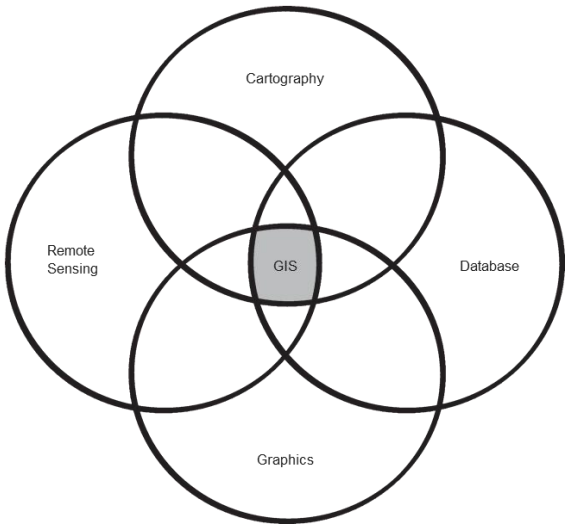

Fig. 5.1: *Interrelationship between GIS disciplines* (Source: Konecny, 2003)

A GIS consists of three main components, as schematically depicted by Konecny (2003) in figure 5.2, which are: a system for data input in several formats; a CPU that contains software suitable for data processing, storage and analysis, facilities for visualization and hard copy output; all the information required for purposes of data inventory, analysis, and presentation, aimed at land monitoring, management and planning.

[318] *According to Konecny (2003), the first theoretical and exploratory attempts for a GIS design started in the 1960s, namely by:*
- *R.F. Tomlinson, who in 1968 created the first Canada Geographic Information System for an agricultural agency (ARDA);*
- *The Experimental Cartography Unit under Bickmore in the UK, which has attempted to automate cartography since 1963;*
- *The Harvard Laboratory for Computer Graphics, which has laid the theoretical foundations for successful industrial GIS developments since 1964, through their creation of Symap (e.g. Jack Dangermond for ESRI and D.F. Sinton for Intergraph);*
- *The Swedish attempts to establish a Land Information System for the district of Upsala.*

These first personal initiatives were followed by the takeover of these ideas by governmental administrations, e.g. by:
- *The US Bureau of Census, from 1967, utilizing DIME files;*
- *The US Geological Survey, creating Digital Line Graphs;*
- *The attempts of the German states and their surveys and mapping coordination body, ADV, creating the ATKIS concept.*

The successful introduction of the technology without subsequent strong industrial development would not have been possible. The leaders in the field from 1969 were:
- *ESRI under Jack Dangermond, in the USA;*
- *Intergraph under Jim Meadlock, in the USA;*
- *Siemens in Germany.*

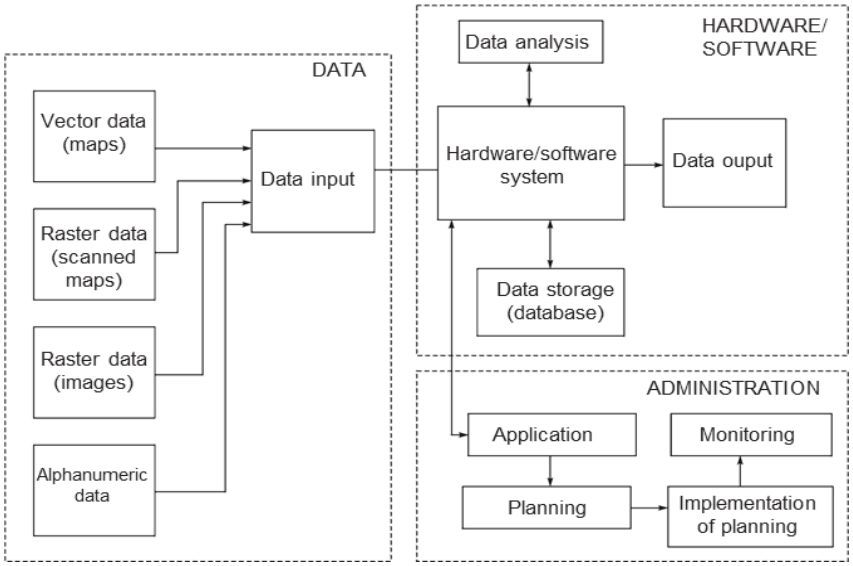

Fig. 5.2: *Concept of a Geographic Information System* (Source: Konecny, 2003)

Regarding input data, the information system is capable of handling data in various formats, as mentioned before, including vector, raster, and alphanumeric as follows:

- *Spatial objects are represented by identifiers. They refers to points, lines or areas administered in vector form. The identification and organization of these objects in coordinate and vector form is subdivided into feature or object classes. These include spatial or topological relations in two or three dimensions.*
- *Data in raster form is also included. A pixel may be assigned an object code, or it may simply consist of the grey levels of an image or a digital elevation model.*
- *The vector or the raster data are also linked to non-graphic information specifying place names and object numbers, which in databases may further be linked to a great variety of coded or alphanumerical attributes (e.g. owners of a parcel, inhabitants of a house, characteristics of a utility feature, statistical data for a defined area)* (Konecny, 2003).

A GIS operates under the assumption that all investigated phenomena will occur in a two-dimensional or three-dimensional Euclidean space, which could be "informally" defined as a model of space in which the locations are represented by coordinates (x and y in a 2D Euclidean plane, and x, y, z in the case of a 3D Euclidean space), distances, and directions, which can be defined through geometric formulas (Huisman, et al., 2009).

In this way, GIS can spatially correlate certain unrelated information by using the spatial position as a key measure. Hence, if we take into account different data representing locations and/or extensions along the Earth's surface, recorded as x, y, and z coordinates (which represent respectively longitude, latitude, and elevation), they could be spatially related to each other and, ultimately, referable to real geographic information on the ground.

Geographic Information Systems offer effective capabilities for integrating multi-sector, multi-level and multi-temporal databases, thus allowing the study of fundamental issues related to the analysis of the Earth's surface including purpose such as the planning, management and monitoring of natural and socio-economic phenomena (Anji Reddy, 2008).

In spatial planning, for instance, GIS is becoming essential for understanding landscape patterns within the geographic space, and then defining the most suitable actions. The development of GIS technologies has provided a wide range of analytical tools for the analysis and management of both urban and natural landscapes. Such tools are capable of depicting digital models of the Earth's surface and quantifying all the different spatial structures, within a territorial system, whose understanding provides a basic requirement for the study of the environment and its changes over time. This new approach to land management and planning has completely transformed the way planners operate.

An urban planner might want to assess the extent of urban fringe growth in her/his city, and quantify the population growth that some suburbs are witnessing. She/he might also like to understand why these particular suburbs are growing and others are not (Huisman, et al., 2009).

In particular, an urban planner might need a set of analytical tools for interpreting spatial data as best as possible, in order to answer key geographical questions such as: demographic trends for specific urban areas; land cover characteristics in a particular portion of the territory; patterns of natural disasters; and distribution of either urban or rural population changes over time.

Currently, GIS provide a digital system for the acquisition, management, analysis and visualization of spatial data about the physical urban environment or demography, which satisfy specific needs such as the pre-processing of data. This includes operations of reformatting, change of projection, resampling and generalisation; support for complex analysis and modelling; and post-processing of results including such as tabulation, report generation and mapping (Anji Reddy, 2008).

In short, according to Anji Reddy (2008), we could argue that *there are mainly four key activities that any urban planners, scientists, resource managers and others are using geographic information for. They observe and measure environmental parameters and develop maps which portray characteristics of the earth. They monitor changes in our surroundings in space and time. In addition, they model alternative actions and process operations in the environment. These four activities are Measurement, Mapping, Monitoring and Modelling, referred to as key activities which can be enhanced by using information systems technologies, like GIS*.

5.1.2. Remote Sensing and GIS Integration

Generally, technology integration, which also often implies the combination of data from different sources, is done in order to obtain the best information possible about a phenomenon under investigation. When the different data sources employed are geometrically registered according to a common geographic coordinate system (any kind of digital cartography such as land cover maps or road network) then the ability to obtain more effective information improves greatly.

In recent years, there has been an increasing interest in providing integration tools in the area of remote sensing, GIS and spatial models (Franklin, 2001). In fact, because most geographic information is available in digital format currently, technology integration and data interchangeability have become the most suitable method for spatial interpretation and analysis.

Currently, as argued by Star, et al. (1997) *GIS has its roots in the stimulus provided by the development of remote sensing, in the late 1960s and early 1970s, as a potentially cheap and effective source of earth observations*. Therefore, the increasing advances since the 70's in the use of remote sensing, GIS, Global Positioning System (GPS) and other ground data collection systems, currently provide a wide range of tools and techniques for spatial analysis and environment management. However, while remote sensing processing techniques are generally highly specialised, more general GIS techniques are used for combining remote sensing data with collateral information (Star, et al., 1997; Anji Reddy, 2008) and analysing spatial patterns.

This produces two main consequences. On the one hand, it makes remote sensing analysts "avid" users of *GIS data as a means to add value to remotely sensed data and analysis* (Franklin, 2001); and on the other hand, as argued by Gahegan and Flack (1999), because RS outcomes are often handled in GIS, the relationship between RS and GIS is that of supplier (remote sensing) and consumer (GIS). Jensen (2005) describes GIS data as "collateral" and "ancillary" as compared to "primary" remotely sensed data (Rogan, et al., 2006).

Whatever the focus may be, the integration of spatial information and the joint use of both RS and GIS technologies has been remarkably encouraged during the last decades by most users of satellite remote sensing and spatial analysts. It is because an integrated approach to spatial analysis enables us to effectively investigate and update datasets, in addition to the great capabilities for forecasting and optimisation of actions.

Such assumptions clarify why surveying and mapping have experienced a significant *transition from discipline-oriented technologies, such as geodesy, surveying, photogrammetry*[319] *and cartography, to the*

[319] *With the advent of high-resolution satellite systems in stereo, the theory of analytical photogrammetry restituting 2D image information into 3D is of increasing importance, merging the remote sensing approach with that of photogrammetry* (Konecny, 2003)

methodology-oriented integrated discipline of geoinformatics, mainly based on GPS positioning, remote sensing, digital photography for data acquisition, and GIS for data manipulation and data output (Konecny, 2003).

Rogan and Miller (2006) argued that the integration of GIS data with remotely sensed imagery is a long-standing matter, which has experienced increasing interest worldwide for several reasons; such as the improvement of digital data quality and availability, at lower costs, for large geographical areas at a global level; growth in demand for accurate information; and the need for automated mapping and map updating, based on expert systems/knowledge-based classification. Moreover, they state that *the integration of remotely sensed and GIS data, referring to GIS data as all non-spectral digital entities, takes four forms*:

- *GIS can be used to store multiple data types;*
- *GIS analysis and processing methods can be used for raster data manipulation and analysis (e.g., buffer/distance operations);*
- *Remotely sensed data can be manipulated to derive GIS data;*
- *GIS data can be used to guide image analysis in extracting more complete and accurate information from spectral data*.

A reasonable approach to the integration of GIS and RS, to enhance each other, is the use of remotely sensed data as primary input for GIS platforms; the use of GIS data as ancillary information in order to improve the products derived from remote sensing; and the joint use of both technologies for spatial analysis and modelling (Wilkinson, 1996; Weng, 2010).

In urban planning, in fact, such integration has been widely recognized for effectively supporting the spatial analysis and modelling either at the national, regional or local level (Konecny, 2003). It is because RS collects multi-spectral, multi-resolution, and multi-temporal data and turns them into information that is significant for the monitoring and understanding of urban growth processes, as well as extracting urban biophysical and socioeconomic variables. Hence, RS derived variables and GIS thematic layers, in conjunction with census data, provide three essential data sources for urban analysis[320] (Weng, 2010).

At any rate, certain criticism is due when approaching the joint use of RS and GIS because the lack of conceptual differences makes the complete integration of GIS and remote sensing somewhat challenging.

In that sense, as argued by Rogan, et al. (2006), some key issues need to be taken into account:

- The incompatibility between certain data types like DEM and census data (Dobson, 1993);
- GIS data space is defined by the values of the direct/indirect variable of interest (e.g., elevation, temperature), while spectral data space consists of a discrete slice of the electromagnetic spectrum, which the remote sensing community needs to address further (Lees, 1996);
- The propagation of inaccuracy at each step of the transformation process from remotely sensed data into GIS information (Gahegan and Ehlers, 2000).

Currently, as is the case in this research, when using remotely sensed data as primary data for GIS analysis, the process of data integration usually includes several analytical procedures such as data acquisition, data processing, data analysis, data conversion, error assessment and final product presentation. At each step, certain inaccuracies could occur so that the accumulation of error may lead to ineffective results.

Performing spatial data analysis operations with data of unknown accuracy, or with incompatible error types, will produce a product with low confidence limits and restricted use in the decision making process (Ross, et al., 1991).

[320] *GIS technology provides a flexible environment for entering, analysing and displaying digital data from the various sources necessary for urban feature identification, change detection, and database development. GIS data for urban applications frequently contain such thematic layers as transportation network, hydrographic features, land use and zoning, basic infrastructure, buildings, and administrative boundaries with different detail. Census data offers a wide range of demographic and socioeconomic information and have been used in various urban geography, planning and environment management studies. The advances in GIS technology provide an effective environment for spatial analysis of remotely sensed data and other sources of spatial data. Integration of remote sensing imagery and GIS (including census) data has received widespread attention in recent years* (Weng, 2010)

5.2. THE QUANTITATIVE APPROACH TO THE SPATIAL ANALYSIS OF LAND OCCUPATION PATTERNS

Spatial analysis refers to a variety of techniques designed to investigate specific phenomena, characterised by the distribution of a number of observations (often linked to geometric entities such as points, lines, or areas) into a well-defined geographical space, and based on different analytical approaches; such as relational, topological or geometric. Currently, as is argued by Martori and Hoberg (2008), spatial analysis deals with changes that occur in the form, location, and distribution of geographical phenomena, including the diversification introduced by the analysis of landscapes with its physical aspects and social implications.

The spatial analysis comes from quantitative geography. This implies the use of statistics applied to the geographical space, which is thus intended as the main environment for analysis. The use of spatial statistics has experienced a significant increase in the last decades, together with an equally rapid development of statistical applications integrated into geographic information systems. Hence, the combined use of statistics and GIS, has provided an essential set of tools for spatial planning (Martori, et al., 2008).

On the other hand, according to Batty (2008), quantitative geography is related to the field of regional science that assumes the location theory as a key matter for the study of economic dynamics, both at urban and regional level. *This is consistent with the complex sciences that dominate the simulation of urban form and function.* In fact, although *most urban models deal with the city in terms of the location of its economic and demographic activities*. There are, clearly, increasing interests to investigate those factors that put such models in relation to urban morphological models (Batty, 2008).

It seems quite reasonable that when we attempt to define the urban environment it is critical to break down the matter into several aspects, all of which cause and effect the final outline of an urban area. We need to refer not only to the physical structure of the urban settlements, but also to other key aspects; such as connectivity, distribution of economic activities, and the social structure. Hence, spatial analysis has to take into account the location, distribution, form and spatial relations of urban growth phenomena on the Earth's surface.

If we consider an urban environment to be a complex system, we could argue, in agreement with Gomez Piñero (1994), that there are at least four ways to analyse a system: functionality, structure, process and form. Functional analysis refers to the contribution that elements within the system provide to the characterization or functionality of the system itself and their position in it; and, where the position has a physical and relative significance in relation to other elements of the system. The analysis of the structure allows us to discover the relationships that occur under the generated configuration, and process analysis is required to explain the mechanisms governing the evolution of the system. Regarding the analysis of the form, it aims to define those components that physically reflect, in the space, the structural relationships behind the functionality, as well as the effects of the process on the system (Gomez Piñero, 1994).

Nowadays, there is a wide agreement that a city, or the urban environment in general, can be analysed and understood by its physical forms, the physical forms being either the shapes of smaller parts that compose the urban space at a local level, such as; buildings, lots, or streets, as well as the external profile of the urban area on the territory, as a whole, which marks the limits between artificial and natural environment.

Whatever the level of analysis, the urban space needs to be understood through investigating shapes, hierarchies, and relationships between solids and voids. It involves analysing the syntax of buildings and open spaces (streets and squares) in relation to each other, as well as spatial interaction among all those variables that define the configuration of urban patterns at the territorial level.

The focus of our investigation is, in particular, to measure the urban form, as it arises from the two-dimensional outline "drawn" upon the territory by the profile of urban settlements. We aim to quantify, geometrically and classify different (physical) patterns of urban land occupation, based on the information detected through the use of remote sensing techniques and stored in digital cartography. The use of Geographic Information Systems (GIS) increases the ability to handle geographic data and spatial measurements.

Currently, measuring and classifying patterns of land occupation rely on two key questions, respectively: spatial metrics and statistics. In particular, spatial (or quantitative) metrics, which are based on descriptive indicators, are used to provide the most exhaustive analysis of the form and structure of urban patterns and the relationships, in terms of distance, between all the patches that are part of the urban system under investigation. On the other hand, statistical methods are used for analysing and synthesizing behaviour patterns of the descriptive indices with the aim of grouping similar urban patterns.

The upcoming sections will address, in detail, the issues concerning either spatial indices as well as statistical techniques; at least those that in our opinion are quite suitable for defining different patterns of land occupation, from a morphological standpoint. The discussion, in fact, does not pretend to be exhaustive about matters regarding spatial metrics and statistical methods, which would likely need more than one essay. However, the work mostly aims to handle those concepts and approaches we have deemed useful for this investigation.

5.2.1. The Statistical Approach for Quantifying Spatial Patterns

Statistics is the field of study concerned with the collection, analysis, and interpretation of uncertain data. Such tasks are fundamental to science and engineering. Really, scientists discover the principles that govern the physical world by analysing data collected in scientific experiments. However, a major difficulty with scientific data is that it is subject to random variation, or uncertainty. That is, when scientific measurements are repeated, they come out somewhat differently each time. To address this question, a knowledge of statistics is essential, in fact, the methods of statistics allow scientists and engineers to design valid experiments and to draw reliable conclusions from the data (Navidi, 2011).

It must be stressed that it would be unreasonable to summarize, in a small number of pages and a couple of chapters, certain complex and articulated issues that are the basis of Statistical Science. However, we need to remember here even if they are just elementary notions, some basic concepts of statistics, as they provide a fundamental approach to spatial analysis, and also because they will provide key tools for quantifying different urban patterns of land occupation within this research.

The statistical approach effectively provides the means for dealing with the spatial analysis of geographical patterns and phenomena, in general. Due to the great number of variables that characterize the environment, and the variability of dynamics, we need suitable tools for synthesizing the main aspects, in which we are interested, and classifying them according to certain assumptions.

In this sense, the statistical techniques applied to spatial analysis, supply effective instruments for understanding the environment. Indeed, a statistical framework provides an objective basis for investigating and comparing observed land use patterns by measuring several quantitative spatial features about the landscape composition and configuration. Hence, we are actually speaking about "spatial statistics", which is a discipline under general statistics, but mostly concerned with the descriptive and inferential analysis[321] of geographic data.

According to such assumptions, when approaching the study of patterns of land occupation based on the analysis of a number of spatial measurements, in the same way as other generic statistical processes, this has to be focused on some primary tasks, such as:

- Problem formulation
- Data gathering
- Exploratory analysis
- Data summary
- Hypothesis formulation
- Modelling and testing

To address these matters, two main groups of statistical techniques will be used, and are briefly discussed here, which are: descriptive statistics, and multivariate statistics. Descriptive statistics in particular are concerned with describing all the experimental data with significant indices, and/or graphs[322]; while multivariate statistics, in general, involve the simultaneous analysis of more than one statistical variable, and how the variables are related

[321] The basic idea behind all statistical methods of data analysis is to make inferences about a population by studying a relatively small sample chosen from it (Navidi, 2011).

[322] Unlike the descriptive statistics, the inferential statistics implicate techniques for inferring about the whole population, but by analysing a sample of the observed data. While descriptive statistics are used for simply describing an observed distribution of data; on the other hand, inferential statistics attempt to make assumptions about the behaviour of any statistical variable, or to test hypotheses about a given phenomenon, based on a predetermined possibility of error. In other words, inferential statistics rely on two main subjects that are estimation and the verification of hypothesis. However, in order to make probabilistic predictions about a given phenomenon, inferential statistics can also use statistical data properly synthesized by descriptive statistics, or employ the same methods as descriptive statistics but applied on data samples (at any rate, descriptive statistics techniques are generally involved for exploratory analysis).

to each other. In addition, it focuses on emphasizing the effective meaning of each variable for the phenomenon under investigation.

5.2.1.1. Descriptive Statistics for Spatial Analysis

Descriptive statistics refers to a set of techniques and instruments used to summarize information and explain the main features of a given data collection. In particular, summaries can be made either on the totality of the observed cases (also termed population) or a finite set of *n* representative units of the whole population (sample). The main concern of descriptive methods is the calculation of numerical summary measurements capable of synthesizing and plotting specific characteristics of a data distribution. *Some of these methods are graphical in nature; the construction of histograms, boxplots, and scatter plots are primary examples* (Devore, 2010).

In other words, descriptive statistics aim to synthesize data through the use of summary indices and graphical tools, in order to highlight the most relevant aspects of the observed phenomenon. This also allows us to make comparisons between different data sets over time, thus allowing us to define changes and/or trends of variables. We could say that descriptive statistics are a collection of measurements that effectively supply the basis of any quantitative analysis, and they focus on three key aspects of data features:

- Location, or central tendency
- Shape of data distribution
- Variability or dispersion

The measurements of location, or of central tendency (also known as first-order statistics), are basically used to define the central value in a data set, i.e. a value that typifies the numerical level of a set of observations. In particular, we should refer to three measurements of location (figure 5.3), which are: Mean, Median, and Mode.

Mean: maybe the most common indicator of central tendency of a variable, calculated by dividing the sum of all observed values by the total number of observations.

Median: the middle value in a set of data numerically ordered from lowest to highest. If the number of cases is odd, then the median is exactly the middle value. On the other hand, for an even number of cases, the median is the average value between the two middle values.

Mode: the most frequent, or repeated, value in the set of data.

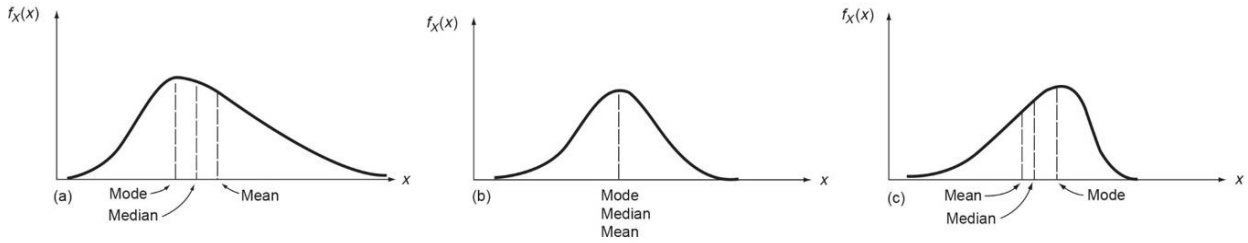

Fig. 5.3: *Relative positions of the mean, median and mode for three distributions: (a) positively skewed; (b) symmetrical; and (c) negatively skewed* (Source: Soong, 2004)

While mean and median are only suitable for numerical data, the mode is appropriate either for numerical or nominal data, such as colour and gender, for instance. Moreover, while the mean is generally a more suitable measure of central tendency (with respect to the median) since it considers all the values in the data set; it is extremely sensitive to outliers. Therefore, in data sets where outliers are present, the median could be preferable because it is not affected by such values, thus providing a more robust indicator.

Regarding the shape of data distribution, descriptive statistics here aim to explain significant features in the shape of the histogram defined by the data. Two main measures of the distribution shape are the index of asymmetry, also known as skewness, and the kurtosis.

Skewness, as also depicted in the previous figure 5.3, indicates the intensity and type of asymmetry of the histogram. Skewness can be positive or negative depending on the shape of the curve. In particular, it is positive

when a unimodal distribution has a dominant tail on the right (sample *a*, in figure 5.3), and it is negative when the distribution has a dominant tail on the left (sample *c*, in figure 5.3). Skewness is null when the mean is perfectly at the center of the distribution (sample *b*, in figure 5.3) (Soong, 2004). On the other hand, the kurtosis is a measure of elongation of the curve of data distribution, i.e. it measures if the shape of the histogram is narrow and pointed, or enlarged and flattened.

The variability or dispersion indices, in descriptive statistics, are second-order statistics that measure the degree of spread of the data with respect to the center value, i.e. the mean. Measures of dispersion are: Range, Variance, and Standard Deviation.

Range: this is the simplest measure of dispersion, calculated as the difference between the largest and the smallest value of the distribution, and it is representative of how data are spread. However, as is for the mean, the range is very sensitive to outliers.

Variance: usually referred to as σ^2, is the most common measurement of dispersion of a distribution around its mean, i.e. it measures the average distance between data population and its mean. Variance, calculated according to equation [5.1], always provides positive values.

$$\sigma^2 = \frac{\sum_{i=1}^{n}(x_i - \bar{X})^2}{n} \qquad [5.1]$$

Where: σ^2 = Variance
x_i = observed value *i*
$\bar{X}$ = mean for all x_i values
n = sample size

As depicted in Figure 5.4, large values of σ^2 imply a large spread in the distribution of data around its mean (as is the case of σ^2_2). Conversely, small values imply a sharp concentration of the mass of distribution in the neighbourhood of the mean (Soong, 2004), i.e. the values tend to be very close to the mean and hence to each other (as is the case of σ^2_1). On the other hand, a variance of zero would indicate that all the values are identical.

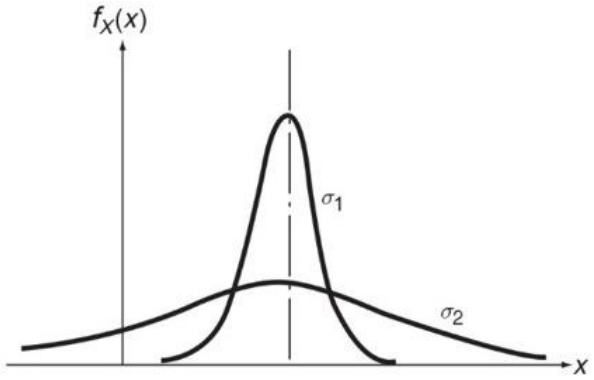

Fig. 5.4: *Density functions with different variances, σ_1, and σ_2* (Source: Soong, 2004)

Standard Deviation: this measure is, probably, the most used index of dispersion. Mathematically speaking, the standard deviation, usually referred to as σ and calculated according to equation [5.2], is the square root of the variance, and indicates how close a value is to the mean of a data set. A standard deviation approaches 0 as the data distribution tends to be very close to its mean value; while a high standard deviation indicates that observations are spread out over a wider range of values.

$$\sigma = \sqrt{\frac{\sum_{i=1}^{n} (x_i - \bar{X})^2}{n}} \qquad [5.2]$$

Where: σ = Standard Deviation
x_i = observed value *i*
$\bar{X}$ = mean for all x_i values
n = sample size

Although data can theoretically spread in different ways around the mean; there are many phenomena, in nature, in which variables tend to be distributed around the central value almost without bias to the left or right (skewness approaches 0), but with different kurtosis. Some examples are height of people, blood pressure, errors in measurements, among others. In such cases, the histogram will draw a quasi-symmetrical curve for data distribution (bell-curve), also known as normal distribution or Gaussian, in which mean, median, and mode are coincident[323].

Normal distributions of data are defined by the mean and the standard deviation (σ), so that if we refer to a normal distribution (actually, many normal distributions exist), the standard deviation will define the percentage of observations that fall within a certain distance from the mean (Figure 5.5), as follows: 68,3% of the values are within one σ (case a), i.e. 1σ on both side of the mean value (actually 1σ covers around 34.1% of the observations); 95,5% are within 2σ (case b); and 99,7% are within 3σ (case c).

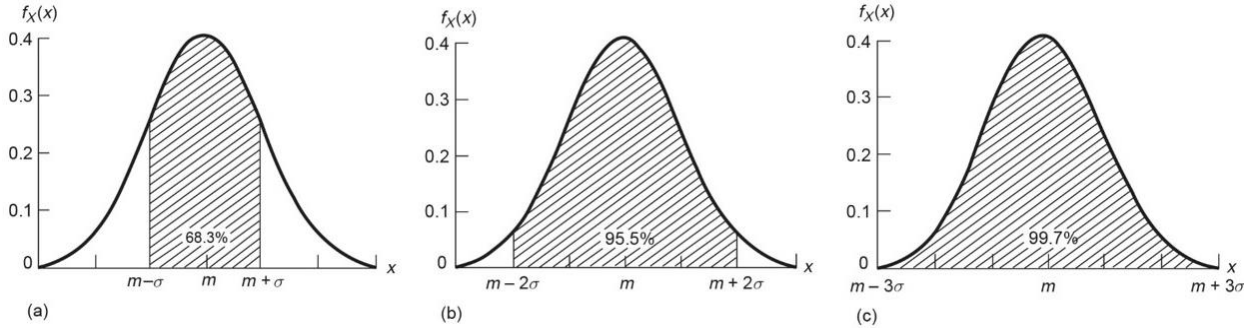

Fig. 5.5: *The Area under the normal density function within the range (a) m ± σ, (b) m ± 2σ, and (c) m ± 3σ*, where *m* is the mean and σ is the standard deviation (Source: Soong, 2004)

Data distribution can also be divided into a number of equal intervals, or quantiles, each one representing a percentage of the whole amount of the observed data. The most commonly used equal distributions are defined by the quartiles, which divide the data distribution into four equal parts so that each quartile represents 25% of the data, the deciles and the percentiles, which divide the data distribution into, ten equal parts and hundred equal parts, respectively.

Two further statistical measurements, derived by standard deviation are: the standard score (or z-score), and the Coefficient of Variation (CV). In particular, the z-score is the number of standard deviations between a value and the population mean, i.e. it reveals how many standard deviations a single value has from the mean. The z-score is calculated as the difference between an observed value and the population mean, divided by the standard deviation. It is negative when the value is below the mean, and positive when greater than the mean. The equation of z-score is also used to standardize series of data with different magnitudes of range, in order to allow comparisons.

[323] In probability theory, the normal distribution, or Gaussian, is a data distribution that occurs frequently, function of the probability that any real observation will fall between two real numbers, and that most of the observations will tend to cluster around the central value (mean), so that the bell-curve will tend to zero on either side.

On the other hand, the coefficient of variation, which is also an index of dispersion, is calculated as the ratio between the mean and the standard deviation. It measures the relative variability about the mean, not the absolute variability. It does not depend on a unit of measurement, and can be used to compare variation for different types of measurements, i.e. it is effective for measuring variability in data populations with different units. A variable with a higher coefficient of variation is more dispersed than a variable with a lower CV.

When descriptive statistics refer to the analysis of distribution of a single variable, thus including its central tendency (mean, median, and mode) and dispersion (range, variance, standard deviation), we speak about univariate analysis. On the other hand, when a sample consists of a pair of variables (often denoted as x, and y), we speak about bivariate analysis. Similarly, a multivariate analysis refers to the simultaneous observation and analysis of more than two variables.

In particular, descriptive statistics for bivariate analysis are used to explain the relationship between pairs of variables, mainly including quantitative measures of dependence such as correlation and covariance. The correlation takes into account two key aspects, that are: type of relationship between variables, i.e. positive (increasing a variable also increases the other) or negative (increasing a variable, the other decreases); and the shape of the relationship, i.e. if it is linear or parabolic, for instance.

In the case of linear correlation, the most commonly used index is the Pearson correlation index (or Bravais-Pearson), also known as Pearson's correlation coefficient *r*, calculated according to equation [5.3], which expresses the existing linear relation between two variables[324], in a range of values that varies between -1.00 and 1.00. The index approaches -1 as the correlation is increasingly negative, and approaches 1 when the correlation is increasingly positive. Pearson's index is 0 when no correlation exists between variables.

$$r = \frac{\sum_{i=1}^{n} (x_i - \bar{X}) * (y_i - \bar{Y})}{\sqrt{\sum_{i=1}^{n} (x_i - \bar{X})^2 * \sum_{i=1}^{n} (y_i - \bar{Y})^2}} \qquad [5.3]$$

Where: r = Pearson Correlation Coefficient
x_i and y_i = pair of observed values *i*
$\bar{X}$ = mean for all x_i values
$\bar{Y}$ = mean for all y_i values

The correlation indicates the tendency of two variables (X and Y) to vary together, i.e. the covariance; therefore the measurement of how much two variables vary mutually also provides a key issue of descriptive statistics under bivariate analysis. In particular, the covariance between a pair of variables is calculated according to equation [5.4], and it can be positive or negative depending on the type of relationship.

$$\sigma_{xy} = \frac{\sum_{i=1}^{n} [(x_i - \bar{X}) * (y_i - \bar{Y})]}{n} \qquad [5.4]$$

Where: σ_{xy} = Covariance
x_i and y_i = pair of observed values *i*
$\bar{X}$ = mean for all x_i values
$\bar{Y}$ = mean for all y_i values
n = sample size

[324] In regression analysis, i.e. the analysis of the mathematical function that links two (or more) variables, the slope of the correlation line also reflects the type of relationship between variables.

5.2.1.2. The Multivariate Analysis: Factor and Cluster Analysis

One of the main fundamentals of spatial analysis is the descriptive approach, based on the use of multivariate analysis, to explain complex spatial phenomena resulting from the interaction of a series of variables with different weights and characteristics. In spatial planning, for instance, the analysis commonly deals with large data sets so that it is critical to effectively summarize such amounts of data, and variables, in order to get the most reliable information about the dynamics of development.

For this reason, since the last century the statistical approach based on multivariate analysis of data has been widely recognized by scientists as an effective tool for understanding dynamics and interactions between urban and non-urban environments. *Multivariate analysis consists of a collection of methods that can be used when several measurements are made on each individual, or object, in one or more samples* (Rencher, 2002).

The multivariate analysis provides statistical approaches capable of performing studies across multiple dimensions by taking into account the effects of each dimension (or variable) upon the phenomenon under investigation, and the relative weights of the variables to each other. Certain dynamics could be not significantly interpreted if variables were analysed separately. In general, multivariate analysis aims to select, synthesize, sort, and classify those factors and features that best explain the phenomenon of interest (our focus is on spatial phenomena), also by excluding misleading (or unnecessary) elements and based on objective criteria.

Depending on the purpose of the study and the type of analysis, there are several multivariate techniques, for instance:

- Multiple regression analysis, used for measuring the degree of linear relationship between one dependent variable and two or more independent variables;
- Logistic regression analysis, sometimes referred to as "choice models", which is a variation of the multiple regression, but allows us to utilize nonmetric (typically binary) dependent variables;
- Discriminant analysis, useful for correctly classifying observations into homogeneous groups;
- Multivariate Analysis of Variance (MANOVA), which examines the relationship between several categorical independent variables and two or more metric dependent variables;
- Canonical correlation, which simultaneously correlates several independent variables and several dependent variables (Richarme, 2001).

At any rate, the investigation here is mostly based on the use of two multivariate techniques in particular which are Factor Analysis and Cluster Analysis, respectively used for summarizing sets of spatial variables and classifying similar patterns of urban models, based on synthetic indices.

The Factor Analysis, or exploratory factor analysis, is probably one of the most common statistical techniques used to extract, from a set of observed variables, a number of synthetic (unobservable) variables, also known as "latent variables" or factors, capable of explaining the covariance and correlations among the variables within the original set. Factors are a linear function of all original variables, but each factor will be more correlated to some of them.

When there are many variables in a research design, it is often helpful to reduce the variables to a smaller set of factors. Rather, the researcher is looking for the underlying structure of the data matrix (Richarme, 2001).

In this sense, the factor analysis allows for such reduction by transforming a set of many variables, most of the time correlated between them, into fewer independent factors that are represented by the eigenvectors of the data correlation matrix, weighted by the eigenvalues. Because the eigenvectors are orthogonal by construction, i.e. not correlated, the analysis is capable of explaining almost all the meanings of the original variables but based on fewer uncorrelated dimensions, and only a little information is lost (the remaining unexplained variation is a known error).

From a mathematical standpoint, being $x_1, x_2, \ldots, x_n$, vectors of observed variables, the formal factor analysis model that links observed and latent variables (factors[325]), is the same as a multiple regression in which each observed vector x is regressed on the common factors $f_1, f_2, \ldots, f_m$, with $m < n$, and a residual error term ε that represents the part of variables not explained by the common factors. The regression coefficients λ_{ij} in the model,

[325] Factors cannot be (directly) measured or observed.

shown in [5.5], are known as factor loadings, and express the degree of dependence among the variables and the underlying factors, i.e. are dependence weights among *x* and *f* (Rencher, 2002; Landau and Everitt, 2004).

$$\begin{aligned} x_1 &= \lambda_{11}f_1 + \lambda_{12}f_2 + \cdots + \lambda_{1m}f_m + \varepsilon_1 \\ x_2 &= \lambda_{21}f_1 + \lambda_{22}f_2 + \cdots + \lambda_{2m}f_m + \varepsilon_2 \\ &\vdots \\ x_n &= \lambda_{n1}f_1 + \lambda_{n2}f_2 + \cdots + \lambda_{nm}f_m + \varepsilon_n \end{aligned} \qquad [5.5]$$

The factor analysis model [5.5] can be written in matrix notation as shown in equation [5.6]:

$$x = \bigwedge f + \varepsilon \qquad [5.6]$$

Where:

$$x = \begin{vmatrix} x_1 \\ x_2 \\ \vdots \\ x_n \end{vmatrix}, \bigwedge = \begin{vmatrix} \lambda_{11} & \lambda_{12} & \cdots & \lambda_{1m} \\ \lambda_{21} & \lambda_{22} & \cdots & \lambda_{2m} \\ \vdots & \vdots & \ddots & \vdots \\ \lambda_{n1} & \lambda_{n2} & \cdots & \lambda_{nm} \end{vmatrix}, f = \begin{vmatrix} f_1 \\ f_2 \\ \vdots \\ f_m \end{vmatrix}, \varepsilon = \begin{vmatrix} \varepsilon_1 \\ \varepsilon_2 \\ \vdots \\ \varepsilon_n \end{vmatrix}$$

As mentioned by Landau and Everitt (2004), *since the factors are unobserved, we can fix their location and scale arbitrarily, so we assume they are in standardized form with mean zero and standard deviation one. We will also assume they are uncorrelated although this is not an essential requirement*.

The factor analysis relies on several approaches for extracting factors; such as, unweighted least squares[326], generalized least squares[327], principal axis factoring[328], alpha factoring[329], image factoring[330], principal components, and maximum likelihood (SPSS, 2006), However, the last two are, without a doubt, the most popular factor extraction methods.

In particular, the principal components[331] method, used for estimating loadings, accounts for the variance shared by the factors, and forms uncorrelated linear combinations of the observed variables in which the first component has maximum variance, while successive components explain progressively smaller portions of the variance and are all uncorrelated (orthogonal). The maximum likelihood method relies on assuming that the

[326] *The Unweighted Least-Squares Method is a factor extraction method that minimizes the sum of the squared differences between the observed and reproduced correlation matrices (ignoring the diagonals)* (SPSS, 2006).

[327] *The Generalized Least-Squares Method minimizes the sum of the squared differences between the observed and reproduced correlation matrices. Correlations are weighted by the inverse of their uniqueness, so that variables with high uniqueness are given less weight than those with low uniqueness* (SPSS, 2006).

[328] *The Principal Axis Factoring is a method of extracting factors from the original correlation matrix, with squared multiple correlation coefficients placed in the diagonal as initial estimates of the communalities. These factor loadings are used to estimate new communalities that replace the old communality estimates in the diagonal. Iterations continue until the changes in the communalities from one iteration to the next satisfy the convergence criterion for extraction* (SPSS, 2006).

[329] *Alpha factoring considers the variables in the analysis to be a sample from the universe of potential variables. This method maximizes the alpha reliability of the factors* (SPSS, 2006).

[330] *Image Factoring is a method based on image theory. The common part of the variable, called the partial image, is defined as its linear regression on remaining variables, rather than a function of hypothetical factors* (SPSS, 2006).

[331] *This name is perhaps unfortunate in that it adds to the confusion between factor analysis and Principal Component Analysis* (Rencher, 2002). Actually, Principal Component Analysis (PCA), like factor analysis is an attempt to explain a set of data depending on a summarized number of dimensions (variables), smaller than the primary. At any rate the procedures used to achieve this goal are essentially quite different in the two methods (Landau and Everitt, 2004). Factor analysis is used to extract latent (underlying) factors, based on the variance shared by the factors. It means that, unlike principal component analysis, the factor analysis begins with a hypothesis about the covariance (or correlational) structure of the variables, where the hypothesis is that a set of fewer latent variables exists and these are adequate to account for the interrelationships of the variables, although not for their full variances (actually, it produces error terms, or variates). On the other hand, principal component analysis extracts factors based on the total variance of variables. It means that PCA is merely a transformation of the data, and no assumptions are made about the form of the covariance matrix from which the data arise. Moreover, this type of analysis has no part corresponding to the specific variates of factor analysis. We could say that PCA is mostly a descriptive statistical technique (Richarme, 2001; Landau and Everitt, 2004).

observed variables have a multivariate normal distribution. The correlations are weighted by the inverse of the uniqueness of the variables, and an iterative algorithm is used (Landau and Everitt, 2004; SPSS, 2006).

According to Landau and Everitt (2004), the application of factor analysis involves two stages:

- *Determining the number of common factors needed to adequately describe the correlations between the observed variables, and estimating how each factor is related to each observed variable (i.e., estimating the factor loadings);*
- *Trying to simplify the initial solution by the process known as factor rotation.*

The initial solution, obtained by applying either Factor Analysis or Principal Component Analysis, may be improved by applying a rotation of factors (or axes). This will enhance the factor's interpretability without changing its underlying mathematical properties or altering the overall structure of a solution, only how the solution is described (Landau and Everitt, 2004). In particular, the rotation is concerned with two main types of approaches, i.e. the orthogonal rotation, which assumes that no correlation exists between the resulting factors, and oblique rotation, used when some relationship is believed to exist (Richarme, 2001). In other words, *rotated factors may be constrained to be independent (orthogonal) or allowed to correlate (oblique), although in practice both will often lead to the same conclusions* (Landau and Everitt, 2004).

The most popular orthogonal rotation method is the Varimax (other methods are the Equimax, and the Quartimax), which forces each factor to have a small number of large loadings, and a large number of small loadings, thus simplifying the interpretation. Indeed, once Varimax rotation is applied, each original variable will tend to be associated with a smaller number of factors (or even just one factor), and each factor will represent a smaller number of variables. On the other hand, in oblique rotations; such as Oblimin, Promax, and Orthoblique, which are more flexible methods, the new axes are free to take any position in the factor space, i.e. these approaches reduce the orthogonality restriction in order to further improve the simplicity of interpretation.

Whatever the approach may be, some prerequisites need to be taken into account prior to carrying out a factor analysis. In order to get more reliable results, the sample has to be made up of at least 50 observations or more (100, for instance), and a minimum of 5 observations per variable have to be provided. It means that the ratio between observations and variables has to be at least 10/1 (Richarme, 2001).

Cluster Analysis refers to statistical techniques concerned with the classification of multivariate observations into groups (clusters). According to Landau and Everitt (2004), classification is, theoretically, a key procedure for all scientific research. In particular, the main purpose of classification is that of reducing a large data set into an optimal number of significant subgroups of individuals (or objects), where the partition is undertaken on the basis of similarity measurements for a given set of variables (Richarme, 2001).

As argued by Richarme (2001), *there are four main rules for developing clusters: the clusters should be different, they should be reachable, they should be measurable, and the clusters should be profitable (big enough to matter)*; moreover, it is desirable to work with uncorrelated variables (e.g. as obtained by factor analysis).

Statistical techniques concerning classification are essentially of two types: Cluster analysis and discriminant function analysis, however, unlike the cluster analysis, the discriminant analysis handles data already classified into groups for deriving rules for classifying unclassified observations, based on their variable values[332].

Regarding cluster analysis, there are two main clustering techniques: hierarchical, also referred to as tree-like approach; and non-hierarchical, which requires a specified number of input clusters (a priori). At any rate, *many clustering techniques begin not with the raw data but with a matrix of inter-individual measures of similarity calculated from the raw data* (Landau and Everitt, 2004). Here, similarity refers to the spatial distance, between variables, and in particular to the Euclidean Distance as *the starting point for many clustering techniques. However, care is needed if the variables are on very different scales, in which case some form of standardization will be needed* (Landau and Everitt, 2004).

Hierarchical techniques rely on iterative procedures that generate a hierarchy of partitions, i.e. the clustering is proceeded by a series of steps in which, progressively, larger groups are derived by joining together smaller groups produced in previous steps. *The initial step involves combining the two individuals who are closest, according to whatever distance measurement is being used. The process goes from individuals to a final stage in which all individuals are combined, with the closest two groups being combined at each stage. At each stage, more*

[332] *Discriminant functions are linear combinations of variables that best separate groups. In discriminant analysis for several groups, we are concerned with finding linear combinations of variables that best separate the k groups of multivariate observations* (Rencher, 2002).

and more individuals are linked together to form larger and larger clusters of increasingly dissimilar elements (Landau and Everitt, 2004).

One of the main goals of such a process is the capability to establish the most optimal number of clusters that naturally exist within the data population, and for a set of given measurements. This is achieved by determining the stage at which the process provides the best description of data (i.e. the best separability), based on the analysis of the tree-like diagram (known as Dendrogram) in which the series of steps are summarized.

Different methods arise from the different possibilities for defining inter-group distance. Indeed, some of the most popular approaches to hierarchical classification are Linkage methods and Ward's method. Linkage methods rely on: a). Complete Linkage, in which the distance between groups is defined as the distance between the most remote pair of individuals (maximum distance), one from each group; b). Average Linkage, in which inter-group distance is taken as the average of all inter-individual distances made up of pairs of individuals, one from each group (Landau and Everitt, 2004); and c). Single Linkage, based on minimum distance. Ward's method, which is a minimum variance method, forms groups based on the minimum increase in the overall within-cluster variance, where the minimum increase refers to a weighted squared distance between cluster centres. *Non-hierarchical classification, is a method of clustering that produces a partition of the data into a particular number of groups (clusters), set by the investigator* (Landau and Everitt, 2004).

As is for the popular K-means technique, non-hierarchical classification is used for clustering a set of *n* observations in an *n*-dimensional space and characterized by *m* variables, into *k* groups, depending on Euclidean distance. An initial number of *k* clusters is defined a-priori, then an iterative process is undertaken to reallocate objects, which are already clustered, in order to minimize differences between observed variables and achieving the best separability. Essentially, the technique seeks to minimize the variability between observations within clusters, and maximize variability among clusters. *After each iteration, cluster mean vectors are updated to new cluster centres. The procedure continues until all individuals in a cluster are closer to their own cluster mean vector than to that of any other cluster* (Landau and Everitt, 2004). Once this stage is reached, further iterations will not improve the results[333]. There is wide consensus that, when one attempts to analyse sets of data depending on clustering procedures, an optimal approach relies on the joint use of both hierarchical and non-hierarchical methods. Generally, hierarchical classification provides a tool for defining the most suitable number of cluster, while non-hierarchical classification is used for minimizing as best as possible the variability within final clusters.

5.2.2. Spatial Metrics for Urban Patterns Analysis

The spatial configuration of urban settlements within a territory, in addition to the most relevant growth dynamics that affect it, are probably the key topics in contemporary debates about spatial planning. *Understanding the urban patterns, dynamic processes, and their relationships is a primary objective in the urban research agenda with a wide consensus among scientists, resource managers and planners, because future development and management of urban areas require detailed information about ongoing processes and patterns* (Bhatta, 2012). On the other hand, a wide panorama of approaches and techniques already exist, and it is often difficult to select the most appropriate information and analysis for supporting decision makers.

Without a doubt, the increasing development of remote sensing technologies and data, in addition to Geographic Information Systems (GIS), during the last decades, has provided further capabilities for measuring, analysing, understanding, modelling the "physical expressions" of urban growth phenomena, in terms of pattern and process (Bhatta, 2012), and based on land use/land cover mapping and change detection over time. As argued by Bhatta (2012), *determining the rate of urban growth and urban spatial configuration, from remote sensing data, is a prevalent approach in contemporary urban geographic studies*.

We strongly agree that a comprehensive understanding of urban phenomena relies on issues of urban pattern (the physical expression) and urban process (evolution over time), and, in particular, through analysing the following key aspects:

[333] An in-depth discussion about non-hierarchical clustering is provided in the previous chapter (4) about remote sensing, at section 4.4.4, where the k-means and the isodata algorithms are considered as key approaches in the field of image processing for undertaking unsupervised classification of pixels in digital data.

- The spatial configuration, i.e. the urban form, either in terms of urban texture and territorial system;
- The magnitude of urban growth, in terms of land consumption with respect to the natural environment;
- The rate of urban growth, in relation to the demographic trend.

A key function in quantifying such urban issues has found the spatial metrics (also known as landscape metrics[334]) implemented and extensively used in landscape ecology during the past decades.

Due to the fact that landscapes provide complex spatial patterns in the distribution of resources, which vary over space and time; and since from different patterns emerge different types of landscapes; quantifying these patterns and their dynamics through the measurement of environmental features; such as connectivity, proximity, and diversity of habitats, for instance, is a key topic in landscape ecology[335].

In general, spatial metrics can be defined as quantitative indices suitable for explaining structures and patterns of landscape (O'Neill et al. 1988; Bhatta, 2012). Herold et al. (2005a) have defined such indices as *measurements derived from the digital analysis of thematic-categorical maps exhibiting spatial heterogeneity at a specific scale and resolution*. Spatial metrics applied specifically to the analysis of urban landscape can be intended as numerical measurements that quantify the spatial patterning of urban land cover (McGarigal and Marks, 1995).

A considerable number of spatial metrics and approaches for quantifying landscape patterns have been developed, improved and tested during the past years, thanks to the work of O'Neill et al. 1988, and other significant contributions have been provided by recognized specialists such as Riitters et al. 1995; Hargis et al. 1998; or McGarigal et al. 2002 (Bhatta, 2012). Facilitated by advances in computer processing and GIS technologies, this has given rise to the development of *literally hundreds of indices of landscape patterns* (McGarigal, 2014).

In this sense, special attention is given to the work undertaken by McGarigal, at the University of Massachusetts (McGarigal and Marks 1995; McGarigal, et al., 2002; McGarigal, 2014), for implementing numerous quantitative measurements in a public domain statistical package known as FRAGSTATS, in which spatial metrics are essentially grouped into three broad categories, depending on the level of aggregation to which land cover is analysed, i.e.:

- Patch analysis. Metrics are computed for every patch (object) in the landscape;
- Class analysis. Metrics are computed for every class (patch set) in the landscape;
- Landscape analysis. Metrics are computed for the entire landscape mosaic, intended as the interaction between all discrete classes, and patches, at once.

There are two main types of metrics for patch, class, and landscape metrics. At the patch level we have indices that measure the spatial character and context of individual patches; and measurements of the deviation of patch values from mean values of class and/or landscape. At the class level, metrics attempt to measure the amount and spatial configuration of the class, and summarize the patch metrics, for the focal class, by providing first and second-order distribution statistics such as mean, area-weighted mean, median, range, standard deviation, and variance of patch attributes.

Therefore, while patch metrics aim to measure structural characteristics of single objects, class metrics measure the aggregate properties of the patches within a class type. This means we can characterize a class by summarizing the patch metrics since the class represents an aggregation of patches of the same type.

Finally, as is for class metrics, there are also two basic types of metrics at the landscape level, i.e. *indices of the composition and spatial configuration of the landscape, and distribution statistics that provide first- and second-order statistical summaries of the patch metrics for the entire landscape* (McGarigal, 2014).

---

[334] *Applied to research fields outside of landscape ecology and across different kinds of environments (in particular, urban areas), the approaches and assumptions of landscape metrics may be more generally referred to as spatial metrics* (Herold et al. 2005a; Bhatta, 2012).

[335] As argued by McGarigal (2014), *landscape ecology by definition deals with the ecology of landscapes. It is the study of landscapes; specifically, the study of landscape patterns, the interactions among the elements of pattern, how patterns and interactions change over time, and the consequences (ecological and socio-economic) of these patterns and changes.* On the other hand*, surprisingly, there are many different interpretations of the term "landscape", thus the disparity in definitions makes it difficult to communicate clearly, and even more difficult to establish consistent management policies.* At any rate, *definitions of landscape invariably include an area of land containing a mosaic of patches or landscape elements. Forman and Godron (1986) defined landscape as a heterogeneous land area composed of a cluster of interacting ecosystems that is repeated in similar form throughout* (McGarigal, 2014). According to Gomez Piñero (1994), the landscape analysis refers to the study of physiognomy of the land surface. The concept of landscape is understood as a geomorphological complex system that occurs in a specific part of the geographic space. Hence, the ecological tradition investigates the spatial effects derived by the interaction between human phenomena and the environment.

Furthermore, as underlined by McGarigal (2014), also as regards the exploration of patch mosaics, there are three main approaches to the analysis, and each of them has different effects on the choice of the metrics and the interpretation of results. Such approaches basically provide different standpoints for assessing landscape patterns, which are a "patch-centric" perspective, a local perspective and a global perspective.

In particular, the patch-centric approach puts the focus on analysing the spatial character of individual patches, instead of the aggregate properties of patches; while the local perspective, or local neighbourhood structure analysis, relies on the use of a "moving window" (of a fixed or variable size and form, depending on the scale of analysis) for calculating metrics around one cell at a time.

If working with raster, a further level of detail should also be taken into account for landscape assessments smaller than the patch, which is the pixel (as the smallest landscape entity), and all related cell-level metrics for neighbourhood analysis. A cell-based approach allows us to assess the environmental systems at the highest possible level of disaggregation, thus allowing a bottom-up analysis of forms and interactions within landscape patterns.

Finally, the global perspective about landscape structure relies on the characterization of the structure of the entire scene, based on selected landscape metrics (McGarigal, 2014).

Whatever the approach, or the level of aggregation (patch, class, or landscape); currently, in the literature, there are plenty of useful metrics for defining the spatial configuration of land cover, either natural or artificial, and the relationships between different objects or events within the environment. However, depending on the specific aspects of landscape to be measured, all metrics can be organised, as proposed by McGarigal and Marks (1995) within the framework of FRAGSTATS, in conceptual groups as follow:

- Area/Density/Edge metrics
- Shape metrics
- Core area metrics
- Isolation/Proximity metrics
- Contrast metrics
- Contagion/Interspersion metrics
- Connectivity metrics
- Diversity metrics

Despite such rationalization provided by FRAGSTATS, the authors warn that there is no "cookbook approach" to dealing with the challenges[336] of a proper use and interpretation of landscape metrics; rather, it depends on the experience of the researcher, or planner, and the specific purposes of the investigation (McGarigal, 2014). Coherently with such assumptions, the analysis is first aimed at calibrating a subset of metrics (then applied to the remotely sensed urban land cover, and by using GIS technologies) capable of setting up a suitable model for delineating patterns of land occupation, i.e. aimed at quantifying both formal and structural configuration of urban settlements on the territory.

The choice of indices is made based on three factors:

- "Spatial Extent", which signifies the degree of urbanization, in terms of absolute amount of surface covered by urban areas (area and perimeter of land occupation), and density, as the ratio between urban/non-urban areas.
- "Spatial Structure", mainly focused on quantifying the degree of fragmentation of urban cover (physical continuity/discontinuity of settlements) in terms of number and relative dimension of patches, as well as the distance between patches that provides a measure of spatial dispersion.
- "Spatial Form", which refers to the geometric shape of the urban patches (the profile of urban boundaries), based on dualism between compact and fragmented form.

All metrics (either for intensity, structure, or form) are measured according to a two-dimensional Euclidean space, and are associated with a circumscribed geographical area, defined according to given spatial boundaries.

[336] *There are numerous challenges too, including: 1) defining a relevant landscape for the phenomenon or question under consideration, 2) gaining a proper theoretical and empirical understanding of metric behaviour to aid in the interpretation of each metric, 3) understanding the theoretical and empirical redundancies among metrics to ensure their parsimonious use, and 4) developing a proper reference framework for ecologically interpreting the computed value of each metric* (McGarigal, 2014).

5.2.2.1. Land Occupation Extent: Area Metrics and Density

As argued by McGarigal (2014), patch (or class) area *is perhaps the single most important and useful piece of information contained in the landscape. This information is the basis for many of the patch, class, and landscape indices*. Besides this, the extent of a patch and/or class, either in terms of cover size or edge length, is one of the most basic landscape pattern measurements affecting many processes (McGarigal, 2014).

At any rate, the absolute amount of the urban land cover class (or land occupation), per se, could not be so explicative about the magnitude of urban growth. For example, if we attempt to provide an analysis of sustainable growth, and we say that a city covers a certain number of square kilometers (or hectares), this measurement is not a negative parameter (or positive) a priori, but rather it needs to be related to other values.

In actuality, when we try to define the dimensions of an urban phenomenon, and we refer to the spatial extent of urban areas as an index of magnitude; a key concept that needs to be considered is the amount of land "consumed" by urban development. In this sense, it is of our opinion that at least four main measurements deserve to be taken into account: a). the total coverage of urbanized areas, in absolute terms; b). the density of land occupation, i.e. the percentage of urbanized area in relation to a reference portion of the territory; c). number of inhabitants; and d). population density (also known as urban density[337]), i.e. the ratio between inhabitants and urban area[338]. However, at this stage, because the objective of the investigation relies on setting up a reliable model for defining urban forms but is strictly based on morphological parameters, population and population density are here discarded[339].

Subsequently, in order to effectively define the extent of urban land occupation, as a key morphological factor concerning urban configuration; area metrics[340], and in particular size and density, will provide some of the most basic information. For such purposes, three measurements are taken into account: patch area; class area; percentage of landscape (named PLAND in FRAGSTATS), which is a measurement of the percentage of landscape occupied by the urban land cover; and the radius of gyration (GYRATE).

Patch area, as argued by McGarigal (2014), *is the simplest measurement of landscape configuration, and represents a fundamental attribute of the spatial character of a patch. Most landscape metrics either directly incorporate patch size information or are affected by patch size. Patch size distribution can be summarized at the class and landscape levels by using mean, median, standard deviation or variance*.

In particular, the Mean of Patch Size (MPS), at the class level, is a function of the number of patches and the total class area. The index provides the average size for all patches in a class, but does not directly provide any information about the number of patches within the class. At present, this index in conjunction with a measurement such as patch density (PD), which is a ratio between number of patches and total area of landscape under investigation, should be more explicit of landscape configuration. Similarly, second-order statistics, such as standard deviation and variation[341] of patch size, may provide further information on landscape configuration (McGarigal, 2014). Class area is the sum of all patch areas within a defined landscape. Here, in particular, it refers to the total amount of area covered by urban land with respect to a limited spatial ambit.

Percentage of landscape is a measure of density. It quantifies the proportional abundance of each patch type in the landscape, i.e. specifies how much of the landscape is composed of a particular patch type (McGarigal,

[337] The term urban density, in spatial planning, refers to the number of people inhabiting a given urbanized area. This measurement provides a key variable in the analysis of several dynamics within urban environments, including economics, sociology, sustainability, or health, for instance. However, it is critical here not to confuse the concept of urban density with the concept of land occupation density, which instead refers to the amount of urbanized area in a given geographical space.

[338] Defining population density could be quite an arduous matter. At present, when working with population density, it would be more reliable to take into account two kinds of densities: a static density and a dynamic density. In fact, because this index is related to the number of persons found within an urban area, it is quite obvious that the number of inhabitants could be quite a variable parameter, for many reasons. First of all, the number of resident inhabitants can vary from one census to another, or alternatively the administrative limits of census can vary; furthermore, dependent on several factors, an important flux of persons move, daily or seasonally, from one city to another. In our opinion, this issue would deserve further investigation that will not be undertaken within this thesis.

[339] On the other hand, population and population density, based on census data per municipality limits, will be taken into account later, in order to provide an assessment analysis of the urban sprawl phenomenon.

[340] Area metrics, here, rely on a set of indices derived by those proposed by McGarigal (2014), under the concept "Area/Density/Edge".

[341] *Patch size standard deviation is a measure of absolute variation, i.e. it is a function of the mean patch size and the difference in patch size among patches. While variability in patch size measures a key aspect of landscape heterogeneity that is not captured by mean patch size and other first-order statistics* (McGarigal, 2014).

2014). Because our focus is on analysing urban land cover, we intend this indicator as a Covering Index (CI) for urban areas, which is the sum of all urban patch areas (a_i) divided by the area of the reference portion of territory, i.e. the landscape under investigation. The Covering Index, calculated according to equation [5.7], approaches 0 when no urban patches are present; instead, CI approaches 100 when the portion of territory under consideration is completely covered by urbanization[342].

$$CI = \frac{\sum_{i=1}^{n} a_i}{A} * 100 \qquad [5.7]$$

Where: CI = Covering Index
a_i = area of patch i
A = total area of a reference portion of territory (landscape)

The radius of gyration, or GYRATE as named in FRAGSTATS, is a measure of the patch extent, i.e. it measures *how far across the landscape a patch extends its reach*. This is a key aspect in spatial analysis because, sometimes, the mere size of a patch might not provide the same meaning as the patch "extensiveness" across the landscape. Instead, the radius of gyration is affected by both patch size and patch compaction (McGarigal, 2014).

GYRATE, according to equation [5.8], is calculated as the mean distance between each cell in a patch and the centroid of that patch, depending on a cell center-to-cell center distance. Such a measurement signifies the average distance needed to reach the patch boundary from a random starting point, and it equals 0 when the patch consists of a single cell, and increases without limit as the patch increases in extent. The maximum level depends on the landscape under investigation, i.e. is achieved when the patch comprises the entire landscape. In other words, *all other things equal, the larger the patch, the larger the radius of gyration; similarly, holding area constant, the more extensive the patch (i.e., elongated and less compact), the greater the radius of gyration* (McGarigal, 2014).

$$GYRATE = \sum_{r=1}^{z} \frac{h_{ir}}{z} \qquad [5.8]$$

Where: GYRATE = Radius of Gyration
h_{ir} = distance between cell *ir* (located within patch *i*) and the centroid of patch *i* (the average location), based on cell center-to-cell center distance
z = number of cells in patch *i*

Although area metrics provide essential information about the magnitude of urban phenomena, some limitations are imposed by the scale of analysis, and the resolution of data employed to extract urban land cover. At any rate, these are critical limits that need to be recognized prior to carrying out a spatial analysis, applying several spatial indices and interpreting results.

5.2.2.2. Urban Form: The Shape Metrics

The basic objectives of spatial planning involve the understanding of forms and dynamics of urban growth, and the possible effects on the territory. In this sense, the ability to identify and compare different forms of land occupation are fundamental topics for spatial analysis.

The scientific discussion about urban form, either in terms of shape, density, amount of land occupation, and/or spatial configuration, is currently based on an increasing array of works that primarily investigate concepts such as the "good form" of a city or the most "sustainable urban form".

Several researchers and urban planners are strongly convinced that the form of a city, or urban area, has a great impact on various aspects of sustainability; such as social equity, accessibility, ecology, economic

[342] The formulation of CI is the same as PLAND, but the term j, which refers to class type, is not present here because just one land cover type, i.e. urbanization, is considered.

performance, pollution and health (Huang, et al., 2007). In this sense we are also quite convinced that the capability of measuring the urban form is a key step to providing suitable analysis about growth dynamics. Likewise, several standpoints need to be taken into account when seeking to quantify as completely as possible such features.

First of all, in terms of metrics, because measuring urban area and density mainly refer to the landscape composition and not the landscape configuration as a result of spatial complexity (McGarigal, 2014), the interaction between size, density, and urban shape should be primarily investigated.

In urban planning and geography, the term "shape" usually refers to a fundamental spatial attribute, which deals with the concept of urban compactness, in opposition to dispersion. Additionally, as argued by Maceachren (1985), geographic shape compactness is of concern in contexts such as urban morphology. In general *the shape of a geometric object is a function of its morphology* (McGarigal, 2014).

Accurate measurement of morphological compactness, according to several approaches, provides suitable information for a wide range of topics of general interest in spatial planning; such as the identification of clustering models in remote sensing images, the understanding of urban sprawl, or the definition of electoral districts, among others. The compactness of urban settlements, which is a key topic in the analysis of urban sprawl, can be measured according to several indices, best known as "shape metrics", which provide numerical values that signify the degree to which a geometrical form is compact (Gillman, 2002; Li, et al., 2013).

Here, in particular, shape complexity refers to the geometry of a two-dimensional urban patch. However, due to the infinite number of possible forms provided by the urban profile on the territory which do not conform to canonical Euclidean geometries, geometry is extremely difficult to capture in a metric. Thus, shape metrics, as overall indices of complexity, measure if a shape tends to be simple and compact or irregular and “complex”, i.e. how much it differs from simple Euclidean geometry (McGarigal, 2014). Saying that, when one attempts to define the geometrical nature of urban patches in a landscape, the key meaning of shape metrics is strongly related to the "edge effect". Specific edge metrics do exist for quantifying edge attributes such as the total edge or edge density, but further landscape measurements are edge-dependent; such as the *core area metrics, which quantify the core area remaining after accounting for adverse penetrating edge effects; the contrast metrics, which quantify the magnitude of contrast along edges due to differences between adjoining patch types* (McGarigal, 2014); and even several shape metrics, as will be considered here, which are based on the relationship between perimeter (edge) and area for measuring shape complexity[343]. As argued by McGarigal (2014), *for simple geometric shapes a readily apparent relationship exists between the perimeter and area of a shape and its compactness*.

Shape comparison is a relevant topic in geography for assessing a broad range of spatial issues (Maceachren 1985). Moreover, as underlined by Chandra, et al. (2009), the notion of compactness in urbanism is *a well-established principle used to guide city planning, evaluate urban settings, and study urban sprawl* (Li, et al., 2013).

Shape here refers to two-dimensional plane objects, not linear entities in one dimension nor three-dimensional objects. In this sense, and according to Li, et al. (2013), shape compactness, in Geographical Information Science, is without a doubt one of the most investigated features for defining several morphological characteristics of planar objects (Angel, et al., 2010), for three main reasons:

- Shape compactness implies maximum accessibility to all parts of a polygon, and increased homogeneity in the distribution of attributes and properties (Tobler, 1970);
- Identification of shape is critical for recognizing and differentiating spatial models as an essential part of the analysis and understanding of current, as well as future, geographical phenomena (Wentz, 1997).
- Compactness, in geography, is a key attribute for the study of spatial objects “observed” by aerial perspective (Li, et al., 2013), and exemplified in a two-dimensional Euclidean space.

For these reasons, the development of effective compactness measurements has been a matter of interest for a number of scientific works during the past century. In fact, already in early 1800 Ritter proposed a

[343] *In landscape ecological investigations, much of the presumed importance of spatial pattern is related to edge effects. Total class edge in a landscape, often is the most critical piece of information in the study of fragmentation, and many of the class indices directly or indirectly reflect the amount of class edge. Similarly, the total amount of edge in a landscape is directly related to the degree of spatial heterogeneity in that landscape. One of the most dramatic and well-studied consequences of habitat fragmentation is an increase in the proportional abundance of edge-influenced habitat. In fact, many of the adverse effects of forest fragmentation on organisms seem to be directly or indirectly related to these so-called edge effects* (McGarigal and Marks, 1995).

measurement of shape compactness, based on a simple ratio between perimeter and area, i.e. an area-perimeter approach (Frolov, 1975; Li, et al., 2013). Because such a simplistic ratio is strongly affected by shape size (a problem with the perimeter-to-area ratio is that it varies with size), squaring the perimeter value, or taking the square root of the area eliminates such inconvenience (Li, et al., 2013; McGarigal and Marks, 1995).

As suggested by Maceachren (1985), *there exist a multitude of measurements that have been developed to, or have potential to, represent shape compactness*, which can be grouped according to four overall categories such as: perimeter-area measurement; single parameters of related circles; direct comparison to a standard shape; and dispersion of elements of a shape's area.

On the other hand, according to McGarigal (2014), *the most common metrics for measuring shape complexity are based on the relative amount of perimeter per unit area, generally indexed in terms of a perimeter-to-area ratio, or as a fractal dimension, and often standardized to a simple Euclidean form (for example, circle or square).* Apart from the most common perimeter-to-area ratio, other measurements emphasize particular morphological features; such as the contiguity index (LaGro, 1991), the linearity index (Gustafson and Parker, 1992), or the elongation and deformity indices (Baskent and Jordan, 1995).

In fact, several variations and improvements, based on precise mathematical forms have been proposed during the last decades to approach area/perimeter as key shape compactness measurement. Within these, without a doubt, some of the most relevant improvements have been the circularity ratio[344], proposed by Miller (1953) for measuring water basins, and the compactness ratio[345] by Richardson (1961). However, the Iso-Perimetric Quotient (IPQ) as proposed by Osserman (1978), and calculated according to equation [5.9], has become one of the most widely accepted compactness measurements within this class of shape metrics[346] (Li, et al., 2013).

$$C_{IPQ} = \frac{4\pi * A}{P^2} \qquad [5.9]$$

Where: C_{IPQ} = Compactness (Iso-Perimetric Quotient)
A = Area of the shape
P = Perimeter of the shape

An example of approaching the measurement of compactness by using a reference shape was proposed by Cole (1964), who made a compactness measurement based on the comparison between the area of a shape (A) and the area of the smallest circle that circumscribes the shape[347] (A_{sc}), according to equation [5.10]. As argued by Li, et al. (2013), Kim and Anderson (1984) termed this the Digital Compactness Measure (DCM). *Like the IPQ, its maximum value, 1, will occur when the shape is a circle. The major drawbacks of this method are that it cannot be applied to shapes with holes, it is not additive and scale-invariant* (Li, et al., 2013).

$$C_{DCM} = \frac{A}{A_{sc}} \qquad [5.10]$$

Where: C_{DCM} = Digital Compactness Measure
A = Area of the shape
A_{sc} = Area of the Smallest circumscribing Circle

[344] The circularity ratio, which involves Area (A) and Perimeter (P) of the shape, is calculated as $4*A/P^2$

[345] This compactness ratio is calculated as $2*\sqrt{(\pi A)}/P$

[346] By adding π in the numerator of Miller's circularity ratio, C_{IPQ} values range between 0 and 1, where a shape with values of C_{IPQ} approaching 1 is considered to be more compact than a shapes approaching 0. In particular, a circle, which is considered the most compact shape will have a compactness value of 1. *The C_{IPQ} is also the square of Richardson's compactness ratio, and although the approach is not very stable for irregular contours* (Santiago and Bribiesca 2009), *it is applicable in computing the compactness index for both vector and raster data, it is easy to compute, and it is not sensitive to size changes* (Li, et al., 2013).

[347] *This is an alternative form of Gibbs's (1961) compactness measurement $4A/L^2$, where L is the longest line between two points on a shape's perimeter* (Li, et al., 2013).

The shape indices employed here are mostly based on those developed within the FRAGSTATS software, which computes complexity measurements basically based on the correlation between area and perimeter, at the patch, class, and landscape level. Different approaches are provided. In particular, some of the most common shape metrics, as developed within FRAGSTATS, and employed here, are: Perimeter-Area Ratio (PARA), Shape Index (SHAPE), Fractal Dimension Index (FRAC), Perimeter-Area Fractal Dimension (PAFRAC), Related Circumscribing Circle (CIRCLE) that equals the 1 minus the Digital Compactness Measurement (C_{DCM}), and Contiguity Index (CONTIG).

Moreover, the distribution of values for such indices can be analysed, at class and/or landscape level, by their first- and second-order statistics such as mean, area-weighted mean, median, range, standard deviation, and coefficient of variation. The mean, for shape index, measures the average patch shape, or the average perimeter-to-area ratio for a particular patch type (class) or for all patches in the landscape. On the other hand, the area-weighted mean[348], at class and landscape levels, is calculated by weighting patch values, according to their size. *Specifically, larger patches are weighted more heavily than smaller patches in calculating the average patch shape for the class or landscape* (McGarigal and Marks, 1995).

Further shape metrics implemented into FRAGSTATS can be categorised depending mainly on two concepts: on the one hand, shape metrics which are compared to a standard shape. In particular, two different circumstances are taken into account: when indices are applied to vector data, shape is compared to a circle (as is for the previous Digital Compactness Measure); while, for raster format, shape is compared to a square standard. On the other hand, in the framework of shape metrics based on the perimeter-area method as a measurement for quantifying the degree of complexity of the planar shapes, a further approach relies on the use of fractal geometry[349], which provides certain advantages because it can be applied to spatial features over a wide variety of scales.

The most basic shape indices as implemented in FRAGSTATS are the Perimeter-Area Ratio (PARA), which equals the ratio between patch perimeter and patch area; and the Shape Index (SHAPE), calculated according to equation [5.11], which *equals the patch perimeter (given in number of cell surfaces) divided by the minimum perimeter (given in number of cell surfaces) possible for a maximally compact patch (in a square raster format) of the corresponding patch area* (McGarigal, 2014).

$$\text{SHAPE} = \frac{P_i}{\min P_i} \qquad [5.11]$$

Where: SHAPE = Shape Index
P_i = Perimeter of patch *i* in terms of number of cell surfaces
min P_i = minimum perimeter of patch *i* in terms of number of cell surfaces

According to Milne 1991, and Bogaert et al. 2000, if a_i is the area of patch *i*, in terms of number of cells, and *n* is the side of a largest integer square, smaller than a_i, and $m = a_i - n^2$, then the minimum perimeter of patch *i*, i.e. $min\text{-}p_i$, will take one of the three following forms (McGarigal, 2014):

- $min - p_i = 4n$, when $m = 0$, or
- $min - p_i = 4n + 2$, when $n^2 < a_i \leq n(1+n)$, or
- $min - p_i = 4n + 4$, when $a_i > n(1+n)$

For large patches, those greater than 100 pixels, for instance, the minimum perimeter asymptotically approaches $4\sqrt{a_i}$, the perimeter of an exact square of size a_i.

SHAPE, as implemented in FRAGSTATS, is the simplest and (perhaps) most straightforward measurement of overall shape complexity, and corrects the size problem that arises in the perimeter-area ratio index, by adjusting for a square (or almost square) standard. SHAPE provides values equal or greater than 1, and in particular it is 1 when the patch is maximally compact (i.e., square or almost square) and increases without limit as patch shape becomes more irregular.

[348] *This index may be more appropriate than the unweighted mean shape index in cases where larger patches play a dominant role in the landscape function relative to the phenomenon under consideration* (McGarigal and Marks, 1995).
[349] *Mandelbrot (1977, 1982) introduced the concept of fractal, a geometric form that exhibits structure at all spatial scales, and proposed a perimeter-area method to calculate the fractal dimension of natural planar shapes* (McGarigal and Marks, 1995).

Besides the SHAPE, as argued by McGarigal (2014), *the degree of complexity of a polygon is characterized by the fractal dimension (D), such that the perimeter (P) of a patch is related to the area (A) of the same patch by* $P \approx VA^D$ *(i.e., log P ≈ ½D*log A). For simple Euclidean shapes (e.g., circles and rectangles),* $P \approx VA$ *and D=1 (the dimension of a line). As the polygons become more complex, the perimeter becomes increasingly plane-filling and* $P \approx A$ *with* $D \rightarrow 2$.

This relationship is used within FRAGSTATS for computing the Fractal Dimension Index (FRAC) for single two-dimensional patches, according to equation [5.12]. An adjusting factor is used, for the perimeter at the numerator, in order to reduce the raster bias. In this way, the values range between 1 and 2, where FRAC approaches 1 for patches providing regular shapes, such as the case of rectangles or other Euclidean geometries. FRAC approaches 2 for highly convoluted shapes, i.e. values greater than 1 specify increasing shape complexity.

$$FRAC = \frac{2 * \ln(0.25 * p_i)}{\ln a_i} \qquad [5.12]$$

Where: FRAC = Fractal Dimension Index
a_i = Area of patch i
p_i = Perimeter of patch i

During the eighties fractal concepts have received widespread attention, including in geography. Since then, geographers, urban planners and others have investigated the relation between fractal structures and urban areas, where the calculation of the global fractal dimension (D) of cities (and surrounding areas), in Europe and the U.S.A., has been carried out. Growth patterns, in turn, show a general increase of D with time for several cities (Encarnação, 2012)

At any rate, the use of Fractal Dimension Index is subject to some restrictions. In fact, as warned McGarigal (2014), caution should be taken when using FRAC as a measurement of patch shape complexity, because varying the cell size of the input image will affect the patch fractal dimension. For example, one patch, if detected according to digital images at different spatial resolution will provide different values of FRAC. Rogers (1993), also claims that the value of the fractal dimension, calculated in this manner, is dependent upon patch size and/or the units used.

As previously mentioned, the Fractal Dimension Index can be computed at the class and/or landscape level by using the mean value of patch, i.e. by averaging FRAC values over all patches within the same class type, for instance; or, alternatively, the index can be averaged based on the area-weighted mean, i.e. FRAC value is weighted depending on the area of each patch within the dataset under investigation.

However, fractal analysis can be applied to the entire landscape mosaic based on a regression approach using the perimeter-area relationship $A=k*P^{2/D}$, where k is a constant and the slope of the line is equal to 2/D (Burrough 1986; McGarigal, et al., 1995). The resulting index, named Perimeter-Area Fractal Dimension (PAFRAC) in FRAGSTATS, is calculated according to equation [5.13], and it equals 2 divided by the slope of regression line, obtained by regressing the logarithm of patch area (A) against the logarithm of patch perimeter (P). As is for the previous Fractal Dimension, PAFRAC values range between 1 and 2, where values greater than 1 signifies an increasing shape complexity for a 2-dimensional landscape mosaic. In particular, PAFRAC approaches 1 for regular (or Euclidean) geometries, and approaches 2 for highly convoluted shapes (McGarigal, 2014).

$$PAFRAC = \frac{2}{\dfrac{\left[n_i \sum_{i=1}^{n} (\ln p_i * \ln a_i)\right] - \left[\left(\sum_{i=1}^{n} \ln p_i\right) * \left(\sum_{i=1}^{n} \ln a_i\right)\right]}{\left(n_i \sum_{i=1}^{n} \ln p_i^2\right) - \left(\sum_{i=1}^{n} \ln p_i\right)^2}} \qquad [5.13]$$

Where: PAFRAC = Perimeter-Area Fractal Dimension
a_i = Area of patch i
p_i = Perimeter of patch i
n_i = number of patches in the landscape of patch type (class) i

Because PAFRAC is based on regression analysis, a certain number of observations are needed in order to get consistent results. Actually, as claimed by McGarigal (2014), *in landscapes with only a few patches, it is not unusual to get values that greatly exceed the theoretical limits of this index. The index is probably only useful if sample sizes are large (e.g., n > 20); although PAFRAC is computed in FRAGSTATS if n > 10)*.

Another approach to shape measurement, also implemented in FRAGSTATS, and alternative to those based on the perimeter-to-area ratio, is provided by the ratio between the area of the patch and the area of the smallest circumscribing circle. This index, calculated according to the above formula [5.10], provides a measurement of overall patch elongation.

In FRAGSTATS, in particular, the index is termed Related Circumscribing Circle (CIRCLE), but because here the equation equals 1 minus the patch area divided by the area of the smallest circumscribing circle. A patch that approximates to a circular shape (i.e. to a compact shape) will have a low related circumscribing circle index. On the other hand, a narrow and elongated patch will have a high related circumscribing index. In other words, *CIRCLE equals 0 for circular patches, and approaches 1 for elongated, linear patches one cell wide* (McGarigal, 2014).

Moreover, in addition to the previous shape metrics, FRAGSTATS also provides an index based on patch cell contiguity (CONTIG), and in particular based on the degree of connection between the pixels in a patch for a given class. This index, which is a cell-centred measure, calculates the amount of contact surface between pixels in a grid, i.e. the common edge, thus providing information about the spatial configuration of a patch depending on the degree of compactness versus the openness of the shape. In other words, and according to LaGro (1991), CONTIG provides an index of patch boundary configuration and thus patch shape.

The contiguity index, computed according to equation [5.14], *is quantified by convolving a 3x3 pixel template with a binary digital image in which the pixels within the patch of interest are assigned a value of 1 and the background pixels (all other patch types) are given a value of zero. The value of each pixel in the output image, computed when at the center of the moving template, is a function of the number and location of pixels, of the same class, within the nine cell image neighbourhood. CONTIG values range between 0 and 1, and in particular it equals 0 for a one-pixel patch and increases to a limit of 1 as patch contiguity, or connectedness, increases* (McGarigal, 2014).

$$CONTIG = \frac{\frac{\sum_{r=1}^{n} c_{ir}}{a_{i*}} - 1}{v - 1} \qquad [5.14]$$

Where: CONTIG = Contiguity Index
c_{ir} = contiguity value for pixel r in patch i
a_{i*} = area of patch i in terms of number of cells
v = sum of values in a 3-by-3 cell template

Although widely recognized as a useful approach in spatial analysis; McGarigal and Marks (1995), warn that some limitations need to be taken into account when using shape metrics. Firstly, all indices based on the use of the perimeter as a key element of the analysis are subject to an "edge effect" that is dependent upon the spatial resolution of the input digital data. That is, when working with raster, the length of perimeter is significantly affected by the stair-stepping pattern of line segments in relation to the pixel size. In this sense, edge-dependent metrics should not be compared among images with different resolutions, unless appropriately weighted depending on the phenomenon under investigation.

Moreover, *shape indices are limited with regards to the differences between how lines are portrayed in vector and raster images*. Additionally, the perimeter-to-area ratio methods are not at all sensitive to patch morphology, instead they are most suitable as measurements of the overall shape complexity. It is because, supposedly, two patches with different shapes may still have an identical area and perimeter.

On the other hand, shape indices not based on perimeter/area ratio are less affected by such limitations. *But these too generally do not distinguish patch morphology, they instead emphasize one or more aspects of shape complexity* such as elongation or circularity. However, it is critical to take into account *that vector and raster images use different shapes as standards* (circle or rectangle)*, thus, the absolute value of these indices differs between vector and raster images* (McGarigal and Marks, 1995; McGarigal, 2014).

5.2.2.3. Urban Structure: The Fragmentation as a Distribution Function of the Area

Analogous to the definition of habitat fragmentation provided by McGarigal (2014), we could define urban fragmentation as a process in which contiguous settlements, or alternatively, a continuous urban area is progressively sub-divided into smaller, geometrically more complex, and more isolated urban fragments. This definition, however, intrinsically assumes the existence of three different dimensions in a complex urban phenomenon, often referred to as urban sprawl. We are speaking about:

- Fragmentation of urban structure, either in terms of number, and relative dimension, of urban patches;
- Fragmentation of the geometrical profile of the patches;
- Dispersion, i.e. the relationship, in terms of distances, between all the patches.

As stated in section 5.2.2.2, some of the most widely recognized spatial metrics for measuring the fragmentation of geometric profile have been taken into account; while the upcoming section will analyse those spatial metrics capable of measuring the urban dispersion based on the physical distance between urban patches.

Here, instead, we focus specifically on measuring the degree of fragmentation of the continuous urban area into multiple smaller patches, i.e. how many patches make up a spatially limited urban structure (or alternatively we could speak about urban landscape), and what is the proportional weight of each patch in terms of size.

As argued by Angel, et al. (2010), the fragmentation of the built-up extent is commonly due to open spaces that "interpenetrate" the urban structure. On the other hand, urban Fragmentation, or scattered development, can be understood as *the relative amount and the spatial structure of the open spaces that are fragmented by the non-contiguous and non-compact expansion of cities into the surrounding countryside*.

An evident reciprocal relationship exists between the urban and natural environment so that the term fragmentation can be referred either to *the way in which open spaces fragment the built-up areas of cities*, as well as *the manner in which the built-up areas of cities fragment the open spaces in and around them* (Angel, et al., 2010).

Spatial metrics, and mainly structural metrics, have found important applications in the last decades in quantifying landscape fragmentation both for urban and natural environment. This is especially due to the increasing development of new technologies for Earth observation and analysis, such as Remote Sensing and GIS, therefore, it has become progressively "easier" to make an effective discrimination between built-up pixels and open space pixels, in a consistent manner at global level. *This makes it possible to study urban fragmentation in a rigorous manner* (Angel, et al., 2010).

Fragmentation indices can be referred to as structural metrics, since they actually measure either the spatial configuration or the physical composition of the patch mosaic, as well as the relative abundance of the patches, thus involving the analysis of changes in the patterns of landscape structure. In terms of urban landscape in particular, we refer to changes in patterns of land occupation.

The structural fragmentation involves the degree of subdivision of a continuous structure into multiple parts and, consequently, it strictly should refer to *the degree to which the landscape is broken up (i.e., subdivided) into separate patches (i.e., fragments), and not the size (per se), shape, relative location, or spatial arrangement of those patches* (McGarigal and Marks, 1995).

Shape fragmentation, as previously mentioned, supposes a different approach in terms of spatial metrics, although certain correlations can be found between structural fragmentation and shape fragmentation when analysing a landscape. Similarly, the degree of fragmentation is often highly correlated to the concept of dispersion (as we will see later), even if the concept and measurement of dispersion mainly involves the analysis of the spatial position of the patches.

As is for shape metrics, one of the main references for the analysis of fragmentation is, undoubtedly, the work provided by McGarigal and Marks (1995) in the FRAGSTATS software. According to this approach, several key indices exist for measuring (directly or indirectly) fragmentation, based on the use of edge metrics, for instance, or the patch density, as a simple ratio between number of patches and total area of landscape, *if numbers of patches (not their area or distribution) is particularly meaningful*. Here, the analysis of fragmentation, although based on FRAGSTATS metrics, takes into account a set of spatial metrics mainly based on the use of the cumulative distribution of patch sizes as an alternative and more explicit measure of subdivision (Jaeger, 2000).

According to the FRAGSTATS approach, we can classify such metrics into two main classes that are the "contagion/interspersion" metrics, which refer more strictly to the degree of subdivision (without taking into account the spatial distribution), and consist of degree of landscape division (DIVISION), splitting index (SPLIT), and effective mesh size (MESH) among others; and "diversity" metrics, which can be understood better as measurements of heterogeneity at landscape level, and consist with the patch richness, Shannon's diversity and evenness, as well as Simpson's diversity and evenness, and the dominance.

We found out, apart from the contagion/dispersion metrics to a certain extent, that also diversity metrics applied at the class level, can be used to measure the degree of fragmentation of a focal patch type (McGarigal and Marks, 1995) due to their capability of discriminating different spatial patterns. According to Jaeger (2000), these metrics can be depicted as *an area distribution function, i.e. they specify the number of patches comprised within a class type, as a function of patch size. This is equivalent to the probability that two randomly chosen places in a region will be found* (or not) *in the same undissected area.*

Mathematically speaking, some of these metrics, such as DIVISION, SPLIT, and MESH, are *different conversions of the second moment of a distribution function of a stochastic variable corresponding to the area distribution function*, known as "coherence" (Jaeger, 2000), and calculated according to equation [5.15]. The degree of coherence (C) is based on the cumulative patch area distribution, and a particular advantage is *its insensitivity to the omission or addition of very small residual areas. This advantage distinguishes the measurements used here from many other fragmentation measurements, especially from the number of patches, and the average patch size, which are sensitive to all patches independently of their sizes* (Jaeger, 2000).

$$C = \sum_{i=1}^{n} \left(\frac{a_i}{A}\right)^2 \qquad [5.15]$$

Where: C = Coherence
a_i = area of patch *i*
A = total area of patch type (class)

The landscape division index (DIVISION) is "simply" the counterpart of coherence. In fact, similar to coherence, it is based on a cumulative patch area distribution. However it is interpreted as *the probability that two randomly chosen pixels, in the landscape, are not situated in the same patch of the corresponding patch type* (or class). Fragmentation here is calculated at class level only (for urban land cover), therefore DIVISION equals 1 minus the sum of the squared values of the ratio among patch areas, and total area of patch type, as shown by equation [5.16].

The values, for DIVISION, range between 0 and 1, where 0 indicates a class type that consists of one single patch; while DIVISION approaches 1 as the number of patches increases, and/or the total patch type area tends to be equally distributed between the patches (McGarigal 2014).

$$DIVISION = 1 - \sum_{i=1}^{n} \left(\frac{a_i}{A}\right)^2 \qquad [5.16]$$

Where: DIVISION = Landscape Division Index
a_i = area of patch *i*
A = total area of patch type (class)

The splitting index (SPLIT), is based on the cumulative patch area distribution, and is defined as *the number of patches one gets when dividing the total region* (land cover type)*, into parts of equal size, in such a way that this new configuration leads to the same degree of landscape division as obtained for the observed cumulative area distribution* (Jaeger, 2000; McGarigal, 2014). The splitting index can be intended as "effective mesh number" of a set of patches[350], i.e. if patches in the set have the same size, SPLIT equals the number of patches.

[350] *SPLIT is interpreted as the effective mesh number, or number of patches with a constant patch size when the corresponding patch type is subdivided into S patches, where S is the value of the splitting index* (McGarigal, 2014)

SPLIT, which is calculated according to equation [5.17], equals the squared area of the total class, divided by the sum of the square of patch areas. In this way, SPLIT values range between 1 and the number of patches as the maximum achievable value. In particular, SPLIT equals 1 when the class consists of one single patch and increases as the class is increasingly subdivided into similar smaller patches.

$$SPLIT = \frac{A^2}{\sum_{i=1}^{n} a_i^2} \qquad [5.17]$$

Where: SPLIT = Splitting Index
a_i = area of patch *i*
A = total area of patch type (class)

The effective mesh size (MESH) is *based on the cumulative patch area distribution and is interpreted as the size of the patches, when the corresponding patch type is subdivided into S patches, where S is the value of the splitting index* (McGarigal, 2014). MESH *is an area-proportionately additive measurement, i.e. characterizes the fragmentation of a region independently of its size. Thus, this index is well suited for comparing the fragmentation of regions of different total size* (Jaeger, 2000).

MESH is computed according to equation [5.18], and it equals the sum of patch area squared, summed across all patches of the corresponding patch type, divided by the total class area, and divided by 10˙000 in order to convert to hectares (McGarigal, 2014). If computed at class level, MESH is highest when the class is made up of one single patch equal to the size of the entire area under investigation, or, alternatively, when all patches have the same area. Indeed, if all patches have the same size, the maximum value of MESH at class level is not sensitive to the number of patches. Thus, it would be more explicit if used in conjunction with other indices. Subsequently, minimum value of MESH is reached when the patch area corresponds to the smallest possible area achievable in the landscape, i.e. such as in the case of using raster data the smallest possible area equals the pixel size.

$$MESH = \frac{\sum_{i=1}^{n} a_i^2}{A} * \left(\frac{1}{10{\cdot}000}\right) \qquad [5.18]$$

Where: MESH = Effective Mesh Size
a_i = area of patch *i*
A = total area of patch type (class)

MESH is redundant with DIVISION, i.e., they are perfectly correlated inversely, although they provide differences in units and interpretation. In fact, DIVISION is interpreted as a probability, whereas MESH is given as an area. Moreover, MESH provides a relative measure of patch structure because it takes into account the patch size distribution of the corresponding class, as well as the amount of landscape area composed of that class. At class level, holding the patch size distribution constant, as the class extent increases, MESH also increases. On the other hand, when computed at landscape level, as the landscape area increases, MESH for the corresponding class decreases (McGarigal, 2014).

As argued by Jaeger (2000), if we take into account two series of patches, of which the first is divided into patches of equal size, and the other is of different patch sizes, but both series have the same number of patches and same relative positions; patch number and average patch size, for instance, cannot distinguish between the two series, while SPLIT, DIVISION, and MESH will reflect structural differences between the two pattern series. In addition, according to McGarigal (2014), these measurements, which are to a certain extent related to the area-weighted mean patch size, have a certain advantage over other conventional measurements of subdivision, such as Mean Patch Size (MPS) or Patch Density (PD), because it is insensitive to omission or addition of very small patches. At any rate, *SPLIT and DIVISION are not area-proportionately additive, thus MESH is the only measurement that is both area-proportionately additive and reflects structural differences. It actually combines the advantages of intrinsic and structural measurements and fulfils more criteria than any other fragmentation measurement* (Jaeger, 2000).

The proportional distribution of land cover classes within the landscape, i.e. the landscape composition, or, alternatively the proportional distribution of total class area between the patches of that class, are both relevant topics to the field of landscape pattern analysis. Among the most recognized indices useful for measuring landscape pattern, the diversity indices provide an effective approach without a doubt.

According to Wen (2010), landscape pattern can be measured with diversity, dominance, evenness and fragmentation. All of these indices, originating from landscape ecology[351], serve to quantify the spatial composition as a key aspect of landscape structure, through measuring features associated with the variety and abundance of patch types within the landscape, but without considering the spatial characteristics, placement, or location of patches within the mosaic (McGarigal, 2014). Here, because the emphasis is on analysing the urban structure with respect to the non-urban land cover, diversity, evenness, and dominance metrics are used to define the degree of fragmentation of urban settlements as a result of an increasing alternation between full and empty space and the relative distribution of urban patch areas.

Diversity indices are, in general, a composite measurement of richness and evenness, and they can be computed according to a variety of forms depending on the relative emphasis placed on these two components (McGarigal, 2014) but, without a doubt, the most significant approaches to the study of landscape diversity are those provided by Shannon and Weaver (1949), and Simpson (1949).

Shannon's Diversity Index (SHDI) is one of the most popular measurements of diversity, in ecology, applied to landscape analysis, and is used here to define the degree of fragmentation of urban structures. As shown in equation [5.19], SHDI equals minus the sum, across all patch types, of the proportional abundance of each patch type, multiplied by the logarithm of that proportion (McGarigal, 2014). If applied at class level, the term P_i is the proportional abundance of each patch within the focal patch type (class).

SHDI provides values equal to, or greater than zero (without limit), where 0 signifies that the landscape, or the class, is made up of one patch only, i.e. there is no diversity. Alternatively, we could say that there is no fragmentation at class level. On the other hand, SHDI increases as the number of different patch types, or the number of patches within a class, increases and/or the proportional distribution of area among patches becomes more equitable.

$$SHDI = - \sum_{i=1}^{n} (P_i * \ln P_i) \qquad [5.19]$$

Where: SHDI = Shannon's Diversity Index

$P_i = \frac{a_i}{A}$ = proportion of the patch type (class) occupied by patch *i*

a_i = area of patch *i*

A = total area of patch type (class)

The Simpson's Diversity Index (SIDI) is another popular diversity measurement that comes from community ecology. SIDI equals 1 minus the sum, across all patch types, of the proportional abundance of each patch type squared, or, according to equation [5.20], at class level SIDI equals 1 minus the sum of the proportional abundance of each patch within the focal patch type (class). The values of SIDI vary between 0 and 1, where, as is for the Shannon's Index, 0 signifies a landscape made up of one patch only, while SIDI approaches 1 as the number of patches, within a class, increases and/or the proportional distribution of area among patches becomes more equitable. Saying that, Simpson's index is somewhat less sensitive to the presence of rare types of structures with respect to Shannon's index, but has an interpretation that is much more intuitive (McGarigal, 2014).

$$SIDI = 1 - \sum_{i=1}^{n} P_i^2 \qquad [5.20]$$

Where: SIDI = Simpson's Diversity Index

P_i = proportion of the patch type (class) occupied by patch *i*

[351] As argued by McGarigal (2014), diversity indices have been largely applied, by landscape ecologists (e.g., Romme, 1982; O'Neill et al., 1988; Turner, 1990a), for measuring the landscape composition as a key aspect of landscape structure.

As underlined by Jaeger (2000), the degree of landscape division (DIVISION) shows a similarity to Simpson's diversity index as defined by McGarigal and Marks (1995). However, when SIDI is applied at landscape level, the sum runs over the proportional area of each patch type in the landscape, not over the proportional area of each patch in the focal class. This means that the area distribution of the patches, within the patch type, is not considered. As a consequence, SIDI would be not suitable as a fragmentation index.

A Modified Simpson's Diversity Index (MSIDI) also exists, which eliminates the intuitive interpretation of the Simpson's index as a probability, thus converting the index into a more generalised diversity measurement, as is the Shannon's diversity index (McGarigal, 2014). As shown in equation [5.21], MSIDI equals minus the logarithm of the sum, across patches, of the squared proportional abundance of each patch in the focal class (instead of the sum, across patch types, of the proportional abundance of each patch type over the landscape, as defined by McGarigal and Marks, 1995).

In the same way as Shannon's diversity, MSIDI also provides values equal to, or greater than zero (without limit), where 0 signifies that the class is made up of one patch only, i.e. there is no diversity (or fragmentation) at class level. On the other hand, MSIDI increases as the number of patches increase within the focal class, and/or the proportional distribution of area among the patches becomes more equitable.

$$MSIDI = -\ln \sum_{i=1}^{n} P_i^2 \qquad [5.21]$$

Where: MSIDI = Modified Simpson's Diversity Index
P_i = proportion of the patch type (class) occupied by patch *i*

The concept of evenness refers to the relative abundance of a quantity, in an observed collection, mostly emphasizing either relative dominance or its complement, i.e. equitability. In other words, evenness defines the degree of deviance from a maximum equipartition of a quantity, which in our case is the amount of urban land occupation in terms of area. *There are many possible evenness (or dominance) measurements corresponding to the many diversity measurements. Evenness is usually reported as a function of the maximum diversity possible for a given richness* (McGarigal, 2014).

The Shannon's Evenness Index (SHEI) measures the degree of homogeneity of area distribution among patches, and in particular when it results in maximal evenness[352]. According to equation [5.22], SHEI equals minus the sum, across all patches, of the proportional abundance of each patch multiplied by the logarithm of that proportion, divided by the logarithm of the number of patches. In other words, SHEI is the observed Shannon's Diversity Index divided by the maximum Shannon's Diversity Index (also known as maximum entropy) for that number of patches.

SHEI provides values that range between 0 and 1, where 0 defines a class that contains only one patch, and approaches 0 as the distribution of area among the different patches becomes increasingly uneven, i.e. one patch is dominant. On the other hand, SHEI equals 1 when distribution of area among patches is perfectly even, which signifies that proportional abundances are the same (McGarigal, 2014).

$$SHEI = \frac{-\sum_{i=1}^{n} (P_i * \ln P_i)}{\ln n} \qquad [5.22]$$

Where: SHEI = Shannon's Evenness Index
P_i = proportion of the patch type (class) occupied by patch *i*
n = number of patches in the focal patch type (class)

The Simpson's Evenness Index (SIEI), as shown in equation [5.23], equals 1 minus the sum, across all patches, of the proportional abundance of each patch in the focal class, squared, and divided by 1 minus 1 divided by the number of patch types. SIEI is conceptually the same as the SHEI, i.e. it provides the degree of homogeneity

[352] In this sense, evenness signifies the complement of dominance (McGarigal, 2014).

of area distribution among patches, and in particular when it results in maximal evenness. Therefore, SIEI also provides values that range between 0 and 1, where it approaches 0 as the distribution of area among the different patches becomes increasingly uneven, and is 0 when only one patch is present; while SIEI equals 1 when distribution of area among patches is perfectly even.

$$SIEI = \frac{1 - \sum_{i=1}^{n} P_i^2}{1 - \left(\frac{1}{n}\right)} \qquad [5.23]$$

Where: SIEI = Simpson's Evenness Index
P_i = proportion of the patch type (class) occupied by patch *i*
n = number of patches in the focal patch type (class)

The Modified Simpson's Evenness Index (MSIEI), according to equation [5.24], equals minus the logarithm of the sum, across all patches, of the proportional abundance of each patch squared, and divided by the logarithm of the number of patch types, i.e. the observed Modified Simpson's diversity divided by the maximum entropy. MSIEI provides values that range between 0 and 1, where the index approaches 0 as the distribution of area among the different patches becomes increasingly uneven. This is 0 when only one patch is present; while MSIEI equals 1 when distribution of area among patches is perfectly even.

$$MSIEI = \frac{-\ln \sum_{i=1}^{n} P_i^2}{\ln n} \qquad [5.24]$$

Where: MSIEI = Modified Simpson's Evenness Index
P_i = proportion of the patch type (class) occupied by patch *i*
n = number of patches in the focal patch type (class)

Evenness can be also reported as its complement, i.e. the Dominance (D). The Dominance, as shown by equation [5.25], is mathematically calculated by subtracting the observed Shannon's Diversity Index from the maximum entropy, which is the logarithm of the number of patches in the focal class. Dominance provides values that range between 0 and the logarithm of the number of patches (*lnn*), i.e. the maximum entropy. Therefore, D approaches 0 for equitability of area distribution in patch increases, and equals 0 when distribution of area among patches is perfectly even. On the other hand, D increases as the dominance of one patch upon the others, in terms of size, is higher.

$$D = \ln n - \left[- \sum_{i=1}^{n} (P_i * \ln P_i) \right] \qquad [5.25]$$

Where: D = Dominance
P_i = proportion of the patch type (class) occupied by patch *i*
n = number of patches in the focal patch type (class)

At certain extents, the urban fragmentation is also intended as the fragmentation of the form, i.e. as the perimeter tends to be more convoluted, an urban settlement provides a more fragmented outline. In that case, shape indices are more suitable to measure such a phenomenon. Here, instead, the fragmentation is intended as the progressive subdivision of the urban settlement into multiple parts, where not just the number of patches is useful to define such a kind of fragmentation, but we also need to know the proportional area distribution for each fragment. It is because, theoretically, very small patches within an urban structure can be compensated when a significantly continuous patch is present.

At any rate the analysis of fragmentation, aimed at measuring the degree of split suffered by urban settlements, could represent a challenge due to the remarkable number of indices that exist, as also reported in this section. Therefore, in this regard, we have drawn four theoretical samples of urban structures, named A, B, C, and D, for which thirteen indices potentially suitable for measuring fragmentation, beside the total class area of the structure, have been computed and plotted (figure 5.6).

Each structure is made up a different combination of patches, either in terms of number and/or size, as follows:

A. Covers a total area of 1˙145 ha, and it is made up 6 patches that respectively occupy an area of 1˙000, 100, 20, 10, 10, and 5 ha;
B. Covers a total area of 445 ha, and it is composed of 10 patches, each one measuring respectively 100, 80, 60, 50, 50, 50, 20, 20, 10, and 5 ha;
C. Covers a total area of 360 ha, and it is composed of 4 patches of 200, 100, 50, and 10 ha;
D. Covers a total area of 610 ha, and it is also made up 4 patches that respectively measure 200, 200, 200, and 10 ha.

For each one of the models, in addition to Coherence (C), Landscape Division Index (DIVISION), Splitting Index (SPLIT), Effective Mesh Size (MESH), Shannon's Diversity Index (SHDI), Shannon's Evenness Index (SHEI), Modified Simpson's Diversity Index (MSIDI), Simpson's Evenness Index (SIEI), Modified Simpson's Evenness Index (MSIEI), and Dominance (D); four further values have been computed that are Class Area (CA), Number of Patches (N), Patch Density (PD), and Mean Patch Size (MPS). Note that the Simpson's Diversity has been omitted because it is redundant with DIVISION at class level.

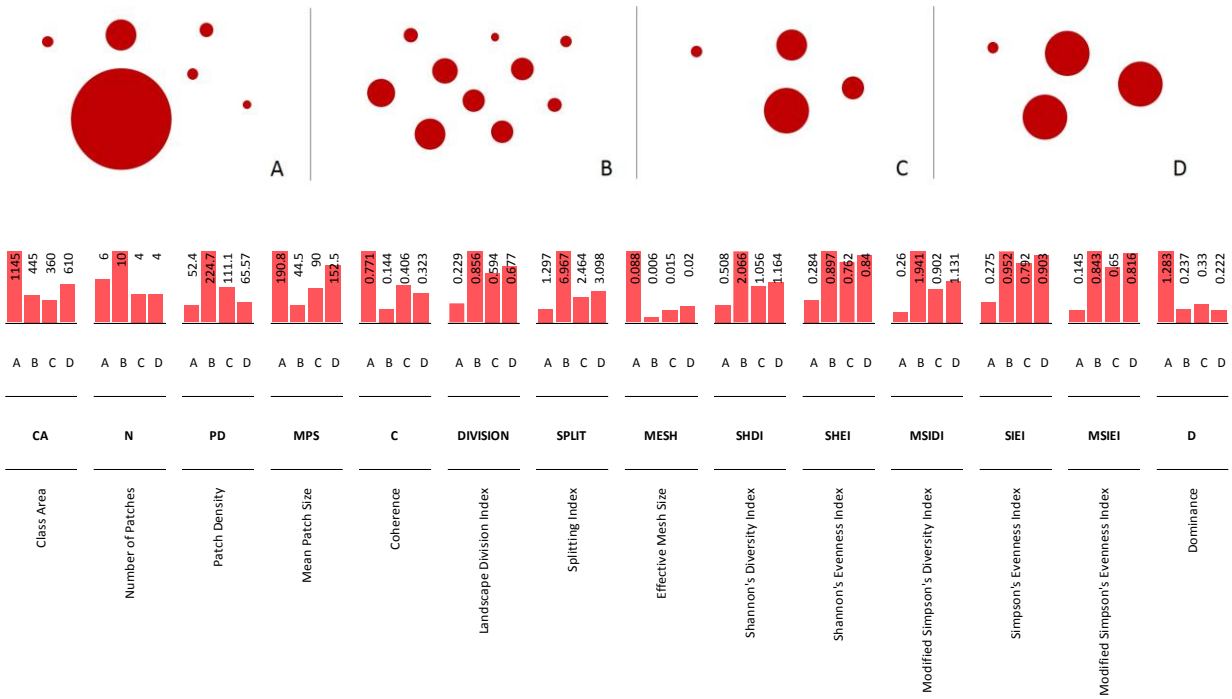

Fig. 5.6: Four theoretical models of urban structures (upper side); values and graphs of a set of widely recognized indices, suitable for the analysis of fragmentation (bottom side), and computed for each model (Source: by Authors)

Class Area (CA), besides its direct interpretive value either in absolute or relative terms, is used in the computations of many other metrics, at class and landscape level, as in the case of shape metrics. Here, in particular, CA provides significant information about the overall dimensions of the models.

Moreover, the summary measures of area, such as the Mean Patch Size (MPS), can also supply useful information about fragmentation by typifying the distribution of area among patches, both at class and landscape level. Generally, *metrics based on the mean patch characteristic offer a fundamentally patch-centric perspective of the landscape structure. In particular, a landscape with a smaller mean patch size, for the target patch type, than another landscape might result in a more fragmented structure. Similarly, within a single landscape, a patch type with a smaller mean patch size than another patch type might be considered more fragmented* (McGarigal, 2014).

Patch density (PD), which is perhaps one of the simplest measurements of composition, can also supply an effective index for landscape structures. In particular, although PD has the same basic utility as the number of patches, it expresses the number of patches on a per unit area basis, so that this facilitates comparisons among landscapes of varying size. Patch Density, at class level, decreases as class area increases. This means that when the number of patches is equal, a smaller structure provides higher PD values.

Moreover, *if numbers of patches, not their area or distribution, is particularly meaningful, then patch density for a particular patch type could serve as a good fragmentation index*. In fact, when the class area remains constant, a greater density of patches for a focal class would signify a more fragmented structure with respect to another structure with a lower patch density (McGarigal, 2014).

5.2.2.4. Urban Dispersion: The Spatial Distribution

Dispersion refers to the tendency for patches, with one in respect to the other, to be distributed in a non-contiguous, or clumped way. Therefore, although dispersion is closely related to the concept of fragmentation, dispersion depends explicitly on the degree to which patches are spatially dispersed, while fragmentation does not report distances between patches but only the degree of patch subdivision. For this reason, in addition to fragmentation measures (spatial composition), the relative position of the patches should be taken into account in order to effectively define spatial structures (spatial configuration).

When we speak about spatial configuration of a set of observations and the quantitative measurements of some of their attributes, we implicitly refer to a two-dimensional mathematical space in which the location of each observation can be specified with respect to both dimensions. Here, as is normal for spatial analysis, the mathematical space is relative to the geographic space, i.e. each observation corresponds to a "real" spatial measurement, on the Earth's surface.

At present, there are several dispersion indices, developed to assess spatial point patterns and applied to the analysis of dispersion for categorical maps; but, without a doubt, the most common and effective approaches are based on measuring distances between patches of the same type. Alternate to dispersion, and according to McGarigal and Marks (1995), we could also speak about isolation/proximity, intended as the tendency for patches to be relatively isolated in space (i.e., distant), from other patches of the same class; but, in the same way, there are many possible isolation/proximity measurements *depending on how distance is defined and how patches of the same class and those of other classes are treated*.

In particular, a common way to represent patch relationships, in terms of distance, is provided by the Euclidean Distance[353], as is the case in this investigation. One of the simplest measurements of patch spatial configuration, extensively used to quantify patch isolation/proximity, is the Euclidean Nearest-Neighbour distance (ENN), also implemented in FRAGSTATS and *defined using simple Euclidean geometry as the shortest straight-line distance between the focal patch and its nearest neighbour of the same class* (McGarigal and Marks, 1995).

When applied to raster format, *ENN equals the distance (h_{ij}) from the focal patch to its nearest neighbour patch of the same type (class), based on patch shortest edge-to-edge distance, and computed from cell center to cell center*. In this way, ENN provides values greater than 0, without limit. In particular, ENN approaches 0 as the distance to the nearest neighbour decreases (minimum values are constrained by the cell size), and increases as the distance, between patches, increases (maximum values depend on the landscape extent) (McGarigal, 2014).

At the class level, the Euclidean Nearest-Neighbour is assessed through the use of its first- and second-order statistics, i.e. the mean, area-weighted mean, standard deviation (SD), and coefficient of variation[354] (CV).

[353] Although other types of distance exist, in quantitative analysis, such as the Manhattan (or Taxicab) distance.
[354] The Coefficient of Variation (CV) is the ratio between the Standard Deviation (SD) and the Mean, for a given value, multiplied by 100.

In particular, the variability of values provided by SD and CV, could provide further information about the spatial patch distribution. *Specifically, a small standard deviation of ENN (ENN_SD), relative to the mean, implies a fairly uniform or regular distribution of patches across landscapes, whereas a large SD relative to the mean implies a more irregular or uneven distribution of patches*[355] (McGarigal, 2014). At any rate, the coefficient of variation (CV) often is preferable to SD for comparing variability among landscapes because CV measures the relative variability of the mean, i.e. the variability as a percentage of the mean, and not the absolute variability[356].

In actuality, an alternative index of dispersion, based on the nearest neighbour distance, and commonly employed in point patterns analysis, is the (well-known) index proposed by Clark and Evans (1954), which is computed as the variance to mean ratio in nearest neighbour distance. In this case, *if the variance is greater than the mean, then the patches are more clumped in distribution than at random, and if the variance is less than the mean, then the patches are more uniformly distributed* (McGarigal, 2014).

Apart from the ENN distance, an additional measurement of dispersion, also based on the shortest Euclidean distance between patches, which has been employed here is the Standard Distance and more specifically an area- weighted standard distance (SD_w), computed according to equation [5.26] (Mitchell, 2005).

$$SD_w = \sqrt{\frac{\sum_{i=1}^{n} w_i (x_i - \bar{X}_w)^2}{\sum_{i=1}^{n} w_i} + \frac{\sum_{i=1}^{n} w_i (y_i - \bar{Y}_w)^2}{\sum_{i=1}^{n} w_i}} \qquad [5.26]$$

Where: SD_w = Weighted Standard Distance
x_i and y_i = coordinates for feature *i*
$\{\bar{X}_w, \bar{Y}_w\}$ = weighted mean center for features
w_i = the weight at feature *i*

In the same way that the standard deviation quantifies the distribution of a set of observed values around their statistical mean, the standard distance provides a single summary measurement of the degree to which features are geographically concentrated, or dispersed, around their geometric mean or median center. Features here are represented by points, so that more dispersed point patterns will have larger standard distances, while clustered points will have smaller standard distances.

When working with land cover patches, if the weighted SD is used, the feature points employed in the computations of distances are patch centroids and the standard distance is weighted based on patch areas. Specifically, the SD_w assumes that data is distributed on a Cartesian plane and provides a single value, in map units, which equals the radius of the circle around the overall centroid of the points system (figure 5.7). This value (or radius) is computed using the geographic mean point of all patches and is the summary measurement of all the distances from the patch centroids, weighted for patch area, to the centroid of the overall system.

[355] *In absolute terms, the magnitude of ENN_SD is a function of the mean nearest-neighbour distance and variation in nearest-neighbour distance among patches. Thus, while SD does convey information about nearest neighbour variability, it is a difficult parameter to interpret without doing so in conjunction with the mean nearest-neighbour distance* (McGarigal, 2014).

[356] *For example, two landscapes may have the same ENN_SD, e.g., 100 m; yet one landscape may have a mean nearest-neighbour distance of 100 m, while the other may have a mean nearest-neighbour distance of 1˙000 m. In this case, the interpretations of landscape pattern would be very different, even though the absolute variation is the same. Specifically, the former landscape has a more irregular but concentrated pattern of patches, while the latter has a more regular but dispersed pattern of patches* (McGarigal, 2014).

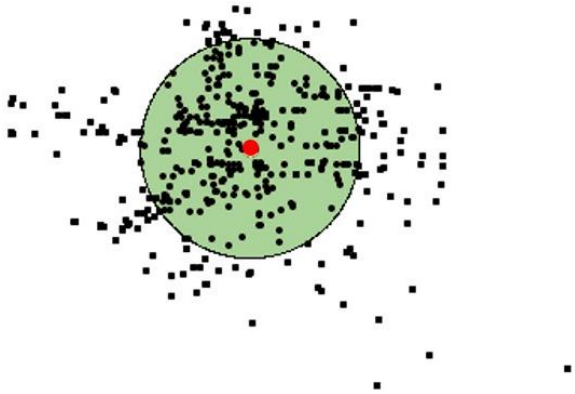

Fig. 5.7: Theoretical example of standard distance, calculated for a generic spatial distribution of points. The circle of radius equal to the value of the SD, and the centroid of the points system (Source: Mitchell, 2005)

A very common measurement used to quantify the spatial configuration of patches, both at class or landscape level, is the Proximity Index of Gustafson and Parker (1992), also implemented in FRAGSTATS and formulated in terms of both size and proximity of neighbouring patches within a local neighbourhood around each patch (search radius of the focal patch); and where such neighbourhood size is specified by the analyst, presumably depending on the phenomenon under consideration.

Note that FRAGSTATS uses the distance between the focal patch and each of the other patches within the search radius, rather than the nearest-neighbour distance of each patch within the search radius (which could be to a patch other than the focal patch), as in Gustafson and Parker (McGarigal and Marks, 1995).

Proximity Index (PROX), as shown in equation [5.27], equals the sum of patch area (a_{is}) divided by the squared nearest edge-to-edge distance[357] (h_{is}), between one patch and the focal patch of all patches of the corresponding patch type, within a specified distance of the focal patch.

This index is dimensionless, and its values vary from 0 to a maximum constrained by the search radius and the minimum distance between patches. In particular, PROX equals 0 when there are no neighbours of the same patch type within the specified search radius; subsequently, PROX increases as the neighbourhood is increasingly occupied by patches of the same type, and, as those patches are closer to each other and more contiguous. At any rate, the absolute value of PROX has little interpretive value; but is more useful as a comparative index (McGarigal, 2014).

$$PROX = \sum_{s=1}^{n} \frac{a_{is}}{h_{is}^2} \qquad [5.27]$$

Where: PROX = Proximity Index
a_{is} = area of patch *is* within specified neighbourhood of patch *i*
h_{is} = distance between patch *is* and patch *is*, based on patch edge-to-edge distance, computed from cell center to cell center

An interesting advantage provided by the proximity index, as also argued by McGarigal and Marks (1995), is that it measures both the degree of patch isolation and the degree of fragmentation for a corresponding patch type (class) within the specified neighbourhood of the focal patch. In fact, all other things being equal, if a patch within the neighbourhood defined by the search radius contains more of the corresponding patch type than another patch, it will have a larger index value. Similarly, all other things being equal, a patch located in a neighbourhood in which the corresponding class is made by a larger, more contiguous, and/or closer distribution of patches, it will have a higher index value.

[357] The edge-to-edge distances are from cell center to cell center.

In addition to those measurements strictly based on patch distances, another key geographic relationship, in spatial analysis, is the connectivity; understood as the total number of borders in common among patches of a same class (i.e. the functional connections among patches).

According to McGarigal (2014), connectivity metrics are generally based on the degree of patch connections (i.e. adjacency); a threshold distance; and a decreasing function of distance that reflects the probability of connection at a given distance. In particular, the Connectance Index (CONNECT), as developed in FRAGSTATS, is defined by the number of functional joinings among all patches within the same patch type, where each pair of patches is either connected or not, depending on a threshold distance (Euclidean distance[358])

Mathematically, as shown in equation [5.28], CONNECT *equals the number of functional joinings between all patches of the corresponding patch type (i.e. the sum of c_{ijk}, where c_{ijk}=0 if patch j and k are not within the specified distance of each other and c_{ijk}=1 if patch j and k are within the specified distance), divided by the total number of possible joinings between all patches of the corresponding patch type, multiplied by 100 to convert to a percentage*. The values of CONNECT range between 0 and 100, where 0 is reached when the focal class consists either of a single patch or none of the patches of the focal class are connected. On the other hand, CONNECT reaches 100 when each patch of the focal class is connected (McGarigal 2014).

$$CONNECT = \frac{\sum_{j=k}^{n} c_{ijk}}{\frac{n_i * (n_i - 1)}{2}} * 100 \qquad [5.28]$$

Where: CONNECT = Connectance Index

c_{ik} = joining between patch *j* and *k* (0=unjoined, 1=joined) of the corresponding patch type *i*, and based on a user specified threshold distance

n_i = number of patches in the landscape of the corresponding patch type (class)

5.3. MORPHOLOGICAL MODELS OF LAND OCCUPATION

In general, we could reasonably argue that an urban area is normally the result of a formal composition that, in turn, depends on socio-economic dynamics. Hence, urban settlements can be understood in terms of size, shape, and spatial distribution, either for the physical dimension or for socio-economic phenomena, at different scales ranging from local to regional level. Often, due to the complexity of the matter, in geography and planning, the analysis of urban areas is based on the use of models as idealized representations of real phenomena, which highlight the most relevant features of urban dynamics.

According to Fricke and Wolff (2002), *the geographical dimension of urban areas, which means the physical expansion of a city, is a fundamental variable of growth phenomena, even if most urban studies focus only on socio-economic data due to the availability of very accurate information deriving from the 10-year censuses or annual national registers in a lot of countries. In order to supply this deficiency, spatial analysis through the use of remote sensing approach is the only way to follow the very rapid urban growth*. The use of morphological techniques provides an effective tool to examine the forms of the urban landscape and rely on different fields; such as statistics, GIS and Remote sensing, Computer science, and Mathematics.

In recent years, research on urban morphology has widely investigated the way in which cities are created, renewed, and extended in space, by providing plenty of spatial metrics and models to understand and describe urban dynamics (for example, Batty, 1998; Batty and Longley, 1994; Longley and Mesev, 1997; Frenkel, 2004; Steiniger, et al., 2007). As argued by Moudon (1997), urban morphological research focuses on three fundamental components, which are form, resolution, and time. In particular, form refers to physical elements such as buildings and their related open spaces, plots or lots, and streets. Resolution refers to the spatial scale to which the form is analysed, i.e. building/lot, street/block, city, or region. Finally, time is regarding the analysis of the continuous transformations and replacement that urban forms undergo during different historical phases.

[358] Euclidean distance is calculated from cell center to cell center

Currently, the analysis of urban settlements is (preferably) undertaken on cartographic sources in digital format[359], such as the land cover/land use maps commonly derived through Remote Sensing techniques and handled using Geographic Information Systems (GIS) platforms. Here, in particular, urban land cover, as derived through remote sensing techniques applied to Landsat imagery at 30 meters, is analysed based on a morphological approach at regional level, and spatial metrics are employed to build suitable models for understanding, classifying and comparing different shapes (patterns) and layouts of land occupation. Actually, someone could argue that the use of traditional metrics, originating from the field of landscape ecology and used for analysing urban areas, is not necessarily optimal for describing different types of urban morphology (Herold, et al., 2005; Vanderhaegen, et al., 2010). However, we strongly believe that the answer to such criticism depends on the aim of the research and the spatial scale of data and analysis, i.e. it is critical to define which metric is most suitable for which analysis.

Indeed, although spatial analysis commonly relies on several dimensions such as *growth rate (of a population or built-up area), density (population density, residential density, employment density), spatial configuration (fragmentation, accessibility, proximity), beside other variables like per-capita consumption of land, land-use efficiency etc.* (Bhatta, 2012); our approach is "purely" morphological, thus we aim to set up spatial models able to synthesize some of the most critical aspects of urban form.

The urban outline (here understood as two-dimensional geometry in a Cartesian plane) is the result of different features, both internal and external, related to the spatial composition and configuration of its component parts. We aim, on one hand, to measure the morphology of the urban profile as a whole and the spatial relationship among urban patches in terms of distance, i.e. the external features; whilst on the other hand, we need to measure those internal features that affect the urban outline such as the morphology of the street network, and the spatial configuration of the built-up pixels, i.e. an analysis at cell level. Once we obtain a suitable set of measurements and models for understanding the urban landscape, from a morphological standpoint, the goal is to provide an automated process to classify similar patterns of land occupation in wide geographic areas. In particular, the focus is on urban areas along the Mediterranean side of Spain.

5.3.1. Scale Factor and Spatial Boundaries: Designing a Reliable Analysis

Regardless of the purpose of the research or the field of analysis, the detection and measuring of spatial patterns (morphological patterns in our case) within a patch mosaic, as is a land cover map for instance, is strictly dependent upon the spatial scale to which a phenomenon is examined. According to the ecology field, the concept of spatial scale encompasses both extent and grain of the landscape under investigation (Forman and Godron 1986; Turner, et al., 1989; Wiens, 1989; McGarigal and Marks 1995).

In particular, "extent" refers to *the overall area encompassed by an investigation or the area included within the landscape boundary. From a statistical perspective, the spatial extent of an investigation is the area defining the population we wish to sample*. On the other hand, "grain" generally refers to the smallest unit allowable for one patch, which in the case of working with raster data, corresponds to the dimensions of the pixel[360] (McGarigal, 2014). Hence, as argued in section 4.5.7.2 of chapter 4, the most appropriate operational scale of analysis will depend on the grain, i.e. on the spatial resolution of the digital data.

In spatial planning, when one discusses the most appropriate scale of analysis, it is critical to define the territorial ambit (or extent) to which an investigation is best suitable, in relation to the most common instruments allowed by urban planning. Spatial analysis associated with planning practices usually refers to four main extents that are the national, regional, municipal (sometimes generically identified as urban level), and local level. With respect to such topics, several limitations often arise in spatial analysis when one attempts to set up models. Limitations linked to the spatial resolution, landscape extent, the operational scale, suitability of metrics, and so on. However, key issues of a phenomenon can be effectively explained, and a reliable analysis can be provided if adequate assumptions are previously taken into account, i.e. stated and clarified.

[359] *Tomlin (1990) saw that if a map could be represented in digital form, then it would be easy to make measurements of its basic elements, specifically the areas assigned and the tedious hand-measurement of area by conducting dots on transparent overlays of known dot density* (Anji Reddy, 2008).

[360] In a map of land cover types, or patch mosaic, the data consists of polygons (vector format) or grid cells (raster format) classified into discrete land cover classes (McGarigal, 2014).

It is widely recognized that generally, in spatial statistics, no method is completely independent of the scale of analysis. Instead, different landscape features are observed depending on spatial scales. Many metrics such as measures of patch or spatial heterogeneity, are strongly dependent on the spatial resolution of the digital data (Bhatta, 2012), i.e. on the spatial measurement scale. In such a case, the spatial scale has a significant effect on determining the spatial pattern of a variable[361]. Interestingly, a series of scale invariant metrics have been developed in ecology. For example, the fractal dimension index for shape analysis, "fixes" the scale dependency of the perimeter-to-area ratio.

Regarding the spatial extent, or landscape, although we conventionally explore a spatial phenomenon by subdividing the geographical space into given areas of analysis, often a phenomenon under investigation is neither exclusively dependent on a sub-territorial space nor on the territory as a whole. Instead, it is more reasonable to state that spatial phenomena depend on and impact dynamics that occur at multiple spatial levels[362]. Hence, the selection of a proper landscape extent (or territorial unit) is quite critical and questionable when calculating spatial indices. There are different approaches to subdivide the study area. In spatial planning, for instance, the physical delimitation of landscape and the agglomeration of urban polygons has traditionally been characterized by two main approaches. On the one hand, there are studies based on functional or economic criteria (Roca et al. 2004), in which the emphasis is placed upon the existing relations and flows within the urbanized territory, in terms of journeys between place of residence and place of work. The other, the delimitation of urban landscape, is based upon physical or morphological criteria[363], where the continuous built-up area or the density of contiguous ambits comprises the basic mechanisms for the delimitation (Bhatta, 2012).

In the latter case, however, the main problem is the lack of census data, which is generally collected and distributed with respect to administrative ambits. *Therefore, how the population or other socioeconomic parameters change over time within the natural boundary cannot be analysed. If the analysis requires consideration of census observations then it must be based on the administrative tracts* (Bhatta, 2012). According to such an assumption, here the analysis of models of land occupation refer to administrative boundaries at the municipal level, based on the official census. Really, there are two levels of analysis, where metrics are applied, i.e. at the municipal level and at the cell level. In the case of analysing morphological patterns at the cell level, the scale is specified by a given distance, around the focal cell, which defines the spatial extent of neighbors in which interactions among built-up pixels are effective. In this case, the overall cell behaviour, for given metrics, is summarized at municipal level. However, because the formation of large peri-urban areas inevitably generates the disappearance of well-defined boundaries either between town and rural area (Antrop, 2004), as well as between adjacent cities in many cases. The disadvantage of such an approach is that the use of administrative limits generates arbitrary ruptures of the urban polygon. Thus, in many cases, it would generate improper results, with respect to the actual physical continuum, more or less notable depending on the number of common urban areas within municipalities.

Indeed, as argued by Bhatta (2012), if we think about the metropolitan space, the area contained within the jurisdictional boundary of a city has little to do with the actual urban agglomeration. In some cases, such as for the city of Barcelona, the municipality does not exactly reflect the real urban extent. The area is very small in comparison with the size of the metropolitan area[364]. Saying that, although in several countries, including Spain and Italy, specific urbanistic instruments exist for managing and planning metropolitan areas. The municipalities outside

[361] *In a low spatial resolution image, individual objects may appear artificially compact or they may get merged together. In an area of low density development where houses are relatively far apart, a spatial resolution of 30 m will produce an estimate of developed land four times that produced using the same underlying data but a spatial resolution of 15 m* (Bhatta, 2012).

[362] *Information may be available at a variety of scales and it may be necessary to extrapolate information from one scale to another. In addition, it may be necessary to integrate data represented at different spatial scales. It has been suggested that information can be transferred across scales if both grain and extent are specified (Allen et al. 1987), yet it is unclear how observed landscape patterns vary in response to changes in grain and extent and whether landscape metrics obtained at different scales can be compared* (McGarigal, 2014).

[363] *In consideration of remote sensing data, physical or morphological criteria are the preferred approach to determine the natural extent of the city* (Bhatta, 2012).

[364] *The Los Angeles metropolitan area, for example, contains 35 independent municipalities. In other cases, for example Beijing, the jurisdictional boundary of the municipality contains an area that is much larger than the built-up area of the city. The official area of the municipality is therefore not a very precise measurement, neither of the built-up area of the city nor of what we intuitively grasp to be the city (Angel et al. 2005). Furthermore, the extent of a city is a dynamic phenomenon and it changes over time. However, the jurisdictional boundary of the city cannot be changed frequently owing to administrative complexities* (Bhatta, 2012).

Universidad Politécnica de Cataluña, Barcelona TECH
Departamento de Tecnología de la Arquitectura
Centro de Políticas de Suelo y Valoraciones
Nicola Colaninno, Josep Roca Cladera

the metropolitan system are not administered at supra-municipal level. Instead, in such cases the municipality itself carries out the land management and planning at urban level, thus strictly limiting the urbanistic interest of city governments within well-defined administrative areas. In this way, all measurements of growth (compactness as opposed to sprawl, or the soil consumption rate, among others) will refer to the planned growth according to the municipal plan, so each municipality will need suitable analysis of its own spatial limits.

It is also critical to take into account that all those measurements related to population data, such as the urban density for instance, which provide fundamental dimensions of the urban growth phenomena, are normally associated with the administrative boundaries due to both census structure and planning practices. Therefore, beyond the criticism of the choice of the most appropriate landscape extent for spatial metrics, we believe that certain interesting conclusions can be derived from the study at municipal level. Besides the effectiveness of the results is that they can be associated to census data, for instance, and are then useful for land management at municipal level and planning. Moreover, here, we mostly aim to suggest a reliable methodological approach to the study of urban morphology, underlining certain key questions and deficiencies that need to be fixed, thus giving rise to future investigations.

5.3.2. Internal and External Factors of Urban Form: Urban Texture, Street Network, and the Urban Agglomeration Profile

Urban form is one of the main characteristics of urban areas. According to Batty, et al. (1994), form means shape, and in this context, shape pertains to the way cities can be observed and understood in terms of their spatial pattern. That said, the spatial pattern of cities is concerned with several physical, demographic and economic features; such as the size of the urban footprint, the degree of soil sealing, transport, social and economic composition, amongst others.

Different combinations of such dimensions produce different patterns of land occupation and urban growth, thus providing spatial structures with different degrees of fragmentation and/or dispersion of urbanised areas within the territory (Kasanko, et al., 2007). In other words, urban pattern is at the same time the cause and effect of other dynamics. In reality, such considerations express the complexity behind the understanding of the urban growth phenomenon that, without a doubt, requires the analysis of several variables. However, within the set of variables, the morphological features provide a key aspect (as also argued by Batty, et al. 1994) where, by ‘‘morphology’’, we mean the spatial configuration and the existing linkages between the different components of a city, both in terms of the relationship between urban patches, as well as the internal structure of each patch.

In this sense, the analysis here aims to measure the spatial composition and configuration of urban patterns with respect to features both internal and external to the urban profile. However, because the terms “internal” and “external” might cause some confusion, it is relevant to clarify that, here, the former term (i.e. internal) refers to the spatial configuration of the built-up pixels within the urban profile (we are speaking at the cell level). Indeed, based on the pixel distributions, we aim to classify different urban textures. In other words, the focus is on how the urban patch is filled.

Apart from the analysis at cell level, the term internal also refers to the street network, as a key structural factor that affects the spatial configuration, or outline, of urban areas. “External” refers to shape, extent, and composition of the urban profile, i.e. the urban agglomeration (intended as a Euclidean geometry drawn upon the territory), in addition to the spatial relationships, in terms of distance, between all the patches that make up the urban agglomeration within a well-defined territorial space. In particular, the spatial limits of such a space are defined by the administrative boundaries of municipality, as previously stated.

5.3.2.1. Urban Texture Classification: Continuous, Discontinuous and Scattered

The objective here is the spatial analysis of the smallest detectable urban component in order to define, as best as possible, those formal features that affect the final outline of the urban model. The analysis relies on measuring those “internal” dynamics, i.e. the spatial relationships that occur among each built-up pixel and its neighbours within the urban settlement, to highlight the morphological differences between types of urban

textures. In particular, the hypothesis is that at least three main textures can be classified at territorial level; a continuous, a discontinuous, and a scattered texture.

It is important to note that the smallest allowable components within an urban space would be buildings, and open spaces between them; but, because the urban land cover here is derived by digital cartography at 30 meters of spatial resolution, i.e. the smallest detectable part is a squared pixel of 30 meters, the analysis provided cannot be assumed as an accurate study at local scale. Indeed, one 30 meter pixel (or cell) theoretically encompasses more than one element at once, being either buildings, open spaces or vegetation, among others. Saying that, the local structure of urban patches at the cell level needs to be quantified prior to analysing the entire city. In fact, although pixels are not buildings, urban patterns detected through raster images strongly depend on the spatial configuration of the pixels.

At present, according to Bhatta (2012), the major limitations provided by the spatial analysis based on the use of metrics is due to the consideration of the external profile of the urban area as a whole, as the only key to understanding, without considering any internal dynamics. On the other hand, the variations of the internal structure, measured in the different parts of the city, often provide further features for understanding urban models. For instance, Wilson et al. (2003) identified three categories of urban growth based on different spatial configurations of pixels, at a given geographical portion, which are: infill, expansion and outlying; with outlying urban growth further separated into isolated, linear branch, and clustered branch growth, as shown in figure 5.8 (Bhatta, 2012).

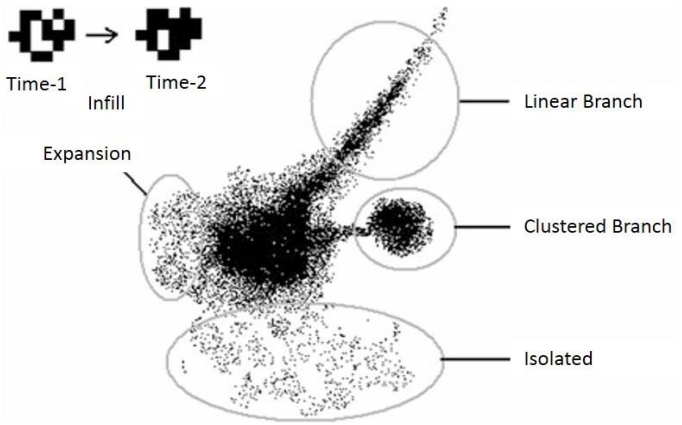

Fig. 5.8: Schematic diagram of urban growth pattern (Source: Bhatta, 2010)

In addition, Angel, et al. (2010) provided an "Atlas of Urban Expansion", in which, besides area metrics and measurements of urban density, five metrics were used to quantify different aspects of urban fragmentation such as openness, city footprint ratio, infill, extension, and leapfrog. All indices have been calculated based on a digital cartography at 30 meters of spatial resolution, derived from classifying Landsat imagery (as is for our study). The spatial configuration of the pixels in particular is examined depending on a circle of 1 square kilometre around each built-up pixel, also known as the walking distance.

Similarly, the internal variations of urban patch type have been quantified here by measuring the local structure, i.e. around each built-up pixel, depending on a given set of spatial indices. Specifically, local patterns are analysed based on a popular approach, which is called the "moving window" (McGarigal and Marks, 1995; Martinuzzi, et al., 2007; Angel, et al., 2010; Bhatta, 2012), i.e. the spatial behaviour of metrics is observed depending on an area (of specified shape and size) surrounding each pixel, which, in our case, is fixed to a square window of 210 meters (a 7x7 array of pixels of 30 meters).

Therefore, each pixel's neighbourhood is examined by passing such a moving window over every positively valued cell in the grid, and across the entire landscape. The value of the class metric, calculated depending on all the pixels in each window (as shown in figure 5.9), is returned to the focal cell.

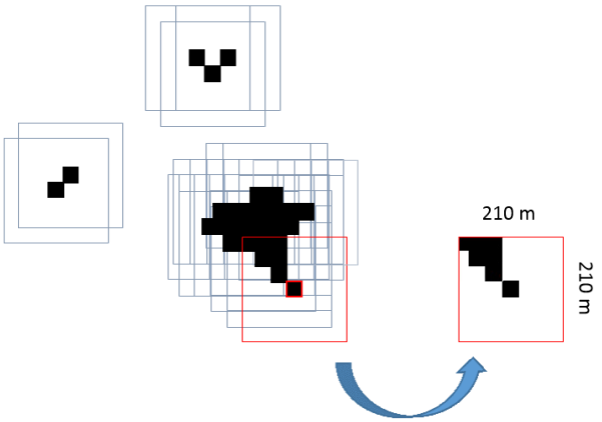

Fig. 5.9: Example of the "moving window" approach for computing spatial metrics at cell level (local structure), and with a square window of 210 meters (Source: By Authors)

However, it is critical to take into account that, as argued by Bhatta (2012), this kind of measurement is *highly dependent on the size of the window and there is no standard rule to define the window size. Further to this, it is influenced by the spatial resolution of the image data and can give varying results*[365]. It means that the results of the analysis should be strictly associated with the resolution of the employed imagery, and therefore to the most appropriate relative operational scale.

Regarding the choice of the window size, which was fixed at 210 meters; firstly, because it was consistent with the approach provided by the N.U.R.E.C.[366] that, in the framework of the "Atlas of Agglomerations in the European Union", published in 1994 and based on Landsat 7 ETM+ imagery, suggested a morphological method to delineate urban continuous areas based on a threshold distance of 200 meters between built-up polygons, intended as the maximum allowable distance within which urbanization can be assumed as a continuum. Here, it is 210 in order to maintain consistency with the pixel size, i.e. we used a distance multiple of 30.

In addition, an empirical examination of the behaviour of several metrics has been undertaken according to different moving window sizes. In our opinion, an array of 7x7 pixels has provided the most reasonable results, at this scale of analysis and with such a spatial resolution. Indeed, this way the moving window is neither too small, thus blind to certain phenomena, nor so big that metrics would be highly generalized, thus losing the character of local analysis.

The spatial metrics addressed in the previous section (5.2.2) have been computed for each built-up pixel, depending on the square window, and tested through several observations in order to find the most reliable indices able to delineate different urban textures, according to our initial hypothesis (continuous, discontinuous, and scattered).

Consequently, four indices have been estimated to be the most consistent with the objective of the analysis at this stage, and then employed to explain those aspects of the urban texture mainly related to compactness; such as density, fragmentation, and degree of physical continuity between pixels of the same type. Table 5.1 summarizes index and code, equation, and related range of values, for Covering Index; Area-weighted Mean for the Radius of Gyration; Mean of Contiguity Index; and the Effective Mesh Size.

[365] *For example, using remote sensing imagery with a spatial resolution of 60 m makes it more likely that small clusters of homogeneous classes will be classified as isolated cells; in comparison, measurement from 30 m resolution image likely appears more scattered. On the other hand, aggregation (resampling) from 30 to 60 m resolution will also cause the pattern at the patch level to become simplified with fewer edges and a higher area-to-perimeter ratio, revealing a more compact urban pattern* (Bhatta, 2012).

[366] Network on Urban Research in the European Community.

SPATIAL INDEX	CODE	EQUATION	VALUES RANGE
Covering Index [5.7]	**CI**	$\frac{\sum_{i=1}^{n} a_i}{A} * 100$	0 < CI ≤ 100
Area-weighted Mean Radius of Gyration [5.8] - Area-weighted Mean (**AM**) -	**GYRATE** (AM)	$\sum_{i=1}^{z} \frac{h_{ir}}{z}$	GYRATE ≥ 0, without limit.
Mean Contiguity Index [5.14] - Mean (**MN**) -	**CONTIG** (MN)	$\frac{\sum_{r=1}^{n} c_{ir}}{a_i *} - 1$ / $v - 1$	0 ≤ CONTIG ≤ 1
Effective Mesh Size [5.18]	**MESH**	$\frac{\sum_{i=1}^{n} a_i^2}{A} * (\frac{1}{10{\cdot}000})$	cell size ≤ MESH ≤ total area of the window

Where: A = Total area of patch type (class)
a_i = Area of patch *i*
h_{ir} = distance between cell *ir* (within patch *i*) and the centroid of patch *i* (the average location)
z = number of cells in patch *i*
c_{ir} = contiguity value for pixel *r* in patch *i*
a_i* = area of patch *i* in terms of number of cells
v = sum of values in a 3-by-3 cell template

Tab. 5.1: Summary of metrics selected for analysis/measurement, and classification, of urban textures at cell level (Source: By Authors; based on FRAGSTATS metrics as provided by McGarigal and Marks, 1995)

Image 5.10 shows a comparison between the spatial behaviour of the indices, for ten hypothetical samples of sets of pixels distributed within a square windows of 210 meters around a focal pixel. High values in each index signify local structures that tend to compactness, where model *C* is the most compact. On the other hand, as values decrease, local structures become more fragmented and/or pixels are less connected among them. In the case of model *D*, for instance, which shows relatively high values for GYRATE and CONTIG, the MESH and CI specify that even though the structure is continuous and quite spread along the window, the model is not as compact as *C*. On the other hand, CONTIG of *D* is lower than CONTIG for *B*, although GYRATE and CI of *D* are higher than *B*, which signifies a greater magnitude of structure *D*, with respect to *B*, but less contiguity among pixels of *D*. The lowest values are provided by structures *A*, *I*, and *L*, which signify low levels of compactness.

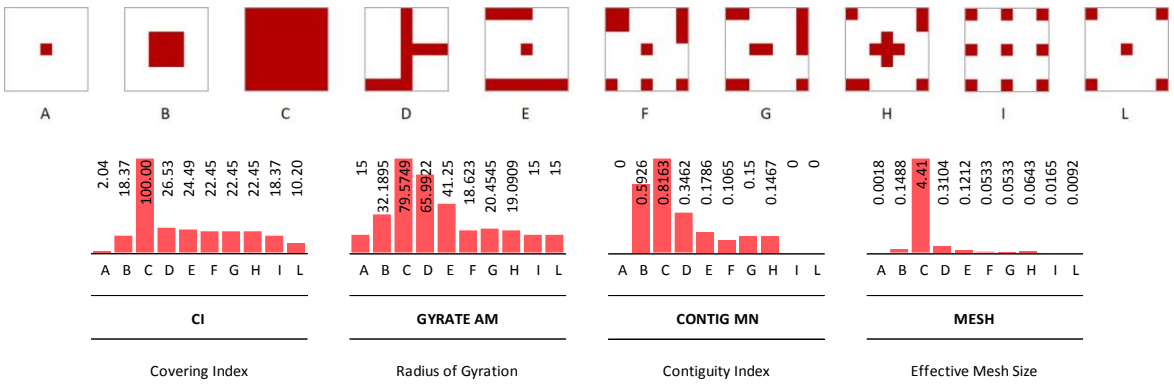

Fig. 5.10: (upper side) Ten hypothetical spatial patterns of pixels within a square window of 210 m around a focal pixel; (lower side) Covering Index, Radius of Gyration, Contiguity, and Effective Mesh Size, for the different patterns (Source: By Authors)

For all of the Autonomous Communities along the Spanish Mediterranean coast, the selected spatial metrics have been calculated for every built-up pixel within the whole urban land cover, here termed "artificial areas" according to the level I of our nomenclature (section 4.5.2), as detected by applying the methodology of remote sensing, provided in chapter 4.

Once pixel values were obtained for each of the indices, they were then categorized into three groups depending on a percentage threshold, i.e. up to the 50% for the lowest values, between 51% and 75% for middle

values, and greater than 75% for high values of indices. An example of the results, after applying CI, GYRATE, CONTIG, and MESH at the artificial area around the city of Terrassa, in Catalonia, is provided in Figure 5.11.

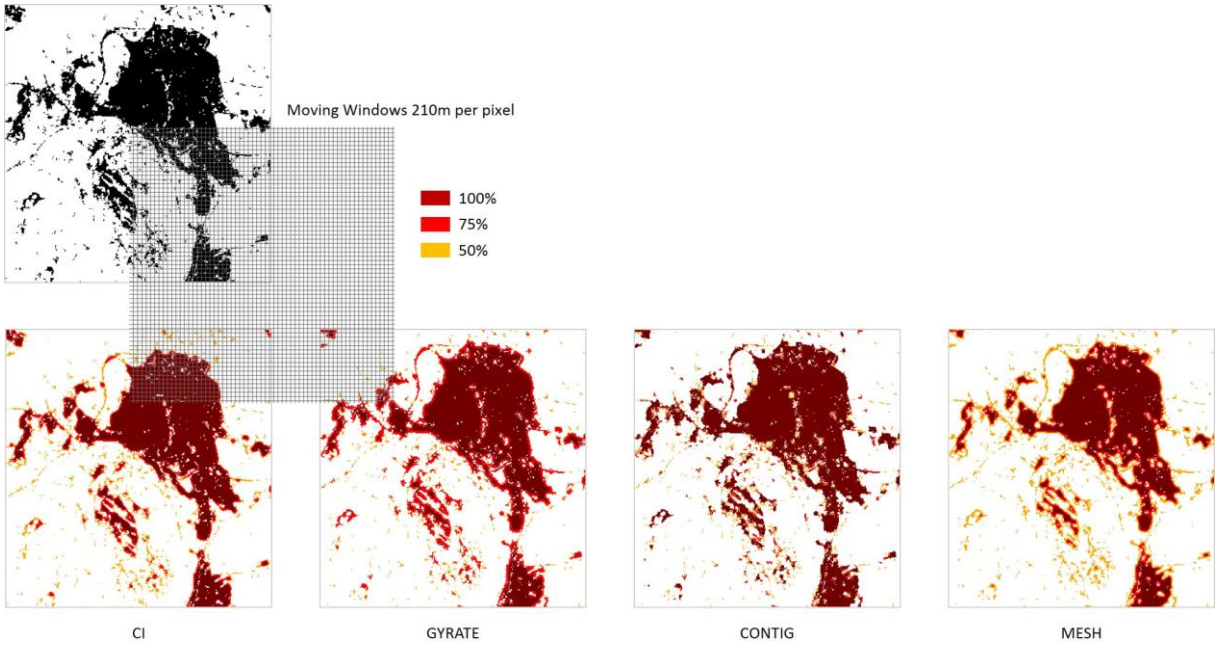

Fig. 5.11: Examples of Covering Index, Radius of Gyration, Contiguity, and Effective Mesh Size, at each built-up pixel depending on a moving window approach for the case of Terrassa, in Catalonia (Source: By Authors)

In order to obtain a synthetic index of compactness for the urban texture, all indices have been first normalized[367] according to a common scale of values that ranges between 0 and 1, and then combined by undertaking a multivariate principal components transformation, based on the covariance matrix and an orthogonal rotation for maximizing the data variance. Such a process defines the most representative common axis for the variables system, which could be identified as our compactness index, and that explains the 93.83% of the total variance of the model.

A filter of spatial correlation is applied to the synthetic index of compactness by calculating the median value among all pixels encompassed within a square buffer of about 1˙000 meters around a focal pixel. Actually, the buffer is an array of 33x33 pixel of 30 meters, i.e. 990x990 meters, in order to keep the consistency with the spatial resolution of input imagery. Such a dimension of the buffer is based on the popular "walking distance" also used by Angel, et al. (2010) for computing metrics of urban fragmentation, such as the openness index.

The effectiveness of the filter consists of reaching a homogenization of values within a given neighbourhood, based on the generalized concept that nearby objects tend to similarity. In addition, it serves to reduce an unsuitable fuzziness of values in the landscape.

Again, a density slice approach is used to quickly classify and visualize the conceptual models of urban texture previously theorized, i.e. continuous, discontinuous, and scattered, dependent on three ranges of values which are, i.e. greater than 75%, between 75 and 51%, and up to 50%, respectively[368], as shown in figure 5.12.

[367] The normalization of each pixel value for a given index is obtained by applying the following equation: $\frac{x_n - x_{min.}}{x_{max.} - x_{min.}}$

[368] The final result of such a classification, as shown in image 5.12, is also reliable for automatically improve the primary land cover classification obtained through applying techniques of remote sensing.

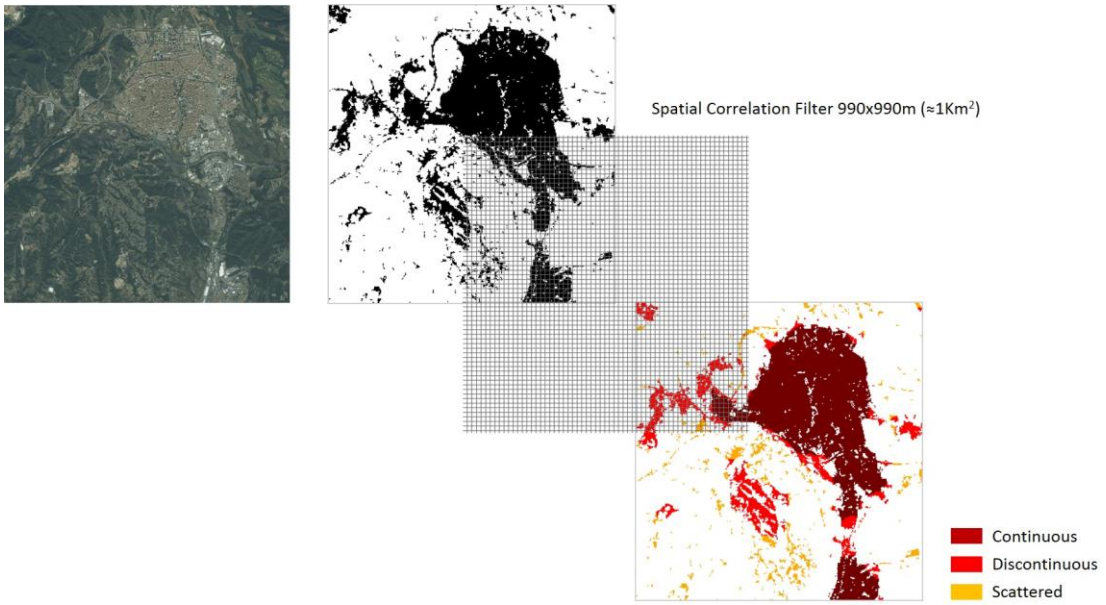

Fig. 5.12: Continuous, Discontinuous, and Scattered texture, classified according to a density slice of the synthetic index of compactness after applying a spatial correlation filter, made from a square buffer of 990x990 meters, around each built-up pixel (Source: By Authors)

5.3.2.2. Measuring the Street Network Morphology: An Approximation

In our opinion, it is quite reasonable to state that a mutual relationship exists in the cities, between urban shapes, measured as the pattern of land occupation of the urban outline, and the morphology of the street network (or urban grid) connected to such outlines. Although geographical constraints also need to be taken into account, in general, *urban shapes affect urban grids by exerting the limitations of where it is possible to extend, while grids affect urban shapes due to growth occurring on outlying streets* (Shpuza, 2007).

The pattern of street networks in a city is highly related to different planning models. For example, if the orthogonal grid structures are common manifestations in planned cities, then *radial organizations and deformed wheels are rather frequent either as stand-alone organizations of street network, or superimposed on infill orthogonal grids*. According to Hillier (1997), the geometric structure of the cities, regardless of dimensions, is often configured as a combination of both orthogonal and radial grids[369], *two of the prime "rationalist" geometric notions by which designers have sought to create ideal cities*. Apart from these two, a further model has to be mentioned, which could be termed as "serpentine", and that basically occurs dependent on *the meandering contour lines in sloped terrains almost parallel to each other* (Shpuza, 2009).

Hence two main questions arise: to what extent do different patterns of street network affect the form of urban profile? And how do we quantify such patterns?

In order to address these questions, at this stage the work focuses on explaining the relationship within morphological features of the urban forms and the spatial configuration of the street network. To do so, we first need to quantify the degree of shape complexity provided by different grid structures within the urban outline,

[369] Two kinds of movements, within the urban grid, have to be taken into account that give rise to the distinctive geometry of the city: *movement from edge to centre (and back again), which is a matter of moving from the peripheral entry points to the city, to a specific destination, and therefore requires an essentially linear form if trip lengths are to be minimised; and movement within urban areas, where the grid must respond not to the need for efficient movement from a specific origin to a specific destination, but the need for efficient movement from all origins to all destinations*. At any rate, although it seems quite clear that the radial structure is generated by the first of these processes, *it is less clear that the 'more or less orthogonal' central grid is generated by the second* (Hillier, 1997).

thus setting up a suitable way to classify the main patterns of street networks. However, the analysis here does not investigate the historical evolution of these models, instead, it focuses on the present situation.

Before taking a step forward, it is appropriate to highlight that, currently, the most popular and effective approach to the analysis of spatial networks is provided by the space syntax, which *originates with the work of a research team led by Bill Hillier at the University of London in the 1970s and 1980s. Hillier's The Social Logic of Space (co-authored with Julienne Hanson) and Space is the Machine, published in 1984 and 1996 (Cambridge University Press) are the seminal references* (Implications, 2006).

Interestingly, the space syntax aims to understand the principles of spatial design both at the urban level, by measuring the connectivity within street networks, as well as at the building level based on the analysis of the internal distribution (connectivity) of the space. At the urban level, the representation of the space relies on a matrix of the "longest and fewest" lines, also known as the axial (or linear) map, and the analysis is made by translating the line matrix into a graph, and using various versions of the 'topological' (i.e. nonmetric) measurement of patterns of line connectivity called "integration" (Hillier and Hanson 1984; Hillier 1996; Hillier, 1999).

Many space syntax studies have addressed the comparative analysis of urban form based on the linear representations of street networks (Shpuza, 2007). However, as argued by Read (1997), space syntax considers neither distance nor direction within the modelling and description of spatial networks, although it doesn't necessarily mean that such variables form no part of the mechanism behind the analysis. *It is quite possible that the sorts of geometries one ordinarily finds in the spatial networks of cities have as a property that - when they are translated into axial maps - have a 'topological distance structure' which correlates with functional patterns in the city*. In actuality, as also argued by Hillier (1999), *far from ignoring geometric and metric properties the 'line-graph' internalises them into the structure of the graph and in doing so allows the graph analysis to pick up the nonlocal*[370]*, or extrinsic, properties of spaces that are critical to the movement dynamics through which a city evolves its essential structures*.

As emphasized by Shpuza (2007), there is little understanding of the effect that morphological features of urban profile, such as shape compactness and/or fragmentation, exert upon the street network configuration and vice versa. Generally, space syntax research on urban environments does not directly address the relationship between settlement shapes and syntactic properties of street networks. Instead, urban grids are mostly considered as independent systems with their own internalized global logic tied to patterns of connectivity between streets (Shpuza, 2007). Here, indeed, the analysis mostly focuses on investigating the formal relationships between the urban outline and the street network pattern. The latter, as is for urban shape, is quantified by using a measurement strictly related to geometrical features of the linear elements that set up the network. In particular, the degree of the formal complexity for each line segment encompassed on two nodes (intersection of lines) is computed according to equation [5.29], which is a ratio between the virtual length and the actual length of the line. The Street Complexity Index ($STREET_{co}$), as formulated here, provides values that range between 0 and 1, where 0 defines a straight line, while the index approaches 1 as a line becomes increasingly convoluted.

$$STREET_{CO} = 1 - \frac{L_v}{L_a} \qquad [5.29]$$

Where: $STREET_{CO}$ = Street Complexity Index
L_a = actual length
L_v = virtual length

Figure 5.13 provides an example of the behaviour of $STREET_{co}$ for three different types of lines, where the black line is the actual length and the red line defines the virtual length. Hence, from left to right, the more convoluted the line, the higher the value of the index. It means that, basically, orthogonal grids of lines tend toward low values of formal complexity; on the other hand, grids of serpentine lines provide high complexity.

[370] *Nonlocal properties are those which are defined by the relation of elements to all others in the system, rather than intrinsic to the element itself* (Hillier, 1999).

In our opinion, such an index provides an interesting approximation to the quick classification of different patterns of street network structures, thus allowing us to investigate the overall kind of relationship (if one exists) between different shapes of urban settlements and different shapes of urban grids.

Fig. 5.13: Sample of the Street Complexity Index ($STREET_{co}$), calculated for three different linear objects (Source: By Authors)

The main strength of the analysis here is that the index of shape complexity of street networks can be applied to automatically classify different patterns of grids at a large scale. Such an approach provides increased statistical reliability for understanding and defining spatial phenomena.

Due to the coarse spatial resolution provided by Landsat satellite imagery, a detailed classification of streets through remote sensing is not practicable. That said, the use of remote sensing for deriving streets through high resolution imagery would be impracticable anyway, if one attempted to do it on a larger scale, because of the multitude of information to be handled.

In order to solve such a question, we have employed here the open and freely accessible information provided by the OpenStreetMap (OSM) project[371], which supplies a database containing, among other information, the road network at global level in a vector format (as two-dimensional linear objects), compatible with the most common GIS platforms. In particular, the OSM is a collaborative world mapping project, started in 2004, with the aim of creating a free editable database[372]. Since 2006, the site has been supported by the OpenStreetMap Foundation, and data is available under the Open Database License.

The establishment and growth of OSM, on the one hand, has been pushed by the increasing need for available geospatial information worldwide, and in several fields. On the other hand, it has been favoured by the growing availability of cheaper portable satellite navigation devices, apart from the recent free availability of a number of satellite data, such as Landsat, among others. Under OSM the *users can freely map any area of the world in a Web 2.0 manner, and the resultant maps become instantly available for free public access across the globe. Users map the world using GPS traces, aerial imagery or their local knowledge. Moreover, the unrestricted use of key-value pairs for tagging all the features provides an excellent means of customized annotations which is an approach suitable for thematic applications* (Pourabdollah, et al., 2013).

Among other uses, the OSM information also supplies useful ancillary data for assessment and enhancement of remotely sensed land cover classifications. All information, which in particular provides data about land use, natural areas, points of interest, railways, waterways, and roads, is recorded into two-dimensional geometric features (points, lines, polygons) and stored according to the Geographic Coordinate System (GCS) and the World Geodetic System 84 (WGS 84). Within the OSM, several road types are codified that vary from motorway, residential, primary, secondary, and tertiary, footway, and cycleway, among others. Due to the coarse scale of analysis employed here, the OSM information about roads has been simplified by keeping just a few types of road, namely living street, pedestrian, residential, and tertiary/residential. In particular, we have focused on those streets strictly related to the urban land cover as detected through remote sensing on Landsat information.

In this way, in addition to the previously mentioned types, further types such as primary, secondary, tertiary and service, have been included only when encompassed within the urban settlement. Indeed, because the interest here is mostly about the relationship between the urban outline and the street network, all external roads

[371] www.openstreetmap.org/

[372] *The success, openness and freedom of OSM has made it a very good examination ground for researchers to study different collaborative mapping characteristics, such as the comparative accuracy and completeness analysis. A statistical comparison of an OSM snapshot in time with official maps was carried within a number of studies*. In particular, the analysis provided by Ather (2009), Kounadi (2009), and Haklay (2010) reveal OSM's relative accuracy and/or completeness. Moreover, it is argued that *by 2010, 29% of England was covered by OSM, and that 80% of the motorways were mapped within 6 meter accuracy compared to Ordnance Survey's dataset* (Pourabdollah, et al., 2013).

have been discarded in order to avoid biased results when summarizing the complexity index at municipal level (or at any other landscape limit).

Image 5.14 shows a sample of the Street Complexity Index calculated for roads in vectorial format (right side), once simplified from the data provided by OSM. Low, middle, and high complexity values are classified according to a density slice approach. In addition, the picture shows the original OSM information (left side)[373].

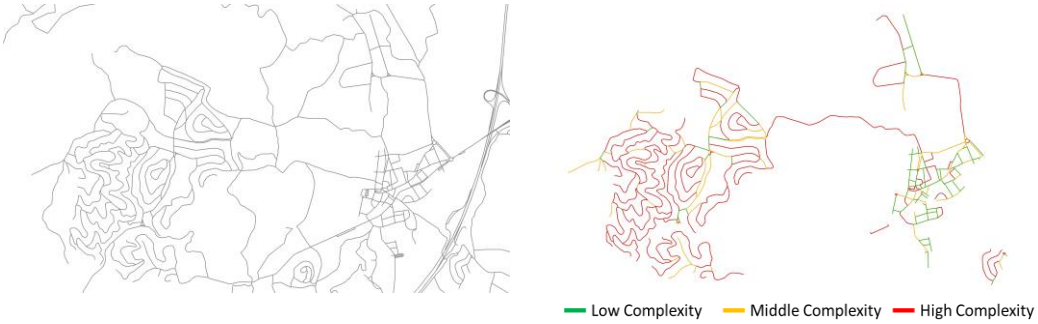

Fig. 5.14: A results sample of the Street Complexity Index (right side); and the original OpenStreetMap information (left side), for the case of Maçanet de la Selva, in Catalonia (Source: By Authors)

A further example of $STREET_{co}$ results is provided in figure 5.15, for the case of Terrassa, consistent with the sample shown in the previous section 5.3.2.1 about the urban texture classification. Again, low, middle, and high complexity values are classified according to a density slice approach. Here, a heuristic examination of the urban grids reveals most clearly two overall patterns of street network. In particular, we find an orthogonal structure, mostly within the consolidated city, generally due to the typical enlargements that occurred during the nineteenth or early twentieth century. This model provides low values of grid complexity, since the strong relation between urban blocks and roads defines regular geometries and provides more connectivity and compactness; although often patches of grids with different orientations are placed next to each other (Shpuza, 2009), due to different historical stages. Likewise, the most contemporary neighbourhoods outside the consolidated city, i.e. the suburbs that arose during the second half of the twentieth century, are often configured in the typical serpentine structure, thus providing less connectivity and less urban compactness.

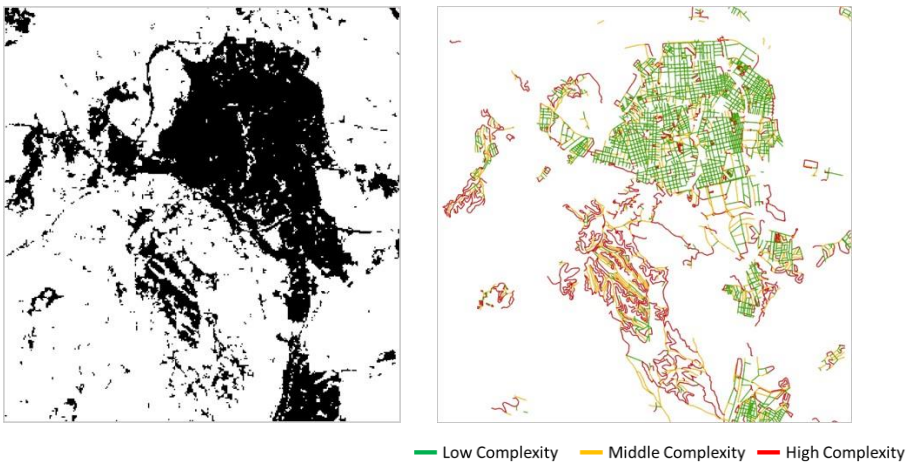

Fig. 5.15: A results sample of the Street Complexity Index ($STREET_{co}$), for the case of Terrassa, in Catalonia (Source: By Authors)

[373] The geographical area under consideration is part of the municipality of Maçanet de la Selva, situated in Catalonia.

5.3.2.3. Urban "voids": Meaning and Detection

Before proceeding with the morphological analysis of the urban profile, also defined as urban agglomeration here, a critical question should be addressed concerning the empty spaces or urban "voids" encompassed within the urban extent. Indeed, the concept of urban extent in a broad sense encompasses not only areas that, in terms of land-use, are really urban such as the residential or industrial uses, but also the in-between lands that, despite being neither impervious nor directly devoted to urban uses such as those previously mentioned, actually form part of the urban environment. We refer to urban green areas, for instance, or other (natural) empty spaces in general, completely surrounded by urbanization, awaiting planning.

When applying morphological metrics, such as those used for this thesis, the variation of areas and the perimeter of the urban profile affect the results of indices and also the interpretation of phenomenon under investigation. This happens for the shape indices, as well as for the index of fragmentation calculated as an area distribution function.

For example, consider the two hypothetical urban configurations *A* and *B* depicted in figure 5.16.

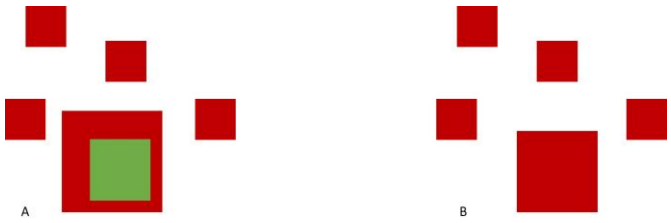

Fig. 5.16: Theoretical models of spatial configuration for two sets of patches *A* and *B*, where *A* is formed by two different patch types while *B* is homogeneous (Source: By Authors)

If we remove the green area from pattern *A*, then both patterns provide the same land cover in terms of area. In such a situation the fragmentation indices of SPLIT or DIVISION, for instance, will provide the same results. On the contrary, the shape indices will vary because the amount of perimeter increases for model *A* due to the hole, thus providing higher shape fragmentation (or less compactness). Indeed, the compactness index [5.9] is about 0.098 for model *A*, and around 0.17 for model *B*. However, if model *A* is calculated without considering the hole, the area of model *A* is greater than *B*, hence SPLIT and DIVISION both increase for model *B* providing, respectively, 2.44 for A and 3.20 for *B*, and 0.59 for A and 0.688 for *B*. This signifies that model *B* now becomes more fragmented than *A*, because such indices are intrinsically weighted for the area distribution among patches (i.e. as the area of one patch increases over the others, fragmentation decreases). Instead, the shape indices now indicate more compactness of *A* with respect to *B*, being that the compactness index is 0.19 for *A* and 0.17 for *B*. Moreover, if the spatial position of the patches does not vary from one model to the other, e.g. the centroids of the patches for both models have the same spatial position. The compactness index is also correlated with the decrease of the average distance between patches, and thus is coherent with the concept of compactness (i.e. the patches are closer to each other).

At this point a doubt arises regarding the most effective approach for computing morphological indices. In other words, is it more reliable to include the holes within the urban profile into the equations or not? The issue is quite speculative. Some studies consider the degree of infill as an index of compactness (Angel, et al., 2010), which is quite reasonable from the urbanistic standpoint. On the other hand, a difference between planned open spaces, e.g. urban parks, and unplanned areas, should be taken into account because the latter category, although urban, presumes discontinuities within the urban outline and the former does not.

A key example here could be the park of Montjuïc in Barcelona, which covers an approximate area of 350 hectares, including the cemetery and all other infrastructures. However, further significant examples can be found around the world; such as the case of Hyde Park in London (about 140 hectares), Tiergarten in Berlin (about 210 hectares), or Central Park in New York (around 341 hectares). In such cases, considering these areas as voids would provide biased values for urban fragmentation and dispersion.

Unfortunately, one common occurrence when one classifies according to a pixel-based approach upon a coarse spatial and spectral information, is that uses cannot be identified well and green areas within the urban

environment reflect similarly to other general areas of vegetation. In fact, a bright vegetation often provides similar values either for evergreen forest, croplands, or urban parks. In the same way, due to the use of the Digital Terrain Model in the classification phase, evergreen forest and croplands can be better separated based on slope; urban green areas cannot be detected based on pixel reflectance[374].

Therefore, based on the use of GIS, a quick automatic method is provided here for reclassifying urban open spaces depending on spatial features and dimensions. Indeed, this is a specific case of GIS and RS integration, which relies on the use of GIS for rectifying the primary results of classification obtained by applying a pixel-based procedure. In particular, GIS is used for handling RS data, for identifying and separating into a further land cover class those patches completely enclosed within urban areas, but not classified according to the urban uses foreseen by the level I of the nomenclature (i.e. artificial areas).

At this point, land cover classification is set up as a binary map, thus providing only two classes, i.e. urban and non-urban polygons (or patches), and two main features are taken into account, which are: patch size (in hectares), and the spatial position of non-urban patches with respect to the urban outline.

Hence, based on empirical assumptions, and according to reasonable speculation about the dimensions of urban parks (see the cases of Barcelona, Berlin, New York, and London as mentioned above), a threshold of 350 hectares, as the maximum allowable area, has been fixed to identify all of those polygons that are potential candidates for urban open spaces. In reality, two thresholds have been identified, i.e. up to 10 hectares (somehow empirical as well), for which all polygons enveloped by urban areas are assumed to be urban open spaces, independent of their spatial position. On the other hand, polygons among 10 and 350 *ha* are assumed to be urban open spaces only if at a distance greater than 100 meters from other (greater) non-urban polygons larger than 350 hectares. Currently, the distance of 100 meters is used to avoid cases in which a narrow strip of urban land, e.g. a highway, separates a great peripheral of undeveloped open space into two smaller parts, thus forcing one of the parts to lie in the urban profile, even if at the margins.

Once such cases are discarded, all non-urban polygons smaller than 350 hectares and completely surrounded by urban areas have been selected as urban open spaces, as depicted in figure 5.17. No further separation is made here between those open spaces that effectively provide urban functions and others that generate urban discontinuities, due to the low spatial and spectral resolution of imagery and for the objective of handling wide geographical areas. At any rate, an infill index (not treated here) could compensate for such a limit by providing an extra variable.

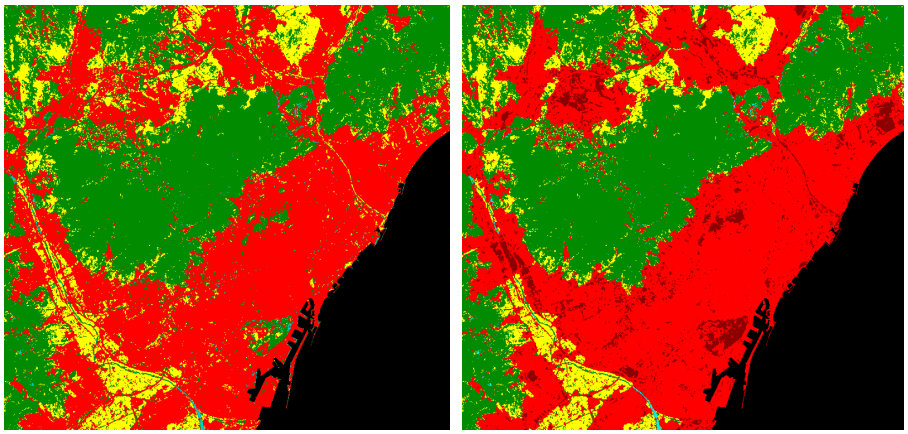

Fig. 5.17: The pixel-based primary classification (left side); and the post-classification process in GIS to obtain an enhanced classification (right side) by separating urban open spaces based on spatial features (Source: By Authors)

[374] Similarly, when classifying based on a pixel-based approach, a critical occurrence is the "misclassification" of golf courses, which often get classified as croplands, due to high reflectance in green and NIR bands. Although an interesting debate should be undertaken about how to consider a golf course, i.e. whether as an artificial or natural area; at any rate, specific research should be undertaken on possible methods of classification (such as the object-based approach) useful for separating golf courses as an additional category. Due to the fact that our analysis is strictly focused on artificial areas, or impervious areas, we have decided to keep off the study of this particular issue, in anticipation of future research.

5.3.2.4. Form and Structure of the Urban Agglomeration: A Generalization at Municipal Level

In the last century, the debate over urban form has generated enormous interest among spatial analysts and planners. In particular, it has focused on the contrast between the "sprawl", often seen as the typical urban model of modern developments in the United States, and the compact urban forms, which are mostly seen in European cities. However, in reality, the European urban model, has experienced an important change in direction since the second half of the last century, at least in some territories. In this respect, several approaches to the measurement of urban forms have been developed to improve the monitoring of urban developments.

Without a doubt, a key approach is the use of quantitative methods, which emerged to aid in more systematic classification and analysis, and which allows us to calculate spatial metrics for capturing several dimensions of urban form. For instance, as highlighted by Huang, et al. (2007), *Torrens and Marina (2000) distinguished varieties of urban form by indicators for density, scatter, leapfrogging, interspersion, and accessibility. Galster et al. (2001) captured eight dimensions of sprawl: density, continuity, concentration, clustering, centrality, nuclearity, mixed uses, and proximity. Ewing et al. (2002) created a sprawl index based on four factors (i.e. residential density, neighbourhood mix, activity strength and accessibility) for US cities. Tsai (2005) employed four quantitative variables (i.e. metropolitan size, activity intensity, distribution degree and clustering extent) to differentiate compactness from sprawl. Others, such as Longley and Mesev, 2000; Filion and Hammond, 2003; Song and Knaap, 2004, employed multi-dimensional indicators to measure compactness within specific neighbourhoods or cities*. For this, Remote Sensing and GIS have provided the best data and tools for analysing urban forms based on spatial metrics. Indeed, *satellite images offer an unprecedented opportunity to develop the more precise comparative indicators that are necessary* (Huang, et al., 2007).

A quantitative approach is also used here in order to set up a model capable of discriminating between different spatial patterns of urban agglomerations, from the morphological standpoint. Actually, if we consider an urban agglomeration as a system of several urban polygons (or patches), then the size, form, and the spatial position of each patch, within the system, defines the physical attributes of such agglomerations. At any rate, the issue of urban morphology requires a critical approach when one attempts to measure the degree of dispersion or, conversely, the compactness of the urban structure. Indeed, we could clearly distinguish some key dimensions of urban morphology mainly according to the form of the profile that an urbanization draws in a territory; the structure in terms of mono-nuclearity/poly-nuclearity, i.e. the number of polygons that make up the urban settlement, in addition to the dimension of each polygon; and the dispersion of the urban system, i.e. the relationship, in terms of the distance, between the patches.

Our assumption is that at least three conceptual dimensions, as depicted in figure 5.18, need to be taken into account when one attempts to explain the form of urban agglomerations. In fact, the morphology of an urban agglomeration can certainly be measured depending on:

I). Fragmentation, which means how many patches make up the agglomeration, and what is the weight of each patch in terms of area;

II). Convolution of the urban outline, or shape fragmentation, i.e. the overall complexity of the urban boundary;

III). Dispersion, i.e. the degree of spread over the landscape, in terms of distance between the patches that make up the agglomeration.

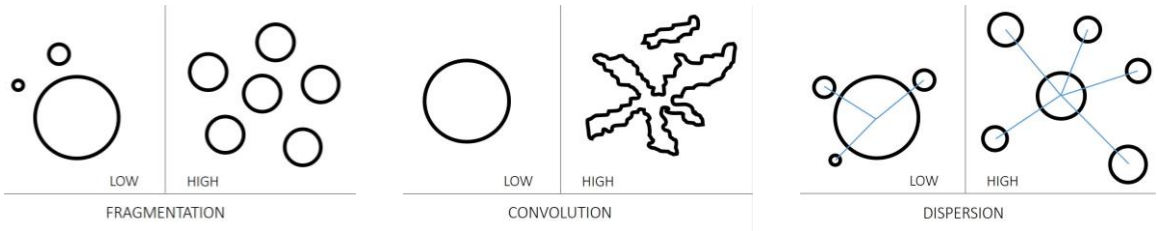

Fig. 5.18: Main conceptual dimensions for defining the morphology of urban agglomerations: Fragmentation, Convolution, and Dispersion (Source: By Authors)

Measuring the urban profile is a fundamental aspect in the analysis of morphological models, but not the only one. In fact, a more exhaustive characterization mostly depends on the relationships that exist between urban profile, urban texture, and street network, which are three factors that mutually affect each other. Consistent with such a statement, Image 5.19 provides a quick comparison between these features, although we will prove it later. Even if the urban profile here is measured based only on the most popular shape index, a relationship is clearly visible, either directly or inversely.

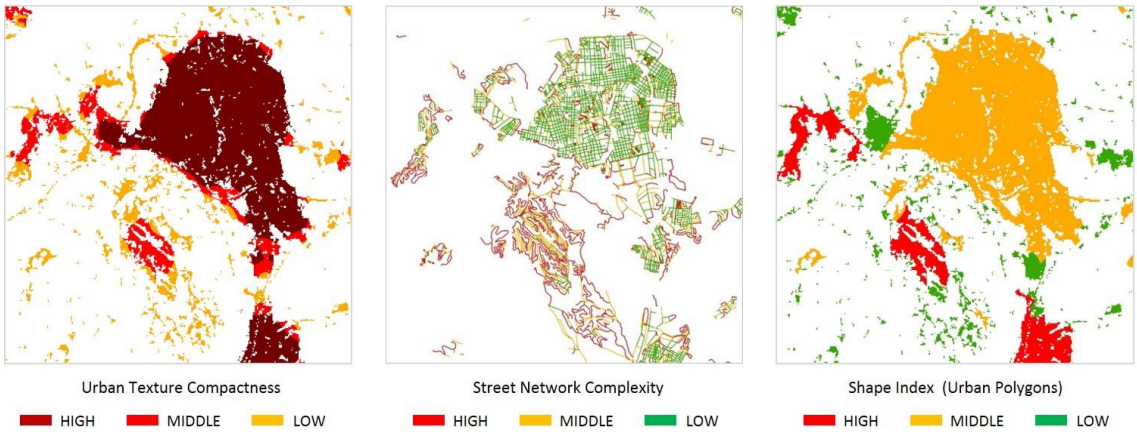

Fig. 5.19: Sample of the urban texture compactness; the street network complexity; and the degree of urban convolution, based on the basic shape index: a visual comparison for the area around the city of Terrassa (Catalonia) (Source: By Authors)

However, as argued in section 5.3.1, we have to face a fairly controversial question when attempting the quantitative analysis of the urban profile, i.e. what is the most suitable geographical ambit to which the spatial metrics have to be referred? As previously stated, several approaches exist, but beyond the criticism regarding the "best choice", we considered here the administrative ambit of municipalities as the space of measurements for a few practical reasons. First of all, there is not yet an international standard or a widely accepted methodology regarding the definition of urban space based on physical criteria. Consequently, there is no standard way to link the census data to a physical division of the urban landscape. Despite several efforts made to identify "real" urban boundaries, the administrative units used to define socio-economic data commonly do not coincide precisely with any physical boundaries. Therefore, one suitable solution to such a question could be the aggregation of administrative ambits dependent on the physical continuum of urban areas, thus achieving a "supra-municipal" administrative ambit derived from morphological issues. This kind of approach was used by the Network on Urban Research in the European Community (N.U.R.E.C), for delimiting urban agglomerations by using the administrative boundaries of communes as basic units (N.U.R.E.C., 1994).

Secondly, although the clipping of an urban continuum with administrative boundaries could generate a "fake" border in some parts of the urban patch, the effective impact of such an approximation on the overall results of the metrics is not yet clearly measured (further investigation would be required at this point). Instead, from the standpoint of urban management and planning, which is commonly undertaken by municipalities or other administrative entities, the use of certain spatial metrics applied at the level of urban continuum could lead to certain generalizations about the results, which could be inconsistent with the phenomenon at the municipal level. For example, consider cases A, B, and C in figure 5.20, in which the urban area is not physically separated, but case A is formed from two municipalities, case B and C by three municipalities, so that the urban polygon is split into smaller independent patches.

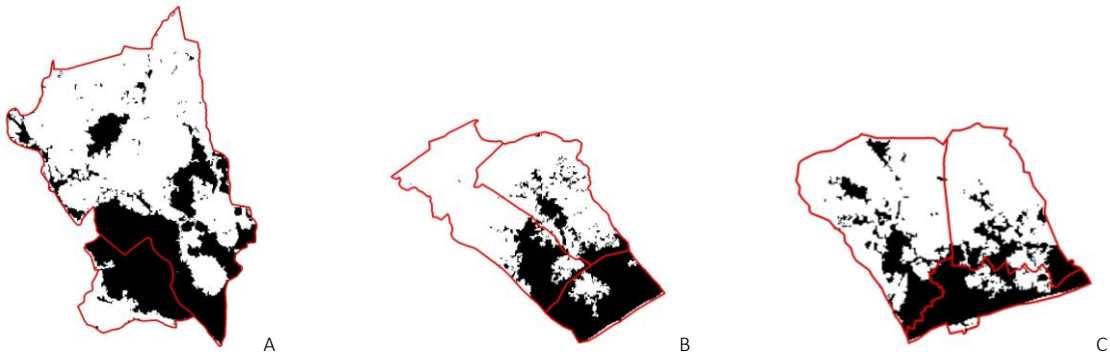

Fig. 5.20: Sample of the interaction between the physical continuum of the urban area, as detected through remote sensing from Landsat TM imagery, and the administrative boundaries for some municipalities in Catalonia (Source: By Authors)

The analysis of the urban profile for the three samples *A*, *B*, and *C*, based on shape metrics, if calculated without considering the administrative division, would give one generalized value for the main patch of each system, even though it is distributed within different municipalities (two or three depending on the case). Hence, the analysis does not consider that different planning procedures have possibly been undertaken. Instead, if we analyse the municipalities separately, at least one of them, in each sample, will provide lower values of shape indices with respect to the others, and this could be consistent with different urban policies.

If we enlarge the geographical window, and take into account the case of the urban continuum of Barcelona, as depicted in figure 5.21, then the issue becomes even more extreme, and the key question is: how representative would the urban shape analysis be for such a physical continuum, with respect to the municipalities that make up this urban area? It probably implies a change of settings and/or metrics in order to define urban phenomena at a different scale and from a different point of view. For the wide analysis undertaken here of the Mediterranean side of Spain and the objective of analysing the urban forms in comparison to certain parameters of land consumption linked to demographic data, we maintain that the simplification of the research at municipal level nonetheless offers a meaningful point of reference and a useful tool for spatial planning at such a scale.

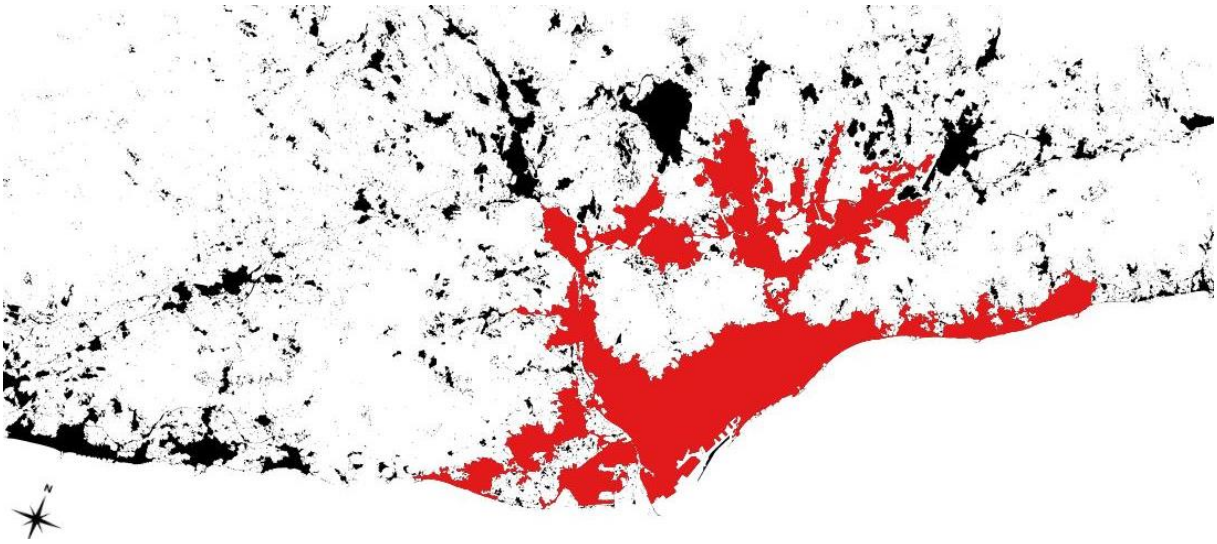

Fig. 5.21: Physical continuum of the urban area around Barcelona, as detected through remote sensing from Landsat TM imagery (Source: By Authors)

Once the spatial limit of urban agglomerations, i.e. the municipality is clarified, a set of 27 spatial metrics of the physical characteristics of urban settlements were selected and computed, among those treated during the previous section 5.2.2. The goal here is to set up a quantitative analysis capable of synthesizing, as best as possible, the three dimensions of the urban form, i.e. fragmentation, convolution, and dispersion, as previously mentioned.

In particular, the quantitative analysis relies on the use of the following indices: Number of patches (NP); Patch Density (PD); Mean and Area weighted Mean Shape Index (SHAPE MN, AM); Mean and Area weighted Mean Compactness Index (Cipq MN, AM); Mean and Area weighted Mean Fractal Dimension (FRAC MN, AM); Mean and Area weighted Mean Circularity index (CIRC MN, AM); Perimeter-Area Fractal Dimension (PAFRAC); Mean, Area weighted Mean Proximity Index (PROX MN, AM); Mean, Area weighted Mean, Coefficient of Variation of Euclidean Nearest Neighbor (ENN MN, AM, CV); Connectivity (CONNECT); Split Index (SPLIT); Division Index (DIVISION); Maximum Entropy (lnN); Shannon's Diversity (SHDI) and Shannon's Evenness (SHEI); Modified Simpson's Diversity (MSIDI), Simpson's Evenness (SIEI), and Modified Simpson's Evenness (MSIEI); Dominance (D); Standard Distance (SD_w).

Certain redundancy could occur when using several indices, and due to the difficulty of interpreting a wide selection of metrics, a factor analysis has been undertaken to synthesize the importance of the spatial metrics into only a few, being the most representative variables concerning the urban form. At this point, the factor analysis has been undertaken for the municipalities of Catalonia, which provides 946 cases. However, due to the coarse resolution of the Landsat TM imagery, some small urban areas have not been detected during the classification phase. The use of panchromatic imagery at 15 meter spatial resolution, as provided by the ETM+ sensor, would possibly allow for a better classification thanks to pansharpened imagery (see section 4.3.3). Of interest, 23 municipalities do not provide urbanized areas, hence the analysis has been undertaken with a final dataset of 920 valid cases.

All metrics have been standardized to standard scores (z-scores) in order to avoid differences in measurement units and weights of the indices. Hence, in order to obtain an effective result, and then for determining the most representative variables within the dataset, communalities and Kaiser-Meyer Olkin (KMO) and Bartlett's test have been taken into account, in addition to the percentage of variance expressed by the factors.

The communalities signify the proportion of variance in the original variables which is expressed by the factor solution, or, in other words, the amount of variance in each of the original variables, expressed by the extracted factors. Mathematically, the communality is the sum of the squared loadings for one variable. To obtain a suitable analysis, the factor solution should express at least half of the original variance of each variable. Therefore, optimal values of each communality should be 0.50 or higher.

The Kaiser-Meyer-Olkin (KMO) is an overall Measurement of Sampling Adequacy (MSA) for the set of variables and it is also assumed to be suitable when it reaches a value of at least 0.50 (or higher). When the overall KMO does not meet the minimum criteria, we might need to take into account the values of sampling adequacy for each individual variable by examining the Anti-Image Correlation Matrix.

The Bartlett's test of Sphericity tests the null hypothesis that the original correlation matrix is an identity matrix, i.e. that all diagonal elements are 1 and all off-diagonal elements are 0, thus this would imply no correlation among the variables. In order to obtain a suitable factor analysis based on the principal components, we need to see some relationship between variables, hence we need this test to be significant by achieving a significance value less than 0.005. Finally, the factor solution is expected to express at least 70/80 percent of variance from the original model.

Based on such indices of suitability, we have repeated the factor analysis several times, and at each iteration the less representative variables have been discarded. In this way, the best factor solution has been reached through the use of a set of ten spatial indices as listed in table 5.2.

SPATIAL INDEX	CODE	EQUATION	VALUES RANGE
Related Circumscribing Circle (1-Digital Compactness Measurement) [5.10] - Area-weighted Mean (**AM**) -	**CIRCLE** (AM)	$1 - \frac{A}{A_{sc}}$	$0 \leq CIRCLE < 1$
Shape Index [5.11] - Mean (**MN**) -	**SHAPE** (MN)	$\frac{p_i}{\min p_i}$	SHAPE ≥ 1, without limit
Fractal Dimension Index [5.12] - Area-weighted Mean (**AM**) -	**FRAC** (AM)	$\frac{2 * \ln(0.25 * p_i)}{\ln a_i}$	$1 \leq FRAC \leq 2$
Landscape Division Index [5.16]	**DIVISION**	$1 - \sum_{i=1}^{n} \left(\frac{a_i}{A}\right)^2$	$0 \leq CIRCLE < 1$
Shannon's Evenness Index [5.22]	**SHEI**	$\frac{-\sum_{i=1}^{n}(P_i * \ln P_i)}{\ln n}$	$0 \leq SHEI \leq 1$
Modified Simpson's Evenness [5.24]	**MSIEI**	$\frac{-\ln \sum_{i=1}^{n} P_i^2}{\ln n}$	$0 \leq MSIEI \leq 1$
Dominance [5.25]	**D**	$\ln n - \left[-\sum_{i=1}^{n}(P_i * \ln P_i)\right]$	$D \geq 0$
Patch Density	**PD**	$\frac{n}{A}$	$PD > 0$
Standard Distance [5.26]	**SD_w**	$\sqrt{\frac{\sum_{i=1}^{n} w_i (x_i - \bar{X}_w)^2}{\sum_{i=1}^{n} w_i} + \frac{\sum_{i=1}^{n} w_i (y_i - \bar{Y}_w)^2}{\sum_{i=1}^{n} w_i}}$	$SD_w \geq 0$
Connectance Index [5.28]	**CONNECT**	$\frac{\sum_{j=k}^{n} c_{ijk}}{\frac{n_i * (n_i - 1)}{2}} * 100$	$0 \leq CONNECT \leq 100$

Where:
- A = Total area of patch type (class)
- A_{sc} = Area of the smallest circumscribing circle
- a_i = Area of patch *i*
- p_i = Perimeter of patch *i*
- $P_i = \frac{a_i}{A}$ = proportion of the patch type (class) occupied by patch *i*
- n = number of patches
- x_i and y_i = Coordinates for feature *i*
- $\bar{X}_w, \bar{Y}_w$ = Weighted mean center for features
- W_i = Weight at feature *i*
- a_{is} = area of patch *is* within specified neighbourhood of patch *i*
- h_{is} = patch edge-to-edge distance between patch *is* and patch *is*
- c_{ik} = joining between patch *j* and *k*

Tab. 5.2: Metrics selected for synthesizing the main morphological dimensions for urban agglomerations, through applying a factor analysis (Source: By Authors; based on FRAGSTATS metrics as provided by McGarigal and Marks, 1995)

The communalities for the final selected metrics are shown in table 5.3, while the overall Kaiser-Meyer-Olkin (KMO) measure of sampling adequacy together with the Bartlett's test are provided in table 5.4. All communalities are greater than 0.60, while the value of the KMO for this set of variables is 0.645, thus signifying that a suitable factor solution is provided. Since the KMO meets the minimum criteria, we left out the examination of the Anti-Image Correlation Matrix.

Moreover, the probability associated with the Bartlett test is < 0.005, which also satisfies the requirements of an appropriate factor analysis. In reality, the value is highly significant thus leading us to reject the null hypothesis because correlations in the data set exist.

Communalities		
	Initial	Extraction
PATCH DENSITY	1.000	0.638
FRAC AM	1.000	0.932
CIRCLE AM	1.000	0.833
CONNECT	1.000	0.754
Shannon EVENNESS	1.000	0.984
Standard DISTANCE	1.000	0.733
SHAPE MM	1.000	0.921
Modified Simpson EVENNESS	1.000	0.948
DOMINANCE	1.000	0.955
DIVISION	1.000	0.903
Extraction Method: Principal Component Analysis.		

Tab. 5.3: Communality values for the final variables employed in the factor analysis (Source: By Authors)

KMO and Bartlett's Test		
Kaiser-Meyer-Olkin Measure of Sampling Adequacy.		0.645
Bartlett's Test of Sphericity	Approx. Chi-Square	13740.882
	df	45
	Sig.	0.000

Tab. 5.4: Kaiser-Meyer-Olkin (KMO) Measure of Sampling Adequacy (MSA), and Bartlett's test (Source: By Authors)

Table 5.5 shows the eigenvalues, the extraction sums of squared loadings, and the rotation sums of squared loadings that was done according to a Varimax rotation. The number of components to consider is chosen based on (a) the eigenvalues associated with each component, and the cumulative proportion of variance expressed by components. In particular, eigenvalues greater than 1.00 are taken into account, hence three components are extracted that express 86% of the total variance of the model, and each component corresponds to one axis in metric space.

Total Variance Explained									
Component	Initial Eigenvalues			Extraction Sums of Squared Loadings			Rotation Sums of Squared Loadings		
	Total	% of Variance	Cumulative %	Total	% of Variance	Cumulative %	Total	% of Variance	Cumulative %
1	**3.818**	**38.184**	**38.184**	**3.818**	**38.184**	**38.184**	**3.682**	**36.818**	**36.818**
2	**3.007**	**30.067**	**68.251**	**3.007**	**30.067**	**68.251**	**3.081**	**30.811**	**67.629**
3	**1.776**	**17.757**	**86.008**	**1.776**	**17.757**	**86.008**	**1.838**	**18.379**	**86.008**
4	.566	5.656	91.664						
5	.386	3.859	95.523						
6	.232	2.317	97.840						
7	.111	1.112	98.953						
8	.081	.812	99.765						
9	.021	.212	99.977						
10	.002	.023	100.000						
Extraction Method: Principal Component Analysis.									

Tab. 5.5: Total variance explained by the factor analysis: eigenvalues, extraction sums of squared loadings, and rotation sums of squared loadings (Source: By Authors)

Finally, table 5.6 provides the component matrix for the rotated solution, according to the Varimax method[375], in which the loadings of the original metrics for each of the extracted factors are displayed. The analysis of the pattern of the factor loadings is the key to interpreting the meaning of the factors and labelling the extracted components, consistent with the input metrics.

The pattern of factor loadings should be also examined to identify variables that have a complex structure, i.e. those variables that have high loadings (0.40 or higher) on more than one component. Generally, this could be a further element to take into account for discarding original metrics but, here, due to few conceptual considerations it has been decided to keep the standard distance index, although it provides a complex structure.

In particular, we labelled component 1 as FRAGMENTATION because, consistent with its factor loadings, this dimension mostly represents the degree of splitting of the urban profile into multiple patches, based on a distribution function of the patch areas. Here, the standard distance provides a factor loading of 0.435 (i.e. a complex structure), but because the standard distance also tends to increase as the number of patches increases, it is reasonable to assume that a small contribution of such a metric to the fragmentation could be conceptually consistent.

Component 2 has been named CONVOLUTION as it basically captures the significance of the shape indices, and expresses either the complexity of the profile or the multiplication of patches. Therefore, the more convoluted the urban profile and the higher the number of patches, the higher the convolution index. The shape index that has provided most significance has been the mean-shape index (SHAPE MN), while the Area-Weighted Mean for CIRCLE and FRAC has resulted in being more significant than the mean simply.

Finally, component 3 has been named DISPERSION as it primarily captures those metrics related to the distance between patches, thus providing a degree of spatial dispersion within a given landscape extent. Actually, the Patch Density (PD) does not directly measure the distance between patches, but by keeping the landscape extent constant, an increase in the number of patches would signify an increase in closeness between patches.

The table also highlights the extraction method, which has been based on the principal component analysis, the rotation method i.e. a Varimax rotation with Kaiser Normalization, and the number of iterations occurred to get the rotated components (tab. 5.6).

Rotated Component Matrix*			
	Component		
	1	2	3
	FRAGMENTATION	CONVOLUTION	DISPERSION
Shannon EVENNESS	0.979	0.154	-0.028
Modified Simpson EVENNESS	0.967	0.034	-0.107
DOMINANCE	-0.895	0.392	0.011
DIVISION	0.866	0.316	0.230
FRAC AM	0.085	0.961	0.030
SHAPE MN	0.028	0.958	-0.047
CIRCLE AM	0.039	0.904	0.121
CONNECT	0.044	0.233	-0.835
Standard DISTANCE	0.435	0.112	0.729
PATCH DENSITY	-0.186	0.278	0.725
Extraction Method: Principal Component Analysis. Rotation Method: Varimax with Kaiser Normalization.			
*. Rotation converged in 4 iterations.			

Tab. 5.6: Rotated component matrix with factor loadings, and component labels (Source: By Authors)

A concrete example of the synthetic indices of fragmentation, convolution, and dispersion (as defined through the factor analysis) is provided in figure 5.22, in which two municipalities for each index have been selected from the urban land cover map of Catalonia, in order to show low and high values of the three main

[375] *To help elucidate the underlying factors, it is a common practice to 'rotate' the selected axes. Both orthogonal and oblique rotations are possible. An orthogonal rotation, such as the Varimax rotation, preserves the relative orientation between axes, but an oblique rotation does not* (Riitters, et al., 1995).

morphological dimensions extracted for measuring the form of the urban agglomeration according to the hypothesis made at the beginning of this section (see previous figure 5.18).

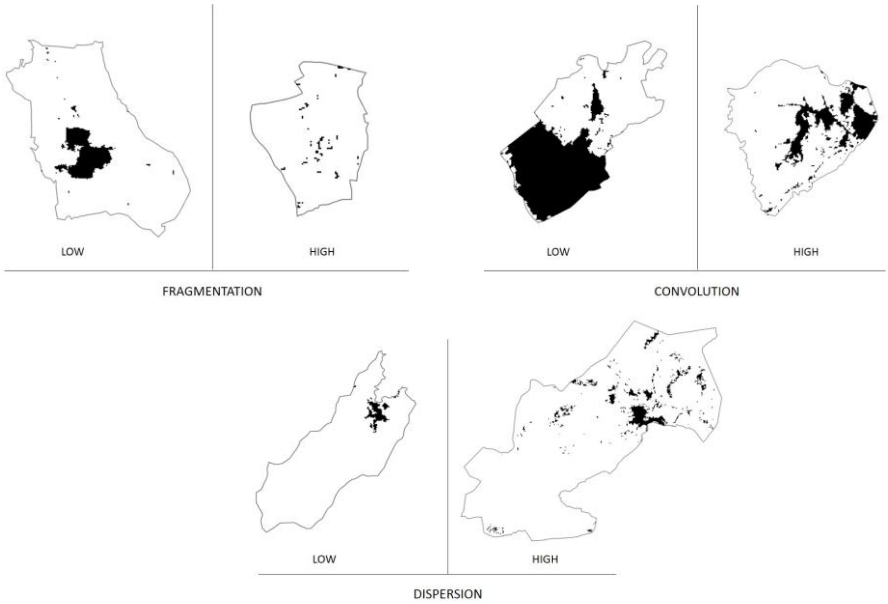

Fig. 5.22: Sample of low and high values for the synthetic indices of fragmentation, convolution, and dispersion (Source: By Authors)

5.3.3. Six Dimensions of Urban Morphology

In tune with other widely recognized investigations that aim to synthesize the main dimensions of the urban phenomenon, such as the eight dimensions of sprawl proposed by Galster (Galster, et al., 2001), or that investigate the interaction between urban shapes and urban grids for discovering robust generic principles that link urban shape properties to properties of street networks (Shpuza, 2007); similarly, the objective at this stage was to find a set of variables able to exhaustively define the main aspects of the urban form (from the morphological standpoint), and investigate the relationship between them. Therefore, in the previous sections we have seen that at least three key aspects need to be taken into account conceptually, which are the urban texture, the street network, and the profile of the urban agglomeration. In addition, we have reported a number of recognized morphological indices (spatial metrics), capable of defining differing aspects of urban morphology, and some statistical approaches that provide useful tools for spatial analysis.

A multivariate factor analysis was used to synthesize the most suitable subset of metrics for monitoring urban landscapes; and we identified a synthetic index for measuring the degree of compactness for urban texture, and three common axes (or dimensions) for measuring the pattern and structure of the urban agglomeration, dependent on the morphological features of the urban profile, and mostly based on area, perimeter, number of parts that make up the urban outline, and distance between them. Moreover, an index of street network complexity has been proposed. Hence, five independent axes of urban pattern and structure have been set up:

- Compactness (urban Texture)
- Street Network Complexity
- Fragmentation (urban settlement)
- Convolution (urban settlement)
- Dispersion (urban settlement)

A correlation analysis between such indices, observed for the municipalities in Catalonia (920 valid cases), is provided in the following images, in which scatter plots are used to show the relative distribution of one index

with respect to another in a two-dimensional Euclidean space. The linear regression between a few indices, the R^2, and the Pearson coefficient of correlation (r), are provided.

In particular, image 5.23 depicts the interaction between the three synthetic indices of fragmentation, convolution, and dispersion of the urban settlement structure, as extracted by applying the factor analysis according to the process argued in the previous section 5.3.2.4.

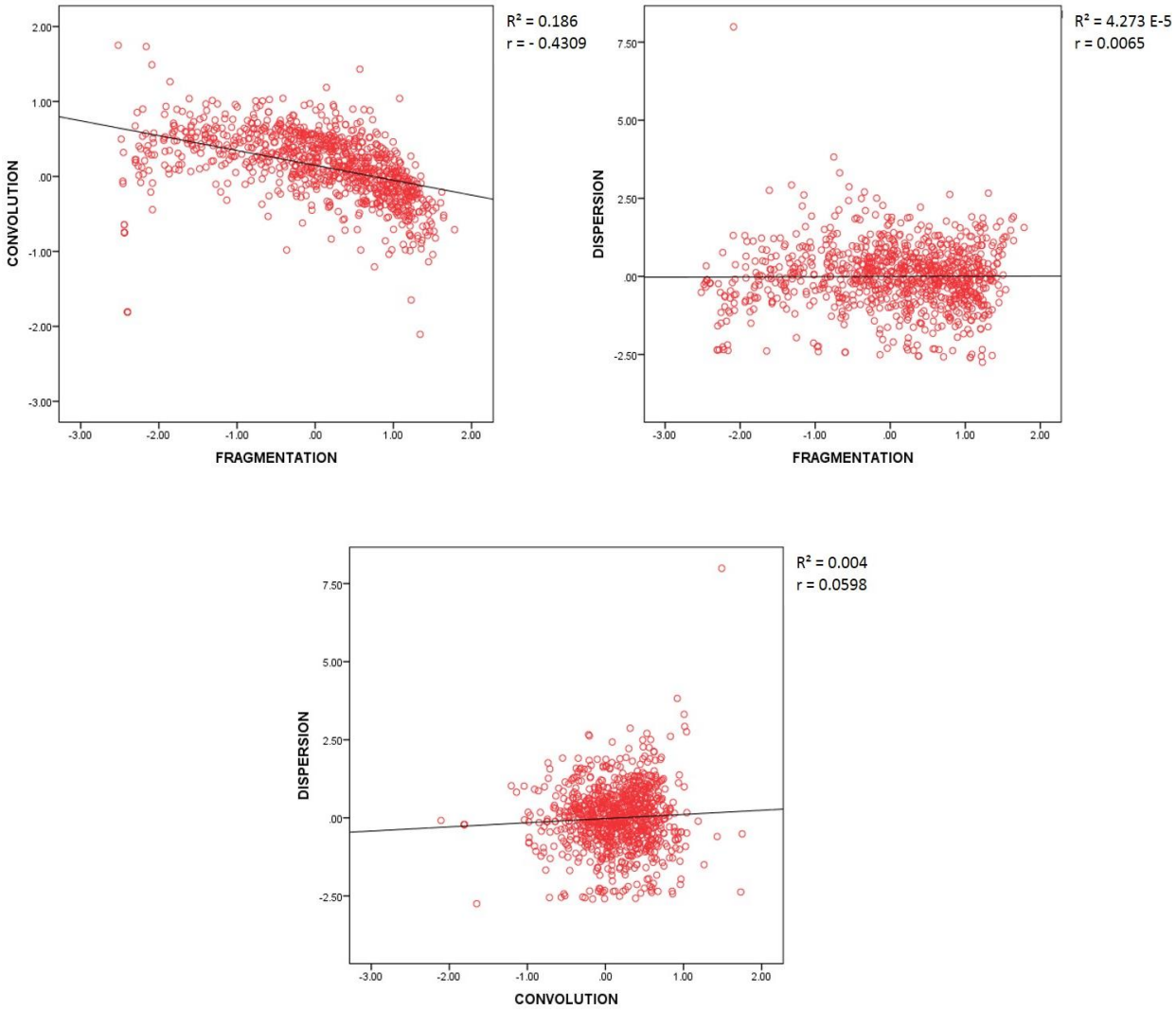

Fig. 5.23: Linear regression analysis and Pearson correlation coefficient (r) between fragmentation, convolution, and dispersion of urban settlement (Source: By Authors)

Consistent with the factor analysis procedure, little or no correlation exists between the indices. Indeed, components were expected to be uncorrelated. Actually, the higher Pearson coefficient occurs between convolution and fragmentation, which provide a value of around -0.43 highlighting a certain small, but negative, correlation. This means that high levels of fragmentation correspond to low values of convolution and vice versa. Although it could appear quite surprising, this probably depends on the fact that the shape metrics of circularity (CIRCLE) and fractal dimensions (FRAC) are weighted for the area of the patch. Therefore, when a large main patch exists within the urban settlement, which provides high values of shape convolution, values of fragmentation are lower because the fragmentation decreases as the dominance, of one or a few patches, increases.

Regarding the correlations between dispersion and fragmentation, and dispersion and convolution, both Pearson coefficients are positive values, which signifies that high dispersion corresponds to high fragmentation and high convolution, which seems quite reasonable. At any rate, this assumption is not really relevant because the correlation coefficients are too low (i.e., around 0.006 for dispersion/fragmentation, and around 0.06 for dispersion/convolution).

Next, images 5.24, 5.25, and 5.26 depict the correlation between settlement shapes (i.e. fragmentation, convolution, and dispersion) and the morphological features of street networks and urban texture.

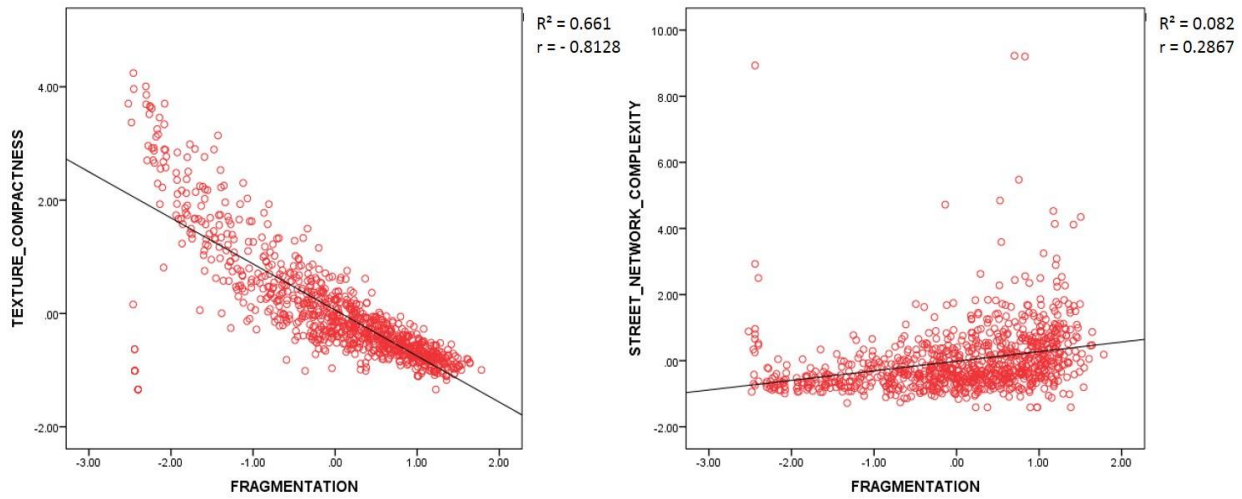

Fig. 5.24: Linear regression analysis and Pearson correlation coefficient (r) between fragmentation and urban texture compactness, and between fragmentation and street network complexity (Source: By Authors)

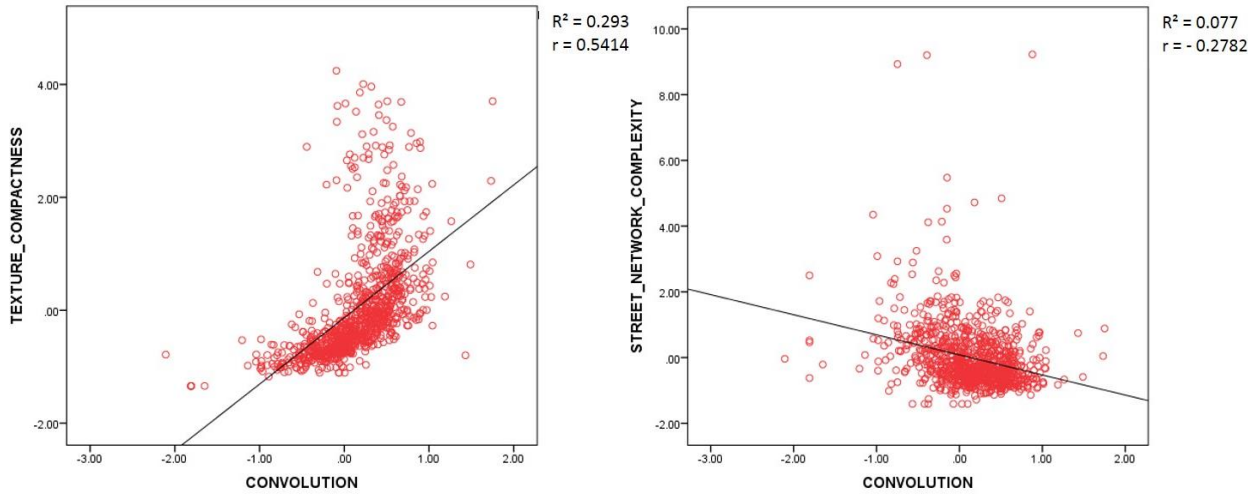

Fig. 5.25: Linear regression analysis and Pearson correlation coefficient (r) between convolution and urban texture compactness, and between convolution and street network complexity (Source: By Authors)

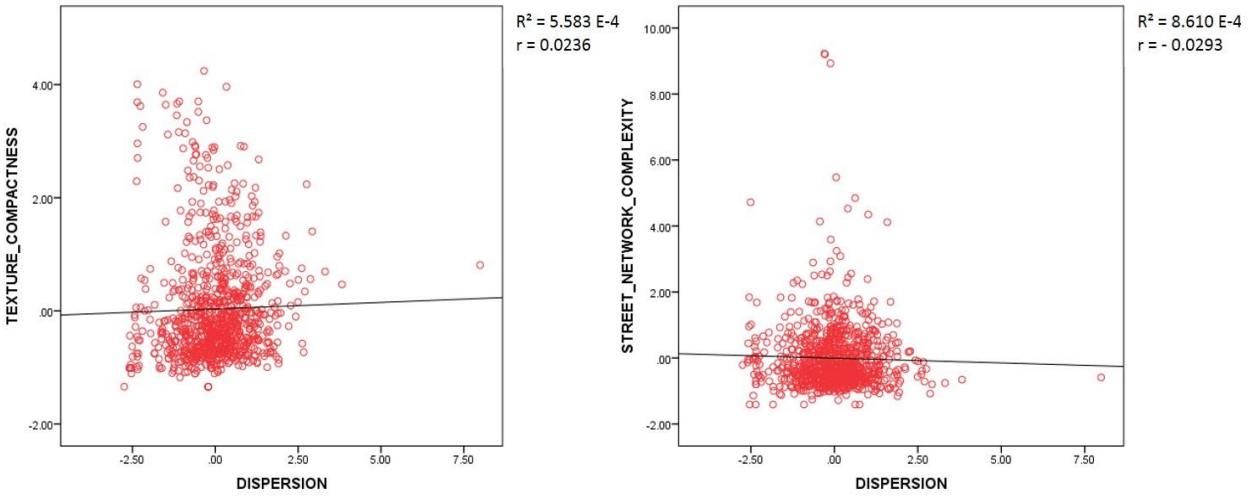

Fig. 5.26: Linear regression analysis and Pearson correlation coefficient (r) between dispersion and urban texture compactness, and between dispersion and street network complexity (Source: By Authors)

The higher correlation here is provided between fragmentation and urban texture, which in particular reaches a value of about -0.81, thus providing a negative correlation. This means that high values of urban settlement fragmentation generally correspond to low values of urban texture compactness and vice versa. On the other hand, little positive correlation of around 0.54 is achieved between convolution and texture compactness. Indeed, as previously discovered, fragmentation and convolution show a negative correlation between them.

Finally, the correlation between urban texture compactness and street network complexity is depicted in figure 5.27, which shows a small negative Pearson coefficient of about -0.31, hence we could possibly say that less compactness of the urban texture could correspond to higher values of street network complexity, and vice versa.

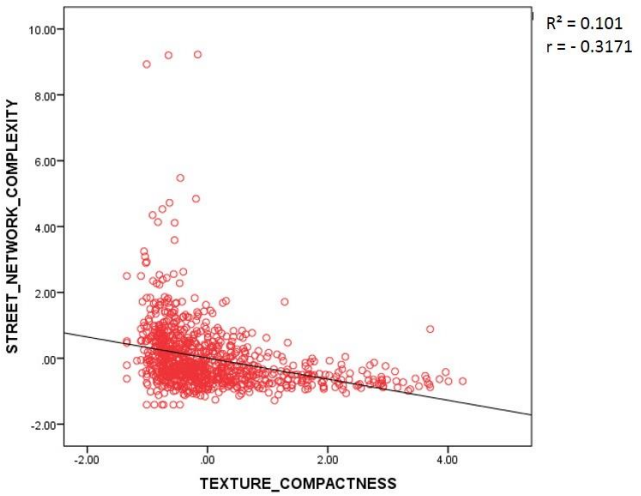

Fig. 5.27: Linear regression analysis and Pearson correlation coefficient (r) between urban texture compactness and street network complexity (Source: By Authors)

Apart from these five morphological dimensions, a further aspect should to be taken into account when one attempts to define the urban form, which is the area of the urban settlement. Indeed, the area is a fundamental measurement of geometry, hence it is relevant for differentiating similar geometries but with

different magnitude. For example, think of two circles, one of them with a radius of 1 and the other with a radius of 50. They are equals in form (i.e. geometrically they are both circumferences), and they have the same circularity index, for instance, but all other parameters such as radius, area, perimeter, are different. Hence, the area also provides a key feature when one is dealing with morphology, and more so if it refers to urban morphology.

Although two cities could theoretically provide similar characteristics with the shape of the profile, or the degree of fragmentation, they cannot be thought of as similar urban structures if greatly different in terms of surface area, due to the important issue of magnitude. Moreover, although the area is used to compute several spatial metrics, no remarkable correlation exists between the urban area and the other morphological dimensions, as shown in Table 5.7, except in the case of texture compactness which provides a positive correlation of about 0.55, i.e. the larger the urban settlement, the higher the compactness of the texture.

		PEARSON COEFFICIENT OF CORRELATION (r)					
	Morphological Dimensions	URBAN AREA	FRAGMENTATION	CONVOLUTION	DISPERSION	TEXTURE COMPACTNESS	STREET COMPLEXITY
1	URBAN AREA	1	- 0.4328	0.2703	0.2691	0.5505	- 0.1643
2	FRAGMENTATION	- 0.4328	1	- 0.4309	0.0065	- 0.8128	0.2867
3	CONVOLUTION	0.2703	- 0.4309	1	0.0598	0.5414	- 0.2782
4	DISPERSION	0.2691	0.0065	0.0598	1	0.0236	- 0.0293
5	TEXTURE COMPACTNESS	0.5505	- 0.8128	0.5414	0.0236	1	- 0.3171
6	STREET COMPLEXITY	- 0.1643	0.2867	- 0.2782	- 0.0293	- 0.3171	1

Tab. 5.7: The Pearson coefficient of correlation between the six dimensions of urban morphology: urban area, fragmentation, convolution, dispersion, urban texture compactness, and street network complexity (Source: By Authors)

Figure 5.28 depicts, in the case of Catalonia, the spatial distribution of the values for the six morphological dimension of the urban form, where red shades provide high values for each of the indexes. The reading of the indices shows a certain similarity of values along the coast and around the city of Barcelona.

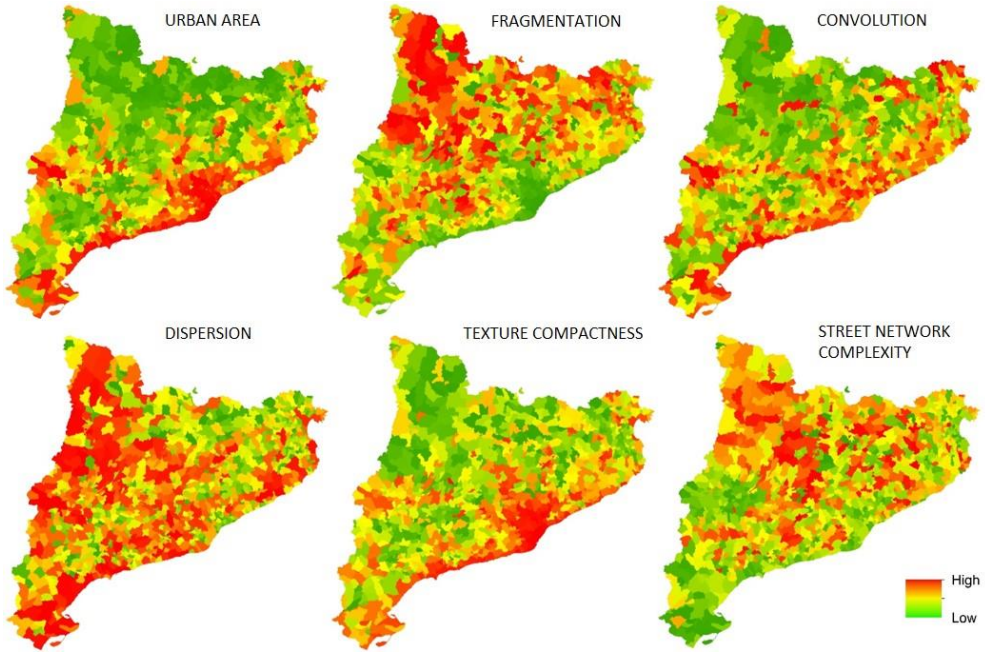

Fig. 5.28: Spatial distribution, for the case of Catalonia, of the six urban morphological dimensions, i.e. the urban area, fragmentation, convolution, dispersion, texture compactness, and street network complexity (Source: By Authors)

5.3.4. Morphological Models: Classification and Analysis of the Urban Forms

Urban form is one of the main characteristics of urban areas which affect its sustainability. It has a bearing on the size of the ecological footprint of the city, degree of soil sealing, transport (length of trips and modal split), air pollution, social segregation, etc. Although there have been and still are debates on to which degree compact urban form is more sustainable than a fragmented and sprawling city (Williams, 2000), *there is a relatively wide consensus among planners and researchers that compactness is desirable from the point of view of sustainable development* (Newton, 2000; Kasanko, et al., 2007).

A key achievement of measuring and classifying urban forms is concerned with the study of the urban sprawl phenomenon, without a doubt one of the main issues debated in the last decades, within the field of the spatial planning. Galster et al. (2001) considered urban sprawl to be both a pattern of urban land use, as well as a process, namely, as the change in the spatial structure of cities over time[376] (Bhatta, 2012). In any case, different degrees of sprawl will affect the final pattern of the physical urban structure. Therefore, although urban sprawl is doubtlessly a wider phenomenon that affects several aspects of urban development, the form is a key variable to understand urban sprawl. For instance, according to Angel, et al. (2010), *it is possible to measure different phenomena of urban growth, over time, through three discrete attributes of urban spatial structure, such as density, as the average population density of the built-up area; fragmentation, calculated as the amount of open space in and around cities that is fragmented by their built-up areas; and urban land cover, as the total land area occupied by cities*[377].

Based on the six dimensions of urban morphology, as defined in the previous section, we now aim to classify different patterns of urban land cover. This will be ranging from more compact, complex models to more fragmented and dispersed ones, and which are dependent on similar behaviour in terms of composition and configuration of the urban profile, degree of compactness of the urban texture, and complexity of the street network. In particular, we expect to find some morphological models able to represent the most relevant aspects of the urban form, by applying an automated process of classification.

The cluster analysis was used here in order to extract homogeneous patterns of urban form for the municipalities within the entire region of Catalonia. A combination of hierarchical and K-Means cluster methods were used for maximizing the effectiveness of the results. First, a hierarchical cluster analysis was used to estimate the most appropriate number of clusters; then a K-Means cluster analysis, based on the previous defined number of groups, was executed to obtain the final classification. *The K-Means method had the advantage that it enabled the group centres to be adjusted iteratively* (Huang, et al., 2007).

Ward's method was used for hierarchical cluster analysis, based on both the Euclidean distance (figure 5.29) and the squared Euclidean distance (figure 5.30) between objects.

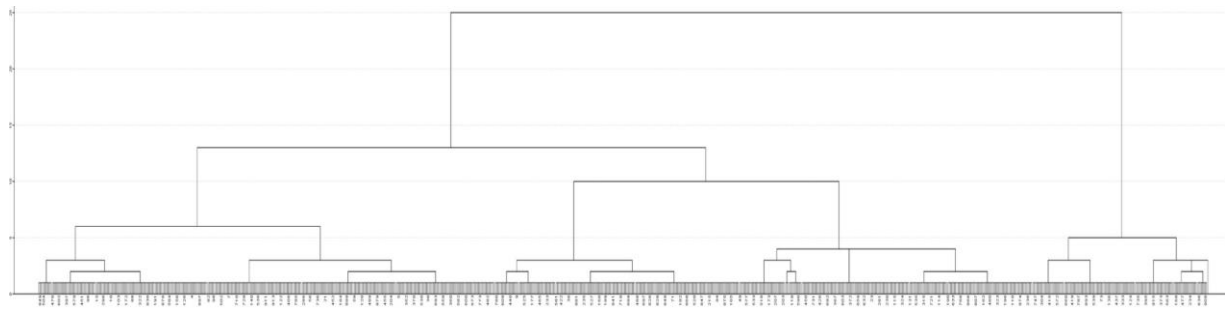

Fig. 5.29: Hierarchical cluster analysis based on Ward's method and the Euclidean distance between objects (Source: By Authors)

[376] *If the sprawl is considered as a pattern, it is a static phenomenon and as a process the sprawl is a dynamic phenomenon* (Bhatta, 2012).
[377] *Even these attributes are correlated with each other and it provides a relatively comprehensive characterization of urban expansion worldwide* (Angel, et al., 2011).

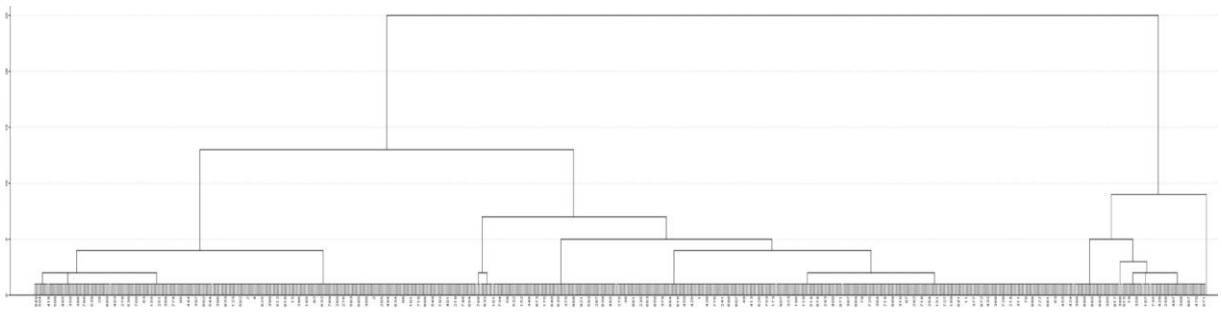

Fig. 5.30: Hierarchical cluster analysis based on Ward's method and the squared Euclidean distance (Source: By Authors)

The dendrograms suggested that a reasonable number of input clusters could range between four and six groups, hence a K-Means cluster analysis (as described in chapter 4 at section 4.4.4) was undertaken either for four, five, and six clusters. The empirical analysis of the results, based on proper knowledge of the geographical area, in addition to the experience of urban morphology matter, has led us to select a six cluster solution as the most suitable for discriminating different urban models.

In this case, convergence is achieved after 46 iterations due to little or no change in cluster centres, and in 923 valid cases, the final distribution of the municipalities in each cluster is the one detailed in table 5.8. While image 5.31 depicts the spatial distribution of the clusters (morphological models) in the case of Catalonia, apart from the urban land cover as detected through the remote sensing procedure.

Number of Cases in each Cluster		
Cluster	1	1
	2	28
	3	97
	4	338
	5	433
	6	26
Valid		923

Tab. 5.8: Number of cases in each cluster, for a K-Means analysis and a six cluster solution (Source: By Authors)

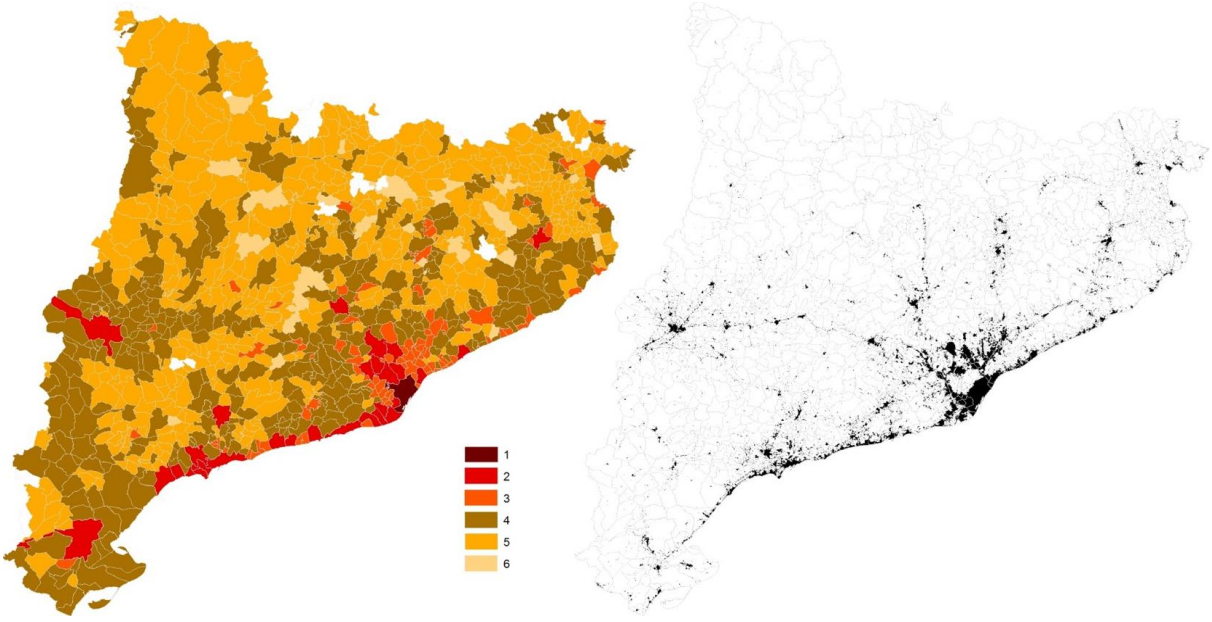

Fig. 5.31: Spatial distribution of clusters (morphological models), and urban land cover, for Catalonia (Source: By Authors)

For each cluster type, a representative sample of morphological models has been provided in figure 5.32, where the model (cluster) 1 is the municipality of Barcelona, model 2 is represented by Terrassa, model 3 is Roda de Berà, model 4 is the municipality of Piera, model 5 is represented by Dosrius, and model 6 is the case of Sant Aniol de Finestres.

Fig. 5.32: Sample of the six morphological models, either for urban agglomeration as well as the street network pattern, as automatically detected for Catalonia through applying a K-Means cluster method (Source: By Authors)

The main morphological features, for each model (cluster), are summarized by the bar-graphs in the next image 5.33, which provides the standardized (z-score) values for the final indices of urban area, fragmentation, convolution, dispersion, texture compactness, and street network complexity.

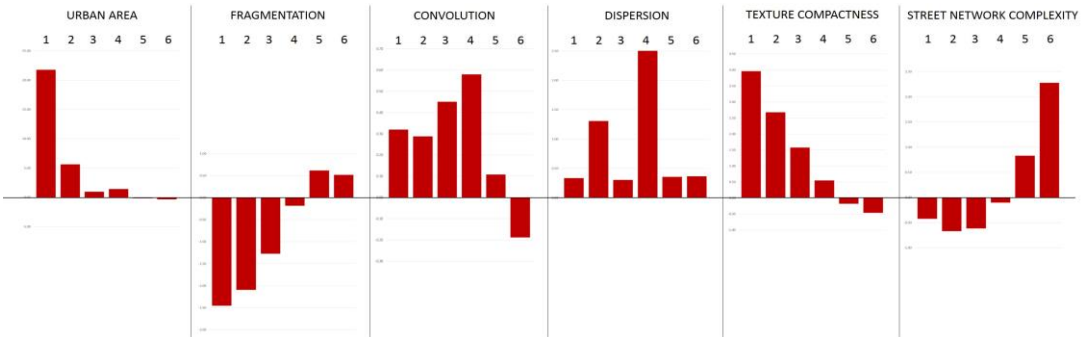

Fig. 5.33: Standardized values either for urban area, fragmentation, convolution, dispersion, texture compactness, and street network complexity, for each urban morphological model (Source: By Authors)

In particular, the bar-graphs highlight that model 1 provides the highest levels for urban area and texture compactness, while achieving the lowest value for fragmentation, besides low values for dispersion and median values of convolution. The street network complexity here is also quite low. Actually, as is the case of Barcelona, the important structure provided by the famous neighbourhood of the "ensanche" creates an important orthogonal grid. Model 2 also provides low fragmentation and street network complexity, but here dispersion increases because the distance between urban patches is higher. Texture compactness is still high as well in the urban area, but less convolution is present than in model 1. Model 3 provides less texture compactness and higher convolution than the two previous models; while in model 4, dispersion and convolution reach the highest values, while the texture compactness decreases and the street network complexity increases due to an increase in the

"serpentine" structure of the streets (Shpuza, 2007). Finally, models 5 and 6 provide the lowest values of texture compactness, urban area, and convolution, but the highest values of fragmentation and street complexity[378].

In the framework of the debate over the modern dynamics of urban development, the indices employed here for defining different models of cities, from the morphological standpoint, play a key role when one attempts to measure the degree of compactness versus urban sprawl. Interestingly, high levels of fragmentation, dispersion and convolution, when combined with high rates of land consumption, probably indicate a process of increasing sprawl (although, as previously highlighted, sprawl is a complex phenomenon that also depends on other dynamics related to socio-economic issues).

The street network complexity can also be considered a "strategic" index here, at least in the case of the geographical area under investigation, as most of the cases suggest a serpentine structure of the street network is related to a fragmented, low density pattern of urban structure, typical of certain suburban areas developed on the Mediterranean side of Spain during the last few decades. If we take into account model (cluster) 6, although it provides the highest values for street network complexity, conversely it provides the lowest values of urban area, which probably could signify that the urban model is not effectively impacting the environment from the standpoint of land consumption.

Alternatively, the degree of compactness for urban texture provides a useful index for discriminating those models that, despite the magnitude of the urban area and the degree of complexity and convolution of the structure, retain certain compactness of the internal structure, as is the case for the city of Barcelona. Therefore, we could infer that the "worst" combination is achieved when high levels of fragmentation, convolution, dispersion, and complexity of the street network, match high values of urban areas (supposedly high land consumption) and low values of urban texture compactness. The next figures 5.34, 5.35, 5.36, 5.37, and 5.38 depict the behaviour of some urban models (for a set of samples in Catalonia), within the two-dimensional Euclidean space built upon the urban texture compactness index combined with each of the other indices, i.e. fragmentation, dispersion, convolution, urban area, and street network complexity.

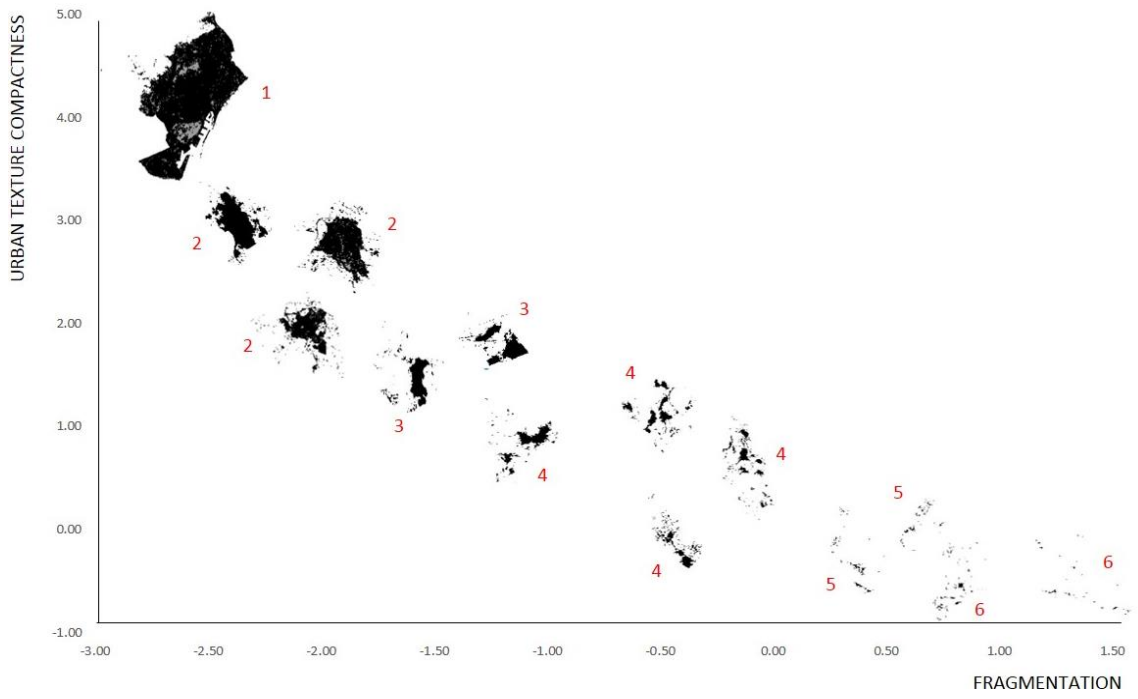

Fig. 5.34: Sample of behaviour for a set of urban morphological models (clusters) in the Region of Catalonia, and within a two-dimensional metric space formed by fragmentation and the urban texture compactness (Source: By Authors)

[378] A previous paper about urban morphological models, mainly focused on the Metropolitan area of Barcelona is provided in: Colaninno, et al., 2009, "The effectiveness of morphology and street networks in determining models of urban growth at different spatial scales of analysis".

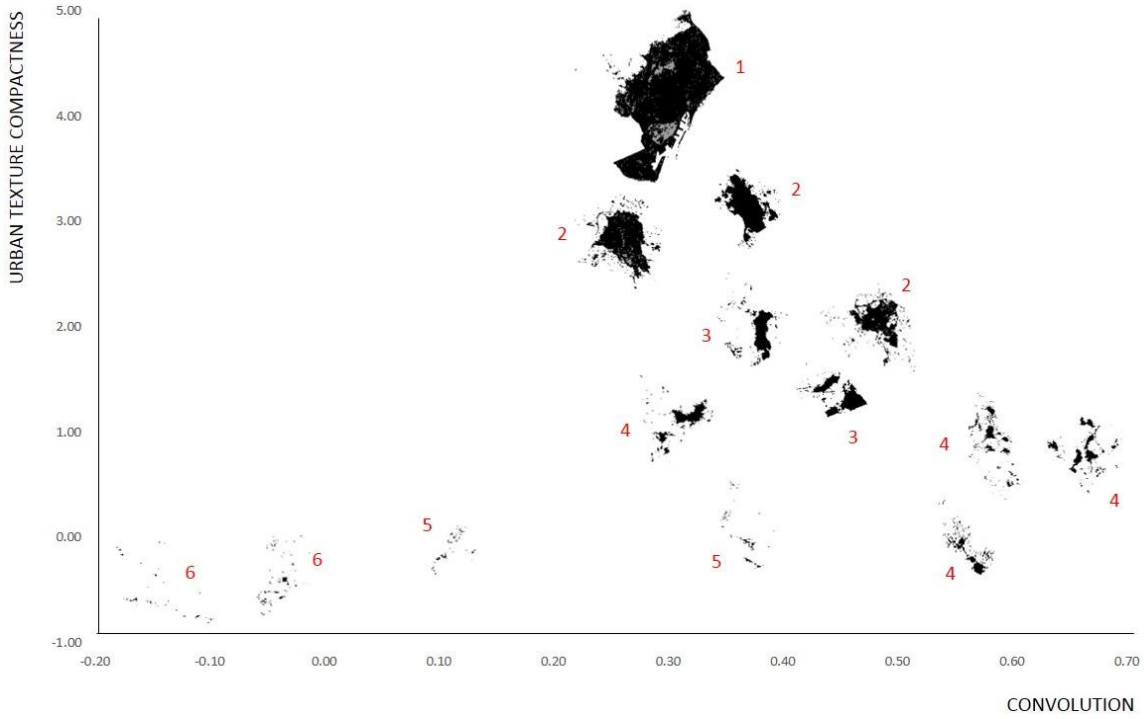

Fig. 5.35: Sample of behaviour for a set of urban morphological models (clusters) in the Region of Catalonia, and within a two-dimensional metric space formed by convolution and the urban texture compactness (Source: By Authors)

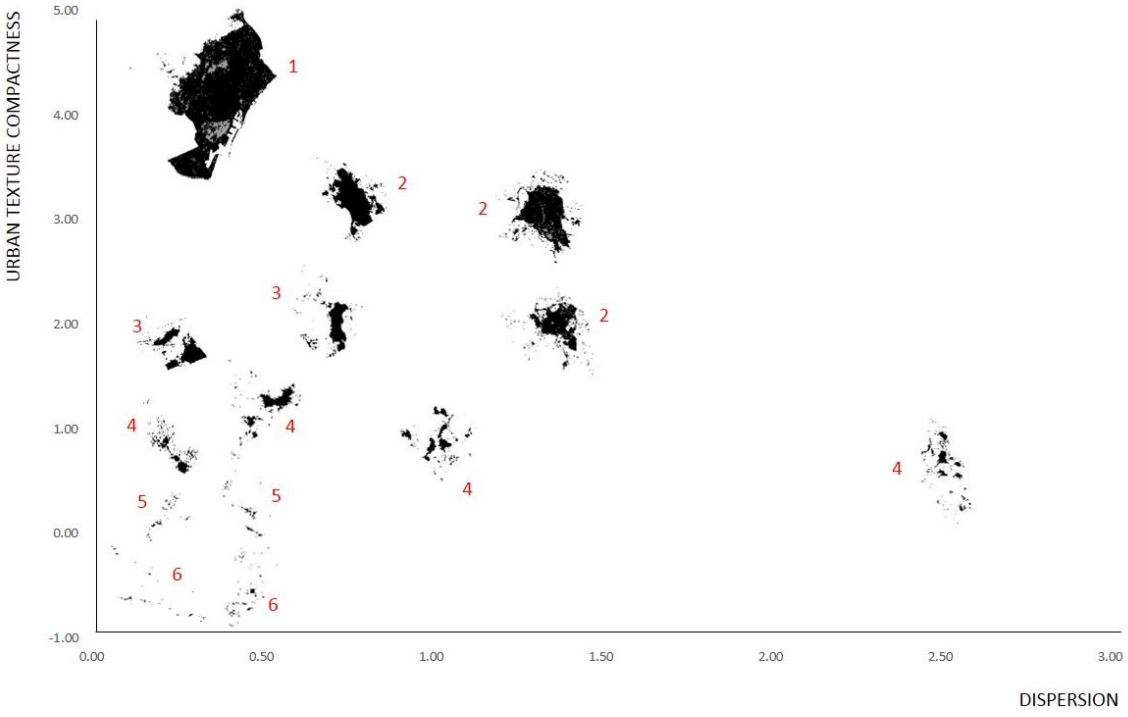

Fig. 5.36: Sample of behaviour for a set of urban morphological models (clusters) in the Region of Catalonia, and within a two-dimensional metric space formed by dispersion and the urban texture compactness (Source: By Authors)

Universidad Politécnica de Cataluña, Barcelona TECH
Departamento de Tecnología de la Arquitectura
Centro de Políticas de Suelo y Valoraciones
Nicola Colaninno, Josep Roca Cladera

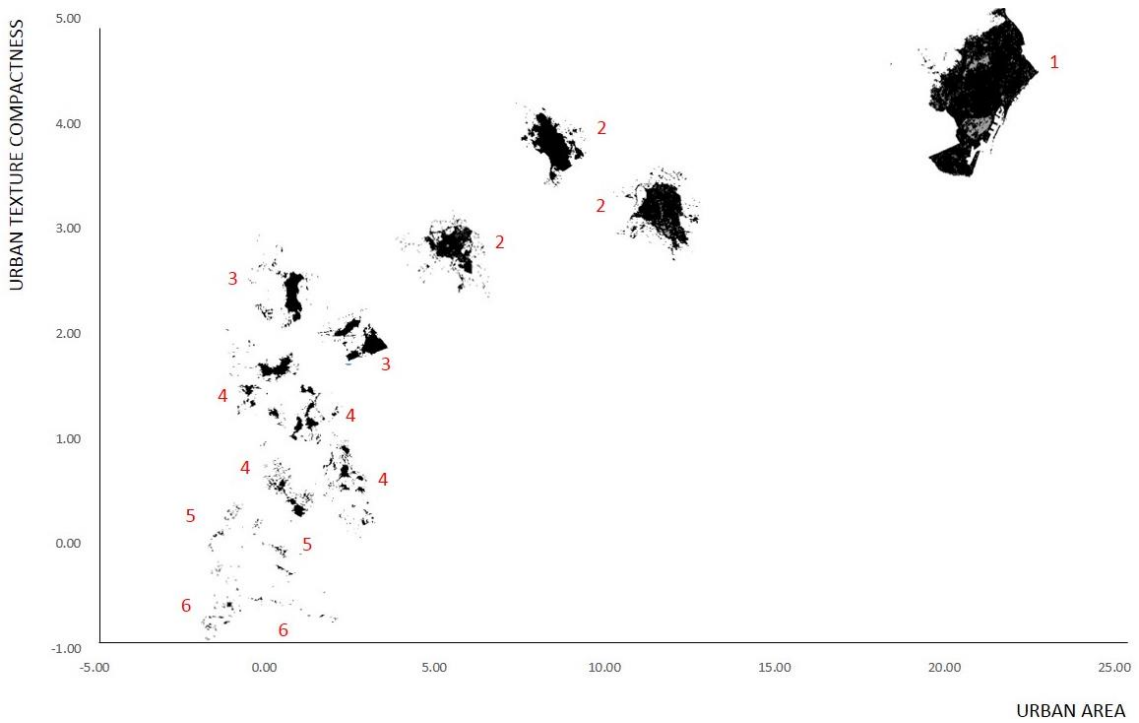

Fig. 5.37: Sample of behaviour for a set of urban morphological models (clusters) in the Region of Catalonia, and within a two-dimensional metric space formed by urban area and the urban texture compactness (Source: By Authors)

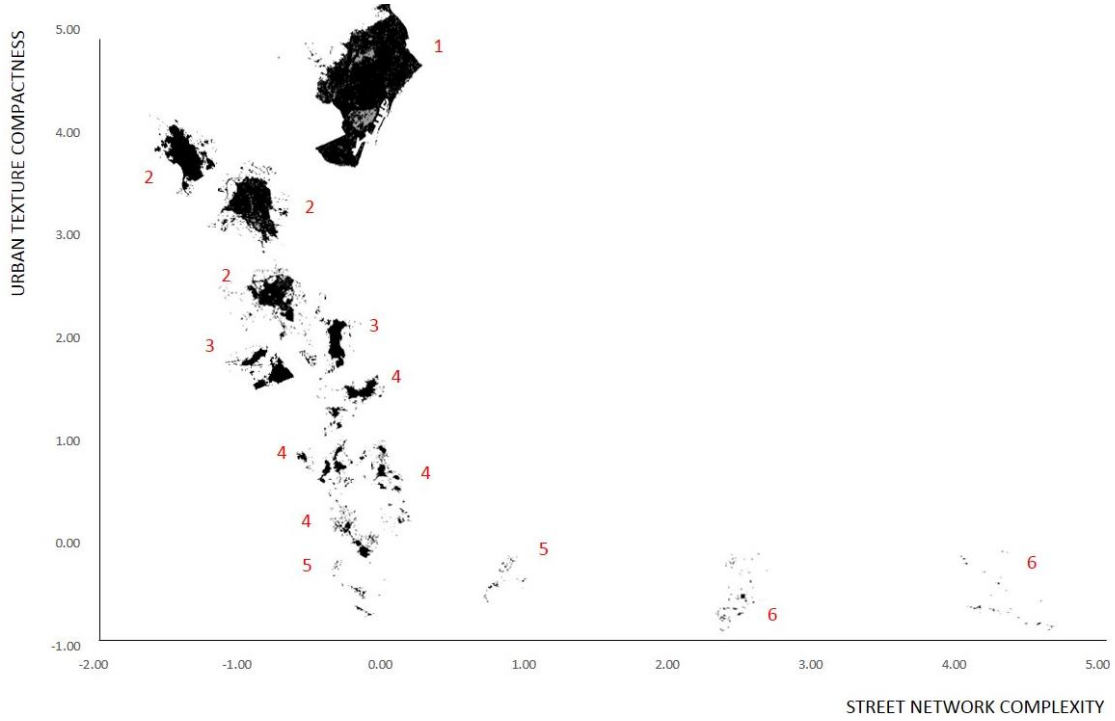

Fig. 5.38: Sample of behaviour for a set of urban morphological models (clusters) in the Region of Catalonia, and within a two-dimensional metric space formed by street network complexity and urban texture compactness (Source: By Authors)

The analysis of the graphs in the previous figures emphasises that, apart from the middle-to-low values of urban texture compactness, models 3 and 4 also provide middle values for fragmentation, convolution, dispersion, and street complexity, although urban area provides relatively low values. On the other hand, model 2, despite higher values of texture compactness and low levels of the street network complexity, provides increased values for urban area, fragmentation, convolution and dispersion.

According to a hypothetical schema of the urban growth process, defined by Herold et al. (2005b) and shown in figure 5.39, *urban area expansion starts with a historical seed or core that grows and disperses to new individual development centres. This process of diffusion continues along a trajectory of organic growth and outward expansion. The continued spatial evolution transitions to the coalescence of the individual urban blobs. This phase transition initially includes development in the open space in interstices between the central urban core and peripheral centres. This conceptual growth pattern continues and the system progresses toward a saturated state. This "final" agglomeration can be seen as an initial urban core for further urbanization at a less detailed zoomed-out extent*[379] (Bhatta, 2012).

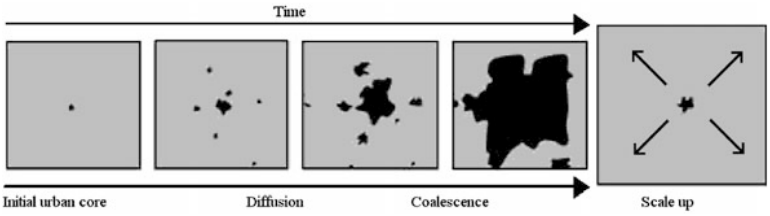

Fig. 5.39: Conceptual sequence of the spatial evolution of urban growth (Source: Herold et al. 2005b; Bhatta, 2012)

In tune with this conceptual scheme, and considering a static spatial extent, we could infer that models 2, 3 and 4 are those matching the stage of "diffusion" depicted in figure 5.38; while the city of Barcelona, due to its stage of development, provides certain degree of "coalescence" typical of mature metropolitan areas. Although model 2 is experiencing a certain consolidation of the central urban core, which is also detectable in the compactness of the urban texture and the street structure, certain dispersion and fragmentation is still present due to a "leapfrogging" growth. However, models 3 and 4 do not provide a dominant central core, which increases fragmentation and dispersion; hence the street network complexity also increases, while texture compactness decreases. Apart from that, model 3 also provides higher values of urban area with respect to model 4.

The analysis of the urban form, as provided here, if combined with other indices such as the population density or mixed uses (Galster, et al. 2001), or the rate of land consumption could lead to a more effective analysis of the urban sprawl phenomenon, and the possible causes and effects related to it.

[379] *In most traditional urbanization-studies this 'scaling up' has been represented by changing the spatial extent of concentric rings around the central urban core* (Bhatta, 2012).

Chapter 6

RELEVANCE AND PERSPECTIVES OF THE RESEARCH: DISCUSSION AND CONCLUSIONS

Most urban models deal with the city in terms of the location of its economic and demographic activities but there is also a move to link such models to urban morphologies which are clearly fractal in structure (Batty, 2008).

This research mainly focused on understanding and measuring the spatial complexity of urban models based on morphological features. Two main objectives in particular were pursued here. First, we aimed to demonstrate the significance of using new technologies, such as RS and GIS, in support of urban analysis, planning and land management. We focused on recognizing the most suitable morphological features capable of exhaustively explaining the key aspects of the spatial complexity. Indeed, we have proposed six morphological dimensions, which are: the urban extent (the urban area); fragmentation, convolution and dispersion of the urban profile, the compactness of the urban texture, and the morphological complexity of the urban street pattern (i.e. how much the street axis differs from the linearity).

The research also emphasizes that the study of urban phenomena relies, intrinsically, on a multidisciplinary approach, contributing to and taking advantage of other disciplines. Apart from that, understanding and modelling urban phenomena currently requires innovative concepts, reliable and diverse data, and feasible methods of analysis or modelling (Cheng, 2003).

In addition to being state of the art for some of the most recognized approaches to urban morphology and projects based on new technologies applied to spatial analysis (Chapter 3); an overview of the urban growth phenomena occurring in Spain during the last few decades, in particular along the Mediterranean side, has been provided based on some recognized studies (Chapter 2). However, the main achievement of the study is to have put forward a general process capable of analysing the territory, from the primary data collection phase based on remote sensing (RS) techniques, to the analysis and mapping of specific urban phenomena based on a statistical approach and geographical information science (GIS).

For this, two proper methodologies have been set up. On the one hand, we have proposed a semi-automatic methodology for classifying land cover for huge geographical areas from satellite data based on recognized RS techniques. On the other hand, we have set up an automatic methodology for classifying similar urban models at the municipal level, based on morphological features and through the use of statistical techniques. Hence, the process and the methodologies proposed here, consistent with the geographical area of interest of this research, have first been calibrated for the case of Catalonia, and then tested for the other Autonomous Communities along the Mediterranean side of Spain, i.e. Valencia, Andalucía, Murcia and Balearic Islands.

Beyond the results, which could be recalibrated to rectify some inconsistencies, the effectiveness of the research relies on the contributions that a conceptual approach to the spatial analysis and the methodological processes can provide to specific scientific fields and planning practice. Actually, in addition to the results of the morphological analysis applied to the whole geographical area, the conclusions in this chapter mainly focus on highlighting the strengths and weaknesses of the study, potentialities, the implications for planning practice and future proposals.

6.1. THE EFFECTIVENESS OF RS & GIS FOR COLLECTING AND PROCESSING SPATIAL DATA

Over the past few decades, the progressive use of new technologies in land management and planning has given rise to a number of pioneering approaches in terms of spatial governance. The possibility of automating the analysis processes and managing large geographical areas and databases, combined with the growing ability to collect territorial information about Land Use/Land Cover globally, have changed the rules.

One of the prime prerequisites for better use of land is information on existing land use patterns and changes in land use over time. Knowledge of the present distribution and area of such agricultural, recreational, and urban lands, as well as information on their changing proportions, is needed by legislators, planners, and State and

local governmental officials to determine better land use policy, to project transportation and utility demand, to identify future development pressure points and areas, and to implement effective plans for regional development (Anderson, et al., 1976).

Indeed, as argued by Weber (2009), *land cover changes reflect the consumption of land (more or less a finite stock) of a given type and the formation of another type resulting from the use of land and from natural drivers (e.g. climate), sometimes in combination (e.g. desertification resulting from overgrazing in arid areas). The observation and analysis of land cover changes is therefore fundamental information used for a wide range of purposes from urban and land planning to agriculture management, forestry, or water management*.

Currently, for informed decision-making and effective land management, governments can obtain an increased knowledge of the physical and social geography of the territory. However, the quantification of dynamic processes of development often requires a large amount of data and a number of spatial analyses, which is not easily accessible, in addition to the high expertise required. Moreover, there still exists a relevant lack of standardization and compatibility between different data sources and approaches.

Remote sensing (RS) and GIS provide effective tools for collecting and processing large amounts of spatial information at a global level and at a different scale of analysis. It also allows the possibility of establishing a common language based on robust scientific bases. Nowadays, several data sources are available due to the number of space missions and national census databases. Moreover, a large amount of such information is freely available. For instance, in the case of the satellite imagery of the Landsat mission, available since the end of the 70's and early 80's, or the Digital Elevation Models derived from the Shuttle Radar Topography Mission (SRTM), available at a global level and at a spatial resolution of 90 and 30 meters per pixel (see Chapter 4).

In addition, a number of commercial and open source software types are available for image processing and management of geographical data. At present, the most common commercial software such as ArcGIS, ENVI, or ERDAS, advanced GIS and RS open source software such as GRASS GIS, and Quantum GIS (QGIS) are currently used by several public institutions and private enterprises. This makes it easier to satisfy the need to establish a globally recognized language and standardize processes for environment monitoring and the spatial analysis.

Although several aspects of the environment can be monitored and analysed based on a technological approach (imagine hydrological analysis, forestry issues, agriculture or natural risks assessment, among others), the study and measurement of urban growth phenomena remain among the major topics concerning RS and GIS applications. In order to collect and handle the necessary information for "measuring" the urban growth phenomena, the data can be derived through satellite and aerial imagery and is widely recognized as suitable at different spatial and temporary scales. Several international projects focused on urban studies rely on the use of such technologies (see Chapter 3).

Remotely sensed imagery also provides a primary data source for monitoring urban growth due to the availability of time series imagery (temporal resolution). *Data sets obtained through remote sensing are consistent over great areas and over time, and can provide information at a great variety of geographic scales. The information derived from remote sensing can help to describe and model the urban environment, leading to an improved understanding that benefits applied urban planning and management* (Bhatta, 2012). Saying that, database management, spatial analysis and modelling, and visualisation (for both raw and processed data) are the main uses of GIS in urban planning.

Indeed, the development of a number of algorithms for image processing and spatial analysis of geographically referenced data provide accurate and consistent methods for obtaining specific indicators capable of measuring the main attributes of urban growth processes, either from the morphological, environmental or socioeconomic standpoint.

Therefore, this research, in addition to the analysis of some relevant methodological approaches to land cover detection and spatial analysis, offers a further methodological approach based on recognized algorithms. In line with other research, this aims to pursue the idea of automation of the processes for collecting and managing information concerning large geographical areas (at a global level) and the normalization of indices and nomenclature for spatial analysis. Moreover, the work indirectly highlights the significance of the use of free imagery and spatial data.

6.1.1. New Technologies for Land Management and Planning

The scientific planning and the management of urban growth need the quantitative measurement of growth patterns. With the progress of modern remote sensing techniques, earth-observation-based monitoring of urban growth has been widely accepted and implemented by national, regional and local governments because it is the prerequisite for comparing spatial and temporal change patterns. This change analysis can be performed with multi-temporal and multi-source imagery. Various methods have been put forward. These methods include spatial, statistical, economic and integrated indicators, often in a comparative analysis setting (Cheng, 2003). However, as argued by Yeh (1999), *urban planning is one of the main applications of GIS. Urban planners use GIS both as a spatial database and as an analysis and modelling tool. The applications of GIS vary according to the different stages, levels, sectors, and functions of urban planning. With the increase in user-friendliness and functions of GIS software and the marked decrease in the prices of GIS hardware, GIS is an operational and affordable information system for planning. It is increasingly becoming an important component of planning support systems. Recent advances in the integration of GIS with planning models, visualisation, and the Internet will make GIS more useful to urban planning. The main constraints in the use of GIS in urban planning today are not technical issues, but the availability of data, organisational change, and staffing* (Yeh, 1999).

The previous statements are the key motivations inspiring this research. Indeed, the first part of the study, related to the field of remote sensing, proposes a relatively quick and semi-automatic procedure for detecting the main land cover classes of interest for land management and planning procedures. Although certain improvements are expected in the final results of the land cover classification[380] based on the interpretation of the analyst, the main idea behind the research is to sing the praises of remote sensing and increase the implementation of *earth-observation-based monitoring* for the urban growth phenomena, and at differing levels of governance (national, regional and local).

Indeed, the findings prove that an analyst could reasonably derive the land cover information (an on-screen human interpretation of the results could be required to improve the accuracy of the results) for a relatively large geographical area (such as the region of Catalonia) in just a few months based on primary (freely available) and widely recognized data sources (such as remotely sensed imagery, either optical Landsat multispectral imagery or radar data from the SRTM Digital Elevation Models). Landsat imagery is proven to be an ideal source for mapping land cover using an operational scale of 1:75˙000, for the spatial resolution of 15 meters/pixel, and 1:150˙000 for the spatial resolution of 30 meters/pixel (as used in our case study), the results achieved by using such information are suitable for land management practices and spatial planning at regional and/or urban level.

Once the final cartographic information concerning land cover, and urban land cover in particular, is obtained; a GIS platform is used to set up a methodology for automatically analyzing and classifying similar urban settlement patterns, dependent on morphological features (in our case). Although certain criticism is due regarding the indices used or the initial hypothesis; the main achievement of the study, at this point, has been to set up a number of synthetic indices capable of quantifying different urban models through the use of statistic analysis.

Urban growth is not a universal process with similar attributes in all world regions but, instead, *it depends on a set of complex phenomena conditioned by various cultural and historical forces in different places* (Laurence and Edward, 1981; Cheng, 2003). The possibility of systematically analyzing some of those aspects, such as the morphology of urban settlements, can be useful in spatial planning for understanding several physical and socio-economic dimensions in different geographical contexts. In this way, *new opportunities come from the advances in complexity science, computer techniques, remote sensing and GIS* (Cheng, 2003).

6.1.2. Spatial Modelling: Exploring the Urban Phenomena

This research has developed a general approach to spatial analysis which falls into two main stages: monitoring and mapping of land cover based on remote sensing techniques (chapter 4); and spatial modelling,

[380] *Image classification and visual interpretation unavoidably contain uncertainties, such as the classification of low density or high-density residential areas that can be treated as fuzzy spatial objects* (Cheng, 2003).

which fundamentally aims to classify a number of similar urban land cover patterns[381] based on morphological features.

In general, spatial modelling is an analytical process concerning sets of indices capable of simplifying and explaining the spatial relationships of geographical features. The main aim is to abstract and represent a specific phenomenon that occurs on the Earth's surface. The increasing availability of geographical data and the capabilities of geographical information systems have enhanced the potential for spatial analysts and planners to study and simulate spatial phenomena that occur in the real world, thus facilitating land management and planning practices.

In the domain of urban planning in particular, urban modelling is a tool for analysing, evaluating, and quantifying urban phenomena and provides a key approach to support decision-making. According to Cheng (2003), *theoretically, urban growth modelling should be considered as an interdisciplinary field as it involves numerous scientific and technical areas, e.g. geographical information science (GIS), remote sensing (RS), urban geography, complexity theory, land use/cover modelling etc.* Hence*, understanding urban growth and applying this knowledge for planning are both closely linked with these areas* (Cheng, 2003).

In line with such assumptions and in terms of spatial modelling, this research focused on setting up a methodological process for exploratory analysis based on spatial indices and statistic analysis, in order to synthesize the main features of urban morphology at a municipal scale. Depending on such features, the study aims to provide a useful instrument for quickly and automatically discriminating between different patterns of urban land cover, thus allowing for the management of relatively large geographical areas.

As a result of the significant environmental impact caused by "uncontrolled" urban expansion that occurred during the last few decades along the Spanish side of the Mediterranean (see Chapter 2), the availability of instruments capable of monitoring certain relevant aspects of the urban expansion based on homogeneous parameters for large portions of the territories resulted in essential resources for planners and policymakers. The urban modelling in this study has produced certain significant quantitative evidence for comparison, evaluation and interpretation of the main forms of land occupation on the Spanish side of the Mediterranean. In particular, the findings of the case studies described in this research have resulted in significant understanding of the main morphological aspects (i.e. relative to the the physical dimension) that characterize urban land cover.

The use of synthetic indices regarding the physical configuration and composition of the urban land cover, dependent on both the internal (urban texture and street pattern) and external (the urban profile) features, allow us to understand the main formal evidence. This is the case of linear patterns, i.e. those urbanizations that spread along the major road networks or along the coast line; compact or fragmented patterns, i.e. those urbanizations formed around a main dominant urban patch or, alternatively, those models consisting of multiple patches of similar weight in terms of land cover area.

The effectiveness of the indices and the analysis are undoubtedly dependent upon the accuracy of the primary data. The consistency of the modelling is strictly related to the initial hypothesis. However, as argued by Cheng (2003), *from the perspective of spatial science, modelling must take both the spatial and temporal dimensions of urban systems into account*. Actually, spatial and temporal modelling together provide the most effective approach to urban planning for simplifying complex dynamics and construct potential scenarios (Cheng, 2003). *The ability to understand and predict changes in land use patterns is necessary, for policymakers, concerned with a variety of public finance, quality of life, and environmental protection issues* (Bell, et al., 2002). In line with this, the research at this phase was basically focused on providing a static analysis of urban morphology, i.e. based on just one temporal observation.

The aim here was the exploratory analysis regarding urban forms, rather than explanatory analysis about urban growth. However, future developments in the research will rely on reproducing the analysis at different temporal stages in order to monitor the growth dynamics of the models over time.

[381] As emphasized by Cheng (2003), *the Oxford English Reference Dictionary defines pattern as "a regular or logical form, order, or arrangement of parts such as behaviour pattern". Two key components are stressed in the definition: elements and the logical ordering among the elements*.

6.2. THE "VALUE" OF THE MORPHOLOGICAL APPROACH IN URBAN ANALYSIS

An important aspect of this research has been to emphasize the "value" of the morphological approach in spatial analysis and, in particular, the effectiveness that such an approach provides for explaining the forms and physical evolution that the urban environment has been experiencing during the modern era.

Indeed, formal paradigms of the modern (Western) city have changed dramatically over the past century. The urban form has gone from physically continuous structures based on a homogeneous spatial syntax to a more fragmented urban system and "opened" towards the more peripheral areas. This openness has certainly caused a change in the scale of the real urban space as well, which is now the result of a juxtaposition of different elements that have become increasingly physically independent and occupy larger land areas.

Within this important morphological change, transport infrastructure (both public and private) has undoubtedly played a central role. As a result, a key part of the "new" physical structure of the urban environment is provided and it is often the only physical link between multiple parts of the same urban environment. Hence, the morphology of the urban space has changed, not only in terms of the urban fabric, but also in terms of territorial structure. The modern city has changed radically. It is more and more scattered around the territory, and dominated by forces that are not related to planning processes. The continuity of urban growth has given way to discontinuity and the urban density decreases dramatically as we move away from the consolidated city. Such dynamics are the basis of one of the most argued, discussed, and analyzed urban growth phenomenon of the modern era: *Urban Sprawl*.

In 1999, Levy argued that *new tools of analysis are needed to understand the new components of the modern urban fabric and their processes of formation* (Levy, 1999). In line with this, the morphological approach to spatial analysis provides effective modelling methods and techniques for analysing the urban growth phenomena (such as complex phenomena) at different spatial scale[382]. In particular, measuring the physical forms of the urban environment provides scientific instruments for inferring the most plausible spatial structure, either in terms of Monocentrism versus Polycentrism or Compactness versus Sprawl (dependent on the scale of analysis).

6.2.1. Urban Morphology and Urban Sprawl

Research in the field of urban morphology is mainly concerned with the study of the different forms that the urban extent "draws" on the territory, either in terms of individual elements, as well as in terms of urban agglomeration as a whole. Without doubt, this provides a useful instrument for dealing with the increasing necessity to measure the modern dynamics of urban growth. The modern urban form has undergone radical changes during the past century. Moreover, technological improvement in the last few decades has further increased the speed of such changes. Cities have exceeded the traditional administrative limits, generating new situations and forms.

As argued by Levy (1999), *there has been a shift from a closed fabric in which the links between the different elements (plot, street, constructed space, and open space) formed a system, to an open fragmented peri-urban fabric. Autonomous, atomized elements do not relate to each other anymore and their scale has changed greatly. In these morphological transformations, the infrastructure of transportation, associated with growing demands for mobility created by post-industrial patterns of employment, has played a dominant role. This infrastructure is an essential part of the new fabric. It has been the primary tool of urban expansion and the principal agent of urban change* (Levy, 1999). This brief analysis, taken from Levy (1999), includes some of the main aspects of the most common modern phenomenon of urban expansion known as sprawl (see section 2.1.2). He actually refers to "morphological transformations", thus implicitly alluding to urban morphology as a key feature of the sprawl.

[382] *Urban morphology is the study of the form of human settlements and the process of their formation and transformation. The study seeks to understand the spatial structure and character of a metropolitan area, city, town or village by examining the patterns of its component parts and the process of its development. This can involve the analysis of physical structures at different scales as well as patterns of movement, land use, ownership or control and occupation* (Wikipedia, 2015).

In fact, Galster, et al. (2001), define the urban sprawl as a phenomenon measurable through the use of eight dimensions which are density, continuity, concentration, clustering, centrality, nuclearity, mixed uses, and proximity. Some of these are strongly related to the morphological features of urban settlement. In particular, urban sprawl is a pattern of expansion that provides low levels in some, or all, of the eight dimensions. This definition gives rise to the possibility that there may be different types and levels of sprawl, depending on different combinations of these variables (Cerda, et al., 2007).

Cheng (2003) stressed the idea that, *faced with the severe negative impacts, urban planners need to rethink the most important development policies and manage urban sprawl and urban growth more scientifically in the future*. He also underlined that, *in the USA, urban sprawl has sparked off a national debate over land use policy that includes smart growth management and growth boundary measures* (Brueckner, 2000; Cheng, 2003).

Criticism is required too when analyzing the urban growth phenomenon. As mentioned by Bhatta (2012), because the term "urban sprawl" has generally a negative connotation, *not all types of modern urban growth can been considered as sprawl;* indeed, *not all urban growth is necessarily unhealthy*. Moreover, *one development that can be considered as sprawl by someone may not be considered by others* (Roca et al. 2004). The urban growth processes based on an "infill growth", for instance, *are generally considered as remedies to sprawl. Therefore, sprawl cannot be characterized by the simple quantification of "the amount of land that has changed to urban uses"* (Bhatta, 2012), but mostly by quantifying the form of such changes.

A set of objective and widely recognized measurements are required. With this in mind, the relevance of the study relies on the effort to arrange a set of objective synthetic indices capable of defining the morphological model for different urban settlements at a given time. In particular, six indices have been synthesized by applying a factor analysis on a set of primary spatial metrics, as detailed in section 5.3.3. In addition to this, an automatic process for classifying similar patterns of urban structures has been designed based on the use of cluster analysis, dependent on an initial hypothesis that assumes the existence of at least six main models (see section 5.3.4). Hence, consistent with previous assumptions, morphological analysis provides a key dimension for measuring the urban sprawl phenomenon and is even more effective if used in conjunction with further spatial features, and applied at multiple temporal stages.

6.2.2. Morphological Models Along the Mediterranean side of Spain: Towards Calibrating a Suitable Analysis about the Urban Growth

A scientific approach to spatial analysis should be based on robust indicators that are widely recognized, quantifiable on a large scale, and suitable for different geographical areas. This means that, for example, the analysis of the urban sprawl phenomenon should be based on a set of indices, or alternatively an overall index of sprawl that is globally accepted and standardized. Usually, the effectiveness of such an approach relies on a spatio-temporal analysis. However, prior to providing a temporal analysis, suitable methodologies and processes are required in order to guarantee the homogeneity of the measurements over time.

From this point of view, the aim of the study was first to propose a set of indices capable of synthesizing the main morphological aspects of the urban settlements. Indeed, the measurement of the urban area in terms of urbanized surface and the complexity of the street network structure in terms of linearity/non-linearity of the street axis provide two primary indices.

Four synthetic (secondary) indexes have been calculated, dependent on widely recognized primary processes of spatial analysis, mainly derived from the field of landscape ecology (see section 5.2.2). Actually, this study can be interpreted as a starting point, more than a point of arrival. In other words, the reasearch aims to emphasize the need for a global effort to define the most suitable parameters for providing effective analysis of urban forms, beyond the results obtained (here, we focus on the territorial level more than the local).

Secondly, the use of (globally) recognized morphological indices, would allow us to determine a limited number of generalized models, depending on ranges of values which could be used as an international standard for objectively measuring certain urban phenomena. Imagine urban sprawl, for instance. How many kinds of sprawl exist? How could we quantify the magnitude of the sprawl phenomenon, in terms of comparison between different cities? Obviously, not all urban aspects can be globally standardized, but some general and basic measurements, if

applied on homogeneous databases, could provide interesting tools for benchmarking and thus, the application of "best practices" in the field of spatial planning.

Our approach to setting up a generalized methodology for analyzing and defining morphological models of land occupation, relies on the following points:

- Problem delineation: defining urban morphological models
- Collecting primary information about urban land cover through remote sensing techniques
- Formulation of the hypothesis: characterising a reasonable number of conceptual models
- Selecting spatial metrics
- Synthesizing the main morphological dimensions
- Automatic classification of similar models based on sampling: testing and evaluation
- Repetition of the classification procedure, dependent on the previously tested parameters.

The test for classification methodology has been conducted for the region of Catalonia (as described in Chapter 5, at the section 5.3), prior to being applied to the whole geographical area under investigation. Image 6.1 shows the urban land cover, detected through remote sensing techniques (as detailed in section 4.5) for Catalonia, for which the computation of metrics and the classification have been applied. The administrative division is according to the provincial level: Barcelona, Girona, Tarragona, and Lerida.

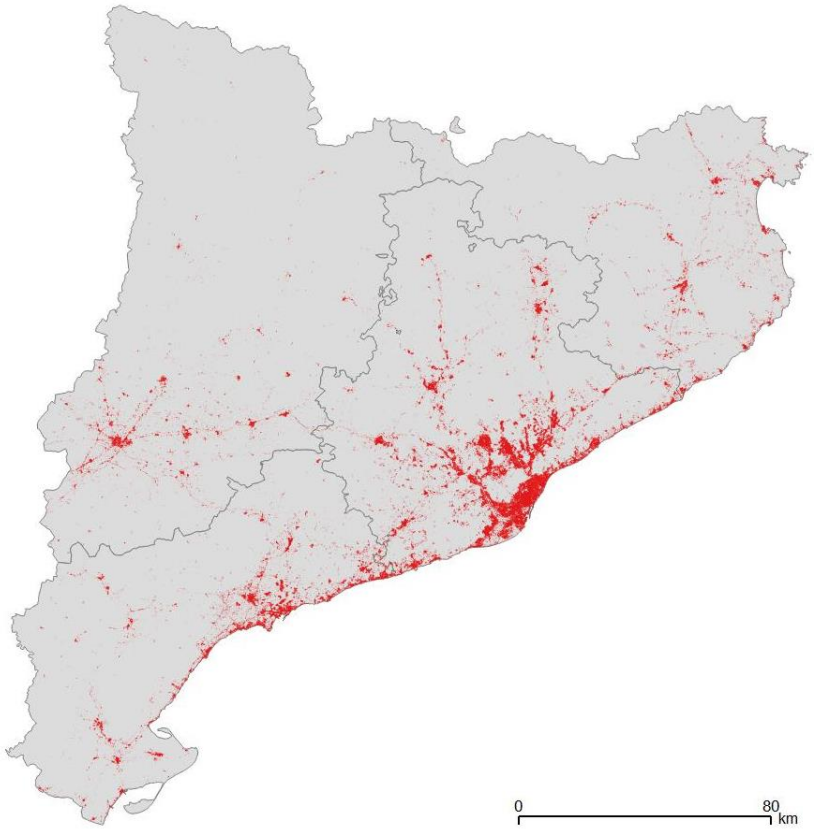

Fig. 6.1: Urban land cover detected by remote sensing for Catalonia (Source: By Authors)

The experiment at this point involves the use of cluster centers, extracted by applying a K-Means cluster analysis for Catalonia and the rest of the Autonomous Communities included in the geographical area under investigation. The values of the cluster centres for each of the six morphological dimensions used in the classification process are provided in table 6.1, plus the number of valid cases (municipalities) in each cluster type.

		Final Cluster Centres - standardized (z-score) Indices -					
CLUSTER	Valid Cases	Urban Area	Fragmentation	Convolution	Dispersion	Texture Compactness	Street Network Complexity
1	1	21.76178	-2.45340	.31935	.33663	3.96071	-.42322
2	28	3.06070	-1.52779	.64606	1.54318	1.92954	-.62940
3	97	.52964	-1.69004	.47700	-.54149	2.06264	-.56350
4	338	-0.01691	-.29513	.30471	.44532	.12909	-.32066
5	433	-.31475	.75256	-.06346	-.33021	-.58047	.17164
6	26	-.33363	.53623	-.38951	-.11316	-.74898	3.92147
Valid	923						

Tab. 6.1: Final cluster centers of the six morphological indices, for Catalonia, and the number of cases in each cluster (Source: By Authors)

The spatial metrics have been calculated for the rest of the Autonomous Communities, and then the six morphological variables. The same process as was used for Catalonia (see section 5.3.3) and based on the urban land cover detected through remote sensing, as shown in figure 6.2[383]. For a total number of 2˙369 cases (municipalities), the urban area of 69 municipalities could not be detected possibly due to the coarse spatial resolution of the Landsat imagery. Hence, a final set of 2˙300 valid cases has been used.

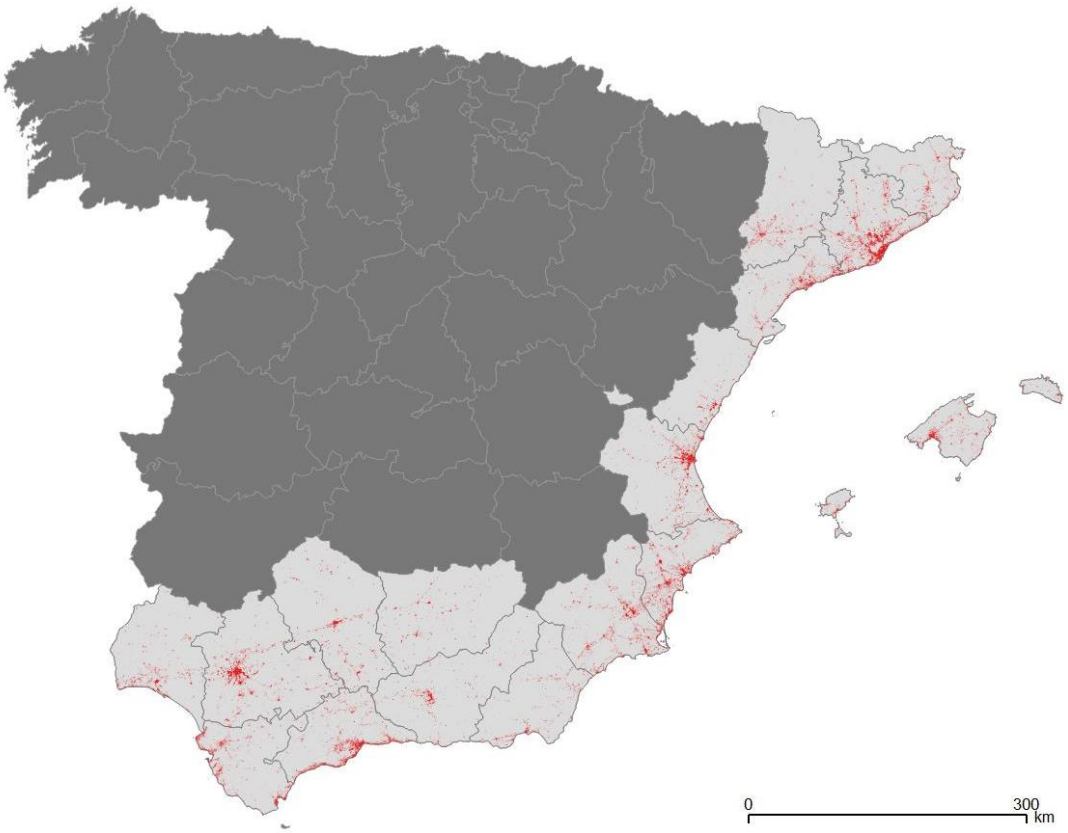

Fig. 6.2: Urban land cover detected through remote sensing for the five Autonomous Communities along the Mediterranean side of Spain. The administrative limits for provinces are also indicated (Source: By Authors)

[383] Maps of urban land cover at a more detailed scale for each province within the area under investigation are provided in Annex I: ATLAS OF LAND COVER 2011 ALONG THE MEDITERRANEAN SIDE OF SPAIN.

Universidad Politécnica de Cataluña, Barcelona TECH
Departamento de Tecnología de la Arquitectura
Centro de Políticas de Suelo y Valoraciones
Nicola Colaninno, Josep Roca Cladera

Once the final indices were obtained, the K-Means cluster analysis was undertaken using the cluster centres derived from Catalonia, as shown in the previous table 6.1. Hence, image 6.3 provides the final result of the classification for the whole geographical area under investigation as well as the spatial distribution of the morphological models described in the section 5.3.4 and depicted in the images 5.32 and 5.33 of the previous chapter.

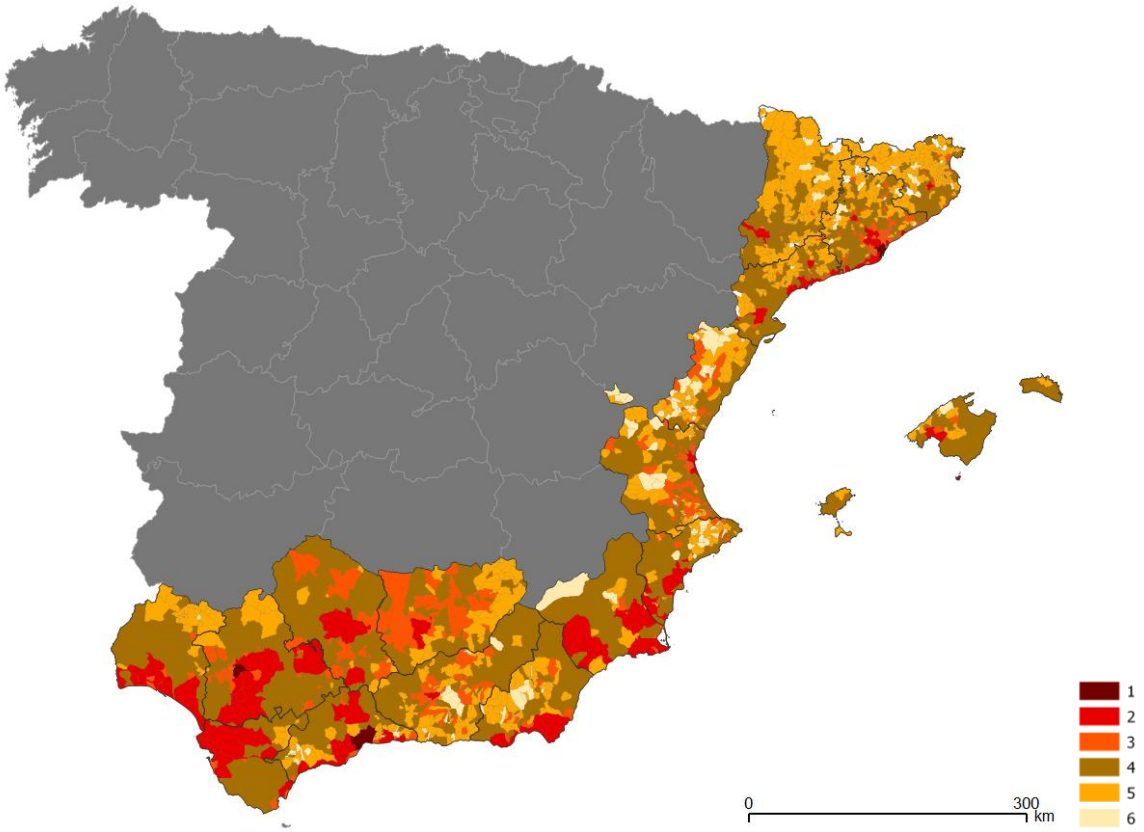

Fig. 6.3: Spatial distribution of the morphological models, at municipal level, for the five Autonomous Communities along the Mediterranean side of Spain. The administrative limits for provinces are also indicated (Source: By Authors)

At this point some considerations must be taken into account with respect to the results obtained regarding the different morphological models observed along the Spanish side of the Mediterranean. In particular, the city of Barcelona, Sevilla and Malaga also provide similar characteristics in terms of urban forms at territorial level, i.e. the highest values of the urban texture compactness and the lowest values of the street network complexity[384]; low fragmentation and dispersion, although the urban agglomeration of Sevilla and Malaga are more fragmented than Barcelona, and the dispersion of Malaga is higher than Sevilla and Barcelona (see figure 6.4).

Model 1 also provides the highest values of urban area, i.e. these are the "biggest" cities in this geographical context in terms of urban land cover extension. In terms of population, Madrid, Barcelona, Valencia, Sevilla, Zaragoza, and Malaga are, respectively, the most populated cities in Spain.

[384] As highlighted in chapter 5, at section 5.3.4, the degree of compactness for the urban texture provides a useful index for discriminating those models that, despite the magnitude of the urban area and the degree of convolution, retain certain compactness of the internal structure as is the case of the city of Barcelona. Therefore, we could infer that the "worst" combination is achieved when high levels of fragmentation, convolution, dispersion, and complexity of the street network match high values of urban areas (supposedly high land consumption) and low values of urban texture compactness. Indeed, a high level of street network complexity, in most of the cases, is related to a fragmented, low density, pattern of urban structure, which is typical of certain suburban areas developed along the Mediterranean side of Spain during the last decades.

Hence, in this scenario, the case of Valencia is a bit surprising in that, although comparable with Barcelona, Sevilla, and Malaga in terms of magnitude, it has resulted in model 2, instead of model 1. However, we strongly stress the idea that the models are based on morphological features, not population. For instance, socio-economic dynamics are not taken into account here either.

Figure 6.4 summarizes the six morphological dimensions, through the use of comparative radar charts, for the cities detected as belonging to the model (cluster) 1, i.e. Barcelona, Seville, and Malaga. All the values have been normalized to a scale ranging between 0 and 1 in order to enhance the interpretability of the values and the comparison between the cases.

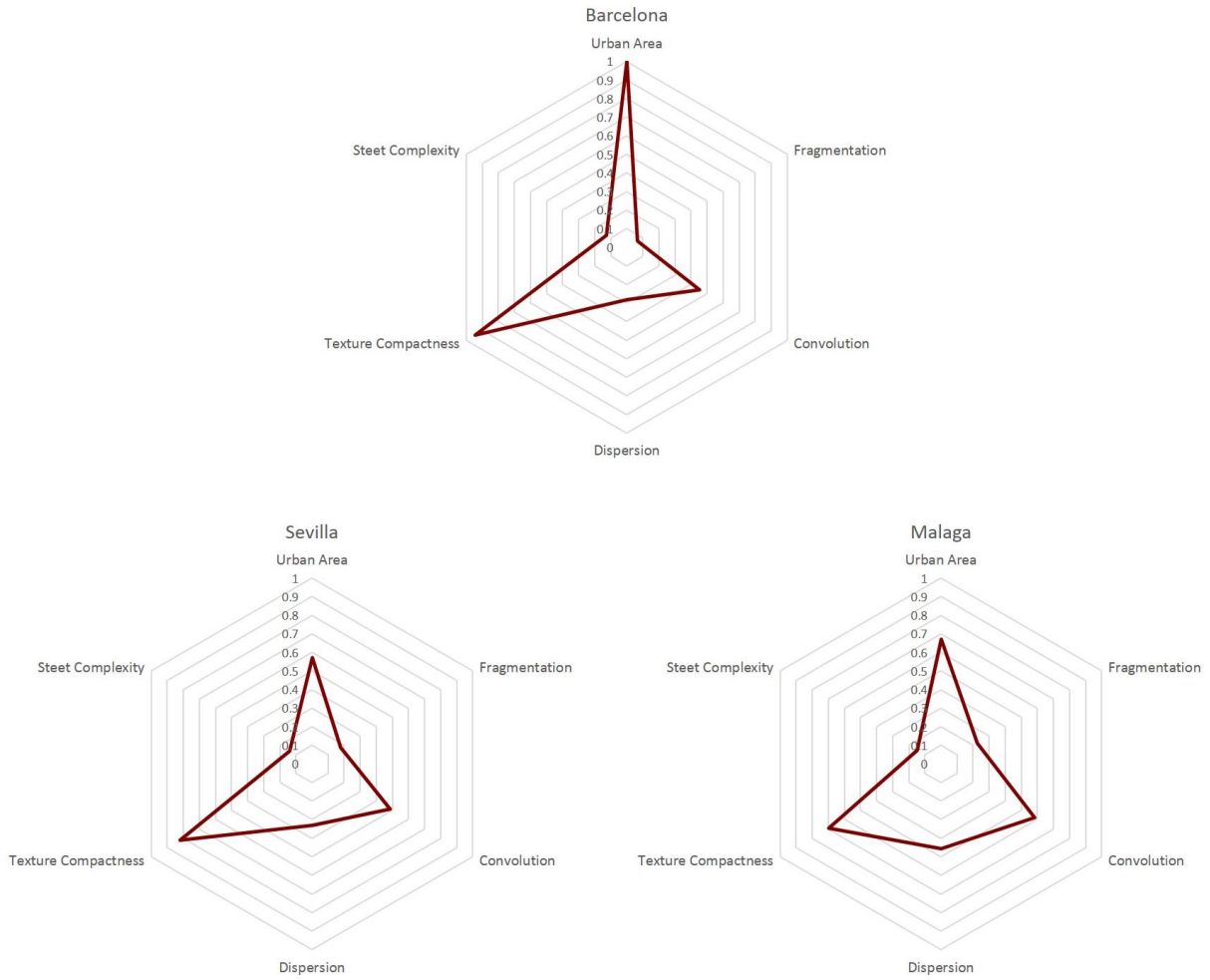

Fig. 6.4: Radar charts of the urban models for Barcelona, Sevilla, and Malaga (i.e. the cluster model 1), based on the behaviour of six morphological dimensions, normalized to a scale 0-1 (Source: By Authors)

As previously mentioned, based on the morphological features considered in this research, the city of Valencia, although among the largest cities in Spain, both in terms of population and urban extension, has resulted in model 2, along with Palma de Mallorca. In particular, as depicted in figure 6.5, the model (cluster) 2, similar to model 1, provides low values for fragmentation and the street network complexity, and average values of convolution and dispersion (actually, Sabadell shows less dispersion than the other samples). On the other hand, the values of texture compactness tend to decrease with respect to model 1 in the cases of Valencia and Palma de Mallorca,. Hence, one could infer that, from a morphological standpoint, these cities are subject to a loss of compactness.

Universidad Politécnica de Cataluña, Barcelona TECH
Departamento de Tecnología de la Arquitectura
Centro de Políticas de Suelo y Valoraciones
Nicola Colaninno, Josep Roca Cladera

Instead, although Terrassa and Sabadell maintain higher values of texture compactness, they provide lower values for urban area. In this case, we have cities smaller than the most consolidated urban structures, such as Barcelona, or Sevilla, but that are undertaking a development affected by dynamics of metropolization. In the case of medium-sized cities, most provide an important dynamism in the urban growth process, and they are growing quite fast and may be considered to have reached an important role within the metropolitan space.

Figure 6.5 summarizes the six morphological dimensions for the cities detected as belonging to model (cluster) 2, i.e. Valencia, Palma de Mallorca, Terrassa and Sabadell. Here again, the values have been normalized to a scale ranging between 0 and 1 in order to enhance the interpretability of the values and the comparison between cases.

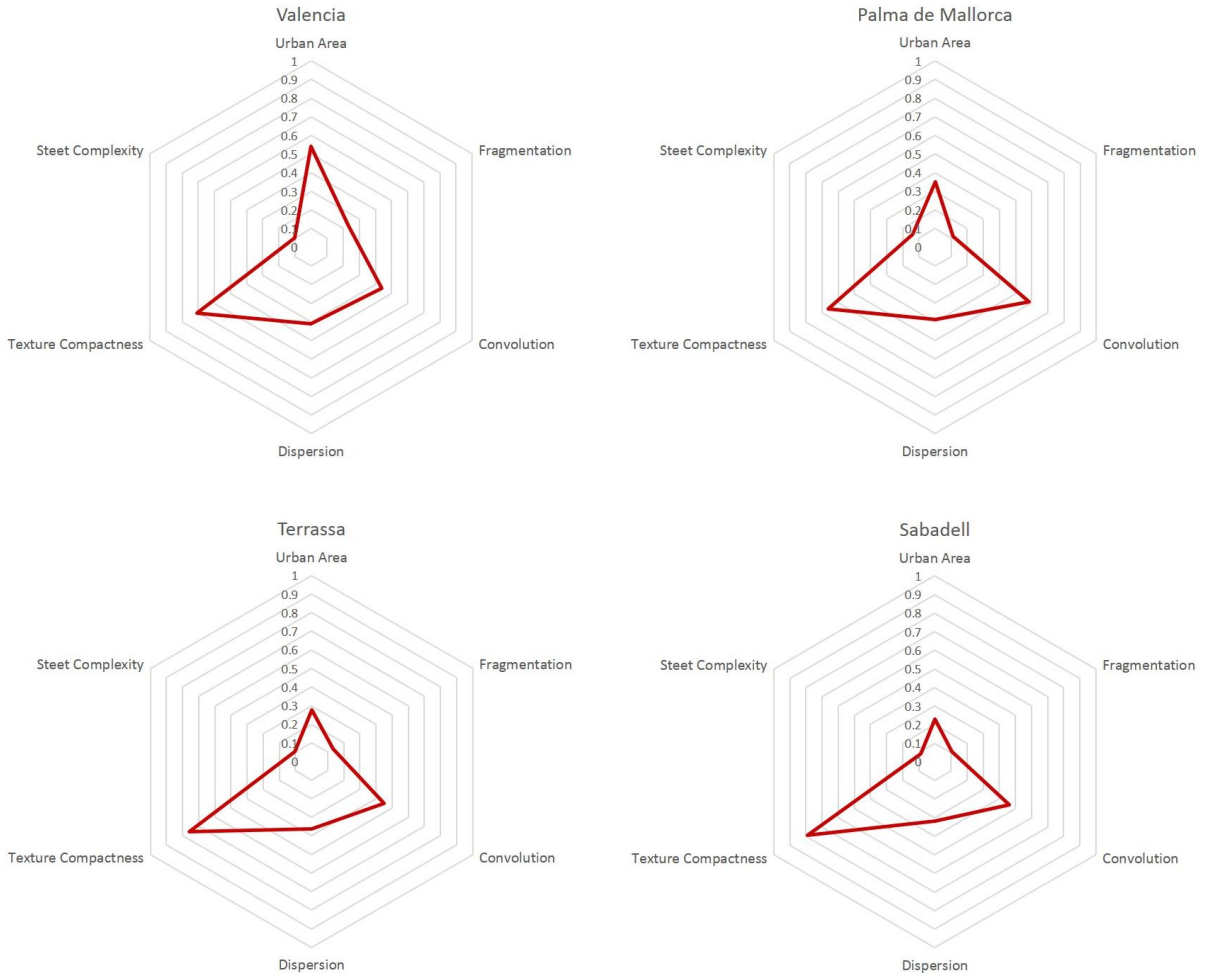

Fig. 6.5: Radar charts of the urban models for Valencia, Palma de Mallorca, Terrassa, and Sabadell (i.e. the cluster model 2), based on the behaviour of six morphological dimensions, normalized to a 0-1 scale (Source: By Authors)

The values of texture compactness and urban area tend to decrease as we move from model 1 toward model 6. Indeed, model 3 provides less texture compactness, with respect to the two previous models, while convolution and fragmentation increase. Models 4, 5, and 6 provide increasing levels of fragmentation and street network complexity, due to an increase in the "serpentine" structure of the streets (Shpuza, 2007), while texture compactness decreases, but convolution does not. Models 5 and 6, in particular, provide the lowest values of urban area, hence the impact in terms of land occupation is quite low.

The next figure (6.6) summarizes the urban outlines (already mentioned in figure 5.32 of Chapter 5), and the six morphological dimensions, using a radar chart representation, for the cities detected as belonging to the

models (cluster) 1, 2, 3, 4, 5, and 6, respectively, i.e. Barcelona, Terrassa, Roda de Berà, Piera, Dosrius, and Sant Aniol de Finestres. According to the previous representation, the values in the radar charts have been normalized to a scale ranging between 0 and 1 in order to enhance the interpretability of the values and the comparison between the cases.

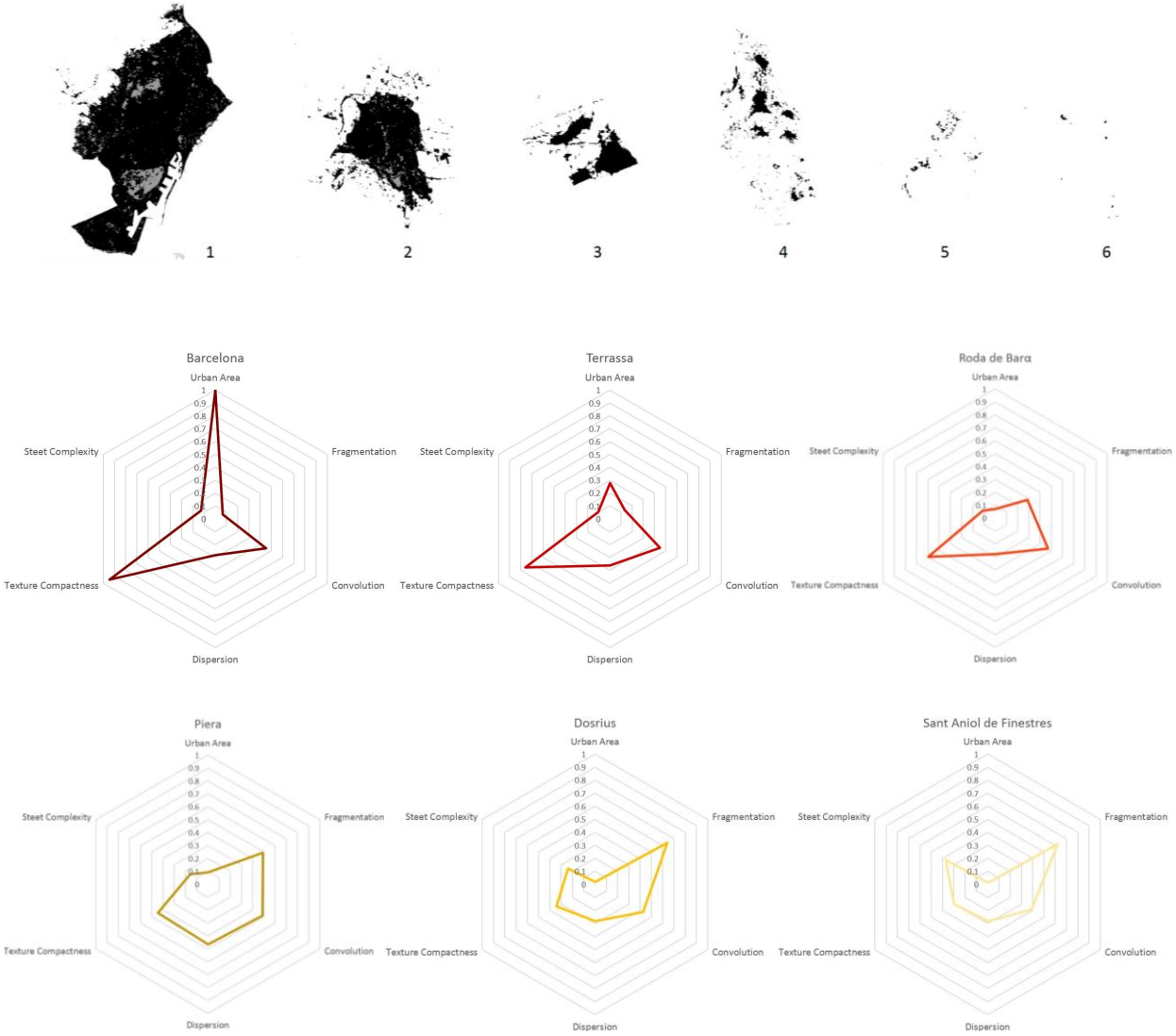

Fig. 6.6: Comparison between the urban outline, and the radar charts of the urban models for Barcelona, Terrassa, Roda de Berà, Piera, Dosrius, and Sant Aniol de Finestres, respectively cluster model 1, 2, 3, 4, 5, and 6, based on the behaviour of six morphological dimensions, normalized to a 0-1 scale (Source: By Authors)

Although only a set of morphological dimensions are used here for defining different urban models, such dimensions play a key role when one attempts to reveal certain fundamental features of urban form in terms of compactness versus urban sprawl. In particular, high levels of fragmentation, dispersion and convolution of the urban outline are highly linked to the sprawl phenomenon. In fact, the use of these dimensions facilitates measuring how the land development process has become more fragmented, for example. Moreover, they provide useful measurements for defining the degree of monocentrism or multi-centrism of the urban form, or even the degree of linearity of the urban pattern when it develops alongside rivers or spreads along major road networks or, as in our case, along the coastline.

Universidad Politécnica de Cataluña, Barcelona TECH
Departamento de Tecnología de la Arquitectura
Centro de Políticas de Suelo y Valoraciones
Nicola Colaninno, Josep Roca Cladera

In the same way, the increasing complexity of the street pattern (the "serpentine" pattern) often occurs in suburban areas characterized by low densities either in terms of population density or urban texture density. Therefore, the index of urban texture compactness (as used here) provides another relevant aspect to measure the sprawl phenomenon. In particular, if low values of urban texture compactness correspond to high values of the urban area (i.e. high land consumption), fragmentation, convolution, dispersion or street network complexity, we could infer that we are probably facing a case of urban sprawl.

Hence, even if this research is based on a synchronic analysis, i.e. it can explain morphological rules at a specific point in time and not the evolution over time, the findings of the cases of study provide some significant understanding about the physical pattern of the urban settlements along the geographical area under investigation. In particular, the analysis delineates a "snapshot" survey of the current models along the Mediterranean coast of Spain. With this survey, it could be possible to provide an initial analysis of those areas affected by urban policies that, during the last decades, have lead to "sprawled forms" instead of preserving the typical Mediterranean model mostly based on urban compactness.

We strongly believe that a comprehensive understanding of the urban sprawl phenomenon should rely on a temporal observation (i.e. a diachronic approach), as well as the use of further measures mainly related to population and functional flows (Marmolejo, et al., 2009; Roca, et al., 2011). For instance, two additional aspects concerning the urban growth phenomena (and the relation with the morphological aspects discussed here, which we aim to investigate further in the the future) are the population density[385], i.e. the number of people in the urban area (net density[386]), and the amount of land consumption, in terms of urban area in a specified geographical context (landscape). As in the example, we report the spatial distribution of the (net) population density[387] in the geographical area under investigation (Fig. 6.7), and the land consumption rate, dependent on the administrative limits of the municipalities (Fig. 6.8).

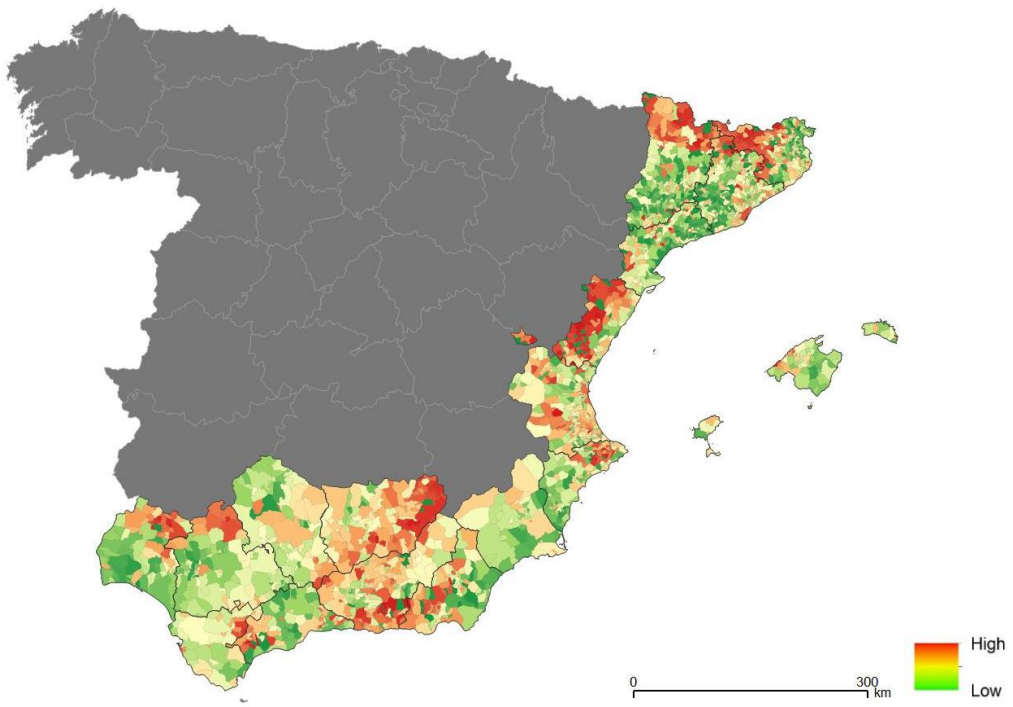

Fig. 6.7: Spatial distribution of the net population density (in 2011), i.e. inhabitants in urban area, along the Mediterranean coast of Spain, and dependent on municipal administrative division (Source: By Authors)

[385] *Population density measures a further generally recognized dimension of compactness or sprawl* (Huang, et al., 2007)

[386] Actually, the population density might be gross or net, depending on whether it refers to the number of inhabitants within the administrative limits, or the number of inhabitants in the urban land cover (Romano, et al., 2010)

[387] Population data has been taken from the National Statistics Institute of Spain (INE) http://www.ine.es/

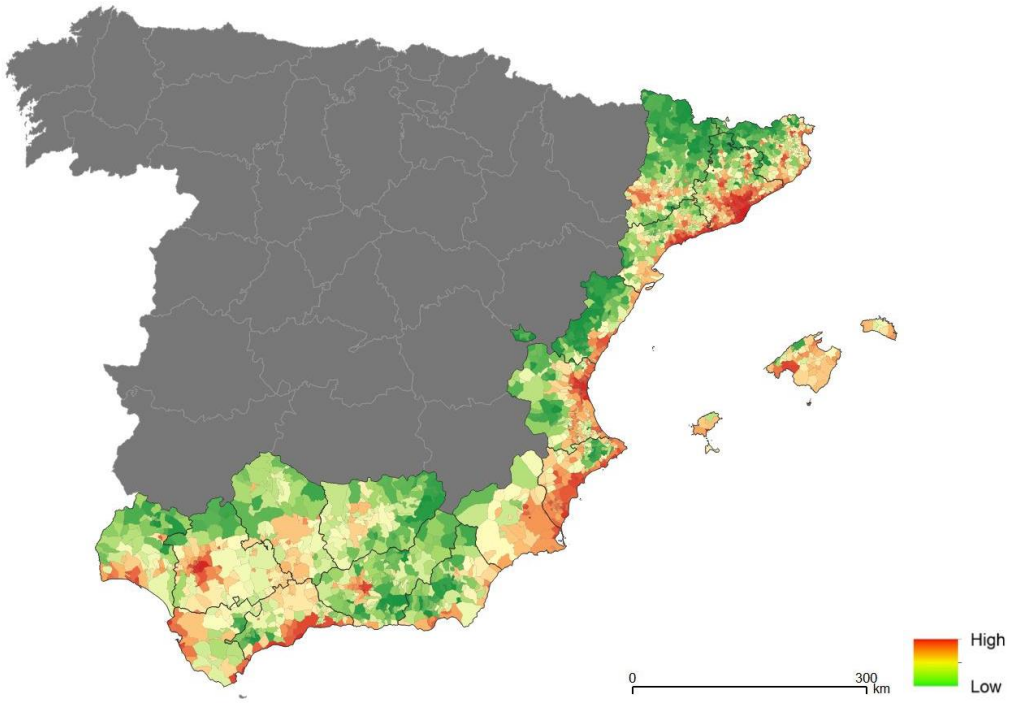

Fig. 6.8: Spatial distribution of the land consumption rate (in 2011), i.e. urban area in a limited spatial extent, along the Mediterranean coast of Spain, and dependent on the municipal administrative division (Source: By Authors)

Although we have not deeply discussed the incorporation of additional indices for urban modeling here, (such as the population density and the land consumption rate) it highlights the need for an integrated approach to urban analysis, i.e. based upon a wider range of features (not only morphological), which could lead to the beginning of a reliable overall sprawl index. In particular, if we look at the next image 6.9, which compares the urban models for the cities of Barcelona, Sevilla, and Malaga, it is clear that the introduction of further features enhances the capability of discriminating different urban models on the basis of a more comprehensive vision.

The city of Barcelona, for instance, provides high levels of urban area and land consumption, but on the other hand provides high level of population density (the urban sprawl often relies on low density values) and high levels of urban texture compactness.

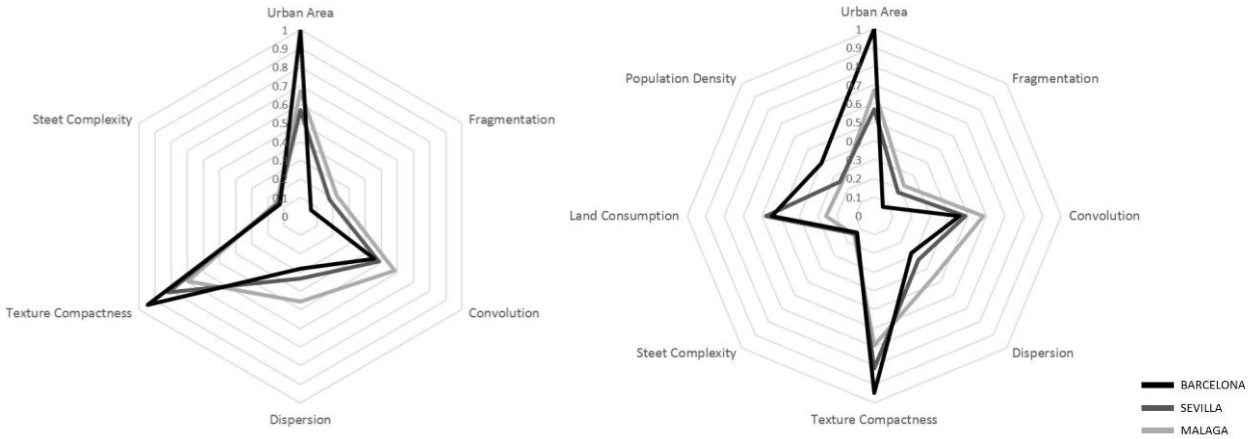

Fig. 6.9: Comparison between the urban models of Barcelona, Sevilla, and Malaga (cluster 1), based on just the six morphological features (left side), and in addition the enhanced set of indices based on including the (net) population density and the rate of land consumption (right side) (Source: By Authors)

6.2.3. Regarding Significant Factors that Affect the Urban Form: Topographic Effect, Coast Effect, and Metropolis Effect

Having set the syntax rules for spatial analysis of urban models, an important aspect to take into account for better understanding of growth dynamics is the analysis of the most significant factors behind the modelling of the urban form. Actually, *the major morphological factors of cities include natural determinants and human-made determinants* (Sun, 2013). Indeed, although the formal rules of the "urban object" are established by humans, the final outline of an urban settlement, besides the socio-economic dynamics, inevitably internalizes topographical and geographical factors[388]. In terms of the form of the urban agglomeration, degree of compactness of the urban texture and the complexity of the street network pattern in the urban environment maintains, to a certain extent, an important relationship with the natural environment that also needs to be investigated in order to exhaustively explain the dynamics of urban development.

The next image 6.10 shows a topographical map of the relief, derived from a SRTM-DEM (top left), and a map of the slope distribution (top right), for the geographical area under investigation. In addition, the urban land cover distribution (below left), and the classification of the morphological models (below right) are also provided.

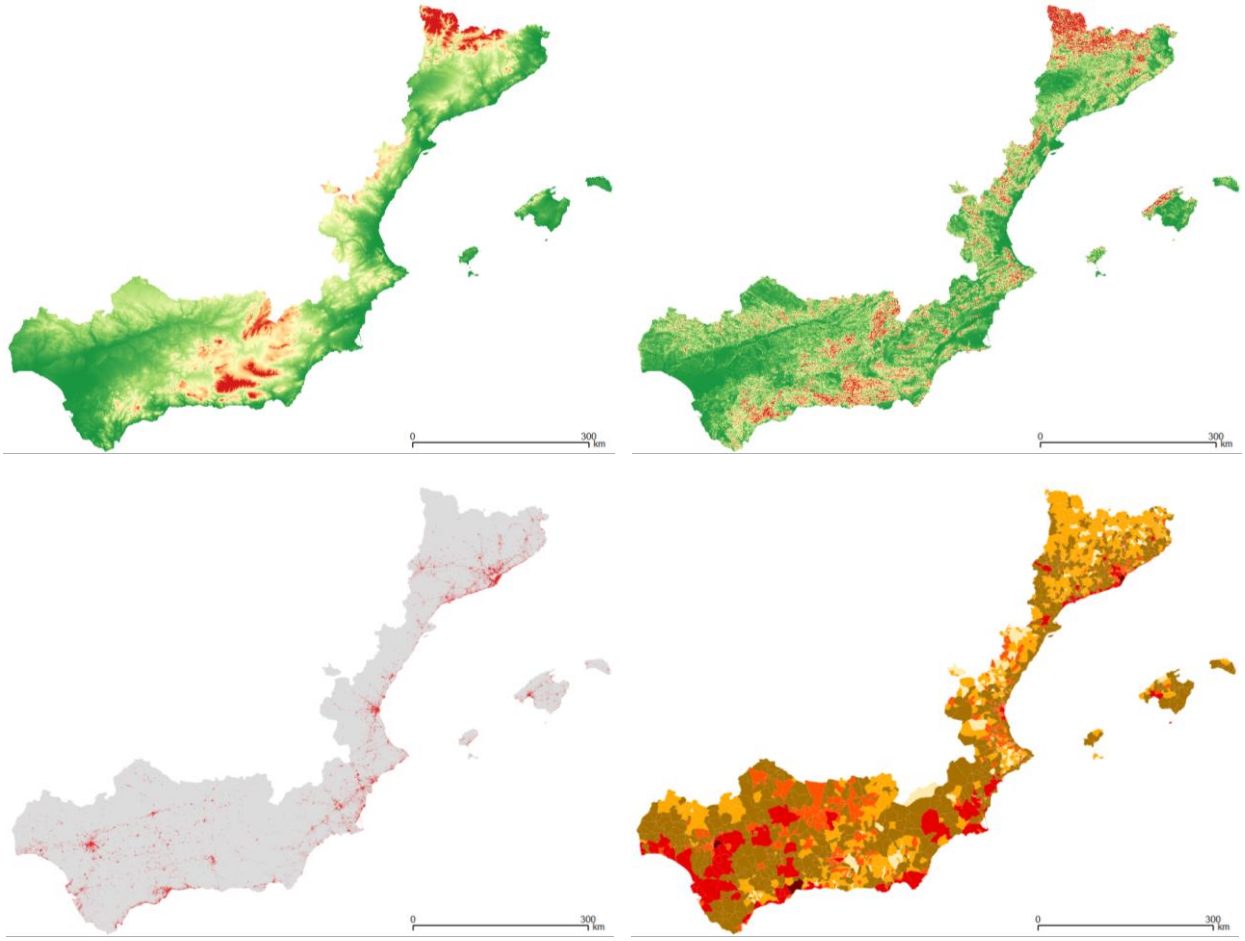

Fig. 6.10: Relief (top left), slope (top right), urban land cover (below left), and distribution of the urban morphological models (below right), along the Mediterranean coast of Spain (Source: By Authors)

[388] Morris (1994) argued that urban forms are dependent on natural occurrences that are basically linked to the geographical location of the cities. In particular, three main determinants depend on the nature of geographical locations, i.e. climate, topography and available construction materials (Morris, 1994; Sun, 2013).

Even if here the relationship between the urban forms and the topography have not been investigated and measured, future developments of the research should tackle such issues (among others). Indeed, if we take a look at the previous image 6.10, it is quite clear that most of the urbanization lies in the greenish colored areas (i.e. the low values) both for the relief map as well as for the slope. Often, the topography of the land defines natural restrictions to urban expansion and rules for the definition of administrative boundaries. Actually, according to Smith (1967), the *topography of a region has an underlying effect for the establishment or expansion of the urban settlements*; on the other hand, Morris (1994), *shows that in history and today, topography is a main part in the creation of urban dimension* (Sun, 2013).

If we build a scatter plot in two dimensions (figure 6.11), in which the x-axis is represented by the slope values (measured as a percentage) and averaged at a municipal level for all of the municipalities included in the area under investigation; and the y-axis provides the urban land occupation rate, measured as the amount of urban area in the municipal boundaries. The result depicts an exponential distribution of the observed data, which results in an abrupt decrease in the land occupation rate with slope values of between 10% and 20%.

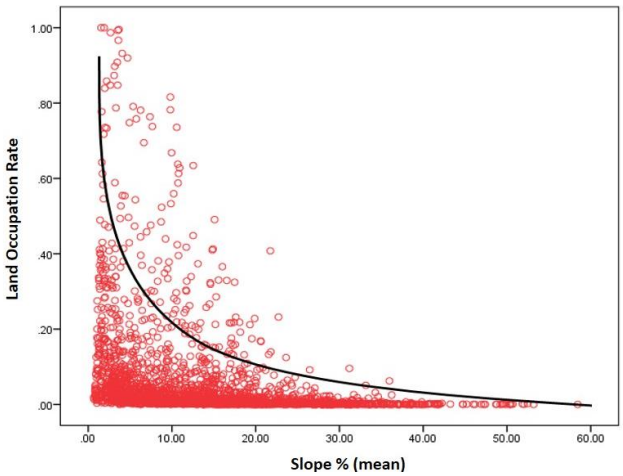

Fig. 6.11: Two-dimensional scatter plot of the relative distribution of the values of slope (averaged at municipal level), and the urban land occupation rate, for the whole geographical area under investigation (Source: By Authors)

A certain linear correlation is shown between two morphological dimensions used to classify different urban models, i.e. urban texture compactness and the street network complexity, with the slope features, as depicted in the graphs at figure 6.12.

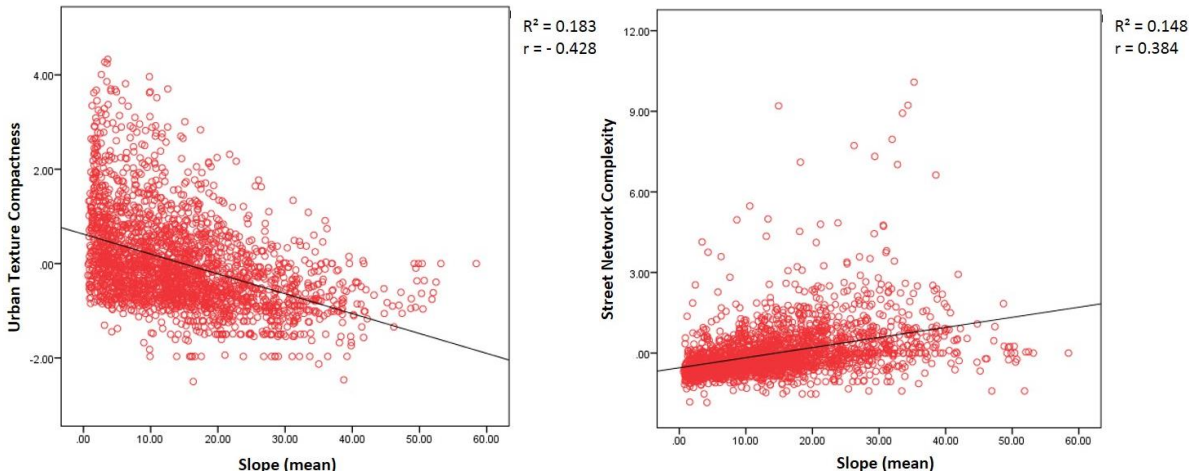

Fig. 6.12: Scatter plots: linear regression analysis and Pearson coefficient between slope and urban texture compactness (left side), and between slope and street network complexity (right side) (Source: By Authors)

Although a very small statistical correlation was found between the other morphological dimensions (i.e. urban area, fragmentation, convolution, and dispersion, and the slope features), some consideration should be given to the relationship between the spatial distribution of the morphological urban models and the topographic features, depicted in the previous figure 6.10. Urban model 2 (the red one) seems to be normally distributed either in areas with low slope, or around urban model (cluster) 1, i.e. cities like Barcelona, Sevilla, or Malaga (in our case study). This also happens for model 3, while model 4 appears more related to areas with low slope . However, models 5 and 6 are more typically found in areas with high slope., These are really just empirical observations (i.e. they are not currently supported by a scientific approach) but several studies have demonstrated (see chapter 2) that an increasing urban pressure has occurred in the last few decades in certain specific areas on the Mediterranean coast of Spain. Hence, we think it is critical to speculate about what the key factors are that have mainly affected such a phenomenon. In line with this speculation, the areas most affected by increasing urban expansion have been the coastal strip and the metropolitan areas. The phenomenon has been particularly relevant in those areas where both characteristics coincide, i.e. the metropolitan areas along the coastal strip, such as the cases of Barcelona, Valencia and Malaga. We are not speaking about the city itself, but mainly about the urban areas around it. Therefore, we could infer that, in addition to a "topographic effect", a "coast effect" and a "metropolis effect" are also relevant aspects to take into account when analyzing the urban growth phenomena.

In particular, "the coast effect" should be analyzed in relation to the production and consumption of leisure activities concerning tourism in certain geographical contexts, as is the case of those under investigation here. Urban areas subject to important seasonal tourist flows have different growth dynamics with respect to others, and often suffer from increased, but discontinuous, human-pressure. In most of the cases, this produces growth dynamics that are unsustainable from different points of view, those environmental and/or soci-economical. Moreover, from the morphological standpoint, coastal cities often reveal an asymmetrical growth in one direction, thus producing a gradual shift of the actual center with respect to the consolidated city center.

On the other hand, "the metropolis effect" is mostly related to socio-economic dynamics: such as the labor market and workflows, services, goods and population distribution, etc. In this way, as is the case for a metropolis, big markets and economic centres affect the spatial distribution and the form of the urban settlements, and their weights in terms of population (Imagine the previously cited cases of Barcelona, Sevilla, or Malaga).

The centripetal pull towards the center of the big cities, in conjunction with a centrifugal pull caused by congestion, productivity, and social issues tend to create concentric rings of urbanization around big cities, which are gradually less dense based on the distances to the center. This produces an exponential behaviour of urban densities and activities (similar to the one represented in the previous image 6.11 about the relation between land occupation and slope). This tends to decrease drastically as we move away from the center. Some important exceptions to the decrease of such a curve are provided by secondary centres (or sub-centers), which thus set up a hierarchical structures (Camagni, 2005) at territorial level.

The larger the central settlement (and the sub-centers) the greater the sphere of influence of the territorial structure, so that human pressure increases within the sphere of influence, and consequently all activities related to the urban development. Conversely, those cities too far from such a structure tend to link their functions to a limited scale basically restricted to the local demand, thus providing different urban forms.

6.2.4. The Mediterranean City: Towards Sprawled Cities?

From a global point of view, as argued by Levy (1999), *the modern city has undergone radical changes in its physical form*, both in terms of territorial expansion as well as in terms of internal physical transformations. The morphological approach to the spatial analysis of the urban environment has provided evidence that the syntax of the "traditional urban fabric" has changed dramatically. *Cities that were dense, compact and continuous have become diffuse, loose and discontinuous*. This has produced a radical shift in the urban model. Indeed, cities changed f*rom a closed fabric to a peri-urban fabric which is open and fragmented*; from a territorial system, made by the different urban elements such as plot, street, constructed space and open space, to an increasing presence of *autonomous and atomized elements which do not relate to each other*. Consequently, *this shift has been accompanied by a significant change in scale, with the appearance of imposing megastructures and relationships between buildings that are now only functional* (Levy, 1999).

The loss of compactness, the dramatic decreasing of the urban densities and the spread of the urban fabric over a more extensive territorial space, form part of a kind of urban phenomenon which began during the past century and has undergone an exponential increase (at global level) predominantly since the second half of the nineteenth century.

Actually, as claimed by Arellano & Roca (2010), *the low density and diffuse forms of urbanization have their origin in the improvement of urban transport systems that emerged throughout the nineteenth century. The appearance of subways was especially a key element that led to the gradual separation of residential and work, causing the incipient process of suburbanization that took place during the last third of the nineteenth century. As it is well known, the generalized use of the car as a way of private transportation in the early decades of the twentieth century reinforced the trend towards the dispersion of the population, generating new forms of suburban development and the construction of the ideal of "mobility and homeownership", which soon spread from the United States to the world* (Arellano & Roca, 2010).

Similarly within the European scenario, by the late sixties, many cities started to undergo an important change in their urban development. The most common phenomenon affecting big cities during these years was a growing decentralization, or de-urbanization, of the urban fabric and the demographic weight. This produced, as a consequence, an increasing loss of population from the inner city, which now tends to move towards the suburban areas (also termed peri-urban). In many cases, the new suburban structures are mainly configured as residential settlements, thus keeping a strong functional relationship with the city centre, The consequence is that the peripheral space suffers a loss of quality, in terms of urban landscape and services, and a generalized loss of identity (Benni, et al., 2007).

These kinds of dynamics, typical of the modern urban development, have been globally summarized with the famous term "urban sprawl". However, certain criticism arises when using such a concept for comparing urban models in different geographical contexts. Actually, as argued in the previous Chapter 2 (section 2.1.2), various forms of urban sprawl could be mentioned, dependent on their formal features. Indeed, as reported by Bhatta (2012), the concept of urban sprawl is quite difficult to define, seen within a number of studies such as those by Johnson (2001), Wilson et al. (2003), Roca et al. (2004), and Angel et al. (2007) among others. He also cites the *conceptual ambiguity of sprawl* underlined by Galster et al. (2001) which argued that *much of the existing literature is "lost in a semantic wilderness"*. Anyway, the term urban sprawl is often simultaneously used for defining patterns of land use, processes of land development, or causes and consequences of particular land-use behaviours. This means that *sprawl is used both as a noun (condition) and as a verb (process)* (Galster, et al., 2001; Bhatta, 2012).

Moreover, sprawl can be measured according to an absolute or relative scale (Bhatta et al. 2010a; Bhatta, 2012), i.e. a "black-and-white" distinction between sprawl and non-sprawl (or compactness) can be provided in absolute terms. A set of attributes can be taken into account and compared (either among different cities, different areas, and/or different temporal stages) when a relative approach to the analysis is undertaken. *In case of relative measurements, whether the city is sprawled or not is generally decided by the analyst, or even left without characterizing the sprawl. It is important to realize that relative measurements, most often fail to draw conclusion on sprawl, and a threshold used in one area cannot be used in other areas reliably* (Bhatta, 2012). At any rate, according to Bhatta (2012), no one has provided any straight answer regarding the optimal built-up growth rate or the per-capita consumption of land in a non-sprawling city. It is certain that we have faced, in the last decades, a unidirectional phenomena of massive and fast urbanization within several metropolitan contexts. Indeed, the sprawling growth phenomena has been not planned and measured properly in most cases.

Even at the European level, in many urban contexts, the classical "Mediterranean model", traditionally based on compactness patterns (such as closeness or mixed use) is giving way to something different. Actually, the challenge is to understand in which direction the urban models are developing, i.e. we need to quantify the present models of development, either at urban or territorial level, and measure the actual advantages and disadvantages. In line with this, we think that it does not make sense to measure urban development in absolute terms (i.e. the black and white approach), but in fact several measurements are required.

As argued by Lewis Mumford (1939), when a city can keep a compact urban structure in its physical form, lifestyle, good connection networks and a close relationship with its natural landscape, it is possible to obtain a good balance between development, living standards, growth and human relationships: stability, continuity,

closeness and mixing[389]. But the question is: What is the most suitable modern urban model able to guarantee such features?

Imagine two "typical" modern urban models, such as those depicted in the next pictures 6.13, and 6.14. Both samples come from Spain, and in particular along the Mediterranean coast, i.e., respectively, along the famous "Costa del Sol" in Andalucia (6.13), and in the urban area of Barcelona (6.14).

Fig. 6.13: Sample of urban sprawl in Spain, Costa del Sol, Andalucía (Sattlberger, 2014)

Fig. 6.14: Residential buildings along the *Gran Via* through *Barcelona* and *Hospitalet de Llobregat* (Source: By Authors)

Although most of the research about the urban sprawl phenomena basically focuses on analyzing those kinds of urban growth based on high levels of land consumption. This is mainly characterized by single-family houses in low-density neighborhoods, and in outlying areas far from the historic city centre (as is the case of the urbanization in the previous figure 6.13).

[389] Lewis Mumford. The City, documentary film. New York, 1939

We would like to ponder another question: Could overly high residential densities (as in the previous figure 6.14) also lead to certain problems of sustainability of urban growth? There are currently many examples of both models around the Mediterranean, which share the same urban space with the traditional city models. Certain areas, due to their differing aspects, either geographical or socio-economic (as highlighted in the previous section 6.2.3), suffer from these kinds of development even more so than others. Therefore, before wondering about the sprawl phenomenon in the Mediterranean area, we first need to quantify all the possible sprawling models, based on robust assumptions. Consequently, we need to understand what the most sustainable alternatives are because, *although accurate definition of urban sprawl is debated, a general consensus is that urban sprawl is characterized by unplanned and uneven patterns of growth, driven by a multitude of processes and leading to inefficient resource utilization* (Bhatta, 2012).

It is also critical to take into account the most common phenomena of modern day urban growth, often indicated as "urban sprawl". For example, the "Città Diffusa" of Indovina (1990) indicates a low density urbanization characterized by a high degree of horizontal connections. "Peri-urbanization", defined as the process of dispersion of urban areas in the territory, suburbanization, or counter-urbanization (Racine, 1967 and Dematteis, 2003, among others), can all be summed up by the concept of "metropolization" proposed by Camagni (1999), which interprets such dynamics of urban expansion (at European level), as "diffuse metropolization", "concentrated metropolization" and "set of urban and regional networks" (Benni, et al., 2007). This means that the analysis of the sprawl phenomenon currently should be interpreted also at territorial level, and not only in terms of urban fabric.

Indeed, for the case of Spain in particular, Nel·lo (2001), argued that the dreaded *misconfiguration*, is then directed at a *new configuration* (though still not achieved), based on different patterns of development, and on a new model of territorial structure which is still in transformation. Therefore, the process of city expansion over the territory produces the generation of a metropolitan space (always broadening). This may be accompanied by phenomena of demographic and economic decentralization, and relative homogenization, following the phases of a typical metropolitan development, i.e.: absolute concentration, relative concentration, relative decentralization and absolute decentralization[390] of population and activities[391]. Among the major Spanish cities, Barcelona, Madrid and Bilbao are in the later stages of this evolution, while these cities are still in the early stages: Sevilla (above all), Valencia, Malaga and Zaragoza (Nel·lo, 2001).

6.3. LIMITATIONS, GAPS AND FUTURE RESEARCH PROPOSALS

This study proposes an overall methodology for the analysis of urban patterns which is fundamentally based on two stages: the first one concerns the collection of primary data about the urban landscape (land cover detection); the second phase uses the previously obtained data to provide a geographical analysis about specific urban phenomenon. More specifically, it is intended to provide a proper description of certain formal (morphological) characteristics regarding the contemporary urban models within a given geographical area. The whole process, in addition to certain theoretical assumptions, relies on a technological approach for collecting and analysing the data which requires the use of two main tools i.e. remote sensing and GIS. In line with this, we have proposed methodological solutions that certainly give interesting results at each stage (i.e. concerning the land cover detection phase as well as the morphological analysis of the urban models). Nevertheless, certain criticism is necessary regarding both the methodological processes and the results at each phase of the analysis. In this section, we aim to highlight the main limitations, gaps and the possible future developments for research.

6.3.1. Land Cover Classification: Non-Site Accuracy and Methodological Suggestions

The first remarkable issue concerns the accuracy of the land cover data obtained through the use of a methodological process, based on remote sensing techniques, which was applied to satellite imagery from the Landsat mission. The Land Cover Base Classification (LCBC), as we have named it, was done for the year 2011 and

[390] Cheshire (1995) highlights the possibility of a phenomena of recentralization after the phase of absolute decentralization (Nel·lo 2001).
[391] See: Hall and Hay (1980); Van Den Berg et al. (1982); Cheshire and Hay (1989); Sau (1995).

for the whole Mediterranean coast of Spain using the administrative limits of the five Autonomous Communities in this area (i.e. Catalonia, Valencia, Murcia, Andalucía, and Balearic Islands). It was first evaluated with respect to other official databases during the previous Chapter 4 (see section 4.6). In particular, we included the European database of land cover known as CORINE (CLC) for the year 2006; the national database provided by the Information System of Land Cover in Spain (SIOSE) 2005; and the *Mapa de Cubiertas de Suelo de Cataluña* (MCSC) 2009, by CREAF, made for Catalonia only.

In addition to the regular accuracy assessment, which is strongly recommended for evaluating the validity of land cover classification systems, we also made non-site accuracy estimation of the results with respect to the other previously mentioned land cover systems (i.e. CLC 2006, SIOSE 2005, and MCSC 2009). The analysis basically consisted of comparing the final percentage of each land cover class at level I of the nomenclature, between the different land cover systems and with respect to the whole geographical area under investigation. In particular, the next image shows the case of Catalonia (6.15)

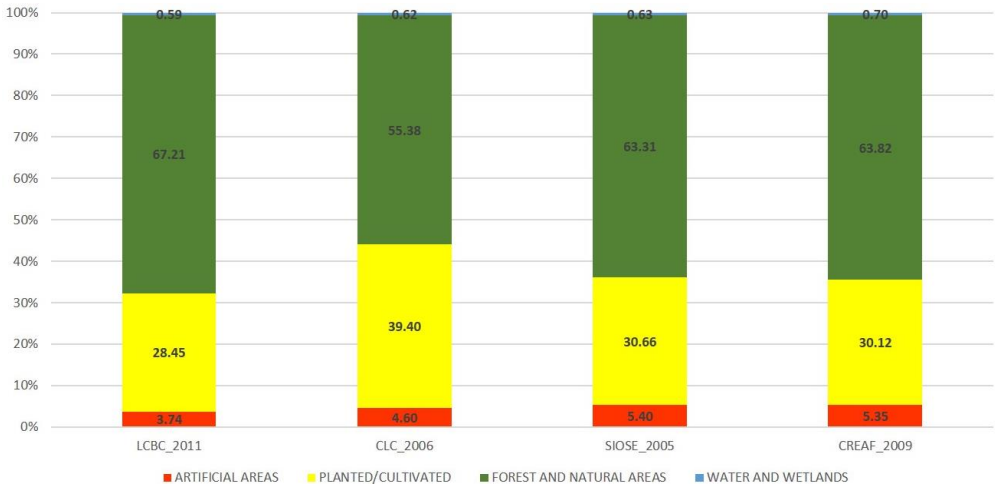

Fig. 6.15: A non-site accuracy assessment for the land cover classification in Catalonia: the Land Cover Base Classification (LCBC) 2011 was compared, respectively, with CORINE Land Cover (CLC) 2006, the Information System of Land Cover in Spain (SIOSE) 2005, and the *Mapa de Cubiertas de Suelo de Cataluña* (MCSC) 2009 from CREAF (Source: By Authors)

The comparison between land cover systems draws attention to some remarkable differences between the results, which require some consideration about several factors: the methodologies behind the classification processes, the imagery used to classify, as well as the final outline of the land cover classes and the most reliable operational scale to which the results can be referred.

In fact, first, it has to be taken into account that our classification system (LCBC) mainly relies on an automatic classification of land covers and photo-interpretation is only used for changing the improperly classified data from one class to another. Meanwhile, the other classification systems employ techniques of photo-interpretation for the on-screen digitizing of the land cover/land use classes. Moreover, in addition to the use of Landsat imagery, they include additional satellite data, such as SPOT and other ancillary data, in order to enhance the classification results. This approach not only allows certain improvements over the detection of the classes but also provides the capability of assigning different uses to the same land cover type, thus allowing parametric classifications, as is the case of the SIOSE system. At any rate, increased processing time and subjectivity of the interpretation also result from such an approach.

An automatic classification based on widely recognized algorithms of image processing allows more objectivity or, at least, allows the possibility of standardizing the results by repeating the classification process based on the same parameters. Besides, time and resources can be saved, thus allowing the management of larger geographical areas. Specifically, if we take a look at the results depicted in the previous figure 6.15, we note that the urban area detected by the LCBC system is significantly lower than the other systems. In the LCBC in particular, the urban area is detected as covering the 3.74% of the whole regional territory of Catalonia, which increases to

4.60% in the CLC, 5.35% in MCSC-CREAF, and 5.40% in SIOSE (although the latter classifications are more dated, i.e. 2006, 2009, and 2005, respectively).

Worth bearing in mind, we stress the idea that the classification proposed here relies on the extraction of land cover classes (not uses) directly based on the automatic interpretation of the pixel. Hence, the spatial resolution of the imagery is a key factor to take into account when assessing the results. Indeed, when one performs an on-screen digitalization of imagery certain subjective assumptions can be applied for discriminating those open spaces surrounded by urbanization. Here, the decision to assign such areas to the urban class, instead of to other categories, is up to the analyst, although certain general criteria could be previously established.

A machine applies an objective process of interpretation of the land cover, based on the physical characteristics of reflectance for each pixel in the image. Therefore, a lower amount of urban areas could be detected in the less urbanized areas (the suburban areas, for instance) than other approaches, simply because empty spaces are not "perceived" as urban (see the samples provided in figure 6.16).

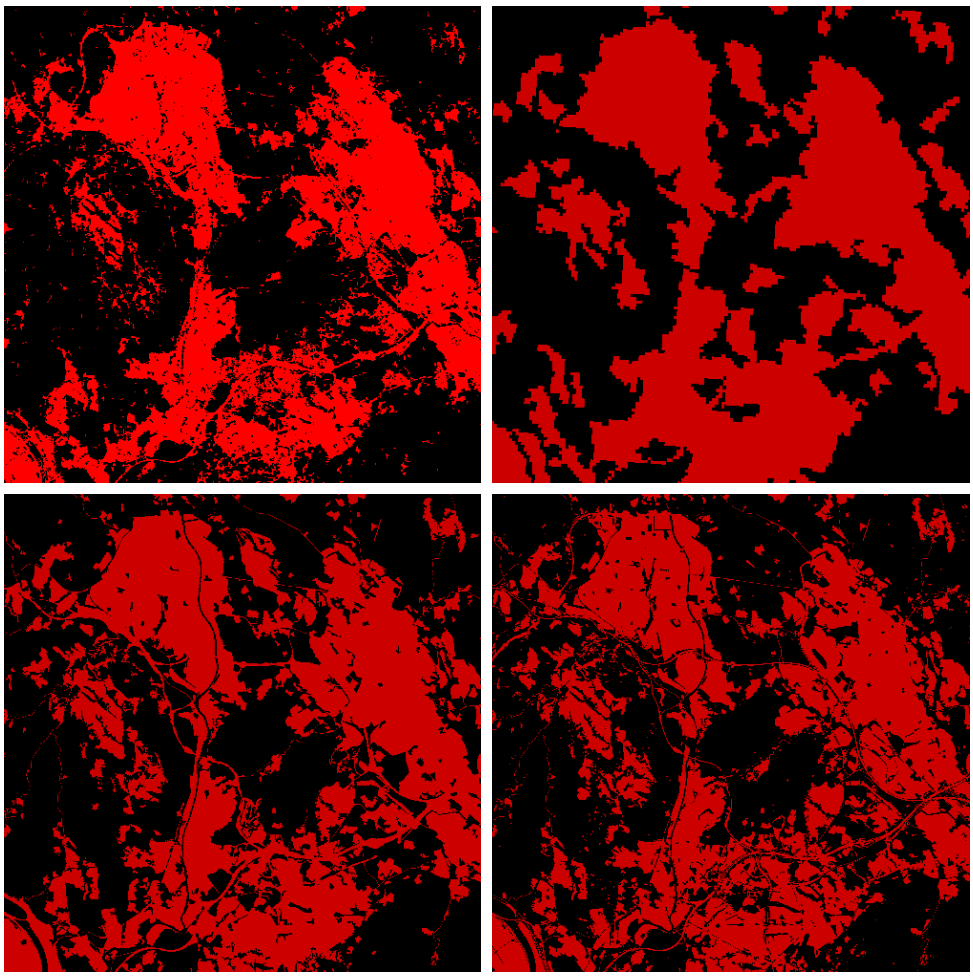

Fig. 6.16: A comparison of the results for the urban land cover classification for a sample in Catalonia, based on four different classification systems: Land Cover Base Classification (LCBC) 2011 (upper left); CORINE Land Cover (CLC) 2006 (upper right); Information System about Land Cover in Spain (SIOSE) 2005 (below left); and *Mapa de Cubiertas de Suelo de Cataluña* (MCSC) 2009 from CREAF (below right) (Source: By Authors)

The use of the "pixelate" results of the classification provided by an automatic process, as in the LCBC, is strictly linked to the operational scale of the analysis, according to the tables 4.10, and 4.11, discussed in the previous Chapter 4 (section 4.5.7.2). Of interest, the on-screen digitizing operations allow the use of the results at even more detailed operational scales, dependent on the imagery and ancillary data used.

Future developments at this point will rely on setting up an automatic methodology based on the spatial relationship between neighbouring areas, and buffering operations capable of providing an appropriate enhancement of the impact of the urban areas on the surrounding areas. This would reasonably produce more homogeneity between the different classification systems, thus improving the comparison.

With regard to the other land cover classes, i.e. planted/cultivated, forest and natural areas, water and wetlands; the most remarkable differences arise in comparison to the system CORINE, in which the planted/cultivated class reaches 39.40% of the total area, instead of 28.45% as is in LCBC, and the forest and natural class decreases to 53.38% with respect to the 67.21% of the LCBC. In terms of both planted/cultivated and forest and natural areas, certain similarity is remarkable if the LCBC system is compared with SIOSE and MCSC-CREAF, which provide, respectively 30.66% of planted/cultivated and 63.31% of forest and natural areas; and 30.12% of planted/cultivated, and 63.82% of forest and natural areas (figure 6.15). Water and wetlands provide similar percentages for LCBC, CORINE, and SIOSE, while higher values are detected in the case of the MCSC-CREAF system, which probably relies on a more detailed analysis[392].

Finally, regarding the classification methodology, future developments could also focus on:

- Investigating other clustering algorithms, such as the Spectral Angle Mapper[393] (SAM), for instance, which is *a physically-based spectral classification that uses an n-D angle to match pixels to reference spectra* (Kruse, et al., 1993; EXELIS, 2015);
- Reviewing the spectral library proposed for classifying Landsat imagery, including testing operations on other geographical areas (see section 4.5.4) and, if necessary, an improvement of the library;
- Reviewing the additional radiometric indices used for enhancing the raw Landsat imagery (section 4.5.5).

6.3.2. The Urban Morphological Analysis: Main Future Improvements

Regarding the morphological analysis, the review and the future improvements will rely on a few key points mainly concerning:

1. The definition of the most suitable landscape extent, as an alternative to the administrative boundaries, for computing the spatial metrics;
2. The embedding of the topographic dimension in the computing of morphological indices; i.e., measurements of area, perimeter, and distances between patches should be computed according to the "real" topographic outline, instead of according to plane geometry;
3. The inclusion of the third urban dimension (i.e. the average height of the built-up area) in the computation of morphological indices (as mentioned in the previous section 6.2.4, about the sprawl phenomenon);
4. The analysis of further indices, linked to the urban growth phenomena, such as the land consumption rate, or the population densities (as mentioned at section 6.2.2), capable of providing an exhaustive description of the urban sprawl if analysed in conjunction with the morphological features;
5. Planning a multi-temporal (dynamic) analysis of the indices, i.e. computing the spatial metrics at multiple temporal stages, in order to measure the evolution of the phenomena.
6. Providing statistical analysis for measuring the actual impact of the “topographic effect”, the “coast effect”, and the “metropolis effect”, on the urban growth phenomena (see section 6.2.3).

With respect to point 1, we have already discussed the “widely” debated issues concerning the most effective scale and spatial boundaries for urban analysis in section 5.3.1 of the previous Chapter. In particular, we have stressed the idea that, because urban planning, demographic data, and the socio-economic information are

[392] Although the different time periods of the classifications could produce certain criticism about comparing these systems, the idea of making the comparison depending on four main classes only, i.e. those at level I of the nomenclature, arose from the desire to compare those classes that, at a territorial level, could reasonably suffer little changes during relatively short time periods.

[393] *The algorithm determines the spectral similarity between two spectra by calculating the angle between the spectra and treating them as vectors in a space with dimensionality equal to the number of bands. This technique, when used on calibrated reflectance data, is relatively insensitive to illumination and albedo effects. Endmember spectra used by SAM can come from ASCII files, or spectral libraries, or you can extract them directly from an image (as ROI average spectra). SAM compares the angle between the endmember spectrum vector and each pixel vector in n-D space. Smaller angles represent closer matches to the reference spectrum. Pixels further away than the specified maximum angle threshold in radians are not classified* (Kruse, et al., 1993; EXELIS, 2015).

often linked to the administrative division of the territory; focusing the investigation on the administrative boundaries certainly provides, an interesting perspective and a useful analysis of certain urban dynamics. At any rate, some variability can occur in terms of administrative division over a time period. For example, in Spain, between 1990 and 2006, the administrative limits changed for a certain number of municipalities (Romano, et al. 2010). Hence, because this issue could affect a multi-temporal analysis, we should investigate further reliable methods for delimiting the urban extent. This can be based on buffering operations, distances from urban patches or other morphological approaches. However, it would be useful to find an effective way to make spatial indices (measured depending on such approaches) interactive with administrative boundaries, in order to allow the use of demographic and socio-economic data.

The availability of the elevation data, using the Digital Elevation Model (DEM), allows us to satisfy the purpose at point 2. This permits the inclusion of the topographic features of the ground contour within the computation of those spatial metrics that rely on use of measurements such as area, perimeter, and/or distances between objects. Indeed, here we computed these measurements using Euclidean geometry. If we take into account the actual ground contours (i.e. we compute the "real" urban profile), the indices could provide significantly different results in most of the cases. A further experiment to conduct would be the comparison of spatial indices computed using Euclidean geometry and the same indices computed for the actual ground contours, in order to evaluate the degree of divergence.

Point 3 concerns the study of urban forms, not only depending on the two-dimensional outline that the city draws on the ground, but instead, by including the third dimension of the city, i.e. the height of the built-up area. Actually, according to Nivola (1999), and as depicted in figure 6.17, urban settlements grow in (only) four directions, i.e. *by crowding (IN), by increased density and height, such as skyscrapers (UP), by sprawl, known in many cases as "oil spill" (OUT), and by subterranean development (DOWN)* (Nivola, 1999; Lavalle, et al., 2002).

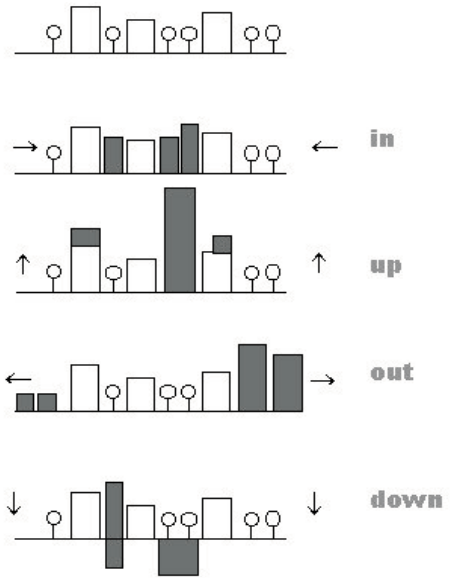

Fig. 6.17: Theoretical scheme of the four possible directions of growth of the urban settlements (Source: Nivola, 1999; Lavalle, et al., 2002)

With regard to the previous scheme about urban growth directions, we have to point out that our study mainly focuses on analysing the forms of the urban outline produced by a two-dimensional growth process, i.e. by crowding ("IN"), and by sprawl ("OUT"). So, what happens with the other dimensions of growth? On one hand, the "DOWN" dimension would be practically impossible to detect through the use of common sensors, either optical or radar. But, on the other hand, the use of high resolution radars or other remote sensing technologies that use laser (LiDAR, for instance) can allows us to detect the elevation values, hence the "UP" dimension of the urban growth. Therefore, the availability of such data enlarges the scenario for the morphological study of the existing urban

models (as also previously pointed out at section 6.2.4, figures 6.13 and 6.14) and the different kinds of urban sprawl as well.

We could speculate about what kind of urban model is provided by a (Mediterranean?) city like Benidorm (figure 6.18), for instance. Is this the "new" model, or future, of the Mediterranean city, or is it even a different example of urban sprawl? Perhaps a "3D sprawl"?

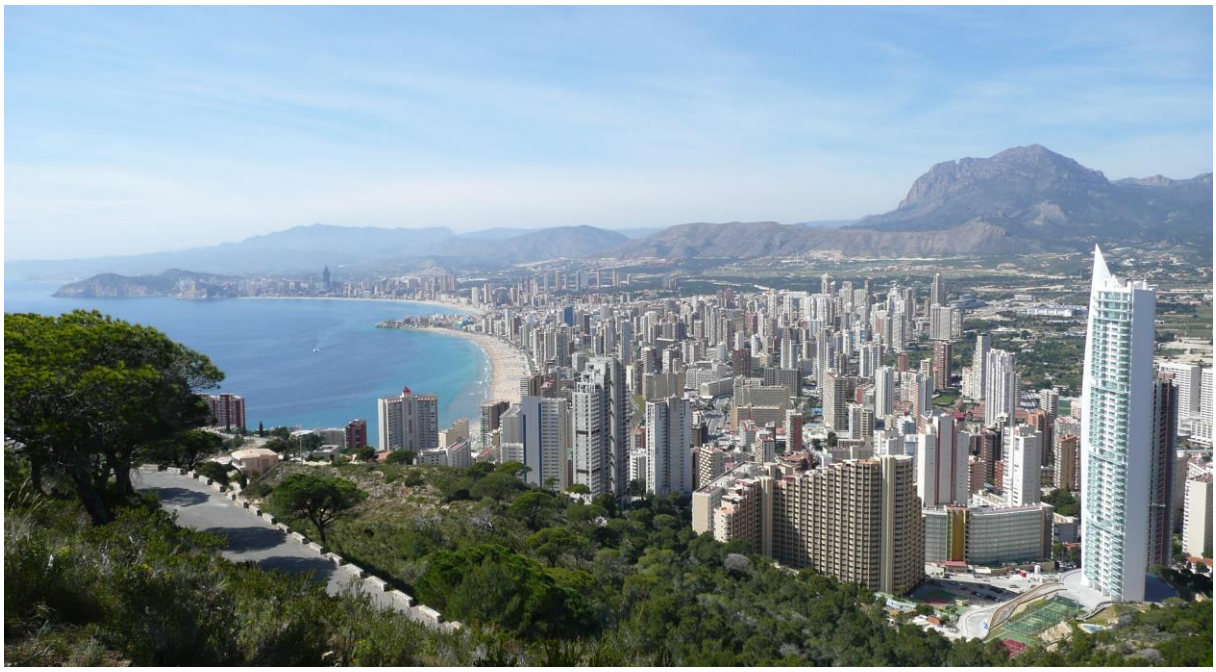

Fig. 6.18: A view over the city of Benidorm, along the Costa Blanca in Alicante, in the Autonomous Community of Valencia (Source: en.wikipedia.org)

The significance of setting up an integrated analysis of the urban growth phenomena, dependent on several dimensions and not only on morphological features (as emphasized at the previous point 4), has already been highlighted in the previous section 6.2.2. We have pointed out the significance of discovering the relationship between the morphological aspects of the urban environment with further indices related to the urban growth phenomena (such as the land consumption rate or the population densities).

It is reasonable to infer that indices of socio-economic structure of the cities are also strongly related to the urban form. Moreover, it is critical to perform adequate testing operations upon indices, in order to observe the weight of each index upon the phenomenon under investigation, i.e. which measurements affect outputs more than others. Indeed, this should be a further issue to investigate.

As emphasized at point 5, a multi-temporal examination is generally necessary when one attempts to provide a reliable analysis of the urban growth phenomena, because we face dynamic processes. Hence, we should provide both exploratory and explanatory analyses. In particular, the exploratory analysis mainly focuses on mapping the actual spatial distribution of any indicators and discovering significant patterns. This approach can compare and evaluate the different patterns of urban outlines according to a synchronic analysis. In contrast, the explanatory analysis aims to investigate the evolution over time of the phenomenon under investigation (diachronic analysis), and explain complex spatial cause-effect relationships. The exploratory analysis can help modellers to develop hypotheses regarding urban growth processes (Cheng, 2003). Moreover, the availability of a multi-temporal observation is also fundamental for spatial simulation methods (such as cellular automata and agent-based modelling).

6.4. FINAL REMARKS

The broader concept of urban development implies changes, growth or decline. The term includes the physical, socio-economic and environmental dimensions. Physically and functionally, urban development includes both new development and urban redevelopment. In contrast to decline, growth involves the transition into urban or non-urban activities and spaces. The physical aspects of urban growth are related to land cover, the functional to land use. Hence, temporal and spatial urban growth indicates the spatial and temporal dimensions of land cover/land use change at the level of the urban landscape (Cheng, 2003).

According to these previous statements, we can exemplify our work as mainly focused on studying the physical dimension of the urban landscape, i.e. based on the analysis of urban land cover. Moreover, as previously emphasized, the analysis relies on a synchronic comparison of different urban land cover configurations in the geographical area that comprises the Spanish (administrative) regions along the Mediterranean coast.

The processes of collecting suitable information concerning the urban land cover, the analysis of spatial metrics, and the classification of a number of similar models of urban configuration, have been based on the integrated use of two main technologies. These are: remote sensing (RS) and the Geographical Information Systems (GIS). Indeed, *as a result of the rapid development of remote sensing (RS) and geographical information sciences (GIS) and techniques, increasingly large-scale studies of urban development have been facilitated* (Masser, 2001; Cheng, 2003).

As argued by Cheng (2003), *we need to develop innovative methodological frameworks for understanding the interaction between spatial patterns and processes*. This research, prior to analysing such an interaction, focused on providing a preliminary perspective of the matter by first understanding the spatial patterns within urban land cover. Since we can consider the morphological dimension of the urban patterns as a key component of the most debated urban phenomenon, i.e. the urban sprawl, we believe that the quantitative approach provided here suggests a suitable estimation of the morphological component of the sprawl. This can evaluate the indicators of fragmentation, dispersion and complexity of the urban land cover, in addition to features of compactness for urban texture and the street network.

Beyond the results, we believe that the main value of the research relies on demonstrating the potential for the integrated use of technologies, such as GIS and remote sensing (RS), in land management and spatial planning. Indeed, this is in line with the current advances in the technological approach towards spatial analysis.

We aimed to suggest a suitable approach for the overall analysis of key environmental aspects (such as vegetation, water, agriculture, and, in particular the built-up environment). These include the generation of primary data about land cover, up to the spatial analysis of different growth dynamics and focused mainly on the urban landscape. In fact, the research provides important background information concerning those basic technical issues for GIS, RS, spatial analysis, and statistics. Our main focus is urban analysis through the use of such technologies and techniques.

This research also demonstrates a way of obtaining and handling spatial data and analysis at global level from scratch, and in many cases by using freely available information and open-source software. Hence, it seems quite obvious that this kind of approach can provide useful tools for environmental monitoring and governing. The main users, at which the research is directed, are urban planners and decision-makers who often need updated and reliable information about the territory for land management and planning.

However, although we proposed a technological approach to the spatial analysis here, it seems only right to stress the idea that technology and data are an indispensable support for urban planning, and that these are only tools that need a human element in order to be really reliable. Actually, as warns Nel·lo (2001), “the simple extrapolation of trends often leads to absurd conclusions, while more complex analysis requires clairvoyance to distinguish between structural and circumstantial elements. Even if this is to be achieved, we must also be able to find out which factors prevail over the others in a fast changing world. This will then help to advance hypotheses regarding which of the numerous and possible futures that could materialise. So, in trying to predict the future based on current trends, there is a risk to project one's own fears, and hopes. The future of a city cannot be predicted, but it can be designed. We cannot say with any certainty how the city will be, but we can decide how we want it to be”.

BIBLIOGRAPHY

Alexander, C. (1965). A city is not a tree. *Architectural Forum*(122), pp. 58–62.

Alexander, C., Ishiwaka, S., Silverstein, M., Jacobson, M., Fiksdahl-King, I., & Angel, S. (1977). *A Pattern Language: Towns, Buildings, Construction.* New York: Oxford University Press.

Allen, T., O'Neill, R., & Hoekstra, T. (1987). Inter-level relations in ecological research and management: some working principles from hierarchy theory. *Journal of Applied Systems Analysis*(14), pp. 63-79.

Alonso, W. (1964). *Location and land use.* Cambridge MA: Harvard University Press.

Anas, A., Arnott, R., & Small, K. (1998). Urban spatial structure. *Journal of Economic Literature*(36), pp. 1426–1464.

Anderson, J. (1971). Land use classification schemes used in selected recent geographic applications of remote sensing. *Photogramm.Eng., 37*(4), pp. 379-387.

Anderson, J., Hardy, E., Roach, J., & Witmer, R. (1976). *A Land Use And Land Cover Classification System For Use With Remote Sensor Data.* United States Department of the Interior. Washington: United States Government Printing Office.

Angel, S., Parent, J., & Civco, D. (2007). Urban sprawl metrics: an analysis of global urban expansion using GIS. *Proceedings of ASPRS 2007 annual conference.* Tampa, 7–11 May. Retrieved from http://clear.uconn.edu/publications/research/tech_papers/Angel_et_al_ASPRS2007.pdf

Angel, S., Parent, J., & Civco, D. (2010). *The Fragmentation of Urban Footprints: Global Evidence of Sprawl, 1990-2000.* Cambridge, MA: Lincoln Institute of Land Policy.

Angel, S., Parent, J., & Civco, D. L. (2010). Ten compactness properties of circles: measuring shape in geography. *Canadian Geographer-Geographe Canadien, 54*(4), pp. 441–461.

Angel, S., Parent, J., Civco, D., & Blei, A. (2010). *Atlas of Urban Expansion.* Cambridge MA: Lincoln Institute of Land Policy. Retrieved from http://www.lincolninst.edu/subcenters/atlas-urban-expansion/

Angel, S., Parent, J., Civco, D., & Blei, A. (2010). *The Persistent Decline in Urban Densities: Global and Historical Evidence of 'Sprawl'.* Lincoln Institute of Land Policy.

Angel, S., Parent, J., Civco, D., Blei, A., & Potere, D. (2010). *A Planet of Cities: Urban Land Cover Estimates and Projections for All Countries, 2000-2050.* Lincoln Institute of Land Policy.

Angel, S., Parent, J., Civco, L., & Blei, A. (2011). *Making Room for a Planet of Cities.* Cambridge: Lincoln Institute of Land Policy.

Angel, S., Sheppard, S., & Civco, D. (2005). *The dynamics of global urban expansion.* Washington, DC: The World Bank, Transport and Urban Development Department.

Angel, S., Sheppard, S., Civco, D., Chabaeva, A., Gitlin, L., Kraley, A., . . . Buckley, R. (2005). *The dynamics of global urban expansion.* The World Bank, Transport and Urban Development Department, Washington, DC.

Anji Reddy, M. (2008). *Remote Sensing and Geographical Information Systems.* Hyderabad: BS Publications.

Antrop, M. (2004). Landscape change and the urbanization process in Europe. *Landscape and Urban Planning, 67*(1-4), pp. 9-26.

Arellano, B., & Roca, J. (2010). The urban sprawl: a planetary growth process? An overview of USA, Mexico and Spain. *6th International Conference Virtual City and Territory.* Mexicali: Universidad Autónoma de Baja California (UABC)/Universitat Politècnica de Catalunya (UPC).

Arino, O., Kalogirou, V., Perez, J., Bontemps, S., Defourny, P., & Van Bogaert, E. (2011). *GLOBCOVER 2009. Products Description and Validation Report.* European Space Agency & Université Catholique de Louvain.

Arnold, C., & Gibbons, C. (1996). Impervious surface coverage: The emergence of a key environmental indicator. *Journal of the American Planning Association*(62), pp. 243-258.

Arribas-Bel, D., Nijkamp, P., & Scholten, H. (2011). Multidimensional urban sprawl in Europe: A self-organizing map approach. *Computers, Environment and Urban Systems*(35), pp. 263-275.

Asami, Y., Kubat, A., Kitagawa, K., & Iida, S. (2002). *Introducing third dimension on space syntax: application on the historical Istanbul.* Center for Spatial Information Science (CSIS). Tokyo: University of Tokyo.

Ascher, F. (1995). *Métapolis ou l'avenir des villes.* Paris: Editions Odile Jacob.

Ather, A. (2009). *A Quality Analysis of OpenStreetMap Data. M.Sc. Thesis.* London, UK: University College London.

Augé, M. (1992). *Non-Lieux. Introduction à une anthropologie de la surmodernité* (La librairie du XXI siècle ed.). Paris: Seuil.

Bakker, W., Feringa, W., Gieske, A., Gorte, B., Grabmainer, K., Heckner, C., . . . Tempfli, K. (2009). *Principles of Remote Sensing.* (K. Tempfli, N. Kerle, G. C. Huurneman, & L. L. Janssen, Eds.) Enschede, The Netherlands: The International Institute for Geo-Information Science and Earth Observation (ITC).

Baldridge, A., Hook, S., Grove, C., & Rivera, G. (2009). The ASTER spectral library version 2.0. *Remote Sensing of Environment*(113), pp. 711–715.

Ball, G., & Hall, D. (1967). *Isodata, a novel method of data analysis and pattern classification.* Menlo Park, California: Stanford Research Institute.

Bannari, A., Huete, A., Morin, D., & Zagolski, F. (1996). Effets de la Couleur et de la Brillance du Sol Sur les Indices de Végétation. *International Journal of Remote Sensing*(17(10)), pp. 1885-1906.

Bardossy, A., & Schmidt, F. (2002). GIS approach to scale issues of perimeter-based shape indices for drainage basins. *Hydrological Sciences Journal (Journal Des Sciences Hydrologiques), 47*(6), pp. 931–942.

Baret, F., & Guyot, G. (1991). Potentials and limits of vegetation indices for LAI and APAR assessment. *Remote Sensing of Environment*(35), pp. 161-173.

Baret, F., Guyot, G., & Major, D. (1989). *TSAVI: A vegetation index which minimizes soil brightness effects on LAI or APAR estimation.* Vancouver, Canada: 12th Canadian Symposium on Remote Sensing and IGARSS'90.

Barredo, J. I., Kasanko, M., Demicheli, L., McCormick, N., & Lavalle, C. (2002). *Modelling the future of cities using cellular automata: the MOLAND methodology.* Thessaloniki: Spatial information and social processes: European and Greek experience in G.I.S.

Barredo, J. I., Lavalle, C., Demicheli, L., Kasanko, M., & McCormick, N. (2003). *Sustainable urban and regional planning: The MOLAND activities on urban scenario modelling and forecast.* European Commission, Joint Research Centre. Luxembourg: Office for Official Publications of the European Communities.

Baskent, E., & G.A., J. (1995). Characterizing spatial structure of forest landscapes. *Canadian Journal of Forest Research*(25), pp. 1830-49.

Batty, M. (1976). *Urban Modelling. Algorithms, Calibrations, Predictions.* Cambridge: Cambridge University Press.

Batty, M. (1998). Urban evolution on the desktop: simulation with the use of extended cellular automata. *Environment and Planning A*(30), pp. 1943-1967.

Batty, M. (2008). *Cities as Complex Systems: Scaling, Interactions, Networks, Dynamics and Urban Morphologies.* University College London (UCL). London: Centre for Advanced Spatial Analysis (CASA).

Batty, M., & Longley, P. A. (1994). *Fractal Cities: A Geometry of Form and Function.* San Diego, CA.: Academic Press.

Batty, M., & Xie, Y. (1996). Preliminary evidence for a theory of the fractal city. *Environment and Planning A*(28), pp. 1745–1762.

Bell, K., & Irwin, E. (2002). Spatially explicit micro-level modelling of land use change at the rural–urban interface. *Agricultural Economics*(27), pp. 217–232.

Bellod Redondo, J. F. (2007). Crecimiento y especulación inmobiliaria en la economía española. *Principios*(8).

Benevolo, L. (1980). *The history of the city.* Cambridge, MA: MIT Press.

Benni, S., Paolinelli, G., Torreggiani, D., & Tassinari, P. (2007). Il mosaico paesistico periurbano: analisi territoriali nel quadro della pianificazione integrata. *Proceedings of the XII International Interdisciplinary Conference: will, freedom and necessity in the creation of landscape cultural mosaic.* Cividale del Friuli. UD.

Berg, L. v., Drewet, R., Klaasen, L. H., Rossi, A., & Vijverberg, C. H. (1982). *A Study of Growth and Decline.* Oxford, New York, Totonto, Sydney, Paris, Frankfurt: Pergamon Press.

Berry, B. (1976). Urbanization and Counter-Urbanization. *Urban Affairs Annual Review*(22).

Berry, B. (1980). Urbanization and Counterurbanization in the United States. *Annals of the American Academy of Political and Social Science, Changing Cities: A Challenge to Planning*(451), pp. 13-20.

Bhatta, B. (2010). *Analysis of urban growth and sprawl from remote sensing data.* Heidelberg: Springer.

Bhatta, B. (2012). *Urban Growth Analysis and Remote Sensing. A Case Study of Kolkata, India 1980-2010* (SpringerBriefs in Geography ed.). Dordrecht: Springer Netherlands.

Bhatta, B., Saraswati, S., & Bandyopadhyay, D. (2010a). Urban sprawl measurement from remote sensing data. *Applied Geography, 30*(4), pp. 731–740.

Birth, G., & McVey, G. (1968). Measuring the color of growing turf with a reflectance spectroradiometer. *Agronomy Journal*(60), pp. 640-643.

Bishop, C. (2006). *Pattern Recognition and Machine Learning.* Singapore: Springer.

Black, T. (1996). The Economics of Sprawl. *Urban Land*(55 (3)), pp. 6-52.

Blaschke, T., & Strobl, J. (2001). What's wrong with pixels? Some recent development interfacing remote sensing and GIS. *GeoBIT/GIS*(6), pp. 12-17.

Blázquez, M., Murray, I., & Artigues, A. A. (2011). La balearización global. El capital turístico en la minoración e instrumentación del Estado. *Investigaciones Turísticas*(2), 01-28.

Bocco, G., Mendoza, M., & Velazquez, A. (2001). Remote sensing and GIS-based regional geomorphological mapping - a tool for land use planning in developing countries. *Geomorphology*(39), pp. 211–219.

Bogaert, J., Rousseau, R., Van Hecke, P., & Impens, I. (2000). Alternative area-perimeter ratios for measurement of 2-D shape compactness habitats. *Applied Mathematics and Computation*(111), pp. 71-85.

Bontje, M. (2001). *The challenge of Planned Urbanization. Urbanization and national urbanization policy in the Netherlands in a Northwest-European perspective.* Amsterdam study centre for the Metropolitan Environment, Department of Geography and Planning. Amsterdam: University of Amsterdam.

Bossard, M., Feranec, J., & Otahel., J. (2000). *CORINE land cover technical guide – Addendum 2000.* European Environment Agency.

Bourne, L. (1989). Are new urban forms emerging? Empirical tests for Canadian urban areas. *The Canadian Geographer*(4), pp. 312-328.

Brazil, L., Cavalcanti, H., & Longo, O. (2014). Cities and sustainability: how to involve the engineers. In S. Zubir, & C. Brebbia, *The Sustainable City VIII: Urban Regeneration and Sustainability* (pp. 405-412). WIT Press.

Brian, B. (1965). The retail component of the urban model. *Journal of the American Institute of Planners, 31*(2).

Brueckner, J. (1987). The structure of urban equilibria: A unified treatment of the Muth-Mills model. In E. Mills, *Handbook of Regional and Urban Economics* (pp. 821-845). New York: Elsevier.

Brueckner, J. (2000). Urban sprawl: diagnosis and remedies. *International Regional Science Review, 23*(2), pp. 160-171.

Brueckner, J., & Fansler, D. (1983). The Economics of urban sprawl: Theory and evidence on the spatial sizes of cities. *Review of Economics and Statistics*(55), pp. 479-482.

Burchell, R., Shad, N., Listokin, D., Philips, H., Downs, A., Siskin, S., . . . ECONorth-west. (1998). *Costs of Sprawl - Revisited.* Washington, DC: National Academy Press.

Burchfield, M., Overman, H., Puga, D., & Turner, M. (2006). Causes of sprawl: A portrait from space. *Quarterly Journal of Economics*(121(2)), pp. 587-633.

Burchfield, N., Overman, H., Puga, D., & Turner, M. (2004). *The Determinants of Urban Sprawl: A Portrait from Space.* University of Toronto.

Burdett, M. (2015). *Economic activity in urban areas*. Retrieved June 2015, from IS Launchpad: Humanities resources: http://islaunchpad.weebly.com/economic-activity-in-urban-areas.html

Burgess, E. (1925). The Growth of the City. In R. Park, E. Burgess, & R. McKenzie, *The City.* Chicago and London: The University of Chicago Press.

Burgess, E. (1925). The growth of the city: an introduction to a research project. In R. Park, E. Burgess, & R. McKenzie, *The Trend of Population* (Vol. XVIII, pp. 85-97). Washington, DC: American Sociological Society.

Burns, M., Moix, M., & Roca, J. (2001). Contrasting Indications of Polycentrism within Spain's Metropolitan Urban Regions. *8th European Estate Society Conference.* Alicante, España.

Burns, M., Romano, Y., & Roca, J. (2011). El consumo de suelo en la franja costera de la Región Metropolitana de Barcelona (1956-2006) y su coherencia con el Pla Director Urbanístic del Sistema Costaner (PDUSC). In J. FARINÓN, *La gestión integrada de zonas costeras ¿Algo más que una ordenacón del litoral revisada?* (pp. 269-290). Valencia: Universitat de València.

Burrough, P. A. (1986). *Principles of Geographical Information Systems for Land Resources Assessment.* Oxford: Clarendon Press.

Butler, M., Mouchot, M., Barale, V., & LeBlanc, C. (1988). *The Application of Remote Sensing Technology to Marine Fisheries: An Introductory Manual.* Rome: FAO.

Büttner, G., & Maucha, G. (2006). *The thematic accuracy of Corine land cover 2000. Assessment using LUCAS (Land Use/Cover Area Frame Statistical Survey).* EEA Technical Report No 7/2006.

Büttner, G., Feranec, G., & Jaffrain, G. (2002). *Corine land cover update 2000, Technical guidelines.* EEA Technical report No 89.

Cabellos Barreiro, M. (2012). ISLAS BALEARES: TENSIÓN ENTRE DESTRUCCIÓN Y PROTECCIÓN. In F. Gaja, *DeCOASTruction. La desconfiguración del litoral mediterráneo español* (pp. 128-253). Valencia: Universitat Politécnica de Valencia.

Camagni, R. (1999). Sostenibilità ambientale e strategie di piano: le questioni rilevanti. In R. Camagni, & R. Camagni (Ed.), *La pianificazione sostenibile delle aree periurbane.* Bologna: Il Mulino.

Camagni, R. (2005). *Economía Urbana.* (M. Girona, Ed.) Barcelona: Antoni Bosch.

Campbell, J. (1983). *Mapping the Land: Aerial Imagery for Land Use Information.* Washington: Association of American Geographers.

Campbell, J. (1996). *Introduction to remote sensing* (2nd Edition ed.). London: Taylor & Francis Ltd.

Campbell, J., & Wynne, R. (2011). *Introduction to Remote Sensing. Fifth Edition.* New York-London: The Guilford Press.

Caniggia, G., & Maffei, G. (1979). *Composizione architettonica e tipologia edilizia/Lettura dell'edilizia di base.* Venezia: Marsilio.

Capper, P. (2011, September 17). *Altea, Costa Blanca, Spain.* Retrieved from Wikimedia Commons: http://commons.wikimedia.org/wiki/File:Altea,_Costa_Blanca,_Spain,_17_Sept._2011_-_Flickr_-_PhillipC_(2).jpg

Carruthers, J. I., & Ulfarsson, G. (2001). Fragmentation and sprawl: Evidence from interregional analysis. *Growth and Change*(33), pp. 312-340.

Casanova, D., Epema, G., & Goudriaan, J. (1998). Monitoring rice reflectance at field level for estimating biomass and LAI. *Field Crops Research*(55), pp. 83-92.

Caselles, V. (1989). An alternative simple approach to estimate atmospheric correction in multitemporal studies. *International Journal of Remote Sensing*(10 (6)), pp. 1127-1134.

Cataldi, G. (1977). *Per una scienza del territorio.* Firenze: Alinea.

Cataldi, G., Maffei, G., & Vaccaro, P. (1997). The Italian school of process typology. *Urban Morphology*(1), pp. 49-63.

CEC. (1993). *CORINE Land Cover technical guide.* Luxembourg: European Union. Directorate-Generale Environment, Nuclear Safety.

Çelik, Z. (1997). *Urban forms and colonial confrontations: Algiers under the French rule.* Berkeley: University of California Press.

Cerda, J. (2012). *Efecto del comportamiento espacio-temporal de la población sobre la estructura de actividades en la ciudad. Un acercamiento a los ritmos urbanos de Barcelona 2001-2006.* Barcelona: Universitat Politècnica de Catalunya (UPC).

Cerda, J., & Marmolejo, C. (2007). *La expansión urbana discontinua analizada desde el enfoque de accesibilidad territorial. Aplicación a Santiago de Chile.* Departament de Construccions Arquitectòniques I. Barcelona: Universitat Politècnica de Catalunya.

Chander, G., Markham, B., & Barsi, J. (2007). Revised landsat-5 Thematic Mapper radiometric calibration. *IEEE GEOSCIENCE AND REMOTE SENSING LETTERS, 4*(3), pp. 490-494.

Chander, G., Markham, B., & Helder, D. (2009). Summary of current radiometric calibration coefficients for Landsat MSS, TM, ETM+, and EO-1 ALI sensors. *Remote Sensing of Environment*(113), pp. 893–903.

Chandra, S., Chhetri, P., & Corcoran, J. (2009). Spatial patterns of urban compactness in Melbourne: an urban myth or a reality. In B. Ostendorf, P. Baldock, D. Bruce, M. Burdett, & P. Corcoran, *Proceedings of the Surveying and Spatial Sciences Institute Biennial International Conference* (pp. 231–242). Adelaide, Australia.

Chapin, F. S., & Weiss, S. F. (1962). *Urban Growth Dynamics in a Regional Cluster of Cities.* New York: JohnWiley & Sons.

Chavez, P. (1989). Radiometric calibration of Landsat Thematic Mapper multispectral images. *Photogrammetric Engineering and Remote Sensing, 55*(9), 1285-1294.

Chen, W., Liu, L., Zhang, C., Wang, J., Wang, J., & Pan, Y. (2004). Monitoring the seasonal bare soil areas in Beijing using multi-temporal TM images. *Geoscience and Remote Sensing Symposium, IGARSS'04 Proceedings, 5*, pp. 3379-3382.

Cheng, J. (2003). *Modelling Spatial and Temporal Urban Growth.* Utrecht University. Utrecht: Faculty of Geographical Sciences.

Cheshire, P. (1995). A New Phase of Urban Development in Western Europe. The Evidence for the 1980's. *Urban Studies, 32*(7), pp. 1045-1063.

Cheshire, P., & Hay, D. (1989). *Urban Problems in Western Europe. An Economic Analysis.* London: Unwin Hyman.

Chow, C. K. (1957). An optimum character recognition system using decision functions. *IREE Trans. Electron. Computers*(6), pp. 247-254.

Christaller, W. (1980). *Le località centrali della Germania meridionale.* Milano: F. Angeli.

Christiansen, P., & Loftsgarden, T. (2011). *Drivers behind urban sprawl in Europe.* Institute of Transport Economics. Oslo: Norwegian Center for Transport Research.

Chuvieco, E., & Huete, A. (2010). *Fundamentals of satellite remote sensing.* New York: Taylor and Francis Group.

Civco, D. L., & Hurd, J. (1997). *Impervious surface mapping for the State of Connecticut.* Seattle, WA: ASPRS/ACSM Annual Convention, 3.

Civco, D. L., Hurd, J., Arnold, C., & Prisloe, S. (2000). *Characterization of suburban sprawl and forest fragmentation through remote sensing application.* Washington, DC: Proceedings of the ASPRS Annual Convention.

Clark, C. (1951). Urban population densities. *Journal of the Royal Geographical Society*(114 (4)), pp. 490-496.

Clark, P., & Evans, F. (1954). Distance to nearest neighbor as a measure of spatial relationships in populations. *Ecology*(35), pp. 445-453.

Clark, R., Swayze, G., Gallagher, A., King, T., & Calvin, W. (1993). *The U. S. Geological Survey, Digital Spectral Library: Version 1: 0.2 to 3.0 microns.* U.S. Geological Survey (USGS).

Clarke, K., & Gaydos, L. (1998). Loose-coupling a cellular automaton model and GIS: long-term urban growth prediction for San Francisco and Washington/Baltimore. *International Journal of Geographical Information Science*(12(7)), pp. 699-714.

Clawson, M. (1962). Urban sprawl and speculation in suburban land. *Land Economics*(38), pp. 99-111.

Clevers, J. (1988). The derivation of a simplified reflectance model for the estimation of leaf area index. *Remote Sensing of Environment*(25), pp. 53-70.

Cohen, J. (1960). A coefficient of agreement for nominal scales. *Educational and Psychological Measurement*(20(1)), pp. 37-46.

Colaninno, N., & Roca, J. (2012). Un desarrollo metropolitano policéntrico: dispersión y compactación en los procesos de crecimiento urbano, a escala territorial. In F. Gaja, *DeCOASTruction. La desconfiguración del litoral mediterráneo español* (pp. 14-75). Valencia: Universitat Politécnica de Valencia.

Colaninno, N., Alhaddad, B., & Roca, J. (2009). The effectiveness of morphology and street networks in determining models of urban growth at different spatial scales of analysis. In M. Ulrich, & D. Civco, *SPIE Proceedings: Remote Sensing for Environmental Monitoring, GIS Applications, and Geology IX, 747813* (Vol. 7478). Berlin, Germany: SPIE - international society for optics and photonics.

Colaninno, N., Cerda, J., & Roca, J. (2011). Spatial patterns of land use: morphology and demography, in a dynamic evaluation of urban sprawl phenomena along the Spanish Mediterranean coast. *51st ERSA congress.* Barcelona.

Cole, J. (1964). *Study of major and minor civil divisions in political geography.* The 20th International Geographical Congress, London.

COMET. (n.d.). *COMET Competitive Metropolises. Agglomeration Delimitation. NUREC Methodology*. Retrieved July 2013, from http://www.oeaw.ac.at/isr/comet/documents/Final_Results/COMET_CTT/delimit/delimit-7.html

Congalton, R. G. (1991). A Review of Assessing the Accuracy of Classifications of Remotely Sensed Data. *Remote Sensing of Environment*(37), pp. 35-46.

Congalton, R., & Green, K. (1999). *Assessing the Accuracy of Remote Sensing Data: Principles and Practices.* Washington, D.C.: CRC Press, Inc.

Congalton, R., & Green, K. (2009). *Assessing the Accuracy of Remotely Sensed Data - Principles and Practices* (Second edition ed.). Boca Raton, FL: CRC Press, Taylor & Francis Group.

Conzen, M. (1960). *Alnwick, Northumberland: a study in town-plan analysis* (Vol. 27). London: Institute of British Geographers Publication, George Philip.

Conzen, M. (1962). The plan analysis of an English city centre. In K. Norborg, *Proceedings of the IGU Symposium in Urban Geography Lund 1960* (pp. 383-414). Lund: Gleerup.

Conzen, M. (1968). The use of town plans in the study of urban history. In H. Dyos, *The study of urban history* (pp. 113-30). London: Edward Arnold.

Conzen, M. (1998). Apropos a sounder philosophical basis for urban morphology. *Urban Morphology*(2), pp. 113-14.

Couch, C., Leontidou, L., & Arnstberg, K. (2007). Introduction: Definitions, Theories and Methods of Comparative Analysis Urban Sprawl . In C. Couch, L. Leontidou, & G. Petschel-Held, *Europe-Landscapes, Land-Use Change & Policy* . Blackwell Publishing.

Crist, E., & Cicone, R. (1984). A physically-based transformation of Thematic Mapper data -- the TM Tasseled Cap. *IEEE Trans. on Geosciences and Remote Sensing, GE-22*(3), pp. 256-263.

Crist, E., Laurin, R., & Cicone, R. (1986). Vegetation and soils information contained in transformed Thematic Mapper data. In *Proceedings of IGARSS' 86 Symposium* (Vols. vol. ESA SP-254, pp. 1465-1470). Paris: ESA Publications Division.

Darin, M. (1998). The study of urban form in France. *Urban Morphology*(2), pp. 63-76.

Dematteis, G. (1986). Urbanization and counter-urbanization in Italy. *Ekistics, 53*(316-317), 26-33.

Dematteis, G. (1998). *Suburbanización y periurbanización. Ciudades anglosajonas y ciudades latinas.* Barcelona: La ciudad dispersa. Suburbanización y nuevas periferias, CCCB. Monclús, F.J. (ed.).

Dematteis, G. (2003). Città diffusa, periurbanizzazione e piani strategici. In C. S. Bertuglia, A. Stanghellini, & L. Staricco, *La diffusione urbana: tendenze attuali, scenari futuri.* Milan: Franco Angeli.

Devore, J. (2010). *Probability and Statistics for Engineering and the Sciences* (Eighth Edition ed.). Boston, MA: Brooks/Cole.

Di Gregorio, A., & Jansen, L. (1997). *A New Concept For A Land Cover Classification System.* Conference Proceedings: Earth Observation And Evolution Classification, 13-16 October Alexandria, Egypt.

Dobson, J. (1993). A conceptual framework for integrating remote sensing, GIS, and geography. *Photogrammetric Engineering and Remote Sensing*(59), pp. 1491-1496.

Donaire, G. (2008, Agosto 28). La superficie construida en la región se ha quintuplicado en medio siglo. *El País*.

Downs, A. (1998). How America's Cities Are Growing: The Big Picture. *Brookings Review*(16 (4)), pp. 8-12.

Duda, R., & Hart, P. (1973). *Pattern classification and scene analysis.* New York: Wiley.

Eastman, R. (2003). *IDRISI Kilimanjaro, Guide to GIS and Image Processing.* Worcester, MA, USA: Clark Labs, Clark University.

Ehlers, M. (2010). Foreword. In Q. Weng, *Remote Sensing and GIS Integration. Theories, Methods, and Applications.* The McGraw-Hill Companies, Inc.

Eiden, G., Kayadjanian, M., & Vidal, C. (n.d.). *Capturing landscape structures: Tools*. (European Union) Retrieved from EUROPEAN COMMISSION - AGRICULTURE: http://ec.europa.eu/agriculture/publi/landscape/ch1.htm

El Nasser, H., & Overberg, P. (2001). *A comprehensive look at sprawl in America.* USA Today.

Elvidge, C., & Simmon, R. (2012). *Earth at Night: Explanation.* Robert Nemiroff and Jerry Bonnell, APOD, NASA.

Elvidge, C., Milesi, C., Dietz, J., Tuttle, B., Sutton, P., Nemani, R., & Vogelmann, J. (2004). U.S. constructed area approaches the size of Ohio. *American Geophysical Union*(85), pp. 233-234.

Elvidge, C., Tuttle, B., Sutton, P., Baugh, K., Howard, A., Milesi, C., . . . Nemani, R. (2007). Global Distribution and Density of Constructed Impervious Surfaces. *Sensors*(7), pp. 1962-1979.

Encarnação, S., Gaudiano, M., Santos, F., Tenedório, J., & Pacheco, M. (2012). Fractal cartography of urban areas. *SCIENTIFIC REPORTS, 2*(527).

Equip Redactor del PTMB. (1999). *Factors clau de la planificació territorial a l'àrea metropolitana de Barcelona. Pla Territorial Metropolità de Barcelona (PTMB).* Barcelona: Tecfoto, S.L.

ESRI. (2006). *A to Z GIS. An illustrated dictionary of geographic information ystems* (Second Edition ed.). (T. Wade, & S. Sommer, Eds.) Redlands, California: ESRI Press.

European Environment Agency. (1995). *CORINE Land Cover- Content.* Commission of the European Communities.

European Environment Agency. (2002). *Corine land cover update 2000. Technical guidelines.* Technical report, European Commission, Joint Research Centre.

European Environment Agency. (2006). *Urban sprawl in Europe. The ignored challenge.* European Commission, Joint Research Centre. Luxembourg: Office for Official Publications of the European Communities.

European Environment Agency. (2007). *CLC2006 technical guidelines.* Luxembourg: Office for Official Publications of the European Communities.

European Environment Agency. (2010). *The European Environment. Thematic Assessment: Land Use.* European Union. Copenhagen: Publications Office of the European Union.

European Environment Agency. (2011). *Analysing and managing urban growth.* European Union, Copenhagen.

European Environment Agency. (2013). *Urban world.* European Union, Copenhagen.

EUROSTAT. (2001). *Manual of concepts on Land Cover and Land Use information systems.* European Commission. Luxembourg: Office for Official Publications of the European Communities.

EUROSTAT. (2012). *NUTS - Nomenclature of territorial units for statistics.* Retrieved from European Commission: http://epp.eurostat.ec.europa.eu/portal/page/portal/nuts_nomenclature/introduction

Ewing, R. (1994). Characteristics, causes, and effects of sprawl: A literature review. *Environmental and urban issues*(21 (2)), pp. 1-15.

Ewing, R., Pendall, R., & Chen, D. (2002). *Measuring sprawl and its impact* (Vol. I). Washington DC: Smart Growth America.

EXELIS. (2015, June 9). *Spectral Angle Mapper (SAM)*. Retrieved from ENVI user guide: http://www.exelisvis.com/docs/SpectralAngleMapper.html

Exelis. (n.d.). *ENVI-Help.* Boulder, Colorado: Exelis Visual Information Solutions.

Fernández Tabales, A., & Santos Pavón, E. (2011). Ordenación del Territorio y Turismo en Andalucía: el tratamiento del espacio turístico en los planes subregionales de ordenación del territorio. In J. M. Jurado Almonte, *Ordenación del Territorio y Urbanismo: conflictos y oportunidades* (pp. 221-243). Sevilla: Universidad Internacional de Andalucía.

Filion, P., & Hammond, K. (2003). Neighbourhood land use and performance: the evolution of neighbourhood morphology over the 20th century. *Environment and Planning B: Planning and Design, 30*(2), pp. 271-296.

Finley, S. R. (2011). *Impervious Surface Mapping Using Satellite Remote Sensing.* University of Minnesota, Department of Forest Resources. Remote Sensing and Geospatial Analysis Laboratory.

Font, A., Oyon, J. L., & Pié, R. (1981). The construction of urban Catalonia. In M. SOLÀ-MORALES, *La identitat del territori català. Les comarques. Quaderns d'Arquitectura i Urbanisme. Número Extra* (pp. 14-25). Barcelona: Universitat Politécnica de Catalunya.

Foody, G. (2002). Status of land cover classification accuracy assessment. (Elsevier, Ed.) *Remote Sensing of Environment*(80), pp. 185-201.

Forman, R., & Godron, M. (1986). *Landscape Ecology.* New York: John Wiley & Sons.

Franklin, S. (2001). *Remote Sensing for Suitable Forest Management.* Boca Raton, FL.: Lewis Publishers.

Freire, S., Santos, T., & Tenedorio, J. (2009). Recent urbanization and land use/land cover change in Portugal - the influence of coastline and coastal urban centers. *Journal of Coastal Research, SI*(56), pp. 1499-1503.

Frenkel, A. (2004). Land-use patterns in the classification of cities: the Israeli Case. *Environment and Planning B: Planning and Design*(31), pp. 711-730.

Fricke, R., & Wolff, E. (2002). The MURBANDY Project: development of land use and network databases for the Brussels area (Belgium) using remote sensing and aerial photography. *International Journal of Applied Earth Observation and Geoinformation*(4), pp. 33-50.

Fricke, R., & Wolff, E. (2002). The MURBANDY Project: development of land use and network databases for the Brussels area (Belgium) using remote sensing and aerial photography. *International Journal of Applied Earth Observation and Geoinformation, 4*(1), pp. 33–50.

Frolov, Y. (1975). Measuring shape of geographical phenomena - history of issues. *Soviet Geography Review and Translation, 16*(10), pp. 676–687.

Fry, J., Coan, M., Homer, C., Meyer, D., & Wickham, J. (2009). *Completion of the National Land Cover Database (NLCD) 1992–2001 Land Cover Change Retrofit Product.* U.S. Geological Survey Open-File Report 2008-1379, USGS.

Fry, J., Xian, G., Jin, S., Dewitz, J., Homer, C., Yang, L., . . . Wickham, J. (2011). Completion of the 2006 National Land Cover Database for the conterminous United States. *Photogrammetric Engineering and Remote Sensing, 77*(9), pp. 858-864.

Fulton, W., Pendall, R., Nguyen, M., & Harrison, A. (2001). *Who sprawls the most? How growth patterns differ across the United States.* Washington, DC: The Brookings Institution.

Gahegan, M., & Ehlers, M. (n.d.). A framework for the modelling of uncertainty between remote sensing and geographic information systems. *ISPRS Journal of Photogrammetry and Remote Sensing*(55), pp. 176-188.

Gahegan, M., & Flack, J. (n.d.). The integration of scene understanding within a geographic information system: a prototype approach for agricultural applications. *Transactions in GIS*(3), pp. 31-49.

Gaja, F. (2008). El “tsunami urbanizador” en el litoral mediterráneo. El ciclo de hiperproducción inmobiliaria 1996-2006. *Scripta Nova. Revista Electrónica de Geografía y Ciencias Sociales, XII num. 270*(66).

Gaja, F. (2012). *DeCOASTruction. La desconfiguración del litoral mediterráneo español.* Valencia: Universitat Politècnica de València.

Gallego, J., & Peedell, S. (2001). Using CORINE land cover to map population density. In E. D., *Towards agri-environmental indicators. Integrating statistical and administrative data with land cover information* (pp. 94-105). Luxembourg: Office for Official Publications of the European Communities.

Galster, G., Hanson, R., Ratcliffe, M., Wolman, H., Coleman, S., & Freihage, J. (2001). Wrestling sprawl to the ground: Defining and measuring an elusive concept. *Housing Policy Debate*(12(4)), pp. 681-717.

García Almirall, P. (1998). *La valoracio urbana en base a les noves tecnologies de sistemes de información geográfica (SIG). L'exemple de l'hospitalet de llobregat.* Barcelona: Universitat Politècnica de Catalunya (UPC).

Garreau, J. (1991). *Edge city : Life on the New Frontier.* New York, London, Toronto, Sydney, Auckland: Anchor Books.

Gauthier, P., & Gilliland, J. (2006). Mapping urban morphology: a classification scheme for interpreting contributions to the study of urban form. *Urban Morphology*(10 (1)), pp. 41-50.

Geoimage. (n.d.). *Satellite Overview*. (Geoimage, Specialists in Satellite Imagery & Geospatial Solutions) Retrieved June 2014, from http://www.geoimage.com.au/satellites/satellite-overview

Gerosa, P. (1999). The philosophical foundations of urban morphology. *Urban Morphology*(3), pp. 44-45.

Gibbs, J. (1961). A method for comparing the spatial shapes of urban units. In J. Gibbs, *Urban research methods* (pp. 99–106). Princeton, NJ: Van Nostrand.

Gillman, R. (2002). Geometry and gerrymandering. *Math Horizons, 10*(1), pp. 10-13.

Ginard Bosch, X., & Murray Mas, I. (2012). *EL TRASFONDO MATERIAL DE LA ECONOMÍA BALEAR (1997-2008): UN PERTINAZ CAMINO HACIA EL COLAPSO.* Sevilla: XIII Jornadas de Economía Crítica. Los costes de la crisis y alternativas en construcción.

Giuliano, G., & Small, K. (1991). Subcenters in Los Angeles Region. *Regional Science and*(21), pp. 163-182.

Glaeser, E. (2005). Four Challenges for Scotland’s Cities. In D. Coyle, W. Alexander, & B. Ashcroft, *New Wealth for Old Nations: Scotland’s Economic Prospects* (pp. 73-95). Princeton: Princeton University Press.

Glaeser, E. e. (2001). Consumer city. *Journal of Economic Geography*(1), pp. 27-50.

Global Land Cover Facility - GLCF. (n.d.). *Global Land Survey Digital Elevation Model (GLSDEM)*. (University of Maryland) Retrieved September 2013, from http://glcf.umd.edu/data/glsdem/

Goetz, S., Wright, R., Smith, A., Zinecker, E., & Schaub, E. (2003). IKONOS imagery for resource management: Tree cover, impervious surfaces, and riparian buffer analysis in the mid-Atlantic region. *Remote Sensing of Environment*(88), pp. 195-208.

Gomez Piñero, J. (1994). Las Técnicas Tradicionales del Análisis Geográfico. *Lurralde. Investigación y Espacio*(17), pp. 341-356.

González Reverté, F. (2008). El papel de los destinos turísticos en la transformación sociodemográfica del litoral mediterráneo español. *Boletín de la A.G.E.*(47), pp. 79-107.

González, A., Moreno, J., Russell, G., & Márquez, A. (2009). Using Kernel Methods in a Learning Machine Approach for Multispectral Data Classification. An Application in Agriculture. In P.-G. P. Ho, *Geoscience and Remote Sensing* (pp. 301-322). In-Teh.

Gonzalez, R., & Woods, R. (2002). *Digital Image Processing.* New Jersey: Prentice Hall.

Gordon, P., Richardson, H., & Wong, H. (1986). The distribution of population and employment in a polycentric city: the Case of Los Angeles. *Environment and Planning A*(18), pp. 161-173.

Gottmann, J., & Harper, R. (1967). *Metropolis on the move: Geographers look at urban sprawl.* New York: John Wiley and Sons.

Greenpeace. (2012). *Destrucción a toda costa 2012. Informe sobre la situación económica y ambiental del litoral. Catalunya.*

Greenpeace. (2012). *Destrucción a toda costa 2012. Informe sobre la situación económica y ambiental del litoral. Islas Baleares.*

Gustafson, E. J. (1998). Quantifying landscape spatial pattern: What is the state of the art. *Ecosystems*, pp. 143-156.

Gustafson, E., & Parker, G. (1992). Relationships between landcover proportion and indices of landscape spatial pattern. *Landscape Ecology*(7), pp. 101-110.

Haklay, M. (2010). How good is volunteered geographical information? A comparative study of OpenStreetMap and Ordnance Survey datasets. *Environment and Planning B*(37), pp. 682–703.

Hall, P. (1997). *Cities of tomorrow: An intellectual history of urban planning and design in the twentieth century.* Oxford: Blackwell.

Hall, P., & Hay, D. (1980). *Growth Centers in the European Urban System.* London: Heinemann.

Halliday, D., Resnick, R., & Walker, J. (2010). *Fundamentals of Physics. 9th Edition.* John Wiley & Sons Inc.

Hargis, C., Bissonette, J., & David, J. (1998). The behavior of landscape metrics commonly used in the study of habitat fragmentation. *Landscape Ecology*(13), pp. 167-186.

Hashemian, M., Abkar, A., & Fatemi, S. (2004). Study of sampling methods for accuracy assessment of classified remotely sensed data. *Proceedings of the 20th International Society for Photogrammetry and Remote Sensing Concress*.

Hasse, J., & Lathrop, R. (2003). Land resource impact indicators of urban sprawl. *Applied Geography*(23), pp. 159-175.

Hebble, E., Carlson, T., & Daniel, K. (2001). Impervious Surface Area and Residential Housing Density: A Satellite Perspective. *Geocarto International, 16*(1).

Hecht, E. (1987). *Optics (2nd ed.).* Addison Wesley.

Heim, C. (2001). Leapfrogging, urban sprawl and growth management: Phoenix, 1950-2000. *American Journal of Economics and Sociology*(60(1)), pp. 245-283.

Herold, M., Couclelis, H., & Clarke, K. (2005a). The role of spatial metrics in the analysis and modeling of urban change. *Computers, Environment and Urban Systems* 29(4), pp. 369-399.

Herold, M., Hemphill, J., Dietzel, C., & Clarke, K. (2005b). Remote sensing derived mapping to support urban growth theory. *Proceedings of ISPRS, XXXVI-8/W27*.

Heymann, Y., Steenmans, C., Croissille, G., & Bossard, M. (1994). *Corine Land Cover. Technical Guide.* Luxembourg: Office for Official Publications of the European Communities.

Hillier, B. (1996). *Space is the Machine.* Cambridge: Cambridge University Press.

Hillier, B. (1997). The hidden geometry of deformed grids. Or, why space syntax works when it looks as though it shouldn't. *Space Syntax First International Symposium Proceedings. London, III*(35), pp. 1-24.

Hillier, B. (1999). The Hidden Geometry of Deformed Grids: Or, Why Space Syntax Works, When It Looks as Though It Shouldn't. *Environment and Planning B: Planning and Design, 26*(2), pp. 169-191.

Hillier, B., & Hanson, J. (1984). *The Social Logic of Space.* Cambridge: Cambridge University Press.

Hillier, B., Penn, A., Hanson, J., Grajewski, T., & Xu, J. (1993). Natural movement: configuration and attraction in urban pedestrian movement. *Environment and Planning B: Planning & Design*(20 (1)), pp. 29–66.

Homer, C., Dewitz, J., Coan, M., Hossain, N., Larson, C., Herold, N., . . . Wickham, J. (2007). Completion of the 2001 National Land Cover Database for the conterminous United States. *Photogrammetric Engineering and Remote Sensing*(73), p. 337–341.

Homer, C., Dewitz, J., Yang, L., Jin, S., Danielson, P., Xian, G., . . . Megown, K. (2015). Completion of the 2011 National Land Cover Database for the conterminous United States-Representing a decade of land cover change information. *Photogrammetric Engineering and Remote Sensing, 81*(5), pp. 345-354.

Horning, N. (n.d.). *Selecting the appropriate band combination for an RGB image using Landsat imagery.* Retrieved September 2013, from Biodiversity Informatics Facility. American Museum of Natural History, Center for Biodiversity and Conservation: http://biodiversityinformatics.amnh.org

Hoyt, H. (1939). *The Structure and Growth of Residential Neighbourhoods in American Cities.* Washington: Federal Housing Administration.

Huang, C., Wylie, B., Yang, L., Homer, C., & Zylstra, G. (2002). Derivation of a tasselled cap transformation based on Landsat 7 at-satellite reflectance. *International Journal of Remote Sensing, 23*(8), pp. 1741-1748.

Huang, J., Lu, X., & Sellers, J. (2007). A global comparative analysis of urban form: Applying spatial metrics and remote sensing. *Landscape and Urban Planning*(82), pp. 184-197.

Hudson, W., & Ramm, C. (1987). Correct formulation of the kappa coefficient of agreement. *Photogrammetric Engineering & Remote Sensing* 53(4), pp. 421-422.

Huete, A. (1988). A soil-adjusted vegetation index (SAVI). *Remote Sensing of Environment*(25), pp. 295-309.

Huete, A., Didan, K., Miura, T., Rodriguez, E., Gao, X., & Ferreira, L. (2002). Overview of the radiometric and biophysical performance of the MODIS vegetation indices. *Remote Sensing of Environment*(83), pp. 195-213.

Huete, A., Liu, H., Batchily, K., & Leeuwen, W. v. (1997). A Comparison of Vegetation Indices Over a Global Set of TM Images for EOS-MODIS. *Remote Sensing of Environment*(59(3)), pp. 440-451.

Huisman, O., & de By, R. (2009). *Principles of Geographic Information Systems. An Introductory Textbook* (Fourth Edition ed.). Enschede, The Netherlands: The International Institute for Geo-Information Science and Earth Observation (ITC).

Ibàñez, J., & Burriel, J. (2009). *Ocupació del sòl a Catalunya: 3a edició del Mapa de Cobertes (MCSC-3).* Generalitat de Catalunya, Departaments de Medi Ambient i Habitatge; Política Territorial i Obres Públiques; Agricultura, Alimentació i Acció Rural. CREAF.

Indovina, F. (1990). *La Città Diffusa.* Venezia, Italia: IUAV, Dipartimento di Analisi Economica e Sociale del Territorio (DAEST).

Irish, R., Barker, J., Goward, S., & Arvidson, T. (2006). Characterization of the Landsat-7 ETM Automated Cloud-Cover Assessment (ACCA) Algorithm. *Photogrammetric Engineering & Remote Sensing, 72*(10), pp. 1179–1188.

Jackson, K. T. (1972). Urban deconcentration in the nineteenth century: A statistical inquiry. In L. F. Schnore, & E. Lampard, *The new urban history: Quantitative explorations by American historians* (pp. 110-142). Princeton: Princeton University Press.

Jackson, R., & Huete, A. (1991). Interpreting vegetation indices. *Preventive Veterinary Medicine*(11), pp. 185-200.

Jacobs, J. (1961). *The Death and Life of Great American Cities.* New York: Vintage Books.

Jaeger, J. (2000). Landscape division, splitting index, and effective mesh size: new measures of landscape fragmentation. *Landscape Ecology*(15), pp. 115-130.

Japan Association of Remote Sensing - JARS. (1999). *Transmittance of the Atmosphere*. (National Space Development Agency of Japan (NASDA) / Remote Sensing Technology Center of Japan (RESTEC)) Retrieved September 2013, from Remote Sensing Note: http://sar.kangwon.ac.kr/etc/rs_note/rsnote/cp1/cp1-11.htm

Japan Association of Remote Sensing. (1999). Retrieved from Remote Sensing Notes: http://stlab.iis.u-tokyo.ac.jp/~wataru/lecture/rsgis/index.htm

Jensen, J. (2004). *Introductory digital image processing: A remote sensing perspective* (3rd edition ed.). NJ: Prentice Hall Logicon Geodynamics, Inc.

Jensen, J. (2005). *Digital Image Processing.* Upper Saddle River, NJ: Prentice Hall.

Jensen, S., & Waltz, F. (1979). *Principal Components Analysis and Canonical Analysis in Remote Sensing.* Proceedings of American Photogrammetric Society. 45th Annual Meeting.

Johnson, M. (2001). Environmental impacts of urban sprawl: a survey of the literature and proposed research agenda. *Environment and Planning A*(33), pp. 717–735.

Kasanko, M., Sagris, V., & Lavalle, C. (2007). Analysing the Compactness of Urban Areas by Using Indicators Derived from Data Acquired by Remote Sensing. *Urban Remote Sensing Joint Event. Paris, France*.

Kasarda, J. D., & Redfearn, G. (1975, November). Differential patterns of city and suburban growth in the United States. *Journal of Urban History*(2(1)), pp. 43-66.

Kasimu, A., & Tateishi, R. (2010). Extraction area at risk of desertification using MODIS and Geophysical data: in Xinjiang Uyghur Autonomous Region of China. *International Conference on Multimedia Technology (ICMT)*, pp. 1-4.

Kaufman, J., & Tanré, D. (1996). Strategy for Direct and Indirect Methods for Correcting the Aerosol Effect on Remote Sensing: from AVHRR to EOS-MODIS. *Remote Sensing of Environment*(55), pp. 65-79.

Kaufman, Y. J., & Tanré, D. (1992). Atmospherically resistant vegetation index (ARVI) for EOS-MODIS. *IEEE Transactions on Geoscince and Remote Sensing*(30), pp. 261-270.

Kauth, R., & Thomas, G. (1976). *The Tasseled Cap - A graphic description of the spectral temporal development of agricultural crops as seen by Landsat.* Proceedings of LARS Symposium on Machine Processing of Remotely Sensed Data, Purdue University.

Kim, C., & Anderson, T. (1984). Digital disks and a digital compactness measured. In *Proceedings of the sixteenth annual ACM symposium on theory of computing* (pp. 117–124). New York: ACM Press.

Knepper, J., & Simpson, S. (1992). *Remote Sensing in Geology and mineral resources of the altiplano and cordillera occidental, Bolivia.* U.S. Geological Survey and Servicio Geologico de Bolivia. U.S. Geological Survey.

Konecny, G. (2003). *Geoinformation. Remote sensing, photogrammetry and geographic information systems.* London and New York: Taylor & Francis.

Kounadi, O. (2009). *Assessing the Quality of OpenStreetMap Data. M.Sc. Thesis.* London, UK: University College of London.

Krüger, M. J. (1979). An approach to built form connectivity at an urban scale: variations of connectivity and adjacency measures amongst zones and other related topics. *Environment and Planning B: Planning & Design*(6), pp. 305–320.

Kruse, F., Lefkoff, A., Boardman, J., Heidebrecht, K., Shapiro, A., Barloon, P., & Goetz, A. (1993). The Spectral Image Processing System (SIPS) - Interactive Visualization and Analysis of Imaging spectrometer Data. *Remote Sensing of Environment, 4*, pp. 145 - 163.

LaGro, J. (1991). Assessing patch shape in landscape mosaics. *Photogrammetric Engineering and Remote Sensing*(57), pp. 285-93.

Land Cover Institute (LCI), USGS. (2012). *The North American Land Change Monitoring System (NALCMS).* Retrieved Mayo 2013, from http://landcover.usgs.gov/nalcms.php

Landau, S., & Everitt, B. (2004). *A Handbook of Statistical Analyses using SPSS.* Boca Raton, Florida: Chapman & Hall/CRC Press LLC.

Lang, J. (1987). *Creating architectural theory: the role of the behavioral sciences in environmental design.* NewYork: Van Nostrand Reinhold.

Larkham, P. (2005). Understanding urban form? *Urban Design*(93), pp. 22-24.

Laurence, J., & Edward, W. (1981). *Urban Development in Modern China.* Boulder: Westview Press.

Lavalle, C., Demicheli, L., Kasanko, M., McCormick, N., Barredo, J., & Turchini, M. (2002). *Towards an urban atlas. Assessment of spatial data on 25 European cities and urban areas.* European Commission, Directorate General Joint Research Centre. Copenhagen: European Environment Agency.

Lavalle, C., Demicheli, L., Turchini, M., Casals-Carrasco, P., & Niederhuber, M. (2002). Monitoring megacities: the MURBANDY/MOLAND approach. In D. Westendorff, & D. Eade, *Development and Cities* (pp. 305-315). Oxfam GB in association with UNRISD.

Lavedan, P. (1926). *Histoire de l'Urbanisme. Antiquité-Moyen Age.* Paris: Laurens.

Leblon, B. (n.d.). *Module 9: Soil and Vegetation Optical Properties.* Retrieved 2014, from Remote Sensing Core Curriculum (RSCC). Volume 4: Applications in Remote Sensing: http://rscc.umn.edu/rscc/Volume4/Leblon/leblon.htm

Lee, K. (1991). *Wetlands detection methods investigation.* Las Vegas, NV: U.S. Environmental Protection Agency; Environmental Monitoring Systems Laboratory.

Lees, B. (1996). Sampling strategies for machine learning using GIS. In M. Goodchild, L. Steyart, B. Parks, M. Crane, C. Johnston, D. Maidment, & S. Glendinning, *GIS and Environment Modelling: Progress and Research Issues.* Ft. Collins, CO.: GIS World.

Levy, A. (1999). Urban morphology and the problem of the modern urban fabric: some questions for research. *Urban Morphology, 3*(2), pp. 79-85.

Levy, A. (2005). New orientations in urban morphology. *Urban Morphology*(9, 50-3).

Li, H., & Reynolds, J. (1993). A new contagion index to quantify spatial patterns of landscapes. *Landscape Ecology*(8), pp. 155-162.

Li, W., Goodchild, M., & Church, R. (2013). An efficient measure of compactness for two-dimensional shapes and its application in regionalization problems. *Internationla Journal of Geographical Information Science, 27*(6).

Li, X., & Yeh, A. (2004). Analyzing spatial restructuring of land use patterns in a fast growing region using remote sensing and GIS. *Landscape and Urban Planning*(69), pp. 335-354.

Lim, H., MatJafri, M., Abdullah, K., & Wong, C. (2009). Air Pollution Determination Using Remote Sensing Technique. In G. Jedlovec, *Advances in Geoscience and Remote Sensing.* InTech, under CC BY-NC-SA 3.0 license.

Lin, W., Wang, Q. F., Zha, S., & Li, J. (2010). Construction and application of characteristic bands of typical land cover based on spectrum-photometric method. *18th International Conference on Geoinformatics*.

Liu, C., Frazier, P., & Kumar, L. (2007). Comparative assessment of the measures of thematic classification accuracy. (Elsevier, Ed.) *Remote Sensing of Environment*(107), pp. 606-616.

Lobley, M., & Winter, M. (2009). Introduction: Knowing the Land. In M. Winter, & M. Lobley, *What is Land For? The Food, Fuel and Climate Change Debate.* Earthscan.

Longley, P., & Masev, V. (2000). On the measurement and generalization of urban form. *Environment and Planning A*(32), pp. 473-488.

Longley, P., & Mesev, V. (1997). Beyond analogue models: space filling and density measurements of an urban settlement. *Papers in Regional Sciences*(76), pp. 409-427.

López, I., & Rodríguez, E. (2010). *Fin de ciclo. Financiarización, territorio y sociedad de propietarios en la onda larga del capitalismo hispano (1959-2010).* Madrid: Traficantes de.

Lösch, A. (1954). *The economics of location.* New Haven: Yale University Press.

Lowry, I. (1988). *Planning for urban sprawl.* Washington, DC: Transportation Research Board.

Lynch, K. (1960). *The image of the city.* Cambridge, MA: MIT Press.

Lynch, K., & Rodwin, L. (1958). A theory of urban form. *Journal of the American Institute of Planners*(24), pp. 201-14.

Maceachren, A. (1985). Compactness of Geographic Shape: Comparison and Evaluation of Measures. *Geografiska Annaler. Series B, Human Geography, 67*(1), pp. 53-67.

Mainigi, J., Marsh, S., Kepner, W., & Edmonds, C. (2002). *An Accuracy Assessment of 1992 Landsat-MSS Derived Land Cover for the Upper San Pedro Watershed (U.S./Mexico).* Arizona Remote Sensing Center; National Exposure Research Laboratory. Tucson, AZ; Las Vegas, NV: United States Environmental Protection Agency (EPA).

Malgorzata, V. (2010). *Data acquisition and integration 6: 6 Remote Sensing.* University of West Hungary Faculty of Geoinformatics. Nyugat-magyarországi Egyetem.

Mandelbrot, B. B. (1977). *Fractals, Form, Chance and Dimension.* New York: W. H. Freeman and Co.

Mandelbrot, B. B. (1982). *The Fractal Geometry of Nature.* New York: W. H. Freeman and Co.

Marambio, A., Corso, J., & Garcia-Almirall, P. (2011). Morphological analysis of Lloret de Mar. A GIS and TLS analysis of the historical centre. *Proceedings of 51th ERSA Congress*.

Marcos Rodríguez, P., Jiménez Navarro, E., & Del Río Paredes, S. (2012). LA URBANIZACIÓN EN EL LITORAL ANDALUZ DURANTE LOS ÚLTIMOS 10 AÑOS. In F. Gaja, *DeCOASTruction. La desconfiguración del litoral mediterráneo español* (pp. 230-351). Valencia: Universitat Politécnica de Valencia.

Maretto, P. (1984). *Realtà naturale e realtà costruita.* Firenze: Alinea.

Marmolejo, C., & Roca, J. (2009). Urban Structure and Polycentrism: Towards a Redefinition of the Sub-centre Concept. *Urban Studies*(46), pp. 2841-2868.

Marmolejo, C., & Stallbohm, M. (2008). En contra de la ciudad fragmentada: ¿Hacia un cambio de paradigma urbanístico en la región metropolitana de Barcelona? *Scripta Nova, revista electrónica de geografía y ciencias sociales, XII*(270(65)).

Marschner, F. J. (1950). *Major laud uses in the United States [map, scale 1:5,000,000].* U.S. Dept. of Agriculture. Agr. Research Service.

Martí, P., & Domínguez, L. (2012). Urban space and its transformation in two Spanish Mediterranean cities: Alicante and Murcia. *1º International Conference on Architecture & Urban Design. Proceedings 19-21*, (p. 8).

Martinuzzi, S., Gould, W., & Gonzalez, O. (2007). Land development, land use, and urban sprawl in Puerto Rico integrating remote sensing and population census data. *Landsc Urban Plan*(79), pp. 288–297.

Martori, J., & Hoberg, K. (2008). Nuevas Técnicas de Estadistica Espacial para la Detección de Clusters Residenciales de Población Inmigrante. *Scripta Nova. Revista Electronica de Geografía y Ciencias Sociales, XII*(263).

Masser, I. (2001). Managing our urban future: the role of remote sensing and geographic information systems. *Habitat International*(25), pp. 503-512.

Mather, P. (1999). *Computer Processing of Remotely-sensed Images.* Chichester: Wiley.

McDonald, J. (1987). The Identification of Urban Employment Subcenters. *Journal of Urban*(21), pp. 242-258.

McFeeters, S. (1996). The use of normalized difference water index (NDWI) in the delineation of open water features. *International Journal of Remote Sensing, 17*(7), pp. 1425–1432.

McGarigal, K. (2014). *FRAGSTATS HELP.* Amherst: University of Massachusetts.

McGarigal, K., & Marks, B. (1995). *FRAGSTATS. Spatial pattern analysis program for quantifying lanscape structure.* Amherst: University of Massachusetts.

McGarigal, K., Cushman, S., Neel, M., & Ene, E. (2002). *FRAGSTATS: spatial pattern analysis program for categorical maps.* Amherst: University of Massachusetts: www.umass.edu/landeco/research/fragstats/fragstats.html

Meaden, G., & Kapetsky, J. (1991). *Geographical information systems and remote sensing in inland fisheries and aquaculture.* FAO Fisheries Technical Paper No. 318, FAO, Fisheries Department, Rome.

Meyer, W., & Turner, B. (1994). *Changes in Land Use and Land Cover: A Global Perspective.* Cambridge: Cambridge University Press.

Milesi, L. (2006). *Il progetto della città aperta. I piani urbanistici secondo il punto di vista estetico* (Vol. Tesi di Laurea). Genova, Italia: Università degli studi di Genova.

Miller, V. (1953). *A quantitative geomorphic study of the drainage basin characteristics in the Clinch Mountain area, Virginia and Tennessee.* New York: Columbia University Department of Geology.

Mills, E. (1967). An aggregative model of resource allocation in a metropolitan area. *American Economic Review*(57), pp. 197-210.

Mills, E. (1973). *Studies in the Structure of the Urban Economy.* London: Johns Hopkins Press.

Milne, B. (1991). Lessons from applying fractal models to landscape patterns. In M. Turner, & R. Gardner, *Quantitative methods in landscape ecology.* New York: Springer-Verlag.

Ministerio de Fomento. (n.d.). *Proyecto SIOSE*. Retrieved May 2013, from http://www.siose.es/siose/index.html

Mitchell, A. (2005). *The ESRI Guide to GIS Analysis: Spatial Measurements and Statistics* (Vol. 2). ESRI Press.

Monclús, J. (1996). *Suburbanización y nuevas periferias. Perspectivas geográfico-urbanísticas.* Workshop: La ciudad dispersa. Suburbanización y nuevas periferias, Barcelona.

Morris, A. (1979). *History of Urban Form: Before the Industrial Revolutions.* London: Longmans Scientific and Technical.

Morris, A. E. (1994). *History of Urban Form before the Industrial Revolutions* (3rd. edition ed.). England: Longman Scientific & Technical.

Moskowitz, H., & Lindbloom, C. (1993). *The new illustrated book of development definitions.* New Brunswick, NJ: Rutgers University, Center for Urban Policy Research.

Moudon, A. (1994). Getting to know the built landscape: typomorphology. In K. Frank, & L. Schneekloth, *Ordering space. Types in architecture and design* (pp. 289-311). New York: Van Nostrand Reinhold.

Moudon, A. (1997). Urban morphology as an emerging interdisciplinary field. *Urban Morphology*(1), pp. 3-10.

Mróz, M., & Sobieraj, A. (2004). Comparison of several vegetation indices calculated on the basis of a seasonal spot xs time series, and their suitability for land cover and agricultural crop identification. *Technical Science*(7), pp. 39-66.

Mücher, C., Stomph, T., & Fresco, L. (1993). *Proposal For A Global Land Use Classification.* Rome: Fao.

Mücher, S., Steinnocher, K., Champeaux, J.-l., Griguolo, S., Wester, K., Heunks, C., & Katwijk, V. v. (2000). Establishment of a 1-Km pan-european land cover database for environmental monitoring. *International Archives of Photogrammetry and Remote Sensing*(XXXIII).

Mumford, L. (1939). The City. New York.

Mumford, L. (1981). *La città nella storia.* (Italian, Trans.) Milano: Bompiani.

Muñiz, I., & Galindo, A. (2005). Urban form and the ecological footprint of commuting. The case of Barcelona. *Ecological Economics*(55), pp. 499– 514.

Muñiz, I., Galindo, A., & García, M. (2003). Cubic spline population density functions and satellite cities delimitation: the case of Barcelona. *Urban Studies*(40 (7)), pp. 1303–1321.

Muth, R. (1968). Urban residential land and housing markets. In H. Perloff, & L. Wingo, *Issues in Urban Economics.* Baltimore, Maryland: Johns Hopkins Press.

Muth, R. (1969). *Cities and Housing.* Chicago: University of Chicago Press.

N.U.R.E.C. (1994). *Atlas of Agglomerations in the European Union* (Vols. I-III). Duisburg (Homberg), Germany.

NASA. (n.d.). *Global Maps: Vegetation*. (C. Ichoku, Editor, & EOS Project Science Office at NASA Goddard Space Flight Center) 2013: http://earthobservatory.nasa.gov/GlobalMaps/view.php?d1=MOD13A2_M_NDVI

NASA. (n.d.). *MODIS Web*. (B. a. Maccherone, Producer, & National Aeronautics and Space Administration (NASA)) Retrieved September 2013, from http://modis.gsfc.nasa.gov/index.php

NASA. (n.d.). *The Landsat Program*. (J. Irons, M. Taylor, L. Rocchio, Producers, & National Aeronautics and Space Administration (NASA)) Retrieved September 2013, from Landsat Science: http://landsat.gsfc.nasa.gov/

Navidi, W. (2011). *Statistics for Engineers and Scientists* (Third Edition ed.). New York: McGraw-Hill.

Nel·lo, O. (2001). *Ciutat de Ciutats* (Vols. Biblioteca Universal, 154). Barcelona, Spain: Empúries.

Nel·lo, O. (2011). El planeamiento territorial en Cataluña. *Cuadernos Geográficos, 47*(2010-2), 131-167.

Neteler, M., & Mitasova, H. (2008). *Open source GIS. A GRASS GIS approach* (Third Edition ed.). Springer.

Newton, P. (2000). Urban Form and Environmental Performance. In K. Williams, E. Burton, & M. Jenks, *Achieving Sustainable Urban Form* (pp. 46-53). London: E&FN Spon.

Nicolau, J. (2002). *Elección en turismo: aplicación probabilística al turismo español.* Alicante: Universidad de Alicante.

Nilsson, K., & Nielsen, T. (2011). *Sustainable urban-rural futures-Need for a coheren EU policy and innovative regional strategies.* PLUREL: Newsletter nr. 8.

Nilsson, N. J. (1965). *Learning Machines Foundations of Trainable Pattern Classifying Systems.* New York: McGraw-Hill Book Co.

Nivola, P. (1999). *Laws of the Landscape: How Policies Shape Cities in Europe and America.* Washington, DC: Brookings Institution Press.

O'Sullivan, D. (2000). *Graph-based Cellular Automaton Models of Urban Spatial Processes.* University of London. London: Bartlett School of Architecture and Planning.

Ogawa, H., & Fujita, M. (1980). Equilibrium land use patterns in a nonmonocentric city. *Journal of Regional Science, 20*(4), pp. 455-475.

OMM. (2011). *La crisis que viene. Algunas notas para afrontar esta década.* Observatorio Metropolitano. Madrid: Traficantes de Sueños.

O'Neill, R., Krummel, J., Gardner, R., Sugihara, G., Jackson, B., Deangelis, D., . . . Graham, R. (1988). Indices of Landscape Pattern. *Landscape Ecology*(1), pp. 153-162.

Orfield, M. (1997). *Metropolitics: a regional agenda for community and stability.* Washington, DC; Cambridge, MA: Brookings Institutions and Lincoln Institute of Land Policy.

OSE. (2011). *SOSTENIBILIDAD EN ESPAÑA 2011.* Observatorio de la Sostenibilidad en España (OSE).

Osserman, R. (1978). Isoperimetric inequality. *Bulletin of the American Mathematical Society, 84*(6), pp. 1182-1238.

Ozdogan, M., & Woodcock, C. (2006). Resolution dependent errors in remote sensing of cultivated areas. *Remote Sensing of the Environment*(103), pp. 203–217.

Peiró, J. B. (2012). El litoral mediterráneo, un balance multidisciplinar, un debate abierto. In F. Gaja i Díaz, & e. al., *DeCOASTruction. La desconfiguración del litoral mediterráneo español.* Valencia: Universitat Politècnica de València.

Peiser, R. (1989). Density and urban sprawl. *Land Economics*(65(3)), pp. 193-204.

Peponis, J., Bafna, S., & Shpuza, E. (2006). Implications. *4*(12). Retrieved from www.informedesign.umn.edu

Perry, C., & Lautenschlager, L. (1984). Functional Equivalence of Spectral Vegetation Indices. *Remote Sensing of Environment*(14(1-3)), pp. 169-182.

Philpot, W. (2011). *Digital Image Processing.* Civil & Environmental Engineering (CEE). Ithaca, NY: Cornell University.

Pinty, B., & Verstraete, M. (1992). GEMI: a non-linear index to monitor global vegetation from satellites. *Vegetatio, 101*, pp. 15-20.

Potere, D., Schneider, A., Angel, S., & Civco, D. (2009). Mapping urban areas on a global scale: which of the eight maps now available is more accurate? *International Journal of Remote Sensing*(30(24)), pp. 6531–6558.

Pourabdollah, A., Morley, J., Feldman, S., & Jackson, M. (2013). Towards an Authoritative OpenStreetMap: Conflating OSM and OS OpenData National Maps' Road Network. *ISPRS International Journal of Geo-Information*(2), pp. 704-728.

Pozuea, J. (2000). Movilidad y planeamiento sostenible: Hacia una consideración inteligente del transporte y la movilidad en el planeamiento y el diseño urbano. *Red de cuadernos de investigación urbanística*.

QGIS Development Team. (2015). QGIS User Guide. *QGIS 2.8 Geographic Information System User Guide*. Retrieved from http://docs.qgis.org/2.8/en/docs/user_manual/

Qi, J., Chehbouni, A., Huete, A., Kerr, Y., & Sorooshian, S. (1994). A Modified Soil Adjusted Vegetation Index. *Remote Sensing of Environment*(48), pp. 119-126.

Racine, J.-B. (1967). Exurbanisation et métamorphisme périurbain. Introduction à l'étude de la. *XXI*(2), pp. 313-342.

Rapoport, A. (1977). *Human aspects of urban form: towards a man-environment approach to urban form and design.* New York: Pergamon Press.

Rapoport, A. (1982). *The meaning of the built environment: a non-verbal communication approach.* Beverly Hills, CA: Sage.

Read, S. (1997). Space syntax and the Dutch City. The supergrid. *Proceedings of Space Syntax Fisrts International Symposium. London, III*(36), pp. 1-20.

Reeves, R. G., Anson, A., & Landen, D. (1975). *Manual of Remote Sensing.* Falls Church, VA: American Society of Photogrammetry.

(2000). *REGIO database - Userr's guide.* Luxembourg: Office for Official Publications of the European Communities.

Rencher, A. (2002). *Methods of Multivariate Analysis* (Second Edition ed.). New York, NY: John Wiley & Sons, Inc.

Richards, J. A., & Xiuping, J. (2006). *Remote Sensing Digital Image Analysis. An Introduction* (4th Edition ed.). Berlin, Germany: Springer.

Richardson, A., & Wiegand, C. (1977). Distinguishing vegetation from soil background information. *Photogrammetric Engineering and Remote Sensing*(43), pp. 1541-1552.

Richardson, L. (1961). A note: measuring compactness as a requirement of legislative apportionment. *Mid-west Journal of Political Science*(5), pp. 70-74.

Richarme, M. (2001). *Eleven Multivariate Analysis Techniques: Key Tools In Your Marketing Research Survival Kit.* Retrieved from Decision Analyst: Strategic Research, Analytics, Modeling, Optimization: http://www.decisionanalyst.com/publ_art/multivariate.dai

Ridd, M. K. (1995). Exploring a V-I-S (vegetation-impervious surface-soil) model for urban ecosystem analysis through remote sensing: comparative anatomy for cities. *International Journal of Remote Sensing*(12), pp. 2165-2185.

Riitters, K., O'Neill, R., Hunsaker, C., Wickham, J., Yankee, D., Timmins, S., . . . Jackson, B. (1995). A factor analysis of landscape pattern and structure metrics. *Landscape Ecology, 10*(1), pp. 23-39.

Roca, J., Arellano, B., & Moix, M. (2011). Estructura urbana, policentrismo y sprawl: los ejemplos de Madrid y Barcelona. *Ciudad y territorio, estudios territoriales, XLIII*(168), pp. 299-321.

Roca, J., Burns, M., & Carreras, J. (2004). Monitoring urban sprawl around Barcelona's metropolitan area with the aid of satellite imagery. *Proceedings of geo-imagery bridging continents, XXth ISPRS congress*.

Rocha, J., Tenedório, J., Estanqueiro, R., & Morgado, P. (2007). Classificação de uso do solo urbano através da análise linear de mistura espectral com imagens de satélite. *Finisterra: Revista Portuguesa de Geografia, XLII*(83), pp. 47-62.

Rock, B., Williams, D., & Vogelmann, J. (1985). Field and airborne spectral characterization of suspected acid deposition damage in red spruce (Picea rubens) from Vermont. *Proceedings, Symposium on Machine Processing of Remotely Sensed Data*, pp. 71-81.

Rogan, J., & Miller, J. (2006). Integrating GIS and Remotely Sensed Data for Mapping Forest Disturbance and Change. In M. Wulder, & S. Franklin, *Understanding Forest Disturbance and Spatial Pattern: Remote Sensing and GIS approaches* (p. 246). CRC Press.

Rogers, A., & Kearney, M. (2004). Reducing signature variability in unmixing coastal marsh Thematic Mapper scenes using spectral indices. *International Journal of Remote Sensing, 25*(12), pp. 2317-2335.

Rogers, C. A. (1993). *Describing landscapes: indices of structure.* Burnaby, British Columbia: Simon Fraser University.

Romano, Y., Colaninno, N., Cerda, J., Roca, J., & Burns, M. (2010). Urban growth dynamics: the relation between land occupation, density and spatial fragmentation. *Geographical information systems and spatial analysis, at ERSA congress Jönköping, Sweden*.

Romme, W. H. (1982). Fire and landscape diversity in subalpine forests of Yellowstone National Park. *Ecological Monographs*(52), pp. 199-221.

Ross, S., Congalton, R., Fenstermaker, L., Jensen, J., McGwire, K., & Tinney, L. (1991, June). Remote Sensing and Geographical Information System Data Integration: Error Sources and Research Issues. *Photogrammetric Engineering & Remote Sensing, 57*(6), pp. 677-687.

Rouse, J. J., Haas, R., Deering, D., Schell, J., & Harlan, J. (1974). *Monitoring the Vernal Advancement and Retrogradation (Green Wave Effect) of Natural Vegetation.* NASA/GSFC Type III Final Report, 371p, Greenbelt, MD.

RS/GIS Quick Start Guides: Landsat Spectral Band Information. (2008).

Rykwert, J. (1988). *The idea of a town: the anthropology of urban form in Rome, Italy and the ancient world.* Cambridge, MA: MIT Press.

Sánchez Morales, J. (2012). LA REGIÓN DE MURCIA EN SU HABITUAL INOPIA. In F. Gaja, *DeCOASTruction. La desconfiguración del litoral mediterráneo español* (pp. 254-299). Valencia: Universitat Politécnica de Valencia.

Santiago, R., & Bribiesca, E. (2009). State of the art of compactness and circularity measures. *International Mathematical Forum, 4*(2), pp. 1305–1335.

Santos, T., Tenedório, J., & Rocha, J. (2006). Comparing pixel vs. object based classifiers for land cover mapping with Envisat-MERIS data. *EARSeL - European Association of Remote Sensing Laboratories.* Warsow.

Sarda, R. (2009). La Estrategia Catalana de Gestión Integrada de Zonas Costeras. In *Gestión Integrada de Zonas Costeras* (pp. 67-97). AENOR.

Satellite Imaging Corporation - SIC. (n.d.). *ASTER Satellite Imagery and Satellite System Specifications*. Retrieved September 2013, from http://www.satimagingcorp.com/satellite-sensors/aster.html

Satellite Imaging Corporation - SIC. (n.d.). *Digital Elevation Models (DEM)*. Retrieved September 2013, from http://www.satimagingcorp.com/svc/dem.html

Sattlberger, C. (2014, January 16). *Aerial series.* Retrieved from http://platformphoto.org/: https://platformphoto.org/2014/01/16/aerial-series-by-chris-sattlberger/_kid0757/

Sau, E. (1995). *El creixement del sistema urbà de Catalunya (1950-1991). De la concentració a la desconcentració metropolitana?* Documents d'Analisi Geografica, 27.

Schell, J. A. (1973). In F. Shahrokhi (Ed.), *Remote Sensing of Earth Resources* (Vol. I, pp. 374-394). Tullahoma, TN: Univ. of Tennessee Space Inst.

Schowengerdt, R. (2007). *Remote Sensing. Models and Methods for Image Processing* (Third Edition ed.). Burlington, MA: Elsevier Inc.

Schuckman, K., & O'Neil Dunne, J. (2014). *Land Cover Classification*. (D. o. Geography, J. A.-E. Institute, Producers, & Pennsylvania State University, College of Earth and Mineral Sciences) Retrieved July 2014, from GEOG 883: Remote Sensing Image Analysis and Applications: https://www.e-education.psu.edu/geog883/node/522

Sebestyen, G. (1962). *Decision-Making Processes in Pattern Recognition.* New York: Macmillan.

Secchi, B. (2007). *Prima lezione di urbanistica* (4th ed.). Laterza.

Secchi, B. (2008, April 17). Le forme della città. *Fahrenheit.* Radio 3. Rdio.Rai, Ferrara.

Self, P. (1961). *Cities in flood: The problems of urban growth.* London: Faber and Faber.

Selkowitz, D., & Stehman, S. (2011). Thematic accuracy of the National Land Cover Database (NLCD) 2001 land cover for Alaska. *Remote Sensing of Environment, 115*(6), pp. 1401–1407.

Shahumyan, H., White, R., Twumasi, B., Convery, S., Williams, B., Critchley, M., . . . Brennan, M. (2009). The MOLAND Model Calibration and Validation for the Greater Dublin Region. *UCD Urban Institute Ireland Working Paper Series*(UCD UII 09/03).

Shannon, C., & Weaver, W. (1949). *The mathematical theory of communication.* Urbana: Univiversity of Illinois Press (UIP).

Shpuza, E. (2007). *Interaction between urban shape and structure* (International Seminar on Urban Form ed.). (morphostudio.net, Ed.) Brasil: Federal University of Minas Gerais e Federal University of Ouro Preto.

Shpuza, E. (2007). Urban shapes and urban grids: a comparative study of Adriatic and Ionian coastal cities. *Proceedings, 6th International Space Syntax Symposium. Istanbul*(009), pp. 1-22.

Shpuza, E. (2009). Evolution of street networks in Adriatic and Ionian coastal cities 1769-2007. (D. Koch, L. Marcus, & J. Steen, Eds.) *Proceedings of the 7th International Space Syntax Symposium*(101), pp. 1-15.

Silleos, N., Alexandridis, T., Gitas, I., & Perakis, K. (2006). Vegetation Indices: Advances Made in Biomass Estimation and Vegetation Monitoring in the Last 30 Years. *Geocarto International, 21*(4), pp. 21-28.

Simpson, E. H. (1949). Measurement of diversity. *Nature*(163), pp. 688-688 .

Sinclair, R. (1967). Von Thunen and urban sprawl. *Annals of the Association of American Geographers*(57), pp. 72–87.

SIOSE. (2011). *Documento Técnico SIOSE 2005, Versión 2.* Ministerio de Fomento, D.G. Instituto Geográfico Nacional. Servicio de Ocupación del Suelo. S.G de Cartografía. Equipo Técnico Nacional SIOSE.

Sitte, C. (1889). *Der Städte-bau nach seinen Künstlerischen Grundsätzen.* (1. J. L'arte di costruire le città. Milano, Trans.) Wien.

Slonecker, E., & Tilley, J. (2004). An evaluation of the individual components and accuracies associated with the determination of impervious area. *GIScience and Remote Sensing*(41(2)), pp. 125-144.

Slonecker, E., Jennings, D., & Garofalo, D. (2001). Remote sensing of impervious surfaces: A review. *Remote Sensing Reviews*(20(3)), pp. 227-255.

Smith, C. T. (1967). *An Historical Geography of Western Europe before 1800.* United Kingdom: Longman Group.

Song, M., & Civco, D. (2002). A Knowledge-Based Approach for Reducing Cloud and Shadow.

Song, Y., & Knaap, G. (2004). Measuring urban form: is Portland winning the war on sprawl? *Journal of the American Planning Association, 70*(2), pp. 210-225.

Song, C., Woodcock, C., Seto, K., Lenney, M., & Macomber, S. (2001). Classification and Change Detection Using Landsat TM Data: When and How to Correct Atmospheric Effects? *Remote Sensing of Environment*(75), 230-244.

Soong, T. (2004). *FUNDAMENTALS OF PROBABILITY AND STATISTICS FOR ENGINEERS.* Chichester, West Sussex, England: John Wiley & Sons, Ltd.

SPSS. (2006). *SPSS Base 15.0 User's Guide.* SPSS Inc.

Stankowski, S. (1972). Population density as an indirect indicator of urban and suburban land-surface modification. *USGS Professional Paper 800-B*, pp. 219-224.

Star, J., Estes, J., & McGore, K. (1997). *Integration of Geographic Information Systems and Remote Sensing.* New York: Cambridge University Press.

Stehman, S. V. (1997a). Selecting and interpreting measures of thematic classification accuracy. (Elsevier, Ed.) *Remote Sensing of Environment*(62), pp. 77-89.

Stehman, S., Wickham, J., Smith, J., & Yang, L. (2003). Thematic accuracy of the 1992 National Land-Cover Data (NLCD) for the eastern United States—Statistical methodology and regional results. *Remote Sensing of Environment, 86*(4), pp. 500–516.

Steiniger, S., Lange, T., Burghardt, D., & Weibel, R. (2007). An Approach for the Classification of Urban Building Structures Based on Discriminant Analysis Techniques. *Transactions in GIS, 12*(1), pp. 31-59.

Story, M., & Congalton, R. (1986). Accuracy assessment: a user's perspective. *Photogrammetric Engineering & Remote Sensing* (52(3)), pp. 397-399.

Strahler, A. H. (1980). The Use of Prior Probabilities in Maximum Likelihood Classification of Remotely Sensed Data. *REMOTE SENSING OF ENVIRONMENT*(10), pp. 135-163.

Strahler, A., Boschetti, L., Foody, G., Friedl, M., Hansen, M., Herold, M., . . . Woodcock, C. (2006). *Global Land Cover Validation: Recommendations for Evaluation ans Accuracy Assessment of Global Land Cover Maps.* European Commission. Luxembourg: Office for Official Publications of the European Communities.

Sun, X. (2013). *Comparative Analysis of Urban Morphology: Evaluating Space Syntax and Traditional Morphological Methods.* Gävle, Sweden: Gävle University College.

Swain, P., & Davis, S. (1978). *Remote Sensing: The Quantitative Approach.* N.Y.: McGraw-Hill.

Swets, D., Reed, B., Rowland, J., & S.E., M. (1999). A weighted least-squares approach to temporal smoothing of NDVI. *Proceedings of the ASPRS 1999 Annual Convention*.

Tarrach, P. (2015, Junio 16). Retrieved from Valenciaplaza.com. Cultura y Sociedad: La ciudad y sus vicios: http://www.valenciaplaza.com/ver/155303/benidorm-arquitectura-turismo-urbanismo.html

Thangavel, C. (2000). An empirical estimation of the effects of some variables on land sub-division in Madras. *Urban Studies, 37*(7), pp. 1145-1156.

The Landsat 7 Compositor. (n.d.). (NASA-National Aeronautics and Space Administration) Retrieved from Goddard Space Flight Center: http://landsat.gsfc.nasa.gov/education/compositor/em.html

Tobler, W. (1970). Computer movie simulating urban growth in Detroit region. *Economic Geography, 46*(2), pp. 234–240.

Tomlin, C. (1990). *Geographic Information Systems and Cartographic Modelling.* Englewood Cliffs, N. J: Prentice Hall.

Torres, P., & Marina, A. (2000). *Measuring Sprawl.* London: Centre for Advanced Spatial Analysis (CASA). University College London.

Travaglia, C. (1989). *Principles of Satellite Imagery Interpretation.* Report of the Twelth International Training Course on the Contribution of Remote Sensing to Marine Fisheries. RSC Series 49, FAO, Rome.

Tsai, Y. (2005). Quantifying Urban Form: Compactness versus 'Sprawl'. *Urban Studies, 42*(1), pp. 141-161.

Turner, B. L., Skole, D., Sanderson, S., & al., e. (1995). *Land-Use and Land-Cover Change: Science and Research Plan.* Stockhdm and Geneva: International Geosphere-Bioshere Program and the Human Dimensions of Global Environmental Change Programme.

Turner, B., Ross, R., & Skole, D. (1993). *Relating Land Use and Global Land-cover Change: a Proposal for and IGBP-HDP Core Project.* Stockholm: International Geosphere-Bioshere Program and the Human Dimensions of Global Environmental Change Programme.

Turner, M. (1989). Landscape ecology: the effect of pattern on process. *Annual Review of Ecology and Systematics*(20), pp. 171-197.

Turner, M. G. (1990a). Spatial and temporal analysis of landscape patterns. *Landscape Ecology*(4), pp. 21-30.

Turner, M., O'Neill, R., Gardner, R., & Milne, B. (1989). Effects of changing spatial scale on the analysis of landscape pattern. *Landscape Ecology*(3), pp. 153-162.

U.S. Department of the Interior | U.S.G.S. (2015). *National Land Cover Database 2011 (NLCD 2011).* Retrieved from Multi-Resolution Land Characteristics Consortium (MRLC): http://www.mrlc.gov/nlcd2011.php

UMass Landscape Ecology Lab. (n.d.). *About Landscape Ecology. What is landscape ecology?* . Retrieved July 2013, from http://www.umass.edu/landeco/about/about.html

UNFPA. (2007). *State of world population 2007. Unleashing the Potential of Urban Growth.* United Nations.

United Nations. (2014). *World Urbanization Prospects: The 2014 Revision, Highlights.* ST/ESA/SER.A/352, Population Division, Department of Economic and Social Affairs.

US Army Corps of Engineers. (2003). *Engineering and Design. REMOTE SENSING* (Vols. Engineer Manual 1110-2-2907). Washington, DC: Department of the Army.

USGS. (2012). *The National Land Cover Database.* U.S. Department of the Interior. U.S. Geological Survey.

USGS. (2013). *Landsat - A Global Land-Imaging Mission.* U.S. Department of the Interior | U.S. Geological Survey. Retrieved from http://pubs.usgs.gov/fs/2012/3072/fs2012-3072.pdf

USGS. (n.d.). *Landsat 8 OLI (Operational Land Imager) and TIRS (Thermal Infrared Sensor)*. (U.S. Department of the Interior | U.S. Geological Survey) Retrieved September 2013, from https://lta.cr.usgs.gov/L8

USGS. (n.d.). *Landsat Processing Details*. (U.S. Department of the Interior | U.S. Geological Survey) Retrieved September 2013, from Landsat Missions: http://landsat.usgs.gov/Landsat_Processing_Details.php

USGS. (n.d.). *Shuttle Radar Topography Mission (SRTM)*. (U.S. Department of the Interior | U.S. Geological Survey) Retrieved September 2013, from https://lta.cr.usgs.gov/SRTM2

USGS. (n.d.). *USGS Global Visualization Viewer: Quick Start Guide*. (U.S. Department of the Interior | U.S. Geological Survey) Retrieved 2011, from Earth Resources Observation and Science Center (EROS): http://glovis.usgs.gov/QuickStart.shtml

Van Den Berg, L., Drewett, R., Klaasen, L., Rossi, A., & Vijverberg, C. (1982). *Urban Europe. A study of Growth and Decline.* Oxford: Pergamon.

Vance, J. (1977). *This scene of man: the role and structure of the city in the geography of Western civilization.* New York: Harper and Row.

Vance, J. (1990). *The continuing city: urban morphology in western civilization.* Baltimore: John Hopkins University Press.

Vancutsem, C., Bicheron, P., Cayrol, P., & Defourny, P. (2007). An assessment of three candidate compositing methods for global MERIS time series. *Canadian Journal of Remote Sensing*(33(6)), pp. 492-502.

Vanderhaegen, S., & Canters, F. (2010). Developing urban metrics to describe the morphology of urban areas at block level. *The International Archives of the Photogrammetry, Remote Sensing and Spatial Information Sciences, XXXVIII-4/C7*.

Vera Rebollo, F. (1990). El auge de la promocidn inmobiliaria en la franja litoral alicantina y sus efecfos en la restructuración de la oferta. *TREBALLS DE GEOGRAFIA*(43), pp. 49-57.

Vespere, G. (2008). *La costa e il sistema costruito: possibili visioni di trasformazione del paesaggio costiero spontaneo nel sud Italia.* Bari: Associazione italiana di scienze regionali: XXIX Conferenza italiana di scienze regionali.

Vidal, C., Gallego, J., & Kayadjanian, M. (2001). Geographical use of statistical data. Methodological overview. In E. D., *Towards agri-environmental indicators. Integrating statistical and administrative data with land cover information* (pp. 11-24). Luxembourg: Office for Official Publications of the European Communities.

Villa, G., Valcarcela, N., Arozarenaa, A., Garcia-Asensioa, L., Caballeroa, M., Porcunab, A., . . . Pecesa, J. (2008). Land Cover Classification: an Obsolete Paradigm. (ISPRS, Ed.) *The International Archives of the Photogrammetry, Remote Sensing and Spatial Information Sciences, XXXVII*(B4), pp. 609-614.

Vitousek, P. M. (1994). Beyond global warming: ecology and global change. *Ecology*(75), pp. 1861-1876.

Vogelmann, J. E., Howard, S., Yang, L., Larson, C. R., Wylie, B. K., & Van Driel, J. N. (2001). Completion of the 1990's National Land Cover Data Set for the conterminous United States from Landsat Thematic Mapper Data and Ancillary Data Sources. *Photogrammetric Engineering and Remote Sensing*(67), pp. 650–662.

Weber, J. (2009, April 27-30). Land Cover Classification for Land Cover Accounting. *14th Meeting of the London Group on Environmental Accounting. Asset Accounting, Land classification*. Cabrera: London Group on Environmental Accounting.

Weier, J., & Herring, D. (2000, August 30). *Measuring Vegetation (NDVI & EVI).* (C. Ichoku, Ed.) Retrieved 2013, from Earth Observatory: http://earthobservatory.nasa.gov/Features/MeasuringVegetation/

Weitz, J., & Moore, T. (1998). Development inside urban growth boundaries: Oregon's empirical evidence of contiguous urban form. *Journal of the American Planning Association*(64 (4)), pp. 424–440.

Wen, Y. (2010). Research on the Spatial Structure and Landscape Patterns for the Land Use in Beijing Suburb based on RS & GIS. In R. Zhu, Y. Zhang, B. Liu, & C. Liu, *Information Computing and Applications. Proceedings of First International Conference, ICICA. Tangshan, China.* Germany: Springer.

Weng, Q. (2010). *Remote Sensing and GIS Integration. Theories, Methods, and Applications.* The McGraw-Hill Companies, Inc.

Wentz, L. (1997). Shape analysis in GIS. *AutoCarto*(5), pp. 204–213.

Wheaton, W. C. (1976). On the optimal distribution of income among cities. *Journal of Urban Economics*(3), pp. 31-44.

White, R., Engelen, C., Uljee, I., Lavalle, C., & Erlich, D. (1999). Developing an Urban Land Use Simulator for European Cities. In *Proceedings of the 5th EC–GIS workshop.*

Whitehand, J. (1999). A century of urban morphology? *Urban Morphology*(3), pp. 1-2.

Whitehand, J. (2001). British urban morphology: the Conzenian tradition. *Urban Morphology*(5), pp. 103-9.

Whitehand, J. (2005). Urban morphology, urban landscape and fringe belt. *Urban Design*(93), pp. 19-21.

Whitehand, J. (2007). *Coenzenian urban morphology and urban landscapes.* Proceedings, 6th International Space Syntax Symposium, Istanbul.

Whyte, L. L. (1968). Introduction. In L. L. Whyte, *Aspects of Form* (pp. 1-7). London: Lund Humphries.

Wickham, J., Stehman, S., Fry, J., Smith, J., & Homer, C. (2010). Thematic accuracy of the NLCD 2001 land cover for the conterminous United States. *Remote Sensing of Environment*(114 (6)), pp. 1286–1296.

Wickham, J., Stehman, S., Gass, L., Dewitz, J., Fry, J., & Wade, T. (2013). Accuracy assessment of NLCD 2006 land cover and impervious surface. *Remote Sensing of Environment*(130), pp. 294-304.

Wickham, J., Stehman, S., Smith, J., & Yang, L. (2004). Thematic accuracy of MRLC-NLCD land cover for the western United States. *Remote Sensing of Environment, 91*(3-4), pp. 452–468.

Wiens, J. (1989). Spatial scaling in ecology. *Functional Ecology*(3), pp. 385-397.

Wilkinson, G. (1996). A review of current issues in the integration fo GIS and remote sensing data. *International Journal of Geographical Information Systems*(10), pp. 85-101.

Williams, K. (2000). Does intensifying cities make them more sustainable? In K. Williams, E. Burton, & M. Jenks, *Achieving Sustainable Urban Form* (pp. 30-45). London: E&FN Spon.

Wilson, E., Hurd, J., Civco, D., Prisloe, S., & Arnold, C. (2003). Development of a geospatial model to quantify, describe and map urban growth. *Remote Sensing of Environment, 86*(3), pp. 275–285.

Wingo, L. (1961). *Transportation and urban land.* Washington, D.C.: Resources for the Future.

Xu, H. (2006). Modification of normalised difference water index (NDWI) to enhance open water features in remotely sensed imagery. *International Journal of Remote Sensing, 27*(14), pp. 3025-3033.

Yang, L., Huang, C., Homer, C., Wylie, B., & Coan, M. (2003). An approach for mapping large-area impervious surfaces: Synergistic use of Landsat 7 ETM+ and high spatial resolution imagery. *Canadian Journal of Remote Sensing* 29(2), pp. 230-240.

Yeh, A. (1999). Urban Planning and GIS. In P. Longley, M. Goodchild, D. Maguire, & D. Rhind, *Geographical Information Systems: Management Issues and Applications* (2nd Edition ed., Vol. II, pp. 877-888). New York: Wiley.

Yeh, A., & Li, X. (2001b). Measurement and monitoring of urban sprawl in a rapidly growing region using entropy. *Photogrammetric Engineering & Remote Sensing, 67*(1), pp. 83-90.

Zamorano, W. (2011). La crisis del modelo urbanístico español. Especial referencia a Andalucía. In J. M. Jurado Almonte, *Ordenación del Territorio y Urbanismo: conflictos y oportunidades* (pp. 246-292). Sevilla: Universidad Internacional de Andalucía.

Zha, Y., Gao, J., & Ni, S. (2003). Use of Normalized Difference Built-up Ondex in automatically mapping urban areas from TM imagery. *International Journal of Remote Sensing, 24*(3), pp. 583-594.

Universidad Politécnica de Cataluña, Barcelona TECH
Departamento de Tecnología de la Arquitectura
Centro de Políticas de Suelo y Valoraciones

Nicola Colaninno, Josep Roca Cladera

ATLAS OF LAND COVER 2011 ALONG THE MEDITERRANEAN SIDE OF SPAIN

With this Atlas we mainly expect to achieve two objectives, that is, if on one hand we want to emphasize the capacity of the new technologies for collecting updated information about the land cover, analysis, and managing large geographic areas; on the other hand we aim to provide some general information about the land cover composition and configuration over a geographic area in Spain which has undergone, mostly during the last decades, certain alarming environmental changes mainly due to the urban development.

In particular the Atlas, which covers the Mediterranean side of Spain, is organized in accordance with the administrative division of the provinces, except for the case of the Balearic Islands where we opted for a division made upon the three main islands (Mallorca, Menorca, and the "tandem" Ibiza/Formentera). According to this, first the Atlas provides a picture of the geographical location of the province, the name, and the Autonomous Community to which it belongs. Moreover, each provincial map provides a metric scale (since the different dimensions of the provinces do not allow to keep the same scale for each case); and the area of each province reported in square kilometers. Finally, four key images are provided which show:

- the satellite image, shown in pseudo-natural colour composite in order to enhance the contrast between green areas and dry areas;
- the land cover classification, according to twenty categories as proposed at level II of our nomenclature and shown in the legend;
- the land cover classification in four categories according to the level I of the nomenclature, and a pie chart showing the percentage share of the four categories, that is: Artificial Areas, Planted/Cultivated, Forest and Natural, Inland Water (the sea is not computed, despite appearing in the picture);
- the Artificial Areas only, as detected by the classification methodology, along with the roads derived from the database of the Open Street Map (OSM), and the Digital Elevation Model (DEM).

The latter, in particular, underlines the relationship between urban development and territorial component, that is, stresses the idea that often the urban fabric tends to occupy flatter and less elevated areas.

Universidad Politécnica de Cataluña, Barcelona TECH
Departamento de Tecnología de la Arquitectura
Centro de Políticas de Suelo y Valoraciones
Nicola Colaninno, Josep Roca Cladera

GERONA (Catalunya)

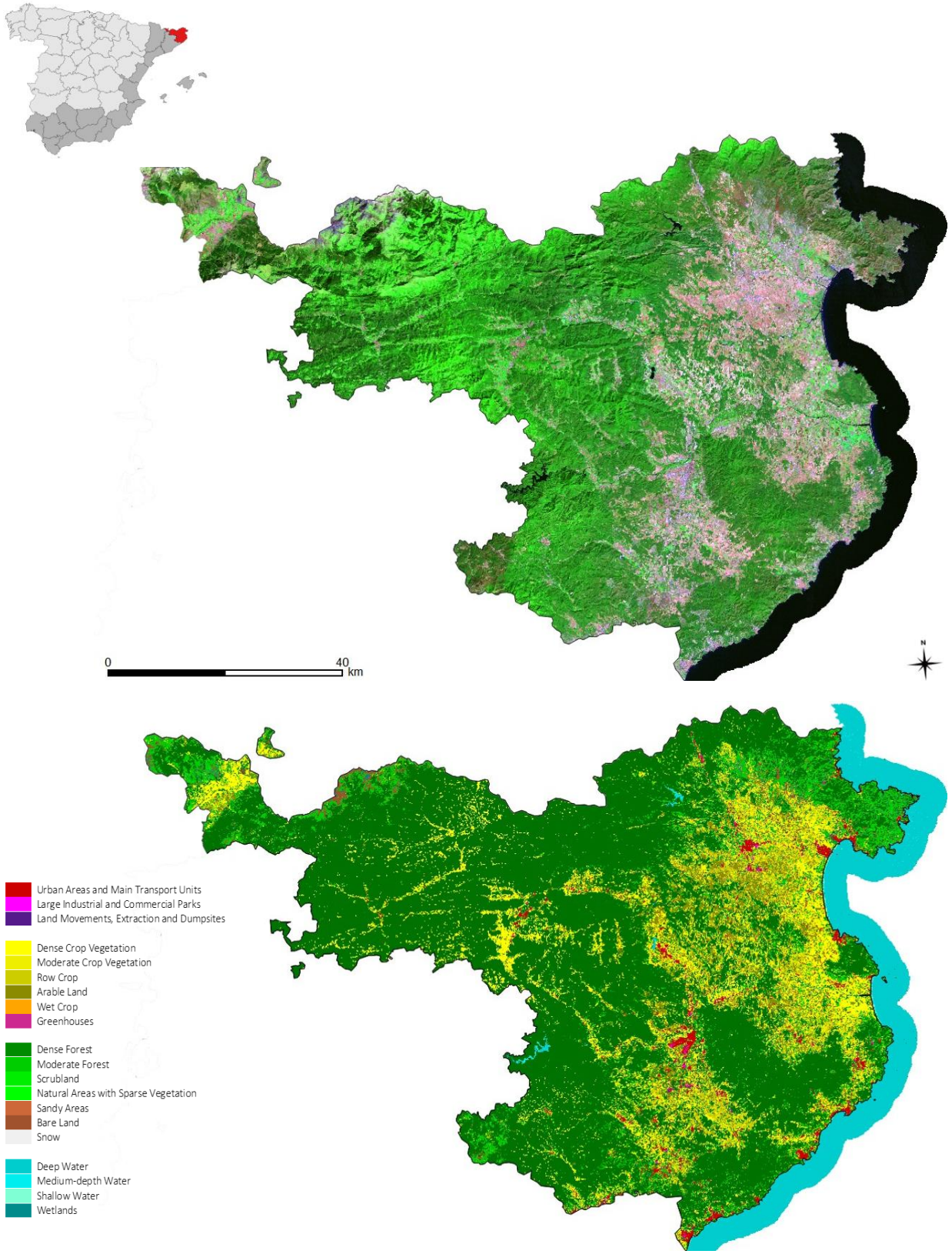

Universidad Politécnica de Cataluña, Barcelona TECH
Departamento de Tecnología de la Arquitectura
Centro de Políticas de Suelo y Valoraciones
Nicola Colaninno, Josep Roca Cladera

Area ≈ 5˙909 Km^2

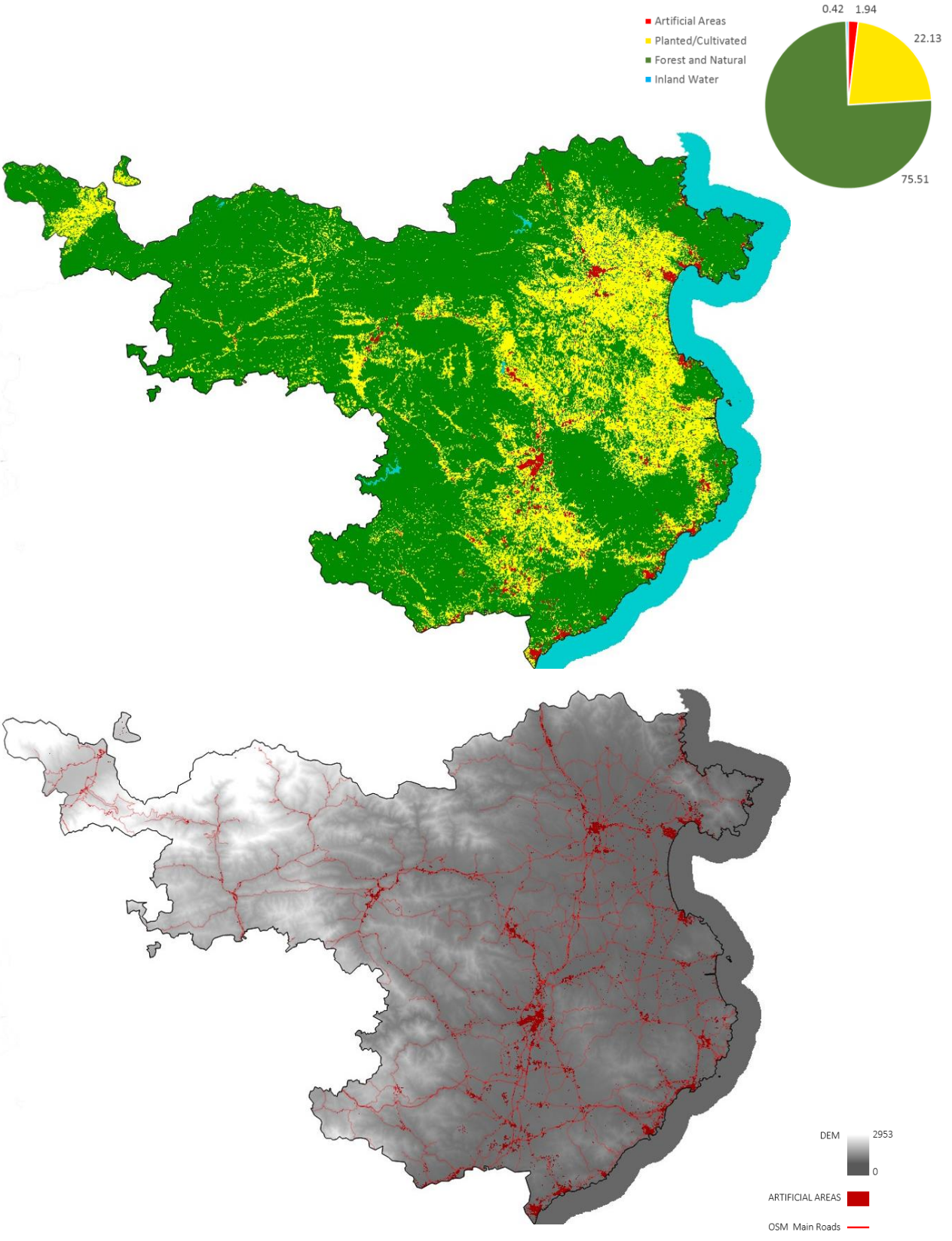

Universidad Politécnica de Cataluña, Barcelona TECH
Departamento de Tecnología de la Arquitectura
Centro de Políticas de Suelo y Valoraciones

Nicola Colaninno, Josep Roca Cladera

BARCELONA (Catalunya)

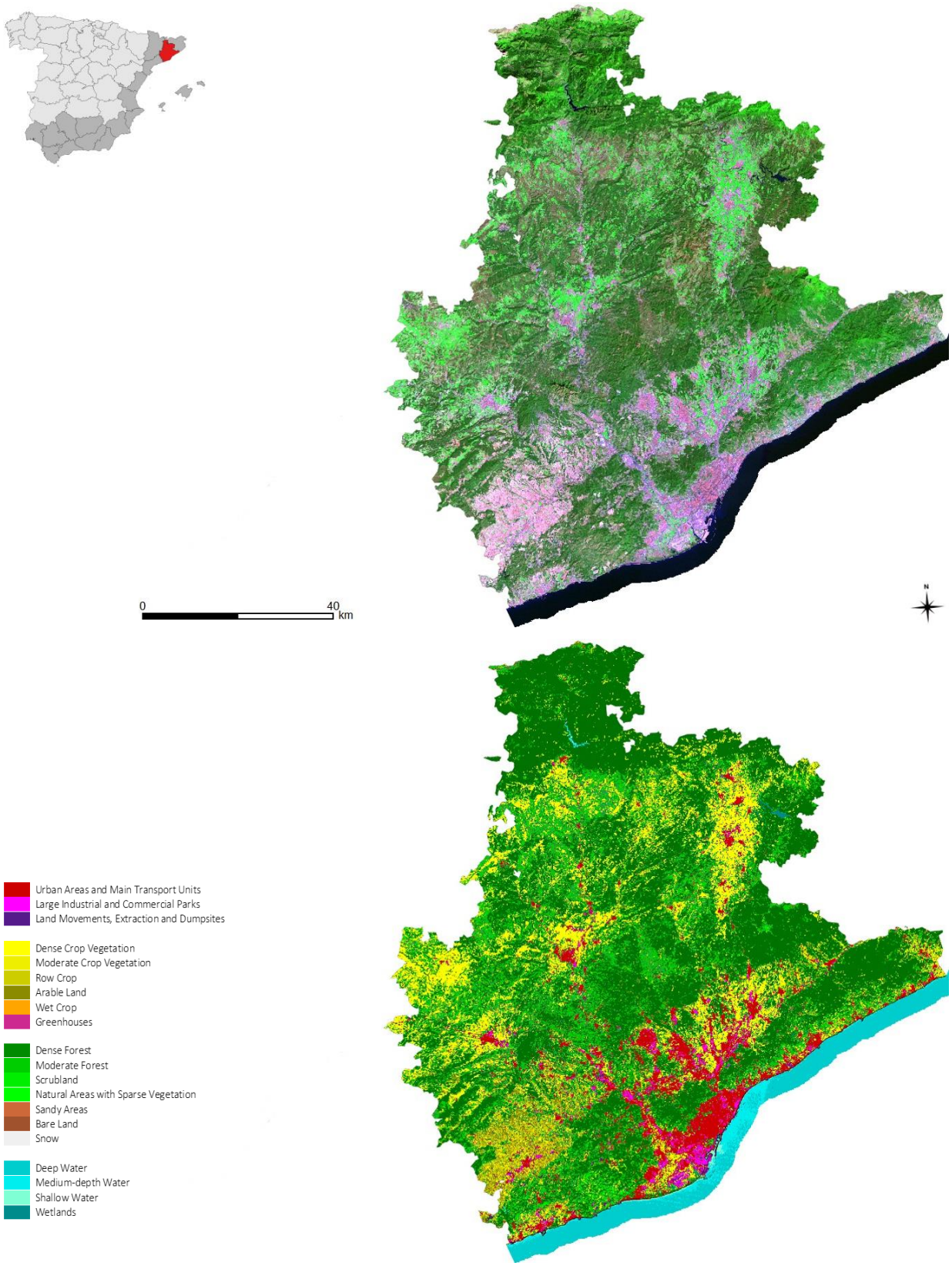

Universidad Politécnica de Cataluña, Barcelona TECH
Departamento de Tecnología de la Arquitectura
Centro de Políticas de Suelo y Valoraciones
Nicola Colaninno, Josep Roca Cladera

Area ≈ 7˙725 Km^2

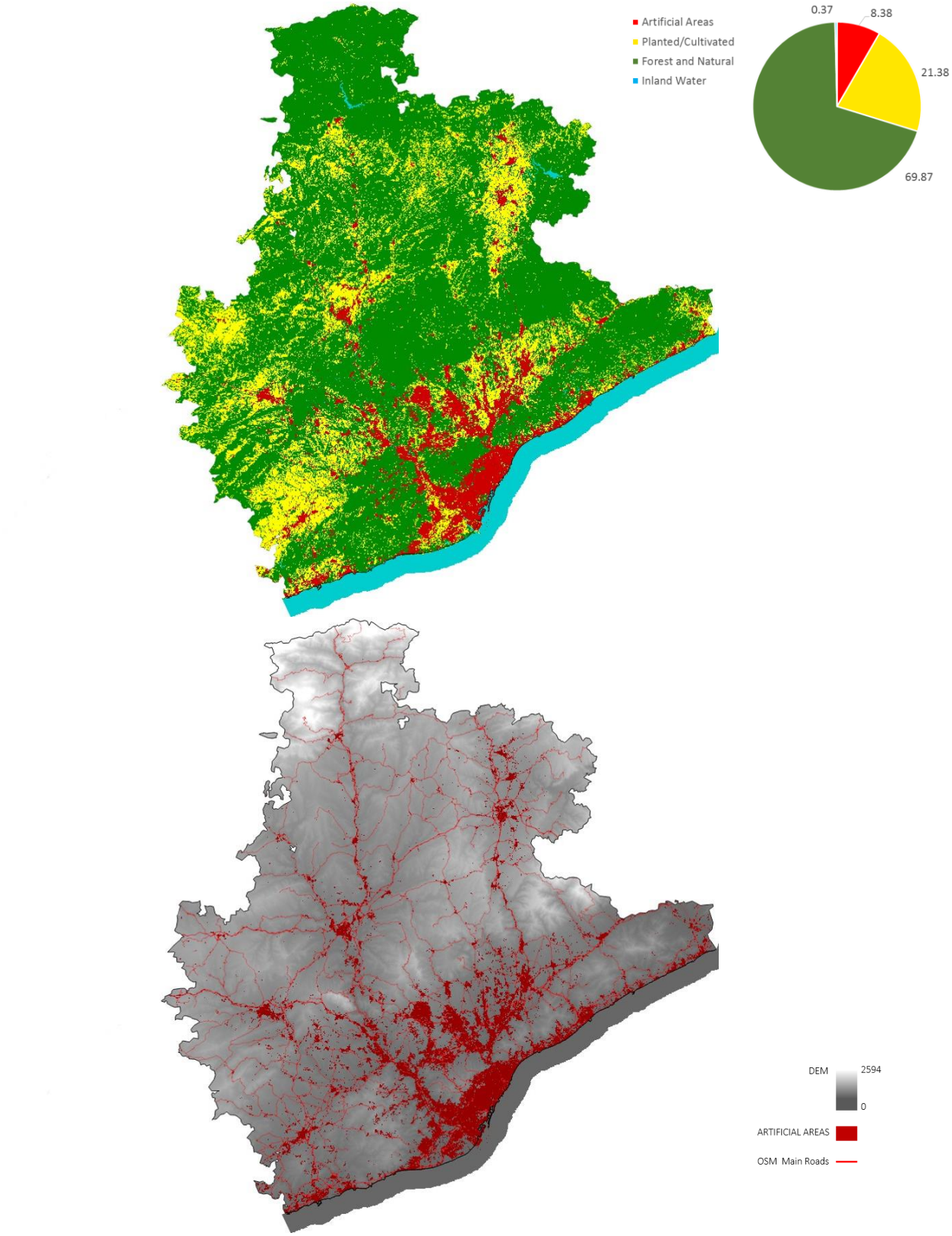

Universidad Politécnica de Cataluña, Barcelona TECH
Departamento de Tecnología de la Arquitectura
Centro de Políticas de Suelo y Valoraciones

Nicola Colaninno, Josep Roca Cladera

LLEIDA (Catalunya)

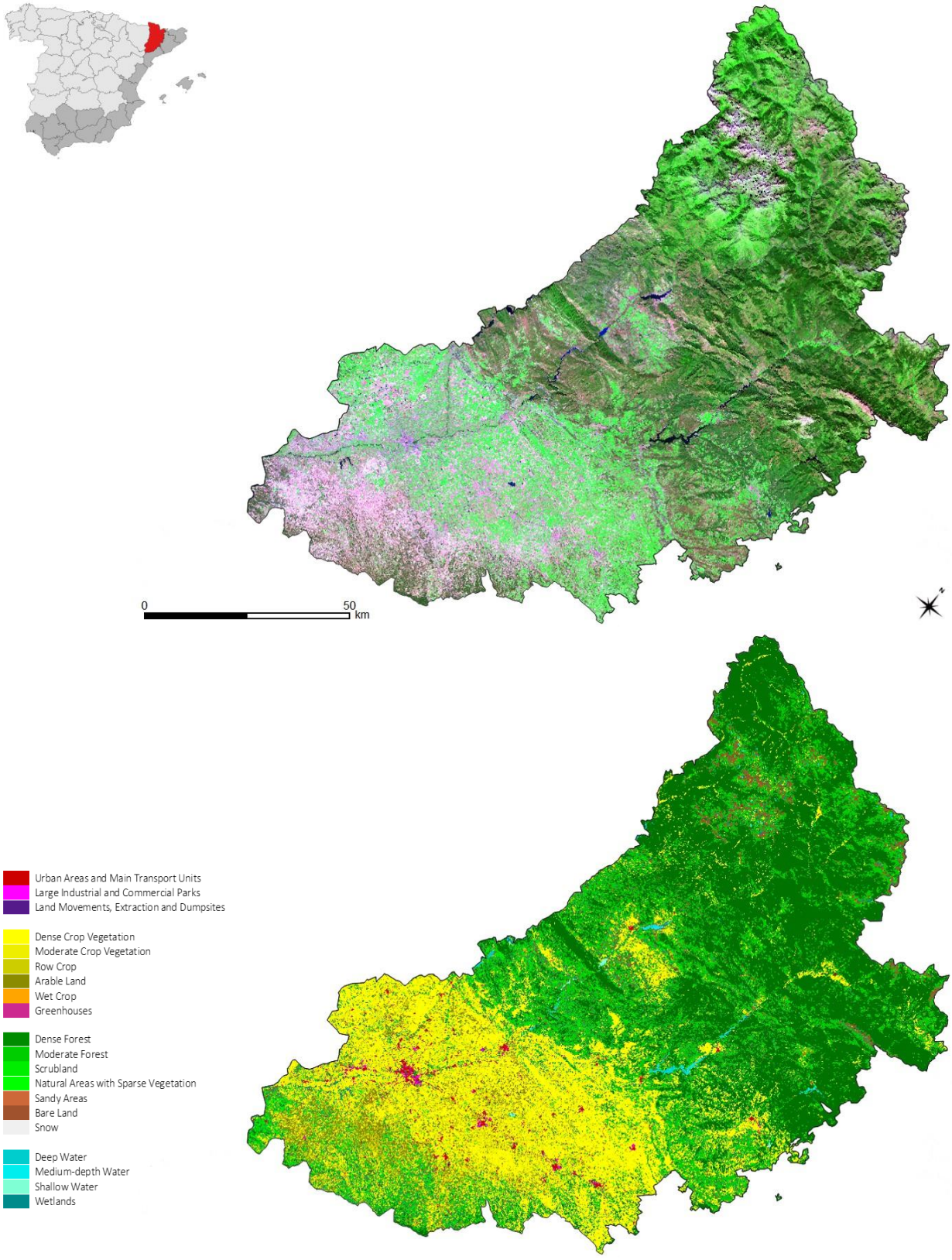

Universidad Politécnica de Cataluña, Barcelona TECH
Departamento de Tecnología de la Arquitectura
Centro de Políticas de Suelo y Valoraciones
Nicola Colaninno, Josep Roca Cladera

Area ≈ 12˙170 Km^2

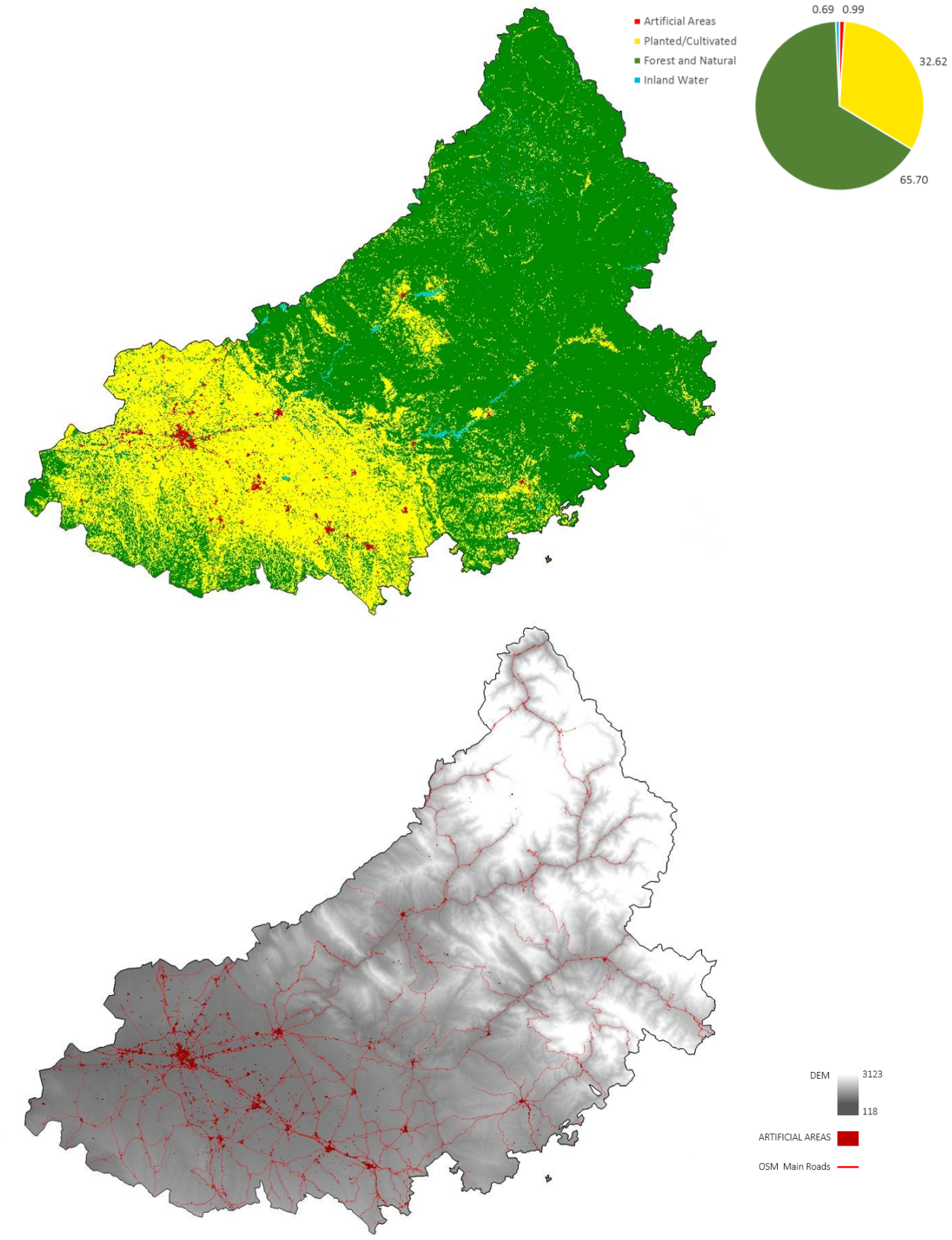

Universidad Politécnica de Cataluña, Barcelona TECH
Departamento de Tecnología de la Arquitectura
Centro de Políticas de Suelo y Valoraciones

Nicola Colaninno, Josep Roca Cladera

TARRAGONA (Catalunya)

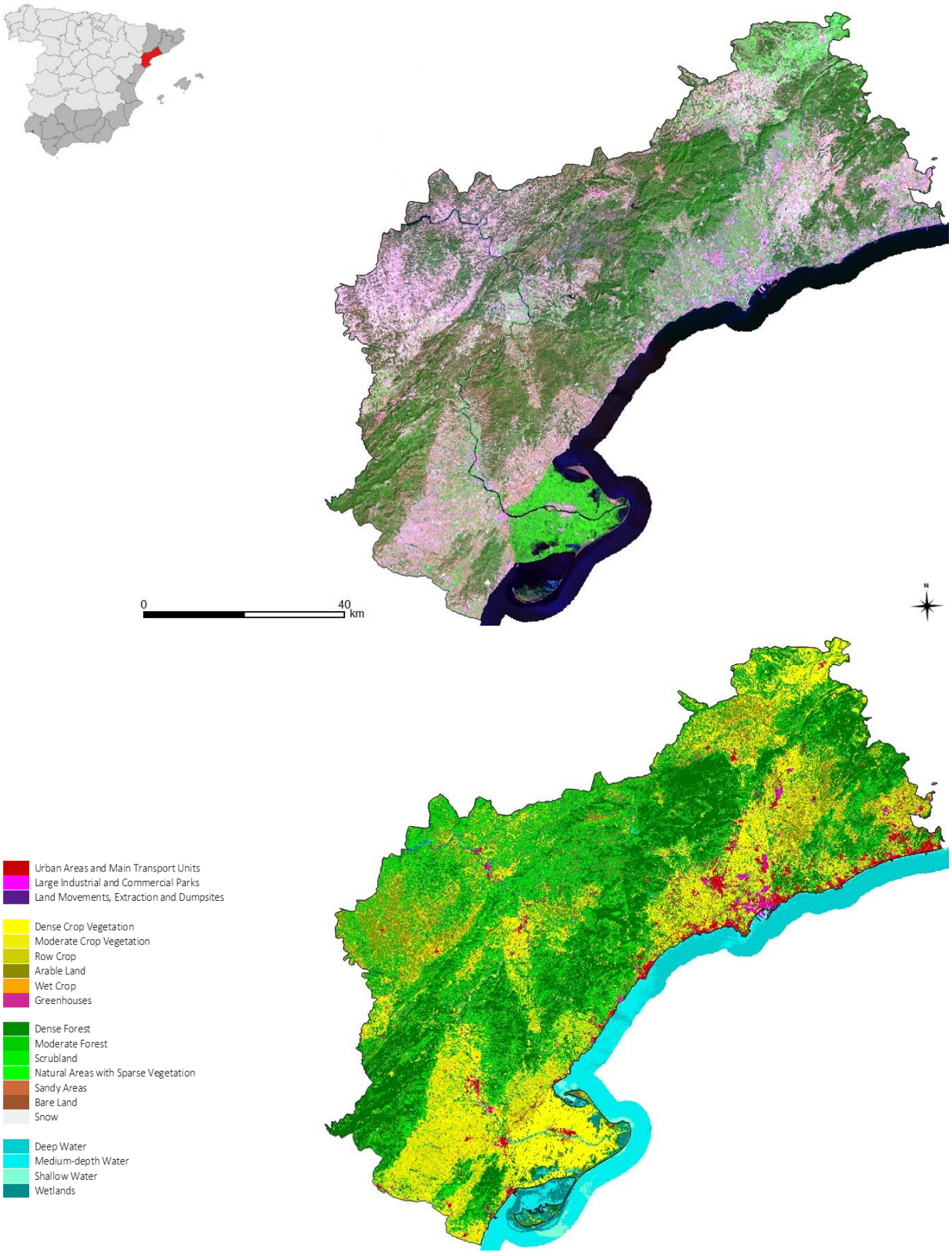

Universidad Politécnica de Cataluña, Barcelona TECH
Departamento de Tecnología de la Arquitectura
Centro de Políticas de Suelo y Valoraciones

Nicola Colaninno, Josep Roca Cladera

Area ≈ 6˙308 Km^2

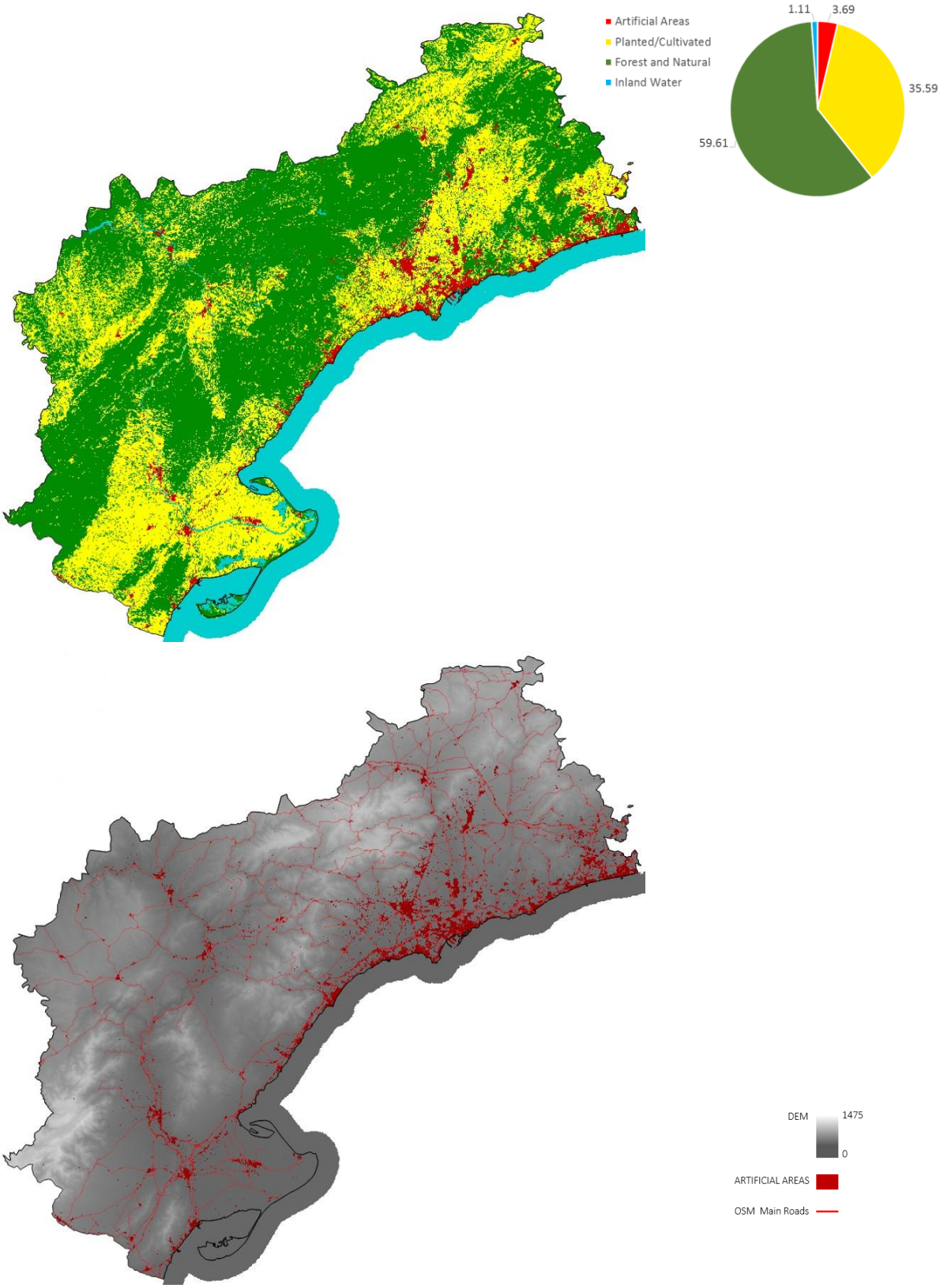

Universidad Politécnica de Cataluña, Barcelona TECH
Departamento de Tecnología de la Arquitectura
Centro de Políticas de Suelo y Valoraciones

Nicola Colaninno, Josep Roca Cladera

CASTELLÓN (Valencia)

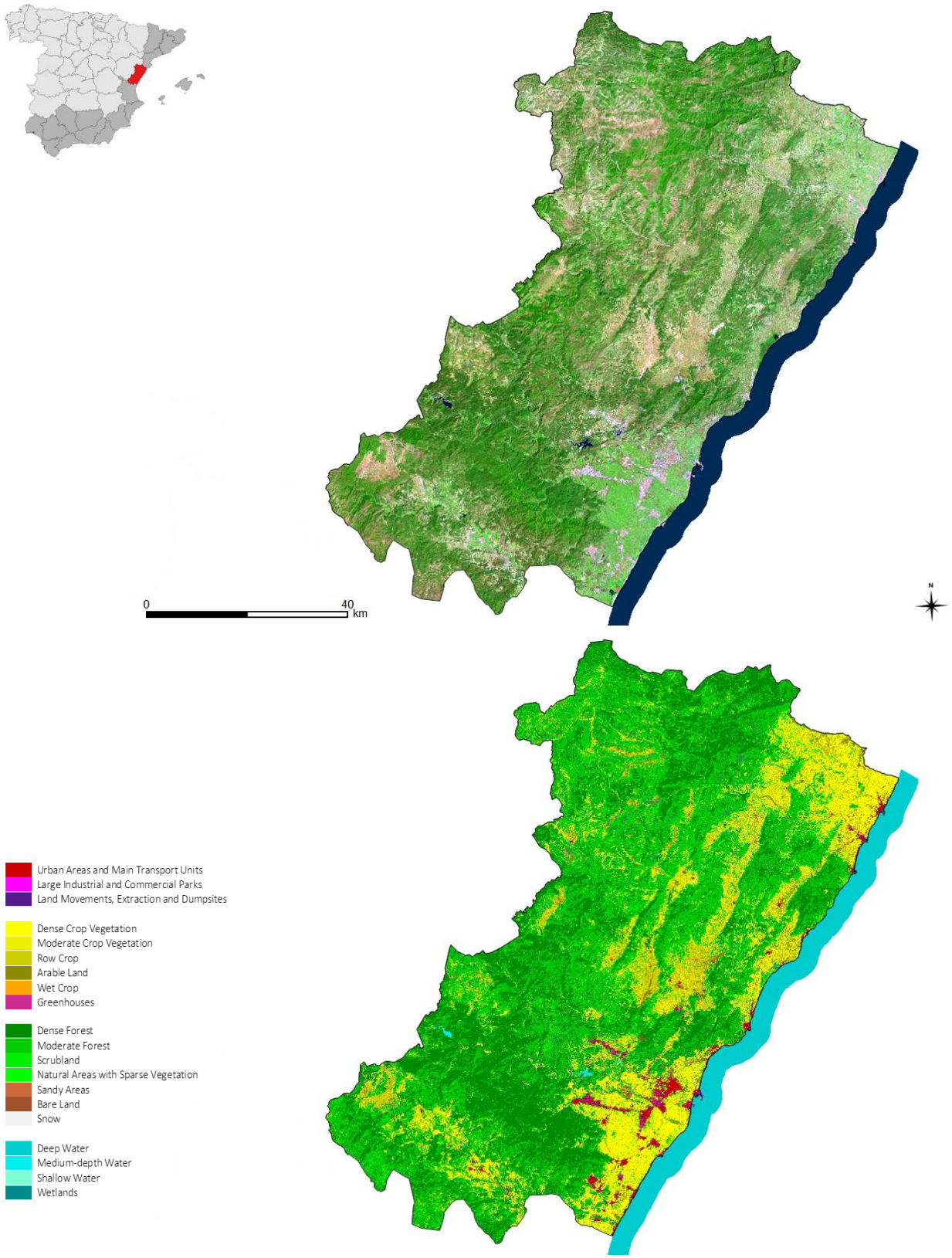

Universidad Politécnica de Cataluña, Barcelona TECH
Departamento de Tecnología de la Arquitectura
Centro de Políticas de Suelo y Valoraciones

Nicola Colaninno, Josep Roca Cladera

Area ≈ 6˙632 Km^2

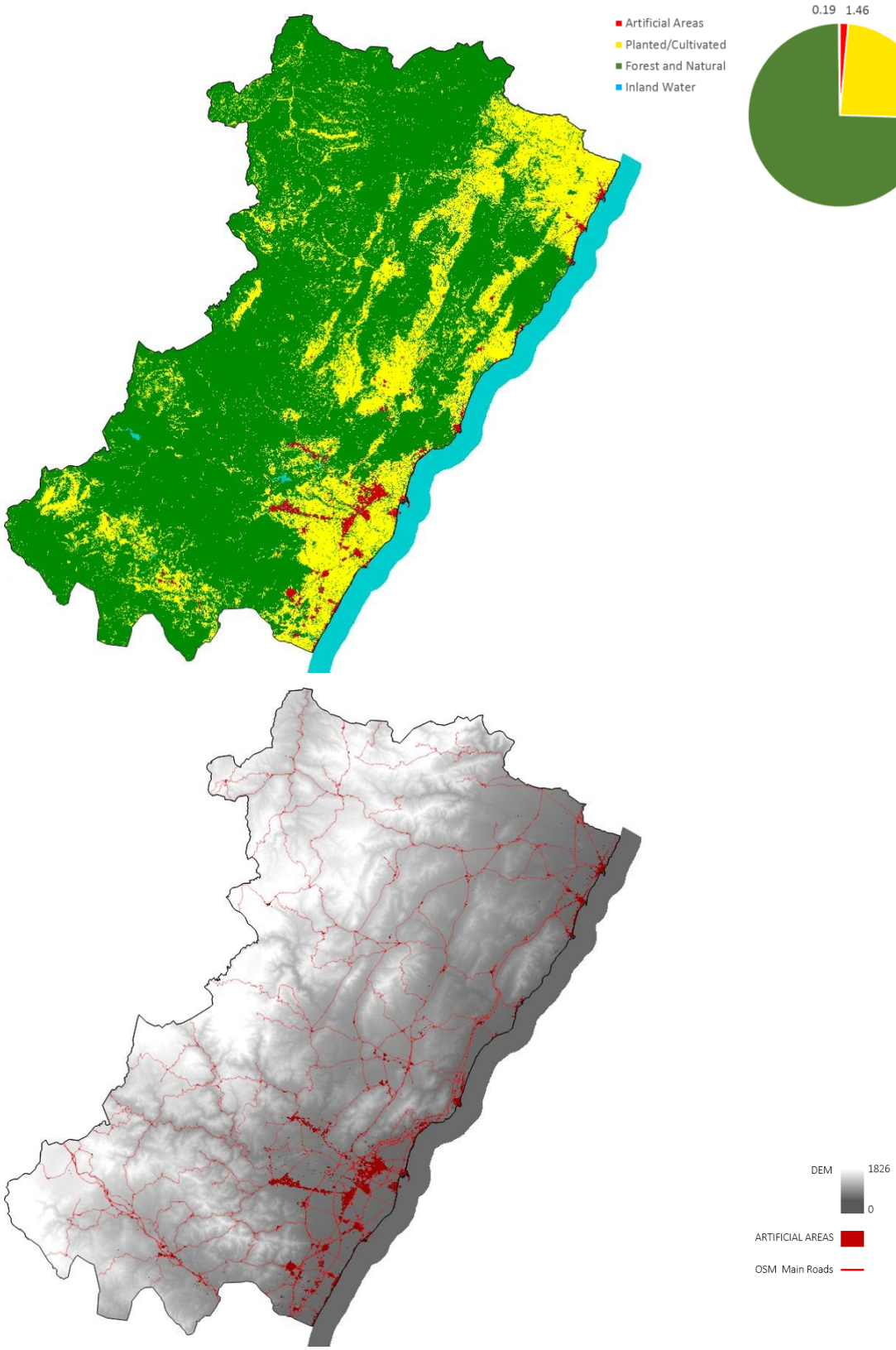

Universidad Politécnica de Cataluña, Barcelona TECH
Departamento de Tecnología de la Arquitectura
Centro de Políticas de Suelo y Valoraciones

Nicola Colaninno, Josep Roca Cladera

VALENCIA (Valencia)

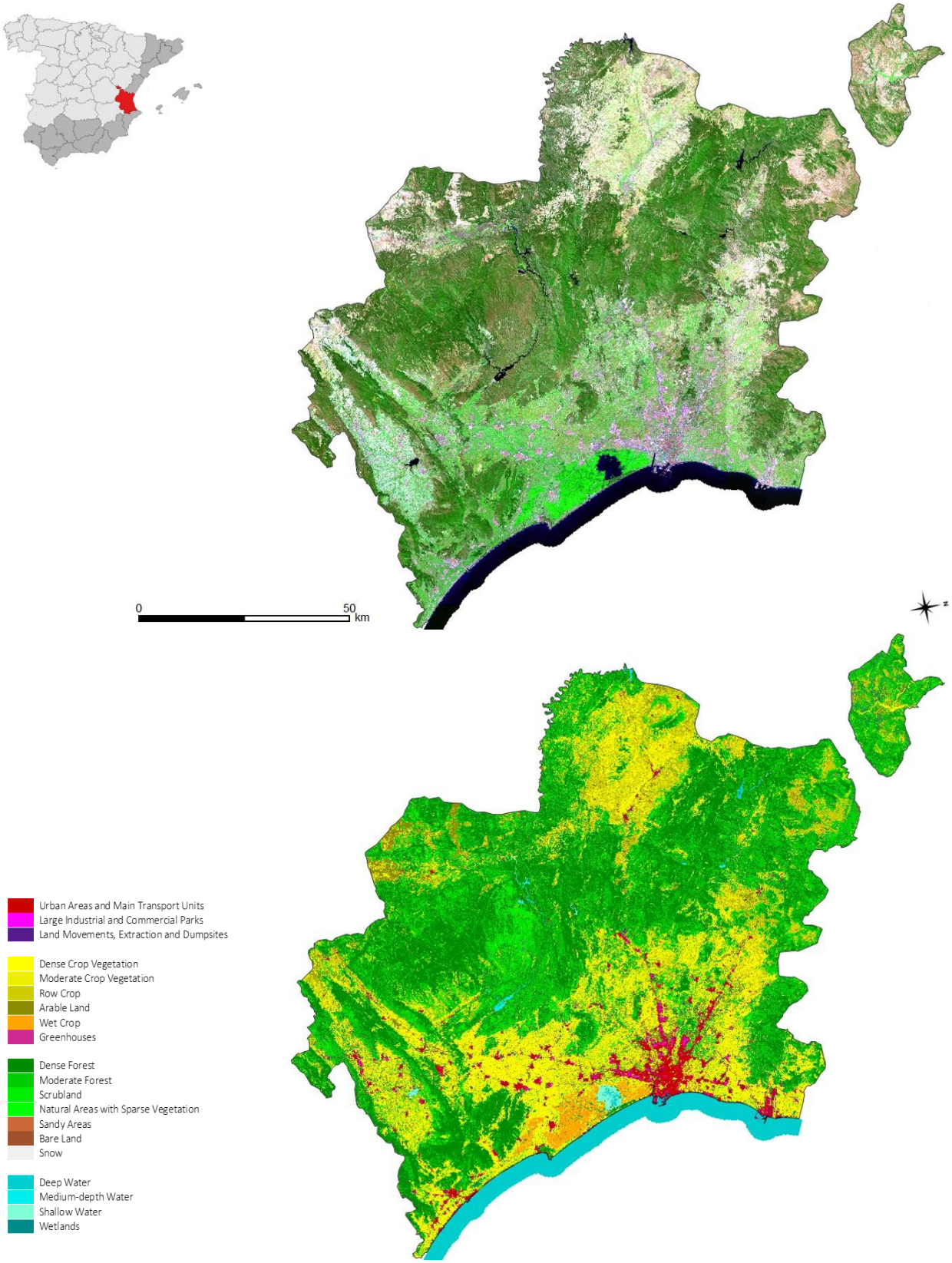

Universidad Politécnica de Cataluña, Barcelona TECH
Departamento de Tecnología de la Arquitectura
Centro de Políticas de Suelo y Valoraciones
Nicola Colaninno, Josep Roca Cladera

Area ≈ 10˙800 Km^2

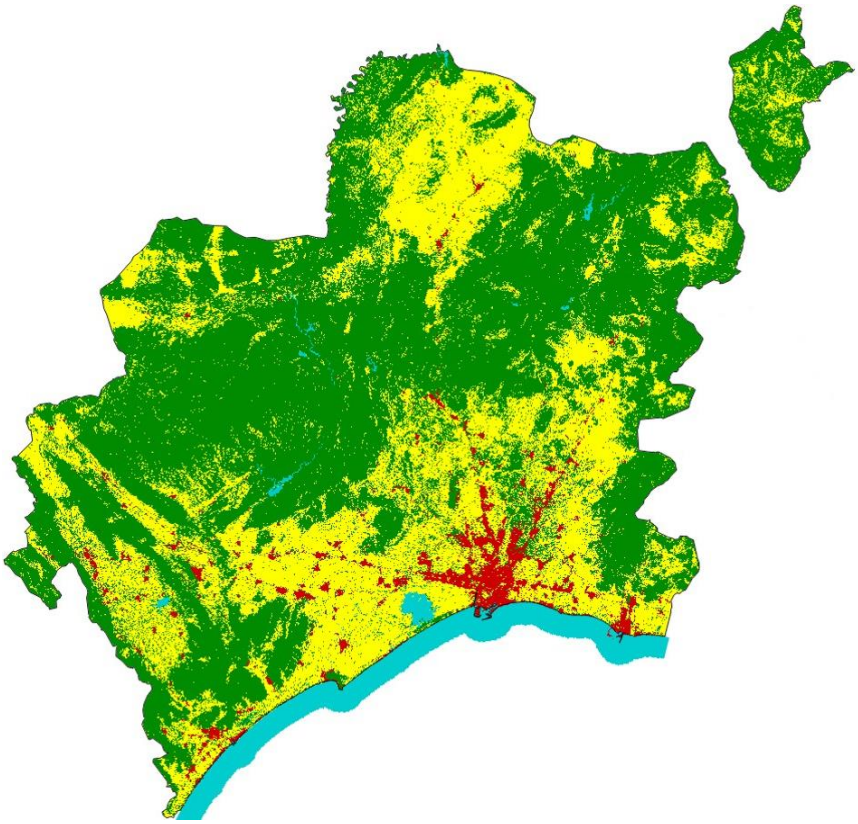

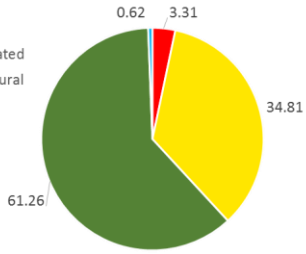

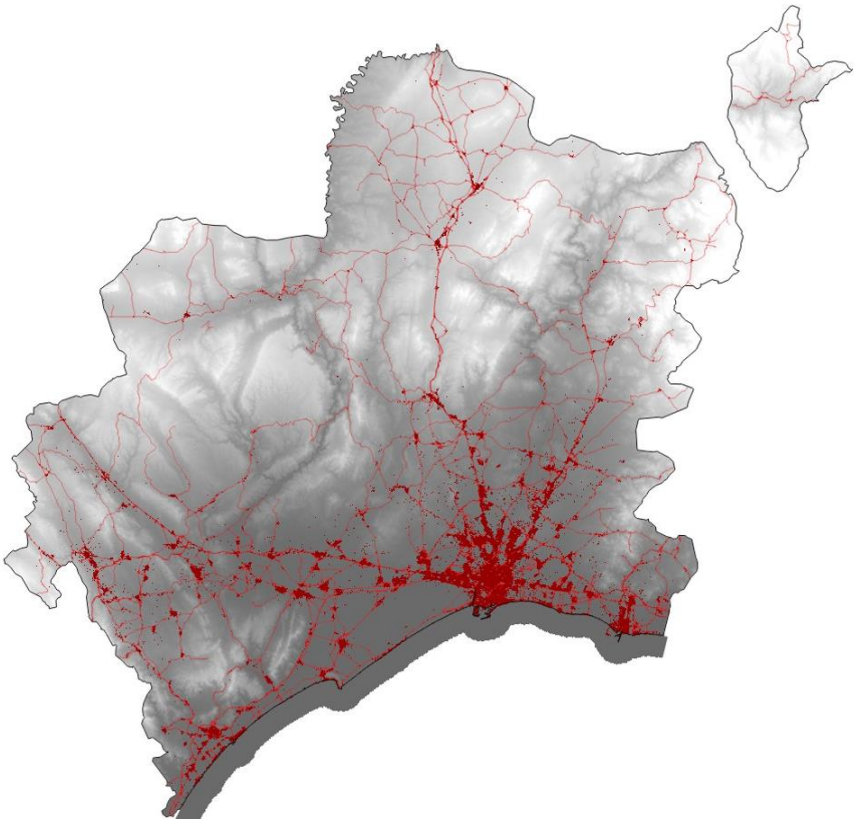

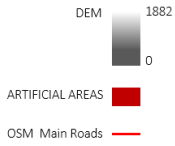

Universidad Politécnica de Cataluña, Barcelona TECH
Departamento de Tecnología de la Arquitectura
Centro de Políticas de Suelo y Valoraciones

Nicola Colaninno, Josep Roca Cladera

ALICANTE (Valencia)

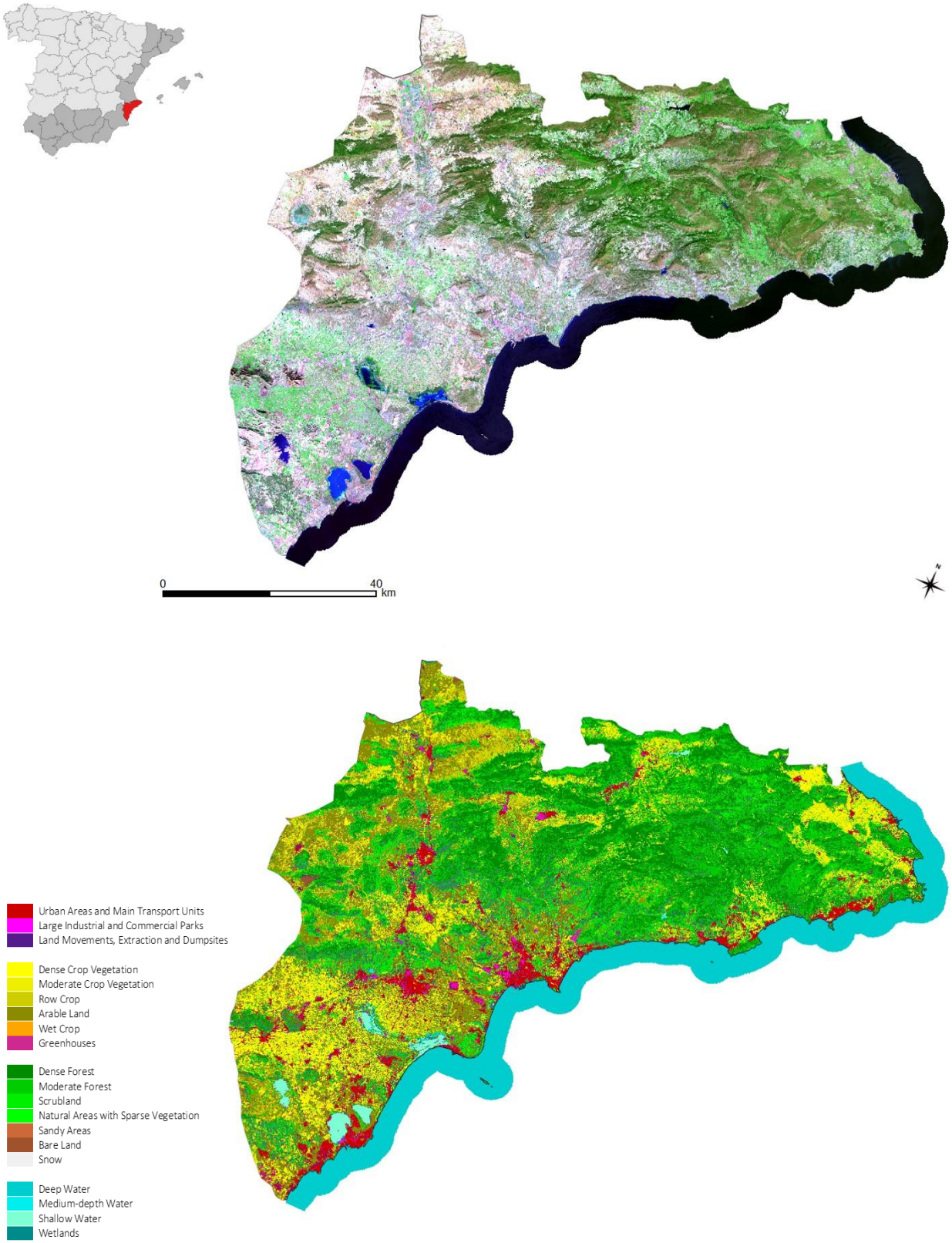

Universidad Politécnica de Cataluña, Barcelona TECH
Departamento de Tecnología de la Arquitectura
Centro de Políticas de Suelo y Valoraciones
Nicola Colaninno, Josep Roca Cladera

Area ≈ 5˙816 Km^2

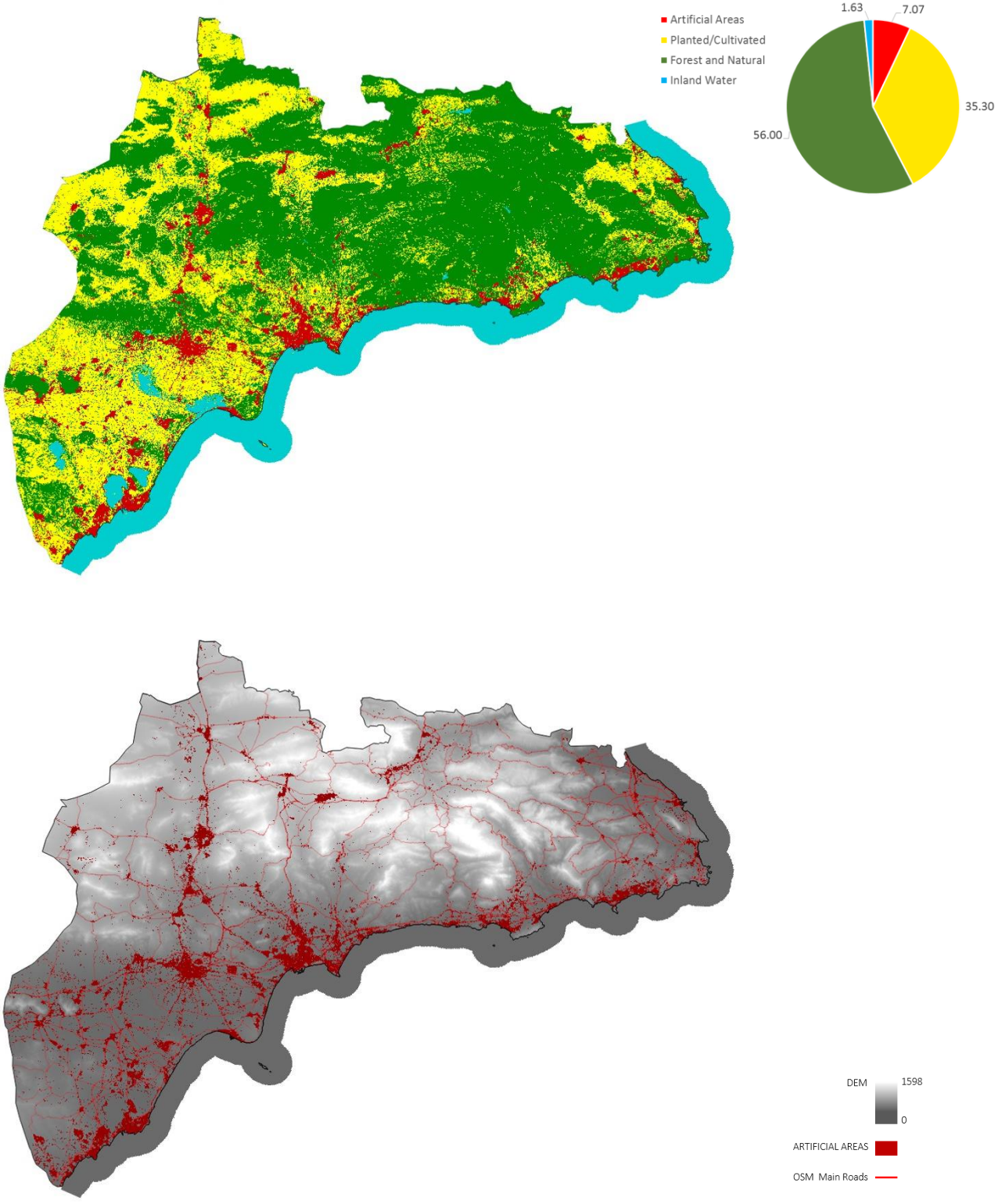

Universidad Politécnica de Cataluña, Barcelona TECH
Departamento de Tecnología de la Arquitectura
Centro de Políticas de Suelo y Valoraciones

Nicola Colaninno, Josep Roca Cladera

MURCIA (Murcia)

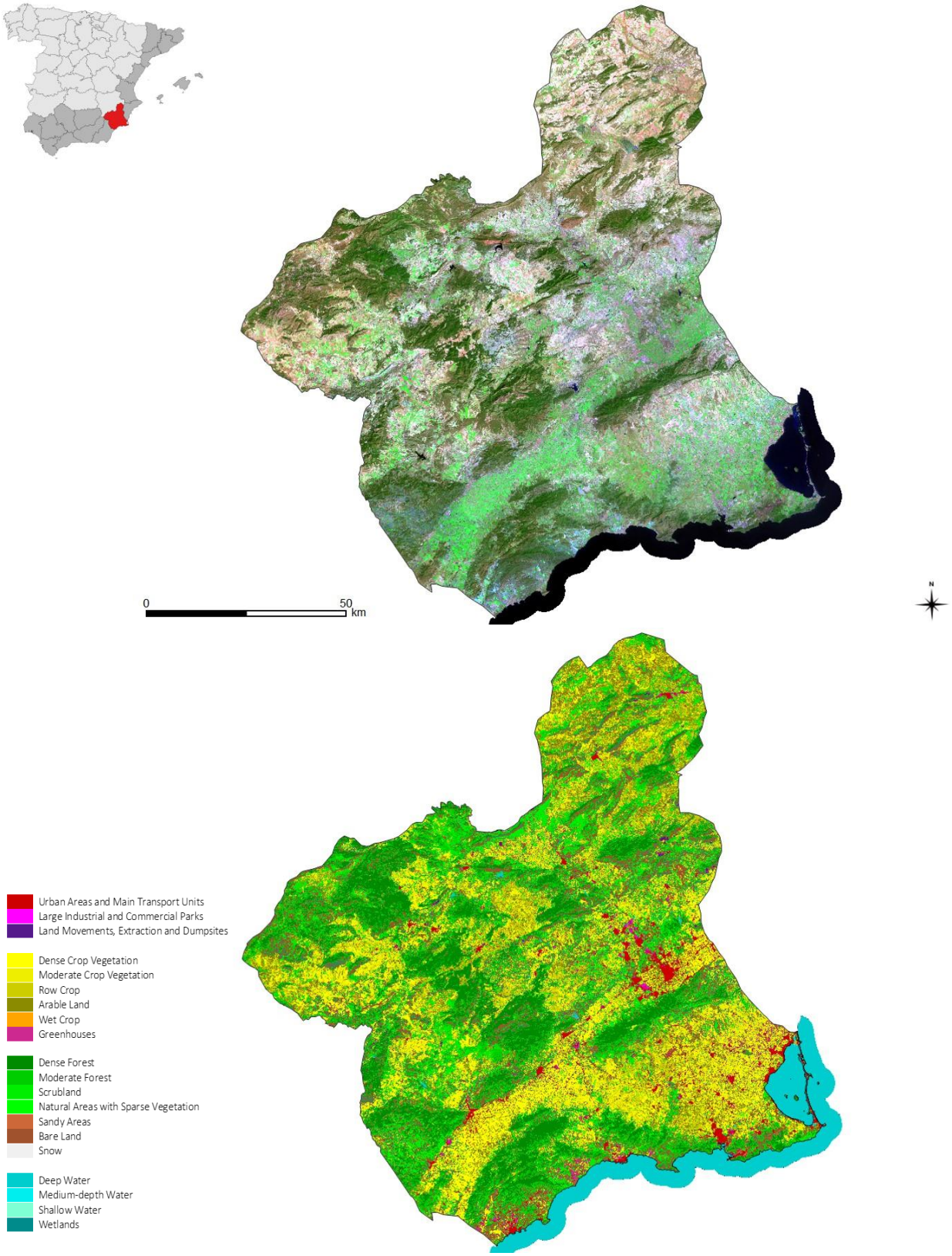

Universidad Politécnica de Cataluña, Barcelona TECH
Departamento de Tecnología de la Arquitectura
Centro de Políticas de Suelo y Valoraciones

Nicola Colaninno, Josep Roca Cladera

Area ≈ 11˙300 Km^2

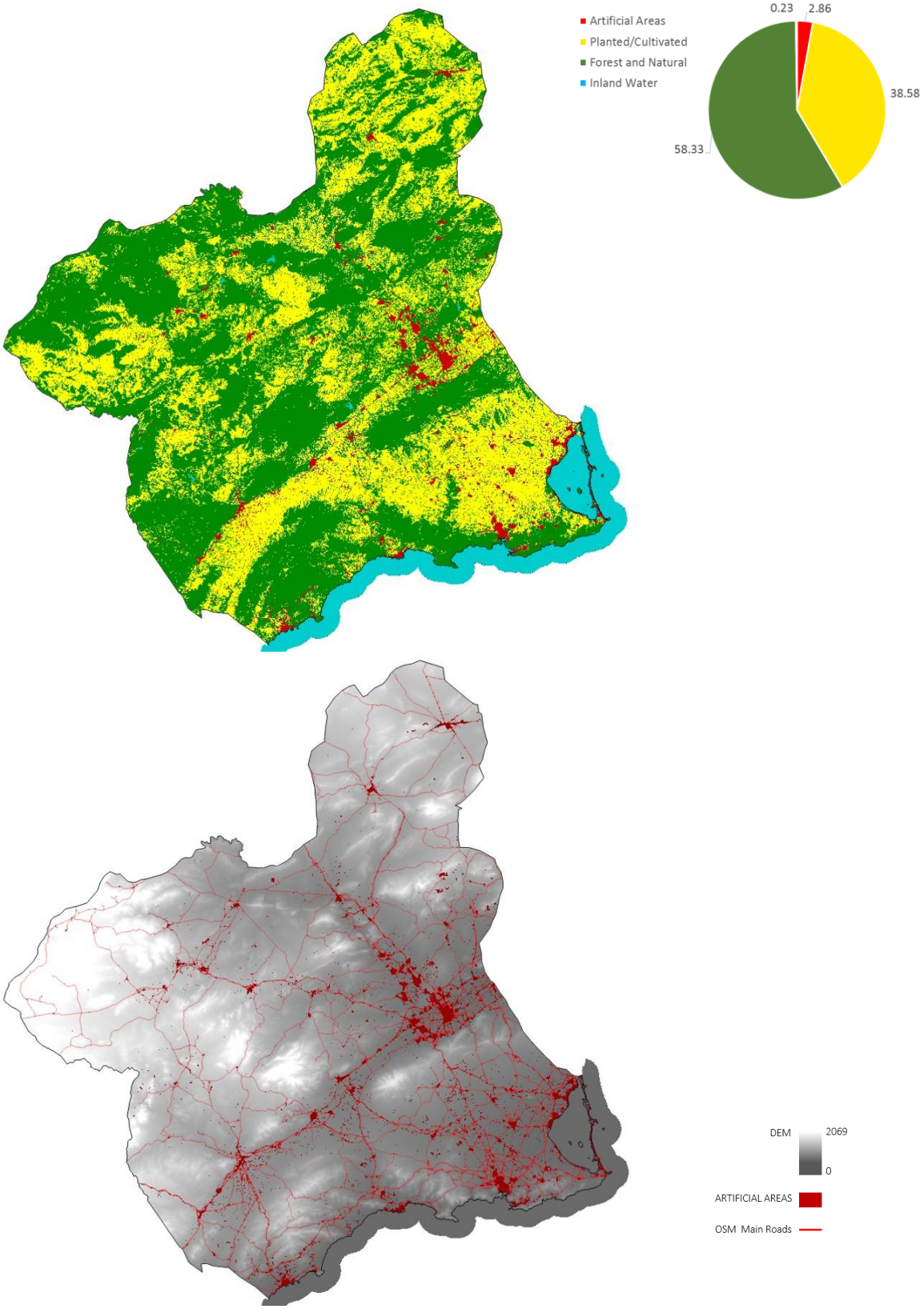

Universidad Politécnica de Cataluña, Barcelona TECH
Departamento de Tecnología de la Arquitectura
Centro de Políticas de Suelo y Valoraciones

Nicola Colaninno, Josep Roca Cladera

ALMERÍA (Andalucía)

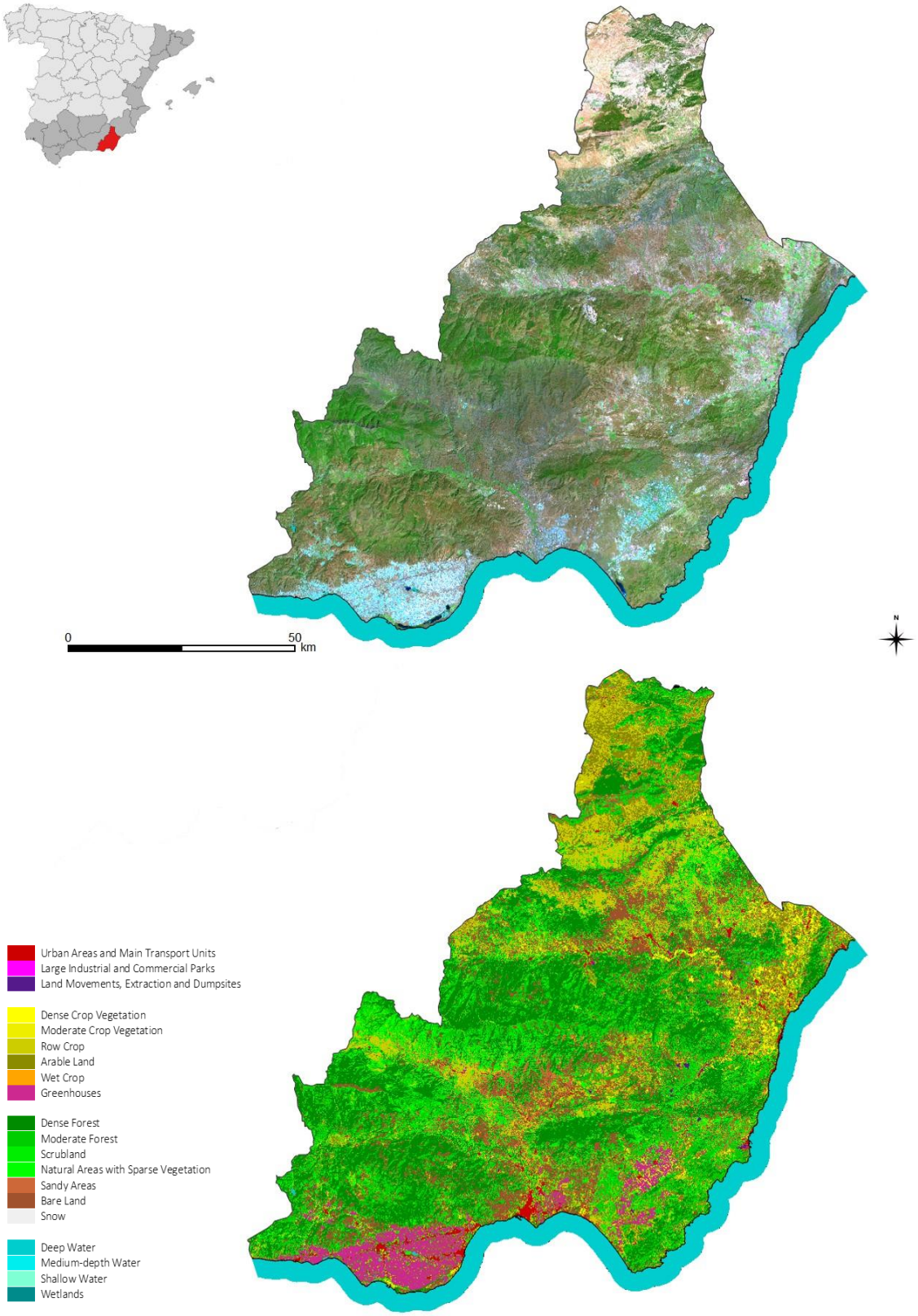

Universidad Politécnica de Cataluña, Barcelona TECH
Departamento de Tecnología de la Arquitectura
Centro de Políticas de Suelo y Valoraciones
Nicola Colaninno, Josep Roca Cladera

Area ≈ 8˙756 Km^2

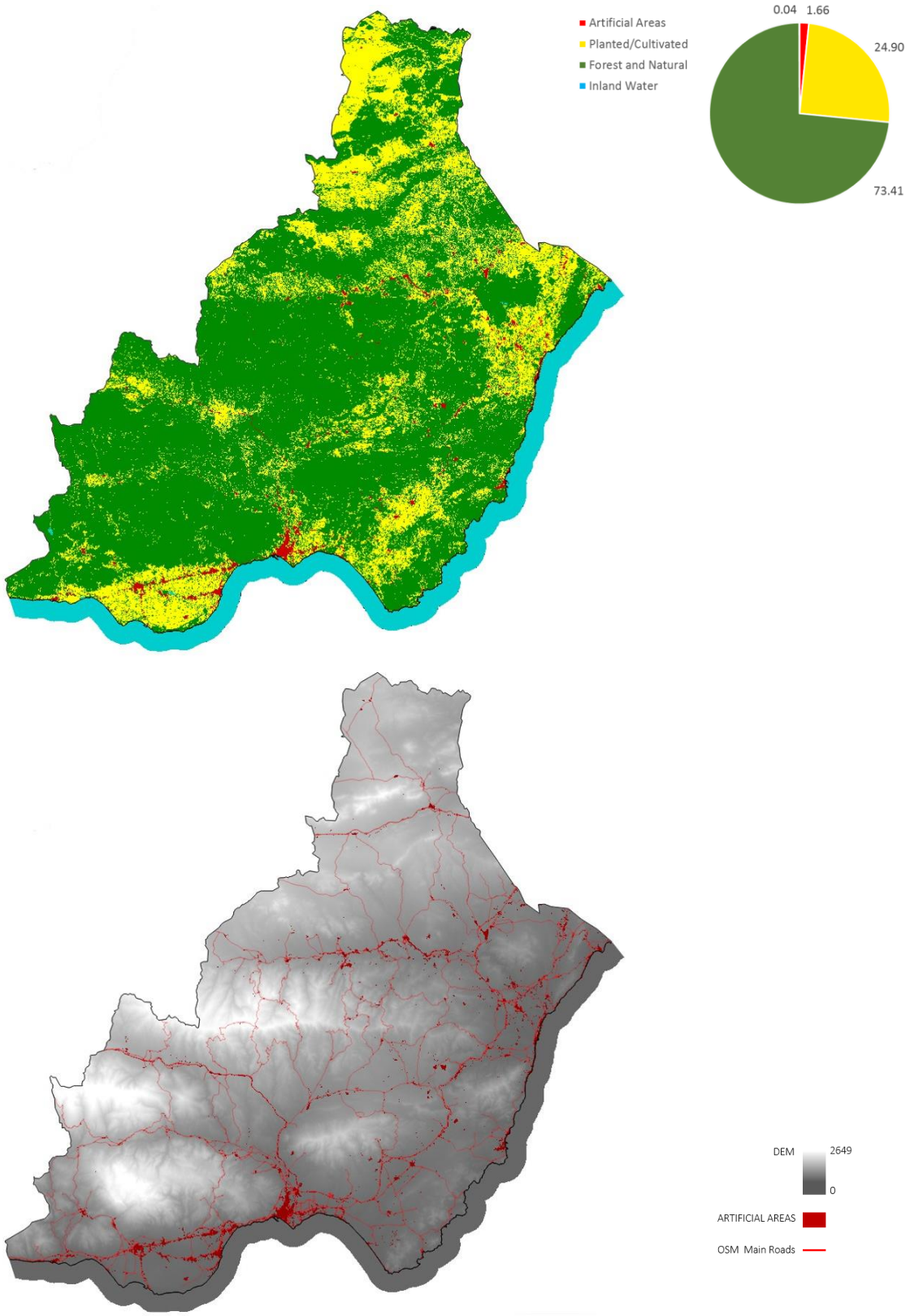

Universidad Politécnica de Cataluña, Barcelona TECH
Departamento de Tecnología de la Arquitectura
Centro de Políticas de Suelo y Valoraciones

Nicola Colaninno, Josep Roca Cladera

GRANADA (Andalucía)

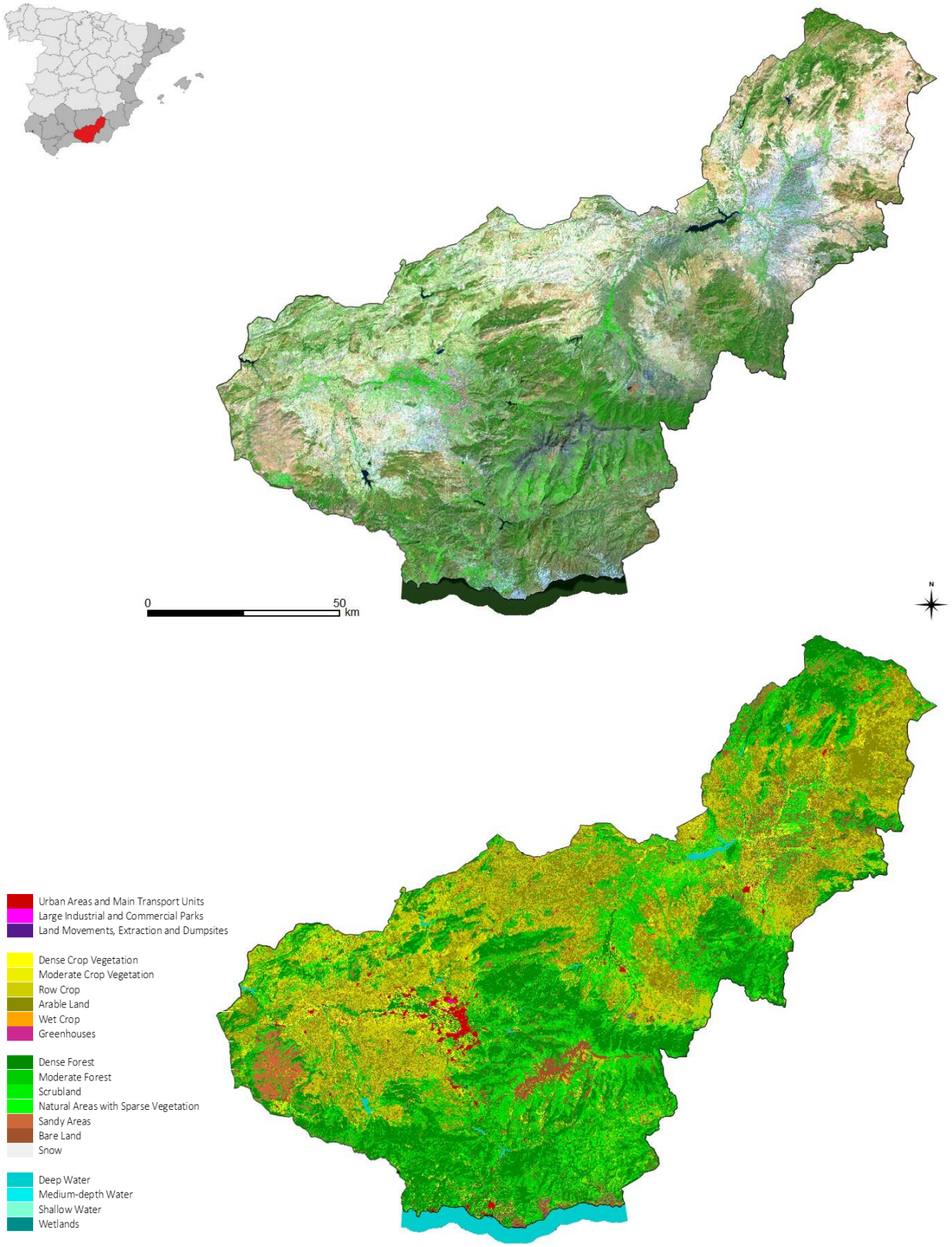

Universidad Politécnica de Cataluña, Barcelona TECH
Departamento de Tecnología de la Arquitectura
Centro de Políticas de Suelo y Valoraciones
Nicola Colaninno, Josep Roca Cladera

Area ≈ 12˙623 Km^2

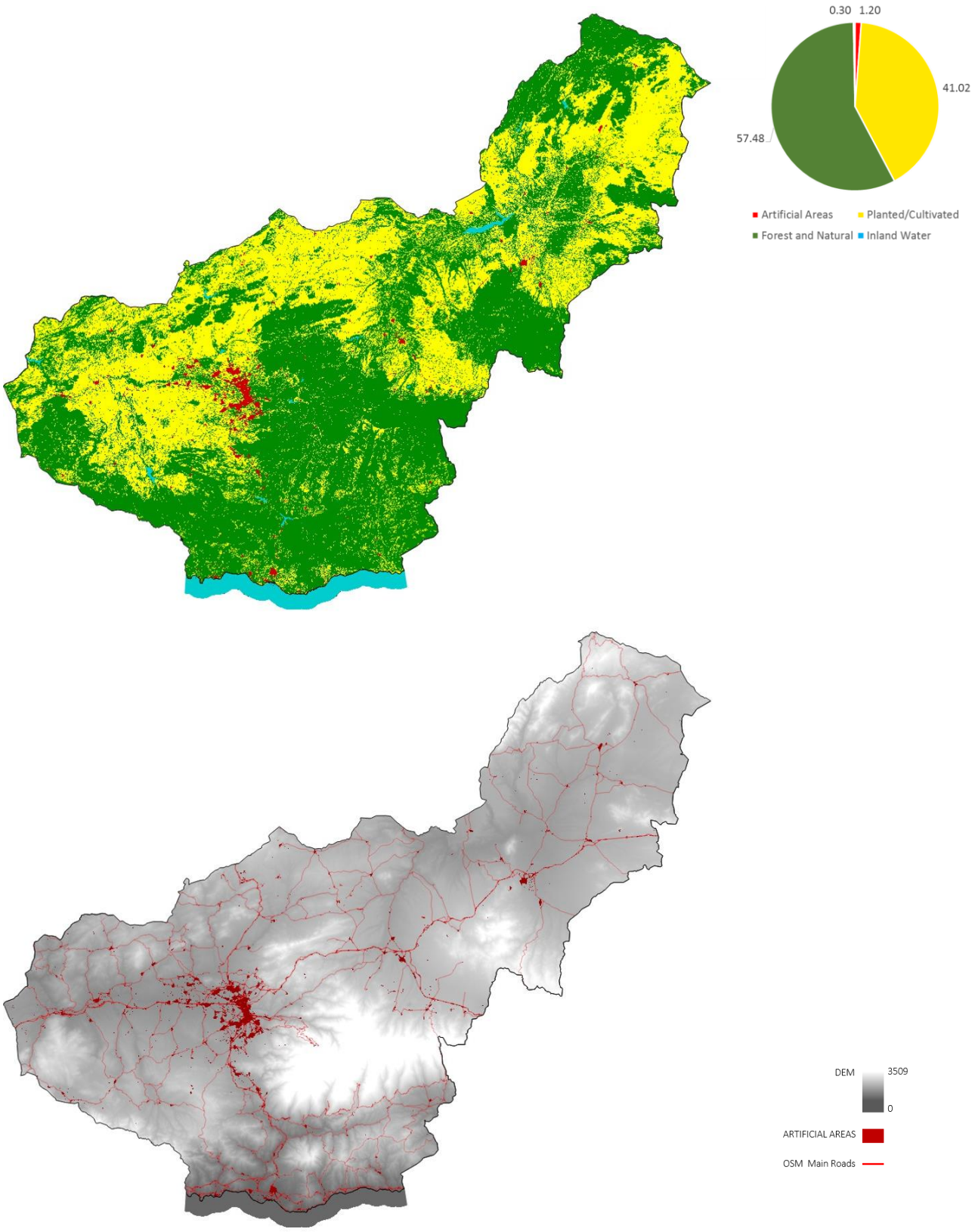

Universidad Politécnica de Cataluña, Barcelona TECH
Departamento de Tecnología de la Arquitectura
Centro de Políticas de Suelo y Valoraciones

Nicola Colaninno, Josep Roca Cladera

JAÉN (Andalucía)

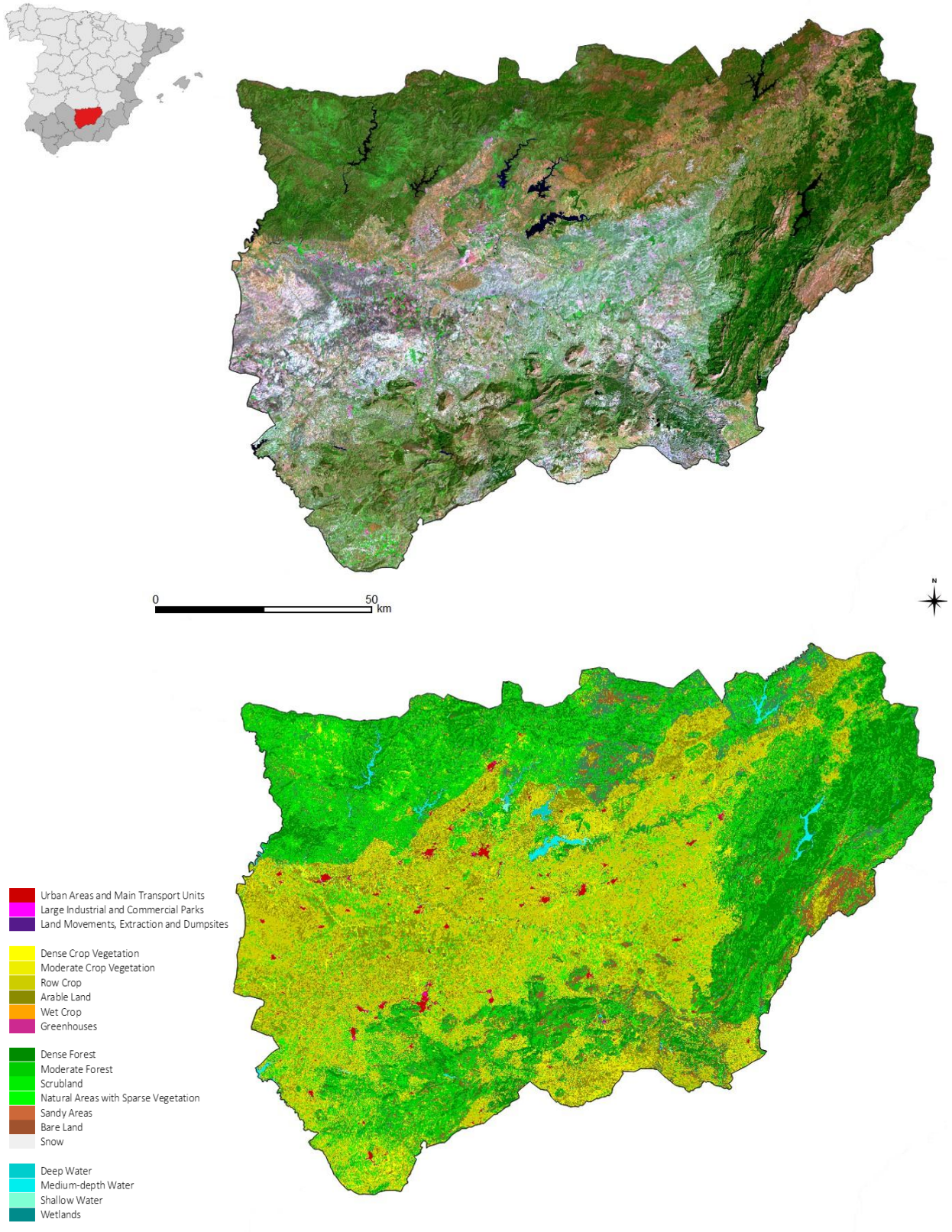

Universidad Politécnica de Cataluña, Barcelona TECH
Departamento de Tecnología de la Arquitectura
Centro de Políticas de Suelo y Valoraciones
Nicola Colaninno, Josep Roca Cladera

Area ≈ 13˙471 Km^2

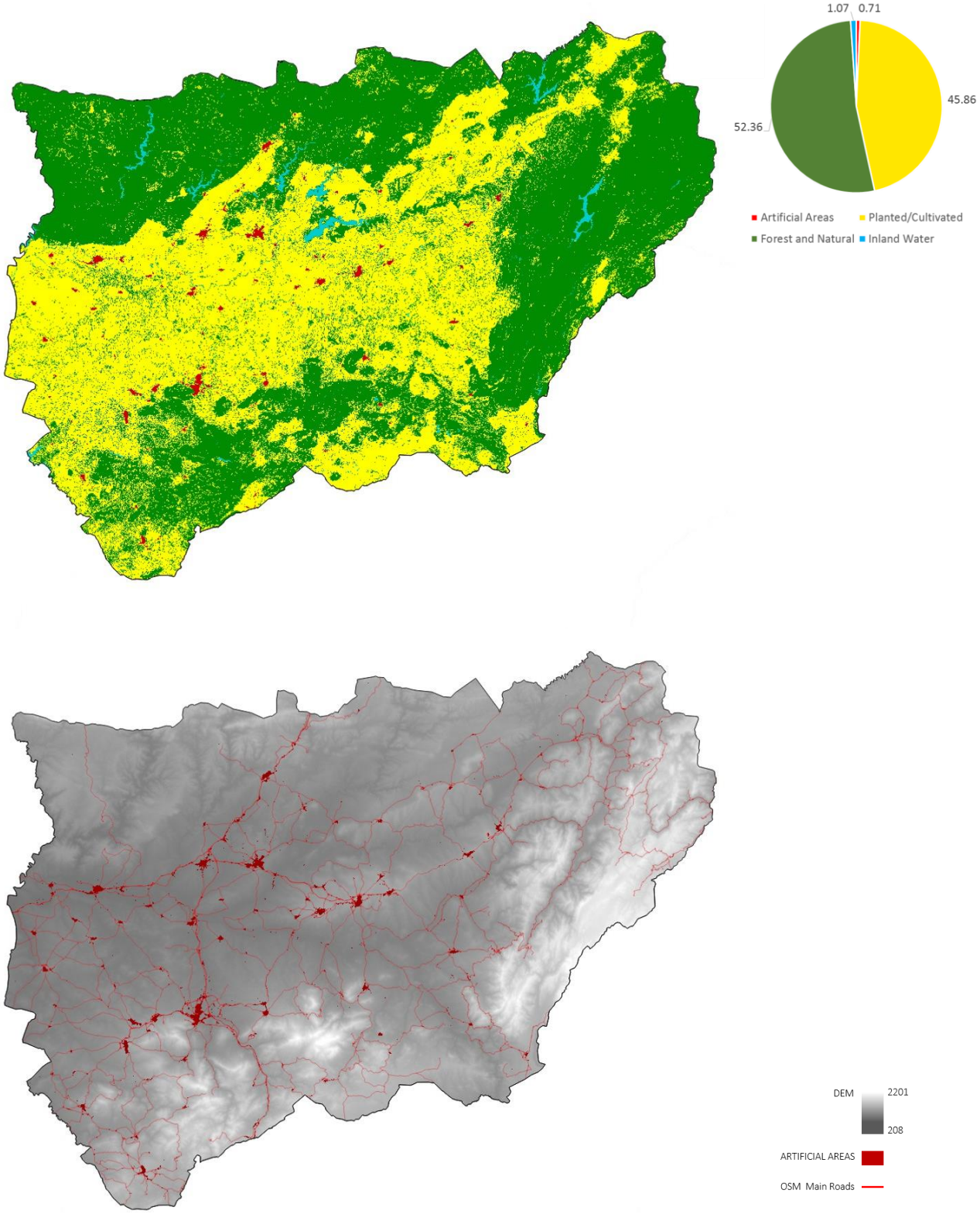

Universidad Politécnica de Cataluña, Barcelona TECH
Departamento de Tecnología de la Arquitectura
Centro de Políticas de Suelo y Valoraciones

Nicola Colaninno, Josep Roca Cladera

CÓRDOBA (Andalucía)

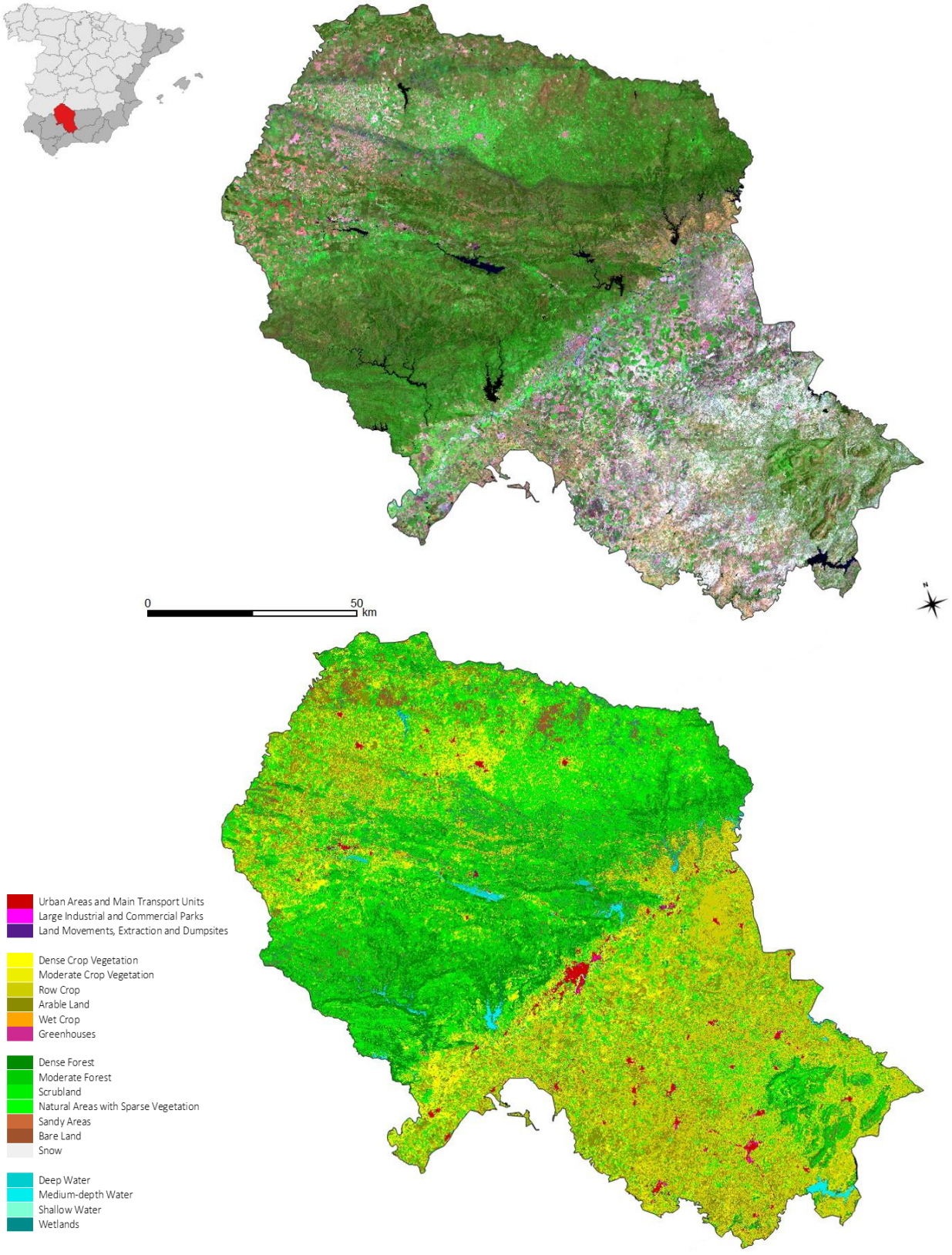

Universidad Politécnica de Cataluña, Barcelona TECH
Departamento de Tecnología de la Arquitectura
Centro de Políticas de Suelo y Valoraciones

Nicola Colaninno, Josep Roca Cladera

Area ≈ 13˙752 Km^2

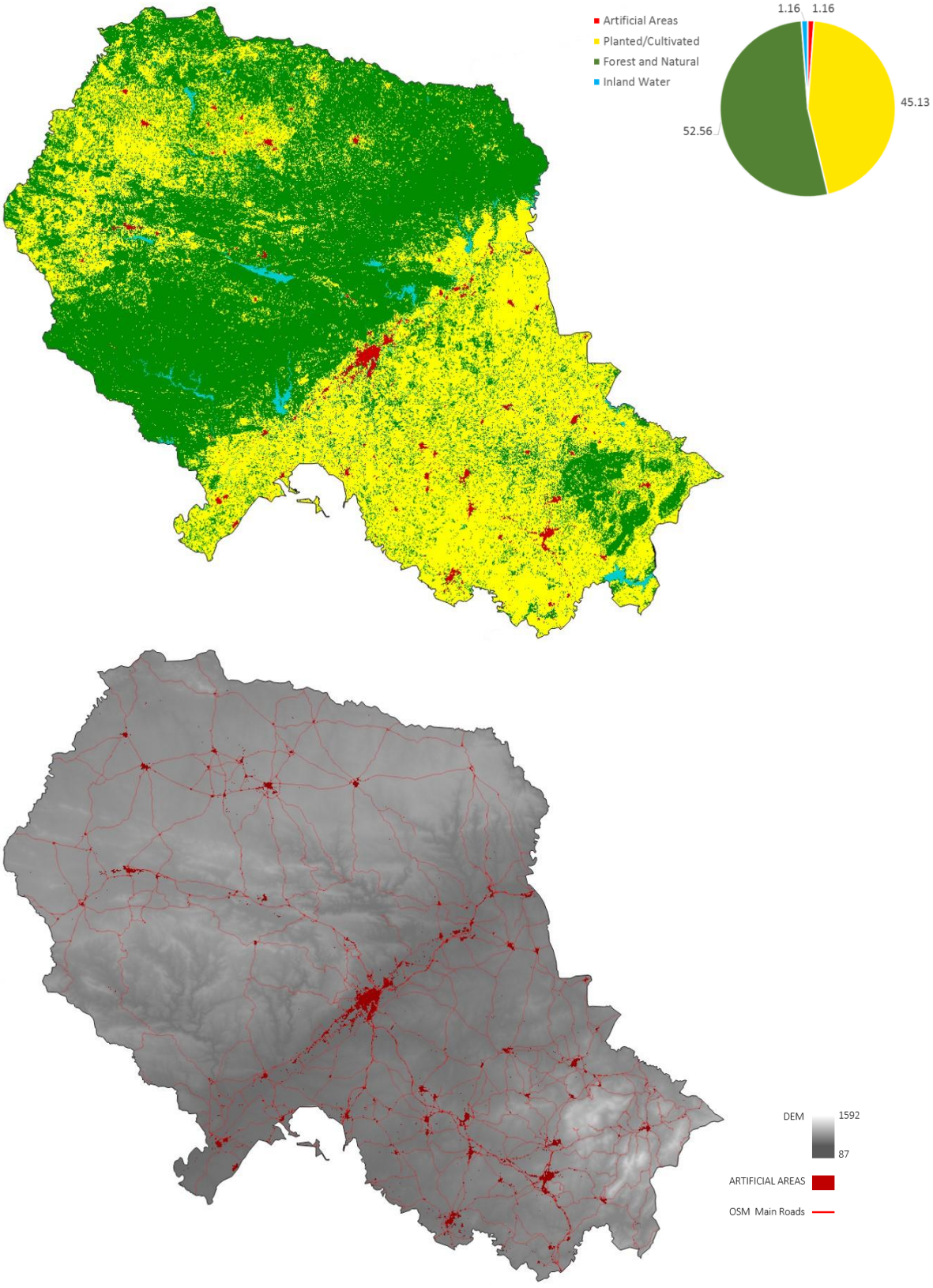

Universidad Politécnica de Cataluña, Barcelona TECH
Departamento de Tecnología de la Arquitectura
Centro de Políticas de Suelo y Valoraciones

Nicola Colaninno, Josep Roca Cladera

MÁLAGA (Andalucía)

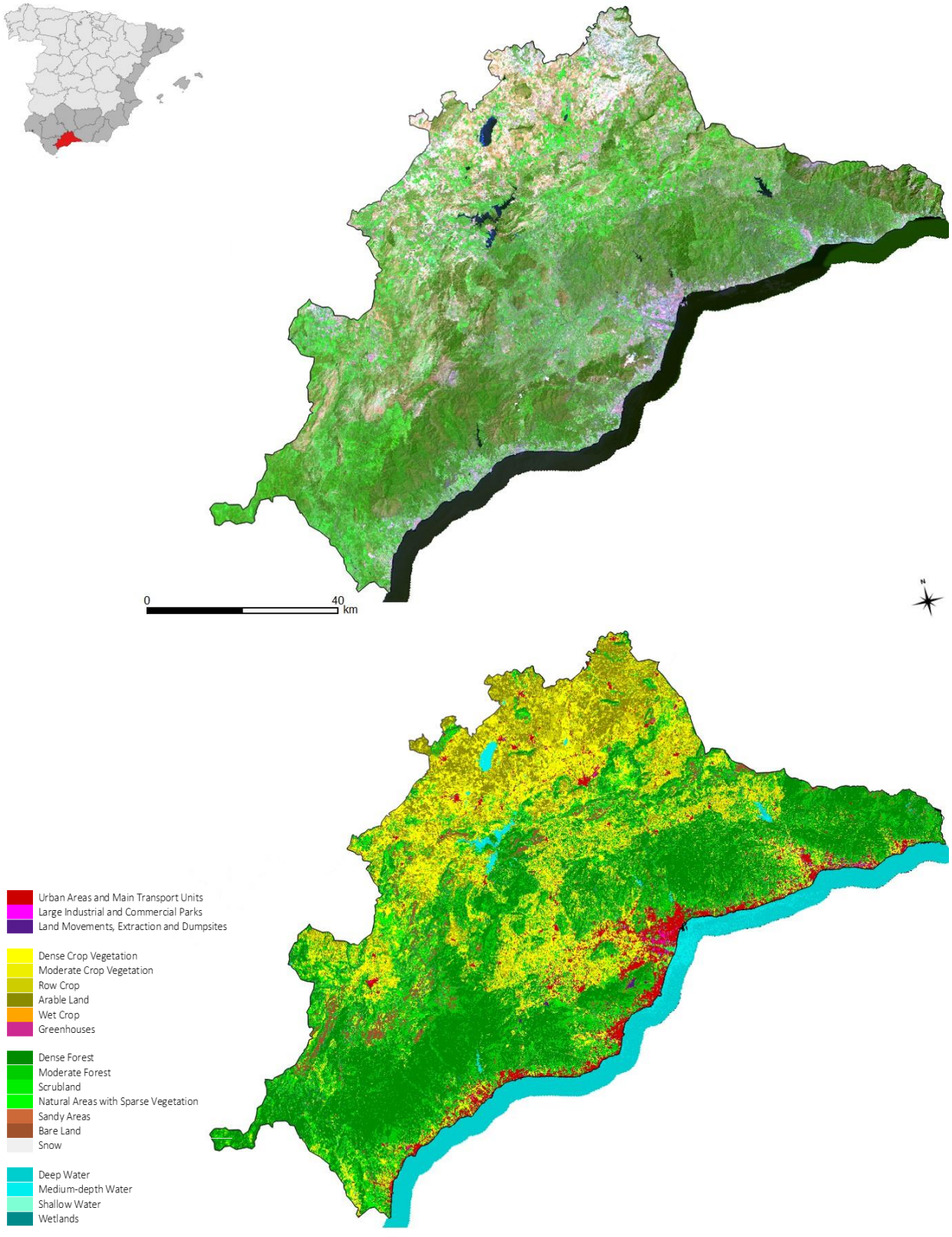

Universidad Politécnica de Cataluña, Barcelona TECH
Departamento de Tecnología de la Arquitectura
Centro de Políticas de Suelo y Valoraciones
Nicola Colaninno, Josep Roca Cladera

Area ≈ 7˙297 Km^2

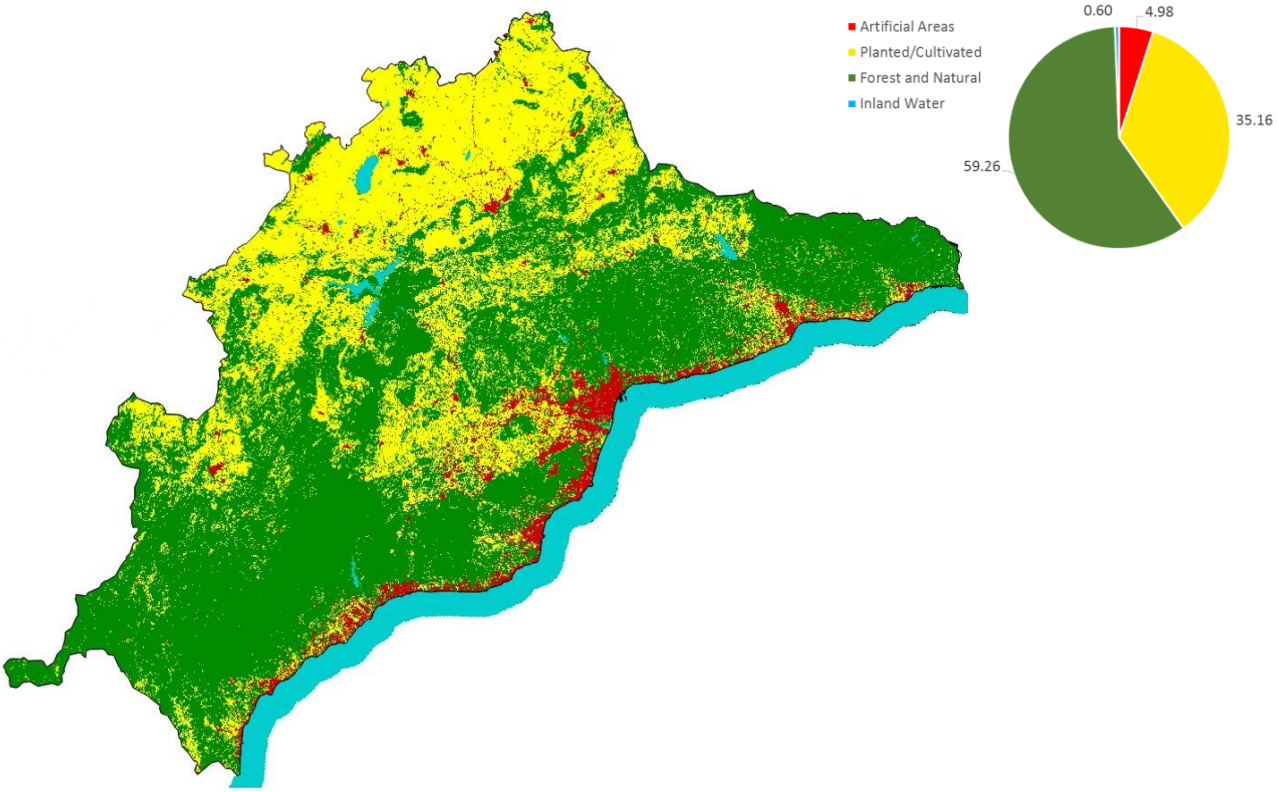

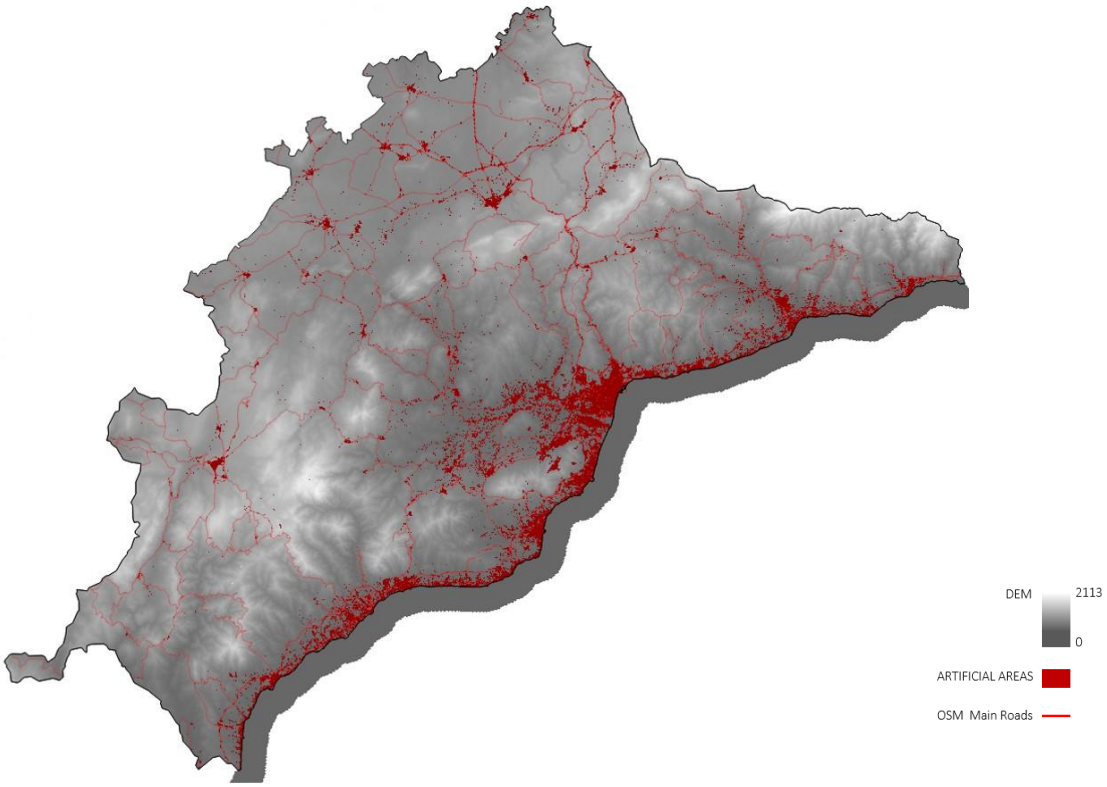

Universidad Politécnica de Cataluña, Barcelona TECH
Departamento de Tecnología de la Arquitectura
Centro de Políticas de Suelo y Valoraciones

Nicola Colaninno, Josep Roca Cladera

CÁDIZ (Andalucía)

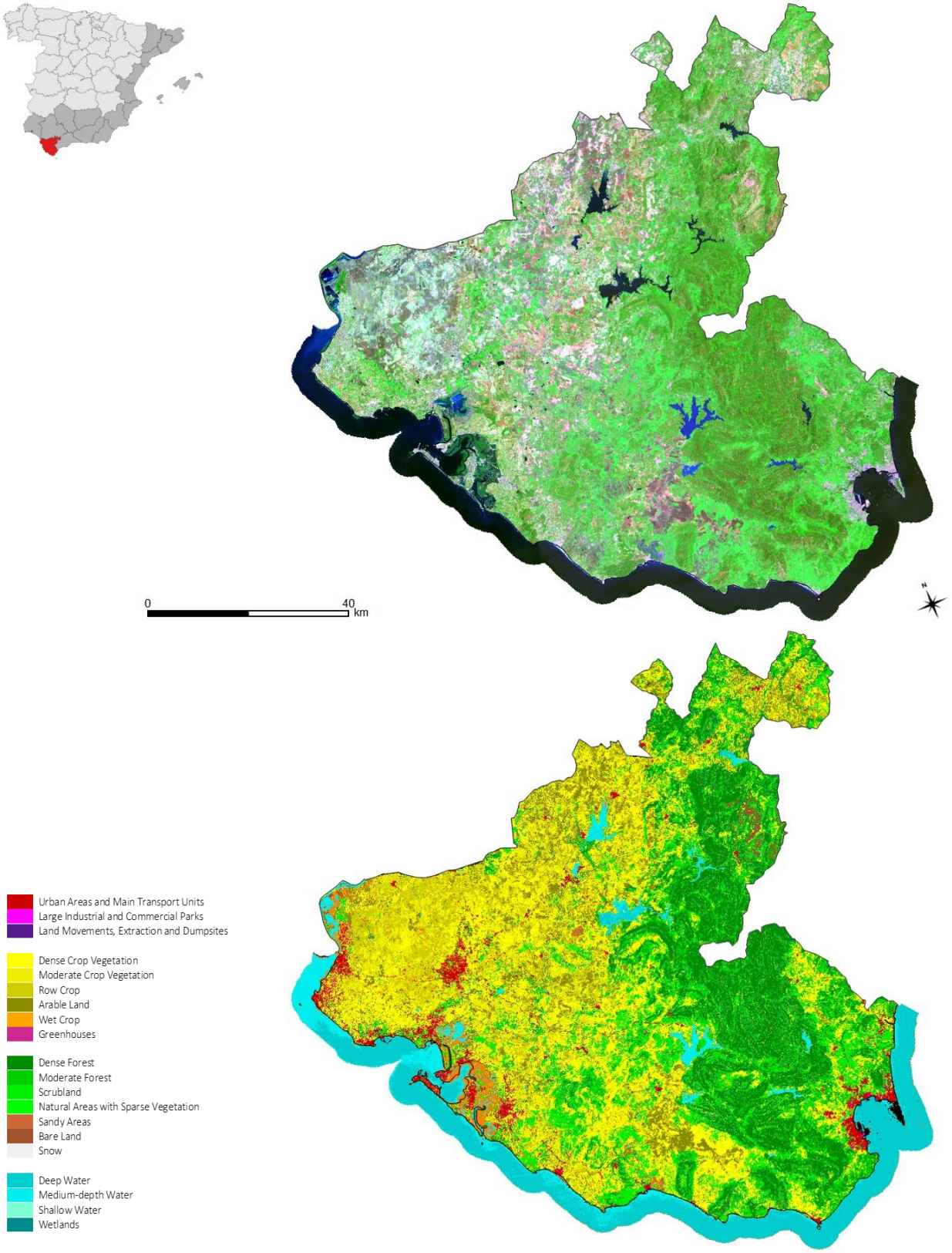

Universidad Politécnica de Cataluña, Barcelona TECH
Departamento de Tecnología de la Arquitectura
Centro de Políticas de Suelo y Valoraciones

Nicola Colaninno, Josep Roca Cladera

Area ≈ 7˙421 Km^2

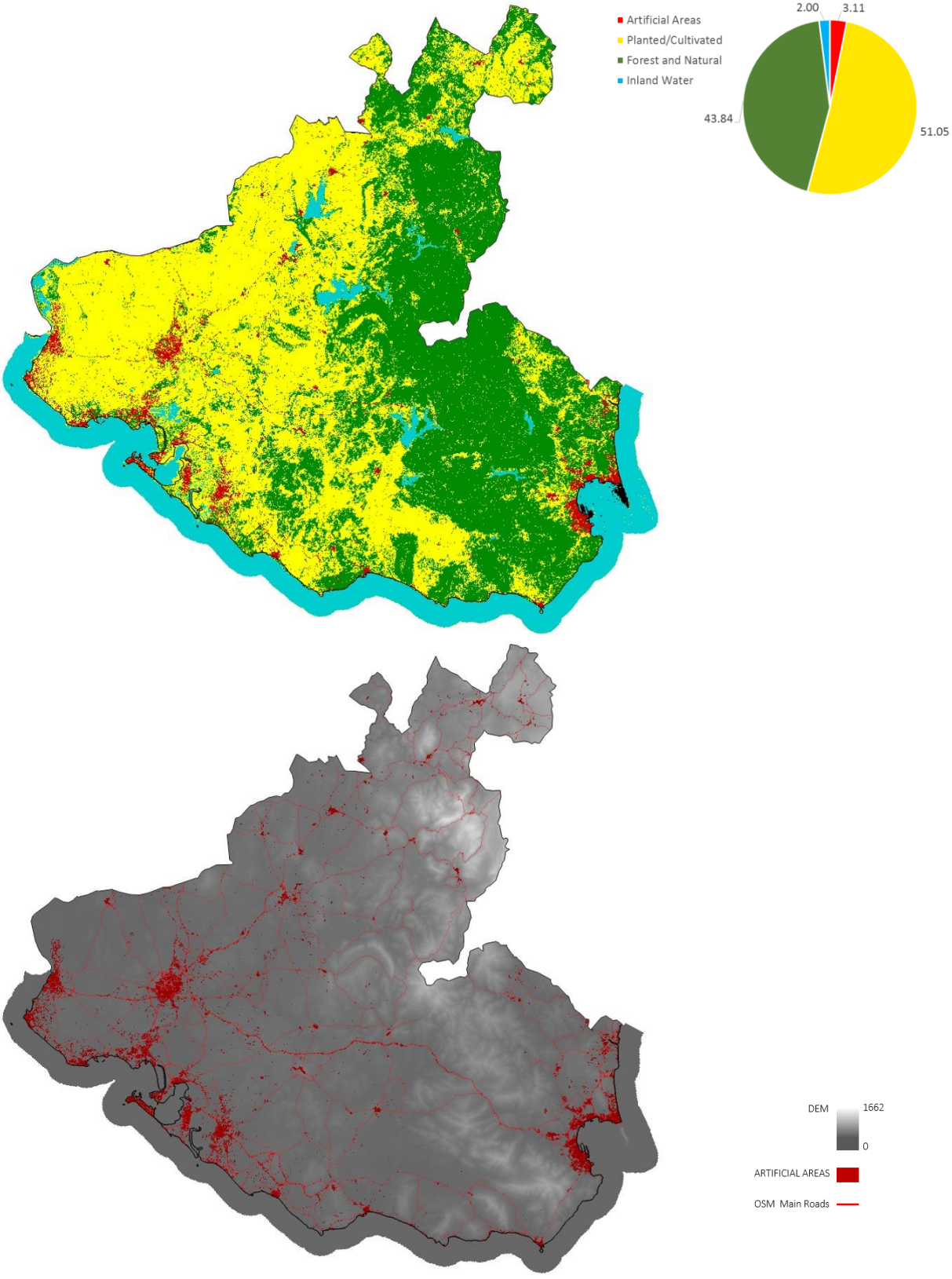

Universidad Politécnica de Cataluña, Barcelona TECH
Departamento de Tecnología de la Arquitectura
Centro de Políticas de Suelo y Valoraciones

Nicola Colaninno, Josep Roca Cladera

SEVILLA (Andalucía)

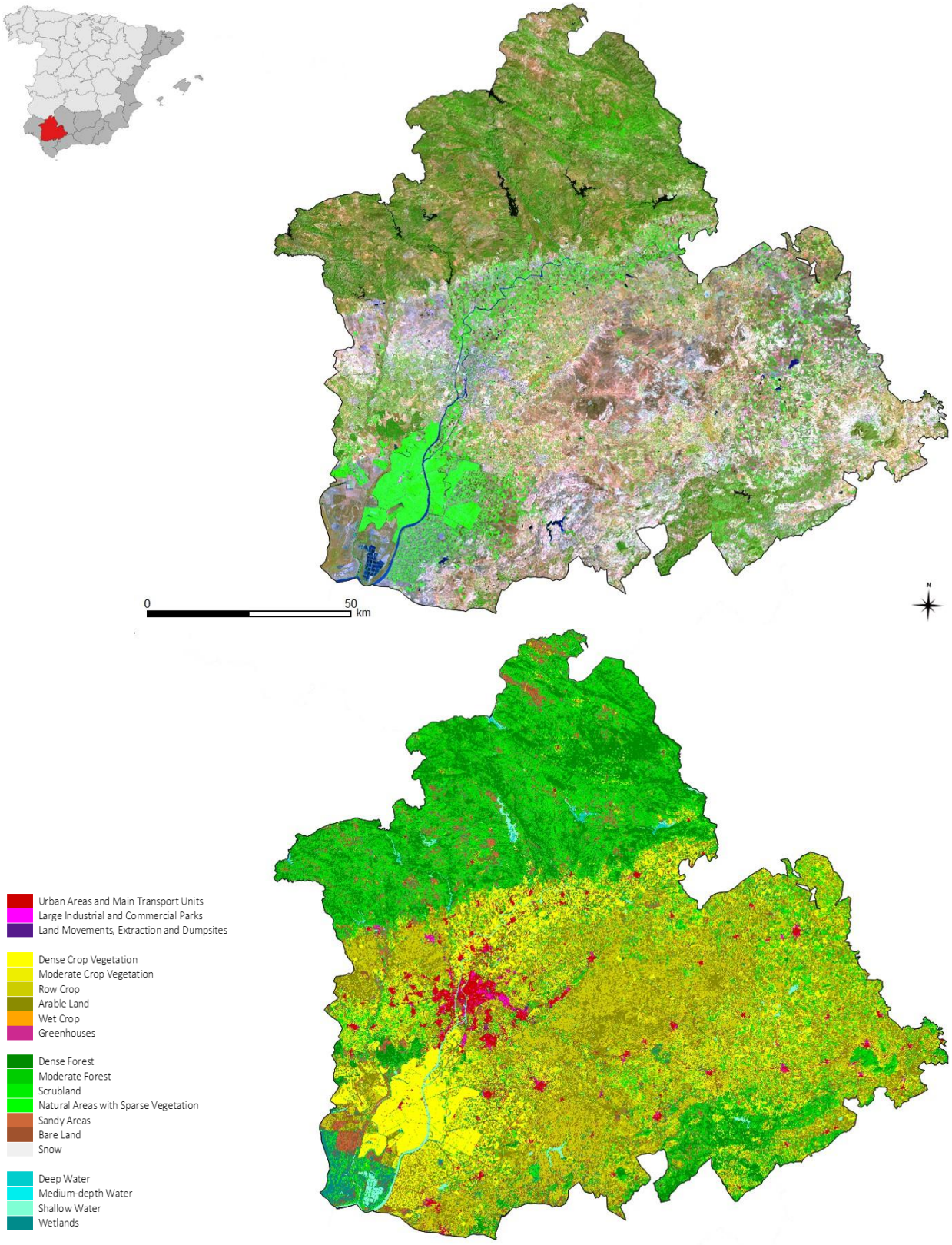

Universidad Politécnica de Cataluña, Barcelona TECH
Departamento de Tecnología de la Arquitectura
Centro de Políticas de Suelo y Valoraciones
Nicola Colaninno, Josep Roca Cladera

Area ≈ 14˙022 Km^2

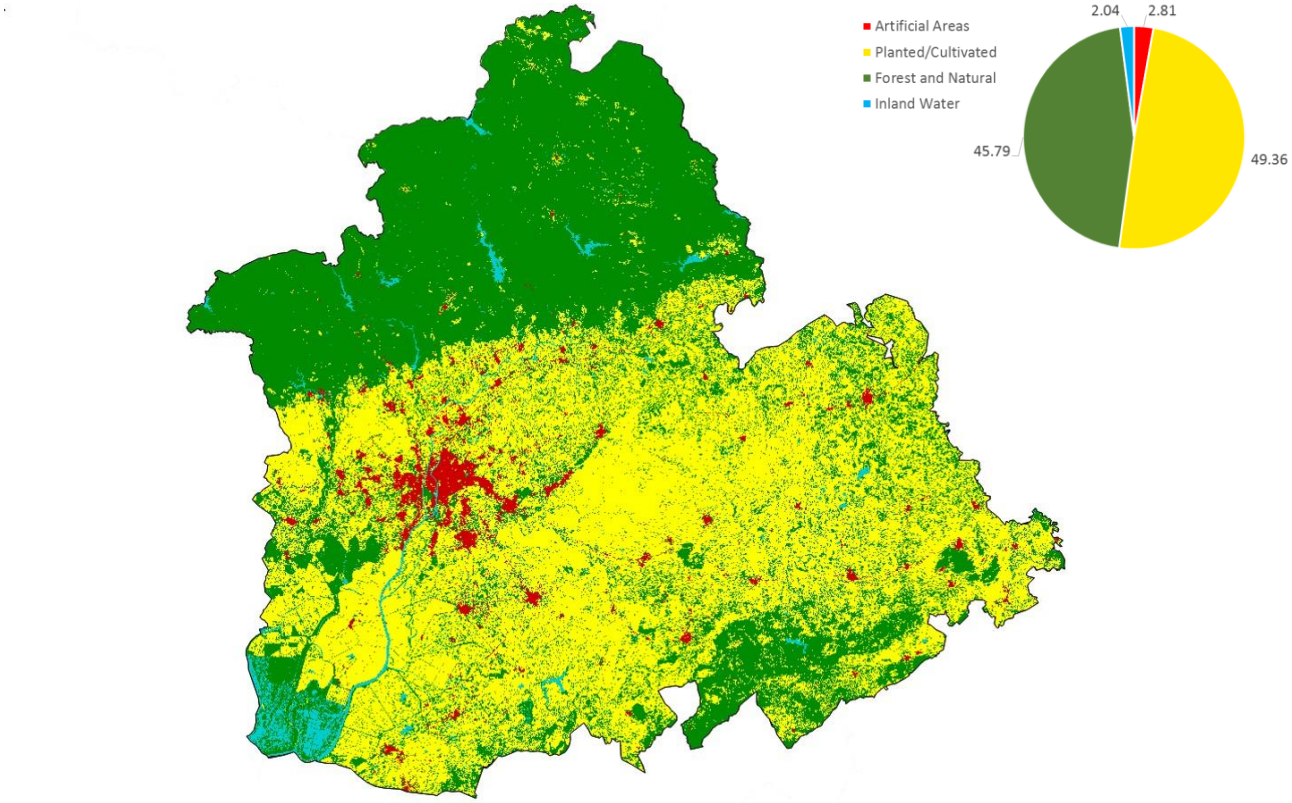

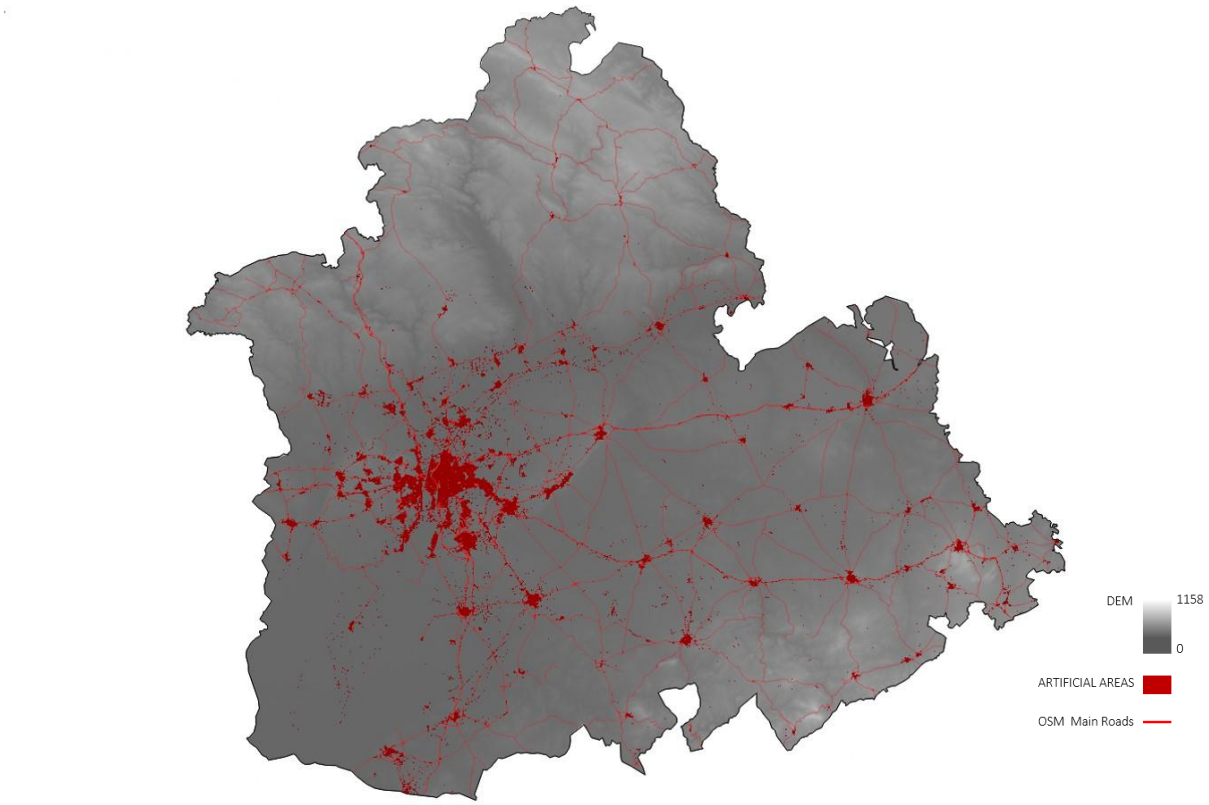

Universidad Politécnica de Cataluña, Barcelona TECH
Departamento de Tecnología de la Arquitectura
Centro de Políticas de Suelo y Valoraciones

Nicola Colaninno, Josep Roca Cladera

HUELVA (Andalucía)

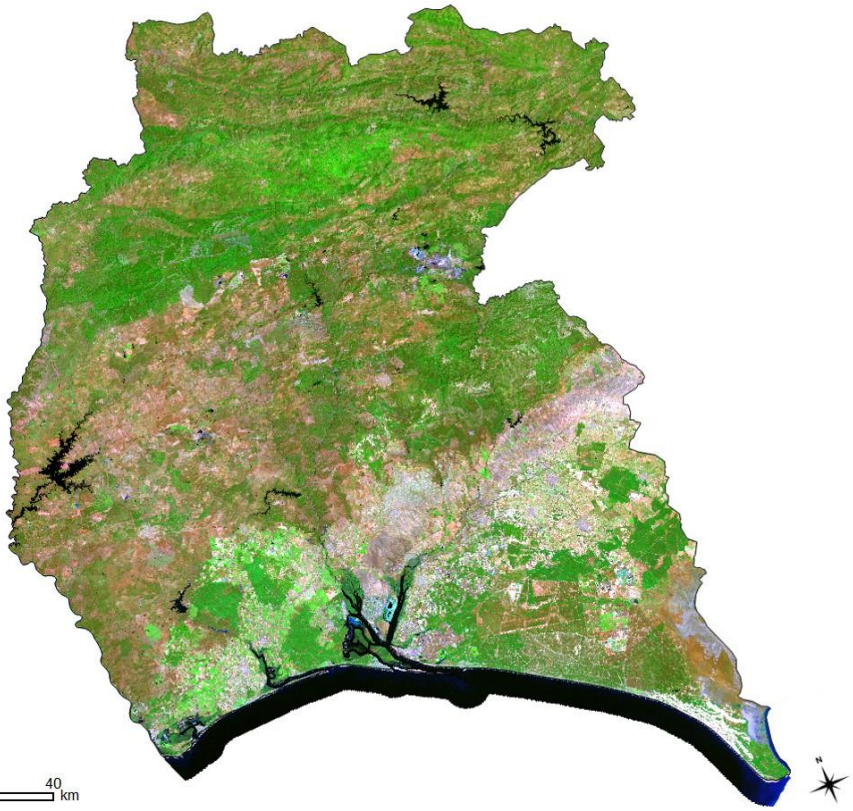

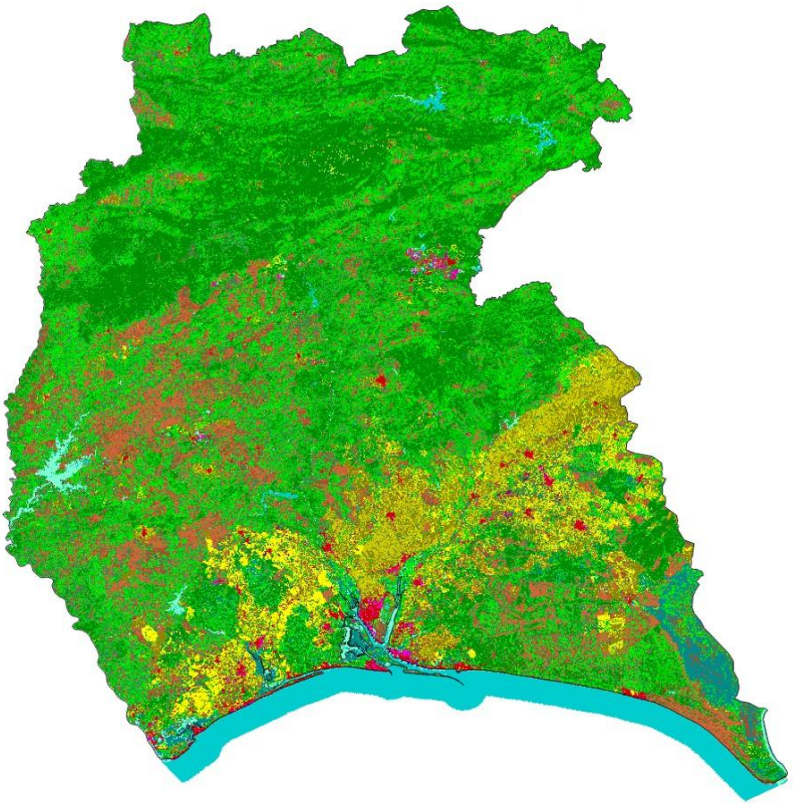

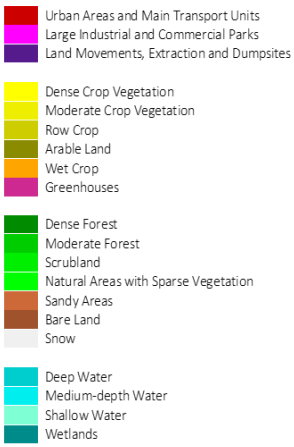

Universidad Politécnica de Cataluña, Barcelona TECH
Departamento de Tecnología de la Arquitectura
Centro de Políticas de Suelo y Valoraciones

Nicola Colaninno, Josep Roca Cladera

Area ≈ 10˙097 Km^2

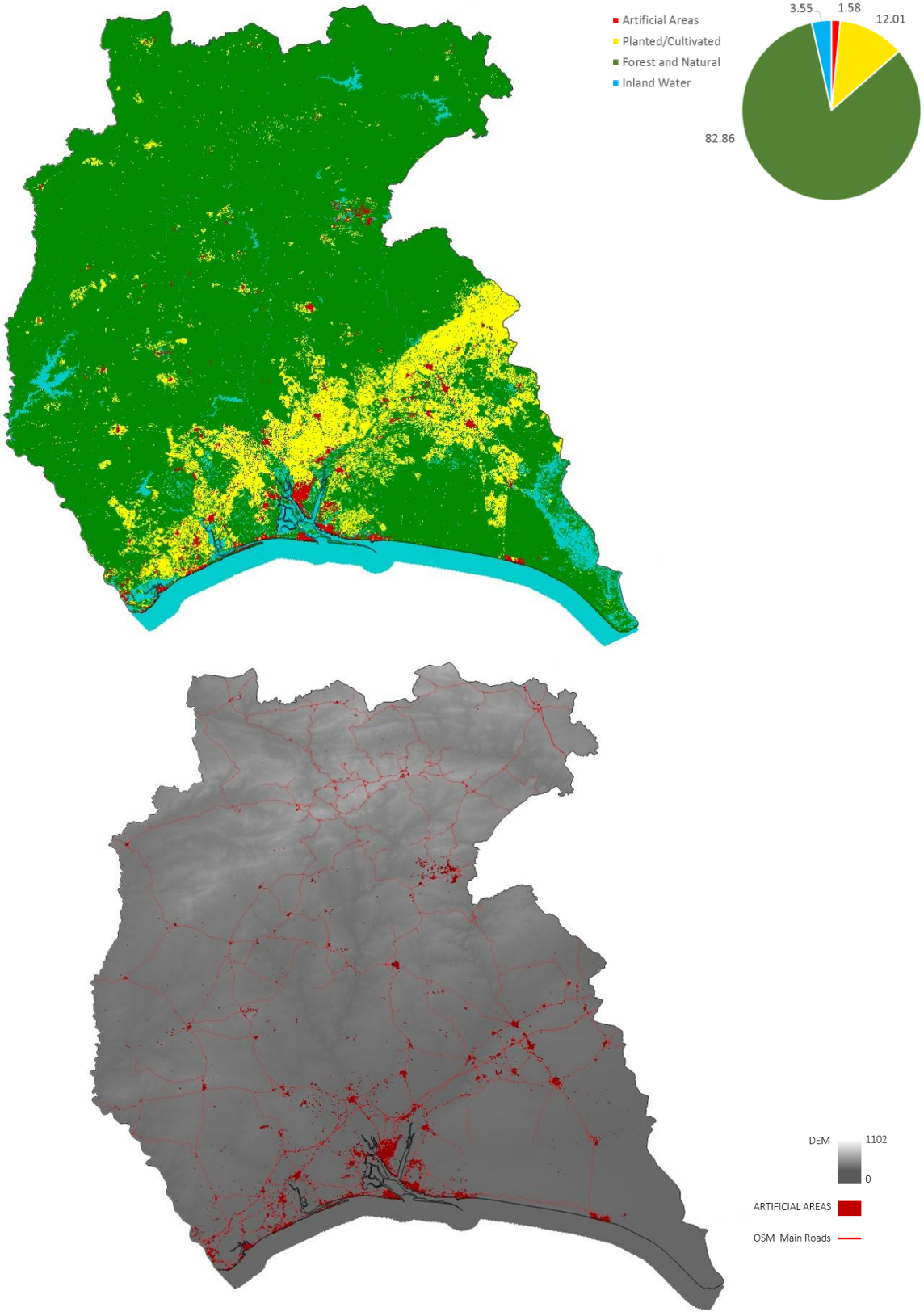

Universidad Politécnica de Cataluña, Barcelona TECH
Departamento de Tecnología de la Arquitectura
Centro de Políticas de Suelo y Valoraciones

Nicola Colaninno, Josep Roca Cladera

MALLORCA and CABRERA (Baleares)

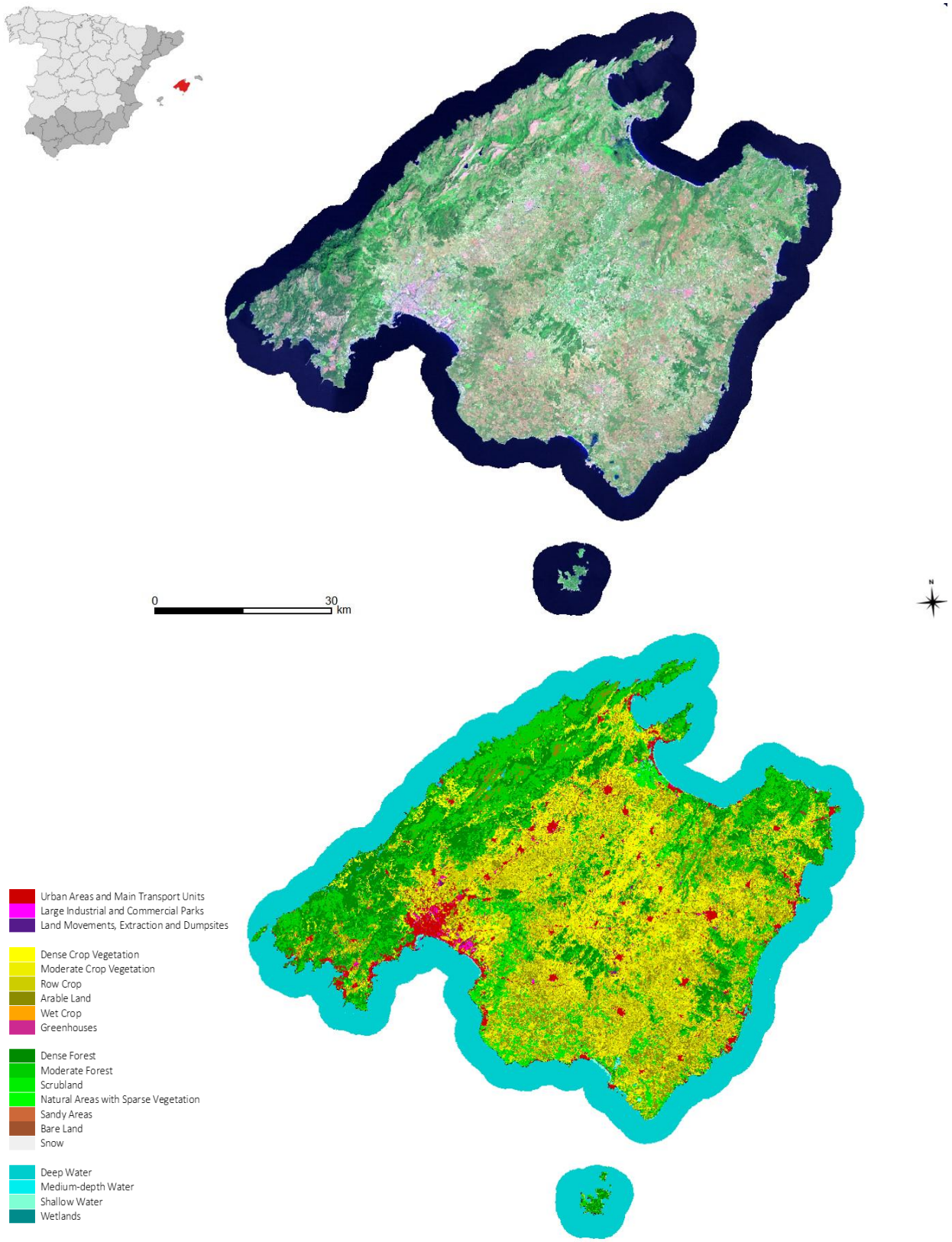

Universidad Politécnica de Cataluña, Barcelona TECH
Departamento de Tecnología de la Arquitectura
Centro de Políticas de Suelo y Valoraciones
Nicola Colaninno, Josep Roca Cladera

Area ≈ 3˙620 Km^2

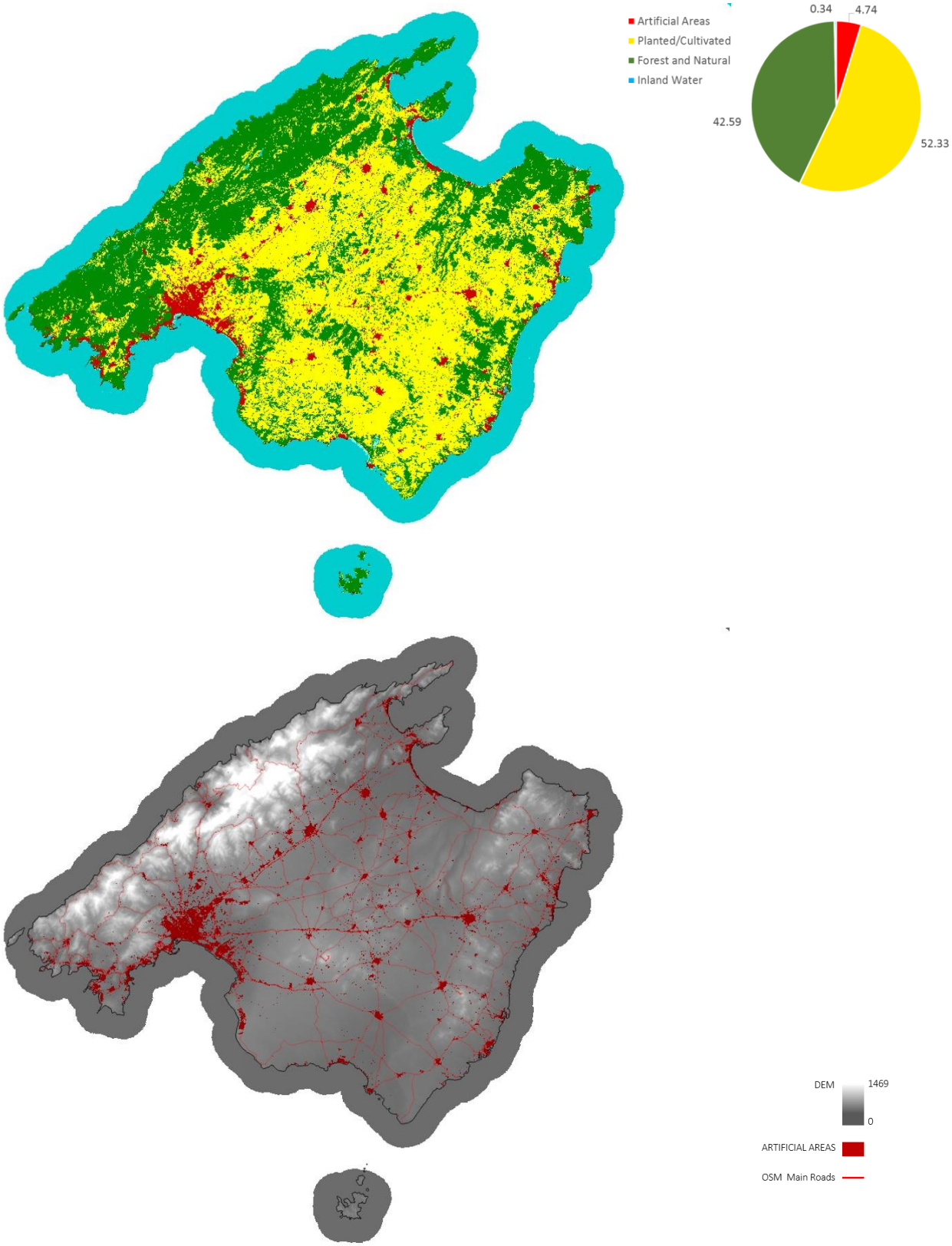

Universidad Politécnica de Cataluña, Barcelona TECH
Departamento de Tecnología de la Arquitectura
Centro de Políticas de Suelo y Valoraciones

Nicola Colaninno, Josep Roca Cladera

MENORCA (Baleares)

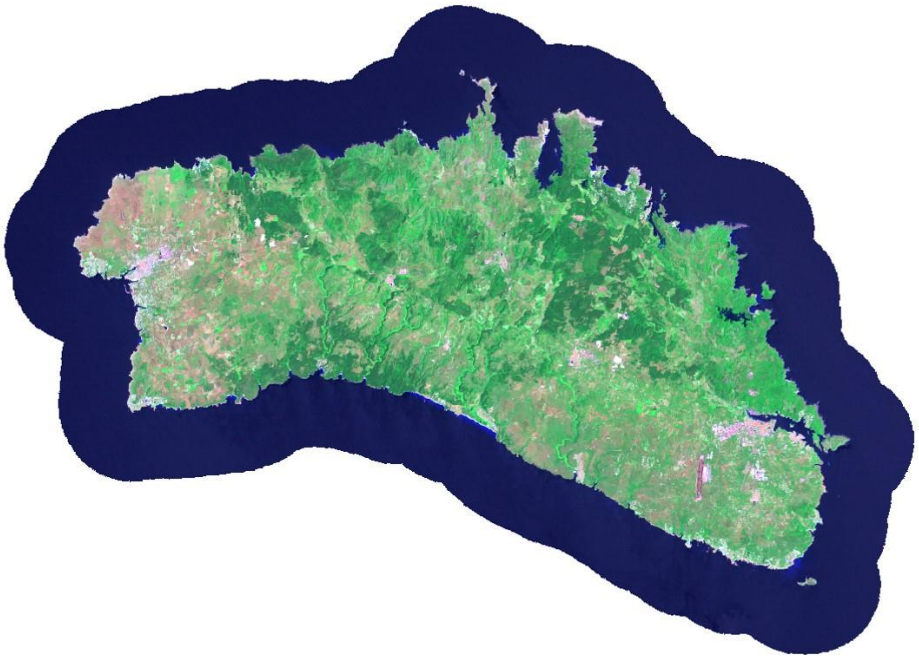

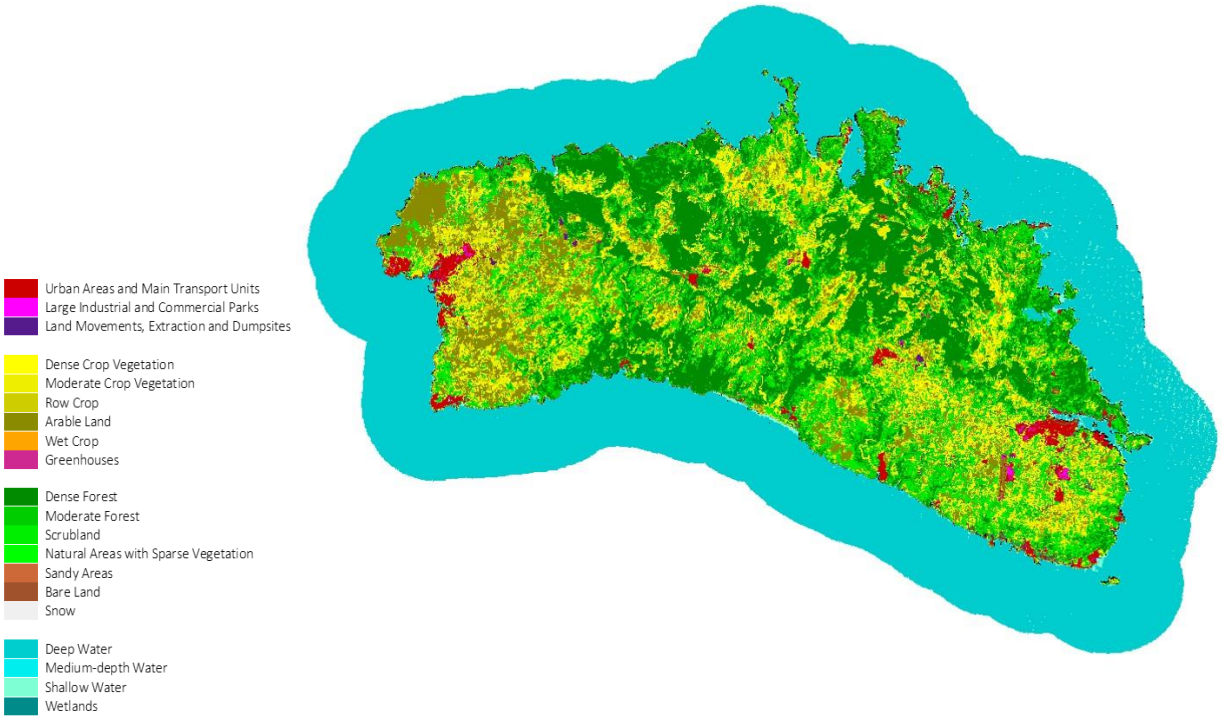

Universidad Politécnica de Cataluña, Barcelona TECH
Departamento de Tecnología de la Arquitectura
Centro de Políticas de Suelo y Valoraciones
Nicola Colaninno, Josep Roca Cladera

Area ≈ 686 Km^2

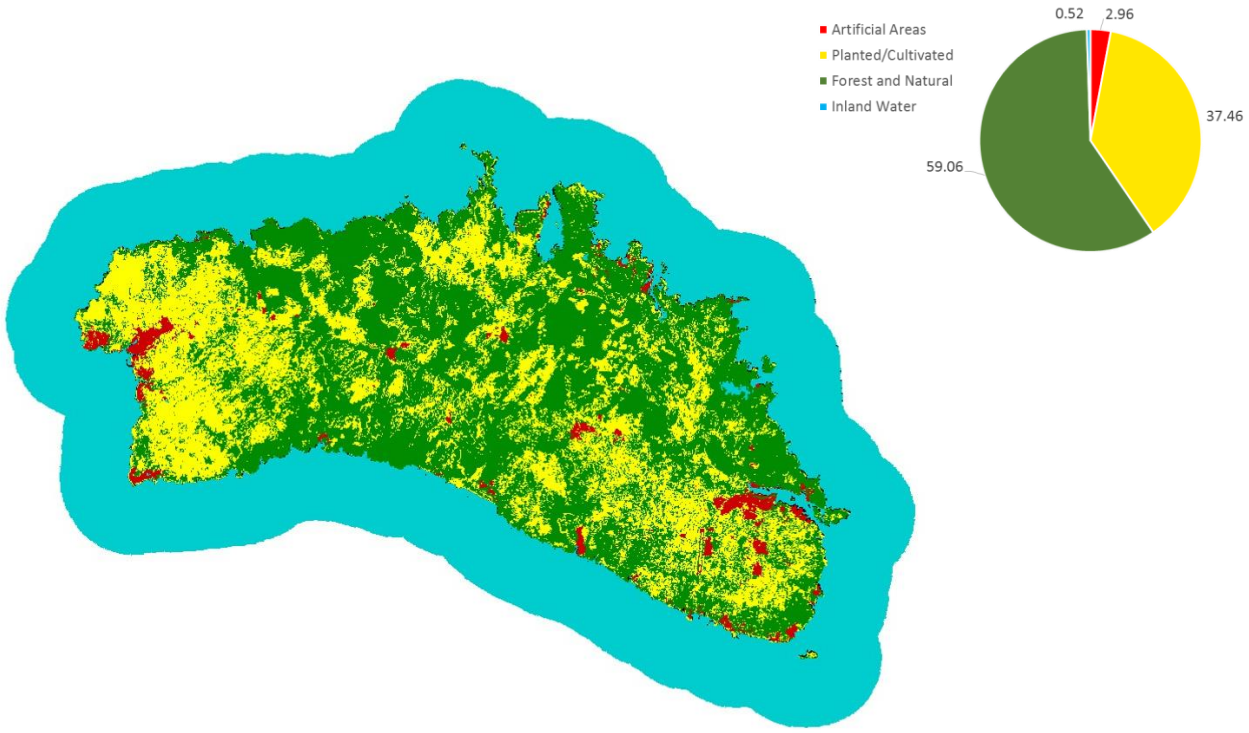

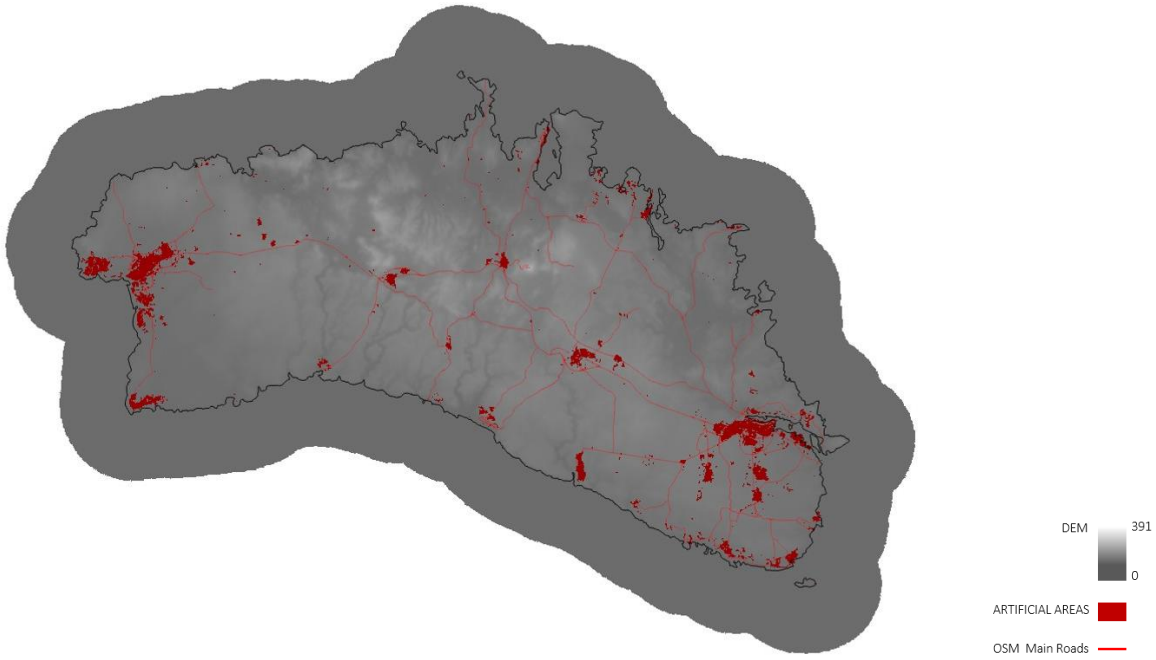

Universidad Politécnica de Cataluña, Barcelona TECH
Departamento de Tecnología de la Arquitectura
Centro de Políticas de Suelo y Valoraciones

Nicola Colaninno, Josep Roca Cladera

IBIZA and FORMENTERA (Baleares)

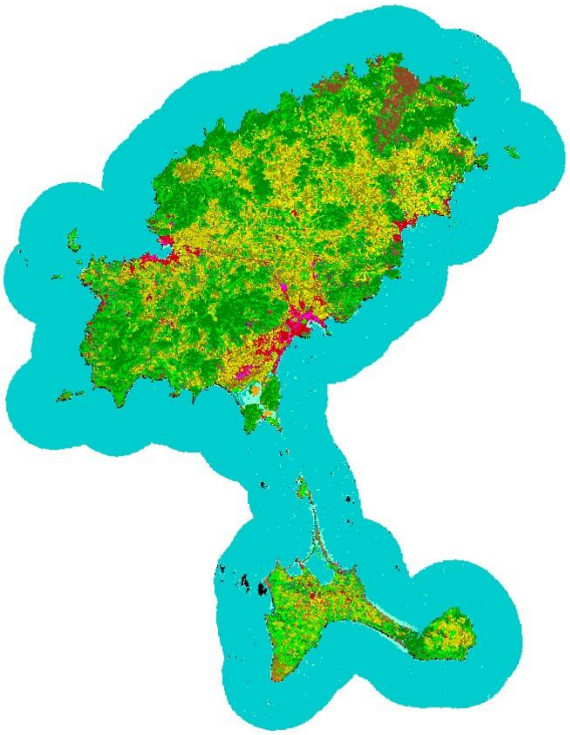

Urban Areas and Main Transport Units
Large Industrial and Commercial Parks
Land Movements, Extraction and Dumpsites

Dense Crop Vegetation
Moderate Crop Vegetation
Row Crop
Arable Land
Wet Crop
Greenhouses

Dense Forest
Moderate Forest
Scrubland
Natural Areas with Sparse Vegetation
Sandy Areas
Bare Land
Snow

Deep Water
Medium-depth Water
Shallow Water
Wetlands

Universidad Politécnica de Cataluña, Barcelona TECH
Departamento de Tecnología de la Arquitectura
Centro de Políticas de Suelo y Valoraciones

Nicola Colaninno, Josep Roca Cladera

Area ≈ 645 Km^2

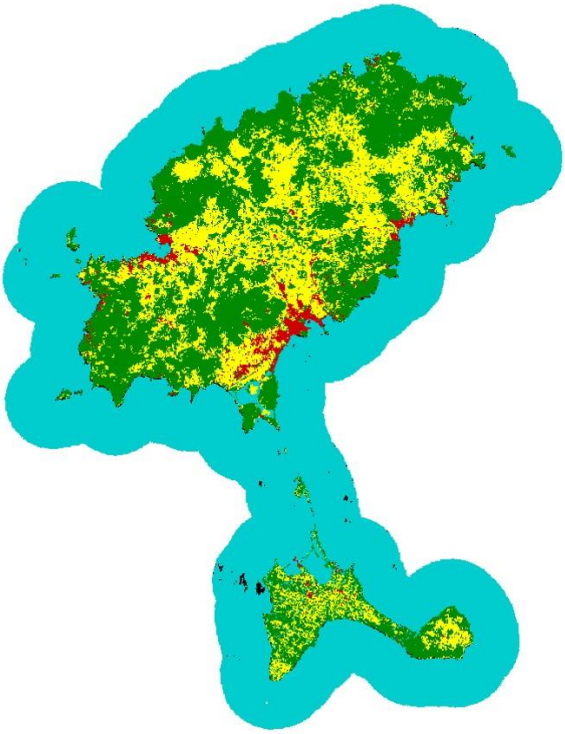

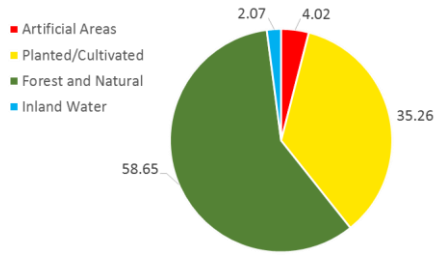

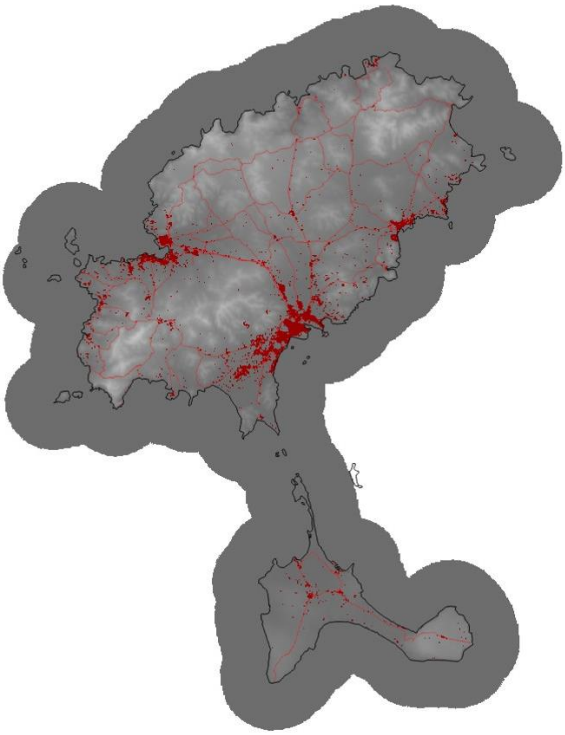

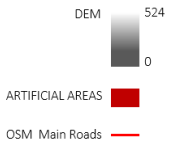

Universidad Politécnica de Cataluña, Barcelona TECH
Departamento de Tecnología de la Arquitectura
Centro de Políticas de Suelo y Valoraciones

Nicola Colaninno, Josep Roca Cladera

Universidad Politécnica de Cataluña, Barcelona TECH
Departamento de Tecnología de la Arquitectura
Centro de Políticas de Suelo y Valoraciones
Nicola Colaninno, Josep Roca Cladera

CLASSIFICATION ACCURACY ASSESSMENT: DETAILED REPORT

CATALUNYA **LCBC 2011/CLC 2006**

Overall Accuracy (%)	80.0228
Kappa Coefficient	0.6105

Class	Ground Truth Accuracy (%)				Total	Errors of Commission (%)	Errors of Omission (%)	Producer Accuracy (%)	User Accuracy (%)
Artificial Areas	51.62	2.32	0.32	4.15	3.49	32	48.38	51.62	68
Planted/Cultivated	19.55	63.3	4.82	12.02	28.58	12.74	36.7	63.3	87.26
Forest and Natural Areas	28.21	34.16	94.58	30.25	67.32	22.2	5.42	94.58	77.8
Water and Wetlands	0.62	0.22	0.28	53.58	0.6	44.89	46.42	53.58	55.11
Total	100	100	100	100	100				

CATALUNYA **LCBC 2011/SIOSE 2005**

Overall Accuracy (%)	85.0355
Kappa Coefficient	0.6910

Class	Ground Truth Accuracy (%)				Total	Errors of Commission (%)	Errors of Omission (%)	Producer Accuracy (%)	User Accuracy (%)
Artificial Areas	50.57	1.40	0.51	1.26	3.49	21.79	49.43	50.57	78.21
Planted/Cultivated	23.28	75.62	6.47	7.95	28.58	18.90	24.38	75.62	81.10
Forest and Natural Areas	25.45	22.89	92.78	30.25	67.32	12.75	7.22	92.78	87.25
Water and Wetlands	0.70	0.10	0.24	60.54	0.6	36.51	39.46	60.54	63.49
Total	100	100	100	100	100				

CATALUNYA **LCBC 2011/CREAF 2009**

Overall Accuracy (%)	84.5575
Kappa Coefficient	0.6798

Class	Ground Truth Accuracy (%)				Total	Errors of Commission (%)	Errors of Omission (%)	Producer Accuracy (%)	User Accuracy (%)
Artificial Areas	50.21	1.65	0.46	1.35	3.49	22.97	49.79	50.21	77.03
Planted/Cultivated	23.89	75.22	7.20	7.96	28.58	20.74	24.78	75.22	79.26
Forest and Natural Areas	25.35	23.03	92.14	32.47	67.32	12.66	7.86	92.14	87.34
Water and Wetlands	0.55	0.10	0.21	58.22	0.60	31.93	41.78	58.22	68.07
Total	100	100	100	100	100				

CATALUNYA **SIOSE 2005/CLC 2006**

Overall Accuracy (%)	83.1325
Kappa Coefficient	0.6794

Class	Ground Truth Accuracy (%)				Total	Errors of Commission (%)	Errors of Omission (%)	Producer Accuracy (%)	User Accuracy (%)
Artificial Areas	70.59	4.17	0.88	3.85	5.40	39.88	29.41	70.59	60.12
Planted/Cultivated	9.45	69.6	4.95	5.96	30.66	10.47	30.34	69.66	89.53
Forest and Natural Areas	19.77	25.95	93.95	23.71	63.31	17.82	6.05	93.95	82.18
Water and Wetlands	0.19	0.22	0.23	66.48	0.63	34.79	33.52	66.48	65.21
Total	100	100	100	100	100				

CATALUNYA **CREAF 2009/SIOSE 2005**

Overall Accuracy (%)	93.7734
Kappa Coefficient	0.8756

Class	Ground Truth Accuracy (%)				Total	Errors of Commission (%)	Errors of Omission (%)	Producer Accuracy (%)	User Accuracy (%)
Artificial Areas	82.10	1.53	0.71	0.31	5.35	17.21	17.90	82.10	82.79
Planted/Cultivated	12.29	90.37	2.76	0.77	30.12	8.01	9.63	90.37	91.99
Forest and Natural Areas	5.50	8.04	96.41	4.29	63.82	4.37	3.59	96.41	95.63
Water and Wetlands	0.11	0.06	0.13	94.63	0.70	14.79	5.37	94.63	85.21
Total	100	100	100	100	100				

CATALUNYA **CREAF 2009/ CLC 2006**

Overall Accuracy (%)	81.7641
Kappa Coefficient	0.6529

Class	Ground Truth Accuracy (%)				Total	Errors of Commission (%)	Errors of Omission (%)	Producer Accuracy (%)	User Accuracy (%)
Artificial Areas	68.00	4.30	0.93	2.79	5.35	41.61	32.00	68.00	58.39
Planted/Cultivated	12.53	67.28	5.41	6.20	30.12	11.99	32.72	67.28	88.01
Forest and Natural Areas	19.19	28.13	93.38	23.48	63.82	18.98	6.62	93.38	81.02
Water and Wetlands	0.29	0.30	0.28	67.53	0.70	40.59	32.47	67.53	59.41
Total	100	100	100	100	100				

Universidad Politécnica de Cataluña, Barcelona TECH
Departamento de Tecnología de la Arquitectura
Centro de Políticas de Suelo y Valoraciones

Nicola Colaninno, Josep Roca Cladera

VALENCIA **LCBC 2011/CLC 2006**

Overall Accuracy (%)	78.9138
Kappa Coefficient	0.6088

Class	Ground Truth Accuracy (%)				Total	Errors of Commission (%)	Errors of Omission (%)	Producer Accuracy (%)	User Accuracy (%)
Artificial Areas	52.87	2.41	0.24	5.75	3.75	33.02	47.13	52.87	66.98
Planted/Cultivated	21.14	63.87	4.43	15.29	31.85	10.46	36.13	63.87	89.54
Forest and Natural Areas	24.81	33.37	95.21	19.39	63.64	25.52	4.79	95.21	74.48
Water and Wetlands	1.18	0.35	0.13	59.57	0.75	36.76	40.43	59.57	63.24
Total	100	100	100	100	100				

VALENCIA **LCBC 2011/SIOSE 2005**

Overall Accuracy (%)	82.7164
Kappa Coefficient	0.6574

Class	Ground Truth Accuracy (%)				Total	Errors of Commission (%)	Errors of Omission (%)	Producer Accuracy (%)	User Accuracy (%)
Artificial Areas	44.23	1.29	0.67	2.54	3.75	22.06	55.77	44.23	77.94
Planted/Cultivated	26.35	78.26	9.90	15.31	31.86	25.1	21.74	78.26	74.86
Forest and Natural Areas	27.95	20.27	89.19	17.70	63.64	12.80	10.81	89.19	87.2
Water and Wetlands	1.47	0.19	0.23	64.45	0.75	39.85	35.55	64.4	60.15
Total	100	100	100	100	100				

VALENCIA **SIOSE 2005/CLC 2006**

Overall Accuracy (%)	79.4986
Kappa Coefficient	0.6279

Class	Ground Truth Accuracy (%)				Total	Errors of Commission (%)	Errors of Omission (%)	Producer Accuracy (%)	User Accuracy (%)
Artificial Areas	78.97	5.38	0.83	4.91	6.61	43.20	21.03	78.97	56.80
Planted/Cultivated	5.95	62.76	4.27	3.87	30.47	8.00	37.24	62.76	92.00
Forest and Natural Areas	14.90	31.62	94.78	25.13	62.22	24.16	5.22	94.78	75.84
Water and Wetlands	0.19	0.24	0.12	66.10	0.70	25.06	33.90	66.10	74.94
Total	100	100	100	100	100				

MURCIA LCBC 2011/CLC 2006

Overall Accuracy (%)	75.2589
Kappa Coefficient	0.5493

Class	Ground Truth Accuracy (%)				Total	Errors of Commission (%)	Errors of Omission (%)	Producer Accuracy (%)	User Accuracy (%)
Artificial Areas	51.43	1.95	0.37	6.91	2.86	44.81	48.57	51.43	55.19
Planted/Cultivated	21.04	63.16	4.37	13.34	38.57	6.24	36.84	63.16	93.76
Forest and Natural Areas	27.09	34.69	95.16	54.19	58.31	35.81	4.84	95.16	64.19
Water and Wetlands	0.45	0.20	0.10	25.56	0.26	66.44	74.44	25.56	33.56
Total	100	100	100	100	100				

MURCIA LCBC 2011/SIOSE 2005

Overall Accuracy (%)	80.8794
Kappa Coefficient	0.6454

Class	Ground Truth Accuracy (%)				Total	Errors of Commission (%)	Errors of Omission (%)	Producer Accuracy (%)	User Accuracy (%)
Artificial Areas	42.19	1.53	0.46	1.87	2.86	33.71	57.81	42.19	66.29
Planted/Cultivated	26.49	71.71	5.07	19.54	38.58	9.29	28.29	71.71	90.71
Forest and Natural Areas	29.34	26.67	94.39	36.15	58.31	24.70	5.61	94.39	75.30
Water and Wetlands	1.99	0.09	0.09	42.44	0.25	69.09	57.56	42.44	30.91
Total	100	100	100	100	100				

MURCIA SIOSE 2005/CLC 2006

Overall Accuracy (%)	84.0152
Kappa Coefficient	0.7019

Class	Ground Truth Accuracy (%)				Total	Errors of Commission (%)	Errors of Omission (%)	Producer Accuracy (%)	User Accuracy (%)
Artificial Areas	75.76	3.07	0.97	8.04	4.49	48.25	24.24	75.76	51.75
Planted/Cultivated	12.16	79.50	7.28	9.22	48.80	6.70	20.50	79.50	93.30
Forest and Natural Areas	11.87	17.35	91.67	51.01	46.52	22.50	8.33	91.67	77.50
Water and Wetlands	0.21	0.08	0.07	31.73	0.18	43.37	68.27	31.73	56.63
Total	100	100	100	100	100				

Universidad Politécnica de Cataluña, Barcelona TECH
Departamento de Tecnología de la Arquitectura
Centro de Políticas de Suelo y Valoraciones

Nicola Colaninno, Josep Roca Cladera

BALEARES **LCBC 2011/CLC 2006**

Overall Accuracy (%)	77.0686
Kappa Coefficient	0.5878

Class	Ground Truth Accuracy (%)				Total	Errors of Commission (%)	Errors of Omission (%)	Producer Accuracy (%)	User Accuracy (%)
Artificial Areas	48.88	2.10	0.46	3.26	4.46	31.43	51.12	48.88	68.57
Planted/Cultivated	24.58	74.02	10.57	11.61	47.92	11.24	25.98	74.02	88.76
Forest and Natural Areas	25.38	23.76	88.49	56.10	47.00	33.68	11.51	88.49	66.32
Water and Wetlands	1.15	0.12	0.47	29.02	0.62	50.25	70.98	29.02	49.75
Total	100	100	100	100	100				

BALEARES **LCBC 2011/SIOSE 2005**

Overall Accuracy (%)	83.4929
Kappa Coefficient	0.7020

Class	Ground Truth Accuracy (%)				Total	Errors of Commission (%)	Errors of Omission (%)	Producer Accuracy (%)	User Accuracy (%)
Artificial Areas	57.77	1.86	0.70	1.29	4.46	26.10	42.23	57.77	73.90
Planted/Cultivated	16.76	89.49	16.80	9.20	47.92	19.90	10.51	89.49	80.10
Forest and Natural Areas	24.43	8.59	82.01	52.01	47.00	11.66	17.99	82.01	88.34
Water and Wetlands	1.04	0.06	0.48	37.50	0.62	53.26	62.50	37.50	46.74
Total	100	100	100	100	100				

BALEARES **SIOSE 2005/CLC 2006**

Overall Accuracy (%)	76.7231
Kappa Coefficient	0.5934

Class	Ground Truth Accuracy (%)				Total	Errors of Commission (%)	Errors of Omission (%)	Producer Accuracy (%)	User Accuracy (%)
Artificial Areas	65.37	2.01	1.10	7.42	5.75	28.32	34.63	65.37	71.68
Planted/Cultivated	15.42	68.87	6.58	1.63	42.78	7.74	31.13	68.87	92.26
Forest and Natural Areas	18.52	29.02	92.23	35.51	50.70	35.91	7.77	92.23	64.09
Water and Wetlands	0.69	0.11	0.08	55.44	0.77	17.34	44.56	55.44	82.66
Total	100	100	100	100	100				

Universidad Politécnica de Cataluña, Barcelona TECH
Departamento de Tecnología de la Arquitectura
Centro de Políticas de Suelo y Valoraciones

Nicola Colaninno, Josep Roca Cladera

ALMERÍA-GRANADA LCBC 2011/CLC 2006

Overall Accuracy (%)	78.2594
Kappa Coefficient	0.5677

Class	Ground Truth Accuracy (%)				Total	Errors of Commission (%)	Errors of Omission (%)	Producer Accuracy (%)	User Accuracy (%)
Artificial Areas	51.18	1.15	0.35	1.32	1.39	51.09	48.82	51.18	48.91
Planted/Cultivated	28.05	64.74	9.19	13.58	34.42	15.46	35.26	64.74	84.54
Forest and Natural Areas	20.30	34.07	90.41	30.30	64.00	24.47	9.59	90.41	75.53
Water and Wetlands	0.47	0.04	0.05	54.80	0.19	24.89	45.20	54.80	75.11
Total	100	100	100	100	100				

ALMERÍA-GRANADA LCBC 2011/SIOSE 2005

Overall Accuracy (%)	81.3871
Kappa Coefficient	0.6087

Class	Ground Truth Accuracy (%)				Total	Errors of Commission (%)	Errors of Omission (%)	Producer Accuracy (%)	User Accuracy (%)
Artificial Areas	42.03	0.55	0.43	0.28	1.39	33.44	57.97	42.03	66.56
Planted/Cultivated	34.56	74.83	13.16	17.07	34.42	26.75	25.17	74.83	73.25
Forest and Natural Areas	23.04	24.61	86.39	34.22	64.00	13.94	13.61	86.39	86.06
Water and Wetlands	0.37	0.00	0.02	48.43	0.19	11.84	51.57	48.43	88.16
Total	100	100	100	100	100				

ALMERÍA-GRANADA SIOSE 2005/CLC 2006

Overall Accuracy (%)	82.6506
Kappa Coefficient	0.6581

Class	Ground Truth Accuracy (%)				Total	Errors of Commission (%)	Errors of Omission (%)	Producer Accuracy (%)	User Accuracy (%)
Artificial Areas	74.54	2.02	0.56	1.73	2.20	55.00	25.46	74.54	45.00
Planted/Cultivated	6.91	68.93	4.90	0.78	33.69	8.05	31.07	68.93	91.95
Forest and Natural Areas	17.87	28.92	94.41	19.53	63.76	20.84	5.59	94.41	79.16
Water and Wetlands	0.69	0.14	0.13	77.97	0.35	40.31	22.03	77.97	59.69
Total	100	100	100	100	100				

Universidad Politécnica de Cataluña, Barcelona TECH
Departamento de Tecnología de la Arquitectura
Centro de Políticas de Suelo y Valoraciones

Nicola Colaninno, Josep Roca Cladera

JAÉN-CÓRDOBA **LCBC 2011/CLC 2006**

Overall Accuracy (%)	73.5856
Kappa Coefficient	0.5014

Class	Ground Truth Accuracy (%)				Total	Errors of Commission (%)	Errors of Omission (%)	Producer Accuracy (%)	User Accuracy (%)
Artificial Areas	55.81	0.55	0.05	0.14	0.94	40.52	44.19	55.81	59.48
Planted/Cultivated	30.86	64.94	7.89	14.31	45.50	6.60	35.06	64.94	93.40
Forest and Natural Areas	11.58	33.98	91.34	11.95	52.45	42.78	8.66	91.34	57.22
Water and Wetlands	1.76	0.52	0.73	73.60	1.12	53.24	26.40	73.60	46.76
Total	100	100	100	100	100				

JAÉN-CÓRDOBA **LCBC 2011/SIOSE 2005**

Overall Accuracy (%)	80.6996
Kappa Coefficient	0.6319

Class	Ground Truth Accuracy (%)				Total	Errors of Commission (%)	Errors of Omission (%)	Producer Accuracy (%)	User Accuracy (%)
Artificial Areas	40.18	0.27	0.09	0.05	0.94	19.01	59.82	40.18	80.99
Planted/Cultivated	44.49	76.88	13.20	4.20	45.50	15.65	23.12	76.88	84.35
Forest and Natural Areas	11.87	22.62	86.27	11.37	52.45	22.14	13.73	86.27	77.86
Water and Wetlands	3.46	0.23	0.44	84.39	1.12	34.71	15.61	84.39	65.29
Total	100	100	100	100	100				

JAÉN-CÓRDOBA **SIOSE 2005/CLC 2006**

Overall Accuracy (%)	81.2343
Kappa Coefficient	0.6374

Class	Ground Truth Accuracy (%)				Total	Errors of Commission (%)	Errors of Omission (%)	Producer Accuracy (%)	User Accuracy (%)
Artificial Areas	76.63	1.54	0.33	0.85	1.89	59.48	23.3	76.63	40.52
Planted/Cultivated	13.43	74.22	3.55	6.59	49.92	2.70	25.78	74.22	97.30
Forest and Natural Areas	9.64	24.03	95.50	18.74	47.33	33.71	4.50	95.5	66.29
Water and Wetlands	0.30	0.21	0.62	73.82	0.87	39.39	26.18	73.82	60.61
Total	100	100	100	100	100				

Universidad Politécnica de Cataluña, Barcelona TECH
Departamento de Tecnología de la Arquitectura
Centro de Políticas de Suelo y Valoraciones

Nicola Colaninno, Josep Roca Cladera

MÁLAGA-JEREZ DE LA FRONTERA **LCBC 2011/CLC 2006**

Overall Accuracy (%)	76.5709
Kappa Coefficient	0.5779

Class	Ground Truth Accuracy (%)				Total	Errors of Commission (%)	Errors of Omission (%)	Producer Accuracy (%)	User Accuracy (%)
Artificial Areas	55.18	3.05	0.78	2.51	4.02	47.76	44.82	55.18	52.24
Planted/Cultivated	23.52	71.37	13.26	32.89	43.18	17.12	28.63	71.37	82.88
Forest and Natural Areas	21.08	25.37	85.50	13.55	51.46	26.81	14.50	85.50	73.19
Water and Wetlands	0.21	0.21	0.46	51.06	1.34	23.63	48.94	51.06	76.37
Total	100	100	100	100	100				

MÁLAGA-JEREZ DE LA FRONTERA **LCBC 2011/SIOSE 2005**

Overall Accuracy (%)	82.2307
Kappa Coefficient	0.6794

Class	Ground Truth Accuracy (%)				Total	Errors of Commission (%)	Errors of Omission (%)	Producer Accuracy (%)	User Accuracy (%)
Artificial Areas	48.14	1.98	1.20	1.15	4.03	35.94	51.86	48.14	64.06
Planted/Cultivated	26.31	84.91	13.73	30.11	43.18	21.44	15.09	84.91	78.56
Forest and Natural Areas	24.80	13.06	84.76	14.48	51.46	13.30	15.24	84.76	86.70
Water and Wetlands	0.75	0.04	0.31	54.26	1.34	16.59	45.74	54.26	83.41
Total	100	100	100	100	100				

MÁLAGA-JEREZ DE LA FRONTERA **SIOSE 2005/CLC 2006**

Overall Accuracy (%)	82.6058
Kappa Coefficient	0.6924

Class	Ground Truth Accuracy (%)				Total	Errors of Commission (%)	Errors of Omission (%)	Producer Accuracy (%)	User Accuracy (%)
Artificial Areas	80.54	3.01	1.63	3.16	5.36	42.71	19.46	80.54	57.29
Planted/Cultivated	6.61	74.29	5.41	3.52	39.95	6.77	25.71	74.29	93.23
Forest and Natural Areas	12.55	22.48	92.30	11.59	52.63	22.77	7.70	92.30	77.23
Water and Wetlands	0.30	0.23	0.67	81.73	2.06	20.39	18.27	81.73	79.61
Total	100	100	100	100	100				

Universidad Politécnica de Cataluña, Barcelona TECH
Departamento de Tecnología de la Arquitectura
Centro de Políticas de Suelo y Valoraciones

Nicola Colaninno, Josep Roca Cladera

SEVILLA-HUELVA **LCBC 2011/CLC 2006**

Overall Accuracy (%)	71.3153
Kappa Coefficient	0.5033

Class	Ground Truth Accuracy (%)				Total	Errors of Commission (%)	Errors of Omission (%)	Producer Accuracy (%)	User Accuracy (%)
Artificial Areas	58.72	1.35	0.40	0.87	2.29	41.31	41.28	58.72	58.69
Planted/Cultivated	17.61	56.58	2.27	6.94	33.66	4.41	43.42	56.58	95.59
Forest and Natural Areas	20.91	41.39	95.87	37.14	61.21	41.26	4.13	95.87	58.74
Water and Wetlands	2.76	0.68	1.46	55.05	2.83	35.29	44.95	55.05	64.71
Total	100	100	100	100	100				

SEVILLA-HUELVA **LCBC 2011/SIOSE 2005**

Overall Accuracy (%)	86.1332
Kappa Coefficient	0.7441

Class	Ground Truth Accuracy (%)				Total	Errors of Commission (%)	Errors of Omission (%)	Producer Accuracy (%)	User Accuracy (%)
Artificial Areas	46.43	1.14	0.47	0.70	2.29	32.32	53.57	46.43	67.68
Planted/Cultivated	30.27	76.67	0.67	1.64	33.67	4.18	23.33	76.67	95.82
Forest and Natural Areas	18.78	21.80	97.86	34.44	61.21	17.79	2.14	97.86	82.21
Water and Wetlands	4.53	0.39	1.00	63.22	2.83	29.36	36.78	63.22	70.64
Total	100	100	100	100	100				

SEVILLA-HUELVA **SIOSE 2005/CLC 2006**

Overall Accuracy (%)	80.0341
Kappa Coefficient	0.6473

Class	Ground Truth Accuracy (%)				Total	Errors of Commission (%)	Errors of Omission (%)	Producer Accuracy (%)	User Accuracy (%)
Artificial Areas	75.06	2.21	0.77	2.28	3.34	48.54	24.94	75.06	51.46
Planted/Cultivated	9.27	70.61	3.93	6.75	42.07	4.54	29.39	70.61	95.46
Forest and Natural Areas	14.98	26.88	94.54	10.00	51.42	31.05	5.46	94.54	68.95
Water and Wetlands	0.69	0.29	0.77	80.97	3.16	14.80	19.03	80.97	85.20
Total	100	100	100	100	100				

Universidad Politécnica de Cataluña, Barcelona TECH
Departamento de Tecnología de la Arquitectura
Centro de Políticas de Suelo y Valoraciones

Nicola Colaninno, Josep Roca Cladera

RS & GIS QUICK GLOSSARY

Because the complexity and the technological level behind the proposed work, we considered appropriate to complement this essay with a glossary as a tool that aims to quickly provide a useful description about most of the technical terms present here (or at least we hope so), either in terms of Remote Sensing and GIS.

In particular, the proposed glossary is based upon the main source used by the author as a reference about the majority of technical terms encountered during this training path, i.e. we used the illustrated dictionary of geographical information systems "A to Z GIS" published by ESRI Press in 2006, and edited by Tasha Wade and Shelly Sommer[394].

Actually, we strongly want to emphasize that, except few variations for some terms, our glossary is a subset of the web version of the illustrated ESRI GIS dictionary which, instead, provides a much more exhaustive collection about the RS and GIS language, and that can be found at:
http://support.esri.com/en/knowledgebase/Gisdictionary/browse

[394] ESRI (2006). A to Z GIS. An illustrated dictionary of geographic information systems (Second Edition). (T. Wade, & S. Sommer, Eds.) Redlands, California: ESRI Press.

A

Absorption: [remote sensing] The amount of electromagnetic energy lost through interactions with gas molecules and matter during its passage through the atmosphere.

Accuracy: [mathematics] The degree to which a measured value conforms to true or accepted values. Accuracy is a measure of correctness. It is distinguished from precision, which measures exactness.

Across-track scanner: [remote sensing] A remote-sensing tool with an oscillating mirror that moves back and forth across a satellite's direction of travel, creating scan line strips that are contiguous or that overlap slightly, thereby producing an image.

Active remote sensing: [remote sensing] A remote-sensing system, such as radar, that produces electromagnetic radiation and measures its reflection back from a surface.

Aerial photograph: [aerial photography] A photograph of the earth's surface taken from a platform flying above the surface but not in orbit, usually an aircraft. Aerial photography is often used as a cartographic data source for basemapping, locating geographic features, and interpreting environmental conditions.

Albedo: [physics] A measure of the reflectivity of an object or surface; the ratio of the amount of radiation reflected by a body to the amount of energy striking it.

Algorithm: [computing] A mathematical procedure used to solve problems with a series of steps. Algorithms are usually encoded as a sequence of computer commands.

Along-track scanner: [remote sensing] A remote-sensing tool with a line of many fixed sensors that record reflected radiation from the terrain along a satellite's direction of movement, creating scan-line strips that are contiguous or that overlap slightly, thereby producing an image.

Alphanumeric grid: [cartography] A grid of numbered rows and lettered columns (or vice versa) superimposed on a map, used to find and identify features. Alphanumeric grids are commonly used as a reference system on local street maps.

Altitude: **1** [coordinate systems] The height or vertical elevation of a point above a reference surface. Altitude measurements are usually based on a given reference datum, such as mean sea level; **2** [map display] The height above the horizon, measured in degrees, from which a light source illuminates a surface. Altitude is used when calculating a hillshade, or for controlling the position of a light source in a scene.

Ancillary data: [digital image processing] In digital image processing, data from sources other than remote sensing, used to assist in analysis and classification or to populate metadata.

Angular unit: [geodesy] The unit of measurement on a sphere or a spheroid, usually degrees. Some map projection parameters, such as the central meridian and standard parallel, are defined in angular units.

Area: **1** [Euclidean geometry] A closed, two-dimensional shape defined by its boundary or by a contiguous set of raster cells; **2** [Euclidean geometry] A calculation of the size of a two-dimensional feature, measured in square units.

Array: **1** [GPS] A set of objects that are connected to function as a unit. In GPS technology, an array of satellites is used to pinpoint locations on the earth; **2** [mathematics] In computing, a fundamental data structure consisting of a variable with multiple, sequentially indexed, cells that can each store a value of the same type. Each cell of the array acts as a variable, and the cells are referenced by an index value for each array dimension. One-dimensional arrays, called vectors, and two-dimensional arrays, called matrices, are most common, but arrays may have more dimensions.

ASCII: [data transfer] Acronym for American Standard Code for Information Interchange. The de facto standard for the format of text files in computers and on the Internet that assigns a 7-bit binary number to each alphanumeric or special character. ASCII defines 128 possible characters.

Aspect: **1** [analysis/geoprocessing] The compass direction that a topographic slope faces, usually measured in degrees from north. Aspect can be generated from continuous elevation surfaces. For example, the aspect recorded for a TIN face is the steepest downslope direction of the face, and the aspect of a cell in a raster is the steepest downslope direction of a plane defined by the cell and its eight surrounding neighbors; **2** [map projections] The conceptual center of a projection system.

Universidad Politécnica de Cataluña, Barcelona TECH
Departamento de Tecnología de la Arquitectura
Centro de Políticas de Suelo y Valoraciones
Nicola Colaninno, Josep Roca Cladera

Aspect ratio: [hardware] The ratio of the width of an image to its height. The aspect ratio of a standard computer monitor is 4:3 (rectangular).

Atlas: [cartography] A collection of maps usually related to a particular area or theme and presented together. Examples of atlases include world atlases, historical atlases, and biodiversity atlases.

Azimuth: 1 [cartography] The horizontal angle, measured in degrees, between a baseline drawn from a center point and another line drawn from the same point. Normally, the baseline points true north and the angle is measured clockwise from the baseline; **2** [analysis/geoprocessing] A compass direction. For example, in some GIS software, the direction from which a light source illuminates a surface is called the azimuth; **3** [navigation] In navigation, the horizontal angle, measured in degrees, between a reference line drawn from a point and another line drawn from the same point to a point on the celestial sphere. Normally, the reference line points true north and the angle is measured clockwise from the reference line.

B

Band: [remote sensing] A set of adjacent wavelengths or frequencies with a common characteristic. For example, visible light is one band of the electromagnetic spectrum, which also includes radio, gamma, radar and infrared waves.

Band ratio: [digital image processing] A digital image-processing technique that enhances contrast between features by dividing a measure of reflectance for the pixels in one image band by the measure of reflectance for the pixels in the other image band.

Bilinear interpolation: [mathematics] A resampling method that uses a weighted average of the four nearest cells to determine a new cell value.

Binary file: [computing] A file that contains data encoded as a sequence of bits (ones and zeros) instead of plain text. A binary file, such as a DLL or an executable file, contains information that can be directly loaded or executed by a computer.

Bit: [computing] The smallest unit of information within a computer. A bit can have one of two values, 1 and 0, that can represent on and off, yes and no, or true and false.

Bitmap: [data structures] An image format in which one or more bits represent each pixel on the screen. The number of bits per pixel determines the shades of gray or number of colors that a bitmap can represent.

Buffer: 1 [spatial analysis] A zone around a map feature measured in units of distance or time. A buffer is useful for proximity analysis; **2** [spatial analysis] A polygon enclosing a point, line, or polygon at a specified distance; **3** [computing] Space on a computer disk or RAM that has been allocated for temporary storage. This temporary storage may also be called a spooler when it is used to hold data in memory before the data is sent to another machine, such as a printer.

Byte: [computing] The smallest addressable unit of data storage within a computer, almost always equivalent to 8 bits and containing one character.

C

C++: [programming] An object-oriented programming language, extended from C.

CAD: [graphics (computing)] Acronym for computer-aided design. A computer-based system for the design, drafting, and display of graphical information. Also known as computer-aided drafting, such systems are most commonly used to support engineering, planning, and illustrating activities

Cadastre: [cadastral and land records] An official record of the dimensions and value of land parcels, used to record ownership and assist in calculating taxes.

Calibration: 1 [accuracy] The comparison of the accuracy of an instrument's measurements to a known standard; **2** [spatial analysis] In spatial analysis, the selection of attribute values and computational parameters that will cause a model to properly represent the situation being analyzed. For example, in pathfinding and allocation, calibration generally refers to assigning or calculating impedance values.

Cartesian coordinate system: [coordinate systems] A two-dimensional, planar coordinate system in which horizontal distance is measured along an x-axis and vertical distance is measured along a y-axis. Each point on the plane is defined by an x,y coordinate. Relative measures of distance, area, and direction are constant throughout the Cartesian coordinate plane. The Cartesian coordinate system is named for the French mathematician and philosopher René Descartes (1596-1650).

Cartographic generalization: [cartography] The abstraction, reduction, and simplification of features so that a map is clear and uncluttered at a given scale.

Cartography: [cartography] The art and science of expressing graphically, usually through maps, the natural and social features of the earth.

Cell: 1 [graphics (computing)] The smallest unit of information in raster data, usually square in shape. In a map or GIS dataset, each cell represents a portion of the earth, such as a square meter or square mile, and usually has an attribute value associated with it, such as soil type or vegetation class; 2 [graphics (computing)] A pixel.

Cell size: [data models] The dimensions on the ground of a single cell in a raster, measured in map units. Cell size is often used synonymously with pixel size.

Cellular automaton: [modeling] A mathematical construction consisting of a row or grid of cells in which each cell has an initial value—from a known and limited number of possible values—and all cells are simultaneously evaluated and updated according to their internal states and the values of their neighbors. The simplest cellular automaton is a row in which each cell has one of two values, such as red or green. In this case, there are eight possible value combinations for a cell and its neighbors. (If a green cell with two red neighbors is notated RGR, then the eight combinations are RRR, RRG, RGR, GRR, RGG, GRG, GGR, GGG.) A set of rules determines whether or not a cell changes value when it is evaluated. A sample rule might be, "A green cell becomes red if it has a red neighbor on both sides." Successive updates, or generations, of a cellular automaton may produce complex patterns. Cellular automata are of interest in spatial modeling and are often used to model land-cover change.

Centroid: [data capture] The geometric center of a feature. For line, polygon, or three-dimensional features, it is the center of mass (or center of gravity) and may fall inside the feature, as shown below for a triangle, or outside the feature, as shown below for a complex line. For multipoints, polylines, or polygons with multiple parts, it is computed using the weighted mean center of all feature parts. The weight for a point feature is 1, for a line feature is its length, and for polygon features is its area.

Change detection: [remote sensing] A process that measures how the attributes of a particular area have changed between two or more time periods. Change detection often involves comparing aerial photographs or satellite imagery of the area taken at different times. The process is most frequently associated with environmental monitoring, natural resource management, or measuring urban development.

Chi-square statistic: [statistics] A statistic used to assess how well a model fits the data. It compares categorized data with a multinomial model that predicts the relative frequency of outcomes in each category to see to what extent they agree.

Class: 1 [data analysis] A set of entities grouped together on the basis of shared attribute values; 2 [data models] Pixels in a raster file that represent the same condition; 3 [computing] A template for a type of object in an object-oriented programming language. A class is used to create objects that share the same structure and behaviour.

Classification: [cartography] The process of sorting or arranging entities into groups or categories; on a map, the process of representing members of a group by the same symbol, usually defined in a legend.

Cluster analysis: [statistics] A statistical classification technique for dividing a population into relatively homogeneous groups. The similarities between members belonging to a class, or cluster, are high; while similarities between members belonging to different clusters are low. Cluster analysis is frequently used in market analysis for consumer segmentation and locating customers, but it is also applied to other fields.

COGO: 1 [coordinate geometry (COGO)] Acronym for coordinate geometry. A method for calculating coordinate points from surveyed bearings, distances, and angles; 2 [coordinate geometry (COGO)] Automated mapping software used in land surveying that calculates locations using distances and bearings from known reference points.

Universidad Politécnica de Cataluña, Barcelona TECH
Departamento de Tecnología de la Arquitectura
Centro de Políticas de Suelo y Valoraciones
Nicola Colaninno, Josep Roca Cladera

Colour composite: [remote sensing] A colour image made by assigning red, green, and blue colours to each of the separate monochrome bands of a multispectral image and then superimposing them.

Colour map: [graphics (computing)] A set of values that are associated with specific colours. Colour maps are most commonly used to display a raster dataset consistently on many different platforms.

Colour model: [graphics (computing)] Any system that organizes colours according to their properties for printing or display. Examples include RGB (red, green, blue), CMYK (cyan, magenta, yellow, black), HSB (hue, saturation, brightness), HSV (hue, saturation, value), HLS (hue, lightness, saturation), and CIE-L*a*b (Commission Internationale de l'Eclairage-luminance, a, b).

Colour ramp: [symbology] A range of colours used to show ranking or order among classes on a map.

Computer-assisted learning: [education] Instruction or training that uses computer-based media instead of hard-copy materials. Computer-assisted learning is generally designed to use the strengths of computer-based media such as the ability to navigate in a nonlinear fashion through the use of hyperlinks.

Conic projection: [map projections] A projection that transforms points from a spheroid or sphere onto a tangent or secant cone that is wrapped around the globe in the manner of a party hat. The cone is then sliced from the apex (top) to the bottom, and flattened into a plane.

Contour interval: [cartography] The difference in elevation between adjacent contour lines.

Contour line: [cartography] A line on a map that connects points of equal elevation based on a vertical datum, usually sea level.

Contrast: [remote sensing] In remote sensing and photogrammetry, the ratio between the energy emitted or reflected by an object and that emitted or reflected by its immediate surroundings.

Contrast stretch: [graphics (computing)] Increasing the contrast in an image by expanding its grayscale range to the range of the display device.

Coordinate system: [coordinate systems] A reference framework consisting of a set of points, lines, and/or surfaces, and a set of rules, used to define the positions of points in space in either two or three dimensions. The Cartesian coordinate system and the geographic coordinate system used on the earth's surface are common examples of coordinate systems.

Coordinate transformation: [coordinate systems] The process of converting the coordinates in a map or image from one coordinate system to another, typically through rotation and scaling.

Coordinates: [coordinate systems] A set of values represented by the letters x, y, and optionally z or m (measure), that define a position within a spatial reference. Coordinates are used to represent locations in space relative to other locations.

Correlation: [statistics] An association between data or variables that change or occur together. For example, a positive correlation exists between housing costs and distance from the beach; generally, the closer a home is to the beach, the more it costs. Correlation does not imply causation. For example, there is a statistical correlation between ice cream sales and crime rates, but neither causes the other. The correlation coefficient is an index number between -1 and 1 indicating the strength of the association between two variables.

Covariance: [statistics] A statistical measure of the linear relationship between two variables. Covariance measures the degree to which two variables move together relative to their individual mean returns.

Cubic convolution: [mathematics] A technique for resampling raster data in which the average of the nearest 16 cells is used to calculate the new cell value.

Cylindrical projection: [map projections] A projection that transforms points from a spheroid or sphere onto a tangent or secant cylinder. The cylinder is then sliced from top to bottom and flattened into a plane.

D

Data: [data management] Any collection of related facts arranged in a particular format; often, the basic elements of information that are produced, stored, or processed by a computer.

Data conversion: [data conversion] The process of translating data from one format to another.

Data format: [data structures] The structure used to store a computer file or record.

Database: [data storage] One or more structured sets of persistent data, managed and stored as a unit and generally associated with software to update and query the data. A simple database might be a single file with many records, each of which references the same set of fields. A GIS database includes data about the spatial locations and shapes of geographic features recorded as points, lines, areas, pixels, grid cells, or TINs, as well as their attributes.

Dataset: [data management] Any collection of related data, usually grouped or stored together.

Datum: [geodesy] The reference specifications of a measurement system, usually a system of coordinate positions on a surface (a horizontal datum) or heights above or below a surface (a vertical datum).

Decimal degrees: [map projections] Values of latitude and longitude expressed in decimal format rather than in degrees, minutes, and seconds.

Degree: 1 [geodesy] A unit of angular measure represented by the symbol °. The earth is divided into 360 degrees of longitude and 180 degrees of latitude; **2** [mathematics] The angle equal to 1/360th of the circumference of a circle. A degree can be divided into 60 minutes of arc or 3600 seconds of arc.

Degrees/Minutes/Seconds: [coordinate systems] The unit of measure for describing latitude and longitude. A degree is 1/360th of a circle. A degree is further divided into 60 minutes, and a minute is divided into 60 seconds.

Delaunay triangulation: [3D analysis] A technique for creating a mesh of contiguous, non-overlapping triangles from a dataset of points. Each triangle's circumscribing circle contains no points from the dataset in its interior. Delaunay triangulation is named for the Russian mathematician Boris Nikolaevich Delaunay.

DEM: 1 [data models] Acronym for digital elevation model. The representation of continuous elevation values over a topographic surface by a regular array of z-values, referenced to a common datum. DEMs are typically used to represent terrain relief; **2** [data models] A format for elevation data, tiled by map sheet, produced by the National Mapping Division of the USGS.

Density slicing: [remote sensing] A technique normally applied to a single-band monochrome image for highlighting areas that appear to be uniform in tone, but are not. Grayscale values (0-255) are converted into a series of intervals, or slices, and different colours are assigned to each slice. Density slicing is often used to highlight variations in vegetation.

Dependent variable: [statistics] The variable representing the process being predicted or modeled, such as crime, foreclosure, or rainfall. The dependent variable is a function of the independent variables. Regression can be used to predict the dependent variable, using known (observed) values to build (calibrate) the regression model. In the regression equation, the dependent variable appears on the left side of the equal sign.

Digital image: [graphics (computing)] An image stored in binary form and divided into a matrix of pixels. Each pixel consists of a digital value of one or more bits, defined by the bit depth. The digital value may represent, but is not limited to, energy, brightness, color, intensity, sound, elevation, or a classified value derived through image processing. A digital image is stored as a raster and may contain one or more bands.

Digital image processing: [remote sensing] Any technique that changes the digital values of an image for the sake of analysis or enhanced display, such as density slicing or low- and high-pass filtering.

Digital number: [remote sensing] In a digital image, a value assigned to a pixel.

Digitizing: [data capture] The process of converting the geographic features on an analog map into digital format using a digitizing tablet, or digitizer, which is connected to a computer. Features on a paper map are traced with a digitizer puck, a device similar to a mouse, and the x,y coordinates of these features are automatically recorded and stored as spatial data.

E

Ecliptic: 1 [astronomy] The great circle formed by the intersection of the plane of the earth's orbit around the sun (or apparent orbit of the sun around the earth) and the celestial sphere; **2** [astronomy] The mean plane of the earth's orbit around the sun.

Universidad Politécnica de Cataluña, Barcelona TECH
Departamento de Tecnología de la Arquitectura
Centro de Políticas de Suelo y Valoraciones
Nicola Colaninno, Josep Roca Cladera

Electromagnetic radiation: [physics] Energy that moves through space at the speed of light as different wavelengths of time-varying electric and magnetic fields. Types of electromagnetic radiation include gamma, x, ultraviolet, visible, infrared, microwave, and radio.

Electromagnetic spectrum: [physics] The entire range of wavelengths (frequencies) over which electromagnetic radiation extends.

Elevation: [geodesy] The vertical distance of a point or object above or below a reference surface or datum (generally mean sea level). Elevation generally refers to the vertical height of land.

Ellipsoid: 1 [Euclidean geometry] A three-dimensional, closed geometric shape, all planar sections of which are ellipses or circles. An ellipsoid has three independent axes, and is usually specified by the lengths a,b,c of the three semi-axes. If an ellipsoid is made by rotating an ellipse about one of its axes, then two axes of the ellipsoid are the same, and it is called an ellipsoid of revolution, or spheroid. If the lengths of all three of its axes are the same, it is a sphere; 2 [geodesy] When used to represent the earth, an oblate ellipsoid of revolution, made by rotating an ellipse about its minor axis.

Encoding: [data conversion] The recording or reformatting of data into a computer format. Data may be encoded to reduce storage, increase security, or to transfer it between systems using different file formats. In GIS, analog graphic data, such as paper maps and images, are encoded into computer formats by scanning or digitizing.

Enhancement: [remote sensing] In remote sensing, applying operations to raster data to improve appearance or usability by making specific features more detectable. Such operations can include contrast stretching, edge enhancement, filtering, smoothing, and sharpening.

Equator: [geodesy] The parallel of reference that is equidistant from the poles and defines the origin of latitude values.

Euclidean distance: [Euclidean geometry] The straight-line distance between two points on a plane. Euclidean distance, or distance "as the crow flies," can be calculated using the Pythagorean theorem.

F

Feature: [cartography] A representation of a real-world object on a map.

Feature extraction: [digital image processing] In image processing, a method of pattern recognition in which patterns within an image are measured and then classified as features based on those measurements.

Filter: 1 [spatial analysis] On a raster, an analysis boundary or processing window within which cell values affect calculations and outside which they do not. Filters are used mainly in cell-based analysis where the value of a center cell is changed to the mean, the sum, or some other function of all cell values inside the filter. A filter moves systematically across a raster until each cell has been processed. Filters can be of various shapes and sizes, but are most commonly three-cell by three-cell squares; 2 [data analysis] A desktop GIS operation used to hide (but not delete) features in a map document or attribute table; 3 [data analysis] A constraint used to define a subset of data.

Floating point: [computing] A type of numeric field for storing real numbers with a decimal point. The decimal point can be in any position in the field and, thus, may "float" from one location to another for different values stored in the field. For example, a floating-point field can store the numbers 23.632, 0.000087, and -96432.15.

Flow direction: [network analysis] The route or course followed by commodities proceeding through edge elements in a network.

Focal analysis: [data analysis] The computation of an output raster where the output value at each cell location is a function of the value at that cell location and the values of the cells within a specified neighbourhood around the cell.

Footprint: [data structures] The extent (often rectangular) of each raster dataset in the mosaic dataset or image service definition. This outline is not always the extent of each raster dataset but can be the extent of the valid raster data within the dataset.

Format: [computing] In computing, the structure and organization of digital information.

Fractal: [mathematics] A geometric pattern that repeats itself, at least roughly, at ever smaller scales to produce self-similar, irregular shapes and surfaces that cannot be represented using classical geometry. If a fractal curve of infinite length serves as the boundary of a plane region, the region itself will be finite. Fractals can be used to model complex natural shapes such as clouds and coastlines.

Frequency: [physics] The number of oscillations per unit of time in a wave of energy, or the number of wavelengths that pass a point in a given amount of time.

Fuzzy classification: [uncertainty] Any method for classifying data that allows attributes to apply to objects by membership values, so that an object may be considered a partial member of a class. Class membership is usually defined on a continuous scale from zero to one, where zero is nonmembership and one is full membership. Fuzzy classification may also be applied to geographic objects themselves, so that an object's boundary is treated as a gradated area rather than an exact line. In GIS, fuzzy classification has been used in the analysis of soil, vegetation, and other phenomena that tend to change gradually in their physical composition and for which attributes are often partly qualitative in nature.

G

Gauss-Krüger projection: [map projections] A projected coordinate system that uses the transverse Mercator projection to divide the world into standard zones 6 degrees wide. Used mainly in Europe and Asia, the Gauss-Krüger coordinate system is similar to the universal transverse Mercator coordinate system. The Gauss-Krüger projection is named for the German mathematician and scientist Karl Friedrich Gauss and the German geodesist and mathematician Johann Heinrich Louis Krüger.

Generalization: **1** [map design] The abstraction, reduction, and simplification of features for change of scale or resolution; **2** [data editing] The process of reducing the number of points in a line without losing the line's essential shape; **3** [data editing] The process of enlarging and resampling cells in a raster format.

Geocentric: **1** [geodesy] Measured from the earth or the earth's center; **2** [astronomy] Having the earth as a center.

Geocentric coordinate system: [coordinate systems] A three-dimensional, earth-centered reference system in which locations are identified by their x-, y-, and z-values. The x-axis is in the equatorial plane and intersects the prime meridian (usually Greenwich). The y-axis is also in the equatorial plane; it lies at right angles to the x-axis and intersects the 90-degree meridian. The z-axis coincides with the polar axis and is positive toward the north pole. The origin is located at the center of the sphere or spheroid.

Geocentric datum: [geodesy] A horizontal geodetic datum based on an ellipsoid that has its origin at the earth's center of mass. Examples are the World Geodetic System (WGS) of 1984, the North American Datum (NAD) of 1983, and the Geodetic Datum of Australia of 1994. The first uses the WGS84 ellipsoid; the latter two use the GRS80 ellipsoid. Geocentric datums are more compatible with satellite positioning systems, such as GPS, than are local datums.

Geocoding: [geocoding] A GIS operation for converting street addresses into spatial data that can be displayed as features on a map, usually by referencing address information from a street segment data layer.

Geocoding process: [geocoding] The steps involved in translating an address entry, searching for the address in the reference data embedded in an address locator, and delivering the best candidate or candidates. These steps include parsing the address, standardizing abbreviated values, assigning each address element to a category known as a match key, indexing the needed categories, searching the reference data, assigning a score to each potential candidate, filtering the list of candidates based on the minimum match score, and delivering the best match. The process requires reference files, input address records, address locators, and software.

Geocomputation: [computing] The application of computer technology to spatial problems, including problems of collecting, storing, visualizing, and analysing spatial data, and of modelling spatial system dynamics.

Geodatabase: [ESRI software] A database or file structure used primarily to store, query, and manipulate spatial data. Geodatabases store geometry, a spatial reference system, attributes, and behavioral rules for data. Various types of geographic datasets can be collected within a geodatabase, including feature classes, attribute tables, raster datasets, network datasets, topologies, and many others. Geodatabases can be stored in IBM DB2, IBM

Universidad Politécnica de Cataluña, Barcelona TECH
Departamento de Tecnología de la Arquitectura
Centro de Políticas de Suelo y Valoraciones
Nicola Colaninno, Josep Roca Cladera

Informix, Oracle, Microsoft Access, Microsoft SQL Server, and PostgreSQL relational database management systems, or in a system of files, such as a file geodatabase.

Geodataset: [ESRI software] Any organized collection of data in a geodatabase with a common theme.

Geodesic: [Euclidean geometry] The shortest distance between two points on the surface of a spheroid. Any two points along a meridian form a geodesic.

Geodesy: [geodesy] The science of measuring and representing the shape and size of the earth, and the study of its gravitational and magnetic fields.

Geographic coordinate system: [coordinate systems] A reference system that uses latitude and longitude to define the locations of points on the surface of a sphere or spheroid. A geographic coordinate system definition includes a datum, prime meridian, and angular unit.

Geographic coordinates: [coordinate systems] A measurement of a location on the earth's surface expressed in degrees of latitude and longitude.

Geographic data: [GIS technology] Information describing the location and attributes of things, including their shapes and representation. Geographic data is the composite of spatial data and attribute data.

Geographic transformation: [coordinate systems] A systematic conversion of the latitude-longitude values for a set of points from one geographic coordinate system to equivalent values in another geographic coordinate system. Depending on the geographic coordinate systems involved, the transformation can be accomplished in various ways. Typically, equations are used to model the position and orientation of the "from" and "to" geographic coordinate systems in three-dimensional coordinate space; the transformation parameters may include translation, rotation, and scaling. Other methods, including one used in transformations between NAD 1927 and NAD 1983, use files in which the differences between the two geographic coordinate systems are given for a set of coordinates; the values of other points are interpolated from these.

Geography: 1 [geography] The study of the earth's surface, encompassing the description and distribution of the various physical, biological, economic, and cultural features found on the earth and the interaction between those features; **2** [geography] The arrangement of the geographic features of an area.

Geoid: [geodesy] A hypothetical surface representing the form the earth's oceans would take if there were no land and the water were free to respond to the earth's gravitational and centrifugal forces. The resulting geoid is irregular and varies from a perfect sphere by as much as 75 meters above and 100 meters below its surface.

Geolocation: [geolocating] The process of creating geographic features from tabular data by matching the tabular data to a spatial location. An example of geolocation is creating point features from a table of x,y coordinates.

Geomorphology: [geography] The study of the nature and origin of landforms, including relationships to underlying structures and processes of formation.

Geoprocessing: [analysis/geoprocessing] A GIS operation used to manipulate GIS data. A typical geoprocessing operation takes an input dataset, performs an operation on that dataset, and returns the result of the operation as an output dataset. Common geoprocessing operations include geographic feature overlay, feature selection and analysis, topology processing, raster processing, and data conversion. Geoprocessing allows for definition, management, and analysis of information used to form decisions.

Georectification: [data editing] The digital alignment of a satellite or aerial image with a map of the same area. In georectification, a number of corresponding control points, such as street intersections, are marked on both the image and the map. These locations become reference points in the subsequent processing of the image.

Georeferencing: [coordinate systems] Aligning geographic data to a known coordinate system so it can be viewed, queried, and analysed with other geographic data. Georeferencing may involve shifting, rotating, scaling, skewing, and in some cases warping, rubber sheeting, or orthorectifying the data.

Geostationary: [astronomy] Positioned in an orbit above the earth's equator with an angular velocity the same as that of the earth and an inclination and eccentricity approaching zero. A geostationary satellite will orbit as fast as the earth rotates on its axis, so that it remains effectively stationary above a point on the equator. A geostationary satellite is geosynchronous, but geosynchronous satellites are not necessarily geostationary.

Geostatistics: [statistics] A class of statistics used to analyze and predict the values associated with spatial or spatio-temporal phenomena. Geostatistics provides a means of exploring spatial data and generating continuous surfaces from selected sampled data points.

GIS: [GIS technology] Acronym for geographic information system. An integrated collection of computer software and data used to view and manage information about geographic places, analyze spatial relationships, and model spatial processes. A GIS provides a framework for gathering and organizing spatial data and related information so that it can be displayed and analyzed.

Gnomonic projection: [map projections] A planar projection, tangent to the earth at one point, projected from the center of the globe. All great circles appear as straight lines on this projection, so that the shortest distance between two points is a straight line. The gnomonic projection is useful in navigation. The gnomonic projection was used by Thales of Miletus, an ancient Greek astronomer and philosopher, to chart the heavens. It is possibly the oldest map projection.

GPS: [GPS] Acronym for Global Positioning System. A system of radio-emitting and -receiving satellites used for determining positions on the earth. The orbiting satellites transmit signals that allow a GPS receiver anywhere on earth to calculate its own location through trilateration. Developed and operated by the U.S. Department of Defense, the system is used in navigation, mapping, surveying, and other applications in which precise positioning is necessary.

Gradient: 1 [geodesy] The ratio between vertical distance (rise) and horizontal distance (run), often expressed as a percentage. A 10-percent gradient rises 10 feet for every 100 feet of horizontal distance; **2** [geodesy] The inclination of a surface in a given direction; **3** [physics] The rate at which a quantity such as temperature or pressure changes in value.

Grey scale: 1 [computing] All the shades of grey from white to black; **2** [graphics (computing)] Levels of brightness used to display information on a monochrome display device.

Greenwich meridian: [astronomy] The meridian adopted by international agreement in 1884 as the prime meridian, the 0-degree meridian from which all other longitudes are calculated. The Greenwich prime meridian runs through the Royal Observatory in Greenwich, England.

Grid: [cartography] In cartography, any network of parallel and perpendicular lines superimposed on a map and used for reference. These grids are usually referred to by the map projection or coordinate system they represent, such as universal transverse Mercator grid.

Ground receiving station: [remote sensing] Communications equipment for receiving and transmitting signals to and from satellites such as Landsat.

Ground truth: [accuracy] The accuracy of remotely sensed or mathematically calculated data based on data actually measured in the field.

GRS80: [geodesy] Acronym for Geodetic Reference System of 1980. The standard measurements of the earth's shape and size adopted by the International Union of Geodesy and Geophysics in 1979.

GUI: [computing] Acronym for graphical user interface. A software display of program options that allows a user to choose commands by pointing to icons, dialog boxes, and lists of menu items on the screen, typically using a mouse. This contrasts with a command line interface in which control is accomplished via the exchange of strings of text.

H

Hectare: [standards] A metric areal unit of measure equal to 10,000 square meters. One hectare is equal to 100 ares or 2.47 acres.

Height: [Euclidean geometry] The vertical distance between two points, or above a specified datum.

Hemisphere: 1 [astronomy] Half of a celestial body, such as the earth; **2** [Euclidean geometry] Half of a sphere.

Heuristic: 1 [computing] In computer science, an algorithm that incorporates a shortcut or simplification for solving a programming problem, such as searching. While a heuristic may run faster than a more rigorous algorithm, there

Universidad Politécnica de Cataluña, Barcelona TECH
Departamento de Tecnología de la Arquitectura
Centro de Políticas de Suelo y Valoraciones
Nicola Colaninno, Josep Roca Cladera

is no guarantee that it will find the best solution; 2 [mathematics] In graph theory, a function used to determine the lowest cost or shortest path between two given nodes in a tree.

High-pass filter: [digital image processing] In digital image processing, a spatial filter that blocks low-frequency (long-wave) radiation, resulting in a sharpened image.

Hillshading: 1 [map design] Shadows drawn on a map to simulate the effect of the sun's rays over the varied terrain of the land; 2 [map design] The hypothetical illumination of a surface according to a specified azimuth and altitude for the sun. Hillshading creates a three-dimensional effect that provides a sense of visual relief for cartography, and a relative measure of incident light for analysis.

Histogram: [statistics] A graph showing the distribution of values in a set of data. Individual values are displayed along a horizontal axis, and the frequency of their occurrence is displayed along a vertical axis.

Histogram equalization: [digital image processing] The redistribution of pixel values in an image so that each range contains approximately the same number of pixels. A histogram showing this distribution of values would be nearly flat.

HSV: [graphics (map display)] A colour model that uses hue, saturation, and value. Hue specifies the perceived colour, such as red or green. Saturation specifies the intensity, or how vivid the colour appears. Value specifies the brightness, or white intensity, with higher values being perceived as lighter.

Hue: [physics] The dominant wavelength of a colour, by which it can be distinguished as red, green, yellow, blue, and so forth.

Hydrography: [geodesy] The measurement and description of water features and their related land areas for the purposes of safe marine navigation.

Hydrology: [geography] The study of water, its behaviour, and its movements across and below the surface of the earth, and through the atmosphere.

Hyperlink: [Internet] A reference (link) from one point in an electronic document to another document or another location in the same document (the target). Activating the link, usually by clicking it with the mouse, causes the browser to display the target of the link.

Hypsometry: 1 [geodesy] The science that determines the spatial distribution of elevations above an established datum, usually sea level; 2 [geodesy] The determination of terrain relief, by any method.

I

IDL: [programming] Acronym for Interface Definition Language. A language used to define COM interfaces. The Microsoft implementation of IDL may also be referred to as MIDL or Microsoft IDL.

Illumination: [cartography] The light incident on a surface or object, either natural or artificial, as determined by the surface's slope and aspect and by the sun's azimuth and altitude.

Image: 1 [data capture] A representation or description of a scene, typically produced by an optical or electronic device, such as a camera or a scanning radiometer. Common examples include remotely sensed data (for example, satellite data), scanned data, and photographs; 2 [ESRI software] In ArcGIS, a raster dataset.

Image coordinate: [data structures] An x,y coordinate pair specifying the location of a pixel, or cell, in terms of its row and column position. The x-coordinate gives the column number (commonly starting from 0 at the left edge of the data), and the y-coordinate gives the row number (commonly starting from 0 at the top of the data).

Image data: [data capture] Data produced by scanning a surface with an optical or electronic device. Common examples include scanned documents, remotely sensed data (for example, satellite images), and aerial photographs. An image is stored as a raster dataset of binary or integer values that represent the intensity of reflected light, heat, or other range of values on the electromagnetic spectrum.

Incident energy: [physics] Electromagnetic radiation that strikes a surface.

Independent variable: [statistics] One or a set of variables used to model or predict the dependent variable. For example, a prediction of annual purchases for a proposed store (the dependent variable) might include independent variables representing the number of potential customers, distance to competition, store visibility,

and local spending patterns. In the regression equation, independent variables appear on the right side of the equal sign and are often referred to as explanatory variables.

Infrared scanner: [data capture] A device that detects infrared radiation and converts it into an electrical signal that can be recorded on film or magnetic tape.

Intensity: [graphics (computing)] In the IHS (intensity, hue, saturation) colour model, the relative brightness of a colour.

Interactive vectorization: [data conversion] A manual process for converting raster data into vector features that involves tracing raster cells.

Interferogram: [remote sensing] A radar image that records interference patterns captured by two antennae a short distance apart.

Interpolation: 1 [mathematics] The estimation of surface values at unsampled points based on known surface values of surrounding points. Interpolation can be used to estimate elevation, rainfall, temperature, chemical dispersion, or other spatially-based phenomena. Interpolation is commonly a raster operation, but it can also be done in a vector environment using a TIN surface model. There are several well-known interpolation techniques, including spline and kriging; 2 [ESRI software] In the context of linear referencing, the calculation of measure values for a route between two known measure values.

Inverse distance weighted interpolation: [mathematics] An interpolation technique that estimates cell values in a raster from a set of sample points that have been weighted so that the farther a sampled point is from the cell being evaluated, the less weight it has in the calculation of the cell's value.

ISO: [standards] Abbreviation for International Organization for Standardization. A federation of national standards institutes from 145 countries that works with international organizations, governments, industries, businesses, and consumer representatives to define and maintain criteria for international standards.

Isobar: [cartography] A line on a weather map connecting places of equal barometric pressure.

Isochrone: 1 [cartography] A line on a map connecting points of equal elapsed time; especially, travel time to or from a given location; 2 [cartography] A line on a map connecting points at which an event occurs, or a state of affairs exists, at the same time.

Isoline: [cartography] A line connecting points of equal value on a map. Isolines fall into two classes: those in which the values actually exist at points, such as temperature or elevation values, and those in which the values are ratios that exist over areas, such as population per square kilometer or crop yield per acre. The first type of isoline is specifically called an isometric line or isarithm; the second type is called an isopleth.

Isometric line: [cartography] An isoline drawn according to known values, either sampled or derived, that can occur at points. Examples of sampled quantities that can occur at points are elevation above sea level, an actual temperature, or an actual depth of precipitation. Examples of derived values that can occur at points are the average of temperature over time for one point or the ratio of smoggy days to clear days for one point.

Iterative procedure: [computing] A repetitive or recurring procedure.

J

Java: [programming] An object-oriented cross-platform programming language developed by Sun Microsystems.

Joining: 1 [database structures] Appending the fields of one table to those of another through an attribute or field common to both tables. A join is usually used to attach more attributes to the attribute table of a geographic layer; 2 [analysis/geoprocessing] Connecting two or more features from different sets of data so that they become a single feature.

JPEG: [graphics (computing)] Acronym for Joint Photographic Experts Group. A lossy image compression format commonly used on the Internet. JPEG is well-suited for photographs or images that have graduated colours.

K

Key: [database structures] An attribute or set of attributes in a database that uniquely identifies each record.

Universidad Politécnica de Cataluña, Barcelona TECH
Departamento de Tecnología de la Arquitectura
Centro de Políticas de Suelo y Valoraciones
Nicola Colaninno, Josep Roca Cladera

Kriging: [spatial statistics (use for geostatistics)] An interpolation technique in which the surrounding measured values are weighted to derive a predicted value for an unmeasured location. Weights are based on the distance between the measured points, the prediction locations, and the overall spatial arrangement among the measured points. Kriging is unique among the interpolation methods in that it provides an easy method for characterizing the variance, or the precision, of predictions. Kriging is based on regionalized variable theory, which assumes that the spatial variation in the data being modeled is homogeneous across the surface. That is, the same pattern of variation can be observed at all locations on the surface. Kriging was named for the South African mining engineer Danie G. Krige (1919-).

L

Label: [cartography] In cartography, text placed on or near a map feature that describes or identifies it.

Land cover: [geography] The classification of land according to the vegetation or material that covers most of its surface; for example, pine forest, grassland, ice, water, or sand.

Land use: [geography] The classification of land according to what activities take place on it or how humans occupy it; for example, agricultural, industrial, residential, urban, rural, or commercial.

Landmark: 1 [geography] Any prominent natural or artificial object in a landscape used to determine distance, bearing, or location; **2** [geography] A building or location that has historical, architectural, or cultural value.

Landsat: [satellite imaging] Multispectral, earth-orbiting satellites developed by NASA (National Aeronautics and Space Administration) that gather imagery for land-use inventory, geological and mineralogical exploration, crop and forestry assessment, and cartography.

Landscape ecology: [environmental GIS] The study of spatial patterns, processes, and change across biological and cultural structures within areas encompassing multiple ecosystems.

LAS: [3D GIS] An industry-standard binary file format that maintains information related to lidar data.

LAS dataset: [database structures] A geodataset that references LAS files and surface constraints, and enables a person to examine LAS files in their native format.

Latitude: [coordinate systems] The angular distance, usually measured in degrees north or south of the equator. Lines of latitude are also referred to as parallels.

Latitude-longitude: [coordinate systems] A reference system used to locate positions on the earth's surface. Distances east–west are measured with lines of longitude (also called meridians), which run north–south and converge at the north and south poles. Distance measurements begin at the prime meridian and are measured positively 180 degrees to the east and negatively 180 degrees to the west. Distances north–south are measured with lines of latitude (also called parallels), which run east–west. Distance measurements begin at the equator and are measured positively 90 degrees to the north and negatively 90 degrees to the south.

Layer: [data structures] The visual representation of a geographic dataset in any digital map environment. Conceptually, a layer is a slice or stratum of the geographic reality in a particular area, and is more or less equivalent to a legend item on a paper map. On a road map, for example, roads, national parks, political boundaries, and rivers might be considered different layers.

Layout: [map design] The arrangement of elements on a map, possibly including a title, legend, north arrow, scale bar, and geographic data.

L-band: [GPS] The group of radio frequencies that carry data from GPS satellites to GPS receivers.

Least-squares adjustment: [surveying] A statistical method for providing a best fit for survey point locations and detecting measurement error by minimizing the sum of the squares of measurement residuals. The method allows many measurements to participate simultaneously in a single computation.

Legend: [symbology] The description of the types of features included in a map, usually displayed in the map layout. Legends often use graphics of symbols or examples of features from the map with a written description of what each symbol or graphic represents.

Library: [programming] In object-oriented programming, a logical grouping of classes, usually with a header section that lists the classes in the library.

Lidar: [remote sensing] Acronym for light detection and ranging. A remote-sensing technique that uses lasers to measure distances to reflective surfaces.

Line of sight: 1 [3D analysis] A line drawn between two points, an origin and a target, that is compared against a surface to show whether the target is visible from the origin and, if it is not visible, where the view is obstructed; **2** [visualization] In a perspective view, the point and direction from which a viewer looks into an image.

Linear dimension: [surveying] A measurement of the horizontal or vertical dimension of a feature. Linear dimensions may not represent the true distance between beginning and ending dimension points because they do not take angle into account as aligned dimensions do.

Linear interpolation: [spatial statistics (use for geostatistics)] The estimation of an unknown value using the linear distance between known values.

Linear unit: [cartography] The unit of measurement on a plane or a projected coordinate system, often meters or feet.

Local analysis: [data editing] The computation of an output raster where the output value at each location is a function of the input value at the same location.

Local datum: 1 [geodesy] A horizontal geodetic datum that serves as a basis for measurements over a limited area of the earth; that has its origin at a location on the earth's surface; that uses an ellipsoid whose dimensions conform well to its region of use; and that was originally defined for land-based surveys. A local datum in this sense stands in contrast to a geocentric datum. Examples include the North American Datum of 1927 and the Australian Geodetic Datum of 1966; **2** [geodesy] A horizontal or vertical datum used for measurements over a limited area of the earth, such as a nation, a supranational region, or a continent. A horizontal datum that is local in this sense may or may not be geocentric. For example, the North American Datum of 1983 and the Geocentric Datum of Australia 1994 are local in that they are applied to a particular part of the world; they are also geocentric. All vertical datums are local in that there is, at present, no global vertical datum.

Log file: [computing] A database file that records changes in data, often used as part of a database restoration.

Logarithm: [mathematics] The power to which a fixed number (the base) must be raised to equal a given number. The three most frequently used bases for logarithms are base 10, base e, and base 2.

Longitude: [coordinate systems] The angular distance, usually expressed in degrees, minutes, and seconds, of the location of a point on the earth's surface east or west of an arbitrarily defined meridian (usually the Greenwich prime meridian). All lines of longitude are great circles that intersect the equator and pass through the North and South Poles.

Lossy compression: [data transfer] Data compression that provides high compression ratios (for example 10:1 to 100:1), but does not retain all the information in the data. In GIS, lossy compression is used to compress raster datasets that will be used as background images, but is not suitable for raster datasets used for analysis or deriving other data products.

Low-pass filter: [remote sensing] A spatial filter that blocks high-frequency (shortwave) radiation, resulting in a smoother image.

M

Major axis: [Euclidean geometry] The longer axis of an ellipse or spheroid.

Majority resampling: [spatial statistics (use for geostatistics)] A technique for resampling raster data in which the value of each cell in an output is calculated, most commonly using a 2x2 neighbourhood of the input raster. Majority resampling does not create any new cell values, so it is useful for resampling categorical or integer data, such as land use, soil, or forest type. Majority resampling acts as a type of low-pass filter for discrete data, generalizing the data and filtering out anomalous data values.

Map: 1 [cartography] A graphic representation of the spatial relationships of entities within an area; **2** [cartography] Any graphical representation of geographic or spatial information.

Map algebra: [data analysis] A language that defines a syntax for combining map themes by applying mathematical operations and analytical functions to create new map themes. In a map algebra expression, the operators are a

Universidad Politécnica de Cataluña, Barcelona TECH
Departamento de Tecnología de la Arquitectura
Centro de Políticas de Suelo y Valoraciones
Nicola Colaninno, Josep Roca Cladera

combination of mathematical, logical, or Boolean operators (+, >, AND, tan, and so on), and spatial analysis functions (slope, shortest path, spline, and so on), and the operands are spatial data and numbers.

Map extent: [cartography] The limit of the geographic area shown on a map, usually defined by a rectangle. In a dynamic map display, the map extent can be changed by zooming and panning.

Map generalization: [cartography] Decreasing the level of detail on a map so that it remains uncluttered when its scale is reduced.

Map topology: [graphics (map display)] A temporary set of topological relationships between coincident parts of simple features on a map, used to edit shared parts of multiple features.

Mask: [cartography] In digital cartography, a means of covering or hiding features on a map to enhance cartographic representation. For example, masking is often used to cover features behind text to make the text more readable.

Matching: [geocoding] In geocoding, the process of linking a record, such as an address, to a set of reference data. The matched record in the reference data is used to determine the location of the input address.

Matrix: [mathematics] A rectangular arrangement of data, usually numbers, in rows and columns. In computer science, a two-dimensional array is called a matrix. In GIS, matrices are used to store raster data.

Mean: [mathematics] The average for a set of values, computed as the sum of all values divided by the number of values in the set.

Measurement error: [surveying] In surveying, the noise that is expected in every measurement. It occurs because the observer makes estimates and uses measuring equipment that is unpredictable in an environment that is also unpredictable.

Measurement residual: [surveying] The difference between a measured quantity and its theoretical true value as determined during each iteration of a least-squares adjustment.

Median: [mathematics] The middle value of a set of values when they are ordered by rank. Half the values in a set are higher than the median, and half are lower. When there are two middle values (if the set has an even number of elements) the median is the mean of these two values.

Merging: [analysis/geoprocessing] Combining features from multiple data sources of the same data type into a single, new dataset.

Meridian: [geodesy] A great circle on the earth that passes through the poles, often used synonymously with longitude. Meridians run north–south between the poles. By convention, meridians are labeled with positive numbers that ascend as one moves eastward from the prime meridian, and negative numbers as one moves westward from the prime meridian until the east and west hemispheres meet at the 180-degree line. Meridians can also, however, be labeled with all positive or negative numbers, including positive numbers increasing westward from the prime meridian.

Metadata: [data transfer] Information that describes the content, quality, condition, origin, and other characteristics of data or other pieces of information. Metadata for spatial data may describe and document its subject matter; how, when, where, and by whom the data was collected; availability and distribution information; its projection, scale, resolution, and accuracy; and its reliability with regard to some standard. Metadata consists of properties and documentation. Properties are derived from the data source (for example, the coordinate system and projection of the data), while documentation is entered by a person (for example, keywords used to describe the data).

Micrometer: [physics] An instrument for measuring minute lengths or angles.

Micron: [physics] One millionth of a meter, represented by the symbol µm. Microns are used to measure wavelengths in the electromagnetic spectrum.

Minimum bounding rectangle: [ESRI software] A rectangle, oriented to the x- and y-axes, that bounds a geographic feature or a geographic dataset. It is specified by two coordinate pairs: xmin, ymin and xmax, ymax.

Minor axis: [Euclidean geometry] The shorter axis of an ellipse or spheroid.

Mixed pixel: [remote sensing] In remote sensing, a pixel whose digital number represents the average of several spectral classes within the area that it covers on the ground, each emitted or reflected by a different type of material. Mixed pixels are common along the edges of features.

Model: 1 [data models] An abstraction of reality used to represent objects, processes, or events; **2** [modeling] A set of rules and procedures for representing a phenomenon or predicting an outcome; **3** [data models] A data representation of reality, such as the vector data model; **4** [ESRI software] In geoprocessing in ArcGIS, one process or a sequence of processes connected together, that is created in ModelBuilder.

MODIS: [satellite imaging] Acronym for moderate resolution imaging spectroradiometer. A bundle of remote-sensing equipment housed on two NASA (National Aeronautics and Space Administration) satellites, Terra and Aqua, in orbit around Earth. These two MODIS-equipped satellites constantly record multiple images of the globe in various wavelengths and resolutions, imaging the earth's entire surface in less than two days.

Monochromatic: 1 [physics] Related to a single wavelength or a very narrow band of wavelengths; **2** [graphics (computing)] A colour scheme made up of lighter and darker shades of the same colour.

Morphology: 1 [geography] The structure of a surface; **2** [spatial analysis] The study of structure or form.

Mosaic: 1 [remote sensing] A raster dataset composed of two or more merged raster datasets-for example, one image created by merging several individual images or photographs of adjacent areas; 2 [visualization] Maps of adjacent areas with the same spatial reference and scale whose boundaries have been matched and dissolved.

Multiple regression: [statistics] Regression in which the dependent variable is measured against two or more independent variables.

Multispectral: [physics] Related to two or more frequencies or wavelengths in the electromagnetic spectrum.

Multispectral image: [remote sensing] An image created from several narrow spectral bands.

Multispectral scanner: [satellite imaging] A device carried on satellites and aircraft that records energy from multiple portions of the electromagnetic spectrum.

Multivariate analysis: [statistics] Any statistical method for evaluating the relationship between two or more variables.

N

NAD 1927: [coordinate systems] Acronym for North American Datum of 1927. The primary local horizontal geodetic datum and geographic coordinate system used to map the United States during the middle part of the twentieth century. NAD 1927 is referenced to the Clarke spheroid of 1866 and an origin point at Meades Ranch, Kansas. Features on USGS topographic maps, including the corners of 7.5-minute quadrangle maps, are referenced to NAD27. It is gradually being replaced by the North American Datum of 1983.

NAD 1983: [coordinate systems] Acronym for North American Datum of 1983. A geocentric datum and graphic coordinate system based on the Geodetic Reference System 1980 ellipsoid (GRS80). Mainly used in North America, its measurements are obtained from both terrestrial and satellite data.

Nadir: 1 [aerial photography] In aerial photography, the point on the ground vertically beneath the perspective center of the camera lens; **2** [astronomy] In astronomy, the point on the celestial sphere directly beneath an observer. Both the nadir and zenith lie on the observer's meridian; the nadir lies 180 degrees from the zenith and is therefore unobservable.

Natural breaks classification: [cartography] A method of manual data classification that seeks to partition data into classes based on natural groups in the data distribution. Natural breaks occur in the histogram at the low points of valleys. Breaks are assigned in the order of the size of the valleys, with the largest valley being assigned the first natural break.

Natural neighbors: [mathematics] An interpolation method for multivariate data in a Delaunay triangulation. The value for an interpolation point is estimated using weighted values of the closest surrounding points in the triangulation. These points, the natural neighbors, are the ones the interpolation point would connect to if inserted into the triangulation.

Nearest neighbour resampling: [mathematics] A technique for resampling raster data in which the value of each cell in an output raster is calculated using the value of the nearest cell in an input raster. Nearest neighbour assignment does not change any of the values of cells from the input layer; for this reason it is often used to resample

Universidad Politécnica de Cataluña, Barcelona TECH
Departamento de Tecnología de la Arquitectura
Centro de Políticas de Suelo y Valoraciones
Nicola Colaninno, Josep Roca Cladera

categorical or integer data (for example, land use, soil, or forest type), or radiometric values, such as those from remotely sensed images.

Network analysis: [network analysis] Any method of solving network problems such as traversability, rate of flow, or capacity, using network connectivity.

Neural network: [computing] A computer architecture modeled after the human brain and designed to solve problems that human brains solve well, such as recognizing patterns and making predictions from past performance. Neural networks are composed of interconnected computer processors that calculate a number of weighted inputs to generate an output. For example, an output might be the approval or rejection of a credit application. This output would be based on several inputs, including the applicant's income, current debt, and credit history. Some of these inputs would count more than others; cumulatively, they would be compared to a threshold value that separates approvals from rejections. Neural networks "learn" to generate better outputs by adjusting the weights and thresholds applied to their inputs.

NoData: [data capture] In raster data, the absence of a recorded value. NoData does not equate to a zero value. While the measure of a particular attribute in a cell may be zero, a NoData value indicates that no measurements have been taken for that cell at all.

Noise: **1** [remote sensing] In remote sensing, any disturbance in a frequency band; **2** [data quality] Any irregular, sporadic, or random oscillation in a transmission signal; **3** [telecommunications] Random or repetitive events that interfere with communication; **4** [data quality] In a raster, irrelevant or meaningless cells that exist due to poor scanning or imperfections in the original source document.

Nonspatial data: [data management] Data without inherently spatial qualities, such as attributes.

Normal distribution: [statistics] A theoretical frequency distribution of a dataset in which the distribution of values can be graphically represented as a symmetrical bell curve. Normal distributions are typically characterized by a clustering of values near the mean, with few values departing radically from the mean. There are as many values on the left side of the curve as on the right, so the mean and median values for the distribution are the same. Sixty-eight percent of the values are plus or minus one standard deviation from the mean; 95 percent of the values are plus or minus two standard deviations; and 99 percent of the values are plus or minus three standard deviations.

Normalization: **1** [data management] The process of organizing, analysing, and cleaning data to increase efficiency for data use and sharing. Normalization usually includes data structuring and refinement, redundancy and error elimination, and standardization; **2** [statistics] The process of dividing one numeric attribute value by another to minimize differences in values based on the size of areas or the number of features in each area. For example, normalizing (dividing) total population by total area yields population per unit area, or density.

O

Oblate ellipsoid: [mathematics] An ellipsoid created by rotating an ellipse around its minor axis. The shape of the earth approximates an oblate ellipsoid with a flattening ratio of 1 to 298.257.

Oblique projection: **1** [map projections] A planar or cylindrical projection whose point of tangency is neither on the equator nor at a pole; **2** [map projections] A conic projection whose axis does not line up with the polar axis of the globe; **3** [map projections] A cylindrical projection whose lines of tangency or secancy follow neither the equator nor a meridian.

Off-nadir: [remote sensing] Any point not directly beneath a scanner's detectors, but rather off at an angle.

Offset: 1 [cartography] In cartography, the displacement or movement of features so that they do not overlap when displayed at a given scale. For example, a road can be offset from a river if the symbols are wide enough that they overlap; 2 [symbology] In symbology, the shift of the origin or insertion point of a symbol in an x and/or y direction.

Orthophotograph: [aerial photography] An aerial photograph from which distortions owing to camera tilt and ground relief have been removed. An orthophotograph has the same scale throughout and can be used as a map.

Orthorectification: [satellite imaging] The process of correcting the geometry of an image so that it appears as though each pixel were acquired from directly overhead. Orthorectification uses elevation data to correct terrain distortion in aerial or satellite imagery.

Outlier: 1 [statistics] An unusual or extreme data value in a dataset. In data analysis, outliers can potentially have a strong effect on results and so must be analysed carefully to determine if they represent valid or erroneous data; 2 [geology] In geology, a feature that lies apart from the main body or mass to which it belongs: for example, a rock or stratum that has been separated from a formation by erosion.

Outline: [data models] The path that follows the boundary of an object. Outlines are also called strokes.

Overlay: 1 [analysis/geoprocessing] A spatial operation in which two or more maps or layers registered to a common coordinate system are superimposed, either digitally or on a transparent material, for the purpose of showing the relationships between features that occupy the same geographic space; 2 [analysis/geoprocessing] In geoprocessing, the geometric intersection of multiple datasets to combine, erase, modify, or update features in a new output dataset.

P

Panchromatic: [remote sensing] Sensitive to light of all wavelengths in the visible spectrum.

Panchromatic image: [remote sensing] A single band image generally displayed as shades of grey.

Panchromatic sharpening: [digital image processing] Sharpening a low-resolution multiband image by merging it with a high-resolution panchromatic image.

Passive remote sensing: [remote sensing] A remote-sensing system, such as an aerial photography imaging system, that only detects energy naturally reflected or emitted by an object.

Passive sensors: [remote sensing] Imaging sensors that can only receive radiation, not transmit it.

Pattern recognition: [digital image processing] In image processing, the computer-based identification, analysis, and classification of objects, features, or other meaningful regularities within an image.

Percent slope: [Euclidean geometry] A measurement of the rate of change of elevation over a given horizontal distance, in which the rise is divided by the run and then multiplied by one hundred. A 45-degree slope and a 100-percent slope are the same.

Photogrammetry: [photogrammetry] The science of making reliable measurements of physical objects and the environment by measuring and plotting electromagnetic radiation data from aerial photographs and remote-sensing systems against land features identified in ground control surveys, generally in order to produce planimetric, topographic, and contour maps.

Pixel: 1 [data models] The smallest unit of information in an image or raster map, usually square or rectangular. Pixel is often used synonymously with cell; 2 [remote sensing] In remote sensing, the fundamental unit of data collection. A pixel is represented in a remotely sensed image as a cell in an array of data values; 3 [graphics (computing)] The smallest element of a display device, such as a video monitor, that can be independently assigned attributes, such as colour and intensity. Pixel is an abbreviation for picture element.

Pixel space: [graphics (computing)] The x,y coordinate space defined by the number of pixels in a computer's display area, with a pixel being a single unit of colour on the screen. Most computer displays support several pixel configurations (800 x 600, 1024 x 768, 1600 x 1200, and so on). The more pixels there are, the smaller each pixel is for a given display size. Since a pixel is a piece of information, a configuration with more pixels can fit more information into a given display area.

Planar coordinate system: [coordinate systems] A two-dimensional measurement system that locates features on a plane based on their distance from an origin (0,0) along two perpendicular axes.

Planar projection: [map projections] A projection that transforms points from a spheroid or sphere onto a tangent or secant plane. Because its directions are often true, the planar projection is also known as an azimuthal or zenithal projection.

Planimetric: [aerial photography] Two-dimensional; showing no relief.

Planimetric map: [cartography] A map that displays only the x,y locations of features and represents only horizontal distances.

PNG: [data structures] Acronym for Portable Network Graphics. A bitmapped graphics format similar to GIF.

Polar orbit: [remote sensing] A satellite orbit with an inclination near 90 degrees that passes over each polar region.

Universidad Politécnica de Cataluña, Barcelona TECH
Departamento de Tecnología de la Arquitectura
Centro de Políticas de Suelo y Valoraciones
Nicola Colaninno, Josep Roca Cladera

Prediction standard error: [spatial statistics (use for geostatistics)] A value quantifying the uncertainty of a prediction; mathematically, the square-root of the prediction variance. (The prediction variance is the variation associated with the difference between the true and predicted value.) As a rule, 95 percent of the time the true value will lie within the predicted value plus or minus two times the prediction standard error if data is normally distributed.

Primary colours: [graphics (computing)] Colors from which all other colors are derived in a particular color system. On a display monitor, these colors are red, green, and blue (RGB). In printing, they are cyan, magenta, and yellow (CMY). In traditional pigments, they are red, blue, and yellow.

Prime meridian: [coordinate systems] In a coordinate system, any line of longitude designated as 0 degrees east and west, to which all other meridians are referenced. The Greenwich meridian is internationally recognized as the prime meridian for most official purposes, such as civil timekeeping.

Prime vertical: [geodesy] In astronomy and geodesy, the vertical circle that passes through an observer's zenith and through the east and west points of the horizon.

PRJ: [ESRI software] Usually a text file named prj.adf that is associated with a coverage, GRID, or TIN. The PRJ file contains the coordinate system information for the data. In a more general sense, PRJ can refer to the coordinate system of data even if the information is not stored in a prj.adf file. For example, "The PRJ of the shapefile is WGS 1984 UTM zone 15 north."

Projected coordinate system: [coordinate systems] A reference system used to locate x, y, and z positions of point, line, and area features in two or three dimensions. A projected coordinate system is defined by a geographic coordinate system, a map projection, any parameters needed by the map projection, and a linear unit of measure.

Projected coordinates: [coordinate systems] A measurement of locations on the earth's surface expressed in a two-dimensional system that locates features based on their distance from an origin (0,0) along two axes, a horizontal x-axis representing east–west and a vertical y-axis representing north–south. Projected coordinates are transformed from latitude and longitude to x,y coordinates using a map projection.

Projection: [map projections] A method by which the curved surface of the earth is portrayed on a flat surface. This generally requires a systematic mathematical transformation of the earth's graticule of lines of longitude and latitude onto a plane. Some projections can be visualized as a transparent globe with a light bulb at its center (though not all projections emanate from the globe's center) casting lines of latitude and longitude onto a sheet of paper. Generally, the paper is either flat and placed tangent to the globe (a planar or azimuthal projection) or formed into a cone or cylinder and placed over the globe (cylindrical and conical projections). Every map projection distorts distance, area, shape, direction, or some combination thereof.

Projection transformation: [data conversion] The mathematical conversion of a map from one projected coordinate system to another, generally used to integrate maps from two or more projected coordinate systems into a GIS.

Prolate ellipsoid: [mathematics] An ellipsoid created by rotating an ellipse around its major axis.

Proximity analysis: [spatial analysis] A type of analysis in which geographic features (points, lines, polygons, or raster cells) are selected based on their distance from other features or cells.

Pyramid: [data structures] In raster datasets, a reduced resolution layer that copies the original data in decreasing levels of resolution to enhance performance. The coarsest level of resolution is used to quickly draw the entire dataset. As the display zooms in, layers with finer resolutions are drawn; drawing speed is maintained because fewer pixels are needed to represent the successively smaller areas.

Q

Qualitative data: [data structures] Data classified or shown by category, rather than by amount or rank, such as soil by type or animals by species.

Quantile: [statistics] In a data distribution, a value representing a class break, where classes contain approximately equal numbers of observations. The p-th quantile, where p is between 0 and 1, is that value that has a proportion p of the data below the value. For theoretical distributions, the p-th quantile is the value that has p probability below the value.

Quantile classification: [data structures] A data classification method that distributes a set of values into groups that contain an equal number of values.

Quantitative data: [data structures] Data grouped or shown by measurements of number or amount, such as population per unit area.

Quantitative geography: [geography] The application of mathematical and statistical concepts and methods to the study of geography.

Query: [programming] A request to select features or records from a database. A query is often written as a statement or logical expression.

R

Radar: [physics] Acronym for radio detection and ranging. A device or system that detects surface features on the earth by bouncing radio waves off them and measuring the energy reflected back.

Radar altimeter: [physics] An instrument that determines elevation, usually from mean sea level, by measuring the amount of time an electromagnetic pulse takes to travel from an aircraft to the ground and back again.

Radar interferometry: [remote sensing] The analysis of interferograms that have been created by IFSAR, or artificially. Radar interferometry involves the comparison of two or more images of the same area taken from different positions and calibrated with surveyed ground points to generate three-dimensional digital elevation models (DEMs), or models demonstrating slight movements of surface features.

Radiation: [physics] The emission and propagation of energy through space in the form of waves. Electromagnetic energy and sound are examples of radiation.

Radiometer: [physics] An instrument that measures the intensity of radiation in a particular band of wavelengths in the electromagnetic spectrum, such as infrared or microwave.

Radiometric resolution: [physics] The sensitivity of a sensor to incoming reflectance. Radiometric resolution refers to the number of divisions of bit depth (for example, 255 for 8-bit, 65,536 for 16-bit, and so on) in data collected by a sensor.

Raster: [data models] A spatial data model that defines space as an array of equally sized cells arranged in rows and columns, and composed of single or multiple bands. Each cell contains an attribute value and location coordinates. Unlike a vector structure, which stores coordinates explicitly, raster coordinates are contained in the ordering of the matrix. Groups of cells that share the same value represent the same type of geographic feature.

Raster dataset band: [remote sensing] One layer in a raster dataset that represents data values for a specific range in the electromagnetic spectrum (such as ultraviolet, blue, green, red, and infrared), or radar, or other values derived by manipulating the original image bands. A raster dataset can contain more than one band. For example, satellite imagery commonly has multiple bands representing different wavelengths of energy from along the electromagnetic spectrum.

Raster postprocessing: [data conversion] In ArcScan, the automatic correction of vector feature results immediately after batch vectorization is completed. Postprocessing involves generalizing lines, straightening angles, and smoothing lines.

Raster preprocessing: [data conversion] Simple raster editing that prepares images for viewing and analysis. Preprocessing includes georeferencing, clipping, positioning, resizing, enhancing, and mosaicking.

Rasterization: [data conversion] The conversion of points, lines, and polygons into cell data.

Rectification: [data conversion] The process of applying a mathematical transformation to an image so that the result is a planimetric image.

Reflectance: [physics] The proportion of incident radiant energy that is reflected by a surface. Reflectance varies according to the wavelengths of the incident radiant energy and the color and composition of the surface.

Regression: [statistics] A statistical method for evaluating the relationship between a single dependent variable and one or more independent variables thought to influence the dependent variable. Regression is used to predict the value of the dependent variable or to determine whether an independent variable in fact influences the dependent variable, and to what extent.

Universidad Politécnica de Cataluña, Barcelona TECH
Departamento de Tecnología de la Arquitectura
Centro de Políticas de Suelo y Valoraciones
Nicola Colaninno, Josep Roca Cladera

Regression coefficient: [statistics] A value associated with each independent variable in a regression equation, representing the strength and type of relationship the independent variable has to the dependent variable. For example, fire frequency might be modeled as a function of solar radiation, vegetation, precipitation, and aspect. A positive relationship between fire frequency and solar radiation is likely (the more sun, the more frequent the fire incidents). When the relationship is positive, the sign for the associated coefficient is also positive. A negative relationship between fire frequency and precipitation is also likely (places with more rain have fewer fires). Coefficients for negative relationships have negative signs. If the relationship is strong, the absolute value of the coefficient is large. Weak relationships are associated with coefficients near zero.

Regression equation: [statistics] The mathematical formula applied to independent variables to best predict the dependent variable being modeled. The notation in regression equations is always Y for the dependent variable and X for the independent variables. Each independent variable is associated with a regression coefficient describing the strength and sign of that variable's relationship to the dependent variable. A regression equation might look like this (where b represents a regression coefficient): $Y = b_0 + b_1X_1 + b_2X_2 + \ldots b_nX_n$

Relief: [cartography] Elevations and depressions of the earth's surface, including those of the ocean floor. Relief can be represented on maps by contours, shading, hypsometric tints, digital terrain modeling, or spot elevations.

Remote sensing: [remote sensing] Collecting and interpreting information about the environment and the surface of the earth from a distance, primarily by sensing radiation that is naturally emitted or reflected by the earth's surface or from the atmosphere, or by sensing signals transmitted from a device and reflected back to it. Examples of remote-sensing methods include aerial photography, radar, and satellite imaging.

Remote-sensing imagery: [remote sensing] Imagery acquired from satellites and aircraft, including panchromatic, radar, microwave, and multispectral satellite imagery.

Rendering: [graphics (computing)] The process of drawing to a display; the conversion of the geometry, colouring, texturing, lighting, and other characteristics of an object into a display image.

Resampling: [mathematics] The process of interpolating new cell values when transforming rasters to a new coordinate space or cell size.

Residual: [statistics] In a regression model, the difference between the observed Y value and the predicted Y value; the unexplained portion of the dependent variable. Predicted values rarely match observed values exactly. The residual is one measure of model fit. Large residuals indicate poor model fit.

Resolution: 1 [cartography] The detail with which a map depicts the location and shape of geographic features. The larger the map scale, the higher the possible resolution. As scale decreases, resolution diminishes and feature boundaries must be smoothed, simplified, or not shown at all; for example, small areas may have to be represented as points; 2 [graphics (computing)] The dimensions represented by each cell or pixel in a raster; 3 [graphics (computing)] The smallest spacing between two display elements, expressed as dots per inch, pixels per line, or lines per millimeter

RGB: [graphics (computing)] A colour model that uses red, green, and blue, the primary additive colours used to display images on a monitor. RGB colours are produced by emitting light, rather than by absorbing it as is the case with ink on paper. Adding 100 percent of all three colours results in white.

RMS error: [spatial statistics (use for geostatistics)] Acronym for root mean square error. A measure of the difference between locations that are known and locations that have been interpolated or digitized. RMS error is derived by squaring the differences between known and unknown points, adding those together, dividing that by the number of test points, and then taking the square root of that result.

R-squared: [statistics] A statistic computed by the regression equation to quantify model performance. The value of R-squared ranges from 0 to 100 percent. If a model fits the observed dependent variable values perfectly, the R-squared value is 1.0, although this is highly unlikely. An R-squared value like 0.49, for example, is far more likely, and means that the model explains 49% of the variation in the dependent variable.

S

Satellite constellation: 1 [remote sensing] The arrangement of a set of satellites in space; 2 [GPS] All the satellites visible to a GPS receiver at one time; 3 [GPS] The set of satellites that a GPS receiver uses to calculate positions.

Saturation: 1 [graphics (map display)] The intensity or purity of a colour; the perceived amount of white in a hue relative to its brightness, or how free it is of grey of the same value; **2** [physics] The point at which energy flux exceeds the sensitivity range of a detector.

Scale: 1 [cartography] The ratio or relationship between a distance or area on a map and the corresponding distance or area on the ground, commonly expressed as a fraction or ratio. A map scale of 1/100,000 or 1:100,000 means that one unit of measure on the map equals 100,000 of the same unit on the earth; **2** [data quality] In reference to double precision, the number of digits to the right of the decimal point in a number. For example, the number 56.78 has a scale of 2.

Scanner: 1 [data capture] A device that captures a print or hard-copy image, such as a text document or map, and records the information in digital format; **2** [remote sensing] A device that records the radiation reflected or emitted by the earth's surface.

SDI: [data sharing] Acronym for spatial data infrastructure. A framework of technologies, policies, standards, and human resources necessary to acquire, process, store, distribute, and improve the use of geospatial data across multiple public and private organizations.

Sensor: [remote sensing] An electronic device for detecting energy, whether emitted or radiated, and converting it into a signal that can be recorded and displayed as numbers or as an image.

Shaded relief image: [visualization] A raster image that shows changes in elevation using light and shadows on terrain from a given angle and altitude of the sun.

Shape: [data models] The characteristic appearance or visible form of a geographic object as represented on a map. A GIS uses points, lines, and polygons to represent the shapes of geographic objects.

Shapefile: [ESRI software] A vector data storage format for storing the location, shape, and attributes of geographic features. A shapefile is stored in a set of related files and contains one feature class.

Signal: 1 [remote sensing] Information conveyed via an electric current or electromagnetic wave; **2** [physics] The modulation of an electric current, electromagnetic wave, or other type of flow in order to convey information.

Signal-to-noise ratio: [remote sensing] The ratio of the information content of a signal to its noninformation content (noise).

Slope: [Euclidean geometry] The incline, or steepness, of a surface. Slope can be measured in degrees from horizontal (0–90), or percent slope (which is the rise divided by the run, multiplied by 100). A slope of 45 degrees equals 100 percent slope. As slope angle approaches vertical (90 degrees), the percent slope approaches infinity. The slope of a TIN face is the steepest downhill slope of a plane defined by the face. The slope for a cell in a raster is the steepest slope of a plane defined by the cell and its eight surrounding neighbors.

Smoothing: [digital image processing] In image processing, reducing or removing small variations in an image to reveal the global pattern or trend, either through interpolation or by passing a filter over the image.

Sonar: [remote sensing] Acronym for sound navigation and ranging. A system or device that measures the time lapse between emitting a sound and receiving a returned echo to determine the location, depth and shape of objects under water. Certain types of sonar consist only of a listening device that picks up sound emitted by underwater objects, such as submarines.

Space coordinate system: [coordinate systems] A three-dimensional, rectangular, Cartesian coordinate system that has not been adjusted for the earth's curvature. In a space coordinate system, the x- and y-axes lie in a plane tangent to the earth's surface, and the z-axis points upward.

Spatial analysis: [spatial analysis] The process of examining the locations, attributes, and relationships of features in spatial data through overlay and other analytical techniques in order to address a question or gain useful knowledge. Spatial analysis extracts or creates new information from spatial data.

Spatial data: 1 [data structures] Information about the locations and shapes of geographic features and the relationships between them, usually stored as coordinates and topology; **2** [data models] Any data that can be mapped.

Spatial modelling: [modelling] A methodology or set of analytical procedures used to derive information about spatial relationships between geographic phenomena.

Universidad Politécnica de Cataluña, Barcelona TECH
Departamento de Tecnología de la Arquitectura
Centro de Políticas de Suelo y Valoraciones
Nicola Colaninno, Josep Roca Cladera

Spatial statistics: [statistics] The field of study concerning statistical methods that use space and spatial relationships (such as distance, area, volume, length, height, orientation, centrality and/or other spatial characteristics of data) directly in their mathematical computations. Spatial statistics are used for a variety of different types of analyses, including pattern analysis, shape analysis, surface modelling and surface prediction, spatial regression, statistical comparisons of spatial datasets, statistical modelling and prediction of spatial interaction, and more. The many types of spatial statistics include descriptive, inferential, exploratory, geostatistical, and econometric statistics.

Spectral resolution: [satellite imaging] The range of wavelengths that an imaging system can detect.

Spectral signature: [physics] The pattern of electromagnetic radiation that identifies a chemical or compound. Materials can be distinguished from one another by examining which portions of the spectrum they reflect and absorb.

Spectrophotometer: [physics] A photometer that measures the intensity of electromagnetic radiation as a function of its frequency. Spectrophotometers are usually used for measuring the visible portion of the spectrum.

Spectroscopy: [physics] The scientific study of how different chemicals and other substances absorb and reflect different parts of the electromagnetic spectrum.

Spheroid: 1 [Euclidean geometry] A three-dimensional shape obtained by rotating an ellipse about its minor axis, resulting in an oblate spheroid, or about its major axis, resulting in a prolate spheroid; **2** [geodesy] When used to represent the earth, a three-dimensional shape obtained by rotating an ellipse about its minor axis, with dimensions that either approximate the earth as a whole, or with a part that approximates the corresponding portion of the geoid.

Spline: [mathematics] In mathematics, a piecewise polynomial function used to approximate a smooth curve in a line or surface.

SPOT: [satellite imaging] Acronym for Satellite Pour l'Observation de la Terre. Earth observation satellites developed by Centre National d'Etudes Spatiales (CNES), the space agency of France. The SPOT satellites gather high-resolution imagery used in natural resource management, climatology, oceanography, environmental monitoring, and the monitoring of human activities.

SQL: [programming] Acronym for Structured Query Language. A syntax for retrieving and manipulating data from a relational database. SQL has become an industry standard query language in most relational database management systems.

Standard deviation: [statistics] A statistical measure of the spread of values from their mean, calculated as the square root of the sum of the squared deviations from the mean value, divided by the number of elements minus one. The standard deviation for a distribution is the square root of the variance.

Standard distance: [spatial statistics (use for geostatistics)] A measure of the compactness of a spatial distribution of features around its mean center. Standard distance (or standard distance deviation) is usually represented as a circle where the radius of the circle is the standard distance.

Stereopair: [photogrammetry] Two aerial photographs of the same area taken from slightly different angles that when viewed together through a stereoscope produce a three-dimensional image.

Stochastic model: [modelling] A model that includes a random component. The random component can be a model variable, or it can be added to existing input data or model parameters.

Street network: [network analysis] A system of interconnecting lines and points that represent a system of roads for a given area. A street network provides the foundation for network analysis; for example, finding the best route or creating service areas.

Stretch: [visualization] A display technique applied to the histogram of raster datasets, most often used to increase the visual contrast between cells.

Syntax: [programming] The structural rules for using statements in a command or programming language.

T

Tangent projection: [map projections] A projection whose surface touches the globe's without piercing it. A tangent planar projection touches the globe at one point, while tangent conic and cylindrical projections touch the globe along a line. At the point or line of tangency, the projection is free from distortion.

Texture: [3D GIS] A digital representation of the surface of a feature.

Thematic map: [map design] A map designed to convey information about a single topic or theme, such as population density or geology.

Thiessen polygons: [Euclidean geometry] Polygons generated from a set of sample points. Each Thiessen polygon defines an area of influence around its sample point, so that any location inside the polygon is closer to that point than any of the other sample points. Thiessen polygons are named for the American meteorologist Alfred H. Thiessen (1872-1931).

Tiling: [data structures] An internal subsetting of a spatial dataset (commonly raster) into a manageable rectangular set, or rows and columns of pixels, typically used to process or analyze a large raster dataset without consuming vast quantities of computer memory.

TIN: [data structures] Acronym for triangulated irregular network. A vector data structure that partitions geographic space into contiguous, nonoverlapping triangles. The vertices of each triangle are sample data points with x-, y-, and z-values. These sample points are connected by lines to form Delaunay triangles. TINs are used to store and display surface models.

Topographic map: [cartography] A map that represents the vertical and horizontal positions of features, showing relief in some measurable form, such as contour lines, hypsometric tints, and relief shading.

Topography: [cartography] The study and mapping of land surfaces, including relief (relative positions and elevations) and the position of natural and constructed features.

Topology: 1 [ESRI software] In geodatabases, the arrangement that constrains how point, line, and polygon features share geometry. For example, street centerlines and census blocks share geometry, and adjacent soil polygons share geometry. Topology defines and enforces data integrity rules (for example, there should be no gaps between polygons). It supports topological relationship queries and navigation (for example, navigating feature adjacency or connectivity), supports sophisticated editing tools, and allows feature construction from unstructured geometry (for example, constructing polygons from lines); **2** [Euclidean geometry] The branch of geometry that deals with the properties of a figure that remain unchanged even when the figure is bent, stretched, or otherwise distorted.

Triangulation: [surveying] Locating positions on the earth's surface using the principle that if the measures of one side and the two adjacent angles of a triangle are known, the other dimensions of the triangle can be determined. Surveyors begin with a known length, or baseline, and from each end use a theodolite to measure the angle to a distant point, forming a triangle. Once the lengths of the two sides and the other angle are known, a network of triangles can be extended from the first.

Trilateration: [surveying] Determining the position of a point on the earth's surface with respect to two other points by measuring the distances between all three points.

U

U.S. Geological Survey: [environmental GIS] Acronym for United States Geological Survey. A scientific agency of the U.S. government, part of the Department of the Interior. The U.S. Geological Survey is a fact-finding research agency that monitors, analyzes, and provides scientific understanding about natural resource issues and conditions, the environment, and natural hazards. The U.S. Geological Survey is the primary civilian mapping agency in the United States. It produces digital and paper map products; aerial photography; and remotely sensed data on land cover, hydrology, geology, biology, and geography.

Univariate analysis: [statistics] Any statistical method for evaluating a single variable, rather than the relationship between two or more variables.

Univariate distribution: [statistics] A function for a single variable that gives the probabilities that the variable will take a given value.

Universidad Politécnica de Cataluña, Barcelona TECH
Departamento de Tecnología de la Arquitectura
Centro de Políticas de Suelo y Valoraciones
Nicola Colaninno, Josep Roca Cladera

Universal polar stereographic: [coordinate systems] A projected coordinate system that covers all regions not included in the UTM coordinate system; that is, regions above 84 degrees north and below 80 degrees south. Its central point is either the north or south pole.

Urban geography: [geography] The field of geography concerning the spatial and cultural patterns and processes of cities and neighborhoods.

UTM: [coordinate systems] Acronym for universal transverse Mercator. A projected coordinate system that divides the world into 60 north and south zones, 6 degrees wide.

V

Variance: [statistics] A numeric description of how values in a distribution vary or deviate from the mean. The larger the variance, the greater the dispersion of values around the mean. The standard deviation for a distribution is the square root of the variance.

Variance-covariance matrix: [surveying] In surveying, the symmetric 3x3 matrix that mathematically expresses the correlation between errors in coordinates x, y, and z.

Variogram: [spatial statistics (use for geostatistics)] A function of the distance and direction separating two locations that is used to quantify dependence. The variogram is defined as the variance of the difference between two variables at two locations. The variogram generally increases with distance and is described by nugget, sill, and range parameters. If the data is stationary, then the variogram and the covariance are theoretically related to each other.

Vector: 1 [data models] A coordinate-based data model that represents geographic features as points, lines, and polygons. Each point feature is represented as a single coordinate pair, while line and polygon features are represented as ordered lists of vertices. Attributes are associated with each vector feature, as opposed to a raster data model, which associates attributes with grid cells; **2** [graphics (computing)] Any quantity that has both magnitude and direction.

Vectorization: [data conversion] The conversion of raster data (an array of cell values) to vector data (a series of points, lines, and polygons).

Vertical geodetic datum: [geodesy] A geodetic datum for any extensive measurement system of heights on, above, or below the earth's surface. Traditionally, a vertical geodetic datum defines zero height as the mean sea level at a particular location or set of locations; other heights are measured relative to a level surface passing through this point. Examples include the North American Vertical Datum of 1988; the Ordnance Datum Newlyn (used in Great Britain); and the Australian Height Datum.

Viewshed: [3D analysis] The locations visible from one or more specified points or lines. Viewshed maps are useful for such applications as finding well-exposed places for communication towers, or hidden places for parking lots.

VMap: [standards] Acronym for Vector Map. A vector-based data product in vector product format (VPF) at several scales divided into groups, referred to as levels. For example, VMap Level 1 includes vector maps at a scale of 1:250,000, and VMap Level 2 includes vector maps at a scale of 1:50,000.

Voronoi diagram: [Euclidean geometry] A partition of space into areas, or cells, that surround a set of geometric objects (usually points). These cells, or polygons, must satisfy the criteria for Delaunay triangles. All locations within an area are closer to the object it surrounds than to any other object in the set. Voronoi diagrams are often used to delineate areas of influence around geographic features. Voronoi diagrams are named for the Ukrainian mathematician Georgy Fedoseevich Voronoi (1868-1908).

W

Watershed: [hydrology] A basin-like terrestrial region consisting of all the land that drains water into a common terminus.

Wavelength: [physics] The distance between two successive crests on a wave, calculated as the velocity of the wave divided by its frequency.

Wavelet compression: [data storage] A lossy method of data compression that uses mathematical functions and is best used in image or sound compression.

Weight: [mathematics] A number that indicates the importance of a variable for a particular calculation. The larger the weight assigned to the variable, the more that variable will influence the outcome of the operation.

Weighted mean center: [spatial statistics (use for geostatistics)] The geographic center of a set of points as adjusted for the influence of a value associated with each point. For example, while the mean center of a group of grocery stores would be the location obtained by averaging the stores' x,y coordinates, the weighted mean center would be shifted closer to stores with higher sales, more square footage, or a greater quantity of some other specified attribute.

WGS72: [geodesy] Acronym for World Geodetic System 1972. A geocentric datum and coordinate system designed by the U.S. Department of Defense, no longer in use.

WGS84: [geodesy] Acronym for World Geodetic System 1984. The most widely used geocentric datum and geographic coordinate system today, designed by the U.S. Department of Defense to replace WGS72. GPS measurements are based on WGS84.

Workflow: **1** [organizational issues] An organization's established processes for design, construction, and maintenance of programs, products, and business objectives; **2** [organizational issues] A set of tasks carried out in a certain order to achieve a goal.

Workspace: 1. [ESRI software] A container for geographic data. A workspace can be a folder that contains shapefiles, a geodatabase, a feature dataset, or an ArcInfo workspace. Other multidimensional data formats such as netCDF or HDF can also be considered workspaces, and are often treated in this manner within GIS software packages.

X

x,y coordinates: [coordinate systems] A pair of values that represents the distance from an origin (0,0) along two axes, a horizontal axis (x), and a vertical axis (y). On a map, x,y coordinates are used to represent features at the location they are found on the earth's spherical surface.

x,y,z coordinates: [coordinate systems] In a planar coordinate system, three coordinates that locate a point by its distance from an origin (0,0,0) where three orthogonal axes cross. Usually, the x-coordinate is measured along the east–west axis, the y-coordinate is measured along the north–south axis, and the z-coordinate measures height or elevation.

x-axis: **1** [coordinate systems] In a planar coordinate system, the horizontal line that runs right and left (east and west of) the origin (0,0); **2** [mathematics] On a chart, the horizontal axis.

XML: [programming] Acronym for Extensible Markup Language. Developed by the W3C, a standardized general purpose markup language for designing text formats that facilitates the interchange of data between computer applications. XML is a set of rules for creating standard information formats using customized tags and sharing both the format and the data across applications.

Y

y-axis: **1** [coordinate systems] In a planar coordinate system, the vertical line that runs above and below (north and south of) the origin (0,0). Numbers north of the origin are positive, and numbers south of it are negative; **2** [coordinate systems] In a spherical coordinate system, a line in the equatorial plane that passes through 90 degrees east longitude; **3** [mathematics] On a chart, the vertical axis.

Z

z-axis: [coordinate systems] In a spherical coordinate system, the vertical line that runs parallel to the earth's rotation, passing through 90 degrees north latitude, and perpendicular to the equatorial plane, where it crosses the x- and y-axes at the origin (0,0,0).

Universidad Politécnica de Cataluña, Barcelona TECH
Departamento de Tecnología de la Arquitectura
Centro de Políticas de Suelo y Valoraciones
Nicola Colaninno, Josep Roca Cladera

Zenith: [astronomy] In astronomy, the point on the celestial sphere directly above an observer. Both the zenith and nadir lie on the observer's meridian; the zenith lies 180 degrees from the nadir, and is observable.

z-factor: [coordinate systems] A conversion factor used to adjust vertical and horizontal measurements into the same unit of measure. Specifically, the number of vertical units (z-units) in each horizontal unit. For example, if a surface's horizontal units are meters and its elevation (z) is measured in feet, the z-factor is 0.3048 (the number of meters in a foot).

Zoning: [local government] The application of local government regulations that permit certain land uses within geographic areas under the government's jurisdiction. Zoning regulations typically set a broad category of land use permissible in an area, such as residential, commercial, agricultural, or industrial. Zoning regulations can also set constraints on building construction within areas, which may affect factors such as the maximum height of structures, minimum setbacks from property lines, the amount of parking that must be provided, or the density of housing.

z-score: [statistics] A statistical measure of the spread of values from their mean, expressed in standard deviation units, where the z-score of the mean value is zero and the standard deviation is one. In a normal distribution, 68 percent of the values have a z-score of plus or minus 1, meaning they lie within one standard deviation of the mean. Ninety-five percent of the values have a z-score of plus or minus 1.96, meaning they lie within two standard deviations of the mean; 99 percent of the values have a z-score of plus or minus 2.58. Z-scores are a common scale on which different distributions, with different means and standard deviations, can be compared.

z-value: [coordinate systems] The value for a given surface location that represents an attribute other than position. In an elevation or terrain model, the z-value represents elevation; in other kinds of surface models, it represents the density or quantity of a particular attribute.

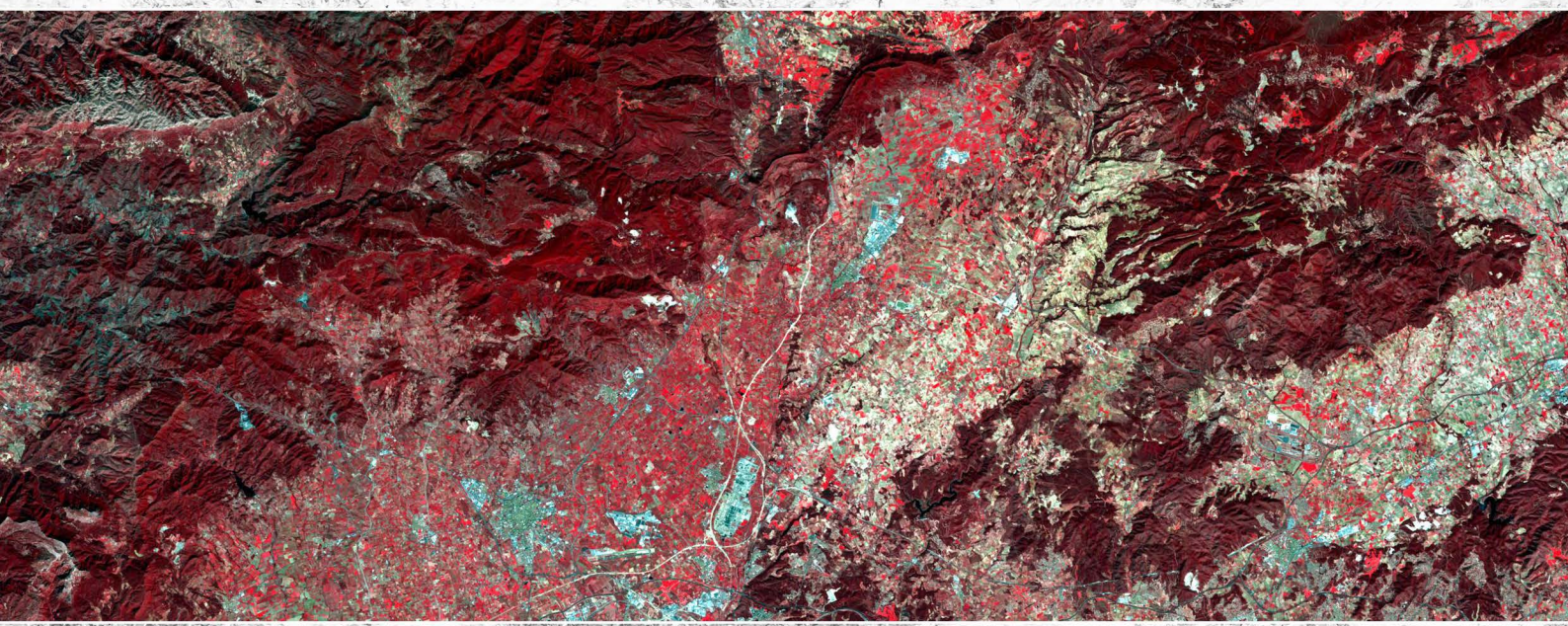

UNIVERSITAT POLITÈCNICA
DE CATALUNYA
BARCELONATECH